Camiel J.F. Boon
Jan Wijnholds   *Editors*

Retinal Gene Therapy

Methods and Protocols

Humana Press

METHODS IN MOLECULAR BIOLOGY

Retinal Gene Therapy

Methods and Protocols

Edited by

Camiel J.F. Boon

*Department of Ophthalmology, Leiden University Medical Center (LUMC),
Leiden, The Netherlands; Department of Ophthalmology, Academic Medical Center,
University of Amsterdam, Amsterdam, The Netherlands*

Jan Wijnholds

*Department of Ophthalmology, Leiden University Medical Center (LUMC),
Leiden, The Netherlands; Netherlands Institute for Neuroscience, Royal Netherlands Academy of Arts and
Sciences (KNAW), Amsterdam, The Netherlands*

✷ Humana Press

Editors
Camiel J.F. Boon
Department of Ophthalmology
Leiden University Medical Center (LUMC)
Leiden, The Netherlands

Department of Ophthalmology
Academic Medical Center
University of Amsterdam
Amsterdam, The Netherlands

Jan Wijnholds
Department of Ophthalmology
Leiden University Medical Center (LUMC)
Leiden, The Netherlands

Netherlands Institute for Neuroscience
Royal Netherlands Academy of Arts
and Sciences (KNAW)
Amsterdam, The Netherlands

Preface

The eye is in the frontline of gene therapy development. As a relatively closed compartment, it is on the one hand relatively isolated and immune-privileged from the rest of the body, yet at the same time well-accessible to surgical intervention and a broad range of clinical examinations of its structure and function. The eye is therefore an attractive target organ for the application of gene therapy. With more than 2000 clinical trials to date for a wide range of genetic diseases, ocular gene therapy offers a promising perspective for the more than currently known 250 retinal disease genes. A preferred delivery system are the adeno-associated viral (AAV) gene therapy vectors for gene augmentation, gene editing, and miRNA delivery, next to the antisense oligonucleotide delivery system. As in preclinical studies, ocular clinical gene therapy studies know their successes and disappointments. The first successful ocular clinical studies for the orphan drug AAV-*RPE65* for Leber congenital amaurosis and retinitis pigmentosa were reported in the literature in 2008. More than a decade later, AAV-*RPE65* retinal gene therapy approaches are evaluated in phase 3 clinical studies and reached market approval. Clinical development of retinal gene therapy is yet a time-consuming process for technological as well financial reasons, but many more successes are expected in the coming decade for ocular gene augmentation, gene editing, miRNA delivery, as well as the antisense oligonucleotide delivery system.

This volume of *Methods in Molecular Biology* describes a spectrum of methods and protocols that can be used for the bench-to-bedside development and evaluation of retinal gene therapy. Methods for the successful delivery of these gene therapy vector systems to the retina are reviewed, as well as assays to test the efficacy in vitro in cell cultures; in vivo on rodents, pigs, and monkey retinas; and on human retinal explants as well as in human clinical studies. Chapters in this book are organized into three major parts: Part I elaborates on the production of retinal gene therapy vectors and testing these in biological assays in vitro. Part II describes assays for gene augmentation and gene editing in vivo on rodent, pig, and macaque retina. Part III highlights clinical protocols and retinal gene therapy vector testing on human retina. Written in the highly successful *Methods in Molecular Biology* series format, chapters include introductions to their respective topics, with step-by-step lists of the necessary materials and reagents, readily reproducible laboratory protocols, and tips on troubleshooting and how to avoid known pitfalls.

The preparation of AAVs is a relatively simple task for the ones skilled in molecular biology, but robust protocols are needed to obtain high-quality high-titer stocks of AAV. In Part I, we have included three of such chapters, Chapters 1–3, describing detailed various techniques to produce microscale and small-scale batches of AAVs with useful notes on the various steps in the production. AAVs have a limited packaging capacity compared to lentiviral vectors, but vectors with multiple gene cassettes enabling cell-specific co-expression of microRNA (miRNA) and protein factors are of high interest. In Chapter 4, we have included such an example that may contribute to the development of combination therapies for various ocular diseases. Other promising retinal gene therapy methods such as the use of antisense oligonucleotides (AONs) to correct pre-mRNA splicing defects involved in inherited retinal dystrophies are described in Chapter 5. Bioavailability and bioactivity of retinal gene delivery system products can be tested in three-dimensional co-culture assays, and these methods and protocols are described in Chapter 6. To test new gene therapy AAV gene

augmentation vectors, there is a need for reliable and sensitive in vitro assays to determine the expression of delivered proteins, which is covered in Chapter 7. In Part II, we highlight assays for gene augmentation and editing in vivo on rodent, pig, and macaque retina. Chapter 8 describes techniques to study the expression of gene therapy vectors upon in vivo electroporation of the developing mouse retina. Clustered Regularly Interspaced Short Palindromic Repeats (CRISPR)-associated protein or CRISPR/Cas gene editing of the adult retina is a powerful technique for correcting inherited ocular disease, and Chapters 9 and 13 describe methods to apply these techniques in preclinical models. Chapters 10 and 11 present protocols to detect the expression of therapeutic protein by fluorescence immunohistochemistry, histological studies using ultrathin sections, and immuno-electron microscopy and confocal laser scanning microscopy. Application techniques to deliver AAV vectors either subretinally or intravitreally into the murine retinas are described in Chapters 9–13 and 15. Very large genes cannot be expressed in a single AAV vector, but some can be expressed using dual-vector technology approaches as described in Chapter 11. Chapter 12 highlights methods for optogenetic retinal gene therapy to express light-sensitive G protein-coupled receptors (GPCRs) in retinal neurons, recording light responses in retinal explants in vitro by multielectrode array (MEA), recording cortical light responses in vivo by visually evoked response (VEP), and testing visually guided behavior in open field test and water maze task in treated mice. Noninvasive diagnostic methods to assess retinal function and morphology in vivo in rodents by electroretinography (ERG) and optical coherence tomography (OCT) are discussed in Chapters 9, 13, and 14. Neutralizing antibodies (NABs) to AAVs may limit the infection capacity when administered intravitreal to the retina, and therefore, Chapters 16 and 17 are included to describe methods to screen rodent and nonhuman primate (NHP) serum for pre-existing NABs, providing useful tips and tricks. Chapters 11 and 18 focus on techniques for subretinal and intravitreal retinal injections in large animal models such as pigs and monkeys. Part III deals with clinical protocols and retinal gene therapy vector testing on human retinal explants and in vivo evaluation of the human retina in the context of retinal gene therapy. Natural as well as recombinant AAVs need to be tested on human tissue for their infection and expression efficacy. Chapter 19 describes iPS-derived human retina production protocols as well as methods to infect retinal cell types with AAVs. Chapters 20 and 21 highlight ex vivo validation on cultured retinal explants obtained from donor retina or from retinal surgery, respectively. Chapters 22–26 describe clinical protocols that can be used in retinal gene therapy studies such as visual acuity testing, electroretinography, visual field testing by Goldmann perimetry, central visual field sensitivity testing by fundus-driven perimetry also known as microperimetry, and spectral domain optical coherence tomography (SD-OCT) and OCT angiography. Methods to test vector shedding have become increasingly important with the number of AAV gene therapy trials that have started, and Chapter 27 describes standard operating protocols for these.

Retinal gene therapy is a broad field of research using various methods and protocols. This book therefore provides a wide range of readers from students to research experts with useful information on ocular gene therapy vector technology, in vitro and in vivo biological assays, and clinical protocols. We hope that the book finds its way in the scientific community to promote further studies for the benefit of children and adults with inherited retinal disease.

We thank all of the contributors for their enthusiastic and valuable contributions, the series editor John Walker, and Springer Nature for their support that made this volume possible.

Leiden, The Netherlands   *Camiel J.F. Boon*
                                                                                                          Jan Wijnholds

Contents

PART I   RETINAL GENE THERAPY VECTOR PRODUCTION
            AND BIOLOGICAL ASSAYS IN VITRO

PART II   ASSAYS FOR GENE AUGMENTATION AND EDITING IN VIVO
             ON RODENT AND MACAQUE RETINA

Contributors

C. Henrique Alves • *Department of Ophthalmology, Leiden University Medical Center (LUMC), Leiden, The Netherlands*

Anne Louise Askou • *Department of Biomedicine, Aarhus University, Aarhus, Denmark*

Callan L. Attwell • *Netherlands Institute for Neurosciences, Amsterdam, The Netherlands*

Alun R. Barnard • *Nuffield Laboratory of Ophthalmology, Nuffield Department of Clinical Neurosciences, John Radcliffe Hospital, University of Oxford, Oxford, UK; NIHR Oxford Biomedical Research Centre, University of Oxford, Oxford, UK; Oxford Eye Hospital, Oxford University Hospitals NHS Foundation Trust, Oxford, UK*

K. Ulrich Bartz-Schmidt • *University Eye Hospital, University of Tübingen, Tübingen, Germany*

Alexander G. Bassuk • *Department of Pediatrics and Neurology, University of Iowa, Iowa City, IA, USA*

Elvir Becirovic • *Department of Pharmacy, Center for Drug Research, Center for Integrated Protein Science Munich CiPSM, Ludwig-Maximilian-University, Munich, Germany*

Michael H. Berry • *Department of Molecular and Cell Biology, University of California Berkeley, Berkeley, CA, USA*

Martin Biel • *Department of Pharmacy, Center for Drug Research, Center for Integrated Protein Science Munich CiPSM, Ludwig-Maximilian-University, Munich, Germany*

Seth Blackshaw • *Solomon H. Snyder Department of Neuroscience, Johns Hopkins University School of Medicine, Baltimore, MD, USA; Department of Neurology, Johns Hopkins University School of Medicine, Baltimore, MD, USA; Department of Ophthalmology, Johns Hopkins University School of Medicine, Baltimore, MD, USA; Center for Human Systems Biology, Johns Hopkins University School of Medicine, Baltimore, MD, USA; Institute for Cell Engineering, Johns Hopkins University School of Medicine, Baltimore, MD, USA*

Camiel J.F. Boon • *Department of Ophthalmology, Leiden University Medical Center (LUMC), Leiden, The Netherlands; Department of Ophthalmology, Academic Medical Center, University of Amsterdam, Amsterdam, The Netherlands*

Thilo M. Buck • *Department of Ophthalmology, Leiden University Medical Center (LUMC), Leiden, The Netherlands*

Bang V. Bui • *Department of Optometry & Vision Sciences, University of Melbourne, Parkville, VIC, Australia*

Leah C. Byrne • *The Helen Wills Neuroscience Institute, University of California, Berkeley, CA, USA; Department of Clinical Studies, School of Veterinary Medicine, University of Pennsylvania, Philadelphia, PA, USA*

Thiago Cabral • *Jonas Children's Vision Care, and Bernard & Shirlee Brown Glaucoma Laboratory, Columbia University Medical Center, New York, NY, USA; Department of Ophthalmology, Columbia University, New York, NY, USA; Department of Ophthalmology, Federal University of Sao Paulo (UNIFESP), São Paulo, Brazil; Department of Ophthalmology, Federal University of Espírito Santo (UFES), Vitória, Brazil*

DING WEN CHEN • *School of Pharmacy, Waterloo Institute of Nanotechnology, University of Waterloo, Waterloo, ON, Canada*

GALAXY Y. CHO • *Jonas Children's Vision Care, and Bernard & Shirlee Brown Glaucoma Laboratory, Columbia University Medical Center, New York, NY, USA; Department of Ophthalmology, Columbia University, New York, NY, USA*

ROB W.J. COLLIN • *Department of Human Genetics, Donders Institute for Brain, Cognition and Behaviour, Radboud University Medical Center, Nijmegen, The Netherlands*

THOMAS J. CORYDON • *Department of Biomedicine, Aarhus University, Aarhus, Denmark; Department of Ophthalmology, Aarhus University Hospital, Aarhus, Denmark*

GISLIN DAGNELIE • *Wilmer Eye Institute, Johns Hopkins University, Baltimore, MD, USA*

DENIZ DALKARA • *INSERM, U968, Paris, France; Sorbonne Universités, UPMC Univ Paris 06, UMR_S 968, Institut de la Vision, Paris, France; CNRS, UMR_7210, Paris, France*

DANIYAR DAULETBEKOV • *University Eye Hospital, University of Tübingen, Tübingen, Germany; Institute for Ophthalmic Research, Centre for Ophthalmology, University of Tübingen, Tübingen, Germany; Nuffield Laboratory of Ophthalmology, University of Oxford, Oxford, UK*

TIMOTHY P. DAY • *The Helen Wills Neuroscience Institute, The University of California at Berkeley, Berkeley, CA, USA*

SAMANTHA R. DE SILVA • *Nuffield Laboratory of Ophthalmology, Nuffield Department of Clinical Neurosciences, John Radcliffe Hospital, University of Oxford, Oxford, UK; Oxford Eye Hospital, Oxford University Hospitals NHS Foundation Trust, Oxford, UK*

MÉLISSA DESROSIERS • *INSERM, U968, Paris, France; Sorbonne Universités, UPMC Univ Paris 06, UMR_S 968, Institut de la Vision, Paris, France; CNRS, UMR_7210, Paris, France*

ELON H.C. VAN DIJK • *Department of Ophthalmology, Leiden University Medical Center (LUMC), Leiden, The Netherlands*

ALLISON L. DORFMAN • *Department of Ophthalmology & Neurology-Neurosurgery, Research Institute of the McGill University Health Centre/Montreal Children's Hospital, Montreal, QC, Canada*

THOMAS L. EDWARDS • *Nuffield Laboratory of Ophthalmology, Nuffield Department of Clinical Neurosciences, John Radcliffe Hospital, University of Oxford, Oxford, UK; Oxford Eye Hospital, Oxford University Hospitals NHS Foundation Trust, Oxford, UK*

RUBEN EGGERS • *Netherlands Institute for Neurosciences, Amsterdam, The Netherlands*

ERICH M.E. EHLERT • *Netherlands Institute for Neurosciences, Amsterdam, The Netherlands; UniQure, Amsterdam, The Netherlands*

M. DOMINIK FISCHER • *University Eye Hospital, University of Tübingen, Tübingen, Germany; Institute for Ophthalmic Research, Centre for Ophthalmology, University of Tübingen, Tübingen, Germany; Nuffield Laboratory of Ophthalmology, University of Oxford, Oxford, UK*

JOHN G. FLANNERY • *The Helen Wills Neuroscience Institute, University of California, Berkeley, CA, USA; Department of Molecular and Cell Biology, University of California, Berkeley, CA, USA; Vision Science, University of California Berkeley, Berkeley, CA, USA*

MARIANNA FOLDVARI • *Vision Science Graduate Group, School of Optometry, University of California, Berkeley, CA, Canada*

ALEJANDRO GARANTO • *Department of Human Genetics, Donders Institute for Brain, Cognition and Behaviour, Radboud University Medical Center, Nijmegen, The Netherlands*

MARINA GARCIA GARRIDO • *Division of Ocular Neurodegeneration, Centre for Ophthalmology, Institute for Ophthalmic Research, University of Tübingen, Tübingen, Germany*

BENJAMIN M. GAUB • *Department of Biosystems Science and Engineering (D-BSSE), Eidgenössische Technische Hochschule (ETH) Zürich, Basel, Switzerland*

MATHIEU GAUVIN • *Department of Ophthalmology & Neurology-Neurosurgery, Research Institute of the McGill University Health Centre/Montreal Children's Hospital, Montreal, QC, Canada*

ALAN R. HARVEY • *School of Anatomy, Physiology and Human Biology, The University of Western Australia, Crawley, WA, Australia; Perron Institute for Neurological and Translational Science, Nedlands, WA, Australia*

ALEX W. HEWITT • *Centre for Eye Research Australia, Royal Victorian Eye and Ear Hospital, East Melbourne, VIC, Australia; Menzies Institute for Medical Research, School of Medicine, University of Tasmania, Hobart, TAS, Australia; Ophthalmology, Department of Surgery, University of Melbourne, East Melbourne, VIC, Australia*

BARBARA HOBO • *Netherlands Institute for Neurosciences, Amsterdam, The Netherlands*

AMY HOLT • *Department of Molecular and Cell Biology, University of California Berkeley, Berkeley, CA, USA*

STEFAN A. HOYNG • *Netherlands Institute for Neurosciences, Amsterdam, The Netherlands; Department of Neurosurgery, Leiden University Medical Center, Leiden, The Netherlands*

SANDY S. HUNG • *Centre for Eye Research Australia, Royal Victorian Eye and Ear Hospital, East Melbourne, VIC, Australia*

EHUD Y. ISACOFF • *Department of Molecular and Cell Biology, University of California Berkeley, Berkeley, CA, USA; Physical Bioscience Division, Lawrence Berkeley National Laboratory, Berkeley, CA, USA; Helen Wills Neuroscience Institute, University of California Berkeley, Berkeley, CA, USA*

JASLEEN K. JOLLY • *Oxford Eye Hospital, John Radcliffe Hospital, Oxford, UK; Nuffield Laboratory of Ophthalmology and Oxford Biomedical Research Center, University of Oxford, Oxford, UK*

SALLY JUSTUS • *Jonas Children's Vision Care, and Bernard & Shirlee Brown Glaucoma Laboratory, Columbia University Medical Center, New York, NY, USA; Department of Ophthalmology, Columbia University, New York, NY, USA*

ANNA E. KING • *Wicking Dementia Research and Education Centre, University of Tasmania, Hobart, TAS, Australia*

JOANNA A. KORECKA • *Netherlands Institute for Neurosciences, Amsterdam, The Netherlands; Neuroregeneration Research Institute, McLean Hospital/Harvard Medical School, Belmont, MA, USA*

PIERRE LACHAPELLE • *Department of Ophthalmology & Neurology-Neurosurgery, Research Institute of the McGill University Health Centre/Montreal Children's Hospital, Montreal, QC, Canada*

BIN LI • *Department of Ophthalmology, Tongji Hospital, Tongji Medical College, Huazhong University of Science and Technology, Wuhan, Hubei Province, China*

FAN LI • *Centre for Eye Research Australia, Royal Victorian Eye and Ear Hospital, East Melbourne, VIC, Australia; Menzies Institute for Medical Research, School of Medicine, University of Tasmania, Hobart, TAS, Australia*

CHYUAN-SHENG LIN • *Department of Pathology and Cell Biology, Columbia University Medical Center, New York, NY, USA*

GUEI-SHEUNG LIU • *Centre for Eye Research Australia, Royal Victorian Eye and Ear Hospital, East Melbourne, VIC, Australia; Menzies Institute for Medical Research, School of Medicine, University of Tasmania, Hobart, TAS, Australia; Ophthalmology, Department of Surgery, University of Melbourne, East Melbourne, VIC, Australia*

DANIEL M. LIPINSKI • *Department of Ophthalmology, Medical College of Wisconsin, Milwaukee, WI, USA; Nuffield Laboratory of Ophthalmology, Department of Clinical Neuroscience, University of Oxford, Oxford, UK*

ROBERT E. MACLAREN • *Nuffield Laboratory of Ophthalmology, Nuffield Department of Clinical Neurosciences, University of Oxford, Oxford, UK; NIHR Oxford Biomedical Research Centre, University of Oxford, Oxford, UK; Oxford Eye Hospital, Oxford University Hospitals NHS Foundation Trust, Oxford, UK; Moorfields Eye Hospital, NHS Foundation Trust, London, UK*

VINIT B. MAHAJAN • *Omics Laboratory, Stanford University, Palo Alto, CA, USA; Department of Ophthalmology, Byers Eye Institute, Stanford University, Palo Alto, CA, USA*

MATTHEW R.J. MASON • *Netherlands Institute for Neurosciences, Amsterdam, The Netherlands*

JIMMY DE MELO • *Solomon H. Snyder Department of Neuroscience, Johns Hopkins University School of Medicine, Baltimore, MD, USA*

STYLIANOS MICHALAKIS • *Department of Pharmacy, Center for Drug Research, Center for Integrated Protein Science Munich CiPSM, Ludwig-Maximilian-University, Munich, Germany*

HARALD M.M. MIKKERS • *Department of Molecular Cell Biology, Leiden University Medical Center (LUMC), Leiden, The Netherlands*

REGINE MÜHLFRIEDEL • *Division of Ocular Neurodegeneration, Centre for Ophthalmology, Institute for Ophthalmic Research, University of Tübingen, Tübingen, Germany*

CHARLOTTE OHONIN • *Department of Ophthalmology, Leiden University Medical Center (LUMC), Leiden, The Netherlands*

HARRY O. ORLANS • *Nuffield Laboratory of Ophthalmology, Nuffield Department of Clinical Neurosciences, John Radcliffe Hospital, University of Oxford, Oxford, UK; Oxford Eye Hospital, Oxford University Hospitals NHS Foundation Trust, Oxford, UK; Moorfields Eye Hospital, London, UK*

MARIA I. PATRÍCIO • *Nuffield Laboratory of Ophthalmology, Nuffield Department of Clinical Neurosciences, John Radcliffe Hospital, University of Oxford, Oxford, UK; Oxford Eye Hospital, Oxford University Hospitals NHS Foundation Trust, Oxford, UK*

KATHLEEN PAULOFF • *Department of Applied Health Sciences, University of Waterloo, Waterloo, ON, Canada*

LUCIE P. PELLISSIER • *Netherlands Institute for Neuroscience, Royal Netherlands Academy of Arts and Sciences, Amsterdam, The Netherlands; Unité Physiologie de la Reproduction et des Comportements, INRA UMR85, Centre National de la Recherche Scientifique*

UMR-7247, Institut Français du Cheval et de l'Équitation, Université François Rabelais, Nouzilly, France

PETER M. QUINN • *Department of Ophthalmology, Leiden University Medical Center (LUMC), Leiden, The Netherlands*

CHRISTOPHER A. REID • *Department of Ophthalmology, Medical College of Wisconsin, Milwaukee, WI, USA*

ANNA N. RUDENKO • *Nuffield Laboratory of Ophthalmology, Nuffield Department of Clinical Neurosciences, John Radcliffe Hospital, University of Oxford, Oxford, UK; Oxford Eye Hospital, Oxford University Hospitals NHS Foundation Trust, Oxford, UK*

DAVID V. SCHAFFER • *The Helen Wills Neuroscience Institute, University of California, Berkeley, CA, USA; Department of Molecular and Cell Biology, University of California, Berkeley, CA, USA; Department of Bioengineering, University of California, Berkeley, CA, USA; Department of Chemical and Biomolecular Engineering, University of California, Berkeley, CA, USA*

CHRISTIAN SCHÖN • *Department of Pharmacy, Center for Drug Research, Center for Integrated Protein Science Munich CiPSM, Ludwig-Maximilian-University, Munich, Germany*

MATHIAS W. SEELIGER • *Division of Ocular Neurodegeneration, Centre for Ophthalmology, Institute for Ophthalmic Research, University of Tübingen, Tübingen, Germany*

JESSE D. SENGILLO • *Jonas Children's Vision Care, and Bernard & Shirlee Brown Glaucoma Laboratory, Columbia University Medical Center, New York, NY, USA; Department of Ophthalmology, Columbia University, New York, NY, USA; State University of New York Downstate Medical Center, Brooklyn, NY, USA*

VITHIYANJALI SOTHILINGAM • *Division of Ocular Neurodegeneration, Centre for Ophthalmology, Institute for Ophthalmic Research, University of Tübingen, Tübingen, Germany*

MAYS TALIB • *Department of Ophthalmology, Leiden University Medical Center (LUMC), Leiden, The Netherlands*

NAOYUKI TANIMOTO • *Department of Ophthalmology, University Hospital Schleswig-Holstein, Kiel, Germany*

MICHEL M. TEUSSINK • *Department of Ophthalmology, Radboud University Medical Center (Radboudumc), Nijmegen, The Netherlands*

THOMAS THEELEN • *Department of Ophthalmology, Radboud University Medical Center (Radboudumc), Nijmegen, The Netherlands*

IVANA TRAPANI • *Telethon Institute of Genetics and Medicine (TIGEM), Pozzuoli, Italy*

YI-TING TSAI • *Jonas Children's Vision Care, and Bernard & Shirlee Brown Glaucoma Laboratory, Columbia University Medical Center, New York, NY, USA; Department of Ophthalmology, Columbia University, New York, NY, USA*

STEPHEN H. TSANG • *Jonas Children's Vision Care, and Bernard & Shirlee Brown Glaucoma Laboratory, Columbia University Medical Center, New York, NY, USA; Department of Ophthalmology, Columbia University, New York, NY, USA; Department of Pathology and Cell Biology, Institute of Human Nutrition, College of Physicians and Surgeons, Columbia University, New York, NY, USA; Edward S. Harkness Eye Institute, Columbia University, New York, NY, USA*

JOOST VERHAAGEN • *Netherlands Institute for Neurosciences, Royal Netherlands Academy of Arts and Sciences (KNAW), Amsterdam, The Netherlands*

MEIKE VISEL • *Department of Molecular and Cell Biology, University of California Berkeley, Berkeley, CA, USA*

ROGIER M. VOS • *Netherlands Institute for Neuroscience, Royal Netherlands Academy of Arts and Sciences, Amsterdam, The Netherlands; InteRNA Technologies BV, Utrecht, The Netherlands*

CHRISTINE WALLRAPP • *BTG International Germany GmbH, Alzenau, Germany*

JIANG-HUI WANG • *Centre for Eye Research Australia, Royal Victorian Eye and Ear Hospital, East Melbourne, VIC, Australia; Ophthalmology, Department of Surgery, University of Melbourne, East Melbourne, VIC, Australia*

JAN WIJNHOLDS • *Department of Ophthalmology, Leiden University Medical Center (LUMC), Leiden, The Netherlands; Netherlands Institute for Neuroscience, Royal Netherlands Academy of Arts and Sciences (KNAW), Amsterdam, The Netherlands*

CHENMIAN WU • *Department of Ophthalmology, Tongji Hospital, Tongji Medical College, Huazhong University of Science and Technology, Wuhan, Hubei Province, China*

WEN-HSUAN WU • *Jonas Children's Vision Care, and Bernard & Shirlee Brown Glaucoma Laboratory, Columbia University Medical Center, New York, NY, USA; Department of Ophthalmology, Columbia University, New York, NY, USA*

YU XU • *Jonas Children's Vision Care, and Bernard & Shirlee Brown Glaucoma Laboratory, Columbia University Medical Center, New York, NY, USA; Department of Ophthalmology, Columbia University, New York, NY, USA; Department of Ophthalmology, Xinhua Hospital affiliated to Shanghai Jiao Tong, University School of Medicine, Shanghai, China*

Part I

Retinal Gene Therapy Vector Production and Biological Assays In Vitro

Chapter 1

Small Scale Production of Recombinant Adeno-Associated Viral Vectors for Gene Delivery to the Nervous System

Joost Verhaagen, Barbara Hobo, Erich M.E. Ehlert, Ruben Eggers, Joanna A. Korecka, Stefan A. Hoyng, Callan L. Attwell, Alan R. Harvey, and Matthew R.J. Mason

Abstract

Adeno-associated viral vectors have numerous applications in neuroscience, including the study of gene function in health and disease, targeting of light-sensitive proteins to anatomically distinct sets of neurons to manipulate neuronal activity (optogenetics), and the delivery of fluorescent protein to study anatomical connectivity in the brain. Moreover several phase I/II clinical trials for gene therapy of eye and brain diseases with adeno-associated viral vectors have shown that these vectors are well tolerated by human patients. In this chapter we describe a detailed protocol for the small scale production of recombinant adeno-associated viral vectors. This protocol can be executed by investigators with experience in cell culture and molecular biological techniques in any well-equipped molecular neurobiology laboratory. With this protocol we typically obtain research batches of 100–200 µL that range in titer from 5×10^{12} to 2×10^{13} genomic copies/mL.

Key words Adeno-associated viral vector, Production, Purification, Serotype, Iodixanol, Amicon centrifugation device

1 Introduction

Adeno-associated virus (AAV) is a nonpathogenic parvovirus belonging to the subfamily of dependoviruses. Dependoviruses cannot replicate autonomously but need a helper virus for their propagation. Adenovirus or herpesvirus can serve as helper virus for AAV. AAV is therefore a "replication defective" virus by nature. The genome of AAV consists of three open reading frames encoding the rep and cap proteins and the assembly activator protein, flanked by inverted terminal repeats (ITRs). The cap genes encode the capsid proteins and the rep genes are required for DNA replication which only occurs in the presence of additional helper functions provided by the helper virus [1].

Over the last three decades protocols have been developed to generate and purify high titer stocks of recombinant adeno-associated viral vectors (rAAV). In early methods to produce rAAV an adenovirus was required as helper virus. As a result, batches of rAAV were contaminated with adenovirus. The identification of the adenoviral genes required for the propagation of rAAV vectors has allowed the creation of a rAAV production system that is entirely plasmid based [2–5]. Today the nine most commonly used rAAV serotypes are produced by dual or triple plasmid transfections in human embryonic kidney (HEK) 293T cells. In the dual plasmid production system the transfer plasmid contains the gene of interest under the control of a promoter flanked by the ITRs from AAV2 and the helper plasmid harbors the AAV2 rep genes, the cap genes of a specific AAV serotype and the adenoviral helper functions [3]. In the triple plasmid production system the rep and cap genes and the adenoviral helper functions resent on two different plasmids [6]. Thus, for each rAAV serotype the helper plasmid harbors the specific cap genes of the desired serotype. Serotypes 1–6 are produced through the dual plasmid system and serotypes 7–9 by means of the triple plasmid system. Large scale production protocols for rAAV in either insect cells [7, 8] or mammalian cells [9] have also been developed. These production systems are mainly used to generate large amounts of rAAV for preclinical or clinical studies.

In this chapter a simple four stage production protocol is provided for the generation of relatively small quantities (100–200 μL) of rAAV with a titer typically ranging between 1×10^{12} and 2×10^{13} genomic copies/mL. The first stage involves the production of rAAV by cotransfection of two or three plasmids (the transfer plasmids mixed with one or two helper plasmids depending on the rAAV serotype) in HEK293T cells. In the second stage rAAV is collected from the transfected cells and concentrated by iodixanol gradient ultracentrifugation. Thirdly, rAAV from the iodixanol gradient is concentrated and separated from cellular proteins by multiple washes and centrifugation in Amicon centrifugal filter devices. Fourth, the titer of the rAAV sample is determined by quantitative PCR (qPCR) on rAAV genomic DNA. This protocol is a modification and extension of original protocols developed earlier and can be completed in 7–8 working days [4, 5, 10, 11]. Finally, we describe our method to deliver rAAV to the brain [12–15] and to the retina by intravitreal injection [16, 17].

2   Materials

2.1   Reagents for Cell Culture and PEI-Mediated Plasmid Transfection

1. DMEM: Dulbecco's Modified Earl's medium supplemented with 10% fetal calf serum (FCS) and 1% v/v penicillin/streptomycin (PS).

Table 1
Overview of helper plasmids used for production of rAAV serotypes 1–9

Serotype	Helper plasmid	References
AAV 1	helper plasmid: PVD20	Grimm et al. [3]
AAV 2	helper plasmid: pDG2	Grimm et al. [5]
AAV 3	helper plasmid: pXR3m1.m2	Grimm et al. [3]
AAV 4	helper plasmid: pXR4m1.m2	Grimm et al. [3]
AAV 5	helper plasmid: pDP5	Grimm et al. [3]
AAV 6	helper plasmid: pDP6	Grimm et al. [3]
AAV 7	helper plasmid 1: p5E18DV2/7	Gao et al. [6]
	helper plasmid 2: pAdΔF6	Gao et al. [6]
AAV 8	helper plasmid 1: p5E18DV2/8	Gao et al. [6]
	helper plasmid 2: pAdΔF6	Gao et al. [6]
AAV 9	helper plasmid 1: pAAV2/9	Vector Core University of Pennsylvania
	helper plasmid 2: pAdΔF6	Gao et al. [6]

2. IMDM: Iscove's Modified Dulbecco's medium supplemented with 10% FCS/1% v/v PS/1% v/v glutamine (GLN).

3. PEI solution: add 500 mg Polyethylenimine (PEI, 25 kDa, linear, powder) to 450 mL H_2O and lower the pH to 2.0 with 12 N HCl to dissolve the PEI. Adjust the pH with 10 M NaOH to 7.0. Adjust the volume to 500 mL yielding a PEI solution of 1 mg/mL. The solution is stored in frozen aliquots after sterilization through a 0.2 μm filter.

4. HEK293T cells: Human embryonic kidney-derived 293T cells.

5. Plasmids: helper plasmids required for each serotype are specified in Table 1.

6. 15 cm tissue culture plate.

2.2 Reagents for rAAV Harvest and Iodixanol Gradient Centrifugation

1. Iodixanol: start with a 60% solution to generate the 15%, 25% and 40% solutions as follows:

   15% iodixanol: dilute 60 mL 60% Iodixanol with 48 mL 5 M NaCl and 48 mL 5× PBS-MK (5× PBS with 5 mM $MgCl_2$ and 12.5 mM KCl), add water to a volume of 240 mL.

25% iodixanol, dilute 67 mL 60% Iodixanol with 32 mL 5× PBS-MK, add water to a volume of 160 mL.

40% iodixanol, dilute 160 mL 60% Iodixanol with 48 mL 5× PBS-MK, add water to a volume of 240 mL.

2. DNaseI: 10 mg DNaseI/mL PBS.

3. D-PBS: Dulbecco's phosphate buffered saline (Gibco).

4. Alternative lysis buffer: 50 mM Tris pH 8.5, 150 mM NaCl, 0.1% Triton X-100, 2 mM $MgCl_2$.

2.3 Reagents for Amicon Filter Centrifugation Concentration

1. D-PBS.

2. D-PBS with 5% sucrose: 5 g sucrose in 100 mL D-PBS, store aliquots at −20 °C.

2.4 Reagents for rAAV Titering

1. Titration DNaseI solution: 250 μg/mL DNAase I in D-PBS supplemented with 3 mM $MgCl_2$.

2. 1 M NaOH for alkaline lysis.

3. Neutralization solution: mix 1 part 1 M Tris pH 8 and 4 parts 1.25 M HCl.

4. Master mix: SYBRgreen solution (Applied Biosystems).

5. Primers: designed against your sequence of interest (*see* **Note 1**).

6. qPCR plate (MicroAmp optical 96-well reaction plate).

7. PCR thermocycler with heated lid.

2.5 Specialist Devices and Equipment for rAAV Production

1. Cell Scraper with a length of 28 cm (Greiner Bio-One).

2. Amicon ultra-15 centrifugal filters 100 k (Merck Millipore UFC910024).

3. Vortex.

4. Ultracentrifuge: a Beckman L-80 ultracentrifuge or equivalent ultracentrifuge.

5. Tabletop centrifuge with inserts for 50 mL tubes, e.g., Eppendorf 5810R centrifuge, and inserts for qPCR plates.

6. 70Ti Beckman rotor.

7. PCR system with heated lid, e.g., Bio-Rad T100.

8. qPCR system, e.g., a 7300 real time PCR system of Applied Biosystems.

9. 19 G needle.

10. 30 G needle.

11. Pasteur pipette.

12. Ultracentrifuge Quick-Seal polypropylene tube (Beckman).

13. Biohazard hood.

14. Metal clamp.

15. Latex or nitrile gloves.

16. Screw-top 1.5 mL tube.

17. Serological pipettes.

2.6 Equipment and Reagents for Delivery of rAAV to the Brain and Retina

1. Sterilized surgical equipment, including a scalpel handle, forceps, fine scissors (fine science tools), a dental drill, cotton swabs, eye ointment, and different size sutures.

2. 50 µL Hamilton for injection of AAV into the vitreal chamber of the eye.

3. Automated microinjection device; Harvard apparatus or Nanojet.

4. Stereotactic apparatus (Kopf).

5. Custom pulled glass capillaries 1.5 mm OD × 0.86 mm ID (#30-0053, Harvard apparatus) with an 80 µm tip diameter.

6. Polyethylene tubing 0.61 mm OD × 0.28 mm ID (#800/100/100 Portex, Smiths medical).

7. Two component epoxy resin (combi rapide, Bison).

8. Mineral oil when using a glass micropipette attached to a Hamilton syringe via polyethylene tubing.

9. Heating pad.

10. Isoflurane equipment, lidocaine (local anesthetics), sterile water (fill needle system), Fynadine (2.5 mg/kg s.c. flunixin).

11. Inhalation anesthesia using a mixture of (0.2 L/min) O_2 and (0.4 L/min) medicinal air containing 1.6% isoflurane.

12. 70% ethanol.

13. PTFE Luer Lock and a cannula with appropriate size to fit the inner diameter of the polyethylene tubing.

3 Methods

3.1 Cell Culture and PEI Transfection

Day 1.

1. Plate $1–1.25 \times 10^7$ HEK293T cells (passage number not higher than 20) per 15 cm tissue culture plate in DMEM in a tissue culture incubator at 37 °C and in 5% CO_2. Prepare eight plates for a typical batch of rAAV (*see* **Note 2**).

Day 2.

2. Check HEK293T cells around 3 PM. The cells should have grown to 70–80% confluency. The transfection efficiency drops significantly when cells are too confluent.

3. Prewarm IMDM in a water bath to 37 °C. Per 15 cm plate you will need 20 mL of IMDM.

4. Replace DMEM with IMDM 2 h before the transfection.

5. Thaw the PEI solution (A) and prepare the plasmid solution (B) for transfection according to Table 2. For AAV 1–6 a two plasmid system is used. For AAV 7–9 a three plasmid system is used (Table 1).

6. Mix A and B (1:1) and vortex immediately. Incubate for 15 min at RT.

7. Add the mixture to the HEK293T cells in IMDM. Per plate add 2 mL of solution in a dropwise fashion. Ensure that the solution is equally distributed over the cells.

8. The plates are returned to the tissue culture incubator and transfected cell are cultured until the next morning (16–18 h after the transfection).

Day 3.

9. Prewarm IMDM in a water bath to 37 °C.

10. Replace IMDM with fresh IMDM, 20 mL per plate. Process one plate at a time to prevent cells from drying out.

11. If the transfer plasmid contains a fluorophore (e.g., GFP) it is possible to check the transfection efficiency under an inverse fluorescence microscope. At this point in time around 30% of the cells should express detectable GFP.

Day 4.

12. Check the condition of the cells under the inverse microscope. Cells should appear viable and the proportion of transfected cells has increased to approximately 60–80% (*see* **Note 3**). For rAAV serotypes 1–6, 8 and 9 rAAV is harvested on day 5. However, for AAV7 we consistently observed that the transfected cells start to detach from the cell culture dish on day 5 and with this serotype we therefore start the rAAV harvest on day 4.

3.2 Harvest of rAAV and Iodixanol Gradient Ultracentrifugation

Day 5.

1. Aspirate medium from the cell culture plates. Two plates at a time.

2. Add 3 mL D-PBS to the first plate. Scape the cells from the first plate with a cell scraper. Aspirate the harvested cells and add this mixture to the second medium free plate and remove the cells by cell scraping. Collect the cell mixture in a 50 mL tube. Repeat this until cells from all plates have been harvested. Total volume of the cell harvest of eight plates should not

Table 2
Preparation of PEI transfection solutions

	Per 15 cm plate	8 plates
Two plasmid system (AAV serotypes 1–6)		
Solution (A)		
PEI	150 μL	1200 μL
NaCl	To 1.5 mL	To 12 mL
Solution (B)		
Helper plasmid	37.5 μg	300 μg
Transfer plasmid	12.5 μg	100 μg
NaCl	To 1.5 mL	To 12 mL
Three plasmid system) (AAV serotypes 7–9)		
Solution (A)		
PEI	150 μL	1200 μL
NaCl	To 1.5 mL	To 12 mL
Solution (B)		
Helper plasmid 1	25 μg	200 μg
Helper plasmid 2	25 μg	200 μg
Transfer plasmid	12.5 μg	100 μg
NaCl	To 1.5 mL	To 12 mL

exceed 17.5 mL because otherwise it cannot be applied on the iodixanol gradient.

3. Freeze-thaw cells three times by freezing in dry ice-cooled ethanol and thawing in a 37 °C water bath until completely thawed.

4. After each freeze/thaw cycle check for large cell clumps in the solution. If these occur vortex the solution to break up cells clumps.

5. Alternative method: Scrape in alternative lysis buffer. Use 16 mL total. This is quicker for harvesting but the detergent can cause bubble formation during the iodixanol gradient step.

6. Add 25 μL DNAseI, incubate for 1 h at 37 °C in a water bath (*see* **Note 4**).

7. Store the cell lysate at −20 °C. Continue with the iodixanol density ultracentrifugation the next day.

3.3 Iodixanol Gradient Centrifugation

Day 6.

1. Defrost the cell lysate in a 37 °C water bath.

2. Centrifuge lysate for 30 min at 3220 × *g* in a table centrifuge.

3. Apply a maximum of 17.5 mL of cell lysate to the bottom of a Beckman ultracentrifuge Quick-Seal polypropylene tube with a Pasteur pipet (*see* **Note 5**).

4. Replace the Pasteur pipette with a new one. This pipette will be used to underlay the iodixanol gradient solutions (Fig. 1).

5. Gently infuse 9 mL of the 15% iodixanol solution under the cell lysate and continue with 5 mL of the 25% and 40% iodixanol solution and finally 3 mL of the 60% iodixanol solution (Fig. 1; *see* **Note 6** [11]).

6. Fill the tube with D-PBS to the bottom of the neck (but not into the neck) to remove any remaining air bubbles. A 1 mL syringe with a 19 G needle can be used for this (*see* **Note 7**).

7. Seal the tube using the electrical tube topper. Ensure that the neck of the Beckman tube is dry because the tube will not seal properly if the neck is wet. Carefully squeeze the sealed Beckman tube to make sure that the tube is indeed fully sealed and not leaking.

8. Centrifuge in Beckman centrifuge in a 70Ti fixed angle rotor for 70 min at 69,000 rpm at 16 °C.

9. After centrifugation open the rotor in the biohazard hood and assemble the first Beckman tube in a metal clamp (*see* **Note 8**).

10. Puncture a small hole in the top of the tube with a 30 G needle. Leave the needle in place.

11. Puncture a hole in the bottom of the tube with a 19 G needle. First gently remove the 19 G needle, subsequently remove the 30 G needle and close the hole with your gloved finger. To collect the iodixanol fractions in **steps 12** and **13** slowly allow air into the centrifuge tube via the hole punctured with the top 30 G needle.

12. Collect the first 2 mL of iodixanol (60% iodixanol) in a 15 mL tube and discard.

13. Collect the next 3 mL of iodixanol (1 mL of 60% and 2 mL of 40% iodixanol). This fraction contains your rAAV.

3.4 Amicon Filter Centrifugation of rAAV, Washing and Concentration

1. Dilute the 3 mL iodixanol solution that contains the rAAV (Subheading 3.3, **step 13**) with 12 mL D-PBS. Mix well.

2. Apply this solution to an Amicon ultra 15 device.

3. Concentrate by centrifugation at $3220 \times g$ for 15 min at RT to reduce the volume to approximately 500 μL. Additional centrifuging time may be necessary.

4. Discard the flow through.

5. Add 15 mL of D-PBS plus 5% sucrose to the concentrated rAAV solution.

17,5 ml Crude lysate

9,0 ml 15% iodixanol

5,0 ml 25% iodixanol

5,0 ml 40 % iodixanol

3,0 ml 60 % iodixanol
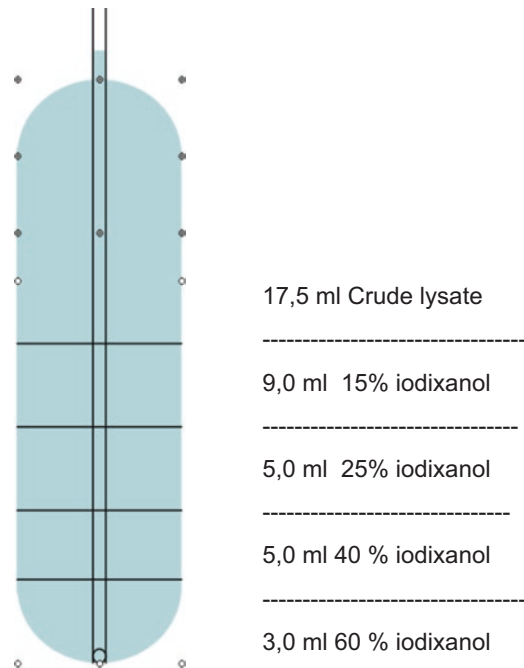
Fig. 1 Illustration of a Beckman Quick seal ultracentrifuge tube and the Pasteur pipet lowered through the neck of the tube to generate the graded iodixanol gradient. We refer to Subheading 3.3 of the protocol for a more detailed description of the procedure to load the crude lysate and create the gradient

6. Centrifuge at $3220 \times g$ for 10 min at RT to approximately 500 μL.

7. Repeat this at least three times (*see* **Note 9**).

8. In the last Amicon wash and concentration step centrifuge until the volume of your rAAV solution is between 150 and 200 μL. Additional centrifuging may be necessary to reduce the volume to this.

9. Transfer your rAAV to a screw-top 1.5 mL tube and store at −80 °C (*see* **Note 10**).

3.5 rAAV Titration   Day 7.

1. Add 2.2 μL of rAAV stock to 85.8 μL of Titration DNAseI solution. Mix well by pipetting and divide in two aliquots of 40 μL in PCR tubes (this is a 1:40 dilution).

2. If necessary spin the samples a few second at $200 \times g$ in the microcentrifuge to collect the sample at the bottom of the tube.

3. Incubate 30 min at 37 °C in the PCR thermocycler with heated lid.

4. Incubate 3 min at 12 °C in the PCR thermocycler with heated lid.

5. Spin down for a few second at $200 \times g$ in the table centrifuge to collect the sample at the bottom of the tube.

6. Add 40 µL of 1 M NaOH and vortex briefly (*see* **Note 11**).

7. Spin the samples a few second at $200 \times g$ in a tabletop centrifuge to collect the sample at the bottom of the tube.

8. Incubate 15 min at 50 °C in the PCR thermocycler with heated lid.

9. Add around 40 µL neutralization solution (exact volume determined previously, *see* **Note 11**) to each sample. Vortex and spin down at $200 \times g$.

10. From each sample take 20 µL and dilute in 180 µL H_2O (1:10 dilution). Keep the samples on ice and continue with **step 11** or freeze at −20 °C and continue later.

11. Prepare a standard curve for the qPCR using a reference plasmid.

12. First make a solution of 10^{10} molecules/mL. For example, using pTR-CGW (FW 3496 kDa), this is 58.4 pg/µL. 16.7 µL of pTR-CGW (1 µg/µL) is diluted in 5 mL H_2O resulting in a 4 ng/µL stock solution. 5895 µL of H_2O is added to 105 µL of the 4 ng/µL stock giving 58.4 pg/µL, or 10^{10} plasmid molecules per mL. Make 1:10 serial dilutions to a final dilution of 10^3 plasmid molecules per mL. These serial dilutions can be stored and used for a number of standard curves in the future. Vortex thoroughly before each use.

13. Prepare reaction mix for the qPCR in qPCR plate. Total volume per reaction is 25 µL. For each reaction: 12.5 µL SYBRgreen master mix, 0.75 µL primer mix (10 µM of forward and reverse primer, *see* **Note 1**), 10 µL rAAV DNA (**step 11**) or 10 µL from the serial dilutions of the standard curve, and finally 1.75 µL H_2O. Spin the qPCR plate at $200 \times g$ for a few second.

14. Place qPCR plate in the qPCR machine and start the cycling: First cycle: 2 min 50 °C, 10 min 95 °C; 40 cycles: 15 s 95 °C, 1 min 60 °C; Dissociation stage: 15 s 95 °C, 1 min 60 °C, 15 s 95 °C, 15 s 60 °C, cool down to RT.

15. Calculate titers from the cycle threshold values using the standard curve, taking into account the dilution steps in the procedure (an initial 1:40 dilution, the 1:3 dilution during alkaline lysis and neutralization and the last 1:10 dilution, giving a final dilution of 1:1200).

3.6 Stereotactic Delivery of rAAV to the Brain

In some jurisdictions, this procedure needs to be performed in a suitable biosafety cabinet.

1. Tubing is connected to the glass needle by application of the two component resin. The opposite side is mounted onto the Hamilton syringe needle, after which the system is back-filled using demi water.

2. The rat is deeply anesthetized with inhalation anesthesia using a mixture of O_2 (0.2 L/min) and medicinal air (0.4 L/min) containing 1.6% isoflurane.

3. The fur on the skull is shaved and the skin surface is cleaned with 70% ethanol.

4. The animal is placed in a stereotactic frame and fixed by ear and tooth bars.

5. A skin incision is made and lidocaine is topically applied to obtain additional local anesthesia.

6. Stereotactic coordinates for intraparenchymal injection are obtained from Paxinos and Watson (*see* **Note 12**).

7. A dental drill is used to drill a small hole in the skull at the intended coordinates.

8. Prior to the injection of the vectors the meninges are punctured with a sharp 30 G needle in order to prevent brain contusion during lowing of the injection needle in the brain parenchyma.

9. A pressure injection of 1 μL rAAV is performed by lowering a glass needle connected to an automatic microinjection device through the hole in the skull to the appropriate depth. The microinjection device is turned on and the vector is injected at a speed of 0.1–0.2 μL/min.

10. After the injection the needle is left in place for 3 min to prevent back-flow of the viral vector solution.

11. Subsequently the needle is gently retracted and the skin is sutured. Per-operative, the animal is kept on a heating pad and an injection of fynadine is administered to obtain adequate analgesia during recovery.

12. If an injectable anesthetic is used the animal should be left on a heating pad for 2–3 h to recover.

3.7 Delivery of rAAV to the Retina: Intravitreal Injections

In some jurisdictions, this procedure needs to be performed in a suitable biosafety cabinet.

1. A sterile pulled glass micropipette (with a relatively shallow profile, tip about 200–300 μm) of known internal diameter (to readily establish volume of injection) is attached via mineral oil

filled polyethylene tubing to a 50 μL Hamilton syringe (preferably via PTFE Luer Lock and a cannula with appropriate size to fit the inner diameter of the polyethylene tubing).

2. Mark the micropipette at the point where the inner total volume from the tip equals the desired volume to be injected. Then aspirate up the rAAV to the mark on the pipette.

3. Under gas/injectable anesthesia, the micropipette is inserted in the peripheral part of an animals' eye (usually via a lower temporal approach), immediately adjacent to the ora serrata. The tip should be angled toward the vitreous humor and back of the eye, taking care to avoid any damage to the retina or lens. For one injection in adult rat, the volume is usually 4 μL, in mice the volume is lower (1–1.5 μL). Occasionally multiple injections into the vitreal chamber are made (e.g., a volume 1.5 μL for each of three injections), to increase the area of transduction but also if different color reporter proteins are used in an attempt to examine the visual topography of retinal projections (*see* **Note 13**) [18]. Inject the AAV vector into the vitreal chamber as slowly as possible.

4. Remove the micropipette from the eye and apply eye ointment with antibiotics as preventive care.

5. Subretinal injections of AAV are also used when there is a need to target outer retina (e.g., photoreceptors). The reader is directed to Qi et al. and Muhlfriedel et al. for further information and useful guidelines [19, 20].

4   Notes

1. Primers for the transgene or the promoter can be used. In most of our rAAV vectors the Woodchuck Hepatitis Virus Posttranscriptional Regulatory Element (WPRE) is present and we therefore often use primers against the WPRE, which allows for reliable intra- and inter-experimental comparison of titers of different stocks.

2. We typically use 8 plates for a single batch of rAAV and this usually results in a batch with a titer between 5×10^{12} and 2×10^{13}. We also have successfully prepared batches of rAAV with similar titers starting with 4 or 12 plates.

3. The viability of the HEK293T cells at the start of the experiment and following the transfection is critical to get high titer stocks. HEK293T cells should be evenly spread across the plate, and without visible cell clumps, for good transfection. This can be achieved by gentle, but thorough, pipetting of the cell suspension prior to plating. The cells should be growing

well (typically requiring 1:10 splits every 3 days). If growth has slowed a new batch of cells should be started.

4. Mix by inversion. DNaseI is somewhat fragile and should not be vortexed.

5. The Pasteur pipette is placed through the neck of the tube and rests on the bottom. The cell lysate and iodixanol layers are then added sequentially from the bottom of the tube.

6. Arrange the tubes of iodixanol with lids off for quick access, in ascending order of concentration. After the first iodixanol solution has been added (15%) the next one should be applied to the top of the Pasteur pipette just as the last of the previous solution enters the neck of the pipette, to minimize the possibility of air entering between the two solutions as they pass through. It often happens that some air is also transferred, resulting in small bubbles. In theory these may disturb the gradient but in practice it appears fairly robust to such disturbances. However there is limited time to load the next solution in the serological pipette. It is advisable therefore not to change the serological pipette between solutions.

7. A few small bubbles invariably remain. This should not cause problems.

8. Experienced virus purifiers may prefer to hold the Beckman tube in one hand and insert the needles with the other rather than using a stand and clamp.

9. DPBS can be used instead of DPBS-sucrose for the first three washes.

10. In general AAV particles are robust to freeze-thawing and we prefer not to make more than 2–3 aliquots. It is advisable not to make small aliquots as this can reduce titer.

11. The final pH is important for the subsequent qPCR and should be ideally around 8. We recommend preparing additional tubes with only D-PBS and 1 M NaOH and then checking the exact volume of neutralization solution required to return the pH to 7–8.5. Check with pH paper or indicator solution. Use the same pipette as you will for the samples.

12. Optimization of the stereotactic coordinates to be used for a particular brain structure includes the injection of a dye, e.g., fast green or methylene blue, and serial sectioning of the brain through the injection area [15].

13. Some researchers remove a small volume of vitreous just prior to the intravitreal AAV injection.

Acknowledgment

References

1. Murlidharan G, Samulski RJ, Asokan A (2014) Biology of adeno-associated viral vectors in the central nervous system. Front Mol Neurosci 7:76

2. Xiao X, Li J, Samulski RJ (1998) Production of high-titer recombinant adeno-associated virus vectors in the absence of helper adenovirus. J Virol 72:2224–2232

3. Grimm D, Kay MA, Kleinschmidt JA (2003) Helper virus-free, optically controllable, and two-plasmid-based production of adeno-associated virus vectors of serotypes 1 to 6. Mol Ther 7:839–850

4. Zolotukhin S, Potter M, Zolotukhin I et al (2002) Production and purification of serotype 1, 2, and 5 recombinant adeno-associated viral vectors. Methods 28:158–167

5. Grimm D, Kern A, Rittner K et al (1998) Novel tools for production and purification of recombinant adenoassociated virus vectors. Hum Gene Ther 9:2745–2760

6. Gao GP, Alvira MR, Wang L et al (2002) Novel adeno-associated viruses from rhesus monkeys as vectors for human gene therapy. Proc Natl Acad Sci U S A 99:11854–11859

7. Mietzsch M, Grasse S, Zurawski C et al (2014) OneBac: platform for scalable and high-titer production of adeno-associated virus serotype 1–12 vectors for gene therapy. Hum Gene Ther 25:212–222

8. Smith RH, Levy JR, Kotin RM (2009) A simplified baculovirus-AAV expression vector system coupled with one-step affinity purification yields high-titer rAAV stocks from insect cells. Mol Ther 17:1888–1896

9. Grieger JC, Soltys SM, Samulski RJ (2016) Production of recombinant adeno-associated virus vectors using suspension HEK293 cells and continuous harvest of vector from the culture media for GMP FIX and FLT1 clinical vector. Mol Ther 24:287–297

10. Hermens WT et al (1999) Purification of recombinant adeno-associated virus by iodixanol gradient ultracentrifugation allows rapid and reproducible preparation of vector stocks for gene transfer in the nervous system. Hum Gene Ther 10:1885–1891

11. Zolotukhin S, Byrne BJ, Mason E et al (1999) Recombinant adeno-associated virus purification using novel methods improves infectious titer and yield. Gene Ther 6:973–985

12. Blits B, Derks S, Twisk J et al (2010) Adeno-associated viral vector (AAV)-mediated gene transfer in the red nucleus of the adult rat brain: comparative analysis of the transduction properties of seven AAV serotypes and lentiviral vectors. J Neurosci Methods 185:257–263

13. Drummond ES, Muhling J, Martins RN et al (2013) Pathology associated with AAV mediated expression of beta amyloid or C100 in adult mouse hippocampus and cerebellum. PLoS One 8:e59166

14. Ruitenberg MJ, Blits B, Dijkhuizen PA et al (2004) Adeno-associated viral vector-mediated gene transfer of brain-derived neurotrophic factor reverses atrophy of rubrospinal neurons following both acute and chronic spinal cord injury. Neurobiol Dis 15:394–406

15. Ruitenberg MJ, Eggers R, Boer GJ et al (2002) Adeno-associated viral vectors as agents for gene delivery: application in disorders and trauma of the central nervous system. Methods 28:182–194

16. Harvey AR, Kamphuis W, Eggers R et al (2002) Intravitreal injection of adeno-associated viral vectors results in the transduction of different types of retinal neurons in neonatal and adult rats: a comparison with lentiviral vectors. Mol Cell Neurosci 21:141–157

17. Hellstrom M, Ruitenberg MJ, Pollett MA et al (2009) Cellular tropism and transduction properties of seven adeno-associated viral vec-

tor serotypes in adult retina after intravitreal injection. Gene Ther 16:521–532

18. You SW, Hellström M, Pollett MA et al (2016) Large-scale reconstitution of a retina-to-brain pathway in adult rats using gene therapy and bridging grafts: an anatomical and behavioral analysis. Exp Neurol 279:197–211

19. Muhlfriedel R, Michalakis S, Garcia Garrido M et al (2013) Optimized technique for subretinal injections in mice. Methods Mol Biol 935:343–349

20. Qi Y, Dai X, Zhang H et al (2015) Transcorneal subretinal injection in mice and its effect on the function and morphology of the retina. PLoS One 10:e0136523

Chapter 2

Small and Micro-Scale Recombinant Adeno-Associated Virus Production and Purification for Ocular Gene Therapy Applications

Christopher A. Reid and Daniel M. Lipinski

Abstract

Over the past two decades recombinant adeno-associated virus (rAAV) vectors have emerged as the gold standard for transferring genetic material to cells of the retina. The ability to effectively produce small batches of rAAV vector at high enough purity for in vitro and in vivo applications in a cost-effective manner is paramount. This is particularly the case when conducting preclinical experiments to screen novel sero-types, promoters or transgenes, where production of numerous vector batches is required. Current vector production methods often produce large quantities of vector, limiting the cost-effectiveness and practical-ity of such screening experiments, which often require only small volumes of vector to carry out. Herein, we describe a method to produce high titer (10^{12}–10^{13} vector genomes (vg)/mL) rAAV vector on small (~100 μL) or micro (~15 μL) scale for in vitro and in vivo applications.

Key words AAV, Manufacture, Purification, Virus vector, Gene therapy, Retina

1 Introduction

Recombinant vectors based upon adeno-associated virus (rAAV), a small, nonpathogenic dependovirus, have demonstrated to be highly effective in transducing cells of the retina in numerous pre-clinical and clinical studies [1, 2]. Numerous methods have been developed for generating rAAV [3–5], with the most common approach involving triple transfection of adherent HEK293T cells with an adenovirus-derived helper plasmid, a plasmid encoding the AAV *rep* and *cap* genes, and a plasmid containing the trans-gene cassette flanked by inverted terminal repeats (ITR) [6–8]. Typically, rAAV production protocols produce large vector vol-umes (~300–500 μl) of high titer (10^{12}–10^{13} vg/mL) vector, which are appropriate for systemic administration or injection in large animal models, but are excessive for in vitro tissue culture experiments or intraocular administration in rodents. Furthermore,

when conducting screening experiments to establish the tropism or specificity of novel vector serotypes or promoters, it is typically necessary to carry out only a small number of injections, leading to vector waste and increased research cost. Here, we describe two methods to produce small quantities of high titer (10^{12}-10^{13} vg/mL) virus in a cost-effective manner (<\$1000): A small-scale preparation which produces ~100 μL of highly pure vector suitable for preclinical in vivo gene therapy applications, and a micro-scale preparation which produces ~15 μL of crudely purified (minimal gradient purification) vector suitable for rapid screening of novel cell-specific promoters or capsid mutants in difficult to transfect cell lines or primary ocular tissue (e.g., retinal explants).

2   Materials

2.1   Small- and Micro-Scale General Materials

1. pHelper plasmid encoding adenovirus helper genes E2A, E4 and Viral Associated RNA.

2. pRep-Cap plasmid encoding rAAV *Rep* and *Cap* genes.

3. pAAV construct containing the transgene cassette consisting of promoter, transgene, and regulatory elements flanked by inverted terminal repeats.

4. A ubiquitously expressing fluorescent reporter plasmid (i.e., CBA-eGFP).

5. Growth Media: Dulbecco's Modified Eagle Medium-DMEM + GlutaMAX supplemented with 10% fetal bovine serum (FBS) and 1% antibiotic/antimycotic solution.

6. Transfection Media: DMEM + GlutaMAX supplemented with 2% FBS and 1% antibiotic/antimycotic solution.

7. 0.01 M phosphate buffered saline (PBS).

8. HEK293T cells (ATCC, #3216).

9. 1 μg/μL Polyethylenimine (PEI) transfection reagent: Linear, molecular weight—25,000 (PolySciences) (*see* **Note 1**).

10. 150 mM NaCl.

11. 10 M HCl.

12. 1× TrypLE or other trypsin–EDTA.

13. Lysis buffer: 150 mM NaCl, 50 mM Tris–HCl, pH 8.5. Filter-sterilize, do not autoclave. Store at room temperature.

14. 100% ethanol.

15. Dry ice.

16. 250 U/μL Ultra-Pure Benzonase nuclease.

17. HBSS/Tween 20: Hanks balanced salt solution (HBSS), no phenol red, containing 0.014% Tween 20.

18. Picogreen lysis buffer: 20 mM Tris–HCl, pH 7.4, 200 mM NaCl, 0.2% SDS. Do not autoclave. Store at room temperature.

19. Quant-iT Picogreen dsDNA Assay Kit: 20× TE, Picogreen Reagent, Bacteriophage Lambda DNA Standard (Thermo Fisher).

20. ddH$_2$O: Autoclaved double distilled H$_2$O.

21. 96-well solid black microtiter plate.

22. Fluorescent plate reader capable of exciting at 485 nm and reading emission at 535 nm.

23. 1% solution of Virkon disinfectant (DuPont).

24. 25% solution of Virkon disinfectant.

25. Inverted light microscope.

26. Vortex tube mixer allowing mixing at high and slow speed, e.g., range 250–2500 rpm.

27. PCR machine/thermal cycler.

2.2 Small-Scale Specific Materials

1. CellBIND Surface Hyperflask Cell Culture Vessel (Corning).

2. 175 cm^2 angled neck cell culture flask with vent cap.

3. 500 mL centrifuge bottles (Nalgene).

4. 50 mL conical bottom "falcon" centrifuge tubes.

5. 25 × 89 mm Quick-Seal Ultra Clear centrifuge tubes (Beckman Coulter).

6. Amicon Ultra-15 100 kDa molecular weight cutoff centrifugal filter units (Millipore).

7. 250 mL glass bottles.

8. 10 mL syringes.

9. 5 mL syringes.

10. 1-in. regular bevel 18-G needles.

11. Microcapilliary pipettes, disposable soda-lime glass, 100 µL blue (Kimble).

12. Syringe-microcapillary "funnel": 10 mL syringe, 1-in. regular bevel 18-G needle, 100 µL blue Kimble disposable soda-lime glass microcapillary pipettes.

13. 5× PBS-MK: 685 mM NaCl, 26 mM KCl, 40 mM Na$_2$HPO$_4$, 10 mM KH$_2$PO$_4$, 5 mM MgCl$_2$. Do not autoclave. Store at room temperature.

14. Opti-Prep density gradient medium (iodixanol).

15. 0.5% Phenol red indicator solution in Dulbecco's Phosphate Buffered Saline.

16. Beckman sealer/tube topper (Beckman Coulter).

17. Type T70 Ti fixed angle rotor (Beckman Coulter).

18. Red aluminum spacer for T70 Ti fixed angle rotor (Beckman Coulter).

19. Optima XE (or "preparation" certified) Ultracentrifuge (Beckman Coulter).

20. Retort stand and clamp.

21. 500 mL plastic or glass beaker.

2.3 Micro-Scale Specific Materials

1. 6-well cell culture plates.

2. 15 mL conical bottom "falcon" centrifuge tubes.

3. 1.5 mL microcentrifuge tubes.

4. Amicon Ultra-0.5 Centrifugal Filter Units Ultracel-100 (Millipore).

5. 1.8 cm blade Cell Scrapers.

3 Methods

All steps should be conducted at room temperature and in a biological safety cabinet, unless otherwise specified. It is recommended that liquid and solid waste produced throughout this protocol be disposed of by bleaching in a 1% solution of Virkon disinfectant (DuPont), which effectively destroys rAAV particles. Due to the necessity to centrifuge vector preparations at several stages during production, it is recommended that an even number (2, 4, 6, or 8) of preparations are made at any one time to facilitate rotor balancing.

3.1 Seeding and Transfection

3.1.1 Small-Scale, One Hyperflask Yields Approximately 100 μL Highly Purified rAAV Vector

1. Seed one T-175 flask with approximately 2.0×10^6 HEK293T cells and allow 2 days for the flask to reach confluency.

2. Once the flask has reached 90–100% confluency, wash the flask with 15 mL of PBS.

3. Detach adherent cells using 10 mL 1× trypsin-EDTA (3–5 min, 37 °C).

4. Transfer cell suspension directly into a 500 mL bottle of complete Growth Media.

5. Slowly pour the bottle of Growth Media containing suspended HEK293T cells into a sterile Hyperflask, being careful not to introduce bubbles.

6. Check cell confluency within the Hyperflask daily using an inverted light microscope daily (*see* **Note 2**); cells are ready for transfection when they reach ~70% confluency, which usually take 2–3 days.

7. Pipette 9.0 mL sterile 150 mM NaCl and 1 mL 1 μg/μL polyethylenimine (PEI) (*see* **Note 1**) into a 50 mL conical bottom "falcon" tube labeled "PEI."

8. Pipette 9.5 mL 150 mM NaCl and 500 μg of plasmid DNA consisting of equimolar amounts of the pHelper, pRep-Cap and transgene plasmids (*see* Table 1) in a 50 mL conical bottom falcon tube labeled "plasmid DNA" (*see* **Note 3**).

9. Add the contents of the "PEI" tube to the "Plasmid DNA" tube in a dropwise manner at a rate of 1 mL/min. It is *critical* during this step to gently agitate the "DNA tube" by swirling throughout the addition of PEI (*see* **Note 4**).

10. Incubate the PEI–DNA complex for 20 min without agitation. During incubation, place one bottle of complete Transfection Media in to a 37 °C water bath to warm.

11. Following incubation, pour the PEI–DNA complex directly into the warmed 500 mL bottle of complete Transfection Media.

12. Remove the Growth Media from the Hyperflask by pouring into a beaker with ~25% Virkon and replace immediately with the Transfection Media containing the incubated PEI–DNA complex being careful not to introduce bubbles.

13. Incubate the flask for 72 h at 37 °C in 5% CO_2 to allow for viral production.

3.1.2 Micro-Scale, One 6-Well Yields Approximately 15 μL Crudely Purified rAAV Vector

1. In Growth Media, seed a single well of 6-well plate with approximately 3.0×10^5 HEK293T cells.

2. Check the plate with an inverted light microscope daily to determine confluency. Cells are ready for transfection when plates reach 70% confluency, which usually take 1–2 days.

3. Pipette 500 μL of prewarmed Transfection Media and 2.7 μg of plasmid DNA (consisting equimolar amounts of pHelper, pRep-Cap, and the transgene plasmid as described in Table 1) into a 15 mL conical bottom "falcon" tube and label "DNA." Pipette 500 μL of prewarmed Transfection Media and 5.4 μg of PEI (*see* **Note 2**) in to a second 15 mL tube and label "PEI." Pipette the contents of the "PEI" tube into the "DNA" tube dropwise and then gently vortex mixing (250 rpm for 15 s) the solution and incubate for 20 min at room temperature.

4. Dilute the DNA-PEI mixture (~1 mL) with Transfection Media to a final volume of 6 mL.

5. Replace the Growth Media in the well with 1 mL of the diluted DNA-PEI mixture and incubate for 72 h at 37 °C in 5% CO_2 to allow for viral production.

Table 1
Plasmid DNA calculation

Plasmid	Plasmid size (kb)	Plasmid DNA (μg)
pHelper	11.6	(11.6)*(B)
pRep-Cap	8.1	(8.1)*(B)
Transgene	X	(X)*(B)
Total size (A)	19.7 + X	
Ratio (B)	500 μg/A	

The total size (base pairs) of each plasmid is summed ("A") and divided by the total amount of plasmid DNA (500 μg for small-scale and 2.7 μg for micro-scale) per prep to produce the ratio of DNA–Base Pair ("B"). The ratio "B" value is multiplied by the size of each plasmid to determine the quantity of each plasmid to add during the transfection

3.2   Purification

3.2.1   Small-Scale Preps

1. Pour out approximately 35% of the media from the Hyperflask into the waste.

2. Replace the cap and vigorously shake (*see* **Note 5**) the remaining media in the Hyperflask to detach the cells.

3. Pour the cell suspension (300–350 mL) into a 500 mL centrifuge bottle.

4. Pellet the cells by centrifugation at ~400 × *g* for 15 min.

5. Pour off the supernatant and resuspend the cell pellet in 15 mL of lysis buffer by pipetting.

6. Transfer the cell suspension to a new 50 mL round bottom centrifuge tube.

7. Tightly seal the tube and immediately freeze the suspension by placing the tube in a slurry of dry ice and 100% ethanol (*see* **Note 6**) for a period of approximately 30 min (*see* **Note 7**). In order to lyse the cells it is necessary to carry out four freeze–thaw cycles. This process is where the cell suspension is rapidly heated and frozen repetitively in order to fracture the cell membranes.

8. Following freezing, place the tube in a 37 °C water bath until all the contents are thawed. This step should take 15–25 min and should be monitored closely (*see* **Note 8**).

9. Immediately following thawing, the cell suspension should be vortex mixed at maximum speed (2500 rpm) for 30 s.

10. Replaced in the dry ice–ethanol slurry for 30 min to refreeze. Repeat this step until the cells have been frozen and thawed four times.

Table 2
Preparation of iodixanol gradient layers

Master mix (mL)						
	Iodixanol	5 M NaCl	5× PBS-MK	H_2O	Phenol red	Total volume
15%	40	32	32	56	0	160
25%	50	0	24	46	0.4	120.4
40%	67	0	20	13	0	100
60%	100	0	0	0	0.4	100.4

11. When the cell lysate has been thawed for the fourth time, add 3 μL of a 250 U/μL stock of Benzonase Nuclease to the lysate to generate a working concentration of 50 U/mL.

12. Incubate for 1 h at 37 °C to degrade cellular RNA and DNA.

13. Pellet the cellular debris by centrifugation at ~24,000 x *g* for 20 min at room temperature.

14. Whilst the cell lysate is centrifuging, prepare the master mix for each iodixanol layer in four autoclaved 250 mL glass bottles, as described in Table 2 (*see* **Note 9**).

15. Set up the syringe-microcapillary "funnel" by placing a quick-seal ultra-clear centrifuge tube into an appropriate test tube rack and insert a 100-μm microcapillary glass pipette into the top until the microcapillary reaches the bottom of the tube. Remove the plunger from a new 10 mL syringe, attach an 18-G needle and insert it into the lumen of the microcapillary tube, as shown in Fig. 1. This forms the syringe-microcapillary "funnel" through which the layers of the density gradient are poured. The density gradient used for purification of the rAAV is poured from the least dense (15%) to the most dense (60%) layer using the syringe-microcapillary "funnel," which allows layers to flow into the tube *underneath* the previous layer (*see* Fig. 1).

16. To pour the gradient, first pipette 7.2 mL of the 15% layer into syringe-microcapillary "funnel" and allow it to run through by gravity flow into the bottom of the centrifuge tube.

17. Once the 15% layer has completely run through the syringe-microcapillary "funnel," the process is repeated by flowing 4.8 mL of the 25% layer, 8 mL of 40% layer, and lastly 4 mL of the 60% layer through the "funnel." The result is discontinuous density gradient consisting of four layers.

18. Remove the syringe and the glass microcapillary tube, taking care not to disturb the gradient (*see* **Note 10**).
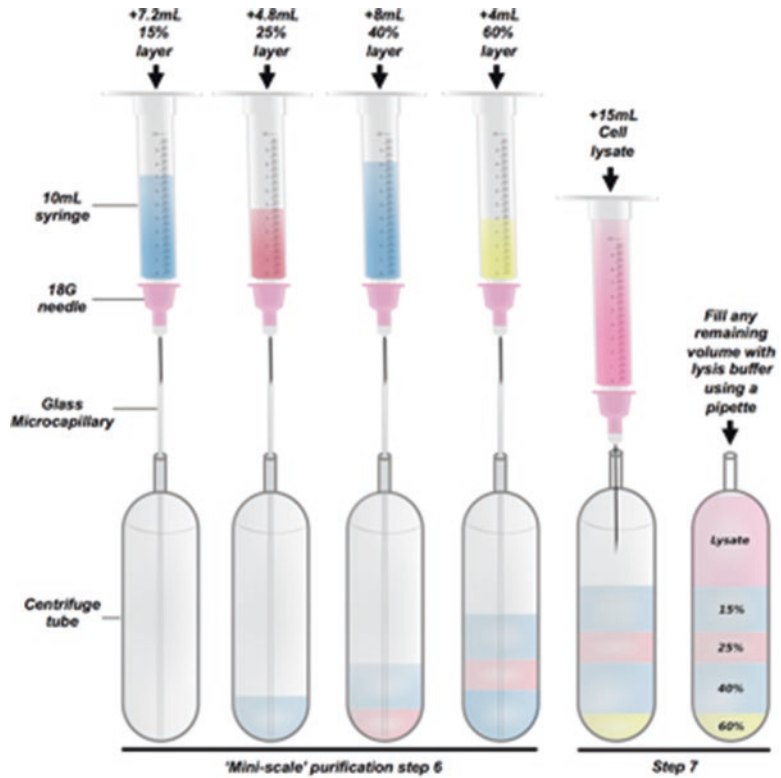
Fig. 1 Preparation of iodixanol gradients. A 10 mL syringe with an 18 G needle is placed in a 100 μm microcapillary glass pipette and placed in an ultra-centrifuge tube. Create the iodixanol gradient by sequentially adding each layer from the lowest percent of iodixanol (15%) to highest (60%). Remove the glass pipette and slowly layer the lysate onto the gradient with a fresh 10 mL syringe and 18 G needle

19. Using a new sterile 18-gauge needle and 10 mL syringe (with plunger), aspirate the supernatant of the lysate from **step 3** and slowly layer the fluid on top of the iodixanol gradient in a dropwise manner. Fill any remaining volume within the centrifuge tube with lysis buffer (*see* **Note 11**).

20. Seal the tube with the tube sealer (*see* **Note 12**).

21. Carefully insert the sealed tube in a T70 Ti fixed rotor, ensuring that the tube cap is in place.

22. Centrifuge at a maximum of ~360,000 x g (we recommend 59,000 rpm when using the T70 Ti rotor) for 1 h and 30 min using a certified "preparatory" ultracentrifuge. Due to the high speed of centrifugation, it is essential that the rotor be properly balanced.

23. Following centrifugation, carefully remove the tube making sure not to disturb the gradient layers and place the tube in a sterilized biological safety cabinet.

24. Secure the centrifuge tube directly above a 500 mL plastic or glass beaker using a retort stand and clamp.

25. Pierce the centrifuge tube at the top (near the neck) with an 18-G needle.

26. Insert a 5 mL sterile syringe attached to an 18-G needle horizontally through the sidewall of the centrifuge tube approximately 2 mm below the 40–60% gradient layer interface.

27. Aspirate ~4–5 mL of the 40% gradient layer being careful not to disturb the interface of the 25% layer (*see* **Note 13**).

28. Inject the aspirated liquid directly into an autoclaved 250 mL glass bottle and dilute with 100 mL sterile room temperature HBSS/Tween-20 (*see* **Note 14**).

29. Pour 15 mL of diluted virus in an Amicon Ultra-15 centrifuge tube with a molecular weight cutoff of 100 kDa and centrifuge at ~4000 × *g* for 15 min using a centrifuge with a swinging bucket rotor.

30. Discard flow through and refill the Amicon Ultra-15 centrifuge tube with vector and repeat the centrifugation until all the vector solution has been added. Following the final centrifugation step, approximately 200–300 µL of vector suspension should remain in the top of the concentrator.

31. Wash the concentrated virus twice with 10 mL of room temperature HBSS/Tween 20.

32. After the second wash, spin the virus for an additional 40 min in order to achieve the highest possible concentration. There should be 120–175 µL of fluid containing the purified rAAV vector.

33. Using a 200 µL pipette, aspirate the concentrated virus and use it to rinse the sides of the concentrator's filter 20 times. Aspirate the final product and place in a 2.0 mL centrifuge tube and store virus at 4 °C until virus is titered.

3.2.2 Micro-Scale Preps

1. Detach the cells from the 6-well using a cell scraper and transfer the cell suspension to a 1.5 mL microcentrifuge tube using a sterile pipette.

2. Centrifuge the tube at ~200 × *g* for 15 min to pellet the cells.

3. Discard the supernatant and resuspend the cell pellet in 500 µL of lysis buffer.

4. Lyse the cells by carrying out four rounds of freeze–thaw as described above.

5. Add 1 µL of Benzonase Nuclease to the tube (500 U/mL final concentration) and incubate the samples at 37 °C for 1 h.

6. Pellet cell debris by centrifuging at ~18,000 × *g* for 20 min.

7. Place 500 µL of 40% iodixanol (*see* Table 2) in a 1.5 mL micro-centrifuge tube. In a dropwise manner, carefully pipette the supernatant on top of the iodixanol layer.

8. Centrifuge for 90 min at ~18,000 × g.

9. Carefully pipette 80% of the 40% iodixanol layer into an Amicon Ultra-0.5 centrifugal filter unit, ensuring not to disturb the supernatant-iodixanol interface.

10. Centrifuge the tube for 15 min at ~18,000 × g.

11. Discard the flow-through and add 400 µL of HBSS/Tween-20 to the centrifuge filter unit.

12. Centrifuge again at ~18,000 × g for 15 min.

13. Repeat this wash/buffer exchange step eight times. Following the final concentration step, the final volume should be 15–20 µL.

14. To elute the virus, invert the centrifugal filter unit into a sterile 2 mL microcentrifuge tube and centrifuge at ~2300 × g for 5 min. Store virus at 4 °C until titered.

3.3 Viral Titering (Small and Micro-Scale Preps)

Titering protocol adapted from Piedra et al. [9]

1. In a 100 µL PCR tube, add 10 µL of Picogreen lysis buffer, 8 µL of autoclaved ddH$_2$O and 2 µL of vector purified using either the small- or micro-scale preparation methods outlined above.

2. Using a PCR machine/thermal cycler, heat the sample to 70 °C for 1 h and then slow cool the mixture down at a rate of 5 °C/min until it reaches 25 °C.

3. In a separate PCR tube, add 10 µL of 1× TE buffer (20× TE buffer stock is provided with picogreen kit), 8 µL of autoclaved ddH$_2$O and 2 µL of purified virus and incubate at room temperature for 1 h; this sample will act as an unlysed control.

4. In parallel, produce a six-point standard curve using Bacteriophage λ DNA (provided with picogreen kit). This is accomplished by diluting 6 µL of 100 ng/µL λ DNA in 94 µL of 1× TE buffer to produce a 6 ng/µL stock followed by one-third serial dilutions. This produces samples for a standard curve ranging from 120 to 0.49 ng per 20 µL of sample.

5. Load a black 96-well plate with 20 µL of each standard in duplicate, as well as the lysed sample, unlysed control and a blank control (20 µL of 1× TE buffer).

6. Dilute Quant-iT Picogreen reagent 1:200 in 1× TE buffer and add 180 µL of the diluted reagent to each well.

7. Incubate the samples for 5 min in the dark and quantify the fluorescence using a plate reader with an excitation of 485 nm and an emission of 535 nm.

8. Subtract the blank control from all samples and generate a line of best fit from the six-point standard using fluorescence values as the Y-axis coordinates and the amount of DNA as the X-axis coordinates. Using the equation of the line of best fit, calculate the rAAV genome concentration. Using the equation below calculate the rAAV titer (*see* **Note 15**).

$$\text{rAAV Titer}\left(\frac{\text{vg}}{\text{mL}}\right) = \frac{\text{rAAVgenome concentration}\left(\frac{\text{ng}}{\text{mL}}\right) \times 1.82\text{E} + 12\left(\frac{\text{bp}}{\text{ng}}\right)}{\text{Length of rAAV genome}\left(\frac{\text{bp}}{\text{vg}}\right)}.$$

9. Aliquot 15 μL of virus each into sterile 2.0 mL centrifuge tubes and store at −80 °C.

4   Notes

1. To prepare 1 μg/μL solution of PEI, dissolve 100 mg of linear PEI in 90 mL of ddH$_2$O in a 250 mL beaker with a magnetic stir bar by constant stirring and heating to ~50 °C (This process can take 2–4 h). Bring solution to pH 7 by adding 10 M HCl drop-by-drop. Adjust final volume to 100 mL with ddH$_2$O and in a sterile biological safety cabinet, filter sterilize through a 0.22 μm membrane. Aliquot 1.0 mL of sterile PEI into 1.5 mL centrifuge tubes and store at −20 °C. Once aliquots are thawed, do not refreeze; use a fresh aliquot each time.

2. Only the bottom 1–2 layers of a Hyperflask can be visualized using an inverted microscope, even when using low power (e.g., 4× or 10×) objectives. As cells were introduced into the Hyperflask in suspension, and cells cannot move between layers, the confluency of the bottom layer can be considered representative of all ten layers.

3. The optimal ratio of plasmid DNA to PEI must be optimized for each batch of PEI manufactured. To this end, in a 12-well plate transfect 1 μg of a ubiquitously expressing fluorescent reporter plasmid (i.e., CBA-eGFP) with varying concentrations of PEI (0.5, 1, 2, and 3 μg). The concentration of PEI that produces the most fluorescent positive cells without causing toxicity is the ratio of DNA: PEI that will be used for transfections.

4. PEI is a cationic polymer that binds DNA to form positively charged complexes capable of entering cells via endocytosis. Excessive agitation of the PEI through vigorous rocking/swirling while adding the plasmid DNA mixture can lead to the formation of toxic precipitates, which can reduce transfection efficiency and lead to cell death.

5. "Vigorous" in this context entails roughly shaking the Hyperflask up and down using both hands, in the manner of a bartender mixing a cocktail. We recommend shaking for at least 1 min in order to dislodge all of the cells. During the shaking process, pause intermittently (approximately every 15 s) to strike the flask firmly on the end with an open palm in order to maximize cell displacement.

6. To make the dry ice/ethanol slurry for rapid freezing, place an 50 mL test tube rack into a white polystyrene-shipping box, fill the box with dry ice to a depth of 2–3 in., and then pour in 100% ethanol until the dry ice is completely submerged. The ethanol will initially produce substantial amounts of white vapor (carbon dioxide) when added to the dry ice—this is normal and will subside.

7. Once frozen, the cell suspension/lysate can be stored in the −80 °C freezer indefinitely.

8. The cell suspension should be incubated at 37 °C only for as long as it takes for the contents to thaw completely. This is to prevent breakdown of the rAAV vector by proteases released during cell lysis.

9. Gradient layers can be stored indefinitely at room temperature. When adding phenol red, the 60% layer should turn a yellow color, while the 25% layer should appear red. The 15% and 40% layers do not have phenol red and should be transparent/clear.

10. If any of the iodixanol layers stop flowing through the syringe, *carefully* insert the plunger into the syringe in order to displace any air bubbles in the microcapillary tube. Remove the plunger and allow the layer to proceed through the glass microcapillary tube by gravity flow.

11. It is imperative that there is no air in the centrifuge tube as this may cause the tube to collapse during ultracentrifugation. Centrifuge tubes should be precisely balanced—this can be checked using a three decimal place electronic balance.

12. It is important to ensure that the centrifuge tube is completely sealed. To check, forcefully squeeze the sealed tube and confirm that no liquid is coming out of the top of the tube.

13. It is better to aspirate less volume than to remove volume from the 25% layer, as this can detrimentally affect downstream buffer exchange. Once aspirated, the vector can be stored in the syringe overnight at 4 °C.

14. It is important to use a glass bottle, as AAV is prone to sticking to plastics.

15. When calculating the titer of a virus encapsulating a self-complimentary genome, the genome length is doubled.

Acknowledgments

References

1. Lipinski DM, Thake M, MacLaren RE (2013) Clinical applications of retinal gene therapy. Prog Retin Eye Res 32:22–47

2. Sengillo JD, Justus S, Tsai YT et al (2016) Gene and cell-based therapies for inherited retinal disorders: an update. Am J Med Genet C Semin Med Genet 172:349–366

3. Powers AD, Piras BA, Clark RK et al (2016) Development and optimization of AAV hFIX particles by transient transfection in an iCELLis(®) fixed-bed bioreactor. Hum Gene Ther Methods 27:112–121

4. Mietzsch M, Casteleyn V, Weger S et al (2015) OneBac 2.0: Sf9 cell lines for production of AAV5 vectors with enhanced infectivity and minimal encapsidation of foreign DNA. Hum Gene Ther 26:688–697

5. Grieger JC, Soltys SM, Samulski RJ (2016) Production of recombinant adeno-associated virus vectors using suspension HEK293 cells and continuous harvest of vector from the culture media for GMP FIX and FLT1 clinical vector. Mol Ther 24:287–297

6. Salvetti A, Oreve S, Chadeuf G et al (1998) Factors influencing recombinant adeno-associated virus production. Hum Gene Ther 9:695–706

7. Clément N, Grieger JC (2016) Manufacturing of recombinant adeno-associated viral vectors for clinical trials. Mol Ther Methods Clin Dev 3:16002

8. Ye GJ, Budzynski E, Sonnentag P et al (2016) Safety and biodistribution evaluation in CNGB3-deficient mice of rAAV2tYF-PR1.7-hCNGB3, a recombinant AAV vector for treatment of achromatopsia. Hum Gene Ther Clin Dev 27:27–36

9. Piedra J, Ontiveros M, Miravet S et al (2015) Development of a rapid, robust, and universal picogreen-based method to titer adeno-associated vectors. Hum Gene Ther Methods 26:35–42

Design and Development of AAV-based Gene Supplementation Therapies for Achromatopsia and Retinitis Pigmentosa

Christian Schön, Elvir Becirovic, Martin Biel, and Stylianos Michalakis

Abstract

Achromatopsia (ACHM) and retinitis pigmentosa (RP) are inherited disorders caused by mutations in cone and rod photoreceptor-specific genes, respectively. ACHM strongly impairs daylight vision, whereas RP initially affects night vision and daylight vision at later stages. Currently, gene supplementation therapies utilizing recombinant adeno-associated virus (rAAV) vectors are being developed for various forms of ACHM and RP. In this chapter, we describe the procedure of designing and developing specific and efficient rAAV vectors for cone- and rod-specific gene supplementation.

Key words Recombinant adeno-associated virus vectors, rAAV vectors, Achromatopsia, ACHM, Retinitis pigmentosa, RP, Gene therapy, Cone photoreceptors, Rod photoreceptors

1 Introduction

In the recent years, gene therapy has seen major developments that have led to a renaissance of the field. This holds in particular true for the subfield of ocular gene therapy. The main reasons for this are our improved understanding of the genetic basis of inherited ocular diseases and the progress in development of efficient and specific gene delivery tools. Recombinant adeno-associated virus (rAAV) vectors have evolved as the "gold standard" gene delivery tool for ocular diseases and rAAV vectors are currently used in a large number of preclinical and clinical studies aiming at developing treatments of previously untreatable genetic eye diseases.

Autosomal recessive retinal disorders are particularly interesting targets for gene therapy. Gene supplementation approaches can be applied to transfer a healthy copy of the disease-causing gene into affected retinal cells. Successful proof-of-concept studies for rAAV-mediated gene supplementation therapy exist for several

inherited blinding eye diseases. The most advanced approaches deal with the treatment of Leber congenital amaurosis type 2 (LCA2), a rare form of childhood blindness [1]. LCA2 is caused by mutations in the gene *RPE65* coding for a central protein of the retinoid cycle and the treatment involves AAV2/2 mediated delivery of the wildtype *RPE65* gene. One promising LCA2 gene therapy product entered Phase III (NCT00999609) and is expected to receive marketing authorization within 2017.

Furthermore, several groups increase their efforts in developing rAAV-based gene supplementation therapies for photoreceptor-specific retinal diseases. One example is achromatopsia (ACHM), a disease characterized by the congenital lack of cone photoreceptor function and subsequent cone degeneration. ACHM patients suffer from severely impaired daylight vision, photophobia, nystagmus, and lack of color discrimination. The majority of ACHM patients carry mutations in *CNGA3* or *CNGB3*, the genes encoding the two subunits of the cone cyclic nucleotide-gated (CNG) channel [2]. Several successful proof-of-concept studies in animal models lacking one of the CNG channel subunits have been performed [3–6] and two Phase I/II clinical trials have been initiated (NCT02610582 and NCT02599922). Other activities for treatment of retinal diseases relate to forms of inherited retinitis pigmentosa (RP) or LCA caused by for example mutations in the photoreceptor-specific genes *PDE6A*, *PDE6B* or *GUCY2D* where Phase I/II clinical trials are expected to begin in 2017/18.

The basic concept of rAAV-based gene supplementation relies on the availability of gene transfer vectors which support efficient, cell-type specific and long lasting transgene expression. This requires the development of a rAAV *cis* vector that carries the future genome of the rAAVs and includes all essential regulatory elements (e.g., promoter, polyA, posttranscriptional regulatory elements). Development and preclinical evaluation of the rAAV-based treatment approach also demands a simple and efficient manufacturing procedure. In this chapter, we will describe in detail all required steps for the design, development and production of rAAVs of gene supplementation therapies for ACHM or RP. The protocol can be easily applied to other target diseases and will also be useful for researchers from other fields.

2   Materials

2.1   rAAV Cis Plasmid Cloning

1. AAV *cis* vector backbone and AAV *trans* plasmids (*see* **Note 1**).

2. QIAquick or other DNA fragment Gel Extraction Kit.

3. Alkaline phosphatase, calf intestinal (CIP).

4. DNA gel loading buffer.

5. DNA ligation kit: T4 DNA ligase, reaction buffer.

6. Agarose gel: e.g., 0.7% agarose in 1× TBE buffer (1 M Tris base, 1 M Boric acid, 0.02 M EDTA).

7. *RecA* deficient competent *E. coli* cell transformation kit: NEB 10-beta or other *RecA* deficient competent *E. coli* cells, SOC medium, control plasmid.

8. LB media: 10 g tryptone, 5 g yeast extract, 10 g NaCl, adjusted to pH 7.0 with 1 M NaOH, autoclaved, and supplemented with antibiotics, e.g., 50 µg/mL ampicillin or kanamycin.

9. Agar plates: 1.5% agar in LB, autoclaved, cooled to 50 °C, supplemented with antibiotics, e.g., 50 µg/mL ampicillin or 30 µg/mL kanamycin, and plated into Petri dishes.

10. Plasmid Miniprep kit.

11. PureLink® HiPure or other plasmid Maxiprep kit.

12. NanoDrop 2000c UV-Vis spectrophotometer.

13. PCR amplification kit: *Taq* polymerase, buffer, and dNTPs.

2.2 rAAV Vector Production

1. HEK-293T cells.

2. Dulbecco's Modified Eagle Medium (DMEM): DMEM containing 10% fetal bovine serum (FBS) supplemented with 100 U/mL Penicillin and 100 µg/mL Streptomycin.

3. 15 × 15 cm cell culture dishes.

4. Pretransfection mix: 270 µg transgene AAV *cis* plasmid, x µg pAd helper plasmid, y µg AAV Rep/Cap plasmid, 15 µl 8 mg/mL Polybrene/Hexadimethrine bromide solution, 1500 µl 10 mg/mL dextran solution, 1500 µl 2.5 M CaCl$_2$, in a final volume of 15 mL double-distilled water. The components listed in Table 1 are added in a 50-mL polystyrene tube. Prepare shortly before transfection.

Table 1
Pretransfection mix for transfection of 15 × 15-cm dishes of HEK293T cells

Reagent	Amount
Transgene AAV *cis* plasmid	270 µg
pAd helper plasmid	x µg
AAV rep/cap plasmid	y µg
Polybrene (8 mg/mL)	15 µL
Dextran (10 mg/mL)	1500 µL
2.5 M CaCl$_2$	1500 µL
Double-distilled water	Up to 15 mL

The following two equations are used to calculate the amount of pAd Helper plasmid and AAV Cap/Rep plasmid needed for the pretransfection mix (Table 1):

$$x(\text{amount of pAd Helper}) = \frac{m(\text{transgene AAV}) \times M(\text{pAd Helper})}{M(\text{transgene AAV})}.$$

$$y(\text{amount of AAV Rep / Cap Helper}) = \frac{m(\text{transgene AAV}) \times M(\text{AAV Rep / Cap Helper})}{M(\text{transgene AAV})}.$$

M = molar mass of a double stranded plasmid.

5. 2× BBS transfection solution: 45 mM BES sodium salt, 280 mM NaCl, 1.5 mM Na_2HPO_4. Adjust pH to 6.95 with 1 M NaOH and sterile filtrate. Prepare 50 mL aliquots and store them at 4 °C for up to 1 year.

6. 50 mL polystyrene tubes.

7. Lysis buffer: 150 mM NaCl, 50 mM TRIS. Adjust pH to 8.5 with diluted HCl and sterile filtrate. Prepare freshly before use.

8. Benzonase.

9. Liquid nitrogen.

10. 15%, 25%, 40%, and 60% iodixanol solutions: Prepare solutions containing 15%, 25%, 40%, or 60% Optiprep in 1 mM $MgCl_2$, 2.5 mM KCl, 1 M NaCl, 1× PBS. Add phenol red (use 1% solution) ad libitum until the solution is visibly colored. Store at 4 °C for up to 1 week.

11. Quick-Seal polypropylene tubes, 39 mL (Beckman).

12. Quick-Seal cordless tube topper kit, 50 Hz (Beckman).

13. Peristaltic pump MINIPULS 3 (Gilson).

14. Long Pasteur glass pipettes.

15. 21-G needles.

16. 5-mL syringes.

17. 0.014% PBS-MK solution: 1 mM $MgCl_2$, 2.5 mM KCl, 0.014% Tween 20 in 1× PBS (e.g., purchased from Sigma; pH 7.4). Sterile filtrate and store at 4 °C for up to 1 week.

18. PBS-MK solution: 1 mM $MgCl_2$, 2.5 mM KCl in 1× PBS (e.g., purchased from Sigma; pH 7.4). Sterile filtrate and store at 4 °C for up to 1 week.

19. ÄKTAprime plus chromatography system (GE Healthcare).

20. HiTrap Q FF sepharose columns, 5 mL (GE Healthcare).

21. Superloop, 50 mL (GE Healthcare).

22. 10 mL syringes.

23. 1.5 mL reaction tubes for fraction collection.

24. Buffer A: 20 mM TRIS, 15 mM NaCl. Adjust the pH to 8.5 with diluted HCl. Store at 4 °C for up to 1 week.

25. Buffer B: 2.5 M NaCl. Adjust the pH to 8.5. Store at 4 °C for up to 1 week.

26. Beckman Coulter J2-MC high speed centrifuge.

27. JA-10 Rotor, Fixed Angle, Aluminum, 6 × 500 mL, 10,000 rpm, 17,700 × g (Beckman).

28. Beckman Coulter Optima LE-80K ultracentrifuge.

29. 70 Ti Rotor, Fixed Angle, Titanium, 8 × 39 mm, 70,000 rpm, 504,000 × g (Beckman).

2.3 Concentration and Titer Determination of rAAVs

1. Amicon Ultra-4 centrifugal filter units, 100 kDa.

2. KAPA SYBR FAST Universal ×2 qPCR MasterMix (Peqlab).

3. MacroAmp® fast optical 96-well reaction plate (Applied Biosystems).

4. MacroAmp® optical adhesive film (Applied Biosystems).

5. StepOnePlus™ real-time PCR system (Applied Biosystems).

6. WPRE PCR primers: Primer forward: AGTTCCGCCGT GGCAATAGG; Primer reverse: CAAGGAGGAGAAAATGA AAGCC.

7. 1.5-mL screw cap reaction tubes.

3 Method

Successful gene therapy requires both high efficiency and cell-type specificity for the expression of transgenes. The AAV vector system allows for optimization and adjustments at different levels to help achieving this goal (Fig. 1). **Notes 2–10** describe recommendations for optimal vector design.

3.1 Cloning of the rAAV Cis Plasmid

Standard molecular biology techniques can be applied for construction and cloning of the rAAV *cis* plasmid. The essential steps are outlined below:

1. Choose the desired AAV *cis* plasmid backbone (*see* **Note 1**).

2. Digest 4 μg backbone plasmid in 40 μl of compatible restriction buffer with the appropriate site-specific restriction enzyme (RE) at the appropriate temperature for at least 1 h.

3. Add DNA gel loading buffer and run the digested DNA on an agarose gel (e.g., 0.7%).
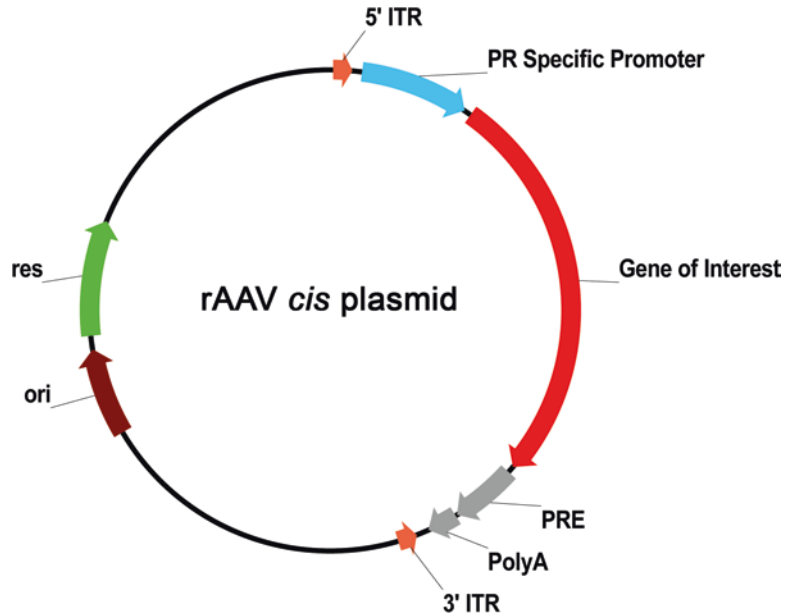
Fig. 1 Map illustrating the composition of a typical rAAV *cis* plasmid for gene supplementation therapies of ACHM and RP. Inverted terminal repeats (ITRs) flank the full gene expression cassette containing the photoreceptor (PR) specific promoter, gene of interest, posttranscriptional regulatory elements (PRE) and polyA sequences. The vector backbone contains a bacterial origin of replication (ori) and a bacterial antibiotic resistance gene expression cassette (res)

4. Cut out the linearized plasmid and purify the DNA using a standard DNA fragment gel extraction kit (*see* **Notes 11** and **12**).

5. Design PCR cloning primers specific for your promoter of choice and your gene of interest with RE recognition sites which are compatible with the multiple cloning site (MCS) of your AAV *cis* plasmid backbone (*see* **Note 13**).

6. PCR amplify the desired promoter sequence and the desired ORF from genomic DNA, cDNA or another appropriate DNA template using a standard PCR amplification kit.

7. Run the PCRs on an agarose gel.

8. Cut out the specific bands and purify the amplified DNA fragments using a standard DNA gel extraction kit.

9. Digest the DNA with the appropriate site-specific RE.

10. Run the digested DNA on an agarose gel.

11. Cut out the specific DNA band and purify the DNA to obtain the RE-digested PCR amplicon, which can be used for ligation into the RE-linearized AAV *cis* plasmid backbone (*see* **step 1**).

12. Ligate the RE-digested promoter and ORF DNA fragments into the RE-linearized AAV *cis* plasmid backbone using a stan-

dard DNA ligation protocol (e.g., mix insert and vector in a molar ratio of 3–1, add T4 DNA ligase in reaction buffer and incubate overnight at 16 °C), (*see* **Note 14** for alternative strategy).

13. Thaw 50 µL *RecA* deficient competent *E. coli* cells (e.g., NEB 10-beta) on ice. Add 3 µL of the ligated product, incubate for 30 min on ice, heat-shock for 45 s at 42 °C, and incubate for 2 min on ice.

14. Plate the transformed bacteria on agar plates containing antibiotics that match the antibiotic resistance encoded on the plasmid backbone and grow them overnight at 37 °C.

15. Pick selected bacterial colonies using sterile pipette tips to inoculate a sterile tube containing 5 mL LB medium plus antibiotics (corresponding to the antibiotic resistance encoded in the AAV *cis* plasmid backbone).

16. Incubate the bacteria overnight at 37 °C in a shacking bacteria incubator.

17. Isolate plasmid DNA by alkaline lysis or plasmid miniprep kit.

18. Verify the identity of correct clones using RE analysis and the composition of the full expression cassette using standard DNA sequencing (*see* **Note 15**).

19. Grow correct clones in LB medium containing proper antibiotics to isolate higher amounts of plasmid DNA using standard plasmid preparation kits under endotoxin-free conditions (e.g., Pure Link® HiPure or other Maxiprep Kit). Determine DNA concentration, e.g., using NanoDrop spectrophotometer.

3.2 rAAV Vector Production

We adapted our protocol on rAAV production based on a previous publication [7].

3.2.1 Transfection of HEK293T Cells

1. 24 h before transfection, split confluent 15-cm dishes of HEK293T cells into 15× 15-cm dishes in DMEM medium.

2. Prepare pretransfection mix shortly before transfection.

3. Add 15 mL 2× BBS dropwise while vortexing the pretransfection mix in the polystyrene tube at maximum speed, are (*see* **Note 16**).

4. Incubate the transfection mix at room temperature for 4–5 min.

5. Remove HEK293T dishes from incubator immediately before transfection.

6. Add 2 mL transfection mix dropwise to each of the 15-cm dishes of approx. 80% confluent HEK293T cells.

7. Incubate transfected cells at 37 °C and 5% CO_2 atmosphere for 24 h.

8. Replace the medium from transfected cells and incubate the plates at 37 °C and 10% CO_2 atmosphere for additional 24 h.

3.2.2 Harvesting of HEK293T Cells

1. 48 h post transfection, harvest the cells by scraping them from each 15-cm dish with a cell scraper. Pool the cell suspensions from the 15 dishes in a 500-mL centrifuge tube and centrifuge at $2000 \times g$ for 15 min at 4 °C (*see* **Note 17**).

2. After medium removal, resuspend the cell pellet in 7.5 mL lysis buffer and transfer it to a 50-mL polystyrene tube.

3. Shock-freeze the cell suspension in liquid nitrogen and thaw it subsequently at 37 °C. Repeat freeze–thaw cycle two additional times (*see* **Note 18**).

3.2.3 Gradient Centrifugation and Purification of rAAVs

1. Add Benzonase to the thawed cell suspension to a final concentration of 50 U/mL and incubate at 37 °C for 30 min.

2. Centrifuge the suspension at $2000 \times g$ for 25 min at 4 °C.

3. Transfer the virus-containing supernatant into a Beckman Quick-Seal polypropylene tube.

4. Generate an iodixanol gradient using a sterile, long glass pipette and a Gilson MINIPULS3 pump. Underlay the virus-containing phase with four separate solutions containing different iodixanol concentrations in the following order: 7 mL 15% iodixanol, 5 mL 25% iodixanol, 5 mL 40% iodixanol and 6 mL 60% iodixanol. To avoid mixing of the layers, the pump should be run at the slowest speed.

5. For centrifugation, fill up the polypropylene tubes and balance them accurately with PBS-MK.

6. Seal the tubes with the Beckman tube topper. Centrifuge at $361,000 \times g$ for 1 h 45 min at 18 °C (70,000 rpm in an Optima LE-80K Beckman ultracentrifuge using a 70 Ti rotor). During centrifugation, the virus-containing fraction accumulates in the 40% phase.

7. After centrifugation, pierce the tube at the top near the seal. To collect the virus-containing phase, pierce the tube through the side at the lower end of the 40–60% interface with a 21-G needle and a 5-mL syringe. During this step, the open site of the needle tip should face the 40% phase. Collect approximately 5 mL of the 40% phase (*see* **Note 18**).

8. For purification, thaw the virus-containing phase on ice.

9. Connect HiTrap Q FF sepharose column and superloop with the ÄKTAprime plus chromatography system.

10. For collection of the purified fractions, load 1.5-mL centrifuge tubes into the tube rack.

11. Adjust the Drop Sync unit of the fraction collector to position 1.

12. Subsequently, equilibrate the HiTrap Q FF sepharose column with 25 mL of buffer A at 10 mL/min flow rate.

13. Select "manual run mode" with 1.0 mL/min flow rate, 1 mL fraction size, and put the measuring curves to starting point via "autozero."

14. Dilute the virus phase 1:1 with buffer A prior to filling the super loop of the ÄKTAprime plus system with a 10 mL syringe.

15. Inject the virus dilution from the superloop into the ÄKTAprime plus system and collect 1 mL fractions in 1.5-mL reaction tubes. During this step, monitor the UV and conductance curves via the Äktaprime software.

16. When the conductance curve reaches basal values, switch the ÄKTAprime plus system to 100% buffer B at 10 mL/min flow rate and 0 mL fraction size to purge the sepharose column from the remaining virus dilution.

17. To wash out the remaining salt from the system, use sterile, double-distilled water at 10 mL/min flow rate.

18. When the conductance curve reaches zero, continue washing for additional 5 min.

19. Pool all 1-mL fractions collected during the plateau phase of the conductance curve (*see* **Note 18**).

3.2.4 Concentration of rAAVs

1. Thaw the purified virus fraction on ice and transfer 4 mL of the fraction to an Amicon centrifugal filter. Centrifuge at $2000 \times g$ for 10 min at 20 °C.

2. Discard the flow-through and repeat **step 1** until the complete virus is loaded to the column and approximately 500 μL remain in the filter unit.

3. Wash out the concentrated rAAV from the membrane with 1 mL 0.014% Tween/PBS-MK by pipetting up and down several times. Centrifuge the virus suspension at $2000 \times g$ at 20 °C until 100 μL of the concentrated virus suspension remains in the filter unit (*see* **Note 19**).

4. Aliquot and store the supernatant in 1.5-mL screw cap tubes (*see* **Note 18**).

3.2.5 Titer Determination of rAAVs

1. For qPCR standard preparation, a small fragment within the WPRE of the rAAV *cis* plasmid needs to be amplified via PCR using an appropriate PCR kit (Primer for: AGTTCCGCC GTGGCAATAGG; Primer rev: CAAGGAGGAGAAAATGAAA GCC). After gel electrophoresis, purify the PCR product and measure the DNA concentration. The DNA copy number can be calculated using for example "DNA copy number and dilu-

tion calculator" (For further information, e.g., *see* ThermoFisher Scientific web page).

2. Using this standard, prepare tenfold serial dilutions ranging from 1×10^5 to 1×10^9 copies/5 μL. Standards can be stored at −20 °C until use.

3. Dilute the rAAV suspension 1:100 with double-distilled water.

4. Perform qPCR with doublets of 5 μL rAAV dilution and standard dilutions using an appropriate qPCR kit (e.g., KAPA SYBR Universal ×2 qPCR Master Mix), 30 pmol/μL primers (compare **step 1**) and double-distilled water according to the manufacturer's protocol.

5. Determine number of rAAV genomes (titer) based on the obtained standard curve using for example the StepOne software implemented protocols (*see* **Note 20**).

4 Notes

1. AAV *cis* vector backbone and AAV *trans* plasmids (encoding for Cap, Rep and adenoviral helper genes) can be obtained from various sources including Penn Vector Core (www.med.upenn.edu/gtp/vectorcore) or from UNC Vector Core (www.med.unc.edu/genetherapy/vectorcore, *see* also ref. 7). Various AAV *cis* vector plasmids are also available from Addgene (https://www.addgene.org).

2. The capacity limit of the rAAV vector genome: Wild type AAV genome size is about 4.6 kb. Optimally, the size of the rAAV genome that comprises the full gene expression cassette flanked by the two inverted terminal repeats (ITR) should not exceed 4.6 kb. However, packaging of intact rAAV genomes of up to 5 kb has been reported [8].

3. rAAV cis vector plasmid backbone: All commonly used DNA plasmid backbones can be used. The DNA plasmid backbone should contain the following functional elements: (a) a bacterial origin of replication and (b) a bacterial antibiotic resistance gene expression cassette. Optimally, the DNA plasmid backbone should exceed the AAV packaging capacity limit (e.g., >5.5 kb) to minimize the possibility of a false or reverse packaging of the backbone [9] into rAAV vector particles.

4. Choice of promoter: Several short promoters have been used in combination with rAAV vectors to drive efficient and specific expression in cone and/or rod photoreceptors. For example, cone-specific transgene expression was demonstrated for a cone arrestin (ARR3 gene) [3], a blue opsin (OPNSW1) [5], or the red/green opsin promoter (OPNMW1) [10, 11]. Rod photoreceptor-specific expression was documented for

rhodopsin (RHO) promoters from different species [12, 13]. In addition, other promoters like rhodopsin kinase 1 (GRK1) [14] or interphotoreceptor retinoid binding protein (RBP3) [15] were also shown to efficiently drive expression in both types of photoreceptors.

5. Optimization of open reading frame (ORF) and utilization of other regulatory elements: If high levels of expression are desired, codon optimization for the target species should be considered (*see* **Note 6**). Additionally, the coding sequence should be followed by a polyadenylation sequence (polyA). Expression levels can also be improved by increasing mRNA stability using posttranscriptional regulatory elements. The most commonly used sequence in various gene vectors is the woodchuck hepatitis virus posttranscriptional regulatory element (WPRE) that increases the size of the polyA tail [16, 17] (*see* **Notes 7** and **8**).

6. In case of clinical applications, it is preferred to generate a "humanized" vector containing human promoter and gene sequences. Note that these adaptations might influence the outcome of preclinical testing in other species (e.g., mice).

7. The WPRE element contains an ORF encoding a truncated peptide of the woodchuck hepatitis virus X protein (WHX). WHX is a transcriptional regulator associated with the development of liver tumors. Although there is no direct evidence for any harmful effects of WPRE in combination with rAAVs we recommend using an element with mutated WHX ORF [17].

8. If the overall size of the transgene and standard regulatory elements exceeds the rAAV packaging capacity, smaller regulatory elements might be used to overcome this limitation. For example, WPRE can be efficiently replaced with smaller polyA sequences (e.g., SV40 polyA [18] or synthetic polyA signal [19]).

9. Choice of AAV capsid: AAV serotypes 5, 7, 8, and 9 are able to efficiently transduce rod and cone photoreceptors [12, 20, 21]. Among those, AAV8 and AAV9 lead to highest transduction rates in different species including mice, pigs, dogs, and nonhuman primates [12, 22–26] (*see* **Note 10**).

10. Apart from wildtype AAV serotypes, novel, engineered AAV capsids might be useful to improve transduction efficacy of photoreceptors (e.g., tyrosine mutant AAV2 [27], 7m8 [28], or Anc80 [29]).

11. Inappropriate high levels of UV light during agarose gel examination or cutting might result in DNA damage and impair efficient ligation of DNA fragments.

12. If the RE chosen for plasmid linearization generate compatible ends vector self-ligation might occur. 5′ dephosphorylation of plasmid DNA using standard enzymes (e.g., CIP) could be used to prevent self-ligation.

13. Obtain high quality primers by choosing appropriate purification techniques offered by the respective company. This can largely exclude mutations of the oligonucleotide sequence which might affect RE cleavage sites.

14. Aside from the described conventional cloning techniques, novel cloning techniques might facilitate subcloning of DNA fragments into rAAV vectors (e.g., NEBuilder).

15. Due to their secondary structure rAAV ITRs can be hardly sequenced by standard Sanger sequencing. Special protocols suitable for sequencing of secondary structure elements in the DNA might be used. Such protocols are typically offered by sequencing companies. In addition, ITR integrity can be verified using SmaI and Eam1105I (or AhdI) RE analysis.

16. BBS quality (in particular the pH) is crucial for good transfection efficiency and should be checked at regular intervals.

17. AAV8 serotype transfected HEK293T cells also secrete the rAAVs to the cell culture medium [30, 31]. This is also the case for other AAV serotypes. Thus, rAAVs can also be purified from the supernatant after the cell harvesting step described in Subheading 3.2.2.

18. At these steps, the harvested material can be stored at −80 °C.

19. As the viscosity of the AAV solution varies between the AAV preparations, in some cases more or longer centrifugation steps are required for the AAV solution to pass the Amicon filter membrane. This should be considered for appropriate time schedule of the experiments. Take care not to overestimate the time needed for the final centrifugation step.

20. Low yield AAV titers can result from various problems during the preparation procedure. Check especially for integrity of the ITRs (*see* **Note 15**) and efficacy of transfection reagents (*see* **Note 16**).

References

1. Scholl HP, Strauss RW, Singh MS, Dalkara D, Roska B, Picaud S, Sahel JA (2016) Emerging therapies for inherited retinal degeneration. Sci Transl Med 8(368):368rv366. https://doi.org/10.1126/scitranslmed.aaf2838

2. Schön C, Biel M, Michalakis S (2013) Gene replacement therapy for retinal CNG channelopathies. Mol Gen Genomics: MGG 288(10):459–467. https://doi.org/10.1007/s00438-013-0766-4

3. Carvalho LS, Xu J, Pearson RA, Smith AJ, Bainbridge JW, Morris LM, Fliesler SJ, Ding XQ, Ali RR (2011) Longterm and age-dependent restoration of visual function in a mouse model of CNGB3-associated achromatopsia following gene therapy. Hum Mol Genet 20(16):3161–3175. https://doi.org/10.1093/hmg/ddr218

4. Komaromy AM, Alexander JJ, Rowlan JS, Garcia MM, Chiodo VA, Kaya A, Tanaka JC,

Acland GM, Hauswirth WW, Aguirre GD (2010) Gene therapy rescues cone function in congenital achromatopsia. Hum Mol Genet 19(13):2581–2593. https://doi.org/10.1093/hmg/ddq136

5. Michalakis S, Muhlfriedel R, Tanimoto N, Krishnamoorthy V, Koch S, Fischer MD, Becirovic E, Bai L, Huber G, Beck SC, Fahl E, Buning H, Paquet-Durand F, Zong X, Gollisch T, Biel M, Seeliger MW (2010) Restoration of cone vision in the CNGA3−/− mouse model of congenital complete lack of cone photoreceptor function. Mol Ther: J Am Soc of Gene Ther 18(12):2057–2063. https://doi.org/10.1038/mt.2010.149

6. Pang JJ, Deng WT, Dai X, Lei B, Everhart D, Umino Y, Li J, Zhang K, Mao S, Boye SL, Liu L, Chiodo VA, Liu X, Shi W, Tao Y, Chang B, Hauswirth WW (2012) AAV-mediated cone rescue in a naturally occurring mouse model of CNGA3-achromatopsia. PloS one 7(4):e35250. https://doi.org/10.1371/journal.pone.0035250

7. Grieger JC, Choi VW, Samulski RJ (2006) Production and characterization of adeno-associated viral vectors. Nat Protoc 1(3):1412–1428. https://doi.org/10.1038/nprot.2006.207

8. Hirsch ML, Agbandje-McKenna M, Samulski RJ (2010) Little vector, big gene transduction: fragmented genome reassembly of adeno-associated virus. Mol Ther: J Am Soc of Gene Ther 18(1):6–8. https://doi.org/10.1038/mt.2009.280

9. Hauck B, Murphy SL, Smith PH, Qu G, Liu X, Zelenaia O, Mingozzi F, Sommer JM, High KA, Wright JF (2009) Undetectable transcription of cap in a clinical AAV vector: implications for preformed capsid in immune responses. Mol Ther: J Am Soc of Gene Ther 17(1):144–152. https://doi.org/10.1038/mt.2008.227

10. Alexander JJ, Umino Y, Everhart D, Chang B, Min SH, Li Q, Timmers AM, Hawes NL, Pang JJ, Barlow RB, Hauswirth WW (2007) Restoration of cone vision in a mouse model of achromatopsia. Nat Med 13(6):685–687. https://doi.org/10.1038/nm1596

11. Komaromy AM, Alexander JJ, Cooper AE, Chiodo VA, Glushakova LG, Acland GM, Hauswirth WW, Aguirre GD (2008) Targeting gene expression to cones with human cone opsin promoters in recombinant AAV. Gene Ther 15(14):1049–1055. https://doi.org/10.1038/gt.2008.32

12. Allocca M, Mussolino C, Garcia-Hoyos M, Sanges D, Iodice C, Petrillo M, Vandenberghe LH, Wilson JM, Marigo V, Surace EM, Auricchio A (2007) Novel adeno-associated virus serotypes efficiently transduce murine photoreceptors. J Virol 81(20):11372–11380. https://doi.org/10.1128/JVI.01327-07

13. Flannery JG, Zolotukhin S, Vaquero MI, LaVail MM, Muzyczka N, Hauswirth WW (1997) Efficient photoreceptor-targeted gene expression in vivo by recombinant adeno-associated virus. Proc Natl Acad Sci U S A 94(13):6916–6921

14. Young JE, Vogt T, Gross KW, Khani SC (2003) A short, highly active photoreceptor-specific enhancer/promoter region upstream of the human rhodopsin kinase gene. Invest Ophthalmol Vis Sci 44(9):4076–4085

15. Beltran WA, Cideciyan AV, Lewin AS, Iwabe S, Khanna H, Sumaroka A, Chiodo VA, Fajardo DS, Roman AJ, Deng WT, Swider M, Aleman TS, Boye SL, Genini S, Swaroop A, Hauswirth WW, Jacobson SG, Aguirre GD (2012) Gene therapy rescues photoreceptor blindness in dogs and paves the way for treating human X-linked retinitis pigmentosa. Proc Natl Acad Sci U S A 109(6):2132–2137. https://doi.org/10.1073/pnas.1118847109

16. Loeb JE, Cordier WS, Harris ME, Weitzman MD, Hope TJ (1999) Enhanced expression of transgenes from adeno-associated virus vectors with the woodchuck hepatitis virus posttranscriptional regulatory element: implications for gene therapy. Hum Gene Ther 10(14):2295–2305. https://doi.org/10.1089/10430349950016942

17. Zanta-Boussif MA, Charrier S, Brice-Ouzet A, Martin S, Opolon P, Thrasher AJ, Hope TJ, Galy A (2009) Validation of a mutated PRE sequence allowing high and sustained transgene expression while abrogating WHV-X protein synthesis: application to the gene therapy of WAS. Gene Ther 16(5):605–619. https://doi.org/10.1038/gt.2009.3

18. Koch S, Sothilingam V, Garcia Garrido M, Tanimoto N, Becirovic E, Koch F, Seide C, Beck SC, Seeliger MW, Biel M, Muhlfriedel R, Michalakis S (2012) Gene therapy restores vision and delays degeneration in the CNGB1(−/−) mouse model of retinitis pigmentosa. Hum Mol Genet 21(20):4486–4496. https://doi.org/10.1093/hmg/dds290

19. Ostedgaard LS, Rokhlina T, Karp PH, Lashmit P, Afione S, Schmidt M, Zabner J, Stinski MF, Chiorini JA, Welsh MJ (2005) A shortened adeno-associated virus expression cassette for CFTR gene transfer to cystic fibrosis airway epithelia. Proc Natl Acad Sci U S A 102(8):2952–2957. https://doi.org/10.1073/pnas.0409845102

20. Lebherz C, Maguire A, Tang W, Bennett J, Wilson JM (2008) Novel AAV serotypes for improved ocular gene transfer. J Gene Med 10(4):375–382. https://doi.org/10.1002/jgm.1126

21. Lotery AJ, Yang GS, Mullins RF, Russell SR, Schmidt M, Stone EM, Lindbloom JD, Chiorini JA, Kotin RM, Davidson BL (2003) Adeno-associated virus type 5: transduction efficiency and cell-type specificity in the primate retina. Hum Gene Ther 14(17):1663–1671. https://doi.org/10.1089/104303403322542301

22. Manfredi A, Marrocco E, Puppo A, Cesi G, Sommella A, Della Corte M, Rossi S, Giunti M, Craft CM, Bacci ML, Simonelli F, Surace EM, Auricchio A (2013) Combined rod and cone transduction by adeno-associated virus 2/8. Hum Gene Ther 24(12):982–992. https://doi.org/10.1089/hum.2013.154

23. Mussolino C, della Corte M, Rossi S, Viola F, Di Vicino U, Marrocco E, Neglia S, Doria M, Testa F, Giovannoni R, Crasta M, Giunti M, Villani E, Lavitrano M, Bacci ML, Ratiglia R, Simonelli F, Auricchio A, Surace EM (2011) AAV-mediated photoreceptor transduction of the pig cone-enriched retina. Gene Ther 18(7):637–645. https://doi.org/10.1038/gt.2011.3

24. Natkunarajah M, Trittibach P, McIntosh J, Duran Y, Barker SE, Smith AJ, Nathwani AC, Ali RR (2008) Assessment of ocular transduction using single-stranded and self-complementary recombinant adeno-associated virus serotype 2/8. Gene Ther 15(6):463–467. https://doi.org/10.1038/sj.gt.3303074

25. Vandenberghe LH, Bell P, Maguire AM, Cearley CN, Xiao R, Calcedo R, Wang L, Castle MJ, Maguire AC, Grant R, Wolfe JH, Wilson JM, Bennett J (2011) Dosage thresholds for AAV2 and AAV8 photoreceptor gene therapy in monkey. Sci Transl Med 3(88):88ra54. https://doi.org/10.1126/scitranslmed.3002103

26. Vandenberghe LH, Bell P, Maguire AM, Xiao R, Hopkins TB, Grant R, Bennett J, Wilson JM (2013) AAV9 targets cone photoreceptors in the nonhuman primate retina. PloS one 8(1):e53463. https://doi.org/10.1371/journal.pone.0053463

27. Petrs-Silva H, Dinculescu A, Li Q, Deng WT, Pang JJ, Min SH, Chiodo V, Neeley AW, Govindasamy L, Bennett A, Agbandje-McKenna M, Zhong L, Li B, Jayandharan GR, Srivastava A, Lewin AS, Hauswirth WW (2011) Novel properties of tyrosine-mutant AAV2 vectors in the mouse retina. Mol Ther: J Am Soc of Gene Ther 19(2):293–301. https://doi.org/10.1038/mt.2010.234

28. Dalkara D, Byrne LC, Klimczak RR, Visel M, Yin L, Merigan WH, Flannery JG, Schaffer DV (2013) In vivodirected evolution of a new adeno-associated virus for therapeutic outer retinal gene delivery from the vitreous. Sci Transl Med 5(189):189ra176. https://doi.org/10.1126/scitranslmed.3005708

29. Zinn E, Pacouret S, Khaychuk V, Turunen HT, Carvalho LS, Andres-Mateos E, Shah S, Shelke R, Maurer AC, Plovie E, Xiao R, Vandenberghe LH (2015) In Silico Reconstruction of the Viral Evolutionary Lineage Yields a Potent Gene Therapy Vector. Cell Rep 12(6):1056–1068. https://doi.org/10.1016/j.celrep.2015.07.019

30. Ayuso E, Blouin V, Lock M, McGorray S, Leon X, Alvira MR, Auricchio A, Bucher S, Chtarto A, Clark KR, Darmon C, Doria M, Fountain W, Gao G, Gao K, Giacca M, Kleinschmidt J, Leuchs B, Melas C, Mizukami H, Muller M, Noordman Y, Bockstael O, Ozawa K, Pythoud C, Sumaroka M, Surosky R, Tenenbaum L, van der Linden I, Weins B, Wright JF, Zhang X, Zentilin L, Bosch F, Snyder RO, Moullier P (2014) Manufacturing and characterization of a recombinant adeno-associated virus type 8 reference standard material. Hum Gene Ther 25(11):977–987. https://doi.org/10.1089/hum.2014.057

31. Vandenberghe LH, Xiao R, Lock M, Lin J, Korn M, Wilson JM (2010) Efficient serotype-dependent release of functional vector into the culture medium during adeno-associated virus manufacturing. Hum Gene Ther 21(10):1251–1257. https://doi.org/10.1089/hum.2010.107

Development of Multigenic Lentiviral Vectors for Cell-Specific Expression of Antiangiogenic miRNAs and Protein Factors

Anne Louise Askou and Thomas J. Corydon

Abstract

Generation of lentivirus (LV)-based vectors holding multiple gene cassettes for coexpression of several therapeutic factors provides potent tools in both gene delivery studies as well as in gene therapy. Here we describe the development of such multigenic LV gene delivery vectors enabling cell-specific coexpression of antiangiogenic microRNA (miRNA) and protein factors and, if preferred, a fluorescent reporter, from RNApol(II)-driven expression cassettes orientated in a back-to-back fashion. This configuration may contribute to the development of new combination therapies for amelioration of diseases involving intraocular neovascularization including exudative age-related macular degeneration (AMD).

Key words DNA cloning, Multigenic vector, Coexpression, Cell-specific expression, Lentivirus, miRNA, Antiangiogenesis, AMD, VEGF, Retina

1 Introduction

Successful gene transfer studies and gene therapy depend on efficient gene delivery vectors allowing coexpression of multiple therapeutic factors. Present approaches to express miRNA clusters and transgenes from a single viral vector may have certain restrictions affecting important issues such as expression levels of the transgene and vector titers. Based on our recent findings [1] we here in detail describe the generation of a versatile LV vector design that facilitates combined expression of therapeutic RNA- and protein-based antiangiogenic factors as well as a fluorescent reporter from back-to-back RNApol(II)-driven expression cassettes. The multigenic LV vector may thus provide potential implications for the future development of gene delivery vehicles for combination therapy of intraocular neovascular diseases, including exudative AMD, which are the principal cause of blindness in the aging population [2, 3]. Exudative AMD is characterized by abnormal choroidal neovessel

development, a process that involves overexpression of vascular endothelial growth factor (VEGF) [4, 5]. Even though present antibody-based anti-VEGF therapy shows great success rates, some patients are only partially responsive or even nonresponsive to the treatment, thereby underlining the demand for new and refined strategies. The complexity of the pathogenic events involved in a multifactorial disease such as AMD, suggests that simultaneous targeting of different pathways, may have synergistic effects and thus improve efficacy as well as reduce the treatment rate [6–8]. The multigenic LV vector described in this chapter has potential in amelioration of exudative AMD since it encodes both anti-VEGF miRNAs and the multifunctional protein pigment epithelium-derived factor (PEDF).

The LV vector was generated by multiple consecutive cloning steps, where the functional elements have been inserted in a simple third generation pCCL-based LV transfer plasmid harboring a PGK-eGFP cassette, here designated pLV/PE. Figure 1 illustrates the cloning design and the consecutive insertions of the elements in the second expression cassette inserted in reverse orientation. The second expression cassette encompasses a retinal pigment epithelium (RPE) specific promoter, the vitelliform macular dystrophy 2 (VMD2) promoter, driving the expression of a single mRNA encoding an intronic miRNA cluster inserted in a modified β-globin intron and the multifunctional protein PEDF. Functionality of the distinctive elements of the multigenic design was verified in different cell culture systems revealing (i) RPE-specific expression, (ii) miRNA-directed downregulation of VEGF, (iii) impairments of angiogenic pathways by codelivery of the gene encoding PEDF, and LV-mediated gene delivery in mouse retina (Fig. 2) [1].

In conclusion, we have generated a multigenic LV vector that may contribute to the development of new combination therapies for amelioration of diseases involving intraocular neovascularization.

2   Materials

Prepare all solutions using ultrapure water.

2.1   Cloning

1. Restriction enzymes: *Mlu*I, *Pst*I, *Xma*I, *Nsi*I, *Bsi*WI, *Sal*I, *Xho*I, *Hind*III, *Eco*RI, *Bam*HI, *Xba*I, and *Sac*II.

2. Calf intestinal alkaline phosphatase (CIP).

3. Compatible enzyme reaction buffers.

4. Loading dye for subsequent gel analysis.

5. Plasmid pLV/PE [9].

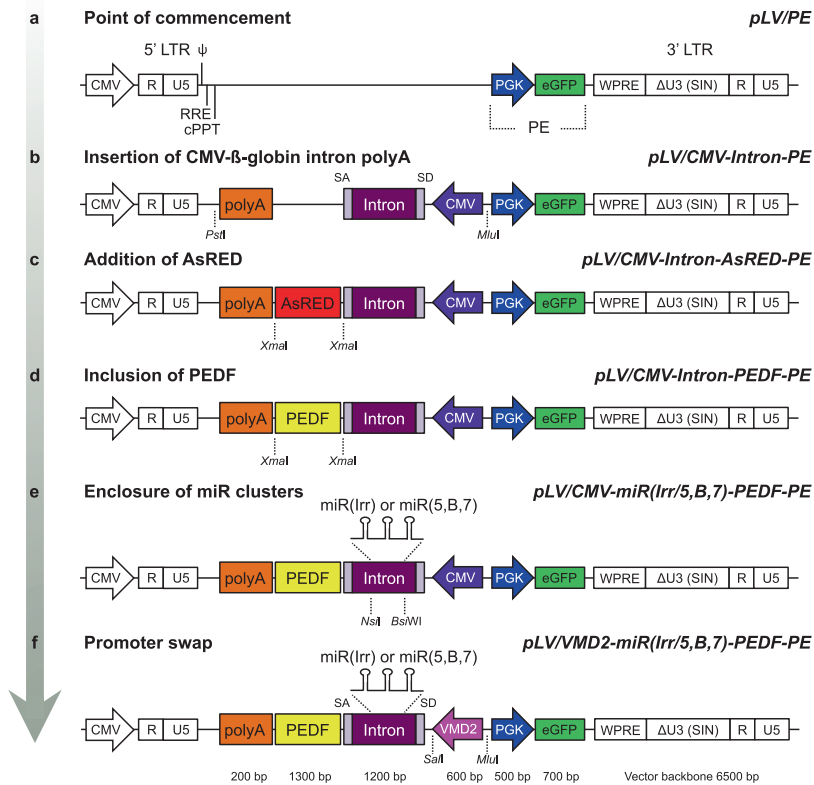6. Plasmid containing CMV-β-globin intron bovine growth hormone (BGH) poly A fragment [1].

Fig. 1 Development of multigenic LV vectors. (**a**–**f**) Schematics representing prominent progression stages during evolvement of the various multigenic LV expression cassettes. Relevant restriction sites used for cloning are shown at the bottom of each figure section. Names of the respective vectors are highlighted in italic on the right hand side. (**a**) Point of commencement: The pLV/PE vector. (**b**) Insertion of CMV promoter, ß-globin intron and polyA using *Pst*I and *Mlu*I. (**c**) Addition of the AsRED sequence using *Xma*I. (**d**) Inclusion of PEDF cDNA sequence using *Xma*I. (**e**) Enclosure of miR(Irr) or miR(5,B,7) clusters using *Nsi*I and *Bsi*WI. (**f**) Interchange of CMV by VMD2 promoter sequence using *Sal*I and *Mlu*I. Approximate sizes (in bp) of relevant elements and the vector backbone are shown. *bp* base pair, *CMV* cytomegalovirus, *cPPT* central polypurine tract, *eGFP* enhanced green fluorescent protein, *LTR* long terminal repeat, *LV* lentiviral, *-PE* PGK-eGFP, *PEDF* pigment epithelium-derived factor, *PGK* phosphoglycerate kinase 1 promoter, *polyA* bovine growth hormone polyadenylation signal, ψ packaging signal, *R* repeat region, *RRE* Rev.-responsive element, *SA* splice acceptor, *SD* splice donor, Δ*U3 (SIN)* self-inactivating deletion in the U3 region, *U5* unique 5′, *VMD2* vitelliform macular dystrophy 2, *WPRE* woodchuck hepatitis virus posttranscriptional regulatory element. Adapted from [1]

7. Plasmid pCM-miR(Irr) [9].

8. Plasmid PEDF cDNA: The plasmid Image clone ID 235156 with a verified PEDF sequence can be ordered at Source Bioscience, Nottingham, UK.

9. Plasmid containing VMD2 or promotor of choice: The promoter of choice can be ordered with for example *Mlu*I and *Sal*I flanking sequences from Genscript or other synthetic DNA supplier.
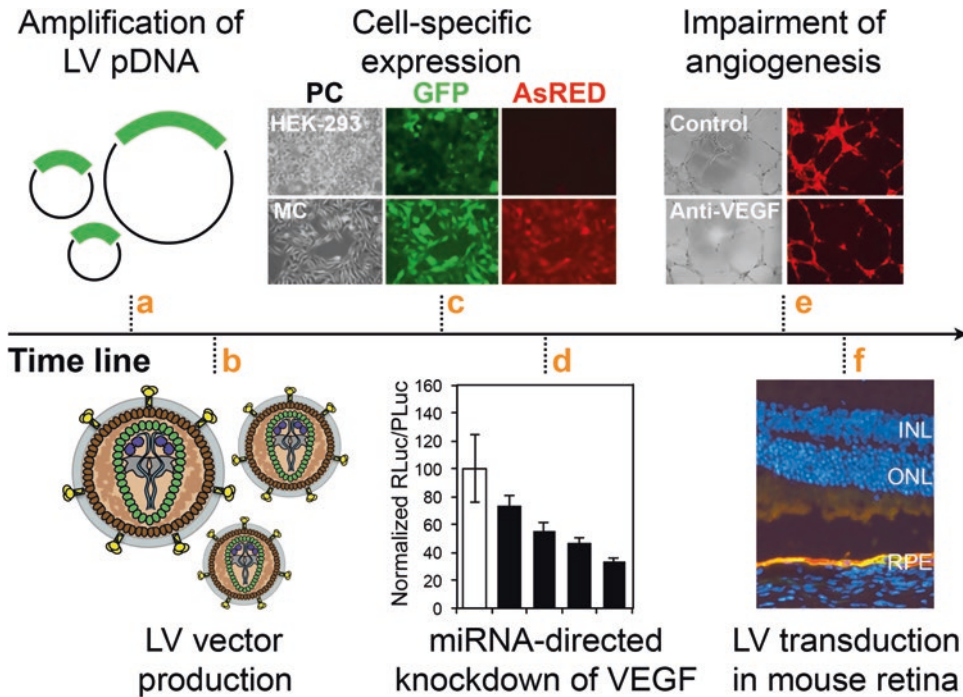
Fig. 2 Validation of multigenic LV vectors. (**a**–**f**) Time line illustrating important steps in the functional valida-
tion of viral vectors. A more comprehensive description of this process can be found in [1, 10, 12]. (**a**)
Amplification and purification of LV-based plasmid DNA carrying the multigenic cassette (Fig. 1). (**b**) Production
of LV vectors following transfection of HEK-293T packaging cells. (**c**) Evaluation of the cell-specific expression
capability of the LV vector as analyzed in HEK-293 and melanoma cells (MC). Cells are transduced with LV/
VMD2-intron-AsRED-PE. The GFP expression, driven by the CMV promoter, is omnipresent whereas the AsRED
reporter, exemplifying synthesis of gene products from the VMD2 driven multigenic cassette, display cell-
specific expression. (**d**) Assessment of miRNA-directed RLuc-VEGF knockdown after transduction of HEK-293
cells demonstrated by using the dual luciferase assay. (**e**) Inhibition of tube formation in transduced HUVECs.
(**f**) Histological investigation of LV transduction in the mouse retina 21 days after subretinal injection of LV/
VMD2-intron-AsRED-PE. The retina is stained with DAPI to show cell nuclei (blue). Expression of GFP (green)
and AsRED (red) reveal localization of the multigenic LV and expression from both cassettes in the RPE cell
layer. *HUVECs* human umbilical vein endothelial cells, *INL* inner nuclear layer, *Irr* irrelevant miR (nontargeting
negative control), *MC* melanoma cells, *ONL* outer nuclear layer, *pDNA* plasmid DNA, *PLuc P. photinus* luciferase,
PC phase contrast, *RLuc Renilla* luciferase, *RPE* retinal pigment epithelium

2.2 Gel Purification   1. 1× TAE: Mix 4.846 g Tris, 1.142 g acetic acid, and 2 mL
0.5 M EDTA pH 8.0 with 800 mL water. Adjust pH to 8.0
with hydrochloric acid and bring the final volume up to
1 L. Sterilize by autoclaving.

2. 7 cm × 10 cm UV-transparent agarose gel trays.

3. Preparative comb for agarose gel trays (containing two pre-
parative and two reference wells).

4. 15-well combs for agarose gel trays.

5. Preparative agarose gel (0.7%): Prepare a 0.7% agarose gel by
adding 0.35 g agarose to 50 mL 1% TAE and heat the solution

to boiling. Leave the solution to cool to approx. 60 °C and add 1.5 μL GelRed or other nucleic acid gel stain. Cast the gel within a 7 cm × 10 cm UV-transparent gel tray and immediately insert a preparative comb (containing two preparative and two reference wells) without introducing air bubbles.

6. Analytical agarose gel (1%): Prepare a 1% agarose gel by adding 0.5 g agarose to 50 mL 1% TAE and heat the solution to boiling. Leave the solution to cool to 60 °C and add 1.5 μL GelRed or other nucleic acid gel stain. Cast the gel within a 7 cm × 10 cm UV-transparent gel tray and immediately insert 1 or 2 (depending on the number of samples to be analyzed) 15-well combs without introducing air bubbles.

7. DNA ladder.

8. QIAquick or other gel DNA extraction kit.

9. Gel loading buffer.

10. NanoDrop spectrophotometer.

2.3 Ligation

1. T4 DNA ligase.

2. Compatible reaction buffer for the T4 DNA ligase.

2.4 Transformation

1. *Escherichia coli* XL2-Blue or other ultracompetent cells.

2. β-Mercaptoethanol.

3. LB medium: Mix 10 g tryptone, 5 g yeast extract, and 10 g NaCl with 800 mL water. Adjust pH to 7.4 and bring the final volume up to 1 L. Sterilize by autoclaving.

4. LB ampicillin medium: LB medium containing 0.1 mg/mL ampicillin.

5. SOC-medium: Mix 19 μL 1 M $MgSO_4$, 19 μL 1 M $MgCl_2$, and 38 μL 20% glucose with 1.8 mL LB medium in a sterile environment. Prepare fresh.

6. 9 cm diameter petridish.

7. LB agar ampicillin plates: Add 15 g agar and bring final volume up to 1 L utilizing LB medium. Autoclave to dissolve agar and sterilize. Let the LB agar solution cool to approx. 45 °C and add 0.1 mg/mL ampicillin. Swirl the flask gently to mix and avoid air bubbles. Pour 10 mL LB agar ampicillin solution into a petri dish and leave at room temperature (RT) to solidify.

2.5 PCR

1. Plasmid pAAV2-siRNA: The plasmid containing AsRED can be ordered at Applied Viromics, Fremont, CA, USA.

2. DNA PCR primers containing suitable restriction sites, e.g., *Xma*I sites at the 5′-end flanking the AsRED gene in plasmid pAAV2-siRNA.

3. Anti-mVEGF miRNAs: Anti-mVEGF miRNAs designated miR(5), miR(B) and miR(7) as partially overlapping

~60-nucleotide oligonucleotides containing suitable restriction sites, e.g., *Xho*I/*Hind*III, *Eco*RI/*Bam*HI, and *Xba*I/*Sac*II, respectively, at the 5′-end [10].

4. High fidelity DNA polymerase and compatible reaction buffer.

5. 10 mM dNTPs: stocks of 10 mM dGTP, dATP, dTTP, and dCTP.

6. PCR tubes.

7. MinElute or other PCR DNA fragment purification kit.

8. Illustra or other MicroSpin G-25 Columns.

3   Methods

Carry out all procedures at RT unless otherwise specified.

3.1   Insertion of CMV-β-Globin Intron BGH PolyA Cassette in pLV/PE (Fig. 1b)

3.1.1   Restriction Digest

1. Mix 10 μg of pLV/PE (Fig. 1a) with reaction buffer and 10 units (U) of *Mlu*I and *Pst*I restriction enzymes in a total volume of 100 μL and place at 37 °C for 1 h to open the vector creating cohesive ends.

2. Add 20 U of CIP to the linearized vector reaction mixture and leave for further 30 min at 37 °C (*see* **Note 1**).

3. In the same way, the CMV-β-globin intron BGH poly A fragment is obtained. Mix 5 μg of plasmid DNA harboring the CMV-intron-poly A with 5 U of *Mlu*I and *Pst*I in a total volume of 100 μL and place at 37 °C for 1 h to cut out the fragment creating compatible cohesive ends. Do not add CIP.

4. Add loading dye to the samples and mix.

3.1.2   Gel Purification

1. The linearized vector and the fragment are purified over a 0.7% preparative agarose gel. Place the gel in submerged horizontal electrophoresis cells using 1× TAE buffer.

2. Apply the restriction digest mixtures to separate wells and run the gel at low voltage (40–70 V) for 1–2 h to separate the DNA bands on the gel.

3. Utilize a UV transilluminator to verify separation.

4. Cut out the DNA bands corresponding to the linearized pLV/PE plasmid and the CMV-intron-poly A fragment.

5. Purify DNA from the agarose gel by applying the QIAquick or other gel extraction kit according to the protocol supplied.

6. Measure the DNA concentration of the two samples for example by applying about 2 μL of DNA solution on a NanoDrop spectrophotometer according to the user's manual.

3.1.3 Ligation

1. Make two ligation mixes: mix fragment and linearized vector in a 3:1 molar ratio.
2. Add 1 U T4 DNA ligase in a total volume of 20 μL in one tube.
3. For the other tube, make the same mix but leave out the fragment and replace with water (negative control, *see* **Note 1**).
4. Mix gently by pipetting and incubate at RT for 1 h.

3.1.4 Transformation

1. Thaw XL2-Blue or other ultracompetent cells on ice.
2. Aliquot 25 μL of cells into each of two tubes placed on ice.
3. Add 0.5 μL β-mercaptoethanol and mix by gently tapping the tubes.
4. Incubate the cells on ice for 10 min, swirling gently every 2 min.
5. Add 1.5 μL of each of the two ligation mixes to separate tubes.
6. Gently tap the tubes and incubate on ice for 30 min.
7. Give the cells a heat-shock by submersing the tubes in a 42 °C water bath for 30 s (*see* **Note 2**).
8. Incubate on ice for 2 min.
9. Add 225 μL of freshly made SOC-medium to each tube and incubate at 37 °C for 1 h with shaking at 225–250 rpm.
10. Plate 50 μL transformation mixture on separate LB agar ampicillin plates.
11. Incubate overnight at 37 °C.
12. Count the colonies on the two plates.

3.1.5 Verification of Insertion by Restriction Digest

1. Pick a number of colonies, e.g., 10, to be screened for insertion of the fragment (*see* **Note 3**).
2. Use a sterile inoculation needle (or tooth pick) to transfer cells from a single, isolated colony to a small tube containing 2–5 mL LB ampicillin medium.
3. Grow culture overnight (12–16 h).
4. Follow the protocol supplied in the QIAprep Spin or other Miniprep kit for purification of plasmid DNA from the cells.
5. For all ten colonies, mix 2 μL of purified plasmid with reaction buffer and 1 U *Mlu*I and *Pst*I restriction enzymes in separate tubes in a total volume of 10 μL.
6. Incubate for 1 h at 37 °C. Prepare a 1% analytical agarose gel and run cut and uncut plasmid DNA from each colony into separate wells for 45 min at 70 V.
7. Utilize a UV transilluminator to verify insertion of the CMV-intron-polyA fragment (positive clone), i.e., plasmid DNA digestion and separation of the vector backbone (approx.

7800 bp) from the *Mlu*I and *Pst*I inserted fragment (approx. 1400 bp). Sequencing further validates DNA purified from one positive clone, and pLV/CMV-intron-PE has been generated.

3.2 Subcloning AsRED in pLV/CMV-Intron-PE (Fig. 1c)

3.2.1 PCR Amplification and Purification of AsRED from Plasmid

1. Design primers for amplification of a red fluorescent protein, AsRED, from the pAAV2-siRNA vector (Applied Viromics, Fremont, CA, USA) plasmid (*see* **Note 4**). Include *Xma*I sites in the primers for subcloning.

2. Mix 20 ng pAAV2-siRNA template DNA, 0.5 µL of a high fidelity DNA polymerase, 0.25 µM of each primer, and 250 µM dNTPs in a sterile PCR tube and bring total volume to 50 µL total with DNA polymerase reaction buffer and water.

3. Mix gently by pipetting and briefly centrifuge the tube.

4. Perform PCR as described in Table 1.

5. Run 2 µL of the PCR reaction mixture on a 1% analytical agarose gel as described in Subheading 3.1.5.

6. Verify amplification of a fragment with a size of approx. 750 bp.

3.2.2 Subcloning of AsRED PCR Product in pLV/CMV-Intron-PE Vector

1. Purify the PCR reaction mixture over a gel as described in Subheading 3.1.2 to recover the AsRED fragment.

2. Generate *Xma*I cohesive ends on the AsRED fragment as well as on the plasmid pLV/CMV-intron-PE by restriction enzyme digestion as described in Subheading 3.1.1.

3. Purify the AsRED fragment using MinElute or other PCR purification kit and the linearized plasmid over a gel using the QIAquick or other gel extraction kit as described in Subheading 3.1.2.

4. Measure the DNA concentration of both fragment and linearized plasmid.

Table 1
Optimized PCR conditions based on target length, DNA polymerase (Herculase II Fusion DNA polymerase), type of template DNA, and primer sequences (*see* Note 5)

Number of cycles	Description	Temperature [°C]	Duration
1	Hot start	95	2 min
	Denaturation	95	20 s
30	Annealing	60	20 s
	Elongation	72	1 min
1	Final extension	72	30 min

5. Perform ligation as described in Subheading 3.1.3.

6. Perform transformation as described in Subheading 3.1.4.

7. Verification is basically performed as described in Subheading 3.1.5, but perform restriction analysis with *Xma*I generating two DNA fragments with a size of 750 and 9100 bp. Sequence the whole fragment between the two *Xma*I sites, and pLV/CMV-intron-AsRED-PE has been generated.

3.3 Subcloning of PEDF in pLV/CMV-Intron-AsRED-PE Vector (Fig. 1d)

1. Design primers including *Xma*I sites for subcloning of PEDF in the pLV/CMV-intron-AsRED-PE (*see* **Note 4**). The PEDF cDNA sequence can be ordered as a clone (Image ID 235156) with a verified sequence from Source Bioscience (Nottingham, UK).

2. Amplify and introduce new restriction sites by performing PCR using the PEDF cDNA as template and verify amplification by running an analytical gel with a small portion of the PCR reaction mixture as described in Subheadings 3.2.1 and 3.2.2.

3. Purify and cleave the PEDF PCR product and the pLV/CMV-intron-AsRED-PE vector with *Xma*I as described in Subheading 3.2, **step 3**.

4. Perform ligation and transformation as described in Subheadings 3.1.3 and 3.1.4, respectively.

5. Verification is basically performed as described in Subheading 3.1.5, but perform restriction analysis with *Xma*I generating two DNA fragments with a size of 1300 and 9100 bp. Sequence the whole fragment between the two *Xma*I sites, and pLV/CMV-intron-PEDF-PE has been generated.

3.4 Subcloning of miR Clusters into pLV/CMV-Intron-PEDF-PE (Fig. 1e)

3.4.1 Insertion of miR(5,B,7) Cluster in pCM-miR(Irr)

1. Design up to three miRNAs targeting your gene of interest. In this vector, three miRNAs are designed to perfectly match the mouse ortholog of the human VEGF$_{165}$. Design of the miR-NAs has been described in a previous study [10]. The three different anti-mVEGF miRNAs, designated miR(5), miR(B) and miR(7), are inserted in the optimized miR-106b cluster driven by a CMV promoter (encoded in a pCDNA3.1-based plasmid, designated pCM-miR(Irr) in this study [11]) by independent replacement of each of the three anti-HIV miRNAs harbored in the original pCM-miR(Irr) plasmid.

2. Generate complete inserts by PCR extension of partially annealed overlapping oligonucleotides. Include restriction sites in oligonucleotides for subsequent cloning. Perform an oligo-extension PCR by mixing 1 μL Taq DNA polymerase, 3 μM of each of oligonucleotide A and B (to generate miR(5)), and 250 μM dNTPs in a sterile PCR tube and bring total volume to 100 μL total with DNA polymerase reaction buffer and water.

Table 2
Optimized PCR conditions for oligo-extension PCR of miRNA sequences for cloning

Number of cycles	Description	Temperature [°C]	Duration
1	Hot start	95	5 min
	Denaturation	95	20 s
30	Annealing	50	20 s
	Elongation	72	20 s
1	Final extension	72	4 min

3. Mix gently by pipetting and briefly centrifuge the tube.

4. Perform PCR as described in Table 2.

5. Verify oligo-extension by gel analysis. Load 5 μL of each of the PCR-extension reactions on a 2% agarose gel together with 5 μL of one of the oligonucleotides. Notice a difference in size from approx. 60 bases in the oligonucleotide to 85 bp in the final extended double-stranded miRNA insert.

6. To insert miRNAs in pCM-miR(Irr) digest the three extended double-stranded miRNA inserts, miR(5), miR(B), and miR(7), with *Xho*I/*Hind*III, *Eco*RI/*Bam*HI, and *Xba*I/*Sac*II, respectively, as described in Subheading 3.1.1.

7. Purify the digested fragments over a column using the Illustra or other MicroSpin G-25 Columns that can be used for rapid purification of DNA greater than ten bases in length.

8. Generate the final plasmid encoding the three anti-mVEGF miRNAs, pCM-miR(5,B,7), by replacing each of the heterologous hairpin entities in pCM-miR(Irr), S1, S2, and S3, one after another with miR(5), miR(B), and miR(7), respectively. The order of replacement is unimportant.

9. pCM-miR(Irr) is digested with the compatible pair of the given restriction enzymes, and the linearized plasmid is purified over a gel as described in Subheading 3.1.2.

10. Ligation and transformation are performed as described in Subheadings 3.1.3 and 3.1.4, respectively.

11. Perform sequencing on positive clones to ensure proper insertion of the miRNA sequences in the final pCM-miR(5,B,7) plasmid.

3.4.2 Insertion of miR(5,B,7) and miR(Irr) Clusters in pLV/CMV-Intron-PEDF-PE

1. Digest pCM-miR(5,B,7) and pCM-miR(Irr) with *Nsi*I and *Bsi*WI and purify the two fragments over a gel as described in Subheadings 3.1.1 and 3.1.2, respectively.

2. Digest pLV/CMV-intron-PEDF-PE with *Nsi*I and *Bsi*WI as well to create compatible cohesive ends for insertion and purify

the linearized plasmid over a gel as described in Subheadings 3.1.1 and 3.1.2, respectively.

3. Perform ligation, transformation, and verify insertion, as described in Subheadings 3.1.3, 3.1.4, and 3.1.5, respectively.

4. To verify insertion, cut with *Nsi*I and *Bst*WI and identify fragments of approx. 700 and 9900 bp on a gel. pLV/CMV-miR(Irr)-PEDF-PE and pLV/CMV-miR(5,B,7)-PEDF-PE have now been generated.

3.5 Swapping the CMV for VMD2 Promoter to Generate pLV/VMD2-miR(5,B,7)-PEDF-PE and pLV/VMD2-miR(Irr)-PEDF-PE (Fig. 1f)

To ensure RPE specific expression from the transgene cassette encoding anti-mVEGF miRNAs and PEDF, the CMV promoter is swapped with the VMD2 promoter. The VMD2 or promotor of choice can be ordered with *Mlu*I and *Sal*I flanking sequences from Genscript or other synthetic DNA supplier for subcloning in the pLV/CMV-miR(5,B,7)-PEDF-PE and pLV/CMV-miR(Irr)-PEDF-PE vectors [1].

1. Cut the plasmid encoding the VMD2 promoter and the pLV/CMV-miR(5,B,7)-PEDF-PE and pLV/CMV-miR(Irr)-PEDF-PE vectors with *Mlu*I and *Sal*I and purify the fragment and two linearized vectors over a gel as described in Subheadings 3.1.1 and 3.1.2.

2. Perform ligation and transformation as described in Subheadings 3.1.3 and 3.1.4.

3. Verify insertion by *Mlu*I and *Sal*I double digestion as described in Subheading 3.1.5 and identify fragments of 600 bp and 10,500 bp on a gel. pLV/VMD2-miR(5,B,7)-PEDF-PE and pLV/VMD2-miR(Irr)-PEDF-PE have now been generated.

Following production of LV vector particles (*see* **Note 6** and Fig. 2a, b) functional analysis of distinctive elements of the multigenic design can be verified in different cell culture systems and in the mouse retina as shown in Fig. 2. In short, the different analyses reveal RPE-specific expression (*see* **Note 7** and Fig. 2c), miRNA-directed downregulation of VEGF (*see* **Note 8** and Fig. 2d), impairment of angiogenic pathways by codelivery of the gene encoding PEDF (*see* **Note 9** and Fig. 2e) and LV-mediated transduction in mouse retina (*see* **Note 10** and Fig. 2f). *See* also [1].

4 Notes

1. Noncompatible cohesive overhangs created by utilizing two different restriction enzymes and addition of CIP to the digested vector prevents religation of the linearized plasmid DNA in a subsequent ligation reaction. Ligation mix without fragment was used as negative control for the transformation.

2. Competent cells are very heat sensitive. Always transfer tubes on ice, and thaw the cells on ice. Furthermore, the duration of the heat pulse is critical, use a timer. Leave plates upside down

wrapped in Parafilm to avoid drying-out. For the experimental DNA, the number of colonies will vary according to the size and form of the transforming DNA, with larger and nonsupercoiled DNA producing fewer colonies. The negative control plate should give rise to very few colonies, preferable <10. Compare the number of colonies on the negative plate to the number on the positive plate. The number of colonies on the positive plate should be many times greater than the number on the negative control plate. If there are no colonies on the positive plate or the number of colonies is comparable to the number on the negative plate, redo the transformation. Include circular plasmid as a positive control for appropriate transformation conditions. The ligation mix can be stored at −20 °C. If retransformation utilizing the same ligation mix is unsuccessful, repeat the ligation and preferably redo restriction digest and purification of DNA fragment and vector.

3. Verification can easily be checked by PCR screening of colonies or by purifying DNA from several colonies followed by restriction enzyme analysis. Digest the DNA with the restriction enzymes used for insertion of the fragment. A successful cloning will regenerate the restriction sites. Alternatively, find a restriction enzyme with a unique restriction sequence inside the inserted fragment. One or two positive colonies should be sent of for sequencing if the inserted fragment was amplified by PCR.

4. The optimal length of a primer is 18–22 nt with a GC content of 40–60%. This should give an ideal melting temperature of the primer between 60 and 65 °C. The melting temperature of the primers should not differ by more than 2 °C, and the annealing temperature should be no more than 5 °C lower than the melting temperature. Avoid strong secondary structures and self-complementarity. If these guidelines are followed, the primers should anneal specifically and simultaneously and efficiently amplify the target product. If addition of new restriction sites is intended, design primers following the above guidelines targeting the 5′ and 3′ end of your target. Add the restriction site to the 5′ end of the primer and remember to add 2–4 additional bases to the 5′ end of the primer depending on the restriction enzyme, to ensure proper digestion of the fragment following PCR amplification.

5. Follow the guidelines supplied by the manufacturer of the DNA polymerase for optimal PCR conditions. The annealing temperature depends on primer design (*see* **Note 4**). The elongation time depends on both the polymerase and the target length.

6. LV vector particles are produced using a 3rd generation LV-packing system. The relevant packing plasmids (in each case three different) and multigenic LV plasmids (Fig. 1) are used

for transfection of HEK-293T cells (Fig. 2a) [1]. For cell studies crude LV preparations (preps) can be harvested and for subretinal injections, the LV preps can be concentrated by ultracentrifugation. The titers of the LV preps can be assessed by determining the HIV-1 p24 concentration by ELISA (*see* also Fig. 2b).

7. RPE-specific expression can be assessed by immunofluorescence analysis of eGFP and AsRED expression in different cell lines (e.g., HEK-293 and melanoma cells) 4 days after transduction with 100 ng p24 LV/VMD2-intron-AsRED-PE (Fig. 2c). This LV vector was generated by replacing the CMV promoter of LV/CMV-intron-AsRED-PE with VMD2.

8. miR-directed downregulation of VEGF can be assessed using a dual luciferase reporter construct [12]. Four-six days after transduction (alternatively, 48 h post transfection), cells are lysed and luciferase levels analyzed using the Dual-Luciferase Reporter Assay System (*see* Fig. 2d).

9. Impairments of angiogenic pathways can be analyzed in a tube formation assay based on human umbilical vein endothelial cells (HUVECs). Approx. 1×10^5 HUVECs are transduced with 100 ng p24 LV/CMV-miR(5,B,7)-AsRED and seeded on a Matrigel (Fig. 2e).

10. Histological analysis of LV transduction can be assessed in the mouse retina 21 days after subretinal injection [10] of 30 ng p24 LV/VMD2-intron-AsRED-PE (Fig. 2f).

Acknowledgment

References

1. Askou AL, Aagaard L, Kostic C et al (2015) Multigenic lentiviral vectors for combined and tissue-specific expression of miRNA- and protein-based antiangiogenic factors. Mol Ther Methods Clin Dev 2:14064

2. Askou AL (2014) Development of gene therapy for treatment of age-related macular degeneration. Acta Ophthalmol 92(Thesis 3):1–38

3. Corydon TJ (2015) Antiangiogenic eye gene therapy. Hum Gene Ther 26:525–537

4. Kliffen M, Sharma HS, Mooy CM et al (1997) Increased expression of angiogenic growth factors in age-related maculopathy. Br J Ophthalmol 81:154–162

5. Spilsbury K, Garrett KL, Shen WY et al (2000) Overexpression of vascular endothelial growth factor (VEGF) in the retinal pigment epithelium

leads to the development of choroidal neovascularization. Am J Pathol 157:135–144

6. Augustin AJ, Puls S, Offermann I (2007) Triple therapy for choroidal neovascularization due to age-related macular degeneration: verteporfin PDT, bevacizumab, and dexamethasone. Retina 27:133–140

7. Singerman L (2009) Combination therapy using the small interfering RNA bevasiranib. Retina 29:S49–S50

8. Tozer K, Roller AB, Chong LP et al (2013) Combination therapy for neovascular age-related macular degeneration refractory to anti-vascular endothelial growth factor agents. Ophthalmology 120:2029–2034

9. Jakobsen M, Stenderup K, Rosada C et al (2009) Amelioration of psoriasis by anti-TNF-alpha RNAi in the xenograft transplantation model. Mol Ther 17:1743–1753

10. Pihlmann M, Askou AL, Aagaard L et al (2012) Adeno-associated virus-delivered polycistronic microRNA-clusters for knockdown of vascular endothelial growth factor in vivo. J Gene Med 14:328–338

11. Aagaard LA, Zhang J, von Eije KJ et al (2008) Engineering and optimization of the miR-106b cluster for ectopic expression of multiplexed anti-HIV RNAs. Gene Ther 15:1536–1549

12. Askou AL, Pournaras JA, Pihlmann M et al (2012) Reduction of choroidal neovascularization in mice by adeno-associated virus-delivered anti-vascular endothelial growth factor short hairpin RNA. J Gene Med 14:632–641

Design and In Vitro Use of Antisense Oligonucleotides to Correct Pre-mRNA Splicing Defects in Inherited Retinal Dystrophies

Alejandro Garanto and Rob W.J. Collin

Abstract

Antisense oligonucleotides (AONs) are small molecules able to bind to the pre-mRNA and modulate splicing. The increasing amount of intronic mutations leading to pseudoexon insertion in genes underlying inherited retinal dystrophies (IRDs) has highlighted the potential of AONs as a therapeutic tool for these disorders. Here we describe how to design and test AON molecules in vitro in order to correct pre-mRNA splicing defects involved in IRDs.

Key words Antisense oligonucleotides, AON, Genetic therapy, Splicing modulation, Pre-mRNA, *CEP290*, Minigene, Inherited retinal dystrophies, Pseudoexon, Intronic mutation

1 Introduction

Inherited retinal dystrophies (IRDs) are a group of genetically and clinically heterogeneous disorders affecting ~1:3000 people worldwide [1–5]. In general terms, IRDs are characterized by the progressive degeneration of the photosensitive cells that ultimately can lead to complete blindness [1–5]. So far, more than 200 genes have been associated with IRDs in all Mendelian inheritance patterns (RetNet: https://sph.uth.edu/Retnet/). Although IRDs are still incurable diseases, gene augmentation therapies have shown promising results in patients suffering from Leber Congenital Amaurosis (*RPE65*) [6] or choroideremia (*CHM*) [7]. These results boosted the development of novel therapeutic interventions for IRDs. One of them is the antisense oligonucleotide (AON)-based splicing modulation approach. AONs are small molecules able to bind to the pre-mRNA and modulate its splicing [8]. The applicability of these AONs is very variable; they can be used to produce exon skipping, exon insertion, transcript degradation,

amongst others [8, 9]. The first clinical trial using AONs was conducted in Duchenne Muscular Dystrophy patients [10]. In particular, the delivery of AONs allowed the skipping of one or multiple exons of the *DMD* gene to reframe the mutated transcript and create a partially functional dystrophin protein [11, 12]. In IRDs, preclinical in vitro and in vivo studies for an intronic mutation in *CEP290* showed that AON delivery (a) led to pseudoexon exclusion both in vitro and in vivo, (b) increased the CEP290 protein levels, (c) corrected a cellular phenotype present in patient-derived fibroblast cells and (d) did not show any morphological alterations or retinal stress response in the mouse retina [13–15]. These data highlight the therapeutic potential of these molecules for IRDs, especially due to the continuous identification of novel intronic mutations that lead to pseudoexon inclusion, as shown in *USH2A* [16] or *OPA1* [17]. In addition, one of the first commercially available AON-based compounds, Vitravene™ or Fomivirsen, was used to treat an ocular disease named cytomegalovirus retinitis [18–21]. In this chapter, we describe how to design efficient AONs based on previous reports and our own experience, how to test them in vitro, and which cellular models are most appropriate for the development of an AON-based therapeutic approach.

2   Materials

2.1   Cellular Models and Culture Conditions

1. Eppstein-Barr virus-transformed lymphoblastoid cells (EBVs) derived from patients. Culture medium: RPMI medium.

2. Fibroblast cells derived from patients. Culture medium: DMEM 20% FCS medium.

3. HEK293T cells (ATCC® CRL-3216™). Culture medium: DMEM 10% FCS medium.

4. RPMI medium: RPMI medium supplemented with 15% fetal calf serum (FCS), 100 U/mL of penicillin, 100 μg/mL streptomycin, and 2% (v/v) 1 M HEPES.

5. DMEM 20% FCS medium: DMEM supplemented with 20% FCS, 100 U/mL of penicillin, 100 μg/mL streptomycin, and 1% (v/v) 100 mM sodium pyruvate.

6. DMEM 10% FCS medium: DMEM medium supplemented with 10% FCS, 100 U/mL of penicillin, 100 μg/mL streptomycin, and 1% (v/v) 100 mM sodium pyruvate.

7. T75 Flasks or similar to grow the cell lines.

8. Trypsin solution for cell dissociation.

9. 1× PBS.

2.2 Minigene Vector and Destination Vector Generation	1. Minigene vector.

2.2 Minigene Vector and Destination Vector Generation

1. Minigene vector.
2. Destination vector.
3. BP-Clonase cloning kit: BP-Clonase, buffer, proteinase K, etc. (i.e. Gateway®enzymes).
4. LR-Clonase cloning kit: LR-Clonase, buffer, proteinase K, etc. (i.e. Gateway® enzymes).
5. Genomic DNA.
6. Primers flanking the region of interest with *attB* sites (underlined). In this chapter we use *CEP290* as an example. Forward primer sequence:5′-ggggacaagtttgtacaaaaaagcaggcttcggccgctc tttctcaaaagtggc-3′ and reverse primer sequence : 5′ggggac-cactttgtacaagaaagctgggtgcttggtggggttaagtacagg-3′. Primers were located in intron 25 and intron 27 of *CEP290*, respectively.
7. High-fidelity *Taq* polymerase PCR kit: High fidelity *Taq* polymerase, dNTPs, buffer, etc.
8. Competent cells (preferably commercial ones).
9. LB medium: Autoclave 10 g NaCl, 10 g tryptone, and 5 g yeast extract in 1 L of deionized water.
10. LB plates: Autoclave 10 g NaCl, 10 g tryptone, 5 g yeast extract, and 15 g agar in 1 L of deionized water.
11. Selection antibiotics (usually Ampicillin and Kanamycin) at 50 mg/mL (this is the stock 1000× concentrated).
12. Mini/Midiprep kit.
13. Electrophoresis equipment and agarose gels.

2.3 RT-PCR

1. RNA isolation kit.
2. cDNA synthesis kit (*see* **Note 1**).
3. Primers located in the flanking exons of the (pseudo)exon to be skipped. In the example described in this chapter: Forward primer (exon 26) 5′ tgctaagtacagggacatcttgc 3′ and Reverse (exon 27) 5′ agactccacttgttctttaaggag 3′.
4. PCR kit: Polymerase, dNTPs, buffer, MgCl₂, water, and Q-solution or DMSO if applies.
5. Electrophoresis equipment and agarose gels.

2.4 Site-Directed Mutagenesis

1. Minigene vector prepared in Subheading 3.2, as an example in this chapter we will use the *CEP290* minigene.
2. Primers to introduce the desired mutation. In the example the c.2991+1655A>G mutation in the *CEP290* minigene:
   Forward primer 5′-cccagttgtaattgtga**g**tatctcatacctatcc-3′ and Reverse primer 5′-ggataggtatgagata**c**tcacaattacaactggg-3′. Mutation is in bold and underlined.

3. *Dpn*I restriction enzyme.

4. High-fidelity *Taq* polymerase PCR kit: High fidelity *Taq* polymerase, dNTPs, buffer, etc.

5. Competent cells (preferably commercial ones).

6. LB medium: Autoclave 10 g NaCl, 10 g tryptone and 5 g yeast extract in 1 L of deionized water.

7. LB plates: Autoclave 10 g NaCl, 10 g tryptone, 5 g yeast extract and 15 g agar in 1 L of deionized water.

8. Selection antibiotics (usually Ampicillin and Kanamycin) at 50 mg/mL (this is the stock 1000× concentrated).

9. Mini/Midiprep kit.

10. Electrophoresis equipment and agarose gels.

2.5 AON Resuspension and Transfection

1. AON stock: Resuspend the AONs at a final concentration of 0.1–1 mM in 1× PBS, that was previously autoclaved twice (*see* **Note 2**).

2. 6-well plates or 12-well plates (*see* **Note 3**).

3. Transfection reagent (i.e. FuGene® or Lipofectamine®).

4. Trypsin solution for cell dissociation.

3   Methods

3.1   Patient Cell Line Strategy

The easiest and most practical way to assess the redirection of pre-mRNA splicing is to directly use patient-derived cells. However, one disadvantage of working with IRD-causing genes is that their expression is often restricted to retinal cells.

3.1.1   Expression of the Gene of Interest

In order to assess whether the use of patient-derived cells is suitable for your studies, we suggest to follow the steps described below:

1. Purchase or isolate (using the RNA isolation kit) RNA from frequently used human-derived cell lines that can be easily obtained from the patients (i.e. fibroblast or EBV-transformed lymphoblast cells).

2. Use 1–2 μg of RNA to synthesize cDNA using the cDNA synthesis kit.

3. Amplify the region of interest by PCR using the PCR kit (*see* **Note 4**).

4. Visualize the PCR products by gel electrophoresis.

5. Confirm that the band corresponds with the region of interest by Sanger sequencing.

3.1.2 Assessing
the Effect of the Mutation
in Patient-Derived Cells

Once the expression of the gene of interest is confirmed in one of the cell lines, it is important to validate that the splicing defect is also present in this particular context, since the splicing pattern can vary between cell types:

1. Grow the cell lines from the patient(s) and control.
2. Isolate RNA using the RNA isolation kit.
3. Use 1–2 μg of RNA for cDNA synthesis using the cDNA synthesis kit.
4. Amplify the region of interest using primers on the flanking exons.
5. Visualize the PCR products by gel electrophoresis.
6. Confirm by Sanger sequencing the content of each band.
7. If the expected effect at pre-mRNA is recapitulated proceed to Subheading 3.3.

3.2 Minigene
Strategy

Unfortunately, in many cases, the gene is not expressed in either fibroblast or lymphoblast cells, or the pre-mRNA defect is retina-specific and it is not observed in these cell lines. Possible alternatives include the generation of minigenes or the reprogramming of fibroblast cells to induced pluripotent stem cells (iPSCs), which subsequently can be differentiated into photoreceptor-like cells (PLCs). However, for the initial screening of multiple AONs we suggest to only use PLCs when no other possibilities are available, since generating such cells is a time- and cost-consuming technique (*see* **Note 5**).

In order to circumvent the issues described, we propose to generate minigenes adapted to our necessities. One may think that a minigene is an artificial system that will not recapitulate what happens in the patient's own cellular context. However, in our experience >90% of the generated minigenes mimic the pre-mRNA defect found in IRD patients [13, 16, 22, 23]. Here, we will use a pCi-Neo-Rhodopsin Gateway®-adapted vector generated in house and described in previous publications [13, 16, 22–24]. Other alternatives are described elsewhere [25–27].

3.2.1 Minigene Design
and Cloning

1. Find the sequence of the gene in the databases (i.e. Genome Browser).
2. Select the region of interest. Since we are describing how to produce pseudoexon exclusion, the region of interest is the intron where the mutation is located. In order to increase the chances of success, it is important, if possible, to include at least the flanking exons (*see* **Note 6**).
3. Design primers with the corresponding sequences for cloning. In our case, we use a home-made vector that has been adapted to the Gateway®-system. For that we will include the *attB* sites

(*see* Subheading 2.2.6) for Gateway® BP cloning in our primers. As an alternative, restriction sites and regular ligation can be used. In this particular case, we have located the forward primer in intron 25 and the reverse primer in intron 27 of *CEP290* [13, 22].

4. Perform a PCR reaction using the high-fidelity *Taq* polymerase PCR kit. Make sure that the elongation time is at least 1 min per each kb of insert.

5. Visualize the PCR product by gel electrophoresis by loading 10% of the PCR reaction. If one single band is obtained at the corresponding size proceed with the purification using any kit for PCR-cleaning. If multiple bands are obtained but the one with the correct size is the most intense, load the entire volume, cut the band, and proceed to gel purification using the kit of your convenience.

6. Quantify the amount of DNA. For Gateway® cloning at least 150 ng are needed in a maximum volume of 5 μL (*see* **Note 7**).

7. Perform the BP reaction to generate the Entry clone as described by the manufacturer of the BP-Clonase cloning kit. Briefly, 1 μL of donor vector (150 ng), 2 μL buffer, 1–5 μL purified DNA (*see* **Note 7**), water up to 8 μL and 2 μL of BP-Clonase™. Incubate for at least 2 h (*see* **Note 8**) at 25 °C. Subsequently, add 2 μL of Proteinase K (supplied with the kit) and incubate for 10 min at 37 °C, in order to stop the reaction.

8. Transform 2–5 μL of the reaction using competent cells (*see* **Note 9**). Transformation will be performed as follows: incubate the reaction with the competent cells for 20 min on ice.

9. Perform the heat shock 30–90 s at 42 °C (*see* **Note 10**).

10. Cool down the cells for 2 min on ice.

11. Subsequently, add 250–1000 μL of SOC medium into the tubes and incubate for 1 h at 37 °C.

12. Plate everything (*see* **Note 11**) on the LB-agar plate containing the corresponding antibiotic (usually entry clones have the kanamycin-resistance cassette).

13. Incubate overnight at 37 °C.

14. Next morning, take out the plates from the incubator.

15. In the afternoon, pick 5–10 colonies per reaction (*see* **Note 12**), and grow overnight at 37 °C in 3–4 mL of LB medium supplemented with the corresponding antibiotic.

16. Perform the plasmid isolation using any miniprep kit available at your laboratory.

17. Verify by restriction analysis that the band pattern is the expected one. As a control, digest the donor vector as well.

18. Sequence the potential good clones in order to make sure that they do not contain new mutations introduced by the *Taq* during the PCR amplification. At this step, we suggest to perform the site-directed mutagenesis to introduce the desired mutations having the same genetic background (*see* Subheading 3.2.2).

19. Once the entry clone has been validated, proceed with the generation of the final destination vector, by performing an LR-reaction. For that use 150 ng of the vector (in this particular case pCI-Neo-Rho), 150 ng of the generated entry clone, 2 μL buffer, water up to 8 μL, and 2 μL of LR-Clonase™.

20. Incubate for at least 2 h at 25 °C (*see* **Note 8**) and proceed with the inactivation of the reaction, transformation, and clone validation as described before, but applying the right corresponding antibiotic.

3.2.2 Site-Directed Mutagenesis

1. Design primers to introduce the mutation. We suggest to design primers where both flanking regions of the mutation contain 15–20 nt. As an example, the primers to introduce the c.2991+1655A>G mutation in the *CEP290* minigene are provided (*see* Subheading 2.4).

2. Perform a 15-cycle PCR with a high fidelity *Taq* polymerase. For that PCR reaction, use 10–35 ng of vector and at least 125 ng of each oligonucleotide (keep primers in excess). Run the PCR program where the elongation step is (at least) 1 min per each kb of the complete plasmid for a total of 12–18 cycles (*see* **Note 13**).

3. Add *Dpn*I directly to the PCR reaction (1 μL per each 10 μL of PCR reaction) in order to digest the original template, and digest at 37 °C for at least 3 h (*see* **Note 14**).

4. Transform 5–10 μL following the protocol described in Subheading 3.2.1.

5. Next day, pick 5–10 colonies and grow them in 3–4 mL of LB medium supplemented with the corresponding antibiotic.

6. Isolate the plasmid by using a miniprep kit.

7. Verify the presence of the mutation by Sanger sequencing (*see* **Note 15**).

3.2.3 Minigene Validation

1. Seed 200,000 HEK293T cells in DMEM 10% FCS medium in each well of a 12-well plate. Seed as many wells as conditions the experiment contains. Usually, at least three wells are needed for the minigene validation: nontransfected cells, cells transfected with the wild-type construct, and cells transfected with the mutant construct.

2. The day after, transfect the cells with 0.6–1 μg of plasmid DNA using a liposome-based transfection reagent (of your convenience) (*see* **Note 16**).

3. Forty-eight hours later, harvest the cells and centrifuge them for 5 min at $100 \times g$.

4. Discard the supernatant, rinse in 1× PBS and centrifuge for 5 min at $100 \times g$.

5. Repeat **step 4** once more.

6. Discard the PBS and (a) store pellets at −80 °C or (b) proceed with RNA isolation using the RNA isolation kit and continue with the steps described below.

7. Use 1 μg of RNA for cDNA synthesis using the cDNA synthesis kit.

8. Prepare a PCR reaction with the PCR kit using the primers located in the flanking exons.

9. By agarose electrophoresis validate the results.

10. Sanger sequence the bands in order to confirm the results.

3.3 Design of the AONs

The design of the AONs is done following previous studies on Duchenne Muscular Dystrophy [28, 29]. In these studies, the authors compared the properties of multiple AONs designed for the *DMD* gene and correlated their properties to their efficacy. In here, we briefly describe this procedure, with additions from our own experience.

1. Select the region of interest and include the ~50 bp flanking the target region.

2. Use the M-fold software to predict the secondary structure of the region (http://unafold.rna.albany.edu/?q=mfold/RNA-Folding-Form).

3. Determine the open and closed structures using the ss-count provided by the M-fold software. Open structures are determined by high ss-count numbers, while closed regions by lower numbers. For instance, a value equal to 0 means that in all the structures this nucleotide is bound to another one, while a high number indicated that this nucleotide is mainly single stranded and not bound to any other nucleotide.

4. Determine regions of 30–40 nt that are partially closed and partially open.

5. Analyze the ESEs of the entire region using the Human Splicing Finder (http://www.umd.be/HSF3/HSF.html) or the ESE finder (http://rulai.cshl.edu/cgi-bin/tools/ESE3/esefinder.cgi?process=home) (*see* **Note 17**).

6. Combine all the information collected from **step 1** and try to find ESE motifs, if possible SC35 with high score (*see* **Note 17**), within the partially closed and partially open regions.

7. Design the AON taking into account the following details:

   (a) Length: 16–25 bp

   (b) 40–60% GC content (http://www.endmemo.com/bio/gc.php)

   (c) Tm > 48 °C (http://www.basic.northwestern.edu/biotools/oligocalc.html)

   (d) Avoid stretches of three or more G's or C's (*see* **Note 18**)

8. Convert the AON in the reverse complement and replace all T's by U's.

9. Determine the secondary structure and free energy of the AONs, by calculating the free energy of the AON alone (and as an AON-AON complex. The ideal free energy is >−4 and >−15, respectively (http://rna.urmc.rochester.edu/RNAstructureWeb/, use the AllSub for the AON alone and the bifold for the AON-AON complex).

10. Calculate the secondary structure of the region of interest using the same software. Of note, only 200 nt can be assessed. Therefore, if the region is longer use the region where the AON is located in the middle.

11. Perform a bifold analysis of the region of interest (**step 10**) and AON.
    Using the free energies obtained in **steps 10** and **11**, calculate the binding energy (optimal 21–28) applying the following formula:
    Binding energy = (Energy Region) − (Energy Region-AON)

12. Finally, assess the uniqueness of the AON by looking at possible targets by performing a BLAT or BLAST.

13. Order the best two or three AONs per each target (*see* **Note 19**).

3.4 Delivery of the AONs into EBV-Transformed Lymphoblast Cells

AONs are small molecules that are able to penetrate easily into the cell. We have observed that 2′*O*-methyl (2′OMe) AONs with a phosphorothioate backbone (coined modAONs in this chapter) are able to redirect splicing better than unmodified AONs in EBV-transformed lymphoblasts, fibroblasts and HEK293T cells (Fig. 1a). In addition, modAONs are able to penetrate into fibroblasts even in the absence of transfection reagent (liposomes). Unmodified AONs however were able to redirect splicing in fibroblast and HEK293T cells, rendering these molecules very useful for screenings since they are cheaper than modAONs. Few aber-

rant transcripts are detected after delivery of the AONs, but liposomes enhanced the uptake as shown in Fig. 1b. In the following steps we describe the delivery of AONs using liposome-based transfection reagent into three different cell lines. A schematic representation of the steps is shown in Fig. 2.

1. Culture in suspension 1.5–1.9 million cells in 2 mL RPMI medium in each well of a 6-well plate.

2. Next day, transfect the AON(s) at the desired concentration (*see* **Note 20**). For that use a liposome-based transfection reagent and follow the manufacturer's instructions (*see* **Note 21**).

3. Harvest the cells 48 h post-transfection by collecting them in a tube and centrifuging for 5 min at $100 \times g$.

4. Remove the PBS and rinse the cells once again in 1× PBS, followed by centrifuging the cells for 5 min at $100 \times g$.

5. Discard the PBS and freeze the pellets at −80 °C or proceed with the RNA isolation (Subheading 3.7).
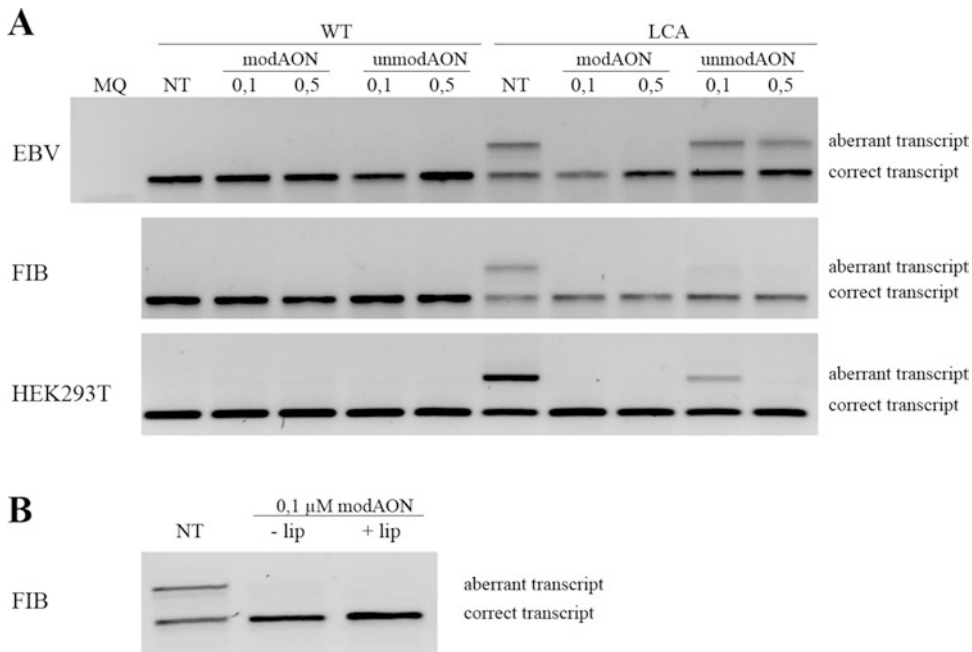
Fig. 1 AON-based splice modulation for *CEP290*. (**a**) AON efficiency in fibroblast, lymphoblast and HEK293T cells. Two concentrations of modified AONs (2' *O*-methyl phosphorothioate) and unmodified AON (coined mod-AON and unmodAON, respectively), were delivered to control and LCA patient lymphoblast-EBV (EBV) and fibroblast (FIB) cells. Same concentrations were delivered to HEK293T cells previously transfected with 750 ng of WT and LCA minigene. The presence of the modAON reduced completely the presence of the aberrant transcript, while the unmodAON was able to redirect splicing in fibroblast and HEK293T cells, but not in lymphoblast-EBVs. (**b**) Delivery of 0.1 μM of modAON to LCA fibroblast with and without liposome-based transfection reagent (FuGene®). ModAONs were already able to penetrate into the cell and correct splicing in the absence of transfection reagent. The use of liposomes enhanced the effect of the modAONs
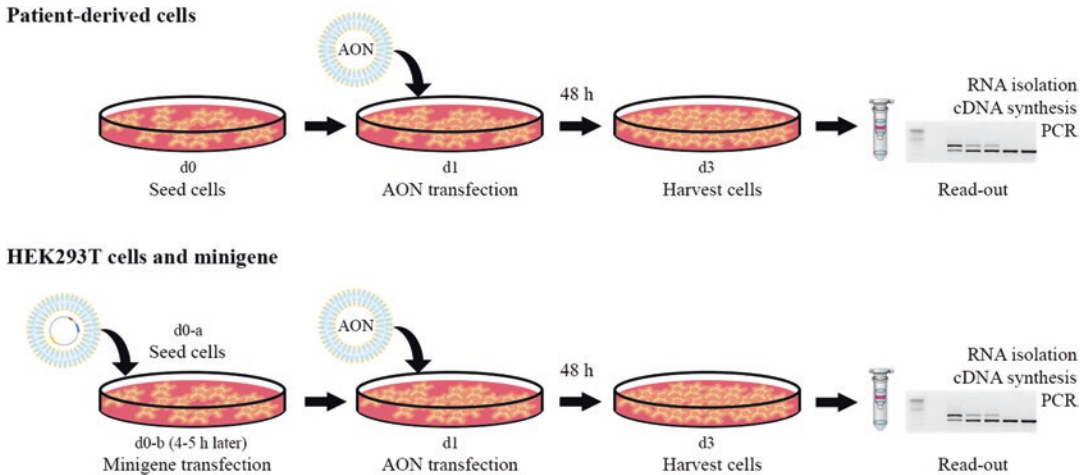
Fig. 2 Schematic representation of the experimental design in patient-derived cells and HEK293T cells. The amount of cells needed is seeded in the corresponding plate with the appropriate medium at day 0 (d0). Next day (day1: d1), AON are transfected into these cells. Forty-eight hours later (day3: d3) cells are harvested and used for different purposes. For HEK293T cells, ~4 h after seeding, when cells start to get attached, minigenes are transfected, 24 h later (d1), AONs are delivered into the cells

3.5 Delivery of the AONs into Fibroblast Cells

1. Seed 100,000 cells/well or 200,000 cells/well in DMEM 20% FCS medium in a 12-well or 6-well plate, respectively.

2. Next day, transfect the AON(s) at the desired concentration (*see* **Note 20**). For that use a liposome-based transfection reagent and follow the manufacturer's instructions (*see* **Note 21**).

3. Harvest the cells 48 h post-transfection by rinsing the cells in 1× PBS and detaching the cells using trypsin. Subsequently, collect the cells in a tube and centrifuge it for 5 min at $100 \times g$.

4. Remove the PBS and rinse the cells once again in 1× PBS, followed by centrifuging the cells for 5 min at $100 \times g$.

5. Discard the PBS and freeze the pellets at −80 °C or proceed with the RNA isolation (Subheading 3.7).

3.6 Delivery of the Minigenes and AONs into HEK293T Cells

1. Seed 200,000 cells/well or 400,000 cells/well in DMEM 10% FCS medium in a 12-well or 6-well plate, respectively.

2. Four hours later, once the cells start to be attached. Transfect 750 ng or 1.5 µg of plasmid in a 12-well or 6-well plate, respectively. Perform the transfection following the information provided with your transfection reagent (*see* **Note 22**).

3. Twenty-four hours later, transfect the AON(s) at the desired concentration as described previously (*see* **Note 20**).

4. Harvest the cells 48 h post-transfection by rinsing the cells in 1× PBS and detaching the cells using trypsin. Subsequently, collect the cells in a tube and centrifuge it for 5 min at $100 \times g$.

5. Remove the PBS and rinse the cells once again in PBS 1×, followed by centrifuging the cells for 5 min at $100 \times g$.

6. Discard the PBS and freeze the pellets at −80 °C or proceed with the RNA isolation (Subheading 3.7).

3.7 AON Efficacy at RNA Level	AON molecules are modulators of pre-mRNA splicing. Thus, a quick and reliable method to evaluate the efficacy of the AONs is to perform an RT-PCR.

1. Design and test forward and reverse oligonucleotides in the flanking exons of the region of interest, when working with patient-derived cells or minigenes containing the flanking exons. In case of working with a minigene construct without flanking exons, design primers in the flanking regions used as artificial exons in your construct.

2. Use the pellets collected in Subheading 3.4 or 3.5 or 3.6.

3. Perform RNA isolation using a kit of your convenience (*see* **Note 23**).

4. Measure the RNA by using nanodrop or Qubit.

5. Use 1 μg of RNA for cDNA synthesis using a cDNA synthesis kit (*see* **Note 3**).

6. Dilute the cDNA to a final concentration of 25 ng/μL.

7. Use 50 ng (for high expressed genes or transfected cells) or 100 ng (low expressed genes) of cDNA for the PCR reaction in a final volume of 25 μL (*see* **Note 4**).

8. Use standard conditions, previously set up in **step 1**.

9. Resolve the PCR products by gel electrophoresis. Load 10, 15, or 25 μL of PCR product for transfected cells, endogenously expressed genes at high-to-medium levels, and low expressed genes, respectively. Mix the PCR product with loading buffer.

10. Assess the content of the bands by Sanger sequencing. In this way the AON efficacy is determined. Using patient-derived cells will allow the measurement of other parameters (*see* **Note 24**). Once multiple AON molecules have been found to be effective, the next step consists in studying which one is the most effective (*see* **Note 25**).

4   Notes

1. For (very) low expressed genes, we strongly suggest to use very sensitive cDNA synthesis kits such as SuperScript® VILO™.

2. The stock solution should be within this range in order to allow accurate pipetting. Usually, the starting dilutions range between 0.1 and 1 μM. Having the stock at 0.1 mM allows to easily pipette the required amount without preparing extra dilutions (i.e. 1 μL AON for 1 mL of medium (0.1 μM) or 10 μL AON for 1 mL of medium (1 μM)).

3. The decision on which kind of plate is needed is based on how much RNA needs to be obtained. For instance, transfected HEK293T cells in a 12 well plate will on average yield to 5–7 μg of RNA in 50 μL; however, the RNA obtained from fibroblast cells cultured in the same way will be in the best scenario 2.5–3.5 μg of total RNA, while in a 6-well plate the amount increases to 5–6 μg of RNA. Lymphoblasts will yield large quantities of RNA; however we prefer to culture them in 6-well plates (the amount of RNA will be 400–500 ng/μL in 50 μL). Another important point is how robust the gene of interest is expressed, for a highly expressed gene no large amounts of RNA are needed for the cDNA synthesis.

4. As mentioned in **Notes 2** and **3**, some genes might be (very) low expressed. Normally, with 20–50 ng of cDNA and 35 cycles is more than enough to detect the expression of the gene. For poorly expressed genes, we suggest to increase the template and use 50–100 ng of cDNA per reaction. If the detection is still low, increase the number of cycles to 40. Of note, this last step might also lead to the increase of nonspecific bands. Other possibilities such as nested PCRs might be useful; however, in our experience one single PCR step delivers more reliable and less variable results.

5. Initially, a group of AONs is screened and it might happen that none of them is able to redirect splicing. In addition, generating iPSCs and differentiating them into photoreceptor cells is a very expensive procedure. On top of that, cells need to be maintained for a large period of time, refreshing the medium every other day, thus needing large quantities of AON. Therefore, we strongly suggest finding other alternatives to perform the AON screening.

6. Size can be a limitation in some cases, however, having the complete intron will increase the chances of positive results and have reliable data. Cloning 7–8 kb of DNA is moderately easy and feasible.

7. In case of larger inserts, it is recommended to increase the amount of DNA to increment the chances of obtaining the correct entry clone. However, the maximum volume of insert still remains equal (5 μL), therefore concentrate your DNA using speedvac or other techniques.

8. For larger inserts leave the reaction for at least 12 h.

9. Home-made competent cells with high transformation efficiencies are useful and cheaper. If you doubt how good the competent cells are, there are multiple providers offering commercial competent cells. For larger fragments, commercial competent cells are highly recommended.

10. Regularly, heat shock step is performed for 60 s, however, when the size of the plasmid (including the insert) turns to be more than 7–8 kb, heat shock should be performed for 90 s to increase the chances of success. Another possibility for large plasmids is electroporation.

11. If 1 mL of SOC medium is used, centrifuge the cells for 1 min at $4000 \times g$; discard the supernatant; resuspend the bacteria in 250 μL of SOC and plate everything onto the corresponding LB plate.

12. The BP reaction is less efficient than the LR. Therefore, more colonies need to be picked at the screening step.

13. Our suggested protocol for site-directed mutagenesis is for 15 cycles, and it can be increased to 18 when no colonies grow on the plate. Some protocols indicate to perform a 20 or even 30 cycles PCR reaction, however this will increase the insertion of undesired mutations.

14. Although 1-h digestion with *Dpn*I should be enough to digest the methylated vector used as a template for the PCR reaction, usually after transformation many colonies contain the original plasmid. We suggest to leave the digestion for at least 3 h to reduce the amount of false positives.

15. In some cases the mutation that is introduced will either create or destroy a restriction site. This can be very useful to validate the clones, allowing to send only for sequencing the real positive ones.

16. We recommend to use 0.6–0.75 μg of plasmid in a 12 well plate to reduce possible artifacts due to overexpression. This is applicable to both WT and MUT minigene constructs.

17. These software tools will allow the detection of multiple types of motifs. In our experience, targeting SC35 is very successful (in our studies >85% success). For that, we design several AONs targeting the two motifs with the highest SC35 scores and that are in the pseudoexon sequence. As indicated in

Subheading 3.3, AON molecules targeting regions outside the (pseudo)exon are not very efficient.

18. Avoid these regions if the sequence allows to move the AON upstream or downstream. Since this is not always possible, if the SC35 motif is the one with the highest score, it is worth to give it a try.

19. All the steps described above are based on previous studies and our own experience. As it was observed also for the *DMD* gene [29], AONs located on the (pseudo)exonic regions were more effective than those in the intronic regions when assessed in vitro. Nevertheless, the steps aforementioned are a tool to try to find the best AON sequence and increase the chances of success. However this is just an in silico prediction and everything needs to be validated in the complete context of a cellular or animal model. In our experience, AONs that did not match all the criteria were able to correct the aberrant splicing. For instance, the most effective AON (5′-AACUGGGGCCAGGUGCG-3′) we found so far to correct the pre-mRNA defect caused by the c.2991+1655A>G mutation in *CEP290* contains a stretch of four G's and has a 70.5% GC content [13, 14]. This AON sequence was used to perform the experiments summarized in Fig. 1.

20. The concentrations depend on the AON itself, the type of cell and the chemistry. We have observed that 0.1 μM for the pseudoexon introduced by the intronic mutation in *CEP290* is enough to redirect splicing in all cell lines. However, using lymphoblast cells carrying an intronic mutation in *CHM*, 1 μM was needed to redirect splicing. We recommend to test two different concentrations (i.e. 0.1 and 1 μM) to validate the AON efficacy. If 0.1 μM already shows rescue, next step will consist in delivering lower concentrations. For large screenings, even though modAON are more stable and efficient, they are also more expensive; hence, unmodified AONs can be very useful. These molecules are cheaper and can redirect splicing in fibroblast or HEK293T cells at almost the same concentration of the one used for modAONs. However, they are not efficient for lymphoblast-EBV cells (Fig. 1a).

21. ModAONs are able to penetrate into the cell in the absence of transfection reagent. However, liposome-based reagents enhance the uptake of these molecules by the cells (Fig. 1b).

22. The simultaneous delivery of the minigene and the AON sometimes yields very variable results, mainly caused by fluctuating levels of the minigenes. These results indicate that AONs somehow interfere with either the transfection of the plasmid or its expression. By delivering separately, the levels of minigene remain equal between the cells nontransfected and transfected with the AON.

23. When performing RNA isolation, several kits have a 15-min step with DNase I. In order to avoid false positive results in your PCR results (i.e. intron inclusion), we suggest to perform a 30-min digestion with DNase I.

24. Using patient-derived cells will allow the measurement of other parameters. For instance, if the gene of interest is highly expressed and a good antibody is available, one possibility is to assess whether the protein levels increase upon transfection. In our published work on the use of AONs for the most recurrent intronic mutation in *CEP290*, we and others found a cellular defect at cilium level that allowed us to also have another readout [13, 15, 30] besides the splicing rescue.

25. Once multiple AON molecules have been found to be effective, the next step consists in studying which one is the most effective. For that, a dose-response in vitro can be performed and use parameters at RNA and/or protein level, and (if possible) using a cellular phenotype as readouts. In addition, it would be also interesting to assess possible off-target effects. However, the expression pattern of a lymphoblast or a fibroblast cell, extremely differs from the one of a photoreceptor cell. Nowadays, the most similar cellular model that we can generate in a lab is the iPSC-derived photoreceptor-like cell [30, 31]. Many research groups have shown that it is possible to create photoreceptor cells in a dish and this technique is being expanded for the study of molecular mechanisms of IRDs and therapeutic assessment of novel approaches. Therefore, it is so far the best model to assess the genetic safety of the AON-based therapeutic intervention by transcriptome analysis.

Having a humanized animal model, carrying the same mutation and preferably with a phenotype, could be an excellent model to assess the rescue of the phenotype in vivo. Previous studies delivering AONs to the mouse retina have shown that it is safe and the potential of AONs to correct splice defects was detectable up to 4 months after a single administration [13, 32, 33]. Nevertheless, when generating an animal model to study splicing defects it is important to take into account that the splice site recognition may differ between species as has been previously shown [22, 34]. Therefore, further in vitro analyses are highly recommended prior to the generation of a mutant animal model.

Acknowledgments

References

1. de Castro-Miro M, Pomares E, Lores-Motta L et al (2014) Combined genetic and high-throughput strategies for molecular diagnosis of inherited retinal dystrophies. PLoS One 9:e88410. https://doi.org/10.1371/journal.pone.0088410

2. Hamel C (2006) Retinitis pigmentosa. Orphanet J Rare Dis 1:40. https://doi.org/10.1186/1750-1172-1-40

3. Hamel CP (2007) Cone rod dystrophies. Orphanet J Rare Dis 2:7. https://doi.org/10.1186/1750-1172-2-7

4. Hartong DT, Berson EL, Dryja TP (2006) Retinitis pigmentosa. Lancet 368:1795–1809. https://doi.org/10.1016/S0140-6736(06)69740-7

5. Sahel JA, Marazova K, Audo I (2014) Clinical characteristics and current therapies for inherited retinal degenerations. Cold Spring Harb Perspect Med 5:a017111. https://doi.org/10.1101/cshperspect.a017111

6. Jacobson SG, Acland GM, Aguirre GD et al (2006) Safety of recombinant adeno-associated virus type 2-RPE65 vector delivered by ocular subretinal injection. Mol Ther 13:1074–1084. https://doi.org/10.1016/j.ymthe.2006.03.005

7. MacLaren RE, Groppe M, Barnard AR et al (2014) Retinal gene therapy in patients with choroideremia: initial findings from a phase 1/2 clinical trial. Lancet 383:1129–1137. https://doi.org/10.1016/S0140-6736(13)62117-0

8. Hammond SM, Wood MJ (2011) Genetic therapies for RNA mis-splicing diseases. Trends Genet 27:196–205. https://doi.org/10.1016/j.tig.2011.02.004

9. Arechavala-Gomeza V, Khoo B, Aartsma-Rus A (2014) Splicing modulation therapy in the treatment of genetic diseases. Appl Clin Genet 7:245–252. https://doi.org/10.2147/TACG.S71506

10. Koo T, Wood MJ (2013) Clinical trials using antisense oligonucleotides in duchenne muscular dystrophy. Hum Mol Genet 24:479–488. https://doi.org/10.1089/hum.2012.234

11. Aartsma-Rus A (2010) Antisense-mediated modulation of splicing: therapeutic implications for Duchenne muscular dystrophy. RNA Biol 7:453–461

12. Aartsma-Rus A, Bremmer-Bout M, Janson AA et al (2002) Targeted exon skipping as a potential gene correction therapy for Duchenne muscular dystrophy. Neuromuscul Disord 12(Suppl 1):S71–S77

13. Garanto A, Chung DC, Duijkers L et al (2016) In vitro and in vivo rescue of aberrant splicing in CEP290-associated LCA by antisense oligonucleotide delivery. Hum Mol Genet 25:2552–2563. https://doi.org/10.1093/hmg/ddw118

14. Collin RW, den Hollander AI, van der Velde-Visser SD et al (2012) Antisense oligonucleotide (AON)-based therapy for Leber congenital amaurosis caused by a frequent mutation in

CEP290. Mol Ther Nucleic Acids 1:e14. https://doi.org/10.1038/mtna.2012.3

15. Gerard X, Perrault I, Hanein S et al (2012) AON-mediated exon skipping restores ciliation in fibroblasts harboring the common Leber congenital amaurosis CEP290 mutation. Mol Ther Nucleic Acids 1:e29. https://doi.org/10.1038/mtna.2012.21

16. Slijkerman RW, Vache C, Dona M et al (2016) Antisense oligonucleotide-based splice correction for USH2A-associated retinal degeneration caused by a frequent deep-intronic mutation. Mol Ther Nucleic Acids 5:e381. https://doi.org/10.1038/mtna.2016.89

17. Bonifert T, Gonzalez Menendez I, Battke F et al (2016) Antisense oligonucleotide mediated splice correction of a deep intronic mutation in OPA1. Mol Ther Nucleic Acids 5:e390. https://doi.org/10.1038/mtna.2016.93

18. Roehr B (1998) Fomivirsen approved for CMV retinitis. J Int Assoc Phys AIDS Care 4:14–16

19. Vitravene Study Group (2002) Safety of intravitreous fomivirsen for treatment of cytomegalovirus retinitis in patients with AIDS. Am J Ophthalmol 133:484–498

20. Vitravene Study Group (2002) Randomized dose-comparison studies of intravitreous fomivirsen for treatment of cytomegalovirus retinitis that has reactivated or is persistently active despite other therapies in patients with AIDS. Am J Ophthalmol 133:475–483

21. Vitravene Study Group (2002) A randomized controlled clinical trial of intravitreous fomivirsen for treatment of newly diagnosed peripheral cytomegalovirus retinitis in patients with AIDS. Am J Ophthalmol 133:467–474

22. Garanto A, Duijkers L, Collin RW (2015) Species-dependent splice recognition of a cryptic exon resulting from a recurrent intronic CEP290 mutation that causes congenital blindness. Int J Mol Sci 16:5285–5298. https://doi.org/10.3390/ijms16035285

23. Sangermano R, Bax NM, Bauwens M (2016) Photoreceptor progenitor mRNA analysis reveals exon skipping resulting from the ABCA4 c.5461-10T-->C mutation in Stargardt disease. Ophthalmology 123(6):1375–1385. https://doi.org/10.1016/j.ophtha.2016.01.053

24. Shafique S, Siddiqi S, Schraders M et al (2014) Genetic spectrum of autosomal recessive non-syndromic hearing loss in Pakistani families. PLoS One 9:e100146. https://doi.org/10.1371/journal.pone.0100146

25. Desviat LR, Perez B, Ugarte M (2012) Minigenes to confirm exon skipping mutations. Methods Mol Biol 867:37–47. https://doi.org/10.1007/978-1-61779-767-5_3

26. Morse R, Todd AG, Young PJ (2012) Using mini-genes to identify factors that modulate alternative splicing. Methods Mol Biol 867:349–362. https://doi.org/10.1007/978-1-61779-767-5_22

27. Pomares E, Riera M, Castro-Navarro J et al (2009) Identification of an intronic single-point mutation in RP2 as the cause of semi-dominant X-linked retinitis pigmentosa. Invest Ophthalmol Vis Sci 50:5107–5114. https://doi.org/10.1167/iovs.08-3208

28. Aartsma-Rus A (2012) Overview on AON design. Methods Mol Biol 867:117–129. https://doi.org/10.1007/978-1-61779-767-5_8

29. Aartsma-Rus A, Houlleberghs H, van Deutekom JC et al (2010) Exonic sequences provide better targets for antisense oligonucleotides than splice site sequences in the modulation of Duchenne muscular dystrophy splicing. Oligonucleotides 20(2):69–77. https://doi.org/10.1089/oli.2009.0215

30. Parfitt DA, Lane A, Ramsden CM et al (2016) Identification and correction of mechanisms underlying inherited blindness in human iPSC-derived optic cups. Cell Stem Cell 18:769–781. https://doi.org/10.1016/j.stem.2016.03.021

31. Tucker BA, Mullins RF, Streb LM et al (2013) Patient-specific iPSC-derived photoreceptor precursor cells as a means to investigate retinitis pigmentosa. eLife 2:e00824. https://doi.org/10.7554/eLife.00824

32. Gerard X, Perrault I, Munnich A et al (2015) Intravitreal injection of splice-switching oligonucleotides to manipulate splicing in retinal cells. Mol Ther Nucleic Acids 4:e250. https://doi.org/10.1038/mtna.2015.24

33. Murray SF, Jazayeri A, Matthes MT et al (2015) Allele-specific inhibition of rhodopsin with an antisense oligonucleotide slows photoreceptor cell degeneration. Invest Ophthalmol Vis Sci 56:6362–6375. https://doi.org/10.1167/iovs.15-16400

34. Garanto A, van Beersum SE, Peters TA et al (2013) Unexpected CEP290 mRNA splicing in a humanized knock-in mouse model for Leber congenital amaurosis. PLoS One 8:e79369. https://doi.org/10.1371/journal.pone.0079369

Three-Dimensional Co-Culture Bioassay for Screening of Retinal Gene Delivery Systems

Ding Wen Chen, Kathleen Pauloff, and Marianna Foldvari

Abstract

Herein we describe a three-dimensional co-culture bioassay protocol designed to assess the therapeutic potential of the proteins expressed from gene delivery transfected cells through the evaluation of expressed protein bioavailability and bioactivity. Using a combination of enzyme-linked immunosorbent assay (ELISA) and immunofluorescent-based neurite length profiling methodologies, the bioavailability of the secreted therapeutic protein in the medium can be quantitated, and the bioactivity of the secreted therapeutic protein can also be evaluated through neurite length profiling, respectively. The versatility and rationale of this bioassay could serve as a useful screening tool in the development of retinal gene delivery systems.

Key words Neurite extension, Neurite length profiling, Immunofluorescent, Retinal gene therapy, Nonviral gene delivery, Co-culture, Brain-derived neurotrophic factor, Neurotrophic factor

1 Introduction

Neurotrophic factor retinal gene therapy is a promising therapeutic approach that aims to provide support and rescue glaucomatous stressed retinal ganglion cells (RGCs) [1]. By delivering neurotrophic factors, such as brain-derived neurotrophic factor (BDNF), to retinal cells surrounding stressed RGCs (i.e., astrocytes) with BDNF-encoded plasmid DNA gene delivery system, transfected retinal cells would become BDNF production focal point, thus providing stressed RGCs with a mean protection and rescue [2]. To simulate the "medic" and "stressed" population interaction in vitro, we have established an astrocyte–neuroblastoma co-culture model where nanoparticle-transfected BDNF-expressing "medic" astrocyte population (cultured in transwell inserts) express and secrete BDNF protein into the medium, while "stressed" BDNF-responsive neuroblastoma population (cultured in reservoir well) receive the secreted BDNF [3]. As SH-SY5Y neuroblastoma exhibits neurite extension in response to BDNF exposure, it serves as a robust BDNF-responsive cellular screening candidate, particularly [4].

Beyond a standard transfection efficiency evaluation using model fluorescent proteins (i.e., green fluorescent protein) as indicators of successful transfection, an incorporation of bioavailability and bioactivity metrics that evaluates expressed therapeutic protein would be advantageous. To evaluate the bioavailability and bioactivity of BDNF protein secreted from BDNF transfected-astrocyte in the coculture system, we have employed two pivotal immunofluorescent and molecular tools: ELISA for the quantitation of the secreted BDNF proteins; and immunofluorescent neurite imaging for the evaluation of neurite extension in response to BDNF exposure [5]. Through the incorporation of ELISA and neurite imaging methodologies, we could effectively evaluate the expressed protein bioavailability and bioactivity, respectively. Altogether, the bioassay serves as a useful tool for screening promising gene delivery systems for retinal gene therapy (Fig. 1).

2   Materials

2.1 Astrocyte–Neuroblastoma Coculture Model

1. Serum-supplemented Dulbecco's Modified Eagle Medium (DMEM) Medium (Complete DMEM/High Glucose medium): 10% fetal bovine serum (FBS) and 1% penicillin/streptomycin (Pen/Strep) in DMEM medium.

2. Serum-supplemented Eagle's Minimum Essential Medium:F12 Medium (Complete MEM:F12 medium): 10% FBS and 1% Pen/Strep in MEM:F12 medium.

3. T75 Tissue Culture Treated Culture Flask, 250 mL, 75 cm^2.

4. 15 mL centrifuge tube.

5. Glass-bottom 12-Well Plate, No. 0 thickness, Uncoated, Sterile (*see* **Note 1**).

6. Polyester (PET) 0.4 μm membrane transwell clear inserts (12-well) with lid and culture plate (*see* **Note 2**).

7. Gene delivery system-treated "medic" retinal cell population: A7 astrocyte cell line (*see* **Note 3**).

8. Oxidatively "stressed" neuronal cell population: SH-SY5Y cell line (ATCC, CRL2266) (*see* **Note 4**).

9. K2 Gene delivery system: K2 transfection reagent consisting of nanoparticles complexed with BDNF-encoded plasmid DNA, containing K2 multiplier (*see* **Note 5**).

10. Phosphate buffered saline solution (PBS): 137 mM NaCl, 2.7 mM KCl, 10 mM Na_2HPO_4, 1.8 mM KH_2PO_4, pH 7.4.

11. PBS with calcium and magnesium (PBS$^{Ca2+Mg2+}$): 1× PBS, 1 mM $CaCl_2 \cdot 2H_2O$, 0.5 mM $MgCl_2 \cdot 6H_2O$, pH 7.4 (*see* **Note 6**).
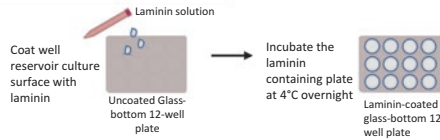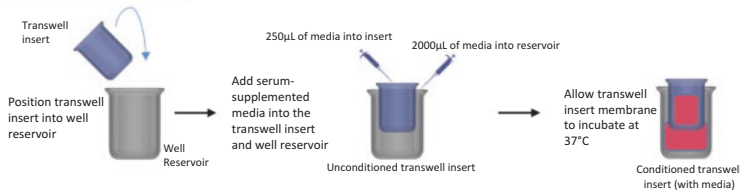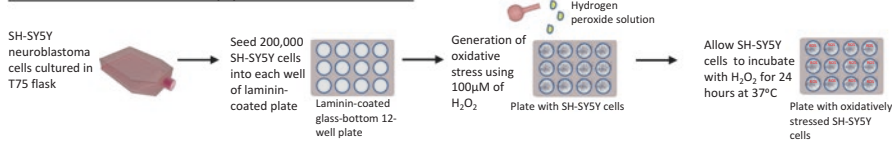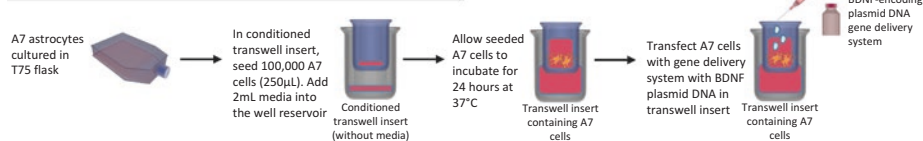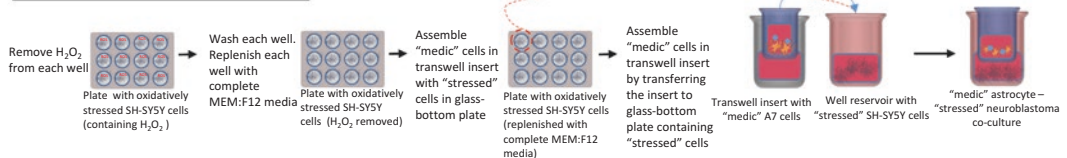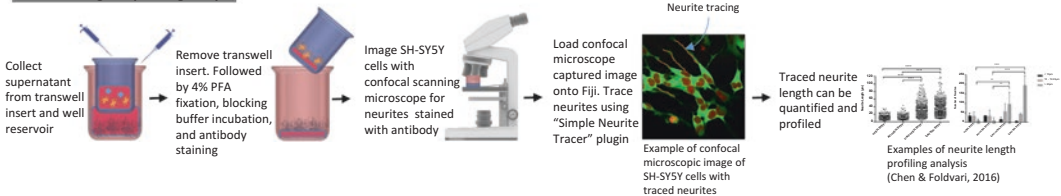
Fig. 1 Summary of the three-dimensional astrocyte–neuroblastoma co-culture model assembly and analysis as outlined in the text

12. Hydrogen peroxide solution: 500 µM hydrogen peroxide in PBS (*see* **Note 7**).

13. 2.5 µg/mL Laminin in PBS$^{Ca2+Mg2+}$ as laminin coating solution.

14. BDNF ELISA Kit.

2.2 Immunofluorescence Staining

1. 4% paraformaldehyde in PBS as fixative solution.

2. Blocking Buffer: 10% FBS and 0.3% Triton X-100 in PBS$^{Ca2+Mg2+}$.

3. Dilution Buffer: 1% bovine serum albumin (BSA), 1% FBS, 0.3% Triton X-100, and 0.01% sodium azide in PBS$^{Ca2+Mg2+}$.

4. Fluorochrome NorthernLights 493 (NL-493) conjugated mouse monoclonal anti-neuron-specific β-III tubulin antibody.

5. Simple Neurite Tracer, a plugin from Fiji software.

6. Confocal scanning laser microscope.

3   Methods

3.1   Astrocyte–Neuroblastoma Co-Culture Model

3.1.1   Culturing of SH-SY5Y Neuroblastoma Cell Line

1. Prewarm complete MEM:F12 media to 37 °C in a water bath.

2. Thaw cyrogenic tube containing SH-SY5Y cell line in a 37 °C water bath.

3. Add 5 mL of the prewarmed complete MEM/F12 medium in a 15 mL centrifuge tube.

4. Transfer thawed cell suspension into the centrifuge tube prepared in the previous step.

5. Pellet the cells by centrifuging the tube at $200 \times g$ for 5 min at room temperature.

6. Aspirate the supernatant and resuspend the cell pellet in 10 mL of complete MEM:F12 media.

7. Gently mix the cell suspension by pipetting up and down gently several times.

8. Transfer the resuspended cell suspension into T75 tissue culture-treated cell culture flask.

9. Incubate the tissue culture flask in an incubator at 37 °C with 5% CO_2.

3.1.2   Culturing of A7 Astrocyte Cell Line

1. Prewarm complete DMEM/High Glucose medium to 37 °C.

2. Thaw cryogenic tube containing A7 cell line in 37 °C water bath.

3. Add 5 mL of the prewarmed complete DMEM/High Glucose medium into 15 mL centrifuge tube.

4. Transfer the thawed cell suspension into the centrifuge tube prepared in previous step.

5. Pellet the cells by centrifuging the tube at $200 \times g$ for 5 min at room temperature.

6. Aspirate the supernatant and resuspend the cell pellet in 10 mL of complete MEM:F12 media.

7. Gently mix the cell suspension by pipetting up and down gently several times.

8. Transfer the cell suspension into T75 tissue culture-treated cell culture flask.

9. Incubate the cell culture flask in incubator at 37 °C with 5% CO_2.

3.1.3   Coating of 12-Well Glass Bottom Plate

1. Thaw laminin stock solution at 4 °C overnight.

2. Prepare working concentration (2.5 μg/mL) of laminin solution in PBS$^{Ca2+Mg2+}$; 1000 μL of laminin solution is needed for each well in the 12-well plate (*see* **Note 8**).

3. Apply laminine coating by pipetting 1000 μL of the prepared laminin solution (2.5 μg/mL) into each well of the glass-bottom plate (*see* **Note 9**).

4. Seal the plate and allow it to incubate at 4 °C overnight (*see* **Note 10**).

5. After overnight incubation, aspirate laminin solution and proceed directly to cell seeding. No washing step is needed.

3.1.4   Seeding and Generation of Stressed Cell Population in 12-Well Glass Bottom Plate

1. In each laminin coated well of the 12-well glass-bottom plate, seed 200,000 cells of SH-SY5Y into each well with a final volume of 2 mL complete DMEM/F12 (*see* **Note 11**).

2. Incubate the plate in incubator for 48 h at 37 °C with 5% CO_2.

3. Next, aspirate media from each well and replenish with fresh prewarmed media (*see* **Note 12**).

4. Prepare working concentration (500 μM) of hydrogen peroxide as described in Subheading 2.

5. Add 500 μL of 500 μM hydrogen peroxide to each well of SH-SY5Y cultured in 2 mL of complete media, resulting in 100 μM of hydrogen peroxide exposure (*see* **Note 13**).

6. Allow the cells to be exposed to the hydrogen peroxide stress at 37 °C for 24 h.

3.1.5   Seeding and Generation of "Medic" Cell Population in Transwell Insert

1. In a separate regular 12-well culture plate, position a 12-well transwell insert into each well.

2. Add 2 mL of prewarmed complete DMEM/High Glucose Media into each of the reservoir wells below the transwell insert (*see* **Note 14**).

3. Add 0.25 mL of complete DMEM/High Glucose Media into the transwell insert. Allow transwell insert to incubate in 37 °C incubator for at least 3 h prior to cell seeding (*see* **Note 15**).

4. Aspirate the conditioning media from the transwell insert and seed 100,000 A7 cells in 250 μL of complete DMEM/High Glucose Media into each transwell insert. Add 2 mL of complete DMEM/High Glucose media into the well reservoir.

5. Allow A7 cells to incubate in the transwell insert for 24 h in 37 °C incubator prior to transfection.

6. Add 3.5 μL of K2 multiplier to each of the transwell insert that are going to be transfected with K2 transfection reagent, 2 h prior to transfection (*see* **Note 16**).

7. Prepare K2 nanoparticles with BDNF plasmid according to the manufacturer's protocol.

3.1.6 Assembly of Astrocyte–Neuroblastoma Co-culture System

1. Carefully aspirate hydrogen peroxide-containing media out of each wells of the 12-well glass bottom plate containing stressed SH-SY5Y cells.

2. Wash each well with complete MEM/F12 media. Be gentle when applying the media. Perform the washing step twice.

3. After the washing step is complete, add 2 mL of the complete MEM/F12 media into each well.

4. Immediately after the replenishment of fresh MEM/F12 complete media into the wells, transwell inserts can be transferred to its respected wells in the 12-wells glass bottom plate.

5. Allow the astrocyte–neuroblastoma coculture to incubate at 37 °C to be analyzed after 24, 48, and 72 h time points.

3.2 Gene Expression, Protein Secretion, and Neurite Extension Profiling Evaluation

3.2.1 ELISA

1. Use a pipette to carefully collect the cell culture medium from both the insert and the wells of the co-culture system.

2. Proceed to ELISA analysis using the BDNF ELISA Kit. Please refer to the kit's manufacturer's protocol for detailed procedure (*see* **Note 17**).

3.2.2 Immunofluorescence Staining and Imaging

1. Carefully set aside the transwell insert and replenish each well of the glass-bottom plate with 600 µL of complete MEM/F12 media (*see* **Note 18**).

2. Add 300 µL of 4% paraformaldehyde directly to the media and allow the "prefixing" to occur for 10 min at room temperature (*see* **Note 19**).

3. Aspirate the paraformaldehyde-containing media and replenish each well with 600 µL of 4% paraformaldehyde directly to each well and allow for fixation of 15 min at room temperature.

4. Remove paraformaldehyde from each well after the incubation period, and add in 400 µL of blocking buffer and incubate for 40 min at room temperature.

5. Aspirate the blocking buffer after incubation has completed.

6. Apply antibody by adding fluorochrome NL-493 conjugated mouse monoclonal anti-neuron-specific β-III tubulin antibody and allow the cells to incubate for 4 h at 37 °C (*see* **Note 20**).

7. After 4 h of incubation, remove the antibody and replenish with 200 µL of PBS$^{Ca2+Mg2+}$.

8. Image each well using using confocal scanning laser microscopy (*see* **Note 21**).

9. Add a scale bar into each captured image as a reference point to determine the pixel/micron ratio (*see* **Note 22**).

10. Individual cells on the captured image can then be traced using Simple Neurite Tracer, a plugin from Fiji software.

3.2.3 Neurite Tracing

1. Open Fiji software.

2. Load images captured using a confocal scanning laser microscope.

3. Load the tracing plugin called "Simple Neurite Tracer".

4. Trace the reference scale bar for the determination of pixel/micron ratio.

5. Begin tracing at the proximal end of the neurite towards the distal end. Repeat for all applicable neurites.

3.2.4 Traced Neurite Quantitation and Profiling

1. Collect all tracing data from all captured images.

2. Convert the collected neurite length data (in pixels) into microns using the pixels/micron ratio.

3. Neurite length data (in microns) can be quantified and profiled using analytical graphing softwares (*see* **Note 23**).

4 Notes

1. Glass-bottom multiwell plates come with different coverslip thickness and surface coatings. For equipment setup, No. 0 thickness coverslip generates the most optimal image quality, while the uncoated coverslip surface is most economical and versatile option. Surface coating can be applied if needed—as utilized in this protocol. The 12-well setup described in this protocol can also be adjusted for different well formats (i.e., 6-, 24-, and 48-well format).

2. Transwell inserts are available in different membrane materials, pore sizes, and plate formats. Pore size of 0.4 μm was the smallest available pore size and it was chosen as it was small enough to prohibit cell migration to take place from the transwell insert, yet large enough for secreted protein to pass through the membrane to the medium beneath. Polyester was chosen as it provides the most optimal optical properties. Alternatively, membrane materials such as polycarbonate and collagen-coated polytetrafluoroethylene can also be used.

3. The "medic" cell population refers to the cell population that are transfected by gene delivery systems carrying the therapeutic gene, which would in turn express therapeutic proteins for the stressed/damaged cell population cultured in the well reservoir. A7 cell line was used as an astrocyte model as it is one

of the gene delivery candidates. Other retinal cells can be substituted as the gene delivery target.

4. The "stressed" cell population refers to the cell population that are to be exposed with hydrogen peroxide to generate an in vitro oxidative stress disease model. Oxidatively stressed cells would then be subject to rescue evaluation by co-culturing with the transfected cell population. SH-SY5Y neuroblastoma cells were used in this case for their BDNF-responsiveness. The subsequent and more decisive model will use an RGC cell line when it becomes available.

5. K2 gene delivery system is a commercially available nanoparticle system that was used as a model system. However, as the purpose of this model system indicates, any experimental or commercial gene delivery system can be used.

6. Using calcium and magnesium containing PBS in washing buffer, blocking buffer, and dilution buffer can reduce the risk of unwanted SH-SY5Y cell detachment through the medium exchanging procedures.

7. A final concentration of 100 μM hydrogen peroxide concentration is required for each well of SH-SY5Y in the 12-well plate. To achieve this concentration, 500 μL of 500 μM hydrogen peroxide will be added to each well containing 2 mL of media, resulting in a final concentration of 100 μM hydrogen peroxide in each well.

8. While culturing of SH-SY5Y does not require coated culture surfaces, it was observed that SH-SY5Y cells only loosely attach to uncoated glass-bottom culture plate and can detach easily from minimal fluid movement in the well (i.e., changing media and washing steps). To prevent this, we have coated the glass-bottom surface with) laminin at a concentration of 0.625 μg/cm² and have found it to be effective in enhancing SH-SY5Y cell attachment to glass-bottom surfaces and remained attached throughout the process.

9. Laminin solution has higher surface tension than a typical water-based solution, hence does not disperse throughout the well resevoir surface easily. Therefore, always visually inspect whether the laminin solution added is sufficient to cover the entire culturing surface.

10. Coating with laminin can done either at 4 °C overnight or at 37 °C for 3 h. If cell seeding is delayed, replenish the laminin-coated wells with 1000 μL of PBS$^{Ca^{2+}Mg^{2+}}$ after laminin coating is completed. Store the plate at 4 °C until needed.

11. An uncrowded and well-dispersed cell population at the time of imaging is key in capturing important neurite length measurements, as overcrowding may mask otherwise available

neurites. As a result, at the time of cell seeding, ensure cells are not in clumps, and that appropriate number of cells are seeded and distributed throughout the culture surface.

12. Be very gentle when adding and removing medium from the wells to reduce the risk of SH-SY5Y cell detachment.

13. Various concentrations of hydrogen peroxide can be used to deliver different levels of acute or chronic oxidative stress.

14. The volume of culture medium in the reservoir wells can be adjusted, but the minimum volume must be sufficient to reach the membrane in the transwell insert in order to ensure protein exchange take places between the transwell insert and reservoir wells.

15. As per manufacturer's suggestion, preconditioning the culture insert with serum-supplemented medium at culturing temperature can improve the attachment of the cells upon seeding into the transwell insert.

16. K2 nanoaprticle system is a two-step gene delivery system. First, the K2 multiplier solution is added directly to the cells prior to nanoparticle treatment. Second, the K2 nanoparticle prepared with the plasmid DNA is added at the required plasmid concentration. Both K2 multiplier and K2 transfection reagent ratios can be adjusted.

17. Protease inhibitor can also be added into the collected media to inhibit protease activity until the content has been analyzed.

18. Medium is added in this step in preparation for the "precondition" procedure as described in the next step.

19. It was observed that direct exposure cultured SH-SY5Y cells to 4% PFA appears to have morphological impact such as cell shrinkage on the cell bodies. Therefore, a "prefixing" step is first is recommended, where 4% PFA (half of the original medium volume, resulting in approximately 2% PFA) is added directly into the culture medium for) 5 min. After 5 min, the cells are fixed using 4% PFA.

20. Fluorochrome NorthernLights 493 conjugated mouse monoclonal anti-neuron-specific β-III tubulin antibody was used in this experiment, but it can be substituted for other conjugated β-III tubulin antibody or an unconjugated antibody used followed by an appropriate secondary antibody.

21. The initial measurement unit for traced neurite length is in the form of pixel(s), which would have to be converted to length through a pixel/unit length ratio. As a result, for every image captured with confocal microscope, ensure that the same magnification objective and image resolution are used and captured, throughout the experiment. This ensures that the pixel-to-length ratio is consistent throughout the experiment

for proper conversion and determination of traced neurite length.

22. For example, a 10 μm scale bar can be added to the corner of a captured image as a reference length. Scale bar can then be traced with the Simple Neurite Tracer plugin. The output of the traced scale bar would be in the unit of pixel which can then be divided by the actual traced scale bar length to obtain a pixel/micron ratio for downstream neurite length conversion (i.e., 5000 pixels per 10 μm results in a 500 pixels/μm ratio).

23. The goal of neurite tracing profiling methodology is to profile and compare the neurite length characteristics exhibited within each treatment group. Examples of neurite profiling strategy):

    (a) Generate a scatter/density plot of the entire neurite length distribution within each treatment group.

    (b) Quantify the number of neurites that falls within each length categories (i.e., number of neurites that are below 10 μm, between 10 and 20 μm, between 20 and 30 μm, etc.).

References

1. Wilson A, Di Polo A (2012) Gene therapy for retinal ganglion cell neuroprotection in glaucoma. Gene Ther 19:127–136

2. Martin KR, Quigley HA, Zack DJ et al (2003) Gene therapy with brain-derived neurotrophic factor as a protection: retinal ganglion cells in a rat glaucoma model. Invest Ophthal Vis Sci 44:4357–4365

3. Chen DW, Foldvari M (2016) In vitro bioassay model for screening non-viral neurotrophic factor gene delivery systems for glaucoma treatment. Drug Deliv Transl Res 6:676–685

4. Foldvari M, Chen DW (2016) The intricacies of neurotrophic factor therapy for retinal ganglion cell rescue in glaucoma: a case for gene therapy. Neural Regen Res 11:875–877

5. Schindelin J, Arganda-Carreras I, Frise E et al (2012) Fiji: an open-source platform for biological-image analysis. Nat Methods 9:676–682

Retinal Gene Therapy for Choroideremia: In Vitro Testing for Gene Augmentation Using an Adeno-Associated Viral (AAV) Vector

Maria I. Patrício and Robert E. MacLaren

Abstract

As gene therapy of choroideremia is becoming a clinical reality, there is a need for reliable and sensitive assays to determine the expression of exogenously delivered Rab Escort Protein-1 (REP1), in particular to test new gene therapy vectors and as a quality control screen for clinical vector stocks. Here we describe an in vitro protocol to test transgene expression following AAV2/2-REP1 transduction of a human cell line. Gene augmentation can be confirmed by western blot and quantification of the fold-increase of human REP1 levels over untransduced controls.

Key words AAV, Gene therapy, Human REP1, Choroideremia, Western blot, Gene augmentation

1 Introduction

Choroideremia (CHM) is an X-linked recessive disease of the retina caused by loss-of-function of Rab Escort Protein 1 (REP1), a key regulator of intracellular trafficking, encoded by the *CHM* gene. Mutations in *CHM* gene cause insufficient REP1 activity to maintain normal prenylation of target Rab GTPases and give rise to cellular dysfunction and ultimately cell death [1, 2]. Phenotypically, this is the basis for a progressive retinal degenerative disease. Affected males typically exhibit night blindness during teenage years, progressive loss of peripheral vision during the 20s and 30s and complete blindness in the 40s. Female carriers have mild but progressive symptoms, most notably night blindness, but may occasionally have a more severe phenotype [3].

Choroideremia may be successfully treated by providing functional copies of the REP1 transgene to the affected cells of the eye [4–6]. Specifically, it has been shown that adeno-associated viral (AAV) vectors may be used to deliver a nucleotide sequence encoding functional REP1 to the eye to treat the disease. Preclinical

work on this particular construct proved human REP1 transgene to be expressed following transduction of the D17 dog osteosarcoma cell line and choroideremia patient fibroblasts [7]. The same AAV vector used in a phase 1/2 clinical trial for choroideremia was then tested in vitro in HT1080 fibrosarcoma cell line to confirm human REP1 expression [6]. Different AAV constructs expressing human REP1 were reported to deliver the protein in vitro following transduction of primary skin fibroblasts providing proof of concept for AAV2/5-mediated gene therapy [8].

Here we describe an in vitro approach to test AAV2/2-REP1 vector for transgene expression. We established a protocol whereby a commercially available cell line is used as a vehicle for transduction with AAV at a standard multiplicity of infection (MOI). Five days post-transduction cells are processed for protein expression analysis, and blotted for REP1 using a commercially available monoclonal antibody raised against the C-terminal 415 amino acids of human REP1 [9]. We demonstrated that AAV2/2-REP1 delivers human REP1 to the cells, and the fold increase above endogenous levels can be detected by western blot and semiquantified using densitometry analysis. This method can therefore be used to show transgene expression from AAV2/2-REP1 clinical batches prior to use in human retinal gene therapy.

2   Materials

2.1   Cell Culture

1. Human Embryonic Kidney (HEK) 293 cell line, maintained in culture at 37 °C in a 5% CO_2 environment.

2. 1× Phosphate buffer saline (PBS), pH 7.4, suitable for cell culture.

3. Complete cell media: Minimum Essential Media (MEM) supplemented with 2 mM L-glutamine, 100 units/mL penicillin, 100 μg/mL streptomycin, 1% nonessential amino acids, and 10% fetal bovine serum (FBS).

4. 1× TrypLE™ Express Enzyme dissociation reagent, no phenol red.

5. Tissue culture-treated T75-cm^2 flasks.

6. Tissue culture-treated 6-well plates.

7. 0.4% Trypan Blue solution.

2.2   Cell Harvesting and Protein Quantification

1. Molecular grade water.

2. 10× radio-immunoprecipitation (RIPA) buffer: 0.5 M Tris–HCl pH 7.4, 1.5 M NaCl, 2.5% deoxycholic acid, 10% NP-40, 10 mM EDTA. Store at room temperature (RT).

3. cOmplete™ Mini EDTA-free Protease Inhibitor cocktail, tablets.

4. Protein quantification kit using the bicinchoninic acid (BCA) method, and bovine serum albumin (BSA) as a standard.

5. Plate reader (562 nm filter, reference filter is optional if available).

2.3 Western Blot (WB)

1. 10× Running buffer: 0.25 M Tris base, 1.92 M glycine, and 1% (w/v) sodium dodecyl sulfate (SDS). Store at RT.

2. 2× Laemmli buffer: 4% SDS, 20% glycerol, 10% 2-mercaptoethanol, 0.004% bromophenol blue and 0.125 M Tris–HCl, pH approx. 6.8. Store in aliquots at −20 °C.

3. Precast 10% polyacrylamide gels.

4. Prestained protein ladder.

5. SDS-PAGE gels tank.

6. PVDF membranes (*see* **Note 1**).

7. Semidry transfer blot system.

8. 1× PBS-Tween® 20 (PBST) solution: 0.1% Tween® 20, 1× PBS. Store at 4 °C.

9. Blocking solution: 3% (w/v) BSA, 1× PBST (*see* **Note 2**). Store in aliquots at −20 °C.

10. Anti-REP1 antibody (mouse monoclonal, clone 2F1, Millipore).

11. Anti-β-actin antibody (or other loading control of choice).

12. Horseradish peroxidase (HRP)-bound secondary antibodies.

13. Enhanced chemiluminescent (ECL) substrate for WB detection.

14. Horizontal plate shaker.

15. Chemiluminescent western blot detection system.

3 Methods

3.1 Cell Seeding

1. Warm up the cell culture media and PBS at 37 °C for 10 min in a water bath.

2. Remove media from cell flask; discard.

3. Add 5 mL of PBS to wash (*see* **Note 3**); discard.

4. Add 1 mL of TrypLE™ Express Enzyme, place cells in the CO_2 incubator for 5 min.

5. Tap flask gently to detach the cells, add 3 mL of medium and resuspend; transfer into a 15 mL Falcon tube.

6. Spin down the cells for 5 min at $300 \times g$ at RT.

7. Discard supernatant; add 1 mL of medium and resuspend the pellet.

8. Prepare 1:10 dilution of trypan blue in PBS to use for cell counting (1 mL trypan blue + 9 mL of PBS).

9. Prepare cell suspension dilution with trypan blue in a 1.5 mL tube for counting.

10. Perform cell counts ($n = 2$) using a haemocytometer and an inverted microscope.

11. Using the mean cell count calculate the volume of cells to use for seeding a density of 8–10E + 05 cells in a 6-well plate (*see* **Note 4**), in a total of 2 mL/well, considering the design below; prepare the total cell suspension in a 15 mL Falcon tube (*see* **Note 5**) (Table 1).

12. Fill in the wells with 1 mL of media. Add 1 mL of cell suspension to every well (total volume 2 mL).

13. Incubate the plate in the CO_2 incubator for 24 h.

3.2 Cell Transduction

1. Calculate the total number of cells to be transduced per well using one of the control wells seeded at Day 1.

2. Warm up all the cell culture media and PBS at 37 °C for 10 min in a water bath.

3. Remove media from the well; discard.

4. Add 1 mL of PBS to wash; discard.

5. Add 250 μL of TrypLE to the well; place the plate in the CO_2 incubator for 5 min.

6. Add 750 μL of PBS to the well; resuspend and transfer the cell suspension into a microtube.

7. Spin down for 5 min at $300 \times g$ at RT.

8. Discard supernatant; add 1 mL of medium and resuspend the pellet.

9. Count cells as in day 1 (*see* Subheading 3.1).

10. Calculate the total amount of cells per well (*see* **Note 6**).

11. Calculate the amount of vector to add per well to have a MOI 10,000 using the formula:
Volume (mL) = (MOI × Number of cells)/Viral concentration, where viral concentration is the number of DNase-resistant particles (DRP)/mL (*see* **Note 7**).

Table 1
Conditions to use when seeding HEK293 cells to test AAV2/2-REP1

# Wells/6-well plate	Condition
1	Endogenous control/Untransduced cells
1	Positive control—cells to add AAV2/2-REP-1 control sample
1	Test sample—cells to add AAV2/2-REP-1 test sample

12. Remove cell media from all wells; discard.

13. Add 1 mL of fresh cell culture media to every well.

14. Pipette the corresponding volume of AAV to each well (*see* **Note 8**).

15. Top up every well with 1 mL of fresh complete cell media.

16. Incubate the plate in the CO_2 incubator for 72 ± 6 h.

17. Renew the cell media in all wells (2 mL/well) and incubate for further 48 h.

3.3 Preparation of Cell Lysates

1. Prepare the lysis buffer by diluting the 10× RIPA solution with molecular grade water.

2. Add cOmplete™ Mini EDTA-free Protease Inhibitor cocktail according to the manufacturer's instructions. Chill on ice.

3. Prepare a cell pellet from each well.

4. Warm up all the cell culture media and PBS at 37 °C for 10 min in a water bath.

5. Remove media from the well; discard.

6. Add 1 mL of PBS to wash; discard.

7. Add 250 µL of TrypLE to the well; place the plate in the CO_2 incubator for 5 min.

8. Add 750 µL of PBS to the well; resuspend and transfer the cell suspension into a microtube.

9. Spin down for 5 min at $300 \times g$ at RT.

10. Discard supernatant (*see* **Note 9**).

11. Add 100 µL of lysis buffer to each cell pellet; homogenize by pipetting up and down. Chill on ice.

12. Sonicate the lysates for 10 s at 20% power using a sonication probe. Chill on ice.

13. Spin the lysates down for 10 min at maximum speed ($\sim$17,000 $\times g$) at 4 °C to clear the lysate.

14. Transfer the supernatant into a new microtube and discard the pellet.

15. Store the lysates at -20 °C for later use, or proceed to protein quantification.

16. Prepare a standard curve using BSA and lysis buffer according to the manufacturer's instructions. Prepare at least two replicates for each point of the standard curve.

17. Prepare at least two replicates of each sample: dilute the cell lysate 1:10 in lysis buffer.

18. Quantify the total amount of protein using the BCA method according to the manufacturer's instructions.

19. Store the lysates at -20 °C for later use, or proceed to western blot.

3.4   *Western Blot*

1. Prepare 1× running buffer: dilute 1 part of 1× running buffer with 9 parts of distilled water. Make fresh every time.

2. Thaw the cell lysates on ice.

3. Calculate the amount of sample to run 20 μg of total protein per lane.

4. Prepare the samples by mixing equal volumes of cell lysate and 2× Laemmli buffer in a microtube.

5. Boil the samples for 5 min at 96 °C in a heat block.

6. Vortex and spin down briefly (10 s, 300 × *g*).

7. Set up the precast gel in the tank and fill it with 1× running buffer.

8. Load the protein ladder and the samples in the gel.

9. Run the gel at 100 V for approximately 100 min.

10. Transfer the gel onto a PVDF membrane (*see* **Note 10**).

11. Transfer the membrane into a tray containing 30 mL of PBST (*see* **Note 11**).

12. Block the membrane in 30 mL of blocking solution for 45 min at room temperature on a plate shaker under gentle agitation.

13. Prepare the primary antibodies using blocking solution (1:2500 for anti-REP1; optimized dilution for the loading control of choice). Vortex briefly.

14. Cut the membrane by the ~60 kDa band: top part to be incubated with anti-REP1 solution, bottom part to incubate with solution to detect loading control of choice (*see* **Note 12**).

15. Incubate the two parts of the membrane with corresponding antibodies solutions for 1 h at room temperature under agitation.

16. Wash the membranes for 3 × 7 min with 30 mL of PBST on a plate shaker.

17. Prepare the secondary antibodies using blocking solution (1:10,000 or the manufacturer recommended concentration). Vortex briefly.

18. Wash the membranes for 3 × 7 min with 30 mL of PBST on a plate shaker. The membranes are now ready for detection.

19. Prepare the ECL substrate according to the manufacturer's instructions.

20. Pipette the ECL substrate over a clean surface.

21. Wipe the excess of PBST and place the membranes flipped over the substrate (protein side should now be facing the substrate).

22. Incubate in the dark for 4 min (*see* **Note 13**).

23. Wipe off the excess of ECL and place the membrane in a clean tray ready for detection (*see* **Note 14**).
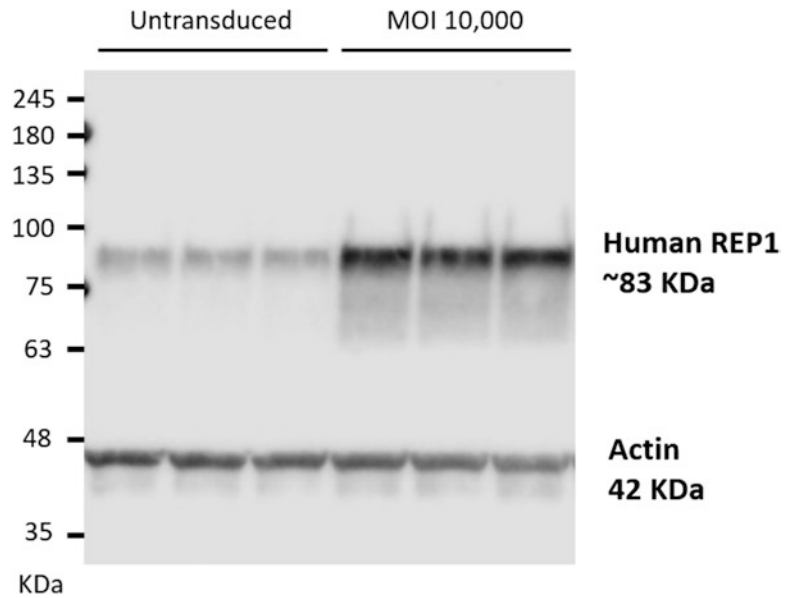
Fig. 1 Representative western blot detection of human REP1 and actin following transduction of HEK293 cells with AAV2/2-REP1. HEK293 cells were transduced with MOI 10,000 of AAV2/2-REP1 at day 1 after seeding (in triplicate). Three untransduced control wells were run in parallel. Cell lysates were prepared 5 days post-transduction and blotted for human REP1 and actin (as loading control). Untransduced cells show endogenous expression of REP1. Cells treated with AAV2/2-REP1 show an augmentation in REP1 protein levels, confirming that the transgene was delivered, translated, and folded correctly in HEK293 cells

24. Acquire images of the detected proteins according to the manufacturer's instructions. Exposure times will vary depending on the instrument and software used (*see* **Note 15**). An example is shown in Fig. 1.

25. Determine the increase of the REP1 band on transduced samples over untransduced controls (*see* **Note 16**).

4   Notes

1. We have found that results are kept more consistent if ready-to-use transfer packs and a semidry transfer system were used (Trans-Blot® Turbo™ blotting system from Bio-Rad). Although not mandatory, the use of ready-to-use transfer packs helps keeping data reliable between experiments, fact that is particularly important if testing viral vectors prior to clinical use.

2. We recommend using a 0.22 μm filter unit to filter any impurities from the blocking solution and avoid unwanted background signal from antibody detection.

3. The volume of PBS is to be adjusted according to the size of the flask used to grown the cells. Here we suggest 5 mL to wash cells in a T75 cm² flask, volume must be optimized accordingly if other sizes are to be used.

4. We found the optimal cell density to achieve approximately 80% confluence 24 h later to be 9.5E + 05 cells. This amount must be optimized prior to any transduction experiment because it is cell line-dependent.

5. We recommend doing triplicates for each condition tested to account for inherent experimental variability. Also at least two extra untransduced wells must be seeded to be used for cell counting at the time/prior to transduction. If available, an AAV vector containing a fluorescent reporter gene can be used to transduce another well, therefore allowing monitoring of transduction efficiency.

6. We would assume the cell number to be similar in all wells having determined the cell number in two separate wells. We have found no significant differences between well plates in our experiments.

7. The viral titre can be found in an AAV Certificate of Analysis (CoA) for GMP stocks or determined 'in house' according to standard protocols.

8. Positioning the plate at a 45° angle helps pipetting the AAV solution into the media. By swirling it gently as it placed horizontally, we have found the viral particles to be well distributed across the entire well.

9. Minimize the amount of remaining liquid by using a P200 tip to aspirate it closely to the cell pellet without disturbing it.

10. If the Trans-Blot® Turbo™ blotting system from Bio-Rad is available, we recommend running the 'mixed weight' program (2.5 A for 7 min). If using other transfer systems, duration of the transfer must be optimized.

11. The protocol can be paused here if the membrane is stored properly: in PBST at 4 °C overnight, or let to dry completely if for a period up to 3 days. If dried, before proceeding with the western blot protocol, the membrane must be activated by submersion in methanol for 2–3 min followed by two washes in PBST. We found no differences in antigen detection when the protocol was stopped at this point.

12. Cut a tiny wedge from the top left corner of each membrane for orientation purposes.

13. This was found to be the optimal incubation time for the ECL in use, should be adapted according to the manufacturer's instructions.

14. Cling film may be used to place the membranes aligned for detection; it will prevent them from drying out if further detections are to be performed.

15. Due to their relative abundance, actin loading control might require a lower exposure time than human REP1. If the signal is too strong, we recommend detecting actin separately from REP1. This will not interfere with post-acquisition processing for band quantification.

16. Although absolute levels of human REP1 in transduced samples over untransduced controls may vary between experiments, we were always able to detect at least a two-fold increase in AAV-treated samples relatively to untransduced controls.

References

1. Seabra MC, Brown MS, Slaughter CA et al (1992) Purification of component A of Rab geranylgeranyl transferase: possible identity with the choroideremia gene product. Cell 70:1049–1057. https://doi.org/10.1016/0092-8674(92)90253-9

2. Seabra MC, Ho YK, Anant JS (1995) Deficient geranylgeranylation of Ram/Rab27 in choroideremia. J Biol Chem 270:24420–24427

3. Edwards TL, Groppe M, Jolly JK et al (2015) Correlation of retinal structure and function in choroideremia carriers. Ophthalmology 122:1274–1276. https://doi.org/10.1016/j.ophtha.2014.12.036

4. Barnard AR, Groppe M, MacLaren RE (2015) Gene therapy for choroideremia using an adeno-associated viral (AAV) vector. Cold Spring Harb Perspect Med 5:a017293. https://doi.org/10.1101/cshperspect.a017293

5. Edwards TL, Jolly JK, Groppe M et al (2016) Visual acuity after retinal gene therapy for choroideremia. N Engl J Med 374:1996–1998. https://doi.org/10.1056/NEJMc1509501

6. MacLaren RE, Groppe M, Barnard AR et al (2014) Retinal gene therapy in patients with choroideremia: initial findings from a phase 1/2 clinical trial. Lancet 383:1129–1137. https://doi.org/10.1016/S0140-6736(13)62117-0

7. Tolmachova T, Tolmachov OE, Barnard AR et al (2013) Functional expression of Rab escort protein 1 following AAV2-mediated gene delivery in the retina of choroideremia mice and human cells ex vivo. J Mol Med 91:825–837. https://doi.org/10.1007/s00109-013-1006-4

8. Cereso N, Pequignot MO, Robert L et al (2014) Proof of concept for AAV2/5-mediated gene therapy in iPSC-derived retinal pigment epithelium of a choroideremia patient. Mol Ther Methods Clin Dev 1:14011. https://doi.org/10.1038/mtm.2014.11

9. Alexandrov K, Horiuchi H, Steele-Mortimer O et al (1994) Rab escort protein-1 is a multifunctional protein that accompanies newly prenylated rab proteins to their target membranes. EMBO J 13:5262–5273

Part II

Assays for Gene Augmentation and Editing In Vivo on Rodent and Macaque Retina

In Vivo Electroporation of Developing Mouse Retina

Jimmy de Melo and Seth Blackshaw

Abstract

In vivo electroporation enables the transformation of retinal tissue with engineered DNA plasmids, facilitating the selective expression of desired gene products. This method achieves plasmid transfer via the application of an external electrical field, which both generates a transient increase in the permeability of cell plasma membranes, and promotes the incorporation of DNA plasmids by electrophoretic transfer through the permeabilized membranes. Here we describe a method for the preparation, injection, and electroporation of DNA plasmids into neonatal mouse retinal tissue. This method can be utilized to perform gain of function or loss of function studies in the mouse. Experimental design is limited only by construct availability.

Key words Electroporation, Gain of function, Gene expression, In vivo, Loss of function, Plasmid, Subretinal injection, Retina

1 Introduction

The functional characterization of genes that are expressed during mammalian retinogenesis, and may regulate retinal development presents several technical challenges. Gene targeting for the purpose of engineering constitutive or conditional loss of function knockouts requires a potentially prohibitive investment in both time and resources. Additionally, retina expressed genes may have essential roles in extraocular tissues, resulting in embryonic mortality in knockout models, precluding ocular analysis. There may also be extraretinal phenotypes that can confound the analysis and interpretation of retinal gene function. The use of conditional knockout Cre-lox models can significantly limit both mortality and extraocular effects, but remains both resource and time intensive. Though knockout models can provide informative loss of function data for a gene of interest, the ability to ectopically express a gene in a controlled gain of function experiment can reveal additional functional effects. Gain-of-function studies are especially valuable for the elucidation of cell fate specification and/or terminal dif-

ferentiation roles in the retina, wherein activation of gene expression may reprogram retinal progenitor cells altering their course of development.

Electroporation is a method that can be used for the rapid and efficient incorporation of DNA plasmids into the neonatal mouse retina [1–9]. The historical development of electroporation began with the discovery that the application of short electrical pulses was sufficient to promote a transient increase in plasma membrane permeability [10]. This induced membrane permeability could be exploited to facilitate the transfer of materials across membranes [10–13]. Further development revealed that electroporation could be utilized as a method of gene transfer into mammalian cells [14]. Continuous technical refinement established electroporation as a robust and reproducible method for in vivo gene transfer in multiple vertebrate species including the mouse [15]. Here we describe a method by which electroporation can be used for in vivo gene transfer in the developing mouse retina.

A DNA solution comprised of isolated and purified engineered plasmid expression constructs is injected into the developmentally transient subretinal space in neonatal mice. Successful injection places the DNA solution between the retinal pigment epithelium and the mitotically active apical neuroretina. Electrical charges are applied using a tweezer-type electrode, thereby facilitating the correct directional orientation of the electrical field such that electrophoresis of the negatively charged DNA moves into the retina and away from the pigmented epithelium. The strength and robustness of gene expression will vary based on differences in plasmid promoter design. We have identified robust plasmid incorporation and gene expression as early as 48 h post electroporation. There is no significant lateral migration of developing cells in the retina. Consequently, electroporation results in distinct electroporated and nonelectroporated regions in the retina. Non-electroporated regions may serve as internal histological controls where appropriate.

Electroporation offers several key advantages over alternative methods for the transformation of retinal tissue. Currently, the size of a gene delivered by retroviral-mediated transduction is limited by the packaging constraints of the viral capsid [16]. Such constraints on gene size are not a factor using electroporation. Furthermore, multiple plasmids can be mixed together in injection solutions to perform combinatorial gene delivery [8, 9]. Plasmid design will vary from study to study. Broadly, retinal electroporation can be used to express a gene of interest under a ubiquitous promoter, such as CAG. Furthermore, plasmids can be designed to disrupt gene function by expressing engineered shRNA constructs or CRISPR/Cas9 plasmids [1, 17]. Loss of function can be further mediated by electroporation of plasmids expressing Cre recombinase into floxed mouse lines [8]. Selective retinal gene expression

can be achieved through the use of cell-class specific gene promoters [2]. Visualization of electroporated cells is typically achieved using bicistronic constructs expressing a fluorescent reporter gene such as GFP, or by co-electroporating a reporter gene expression plasmid.

2   Materials

This protocol describes a procedure for the purification and concentration of plasmid DNA with the objective of obtaining an injectable DNA solution at a concentration of 5 μg of DNA per μL of solution. The protocol then describes the injection of this purified DNA solution into the subretinal space and the application of electrical pulses for the purpose of transforming the retinal tissue. All prepared solutions should be made with ultrapure water (ASTM Type I standard) and be prepared such that they follow any applicable guidelines for their use in animal procedures. All steps may be performed at room temperature unless otherwise indicated. All governmental and institutional waste disposal regulations should be followed when disposing laboratory waste products.

2.1 Plasmid Preparation

1. Phenol: Phenol that is Tris-equilibrated 10 mM Tris–HCl, pH 8.0, 1 mM EDTA.
2. Chloroform: >99% chloroform anhydrous.
3. 3 M Sodium acetate: 3 M sodium acetate molecular biology grade, pH 5.5.
4. Ethanol: Absolute ethanol, molecular biology grade 200 Proof.
5. 80% v/v Ethanol: 8 parts of absolute ethanol is diluted (v/v) with 2 parts ultrapure water.
6. 1× PBS: Phosphate buffered saline pH 7.4.
7. 1% Fast Green FCF: Dissolve 1% w/v Fast Green FCF into 1% (v/v) >99.7% acetic acid in ultrapure water.
8. Plasmid DNA purification kit (Qiagen Maxi-Kit or similar).

2.2 Subretinal Injection of DNA

1. Sharp beveled 30 gauge needle: Precision glide beveled 30 gauge needles (BD).
2. 70% Isopropyl alcohol prep: Isopropyl alcohol prep pads Curity 70% Isopropyl alcohol (Covidien).
3. 33 gauge blunt ended needle: Exmire microsyringe, needle outer diameter 0.52 mm, inner diameter 0.13 mm (Ito Corporation, Shizuoka, Japan).
4. Stereomicroscope.
5. Hemostat: Surgical tool used for paw pinch tests.
6. Ice in a box.
7. Thin latex barrier to prevent direct contact of mouse pups with the ice.

2.3 Electroporation	1. Electroporator Model ECM 830 (BTX-Harvard Apparatus) (*see* **Note 1**).
	2. Tweezertrodes: 10 mm tweezer electrode diameter Stainless steel (BTX-Harvard Apparatus).
	3. 110 V Heat lamp (Braintree Scientific).
	4. Clean tissue-lined container.
	5. Mouse pups postnatal day 0 (P0) to P4.
2.4 Fixation and Cryoembedding	1. 4% paraformaldehyde (PFA): Add 4% (w/v) paraformaldehyde into 1× PBS pH 7.4, add 20 μL 10 N NaOH and incubate at 65 °C until dissolved. Cool to room temperature and adjust pH to 7.4 and filter pass to remove any particulate.
	2. 30% Sucrose: Add 30% (w/v) sucrose into 1× PBS pH 7.4 and stir over moderate heat until dissolved. Cool to room temperature and filter pass before use.
	3. O.C.T. compound: Tissue-Tek (Sakura Finetek USA).
	4. Optional Fluorescent stereomicroscope or inverted fluorescent microscope.
	5. Molds for O.C.T. embedding.
	6. Dry ice chilled methylbutane to freeze the O.C.T. filled molds.
	7. Cryotome.
	8. −80 °C freezer.

3   Methods

The following methods include a description of a surgical procedure where DNA solution is injected into the subretinal space of neonatal mice followed by the application of an electrical field. All animal procedures must be approved and performed under the specific guidelines of any and all applicable governmental and institutional regulators. Injections are performed with the aid of a stereomicroscope, the make and model of which may vary based on the preferences of the research group. Variations to the methods may be required based on the specific animal research policies at any given institution.

3.1 Plasmid Preparation	1. Aliquot 100 μg of plasmid DNA solution. Plasmids should be cultured, isolated and purified such that the stock concentration ranges from 2 to 5 μg/μL with sufficient volume for isolation of 100 μg of DNA. Acquisition of this amount of plasmid DNA typically necessitates preparation with a Plasmid Maxi-Kit or similar method.
	2. Dilute the volume of DNA to 100 μL for ease of calculation and manipulation.

3. Add 67 μL of phenol to the 100 μL diluted plasmid DNA preparation in order to obtain a 60% (v/v) DNA–40% phenol ratio (*see* **Note 2**). Mix the tubes thoroughly by inversion; do not mix the samples by pipetting or by vortexing as this may cause excessive shearing of the plasmid DNA.

4. Spin the DNA–phenol mixture for 5 minutes (min) in a microcentrifuge designated for the use of organic solvents at $16,000 \times g$ at room temperature.

5. Collect the 100 μL of aqueous supernatant and transfer to a fresh 1.5 mL centrifuge tube. The organic layer may be discarded. Add 67 μL of chloroform to the 100 μL of aqueous solution in order to obtain a 60% (v/v) DNA–40% chloroform ratio (*see* **Note 2**).

6. Spin the DNA–chloroform mixture for 5 min in a microcentrifuge designated for the use of organic solvents at $16,000 \times g$ at room temperature.

7. Collect the 100 μL of aqueous supernatant and transfer to a fresh 1.5 mL centrifuge tube. The subnatant organic layer may be discarded. Add 10 μL of 3 M sodium acetate to the 100 μL of DNA solution, mix gently by inversion and then add 250 μL of 100% ethanol. Mix the solution thoroughly by inversion. Avoid pipetting or vortexing as this may cause excessive plasmid shearing. The plasmid DNA should precipitate out of solution during the mixing (*see* **Note 3**).

8. Spin the DNA–ethanol solution in a microcentrifuge at 4 °C for 10 min at $16,000 \times g$.

9. A large white pellet should be visible at the bottom of the centrifuge tube. Pour off the aqueous solution with care so as not to lose the DNA pellet. Add 350 μL of 70% ethanol to the tube and gently invert the tube to rinse the DNA pellet (*see* **Note 4**).

10. Spin DNA–ethanol solution in a microcentrifuge at 4 °C for 5 min at $16,000 \times g$.

11. Pour off the 70% ethanol solution with care so as not to lose the DNA pellet. Air-dry the pellet. Excess ethanol may be aspirated off by pipetting to speed the process. Do not excessively dry out the DNA pellet because this will make it difficult to resolubilize (*see* **Note 5**).

12. Dissolve the DNA pellet into 20 μL of 1× PBS to achieve a final concentration of 5 μg/μL of plasmid DNA (*see* **Note 6**).

13. Add 2 μL of Fast Green FCF (1% stock) in order to achieve a final dye concentration of 0.1%. Fast Green FCF serves as an injection tracer facilitating observation of the spread of the injection solution into the subretinal space (*see* **Note 7**).

3.2   Subretinal Injection of DNA

1. Hypothermic anesthesia will be used to anesthetize neonatal (postnatal day (P)0) mice prior to subretinal injection of DNA and electroporation (*see* **Note 8**). Pups are placed on a bed of ice for several minutes with constant monitoring (Fig. 1a). A thin latex barrier should be placed between the pups and the ice to prevent freeze damage to the skin. Pups must not be buried in the ice as this may increase mortality. The duration of ice exposure that any given pup may require to ensure appropriate hypothermic analgesia will vary from animal to animal. Typically, 5 min is sufficient but mice should be carefully monitored as individuals may respond very quickly or may require longer exposure. A paw pinch test using a hemostat may be conducted to check for a withdrawal reflex, when the withdrawal reflex is not identifiable the pup is ready for the procedure.

2. Prior to injection of DNA into the subretinal space, the eye must be opened using sharp beveled 30 gauge needle. Swab the eye to be injected with a 70% isopropyl alcohol prep, and with the assistance of a stereo microscope identify the fused junctional epithelium where the eyelids of the eye to be injected come together.

3. Using the sharp beveled 30-gauge needle, carefully open the eye by cutting along the fused junctional epithelium (Fig. 1b). This can be achieved by gently slicing along the junction with the sharp edge of the needle. Do not use a sawing, poking or stabbing motion to open the eye. Avoid applying excessive force; too much pressure may result in the penetration of the underlying eye. Furthermore, avoid cutting past the range of the fused eyelid junction. This may result in significant bleeding which will obscure the eye increasing the difficulty of the following injection.

4. Because the injection needle is blunt ended, it is necessary to make a small incision in the sclera at the point of injection to facilitate insertion of the injection needle into the eye. Use the tip of a 30-gauge beveled needle to make an incision in the sclera adjacent to the corneal limbus at the site where the blunt ended needle will penetrate the eye. Do not penetrate too deeply in order to avoid damaging the lens with the sharp tip of the beveled needle.

5. Draw 0.6 μL of DNA solution into the 33 gauge blunt ended Exmire microsyringe injection needle. The gradients incorporated into the barrel of the syringe may be used to measure the volume drawn (*see* **Note 9**). Insert the needle into the incision generated in the previous step. The opposing scleral wall will provide resistance once the needle has passed through the vitreous humor and retina. Care should be taken to avoid penetrating
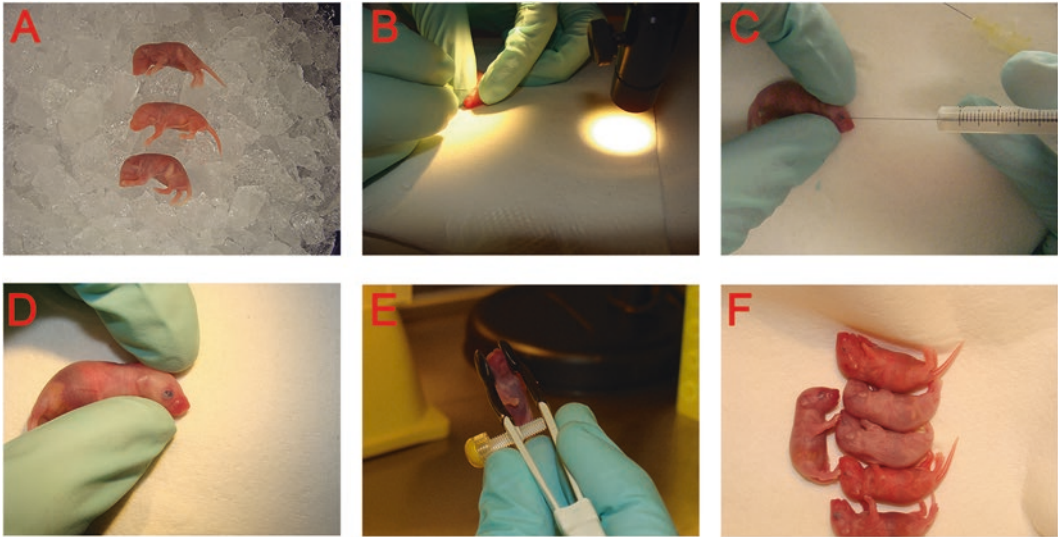
Fig. 1 Images of key steps in protocol. (**a**) Ice anesthesia of neonatal pups. (**b**) Surgical opening of the eye and scleral incision. (**c**) Manual injection of DNA/Fast Green solution. (**d**) Efficient spread of Fast Green in subretinal space following successful injection. (**e**) Electroporation with tweezertrodes. (**f**) Recovery following surgery under heat lamp

or scratching the lens as the needle is passed through the eye. A ruptured lens may contribute to ocular dysplasia as the eye develops making retinal analysis difficult or impossible.

6. Slowly inject 0.3 μL of DNA solution into the subretinal space (Fig. 1c). The experimenter should execute a controlled and even ejection of solution from the syringe so that the DNA solution does not overflow the subretinal space and become deposited into the vitreous chamber of the eye. Successful subretinal placement of the DNA solution will produce an even spread in a portion of the subretinal space which will be readily observable by the Fast Green FCF injection tracer (Fig. 1d). The experimenter will be able to discriminate areas of retina with and without underlying Fast Green FCF stained solution. Gradual rotation of the head of the pup under the microscope should help make these regions discernable.

3.3 Electroporation

1. Electroporation is performed on injected pups using a tweezertrode. The tweezertrode should be immersed in 1× PBS prior to application on injected pups. Wetting the tweezertrode with 1× PBS is performed to maximize the electrical conductivity from the tweezertrode to the pup. The tweezertrode may then be applied to the head of the injected pup (Fig. 1e). The electrodes should be oriented such that the positive pole electrode is placed over the injected eye and the negative pole electrode is placed over noninjected eye. This placement

ensures that the electrical field is oriented such that electrophoresis will drive the injected DNA solution from the subretinal space into the retina.

2. Apply the electrical pulses using the pulse generator (electroporator). For electroporation of neonatal (P0–P4) mouse pups the electrical paradigm should be set as follows: 5 square pulses, each pulse is set at 80 V and 50 ms in duration. There should be a 950 ms interval between pulses.

3. Using a 70% isopropyl alcohol prep clean the area around the injected/electroporated eye. The electroporated pups must now be allowed to recover from the hypothermic anesthesia (Fig. 1f). Place the pups in a clean, tissue-lined container beneath a heat lamp (*see* **Note 10**). Allow the pups to remain under the heat lamp until full mobility and normal pink coloring of the pups has returned to each animal. The duration of time under the light may vary for each individual animal. Upon full recovery, return the electroporated pups to their mother and monitor over the next 1–2 days for signs of distress.

3.4 Fixation and Cryoembedding

1. The end point for each electroporation experiment is subject to the requirements of the specific study and will vary accordingly. Reporter expression off of CAG based plasmid constructs can be visualized within 2 days of electroporation, however the expression profile for any given plasmid construct may vary and should be determined empirically.

2. Euthanize the electroporated animals at the desired timepoint. All methods utilized for the euthanasia of animals should adhere to all governmental and institutional guidelines. Dissect out the electroporated eye and fix in 4% paraformaldehyde with rotational agitation at 4 °C for approximately 50 min. The optimized fixation time for any given endpoint can vary and should be determined by the individual research group.

3. Carefully dissect out the retina from the fixed eye in cold 1× PBS by removing the sclera, cornea, lens, choroid and retinal pigmented epithelium. If a fluorescent reporter has been used as part of the experimental design, the dissected retinas can be analyzed under a fluorescent stereomicroscope or inverted fluorescent microscope to grossly determine the electroporation efficiency. Dissected retinas can then be transferred into 30% sucrose solution and incubated overnight with rotational agitation at 4 °C.

4. Half of the sucrose solution can be removed and replaced with O.C.T. cryo-embedding media. The 50% sucrose/50% O.C.T. solution can be incubated with rotational agitation at 4 °C until the solution reaches a homogeneous consistency. The retinas can then be embedded into O.C.T. filled molds and

frozen over dry ice chilled methylbutane. The embedded retinas can be stored at −80 °C. Retinas may now be sectioned on a cryotome and captured onto glass slides (*see* **Note 11**).

---

4   Notes

1. The specific make and model of the electroporation system is subject to system availability and/or the preferences of the research group performing the studies. Electroporators marketed by manufacturers different from that outlined in this protocol are perfectly acceptable given that they can achieve the pulsing paradigm outlined in Subheading 3.3, **step 2**.

2. All use of organic solvents should be performed under appropriately ventilated hoods. Disposal of organic solvents should follow all governmental and institutional regulations.

3. Due to the relatively large amount of DNA (100 µg) in the solution, the precipitation of the DNA should be readily observable after mixing by inversion. Failure to see a cloudy/stringy white precipitate should be taken as a sign that an error may have occurred earlier in the process, and that the plasmid DNA may have been lost in washes or transfers.

4. The pellet may become dislodged from the bottom of the tube following inversion, this is not problematic. Simply ensure that the pellet is resubmerged in the 70% ethanol by gently tapping the tube before the following centrifugation step.

5. The importance of not overdrying the DNA pellet cannot be emphasized enough. Excessively dried pellets will not dissolve readily into the 1× PBS injection solution. Attempts to improve solubilization by mixing the pellet into solution through pipetting or vortexing may cause plasmid shearing which can impact plasmid performance following electroporation. The pellet will appear white and opaque following the alcohol wash step and will become transparent as it dries. Transparency will be observed first at the outer edges of the pellet with the center mass of the pellet remaining opaque. Upon removal of the excess ethanol the pellet should monitored while drying. Once the outside edges of the pellet begin to clear the pellet is ready to be dissolved into 1× PBS. Do not wait for the center mass to clear as this will overdry the pellet.

6. The final concentration of plasmid required for optimal electroporation efficiency may need to be determined empirically for any given construct. We generally observe excellent electroporation efficiency injecting CAG promoter based plasmids at a concentration of 5 µg/µL. However, injection

concentrations ranging from 1.25 to 6 μg/μL have yielded successful electroporation results.

7. The use of an injection tracer is of value primarily within albino mouse strains. If electroporation is being performed on pigmented mice, the inclusion of Fast Green FCF may not be of significant value as a tracer and can be omitted at the experimenter's discretion.

8. Hypothermia is generally acceptable for procedures requiring <10 min in mouse pups up to age P5. Once practiced the process of eye opening, incision, injection and electroporation takes approximately 3 min, which will not allow the pup enough time to recover.

9. Although only 0.3 μL will be injected into the subretinal space, excess injection solution should be drawn into the needle for each injection to ensure that the air which is present in the barrel of the metal needle portion of the syringe and which gets drawn into the syringe preceding the injection solution does not get injected into the eye. This can result in the creation of an air bubble in the subretinal space, which may cause retinal detachment and dysplasia.

10. Alternatively the pups may be allowed to recover by placing them on a slide warmer. If a slide warmer is used the experimenter should ensure that an appropriate pad is placed between the pups and the metal surface of the slide warmer.

11. The specific make and model of cryotome used for sectioning may vary based on availability or the preferences of the experimenters. Section thickness may range from 15 to 25 μm and will also be determined by the experimenter subject to the requirements of the specific study. It also is recommended that sections be captured on positively charged slides for better tissue adherence. Slides containing captured sections may be stored between –20°C and –80°C depending on the duration of storage necessitated and the requirements of the specific research group.

References

1. Matsuda T, Cepko CL (2004) Electroporation and RNA interference in the rodent retina in vivo and in vitro. Proc Natl Acad Sci U S A 101:16–22. https://doi.org/10.1073/pnas.2235688100

2. Matsuda T, Cepko CL (2007) Controlled expression of transgenes introduced by in vivo electroporation. Proc Natl Acad Sci U S A 104:1027–1032. 0610155104 [pii]

3. Onishi A, Peng GH, Hsu C et al (2009) Pias3-dependent SUMOylation directs rod photoreceptor development. Neuron 61:234–246. https://doi.org/10.1016/j.neuron.2008.12.006

4. Onishi A, Peng GH, Poth EM et al (2010) The orphan nuclear hormone receptor ERRbeta controls rod photoreceptor survival. Proc Natl Acad Sci U S A 107:11579–11584. https://doi.org/10.1073/pnas.1000102107

5. Onishi A, Peng GH, Chen S et al (2010) Pias3-dependent SUMOylation controls mammalian cone photoreceptor differentiation. Nat Neurosci 13:1059–1065. https://doi.org/10.1038/nn.2618

6. de Melo J, Peng GH, Chen S et al (2011) The Spalt family transcription factor Sall3 regulates the development of cone photoreceptors and retinal horizontal interneurons. Development 138:2325–2336. https://doi.org/10.1242/dev.061846

7. de Melo J, Blackshaw S (2011) In vivo electroporation of developing mouse retina. J Vis Exp (52):pii:2847. https://doi.org/10.3791/2847

8. de Melo J, Zibetti C, Clark BS et al (2016) Lhx2 is an essential factor for retinal gliogenesis and notch signaling. J Neurosci 36:2391–2405. https://doi.org/10.1523/JNEUROSCI.3145-15.2016

9. de Melo J, Clark BS, Blackshaw S (2016) Multiple intrinsic factors act in concert with Lhx2 to direct retinal gliogenesis. Sci Rep 6:32757. https://doi.org/10.1038/srep32757

10. Neumann E, Rosenheck K (1972) Permeability changes induced by electric impulses in vesicular membranes. J Membr Biol 10:279–290

11. Turnbull RJ (1973) Letter: an alternate explanation for the permeability changes induced by electrical impulses in vesicular membranes. J Membr Biol 14:193–196

12. Zimmermann U, Schulz J, Pilwat G (1973) Transcellular ion flow in Escherichia coli B and electrical sizing of bacterias. Biophys J 13:1005–1013. S0006-3495(73)86041-2 [pii]

13. Kinosita K, Tsong TY (1977) Voltage-induced pore formation and hemolysis of human erythrocytes. Biochim Biophys Acta 471:227–242. 0005-2736(77)90252-8 [pii]

14. Neumann E, Schaefer-Ridder M, Wang Y et al (1982) Gene transfer into mouse lyoma cells by electroporation in high electric fields. EMBO J 1:841–845

15. Swartz M, Eberhart J, Mastick GS et al (2001) Sparking new frontiers: using in vivo electroporation for genetic manipulations. Dev Biol 233:13–21. https://doi.org/10.1006/dbio.2001.0181

16. MacLaren RE, Bennett J, Schwartz SD (2016) Gene therapy and stem cell transplantation in retinal disease: the new frontier. Ophthalmology 123(10S):S106. S0161-6420(16)30509-7 [pii]

17. Latella MC, Di Salvo MT, Cocchiarella F et al (2016) In vivo editing of the human mutant rhodopsin gene by electroporation of plasmid-based CRISPR/Cas9 in the mouse retina. Mol Ther Nucleic Acids 5:e389. https://doi.org/10.1038/mtna.2016.92

Chapter 9

Methods for In Vivo CRISPR/Cas Editing of the Adult Murine Retina

Sandy S. Hung, Fan Li, Jiang-Hui Wang, Anna E. King, Bang V. Bui, Guei-Sheung Liu, and Alex W. Hewitt

Abstract

Clustered Regularly Interspaced Short Palindromic Repeats (CRISPR)/CRISPR-associated protein (Cas) is used by some bacteria and most archaea to protect against viral phage intrusion and has recently been adapted to allow for efficient editing of the mammalian genome. Whilst CRISPR/Cas-based technology has been used to modify genes in mammalian cells in vitro, delivery of CRISPR/Cas system into mammalian tissue and/or organs is more difficult and often requires additional vectors. With the use of adeno-associated virus (AAV) gene delivery system, active CRISPR/Cas enzyme can be maintained for an extended period of time and enable efficient editing of genome in the retina in vivo. Herein we outline the method to edit the genome in mouse retina using a dual AAV vector-mediated CRISPR/Cas9 system.

Key words CRISPR/Cas9, Genome editing, Gene delivery, AAV, Retina

1 Introduction

Many inherited retinal degenerations are progressive sight-threatening disorders caused by well-defined genetic mutations [1]. Although numerous variants across many loci have been found to cause specific retinal disease, all of these conditions currently remain untreatable [1]. CRISPR/Cas-based technology opens the prospect for anticipatory therapies through the direct correction of genetic mutations retinal cells [2]. Generally, there is firm public support for the clinical application of such technology [3]. Editing disease-causing mutations in genomic DNA through a single guide RNA (sgRNA)/Cas endonuclease complex can cause DNA breaks which are subsequently repaired through nonhomologous end joining (NHEJ) or when accompanied by an additional DNA template, homology-directed repair (HDR) [4]. During NHEJ

Guei-Sheung Liu and Alex W. Hewitt contributed equally to this work.

the inadvertent incorporation of insertions and/or deletions (indels) of DNA fragments can cause frameshift mutations, which lead to knockout of the targeted gene. On the other hand, HDR-mediated repair can be used to generate single nucleotide corrections as well as to potentially introduce larger sequences by providing a DNA template with flanking homology sequences. Genes modified using CRISPR/Cas technology remain under their normal endogenous expression control elements without the random integration or exogenously introduced transgene as found in conventional gene therapy methods [2].

Vectors derived from small AAV are a very useful delivery system for the treatment of eye diseases since many of the AAV serotypes are able to transduce a variety of ocular cell types in a stable manner with high efficiency [5]. In addition, AAVs have a relatively reduced immunoreactivity in the eye compared to other viral transduction methods, such as adenovirus. However, due to limitations of its cargo capacity, a single AAV vector is unable to package the Cas9 nuclease from the bacterial species Staphylococcus pyogenes (SpCas9, size ~4.2 kb), the most commonly used CRISPR-Cas system, with its accompanying sgRNA. Therefore, a dual AAV vector system was used in the first description of SpCas9-mediated in vivo genome editing in the adult mouse retina [6].

In this chapter, to outline the steps required for CRISPR/Cas-mediated gene editing in the retina using a dual viral delivery system, we designed sgRNA constructs to disrupt a yellow fluorescent protein (YFP) in vitro and in vivo in a transgenic mouse. This methodology can be readily adapted to single AAV system using smaller Cas9 orthologues [7].

2   Materials

2.1   sgRNA Design and Vector Construction

1. sgRNA design programs:
   (a) Benchling: https://benchling.com/
   (b) Zhang lab (Broad Institute): http://crispr.mit.edu/
   (c) CRISPR RGEN Tools: www.rgenome.net/
2. Oligonucleotides and primers.
3. CRISPR constructs were obtained from Addgene and were gifts from Dr Feng Zhang (Broad Institute, USA). The AAV transfer vectors used were pX551 (Addgene plasmid#60957), which contains the SpCas9, and pX552-mCherry (modified from Addgene plasmid#60958), which contains the sgRNA scaffold and mCherry reporter gene.
4. T4 DNA ligase and T4 DNA ligase buffer. (New England Biolabs)
5. T4 polynucleotide kinase. (New England Biolabs)

6. Thermal cycler.

7. SapI restriction enzyme. (New England Biolabs)

8. CutSmart buffer (New England Biolabs).

9. Calf intestinal alkaline phosphatase. (New England Biolabs)

10. 1% Agarose gel in electrophoresis buffer.

11. QIAquick or other Gel Extraction kit.

12. UltraPure DNase/RNase-free distilled water.

13. PlasmidSafe ATP-dependent exonuclease (Epicentre).

14. 10× PlasmidSafe buffer.

15. 10 mM ATP. (New England Biolabs)

16. DH5α chemically competent *E. coli*. (Life Technologies)

17. SOCS media (Sigma-Aldrich).

18. Luria Broth Base (LB media) supplemented with 100 μg/mL ampicillin. Prepare from a 100 mg/mL sodium ampicillin stock.

19. LB agar plates: LB agar plates supplemented with 100 μg/mL ampicillin.

20. Plasmid QIAprep or other spin miniprep kit.

21. U6 sequencing primer (5′-GAGGGCCTATTTCCCATGAT TCC-3′).

2.2 Cell Culture and Transfection

1. HEK293D was a gift from Prof Ian Alexander (Children's Medical Research Institute, Australia). HEK293A (catalogue no. R70507, Life Technologies) and NIH3T3L1 cells (catalogue no. ATCC CL173; American Type Culture Collection) were transduced with pAS2.EYFP.puro lentivirus (RNAiCore; Academia Sinica) to generate YFP-expressing cell lines (HEK293A-YFP and NIH3T3L1-YFP) for the in vitro tests.

2. DMEM/10% FBS culture medium: Dulbecco's modified Eagle's medium (DMEM; Life Technologies) supplemented with 10% fetal bovine serum (FBS; Sigma-Aldrich) and 2 mM L-glutamine.

3. DMEM/2% FBS maintenance medium: DMEM supplemented with 2% FBS and 2 mM L-glutamine.

4. Dulbecco's phosphate-buffered saline without Ca^{2+} and Mg^{2+} (DPBS-; Life Technologies).

5. 0.25% Trypsin–EDTA: 0.25% Trypsin–EDTA (Life Technologies) containing phenol red.

6. IMDM/10% FBS transfection medium: Iscove's Modified Dulbecco's Medium (IMDM; Life Technologies) supplemented with 10% FBS.

7. Lipofectamine 2000 (Life Technologies).

8. Fugene HD (Promega).

9. Opti-MEM® I reduced serum medium (Life Technologies).

2.3 Indel Assay

1. QIAamp or other DNA mini kit.

2. SURVEYOR assay kit (Integrated DNA Technologies).

3. KOD or other high fidelity thermostable DNA polymerase.

4. 1× hybridization buffer: 10 mM Tris–HCl pH 8.8, 1.5 mM $MgCl_2$, 50 mM KCl.

5. 1.8% agarose gel: 1.8% agarose gel in 0.5× Tris/Borate/EDTA (TBE) buffer.

6. GelRed nucleic acid gel stain (Biotium).

7. QuickExtract DNA Extraction Solution (Epicentre).

8. Taq DNA polymerase with ThermoPol buffer (New England Biolabs).

9. pCR2.1-TOPO TA cloning kit (Life Technologies): Cloning kit containing salt buffer (1.2 M NaCl, 0.06 M $MgCl_2$), pCR™2.1-TOPO® vector in storage buffer, 10× PCR Buffer, dNTP Mix.

10. YFP indel PCR primers (Forward primer: 5′-ATGGTGAGCAAG GGCGAGGA-3′; Reverse primer: 5′-TTACTTGTACAGCTC GTCCA-3′).

11. FACS sorter (FACS ARIA-I, BD).

12. ONE shot top10 or other competent bacteria.

13. LB agar X-gal/IPTG plates: Before plating, supplement 100 mL of 50 °C fluid LB agar with 100 μg/mL ampicillin, 100 μl 20 mg/mL X-gal solution, and 100 μl 100 mM IPTG solution.

14. M13 forward (−20) sequencing primer (5′-GTAAAACGA CGGCCAG-3′).

15. EcoRI restriction enzyme. (New England Biolabs)

2.4 Viral Production

1. AAV2 packaging system (pXX2 [packaging/capsid plasmid] and pXX6 [helper plasmid], a gift from Prof. Richard J. Samulski, University of North Carolina, USA) [8].

2. 10% TE buffer (1 mM Tris–HCL, 0.1 mM EDTA, pH 8).

3. 2× Hepes-buffered saline (HBS; 280 mM NaCl, 50 mM HEPES, pH 7.1).

4. AAVpro® AAV2 purification kit (Clontech Laboratories) containing AAV Extraction Solution A, AAV Extraction Solution B, Equilibration Buffer, Washing Buffer, Elution Buffer, prepacked AAV purification columns, Filter Device, SD Buffer, Suspension Buffer, Collection tubes.

5. Wizard® SV or other Gel and PCR clean-up kit. (Promega)

6. Primers for AAV titration (pX551 Forward primer: 5′-CCGAA GAGGTCGTGAAGAAG-3′, pX551 Reverse primer: 5′-GCC TTATCCAGTTCGCTCAG-3′, pX552 Forward primer: 5′-TG TGGAAAGGACGAAACACC-3′, pX552 Reverse primer: 5′-TGGTCCTAAAACCCACTTGC-3′).

7. Fast SYBR green master mix (Life Technologies).

8. StepOne™ or other Real-Time PCR System.

9. 1.5 mL Eppendorf tubes.

2.5   Intraocular Injection

1. 30-gauge needle (30 G × 1 in.; BD, ice cold).

2. Hand-pulled glass micropipette (6 in., 1.0 mm OD; Life technologies).

3. Sutter P-97 pipet puller.

4. Winged infusion set.

5. Clay material. Clay to connect the pulled 100 μm diameter micropipette needle to the winged infusion set.

6. UMP3 ultra micro pump with controller (World Precision Instruments).

7. 10 mL syringe.

8. 10 μL Hamilton syringe.

9. Anesthetic cocktail: 1.6 mL 100 mg/mL Ketamine, 1.6 mL 20 mg/mL xylazine, and 6.8 mL 0.9% w/v sodium chloride.

10. Isoflurane.

11. Curved dressing forceps.

12. 0.5% w/v chloramphenicol Chlorsig or other antibiotic Eye Drops.

13. 0.9% w/v sodium chloride (sterile saline).

14. Heating pad to maintain normal body temperature.

2.6   Retinal Tissue Processing

1. 4% paraformaldehyde (PFA; ProSciTech), ice-cold.

2. NucBlue® Live ReadyProbes® reagent (Life Technologies).

3. Fluorescence mounting medium (Dako).

4. Coverslips (22 × 22 mm; Fisher Scientific).

5. Papain dissociation system (Worthington Biochemical Corporation).

6. 350 mg/kg Lethabarb (pentobarbital).

7. Phosphate-Buffered Saline (PBS).

8. 1% Triton X-100.

9. 75% ethanol.

10. Small micro scissor.

11. Blunt-edged forceps.

12. Microscopic slide.

13. Microscope slide storage box.

14. Kimwipes.

2.7 Electro-
retinography
and Optical Coherence
Tomography

1. Electrode wire (0.3 mm diameter 99.9% Silver round wire, A&E Metal Merchants).

2. Insulating tape (Masking tape).

3. Tape or Velcro.

4. 9 V Chloriding battery (Energizer).

5. Platinum electrode leads (Grass Telefactor).

6. Electrode holders (Micromanipulators, World Precision Instruments).

7. Ground electrode: F-E2-30 (Needle electrode, Grass Telefactor).

8. Headlight for preparation (Energizer HD+ LED headlight, Energizer).

9. 0.5% Tropicamide Dilating agent.

10. 0.5% Proxymetacaine corneal anesthesia.

11. 1% Sodium carboxymethylcellulose contact gel.

12. Light stimulus via Ganzfeld integrating bowl (36 cm diameter, 13 cm aperture size, Photometric Solutions International).

13. Bioamplifier (ML 135, ADInstruments).

14. Data acquisition system (Powerlab ML 785 data acquisition system, ADInstruments).

15. Data Acquisition software (Scope Software, version 3.7.6, ADInstruments).

16. Computer: Personal computer (Windows based) for recording signals for offline analysis.

17. Temperature maintenance (Circulating water bath, LAUDA-Brinkmann).

18. Faraday Cage (2 × 1.2 × 1.2 m, Photometric Solutions International).

19. Analysis Software (R statistical environment current version 3.3.2, for data analysis).

20. Spectral domain optical coherence tomography (SD-OCT, Envisu R2200 VHR, Bioptigen Inc.).

21. Mouse platform (Bioptigen Inc.).

22. Ocular lubricant (Systane, Alcon Laboratories).

23. Analysis software (FIJI [https://fiji.sc/]).

2.8 Plasticware	1. T170 tissue culture flask.
	2. T75 tissue culture flask.
	3. 100 × 20 mm TC culture dish.
	4. 14 mL polypropylene round-bottom tube.
	5. 6 well clear flat bottom TC-treated multiwell cell culture plate.
	6. 12 well clear flat bottom TC-treated multiwell cell culture plate.
	7. 5 mL round bottom polystyrene test tube with cell strainer snap cap.
	8. Cell scraper.

3 Methods

3.1 sgRNA Selection and In Vitro Validation

3.8.1 sgRNA Design and Cloning

1. Put the target genome sequence into the sgRNA online programs and select the top three 20 nt sgRNA target sequences.

2. To clone the YFP-targeting sgRNA into pX552 plasmid, order top and bottom complementing oligonucleotides with SapI restriction enzyme overhangs (Fig. 1a) [9]. Cloning strategy follows the protocol from Dr Feng Zhang's laboratory.

3. Anneal and phosphorylate the sgRNA oligos in a 10 μL reaction containing: 1 μL 100 μM top oligo, 1 μL 100 μM bottom oligo, 1× T4 DNA ligase buffer, 10 U T4 polynucleotide kinase. Incubate the reaction mix at 37 °C for 30 min to phosphorylate the oligos followed by denaturation at 95 °C for 5 min and ramping down to 25 °C at a rate of 5 °C per minute to anneal the sgRNA oligos.

4. Dilute the annealed oligo 1:50 in nuclease-free water.

5. Digest 2 μg of pX552 plasmid in a 50 μL reaction with 10 U SapI restriction enzyme and 1× CutSmart buffer. Incubate at 37 °C for 1 h to overnight.

6. Add 10 U calf intestinal alkaline phosphatase to the reaction and incubate for an additional hour at 37 °C to dephosphorylate the digested ends of the vector to prevent religation of the empty vector.

7. Run the digested pX552 plasmid on a 1% agarose gel and gel purify the DNA fragment with the Gel Extraction kit following manufacturer's instructions. Elute in a final volume of 30 μL nuclease-free water.

8. To ligate the annealed sgRNA oligo to the SapI-digested pX552 plasmid, set up the following 10 μL reaction mixture: 25 ng SapI-digested pX552 plasmid, 1 μL diluted annealed sgRNA oligo, 1× T4 DNA ligation buffer, and 800 U T4 DNA ligase. Incubate at 16 °C overnight.

A.

Additional G for U6 promoter

SapI overhang   ↓   sgRNA guide target sequence

Top oligo   5`- ACCGNNNNNNNNNNNNNNNNNNNNNNNN -3`

Bottom oligo   3`- CNNNNNNNNNNNNNNNNNNNNNNNNCAA -5`

Reverse complementary to   SapI overhang
sgRNA guide target sequence

B.

C.
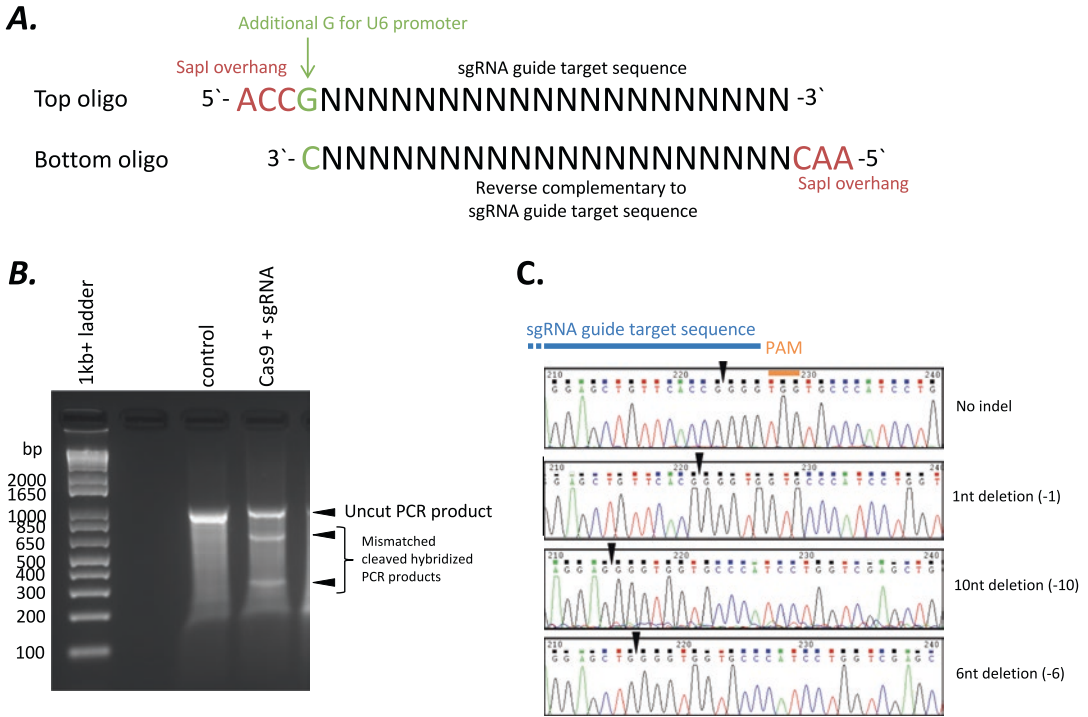
Fig. 1 CRISPR cloning and in vitro testing set up. (**a**) sgRNA design for cloning into the SapI site in the pX552-mCherry construct. Note if sgRNA guide sequence begins with a G, the additional G for U6 promoter priming will not be required. (**b**) An example of SURVEYOR assay results after cleavage of mismatched sites of SURVEYOR hybridized PCR products. The mismatch is caused by any indel introduction at the sgRNA cleavage site. The PCR fragments are resolved on a 1.8% TBE agarose gel. (**c**) Example of sequencing results from TA cloning. The frequency of each type of indel introduced is then plotted on a graph to look at the spectrum of indels generated by the particular sgRNA

9. Digest residual linearized DNA with PlasmidSafe exonuclease by adding the following to the ligation reaction mix: 1.5 μL 10× PlasmidSafe buffer, 1.5 μL 10 mM ATP, 10 U PlasmidSafe exonuclease, and 1 μL nuclease-free water. Incubate at 37 °C for 30 min and inactivate the enzyme by incubation at 70 °C for 30 min.

10. Transform the ligation mixture into DH5α chemically competent *E. coli* following manufacturer's protocol. Briefly, add 5 μL of the ligation mixture to 50 μL DH5α bacteria and incubate on ice for 30 min. Heat-shock to transform the bacteria by incubating at 42 °C for 20 s. Immediately transfer the bacteria mixture back on ice for approximately 2 min. Add 500 μL SOCS media and incubate at 37 °C for 1 h with shaking at 225 rpm. Pellet bacteria and spread on LB agar plates with 100 μg/mL ampicillin. Incubate the plate overnight at 37 °C.

11. The following day, pick several bacterial colonies for miniprep cultures (5 mL LB media with 100 μg/mL ampicillin) and incubate at 37 °C overnight with 225 rpm shaking.

12. Extract the plasmid DNA using the spin miniprep kit following manufacturer's instructions. Elute plasmid DNA in 50 μL nuclease-free water.

13. Validate the sgRNA sequence by sequencing the plasmid with the U6 sequencing primer.

3.1.1 Transfection of HEK293A-YFP Cells with the CRISPR Constructs

1. The day before transfection, seed 0.75×10^5 HEK293A-YFP per well of 12-well plates in DMEM/10% FBS culture media. The following day, change media on the cells before setting up transfection reaction.

2. Set up the transfection reaction with 500 ng pX551 and 500 ng pX552-mCherry containing the cloned YFP-targeting sgRNA in 47 μL Opti-MEM. Mix the reaction mixture.

3. Add 3 μL of Fugene HD, vortex to mix the reaction thoroughly and pulse spin. Incubate at room temperature for 10 min to allow for DNA transfection complex formation.

4. Add the transfection mixture to the cells dropwise and mix into the medium by swirling the plate several times before placing the plate in 37 °C incubator with 5% CO_2.

5. Change the media the following day.

6. On the third day after transfection harvest the cells for genomic DNA using the DNA mini kit following the manufacturer's protocol and eluting in 30 μL nuclease-free water.

3.1.2 SURVEYOR Assay to Detect CRISPR/Cas9 Cleavage

1. To determine and compare the cleavage activity of the sgRNA and SpCas9 complex in the HEK293A-YFP cells, we used the SURVEYOR assay with PCR products amplified from the extracted genomic DNA spanning the hypothesized cleavage area. For each sgRNA tested set up 2–4 tubes of PCR reaction using KOD polymerase following manufacturer's protocol.

2. Run the PCR reaction on an agarose gel and purify the PCR fragment using the Gel Extraction kit following manufacturer's instructions. Elute in a final volume of 30 μL nuclease-free water.

3. To set up the SURVEYOR assay, take 200–400 ng of the PCR sample to hybridize in 1× Hybridisation buffer (10 mM Tris–HCl pH 8.8, 1.5 mM $MgCl_2$, 50 mM KCl) in a total of 20 μL reaction. To hybridize the PCR products, first dissociate the oligos by heating at 95 °C for 10 min and anneal by ramping down to 25 °C (at 5 °C per minute).

4. After the heteroduplex formation of the PCR product add the following from the SURVEYOR assay kit to each 20 μL reaction: 2.4 μL 0.15 M $MgCl_2$ solution, 1 μL SURVEYOR

Enhancer S, and 1 μL SURVEYOR Nuclease S. Incubate the reaction mix at 42 °C for 1 h.

5. To terminate the reaction add 2.5 μL of the Stop Solution.

6. To resolve the PCR fragments run the samples on a 1.8% agarose gel. SURVEYOR nucleases cleaves mismatched sites in DNA heteroduplexes, therefore any CRISPR-Cas9 mediated cleavage generated indels in the genomic DNA can be detected through mismatches with the control samples (Fig. 1b).

3.1.3 TA-Cloning to Determine CRISPR-Mediated Indel Frequency In Vitro

1. Plate NIH3T3L1-YFP cells at 1.2×10^5 cells per well of the 6-well plate in DMEM/10% FBS media and culture at 37 °C with 5% CO_2.

2. Change the media on the cells to 1.5 mL per well the following day before setting up the transfection mix.

3. Set up the transfection reaction mixture with 1.5 μg of the pX551 and pX552-mCherry containing the cloned YFP-targeting sgRNA each in 150 μL total reaction in Opti-MEM. Add 7 μL Fugene HD, mix and pulse-spin the reaction mixture. Incubate at room temperature for 10 min to allow for the DNA transfection complex to form.

4. Add the DNA transfection complex dropwise to the cells.

5. Twenty-four hours post-transfection, change the media on the cells.

6. Three days post-transfection, FACS sort mCherry positive cells and extract genomic DNA using 30 μL QuickExtract DNA extraction solution. Heat the samples to 65 °C for 20 min, 68 °C for 20 min and lastly at 98 °C for 20 min (*see* **Note 1**).

7. Amplify a PCR product spanning the YFP cleavage site using Taq DNA polymerase with ThermoPol Buffer following the manufacturer's protocol.

8. Use 4 μL of the PCR reaction in the TOPO TA cloning reaction with 1 μL salt solution and 1 μL of the TOPO vector. Incubate at room temperature for 10 min.

9. Transform 2 μL of the TOPO TA cloning reaction into ONE shot TOP10 competent bacteria following manufacturer's protocol.

10. Plate bacteria on LB ampicillin agar plates supplemented with X-gal/IPTG to allow for blue/white LacZ selection. Incubate plates at 37 °C overnight.

11. Pick 50–100 white bacteria colonies for miniculture overnight at 37 °C with shaking at 225 rpm.

12. Extract the plasmid DNA using the spin miniprep kit following manufacturer's instructions. Elute plasmid DNA in 50 μL nuclease-free water.

13. Set up diagnostic digests with EcoRI restriction enzyme to confirm ligation of inserts before submitting samples for sequencing with M13 sequencing primer.

14. Analyze the sequences, tally and graph the number and frequency of the indels (Fig. 1c).

3.2 Recombinant AAV2 Production

3.2.1 Production of AAV2 Utilizing Calcium Phosphate Transfection

1. Twenty-four hours before transfection, seed HEK293D cells in DMEM/10% FBS culture medium into 50 tissue culture dishes (100×20 mm) at 7×10^6 cells/dish (*see* **Note 2**).

2. Remove old medium and leave ~1 mL to cover the cell sheet and add 9 mL transfection medium (IMDM/10% FBS) 2 h before transfection (*see* **Note 3**).

3. Triple plasmid transfection (25 μg DNA/dish: 5 μg transfer vector [pX551 or pX552-mCherry containing the cloned YFP-targeting sgRNA], 5 μg packaging/capsid plasmid [pXX2] and 15 μg helper plasmid [pXX6]) can be performed with the Calcium Phosphate method.

   (a) Prepare transfection solution A and B in the following order in a 50 mL falcon tube (Table 1), respectively (the following volume is used to transfect 50 tissue culture dishes):

   (b) Aliquot 2 mL of solution A and B to separate 14 mL poly-propylene round-bottom tubes, respectively.

   (c) Add solution B dropwise to solution A to precipitate the DNA with P200 pipette while gently agitates to mix the cocktail (*see* **Note 4**).

   (d) Incubate the cocktail for 20–30 min at room temperature and pipette 1 mL dropwise into each of the 50 tissue culture dishes (100×20 mm) of HEK293D cells.

   (e) Twenty-four hours post-transfection, remove old medium and leave ~1 mL to cover the cell sheet and add 11 mL maintenance medium (DMEM/2% FBS).

   (f) Forty-eight hours post-transfection, harvest the HEK293D cells as described below in Subheading 3.2.2.

3.2.2 Isolation, Purification and Concentration of AAV2

1. Using a cell scraper, scrape the transfected HEK293D cells from each culture dish and place in 50 mL falcon tubes.

2. From this step, follow the modified manufacturer's instructions to extract AAV2 vectors. Briefly, centrifuge cells at $1750 \times g$ for 10 min at 4 °C. Remove the supernatant, leaving approximately 5 mL. Loosen the cell pellets by tapping and collect all cells in a single 50 mL falcon tube. Centrifuge at $1750 \times g$ for 10 min at 4 °C. Completely remove the supernatant and collect the cell pellet.

3. Loosen the cell pellet completely by tapping or vortexing.

Table 1
Solution preparation for triple plasmid transfection

Order to add reagent	Reagent	Amount
Solution A		
1	2× HBS	24.8 mL
2	NaH_2PO_4	250 μL
Solution B		
1	10% TE	Add to 25 mL
2	Transfer vector	125 μg
3	pXX2	125 μg
4	pXX6	375 μg
5	2 M $CaCl_2$	3.1 mL

4. Add 10 mL of AAV Extraction Solution A.

5. Suspend the cells by vortexing for 15 s and leave the tube for 5 min at room temperature. Then vortex for 15 s.

6. Centrifuge extracts at 2000–14,000 × g for 10 min at 4 °C. If the titer of the recovered AAV2 vector is low, the efficiency may be increased by repeating **steps 5** and **6**.

7. Recover the supernatant in a new sterile 50 mL falcon tube and add 1 mL of AAV Extraction Solution B. The mixture can be stored at −80 °C at this point. If sample is not stored, continue promptly to **step 8**. If sample has been stored at −80 °C, thaw quickly in a 37 °C water bath before proceeding to the next step.

8. Add 1 mL of SD Solution and incubate for 30 min at 37 °C. Then centrifuge at 2000–14,000 × g for 10 min at 4 °C, collect the supernatant as the crude AAV2 vector solution.

9. Set up the prepacked AAV purification column.

10. Remove and top and bottom caps and drain the excess solution. Equilibrate the column with 10 mL of Equilibration Buffer.

11. Add the crude AAV2 vector solution from **step 8** to the column and allow the solution to flow through.

12. Wash the column with 10 mL of the Washing Buffer.

13. Elute the AAV2 vectors with 3 mL of Elution Buffer in a sterile 15 mL centrifuge tube.

14. Set up the Filter Device in the collection tube. Add 500 μL of the eluted AAV2 vector solution from **step 12** to the Filter Device and centrifuge at 2000 × g for 10 min at 4 °C. Discard the flow-through.

15. Repeat **step 13** until all viral solution has been applied to the Filter Device. Ensure that the final volume of solution in the Filter Device is <100 μL.

16. Apply 400 μL of Equilibration Buffer to the Filter Device. Centrifuge at 2000 × g for 20 min at 4 °C, and discard the flow-through. Ensure that the final volume of fluid in the Filter Device is <100 μL.

17. Add 200 μL of Suspension Buffer to the Filter Device and pipette at least 100 times to wash the membrane of the Filter Device. The amount of Suspension Buffer to recover the AAV2 vectors can be adjusted to reach a desirable final titer to suit different settings.

18. Invert the Filter Device and recover the Suspension Buffer in a new collection tube. Centrifuge at 1000 × g for 1 min at 4 °C. The solution recovered is the purified and concentrated rAAV2 particles.

3.2.3 Preparation of Standards

1. Prepare 1 μg of linearized vector plasmid by restriction digest. Purify the linearized plasmid with purification kit (PCR clean-up systems).

2. Assay the concentration of the linearized plasmid by spectro-photometry. To make up the 1×10^9 vg/5 μl of the standard in 500 μL of TE buffer, refer to the formula as below.

$$\text{The amount of linearized plasmid in } 500 \text{ μL of TE buffer} = \frac{\text{vector plasmid length} \times 660}{6.022 \times 10^3} \quad (1)$$

3. Make a serial tenfold dilution in TE buffer by adding 100 μL of 1×10^9 vg/5 μl linearized plasmid to 900 μL of TE buffer. Successfully dilute the rest of the series to yield a total of eight dilutions.

3.2.4 AAV2 Titration by Quantitative PCR

1. Make 10,000- and 100,000-fold dilution of AAV2 vectors in TE buffer.

2. Prepare the quantitative PCR master mix in a 1.5 mL Eppendorf tube as seen in Table 2 (25 μL/reaction).

3. Dispense 20 μL of PCR master mix into triplicate wells of a 96-well plate. Dispense 5 μL of each standard and 10,000- and 100,000-fold dilution of AAV2 vectors from **step 1**.

4. Seal the 96-well plate using ultraclear cap film, load the plate in the real-time PCR machine, and run using the program seen in Table 3.

Table 2
PCR mastermix for AAV2 titration

	Volume (μL)
dH$_2$O	7.3
Fast SYBR green master mix	12.5
Forward primer (100 μM)	0.1
Reverse primer (100 μM)	0.1
Standards or diluted vectors	5.0

Table 3
PCR settings for AAV2 titration

Cycle number	Denature	Anneal/extend
1	95 °C, 10 min	
2–40	95 °C, 15 s	60 °C, 60 s

5. Calculate the final AAV2 vector genome copy using the formula as below:

$$\text{Titer}\left(\text{viral genome} / \text{mL}\right) = \left(C_1 \times 10{,}000 + C_2 \times 100{,}000\right) \times 100 \text{ vg} / \text{mL}$$

Where C_1 and C_2 is average copy number of respective 10,000- and 100,000-fold diluted AAV2 vectors from quantitative PCR runs.

3.3 In Vivo AAV Delivery in Mouse Retina

1. Make a 100 μm diameter needle by manually pulling a glass capillary tube with a Sutter P-97 pipet puller. The end of the capillary tube will be heated and pulled until it reaches the desired diameter (100 μm).

2. Connect the 100 μm diameter needle to a winged infusion set by a bit clay (removing the needle from the tubing).

3. Fill a 10 mL syringe with sterile saline and connect to another end of winged infusion set (trim the tip of capillary needle to allow for flow per se). Eject sterile saline to fill the dead space in the tubing and capillary needle.

4. Dissemble 10 mL syringe and connect the winded infusion set to 10 μL Hamilton syringe which is mounted to a UMP3-2 Ultra Micro Pump. Next, aspirate approximately 1 μL of air, into the tip of the capillary needle. This will separate the saline

from the injection substances and provide a visible cue indicating the end of the injection during the surgical procedure.

5. Aspirate injection substance containing the desired volume of viral vectors. The amount can be 1 μL for mouse.

6. Anesthetize mouse by allowing mouse to inhale isoflurane. Pull apart the eyelids with curved dressing forceps to expose the eye for injection.

7. Prior to injection, make a guide tunnel by carefully inserting a 30-gauge needle directly into the sclera away 1 mm from limbus of mouse. Do not go too deep or you may hit the lens or retina.

8. Inject 1 μL of viral vectors through the guide hole into the vitreous by Ultra Micro Pump.

9. After surgery, apply one drop of Chlorsig and wake the mouse from anesthesia. The mouse should be kept on a heating pad to maintain normal body temperature during the procedure.

3.4 In Vivo Validation of Retinal Genome Editing

3.4.1 Retinal Wholemount

1. Mouse is euthanized by intraperitoneal injection of pentobarbital (350 mg/kg Lethabarb).

2. Enucleate the eyeball and fix with ice-cold 4% PFA for 1 h, and then transfer into Phosphate-Buffered Saline (PBS) (*see* **Note 5**).

3. Remove the cornea in a circular way along the ora serrate using small micro scissor. Gently pull out the lens and remove as much vitreous as possible by blunt-edged forceps (*see* **Note 6**).

4. Place the eyecup onto a microscopic slide with PBS. To achieve a flat preparation, make four incisions from the periphery half way to the optic nerve head by micro scissors. Carefully detach the retina from the eyecup using forceps and separating bluntly from optic nerve head to periphery retina.

5. Staining of retina:

    (a) Fix the retina with 75% ethanol at 4 °C for 30 min and wash twice with PBS.

    (b) Incubated the retina with 1% Triton X-100 at room temperature for 20 min, then wash twice with PBS.

    (c) Use NucBlue® Live ReadyProbes® reagent (1 drop in 1 mL PBS) to stain the nucleus for 10 min at room temperature. Wash with PBS afterward.

    (d) Carefully dry the area around retina with Kimwipes. Apply a drop of mounting medium to preserve fluorescence, cover with coverslip and keep in a storage box at 4 °C for longer use.

6. Retinal cell quantification (percentage of YFP disruption) is performed using individual fluorescent images captured at
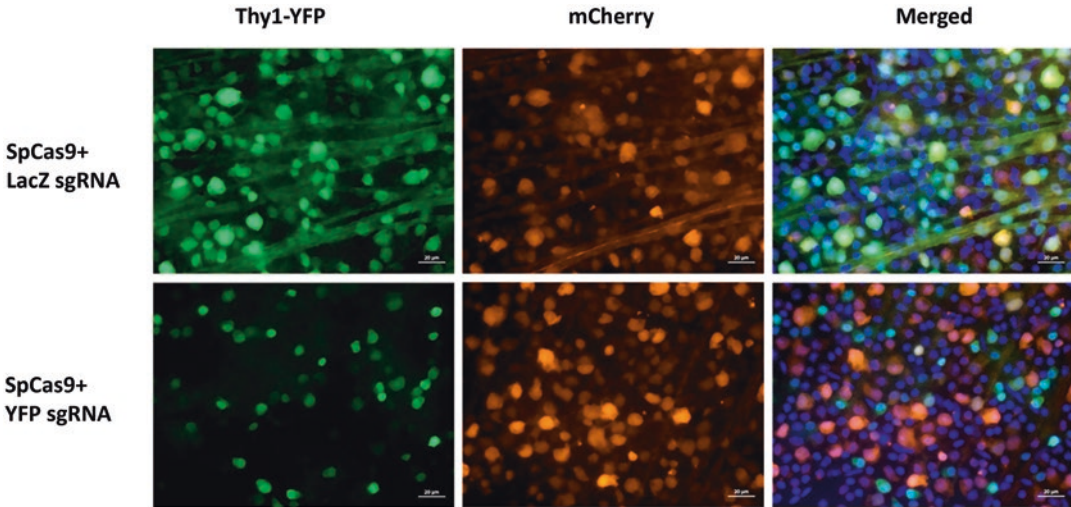
Fig. 2 CRISPR/Cas-mediated gene editing of retinal cells in vivo. Higher magnification of flat-mount images, displaying differences in YFP expression following AAV2-mediated delivery of SpCas9/LacZ-sgRNA (upper images) or SpCas9/YFP-sgRNA (lower images). Scale bar: 20 μm

×400 magnification. The efficiency of YFP disruption is determined by the proportion of YFP-negative cells among mCherry-expressing cells (Fig. 2).

3.4.2 Retinal Dissociation and FACS

1. After removing the cornea, lens, and vitreous from enucleated eye ball, the retina is dissected out and place in a 1.5 mL centrifuge tube with cold PBS.

2. Retinal dissociation is performed using Papain dissociation system following the manufacturer's protocol for dissociation medium preparation and dissociation procedure [10].

3. AAV2 transduced retinal cells (mCherry positive) are sorted by FACS from three dissociated retinas.

4. The percentage of YFP disruption is quantified by FACS and sorted cells are subjected to TA-cloning assay for validating the CRISPR-mediated indel frequency as described previously Subheading 3.1.3, **step 3**.

3.5 Retinal Function and Morphology Assessment

3.5.1 Electroretinography for Retinal Function Assessment

Dark-adapted full-field ERG was utilized to examine retinal function as described previously [11, 12].

1. For recording from both eyes, four electrodes are needed. Prepare electrodes by attaching silver wire to platinum leads. Use masking tape to insulate the connections leaving a 1 mm rounded tip of silver wire exposed to make contact with the eye. For the reference electrodes, create a 4–5 mm diameter loop for the electrode to slide around the equator of the eye without squeezing the eye.

2. Chloride the silver tips by immersing them into 0.9% saline and connecting the leads to a 9 V battery and completing the circuit using another length of conductive wire. Chloride for 10 s until the silver wire is coated with a layer of white salt. Prior to use, lightly dust off any excess salt, which can damage the cornea.

3. Mice are dark-adapted overnight (12 h) prior to recording [13].

4. Unwanted light exposure is minimized during anesthesia and electrode setting to ensure maximal retinal sensitivity and optimize recording of ganglion cell response. Throughout preparation use a headlight to provide dim red illumination. This helps to maintain dark-adaptation prior to signal recording.

5. Anesthetize mice using an intraperitoneal injection of ketamine (60 mg/kg) and xylazine (5 mg/kg).

6. Dilate pupils using one drop of 0.5% tropicamide and place a drop of 0.5% proxymetacaine onto each eye for corneal anesthesia. Leave for 5 s and dab off any excess fluid from the margin of the eyelids.

7. Place mice on a platform warmed using circulating heated water (Lauda). Electrically warmed heating pads will generate electrical noise.

8. Insert the needle electrode into the tail about half way up.

9. Gently place the loop electrodes around each eye, using tape or Velcro to ensure that the loops remain around the equator of the eyes. Ensure that the loops do not squeeze the eyes as this will increase eye pressure, which can cause a reduction in the ERG.

10. Using micromanipulators to allow for fine adjustment position the tips of the active electrodes to gently touch the corneal apex. Place a small drop of contact gel onto the active electrode tip to improve electrical contact and maintain corneal hydration. Avoid letting the lubricant make contact with both active and reference electrodes. Connect all leads.

11. Move the stimulus so that the eyes are in the plane of the Ganzfeld sphere. Close the faraday cage.

12. Allow at least 5 min for redark adaption, to let the eye recover full scotopic sensitivity after electrode placement.

13. Stimuli are delivered starting with the dimmest light level (-6.35 log cd·s/m^2) and progressing to the brightest (2.07 log cd·s/m^2). Signal averaging may be needed to remove random noise arising from animal (breathing and other small in voluntary movements) and environment related sources of noise. Average enough signals for a signal to noise ratio of >5.

14. Signals are acquired using a data acquisition system (ML785 Powerlab 8SP) using Scope™ software with 2560 points at a 4-kHz sampling rate with band-pass filter settings of 0.3–1000 Hz (−3 dB).

15. The very first electronegative component of the ERG waveform (the a-wave) in response to the brightest stimuli can be modelled using a delayed-Gaussian function (Fig. 3a), which describes the underlying P3 generated by the photoreceptors [14]. The maximal amplitude (designated RmP3) returned by this model reflects photoreceptor function (number of photoreceptors, outer segment length or density of nonspecific cationic channels). The second and largest component of the ERG waveform (the b-wave) is the combination of the photoreceptoral and an ON bipolar cell component. Subtracting the delayed-Gaussian model from the raw ERG waveform reveals a putative ON bipolar cell response (P2). The amplitude of each P2 waveform can be plotted as a function of intensity and modeled with classical agonist-receptor characteristics using a hyperbolic curve [15]. This model returns a maximum amplitude, which provides an index of bipolar cell integrity. The small high frequency wavelets that overlie the P2 leading edge, known as oscillatory potentials (OPs), can be isolated from the P2 using a digital band-pass filter (50–180 Hz, −3 dB), to provide an index of amacrine cell derived inner retinal inhibitory pathways. Finally, the positive STR (pSTR), which can be measured near absolute light threshold is a good indicator of retinal ganglion cell function in rodents (Fig. 3a) [11].

3.5.2 Optical Coherence Tomography for Retinal Morphology Assessment

1. Place the animal in the mouse platform add a drop of ocular lubricant to smooth the corneal surface.

2. For retinal imaging choose the mouse retinal lens and the "Mouse Porter". Enter animal identification details. Choose the appropriate reference arm position for the mouse retina as directed by the manufacturer.

3. Choose a scan pattern, for example 1.4 × 1.4 mm volume scan with a depth of 1.7 mm (1000 A-scans per B-scans, 200 horizontal B-scans evenly spaced in the vertical dimension).

4. Align the optical axis of the eye along the objective lens. Move the objective lens to within 10–15 mm from the eye.

5. Choose "free run" which provides simultaneously a vertical B-scan along with an en-face image. Align the eye such that the region of interest (e.g., the optic nerve) is located at the center of the imaging area.

6. Once the region of interest is centered, stop "free run" and choose "Aim", which allows both vertical and horizontal B-scans through the center of the imaging area to be viewed at the same time. Adjust horizontal and vertical B-scan so that they are both straight. Acquire the volume.
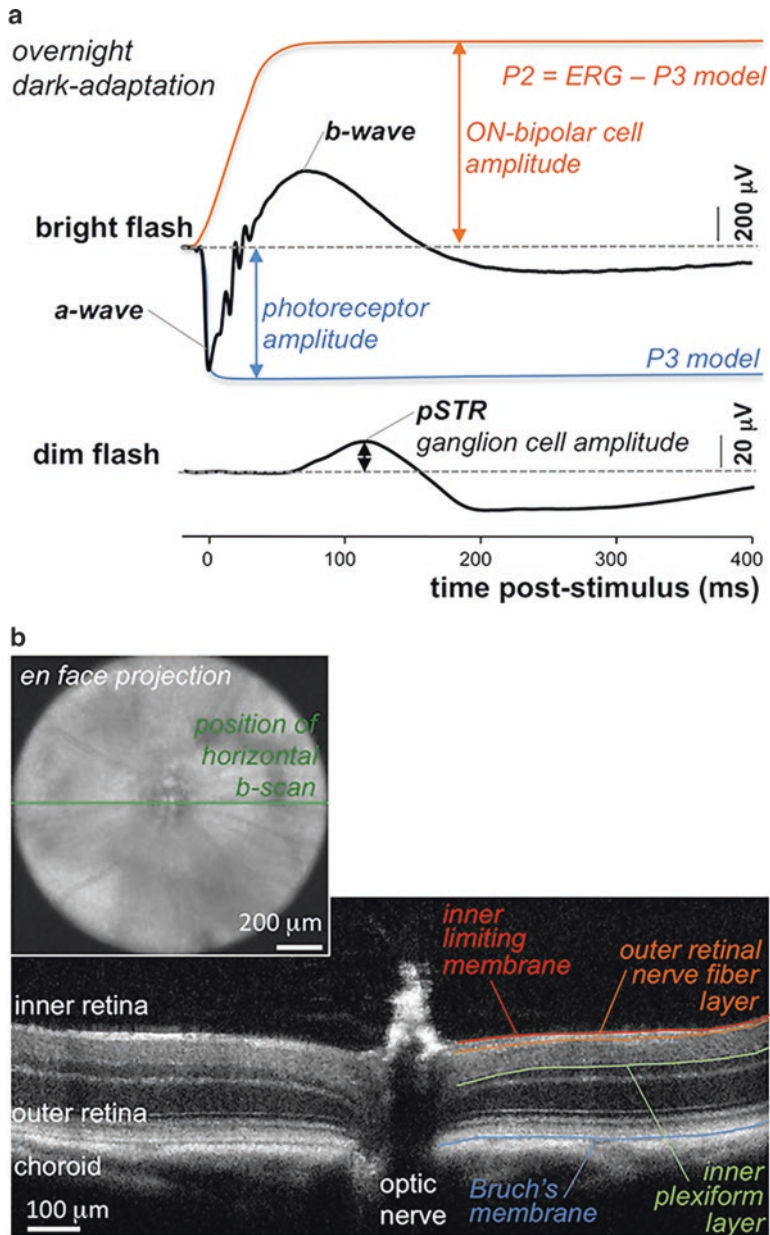
Fig. 3 Retinal function and morphology assessment. (**a**) Scotopic ERG response analysis. (**b**) Optical coherence tomography analysis

7. Image analysis can be undertaken via automated segmentation or manual segmentation. Manual segmentation by a masked observer can be undertaken using FIJI software (https://fiji.sc/). B-scans through the center of the optic nerve are analyzed by manually tracing the inner boundary of the retinal nerve fiber layer (inner limiting membrane), the outer boundary of the

retinal nerve fiber layer, the inner plexiform layer and Bruch's membrane. From these boundaries Total retinal thickness (inner limit membrane to retinal pigment epithelium), retinal nerve fiber layer (RNFL; inner retinal surface to nerve fiber layer) and ganglion cell complex (GCC) thickness (inner retinal surface to inner plexiform layer). Thicknesses across a region of 200–400 μm from the center of the optic nerve and from both nasal and temporal retina are averaged (Fig. 3b).

4 Notes

1. Genomic DNA extraction using the QuickExtract solution results in a crude genomic prep and is used for low starting cell numbers. If there are sufficient cell numbers after FACS sorting the DNA mini kit (e.g., QIAamp) can be used instead to obtain purer genomic DNA extracts.

2. Do not allow cells to become overconfluent as the transfection ability will be compromised. If cells do become overconfluent, passage several times at a sub-confluent level before using for transfection.

3. Cells are very sensitive and fragile. Change medium on 4–5 dishes at a time, and leave 1 mL of old medium on cells so they do not dry out. Remove and replace with 9 mL medium, very gently using 25 mL disposable pipette.

4. Precipitate should be very fine and solution should look like diluted milk.

5. If the dissection cannot be performed immediately after enucleated, eyes should be fixed in 4% PFA for 1 h and then kept in PBS at 4 °C. It is highly recommended that the retina dissection should be performed as soon as possible after enucleation, best within 3–5 days; otherwise the eyes generally become too soft to dissect well.

6. To achieve high-quality retinal images, it is essential to remove as much vitreous as possible without retinal damage.

Acknowledgments

References

1. Chiang JP, Trzupek K (2015) The current status of molecular diagnosis of inherited retinal dystrophies. Curr Opin Ophthalmol 26:346–351. https://doi.org/10.1097/ICU.0000000000000185

2. Hung SS, McCaughey T, Swann O et al (2016) Genome engineering in ophthalmology: application of CRISPR/Cas to the treatment of eye disease. Prog Retin Eye Res 53:1–20. https://doi.org/10.1016/j.preteyeres.2016.05.001

3. McCaughey T, Sanfilippo PG, Gooden GE et al (2016) A global social media survey of attitudes to human genome editing. Cell Stem Cell 18:569–572. https://doi.org/10.1016/j.stem.2016.04.011

4. Mali P, Yang L, Esvelt KM et al (2013) RNA-guided human genome engineering via Cas9. Science 339:823–826. https://doi.org/10.1126/science.1232033

5. Day TP, Byrne LC, Schaffer DV et al (2014) Advances in AAV vector development for gene therapy in the retina. Adv Exp Med Biol 801:687–693. https://doi.org/10.1007/978-1-4614-3209-8_86

6. Hung SS, Chrysostomou V, Li F et al (2016) AAV-mediated CRISPR/Cas gene editing of retinal cells in vivo. Invest Ophthalmol Vis Sci 57:3470–3476. https://doi.org/10.1167/iovs.16-19316

7. Ran FA, Cong L, Yan WX et al (2015) In vivo genome editing using Staphylococcus aureus Cas9. Nature 520:186–191. https://doi.org/10.1038/nature14299

8. Xiao X, Li J, Samulski RJ (1998) Production of high-titer recombinant adeno-associated virus vectors in the absence of helper adenovirus. J Virol 72:2224–2232

9. Swiech L, Heidenreich M, Banerjee A et al (2015) In vivo interrogation of gene function in the mammalian brain using CRISPR-Cas9. Nat Biotechnol 33:102–106. https://doi.org/10.1038/nbt.3055.

10. Feodorova Y, Koch M, Bultman S et al (2015) Quick and reliable method for retina dissociation and separation of rod photoreceptor perikarya from adult mice. MethodsX 2:39–46. https://doi.org/10.1016/j.mex.2015.01.002

11. Bui BV, Fortune B (2004) Ganglion cell contributions to the rat full-field electroretinogram. J Physiol 555(Pt 1):153–173. https://doi.org/10.1113/jphysiol.2003.052738.

12. Liu HH, Bui BV, Nguyen CT et al (2015) Chronic ocular hypertension induced by circumlimbal suture in rats. Invest Ophthalmol Vis Sci 56:2811–2820. https://doi.org/10.1167/iovs.14-16009

13. Behn D, Doke A, Racine J et al (2003) Dark adaptation is faster in pigmented than albino rats. Doc Ophthalmol 106:153–159

14. Hood DC, Birch DG (1994) Rod phototransduction in retinitis pigmentosa: estimation and interpretation of parameters derived from the rod a-wave. Invest Ophthalmol Vis Sci 35:2948–2961

15. Fulton AB, Rushton WA (1978) Rod ERG of the mudpuppy: effect of dim red backgrounds. Vision Res 18:785–792

Chapter 10

AAV Gene Augmentation Therapy for *CRB1*-Associated Retinitis Pigmentosa

C. Henrique Alves and Jan Wijnholds

Abstract

Mutations in the *CRB1* gene account for around 10,000 persons with Leber congenital amaurosis (LCA) and 70,000 persons with retinitis pigmentosa (RP) worldwide. Therefore, the *CRB1* gene is a key target in the fight against blindness. A proof-of-concept for an adeno-associated virus (AAV)-mediated *CRB2* gene augmentation therapy for *CRB1*-RP was recently described. Preclinical studies using animal models such as knockout or mutant mice are crucial to obtain such proof-of-concept. In this chapter we describe a technique to deliver AAV vectors, into the murine retinas, via the subretinal route. We also present protocols to detect expression of the therapeutic protein by fluorescence immunohistochemistry and to perform histological studies using ultra-thin sections stained with toluidine blue. These techniques in combination with electroretinography and visual behavior tests are in principle sufficient to obtain proof-of-concept for new gene therapies.

Key words Gene therapy, Adeno-associated virus (AAV), *CRB2*, Retinitis pigmentosa, Subretinal injection, Immunohistochemistry and eye histology

1 Introduction

Human gene therapy as a medicine, using adeno-associated virus (AAV) as a delivery system, became a reality in 2012 when Glybera® (alipogene tiparvovec) received a market approval from the European Medicines Agency (EMA) [1]. AAV gene therapy also holds great promise to treat retinal dystrophies proved by the great number of successful reports recently described in the literature, amongst them are potential treatments for: Leber congenital amaurosis type 2 (LCA2) (*RPE65*) [2], Choroideremia (*CHM* or *REP-1*) [3], Achromatopsia (*CNGA3*) [4], wet age-related macular degeneration (AMD) (*VEGFR1*/FLT) [5], Leber hereditary optic neuropathy (LHON) (*ND4*) [6], and autosomal recessive retinitis pigmentosa (arRP) (*MERTK*) [7]. Most of these studies involved

gene transfer to a single cell type and short coding sequences (under 4 kb) encoding enzymes, channels or secreted factors. Mutations in the Crumbs homologue-1 (*CRB1*) gene cause severe autosomal recessive retinal dystrophies such as LCA8 and RP12. These are the genetic cause of chronic and disabling vision disorders in approximately 80,000 patients worldwide [7–9].

The development of a gene therapy to *CRB1*-retinopathies seems more of a challenge compared to the genes previously mentioned due to its large cDNA (4.2 kb) which approaches the AAV packaging limit (~4.7–4.9 kb). The *CRB1* gene encodes a large transmembrane protein, of 1402 amino acids, with a large extracellular domain consisting of epidermal growth factor (EGF) and laminin-globular domains, a single transmembrane domain and a small intracellular C-terminus of 37 amino acids [10]. However, using vector optimizations such as a short promoter and synthetic polyadenylation sequence, and codon optimization it is possible to efficiently package human *CRB1* cDNA in AAV vectors and to express CRB1 in vivo [11]. Another strategy to overcome the size limitation is to use the 3.85 kb codon-optimized *CRB2* cDNA as replacement [12]. The CRB2 protein is highly similar to CRB1 in structure, although it has a shorter extracellular domain, and studies performed in mice suggest that in the retina it has similar functions in maintenance of cell to cell adhesion [12–15]. In the retina, both CRB1 and CRB2 localize to the subapical region, above the adherens junctions at the outer limiting membrane. In human retinas, CRB1 is located in Müller glial cells and cone and rod photoreceptors, while CRB2 is localized at the subapical region in Müller glial cells but not photoreceptors [16–18]. In mice, the protein expression pattern is reversed [19]. Expressing the therapeutic vector in at least three different cell types requiring CRB function, Müller glial cells, rod and cone photoreceptors, also constitutes a challenge. This obstacle is overcome using an ubiquitous promoter, that drives expression in the three cell types using a AAV capsid that is able to efficiently transduce all three cell types, as for example, AAV2/9 or AAV2/ShH10^{Y445F}, when injected subretinally [11, 12, 20, 21].

In this chapter we describe protocols to deliver AAV vectors into the mouse eye via the subretinal route and how to process the eyes in order to perform fluorescence immunohistochemistry and histological analysis in ultra-thin sections stained with toluidine blue. As example, we present AAV2/ShH10^{Y445F} mediated expression of human *CRB2* injected subretinally into the eye of a mouse lacking *Crb2*. CRB2 protein was detected by fluorescence immunohistochemistry in retinal frozen sections. Moreover, to demonstrate the potential of the histology protocol described in this chapter, we show, as example, light microscope images from control and *Crb2* cKO retinas from 1- and 3-month-old mice.

2   Materials

2.1 Anesthesia	1. Anesthesia mixture: 100 μL Ketamine, 25 μL Xylazine, 375 μL 0.9% NaCl.

2. 0.9% NaCl in sterile H_2O.

3. 1.5 mL microcentrifuge tube.

4. 1 mL syringe.

5. 25 G needle.

2.2   Eye Injection

2.2.1   Mice

1. Post-natal day 23 *Crb2* conditional knockout mice crossed with *Chx10*-Cre transgenic mouse line (*Crb2* cKO) and the respective controls (*see* **Note 1**).

2.2.2   Viral Vectors

1. AAV2/ShH10^{Y455F}-CMV-h*CRB2* virus vector stock: $>10^{10}$ genomes copies/μL AAV2/ShH10^{Y455F}-CMV-h*CRB2*.

2. AAV2/ShH10^{Y455F}-CMV-*GFP* virus vector stock: $>10^{10}$ genomes copies/μL AAV2/ShH10^{Y455F}-CMV-*GFP*. The individual purified virus concentrated stocks in PBS are stored at −80 °C (*see* **Notes 2** and **3**).

3. Virus vector mix: 1×10^{10} genomes copies/μL AAV2/ShH10^{Y455F}-CMV-h*CRB2* containing 1×10^9 genomes copies/μL AAV2/ShH10^{Y455F}-CMV-*GFP*.

2.2.3   Solutions, Materials, and Supplies

1. Appropriate personal protective equipment: gloves, eyes safety goggles, lab coat, FFP2 respirator mask covering the mouth and nose.

2. Absorbent pads.

3. 1% Fast green FCF solution.

4. 0.1% Poloxamer-188.

5. Anesthesia.

6. 5 μL model 75 RN Hamilton syringe and a custom made 34 gauge needle (HAM7803-05-RN NEEDLE(33/10mm/4 angle 40°)S.

7. Operating microscope.

8. Small #5 skin-forceps.

9. 5 mg/mL Tropicamide.

10. ViscoTears® polyacrylic acid eye gel carbomer.

11. 7–10 mm in diameter glass cover slips.

12. 10 mg/mL Chloramphenicol ointment.

13. Cotton swab.

14. Heating mat.

2.3 Immuno-histochemistry

2.3.1 Solutions

1. Yellow tissue marking dye.

2. Phosphate buffered saline (PBS): 2.6 mM KH_2PO_4, 26 mM Na_2HPO_4, 145 mM NaCl, pH 7.2.

3. 4% Paraformaldehyde (PFA): 4% PFA in PBS.

4. 15% Sucrose: 15% sucrose in PBS.

5. 30% Sucrose: 30% sucrose in PBS.

6. Preincubation buffer: 1% Bovine serum albumin (BSA, fraction V), 10% normal serum, 1% Triton X-100 solution in PBS (*see* **Note 4**).

7. Primary antibody incubation buffer: 1% BSA, 3% normal serum, 1% Triton X-100 solution in PBS (*see* **Note 4**).

8. Secondary antibody incubation buffer: 1% normal serum in PBS (*see* **Note 4**).

9. Aluminum foil.

10. Normal goat serum.

11. Rabbit anti-mouse CRB2 antibody.

12. Cyanine Cy™3 labeled goat anti-rabbit IgG affinipure F(ab′)$_2$, fragment (H+L).

2.3.2 Materials and Supplies

1. 2 mL Microcentrifuge tubes.

2. Cryo-embedding media, Tissue-Tek® O.C.T. compound.

3. $10 \times 10 \times 5$ mm Cryomold® biopsy, square.

4. Dry ice.

5. Cryotome cryostat.

6. 25×75 mm Microscope slides Superfrost® Plus.

7. Antibodies.

8. Vertical staining jar.

9. Humidified chamber.

10. Orbital shaker.

11. 24×50 mm Glass coverslips.

12. VECTASHIELD® hardSet antifade mounting medium with DAPI.

13. Fluorescence or confocal laser scanning microscope.

2.4 Histology

2.4.1 Solutions

1. PBS.

2. 4% PFA: 4% PFA in PBS.

3. 30, 50, 70, 90, and 96% Ethanol.

4. Technovit® 7100 embedding kit: 500 mL Glycol Methacrylate monomer, 5×0.6 g packs Hardener I, and 40 mL Hardener II.

5. Technovit® 3040 powder, yellow.

6. Technovit® universal liquid.

7. Technovit infiltration solution (Technovit 1): 1 sachet Hardener I (1 g) with 100 mL Glycol Methacrylate monomer Technovit® 7100

8. Technovit polymerization solution (Technovit 2): 15 mL Technovit 1 with 1 mL Hardener II, freshly prepared.

9. 0.5% Toluidine blue in H_2O.

2.4.2 Materials and Supplies

1. 2 mL microcentrifuge tubes.
2. Small glass recipient.
3. Histoblocs for histoform S.
4. $10 \times 16 \times 6.5$ mm Histoform S Teflon embedding form.
5. Microtome.
6. TC65 disposable tungsten carbide blades.
7. 22×75 mm microscope slides.
8. Coplin staining jar.
9. Entellan® mounting medium.
10. 24×50 mm glass coverslips.
11. Light microscope.

3 Methods

3.1 Eye Injection

3.1.1 Preparation of the Virus

1. Centrifuge the purified virus stock suspensions shortly and store the collecting tube on ice (*see* **Note 5**).

2. Prepare the mix of 1×10^{10} genomes copies/μL AAV2/ShH10^{Y445F} CMV-*CRB2* containing 1×10^9 genomes copies/μL AAV2/ShH10^{Y445F} CMV-*GFP* from the virus stocks. The addition of AAV2/ShH10^{Y445F} CMV-*GFP* will help to identify the injection area during fluorescence microscopy.

3. Add fast green to the virus preparation at a final concentration of 0.1%, addition of the fast green will help to evaluate the success and place of the injection (*see* **Note 6**).

3.1.2 Anesthesia and Preparation of Mice

1. Weigh the mouse.

2. Anesthetize the mouse by intraperitoneal injection of 5 μL anesthesia mixture per gram body weight. The final concentrations of anesthetics will be 100 mg/kg Ketamine and 5 mg/kg Xylazine. The mouse will develop adequate anesthesia in approximately 5 min.

3. For pupillary mydriasis apply tropicamide eye drops. The pupil is fully dilated within 2–3 min.

3.1.3 Subretinal Injection   Subretinal injection is performed under direct visualization using an operating microscope.

1. Wash the needle and the syringe with PBS containing 0.001% Poloxamer-188, to prevent AAV aggregation.

2. Fill the syringe with 1 μL vector suspension. Prime the needle in order to remove any air bubbles (*see* **Note 7**).

3. Place the mouse over an absorbent pad and position the animal with its nose pointing to the right size of the surgeon and its eye facing up toward the ring light and the microscope over a heating map.

4. Fixing the eye holding the tunica conjunctiva with forceps, in order to pop the eye up.

5. Add gel carbomer on the cornea and cover it with a glass coverslip (Fig. 1).

6. Place the needle at the inferior site of the ora serrata. The tip of the needle should be positioned with the aperture turned down (Fig. 1).

7. Advance the needle *ab externo* transsclerally into the subretinal space. Penetrate slowly the retina until the tip of the needle is visible underneath of it.
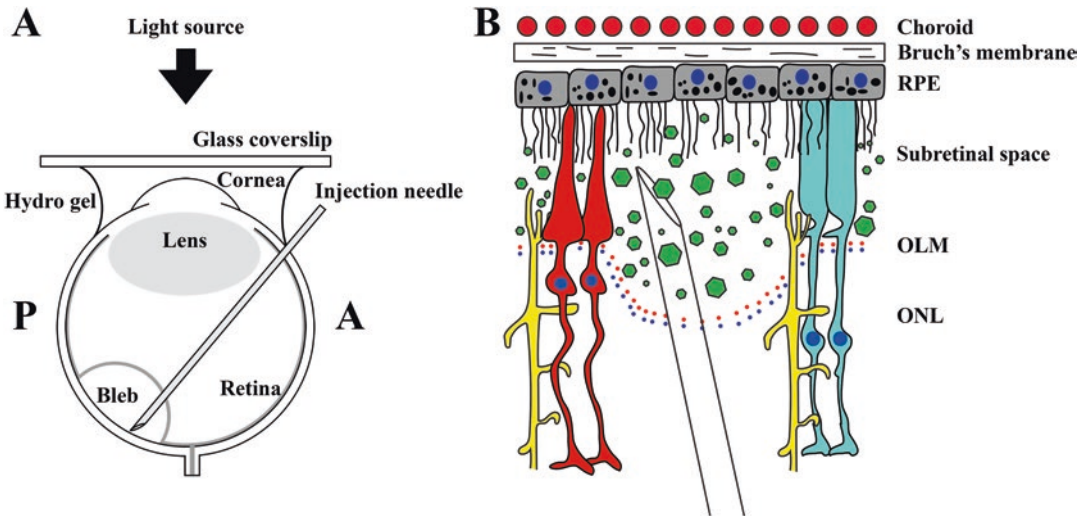
Fig. 1 Schematic representation of the subretinal injection. Technical setup for the intraocular injection. Using an operating microscope and under illumination the fundus is visualized by means of a glass coverslip over a drop of hydrogel on the cornea (**a**). Subretinal injections are performed transsclerally. *A* anterior, *P* posterior. The needle is placed in the subretinal space, when a certain volume, of a virus preparations, is injected the retina will detach from the retinal pigment epithelium (RPE) creating a bleb. The virus will then be in contact with photoreceptors (cones and rods), RPE, and Müller glial cells (**b**). *INL* inner nuclear layer, *OLM* outer limiting membrane, *ONL* outer nuclear layer, *RPE* retinal pigment epithelium

8. Slowly inject 1 μL of the fluid subretinally, a green bleb under the retina will appear once the injection is placed correctly.

9. To reduce outflow keep the needle in place for a few seconds, and then withdraw it slowly.

10. Clean the eye with a small cotton swab and apply chloramphenicol ointment to the cornea to prevent drying eyes.

11. Rinse the needle three times with PBS containing 0.001% Poloxamer-188, followed by three times with sterile water. Disassemble the syringe/needle and let it dry.

12. Keep the animals on a heating map until they are fully recovered from the anesthesia.

13. Take notes about the injection site, bleb formation and as well as any side effects.

3.2 Immuno-histochemistry

The analysis of the therapeutic protein expression can be performed by fluorescence immunohistochemistry in frozen sections. Please note, that the time required to obtain high levels of expression of the transgene depends on the transgene itself and on the AAV capsid used. In this particular example we analyzed the CRB2 expression 2 months after injection of 10^{10} genome copies per μL of ShH10^{Y445F}-CMV-*CRB2* into the subretinal space of mouse retinas lacking CRB2.

3.2.1 Tissue Processing

1. Euthanize the mouse.

2. Mark the top dorsal part of the eye by placing a small drop of yellow tissue marking dye on the sclera and let it dry for a few seconds.

3. Enucleate the eye with a small curved end scissor.

4. Fixation: place the eye in a 2 mL microcentrifuge tube with approximately 1.5 mL of 4% PFA for 20 min at room temperature (~20 °C) (*see* **Note 8**).

5. Wash the eye shortly in PBS.

6. Sucrose embedding: incubate the eye in 15% sucrose for 30 min.

7. Incubate the eye in 30% sucrose for approximately 60 min (until the eye has sunk).

8. Blocking: orientate the eye by placing the top dorsal part, marked previously, of the eye facing the top of the cryomold and the cornea the left size (Fig. 2).

9. Cover the eye with cryo-embedding media and freeze it by placing the cryomold over dry ice until the tissue is frozen completely.

10. Wrap in aluminium foil and store at −80 °C until ready for sectioning.
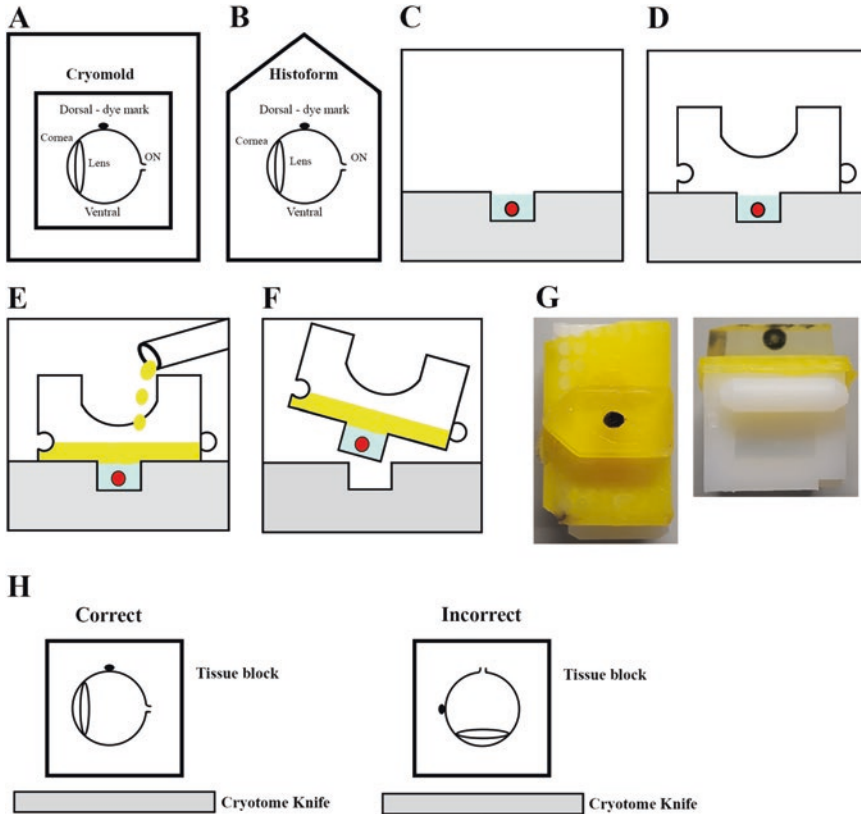
Fig. 2 Schematic representation of the correct orientation of the eye during the embedding in cryomold (**a**) or in the histoform (**b**). Schematic representation of the blocking procedure (**c**–**f**). Photography of a Technovit block (**g**). Schematic representation of the orientation of the eye relatively to the cryotome knife (**h**). The lens should face perpendicular to the knife. *ON* optic nerve

11. Sectioning: transfer the frozen tissue block to a cryotome cryostat (e.g., −20 °C) prior to sectioning and allow the temperature of the frozen tissue block to equilibrate to the temperature of the cryotome cryostat.

12. Orientate the tissue block in a way that the cornea is perpendicular to the knife, to reduce the contact area between knife and lens. Beware of the dorsal-ventral orientation of the sections.

13. Section the frozen tissue block into a desired thickness (typically 7–10 μm) using a cryotome (*see* **Note 9**).

14. Place the tissue sections onto glass slides.

15. Air-dry the sections for at least 1 h.

16. Store the sections at −80 °C until needed.

3.2.2 Immuno-histochemistry (See Note 10*)*

1. Thaw the sections for 30 min at room temperature.

2. Rehydrations: incubate the slides in PBS for 20 min. Once rehydrated do not to let the sections dry.

3. Prepare the preincubation and primary antibody incubation buffers needed during this incubation period (*see* **Note 11**).

4. Blocking: incubate the sections in a humid chamber with ~150 μL of preincubation buffer per slide for 1 h at room temperature. Once the secondary antibody used in this example was raised in goat we use normal goat serum.

5. Remove the preincubation buffer by passing the slides by PBS.

6. Primary antibody incubation: dilute the primary antibody to the desired concentration in the primary antibody incubation buffer and add ~150 μL to each slide (*see* **Note 12**). In this example we use an home-made rabbit anti-mouse CRB2 antibody (1/1000, EP13[17]).

7. Incubate the slides with the first antibody for 16 h at 4 °C (*see* **Note 13**).

8. Washing: wash the sections three times 10 min each in PBS with gentle shaking.

9. Secondary antibody incubation: add the fluorophore-conjugated secondary antibody, with specificity against the primary antibody, to the secondary antibody incubation buffer and incubate for 1 h, in the dark, at room temperature (*see* **Note 14**). In this particular example we used a Cyanine Cy™3 goat anti-rabbit IgG (1/500).

10. Washing: wash the sections two times 10 min each in PBS with gentle shaking.

11. Remove the excess of fluid and add a drop mounting medium and cover with a coverslip.

12. Visualize the staining under a fluorescence or a confocal laser scanning microscope (Fig. 3).

3.3 Confocal Microscopy

Immunohistochemistry followed by fluorescence or confocal microscopy is a useful method to study protein expression and localization in tissues after transduction with a gene therapy viral vector. As a standard method we perform three colors microscopy using DAPI as a counter-staining of the nuclei, GFP-autofluorescence or Alexa Fluor®488 or Cy™2 in combination with Alexa Fluor®555 or Cy™3. Before performing immunohistochemistry we used fluorescence microscopy to fast access the quality of the cryo-sections or GFP-expression by simply rehydrating the cryo-sections and mounting the slides with a mounting medium containing DAPI. Thereafter, immunohistochemistry and confocal microscopy are performed. This last one offers several advantages over conventional optical microscopy, including controllable depth of field, the elimination of image degrading out-of-focus information, and the ability to collect serial optical sections from thick specimens. Hereby, we described a simple protocol to perform confocal imaging.
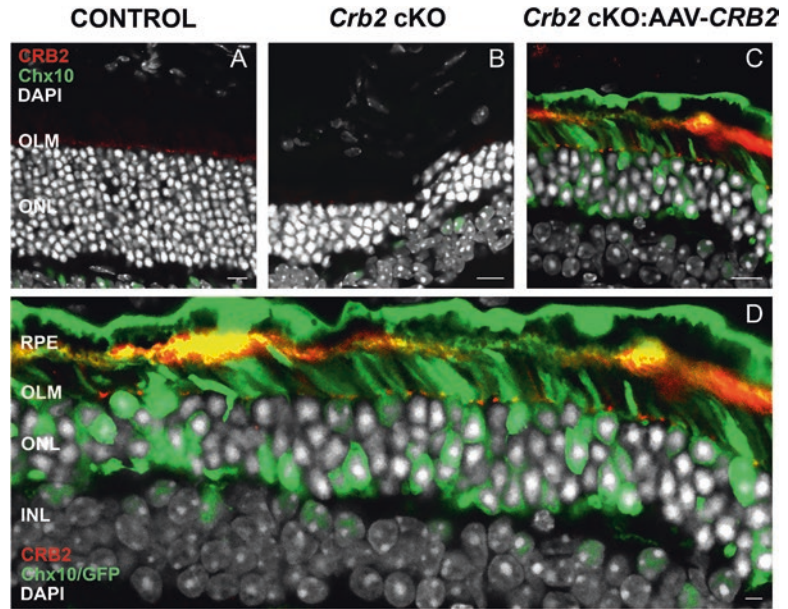
Fig. 3 Efficient expression of human CRB2 after AAV-*CRB2* injection in *Crb2* cKO retinas. Endogenous mouse CRB2 expressed at the subapical region in wild type retinas (**a**) and did not express in *Crb2* cKO retinas (**b**). After 2 months post-injection in *Crb2* cKO retinas of 10^{10} genome copies of subretinally AAV2/ShH10^{Y445F}-CMV-*CRB2* (targeting photoreceptors, Müller glial cells, and RPE) (**c**, **d**) in addition to 10^9 genome copies of the *GFP* virus. CRB2 protein was detected at the subapical region and in the apical membrane of RPE cells. *Crb2* cKO retinas displayed Cre-GFP positive bipolar cells due to the *Chx10* promoter. *INL* inner nuclear layer, *ONL* outer nuclear layer, *RPE* retinal pigment epithelium. Scale bar: 10 μm

We perform confocal microscopy using a Leica SP8 microscope with hybrid detectors (HyD), using the LAS AF software. As standard procedure we perform 3-colors sequential image recording using the between frames method.

1. Turn on the lasers: access the "Configuration" mode by clicking the Laser icon, activate the necessary lasers: UV-405 nm, visible-488 nm and -552 nm by clicking on their on/off button.

2. Select the appropriate beam splitter, or use autoselect.

3. If not in place, select 40× (oil) objective (*see* **Note 15**).

4. Set Parameters in "Acquisition" Mode: Format, or number of pixels in the scan area by selecting XYZ Format to the desired scan format (1024 × 1024 pixels).

5. Set scan Speed to 200 Hz.

6. Set the Pinhole to 1 Airy Unit.

7. Averaging six lines to remove noise from high gain settings (*see* **Note 16**).

8. Set Zoom to 1.

9. Set the sequential acquisition: Click SEQ in the "Acquisition" Mode to open the Sequential Scan control window.

10. Click twice Plus in the "Sequential Scan" control window to add another two sequences.

11. For Scan1 set all laser powers to zero except the 552 nm laser, turn on the HyD detectors by clicking ON. Select the fluorochrome Alexa 555 to see the emission spectrum.

12. For Scan2 set all laser powers to zero except the 488 nm laser, turn on the HyD detectors by clicking ON. Select the fluorochrome Alexa 488 to see the emission spectrum.

13. For Scan3 set all laser powers to zero except the 405 nm laser, turn on the HyD detectors by clicking ON. Select the fluorochrome DAPI to see the emission spectrum.

14. Define the emission wavelength range to be collected by moving the sliders (gates). Do not overlap detector range with active laser line; minimal distance 8–10 nm.

15. Select "Switching" mode to switch between frames.

16. Using the "Live scanning" mode, adjust focus.

17. Adjust the detector gain and the offset values as well as the intensity of the excitation wavelengths. Move emission-bar underneath emission spectrum (at least 10 nm right of the laser line). Open up laser power a few %. Set gain to 10% (minimum level).

18. Use QLUT to judge over/under exposition.

19. Rotate the scan field in order to have the images in the same orientation; this can be achieved by use the slider, numerical factor, or control panel knob.

20. Stop the Live scan.

21. Click Start to start the sequential scan.

22. With the buttons Load and Save in the Sequential Scan dialog, you can load a previously saved sequential scan setting or save the current setting.

3.4 Histology

While frozen sections are of advantage to perform fluorescence immunohistochemistry the same does not hold for histological studies, due to the physical process of freezing and cryo-sectioning it might be difficult to obtain consecutive high quality sections that allow to analyze the retinal structure in detail. We recommend to use instead ultra-thin sections of eyes embedded in glycol methacrylate (Technovit®) stained with toluidine blue, a basic thiazine

metachromatic dye with high affinity for acidic tissue components. Using this protocol it is possible to obtain consecutive sections as thin as 1 μm. Thinner sections provide improved detail. Also, the matrix provides good support to cellular components, offering improved morphology.

3.4.1 Eye Processing

1. Euthanize the mouse.

2. Mark the top dorsal part of the eye by placing a small drop of yellow marking dye and let it dry for a few seconds.

3. Enucleate the eye with a small curved end scissor.

4. Place the eye in a 2 mL microcentrifuge tube with approximately 1.5 mL 4% PFA for 20 min at room temperature.

5. Wash the eye shortly in PBS.

6. Dehydration: incubating the eye in 30% ethanol for 30 min at room temperature.

7. 50% ethanol for 30 min.

8. 70% ethanol for 30 min.

9. 90% ethanol for 30 min.

10. 90% ethanol for 30 min.

11. 96% ethanol for 30 min.

12. 96% ethanol for 30 min.

13. Transfer the eye to a small glass recipient.

14. Preinfiltration: prepare the final concentration of the dehydration series in equal parts with basic solution Technovit® 7100 (e.g., 2 mL 96% ethanol:2 mL of Technovit® 7100 basic solution), incubate the eye 30 min at room temperature.

15. Prepare Technovit infiltration solution (Technovit 1) by dissolving 1 sachet containing 1 g of Hardener I in 100 mL Technovit® 7100 in a clean (detergent-free) glass or polyethylene container for approximately 10 min (*see* **Note 17**).

16. Infiltrate the specimens with Technovit 1 for 16 h at room temperature in 3–4 mL of the infiltration solution.

17. Polymerization: prepare fresh Technovit polymerization solution (Technovit 2) by mixing 15 mL Technovit 1 with 1 mL Hardener II.

18. Fill the histoform embedding form cavities halfway with the Technovit 2 polymerization solution using a disposable pipette, position the prepared specimen therein and fill the form (warning: only the cavity, not the entire recess). Let polymerize for 2 h at room temperature. The slightly sticky surface (inhibition layer) can be removed with a lint-free disposable cloth.

19. Orientate the eye by placing the top dorsal part, marked previously, of the eye facing the top of the histoform and the cornea the left size (Fig. 2c).

20. Blocking and archiving: once the Technovit 2 has hardened, place the histobloc support element in the opening in the Teflon embedding form.

21. Mix the Technovit® 3040 powder to Technovit® universal liquid until it is as viscous as possible (mixing ratio 2–3 volumetric parts of powder to 1 volumetric share of liquid). Pour the mixed material into the opening in the histobloc (Fig. 2d–f).

22. Wait for 5–10 min till the Technovit hardens and the histobloc tightly binds to the specimen.

23. Remove the block with the specimen from the Teflon mold.

3.4.2 Sectioning and Toluidine Blue Staining

1. Tightly clamp the blocks in the totem cam devices on the rotation microtome.

2. Cut thin sections, 1–3 μm thick.

3. Using forceps collect every fifth section, so the sections are 5 or 15 μm apart of each other.

4. Place section floating in distilled water on a microscope slide. Let dry for 16 h at 60 °C.

5. Place the de-plasticized sections in the 0.5% toluidine blue stain solution for 15–30 s. A 1 μm-section must be stained longer than a 5 μm section for the desired stain intensity.

6. Wash the slides under abundant tap water and let dry again for several hours at 60 °C until completely dried.

7. Mount the slides using Entellan® mounting medium, and let them dry for several hours.

8. Visualize the staining under a light microscope (Fig. 4).

4   Notes

1. In *Crb2* cKO mice, CRB2 is ablated from progenitor cells [15], in these mice Chx10-*Cre* is fused to *GFP*. In adult mice Cre-GFP protein expression is detected in bipolar cells.

2. The addition of Poloxamer-188 solution at a final concentration of 0.001% to the viral preparation will decrease aggregation of the virus and prevent sticking of the virus to plastics and to the needle/syringe, preventing the loss of viral particles during preparation and injection. Moreover, pipette tips and syringe/needle should be rinsed with 0.001% Poloxamer-188 in PBS before pipetting the virus.

3. The pAAV2-*GFP* plasmids consist of the flanking inverted terminal repeats (ITRs) of AAV2, the full-length CMV promoter, the *eGFP* cDNA, the woodchuck post-transcriptional regulatory element and the SV40 polyadenylation sequence. The pAAV2-*CRB2* plasmids consist of the flanking ITRs of AAV2, full-length CMV driving expression of the human codon optimized *CRB2* cDNA, with or without a synthetic and short intron sequence and a 48 bp synthetic polyadenylation sequence [12].

4. Prepare always fresh solutions. A 20% BSA solution can be prepared, aliquoted and stored at −20 °C.

5. Centrifuge the purified virus suspension shortly and store the collecting tube on ice.

6. The addition of fast green to the virus preparation will allow to visualize the injection place, if subretinal the dye will be confined in the bleb, however if intravitreal the entire vitreous cavity will become green.

7. The syringe filling with AAV should be performed inside of a biosafety cabinet class 2. Prime the needle/syringe in order to remove any air bubble in the solution.

8. The time of fixation for 20 min with 4% PFA is critical for some antibody staining's. In a comparison of wild type against *Crb1* knockout retinas lacking CRB1, excessive fixation caused unspecific staining of cones by anti-CRB1, whereas antigen retrieval caused unspecific staining at the outer limiting membrane in *Crb1* knockout retinas.

9. Use an angle of 6°. The suggested cryostat temperature is between −18 and −21 °C. The section will curl if the specimen is too cold. If it is too warm, it will stick to the knife. The integrity of the anti-roll glass is important to have high quality sections.

10. Carry out incubations in a humidified chamber to avoid tissue drying out, which will lead to nonspecific binding and high background staining. A shallow plastic box with a sealed lid and wet tissue paper in the bottom is an adequate chamber. Keep slides off the paper and lay flat so that the reagents do not drain off.

11. The secondary antibody may cross react with endogenous immunoglobulins in the tissue. Minimize this by pretreating the tissue with normal serum from the species in which the secondary was raised. The use of normal serum before the application of the primary also eliminates Fc receptor binding of both the primary and secondary antibody. BSA is included to reduce nonspecific binding caused by hydrophobic interactions.
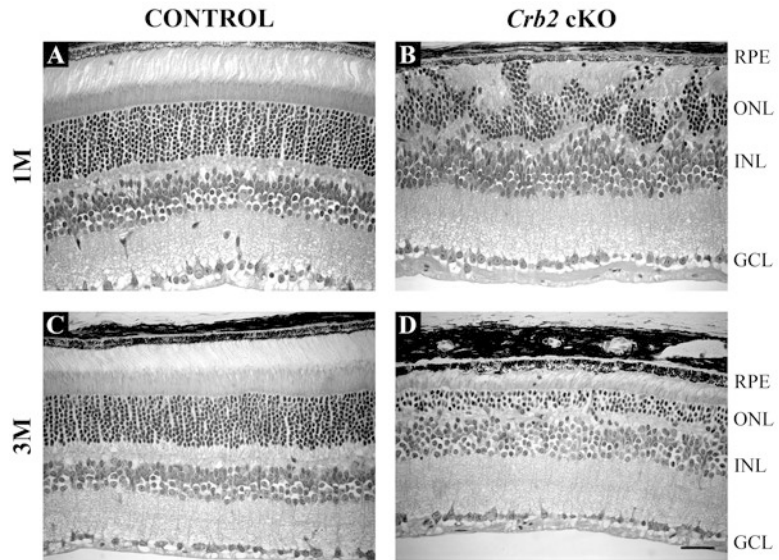
Fig. 4 Loss of CRB2 results in retinal disorganization. Toluidine-stained light microscope pictures, of retina sections, from the control (**a**, **c**) and from the *Crb2* cKO (**b**, **d**) at different ages: (**a**, **b**) 1 M; (**c**, **d**) 3 M. Control retinas showed no abnormalities. *Crb2* cKO showed progressive loss of photoreceptors and disruptions of the outer limiting membrane. Scale bar: 20 μm. *GCL* ganglion cell layer, *INL* inner nuclear layer, *ONL* outer nuclear layer, *RPE* retinal pigment epithelium

12. Dilute the primary antibody to the manufacturer's recommendations or to a previously optimized dilution.

13. Appropriate controls are critical for the accurate interpretation of results. A negative control should be included using the incubation buffer with no primary antibody to identify nonspecific staining of the secondary reagents. Additional controls can be employed to support the specificity of staining generated by the primary antibody. These include absorption controls, isotype matched controls, tissue type controls. In this particular case the use of a knockout (negative control) and a wildtype retina (positive control) is very useful to test the specificity of the staining. Note, that degenerating retinas normally present higher fluorescence background.

14. To perform multicolor immunohistochemistry we recommend the use of Alexa Fluor®488 or Cy™2 in combination with Alexa Fluor®555 or Cy™3 conjugated to the secondary antibodies. This combination allows a good separation of the excitation emission spectrum. It is also possible to combine the previous two antibodies with others, e.g., Alexa Fluor®649 or Cy™5.

15. If more detail is need a 63× objective can be used if available, however the software also offers the possibility to perform digital zoom, in our case digital zoom of 2× works well and avoids the need to change the objective.

16. The accumulation sums up the intensities of several passes and may lead to saturation of the data space.

17. When sealed, the Technovit 1 infiltration solution is stable for a maximum of 4 weeks at 4 °C.

Acknowledgment

References

1. Glybera (2012) http://www.ema.europa.eu/ema/index.jsp?curl=pages/medicines/human/medicines/002145/human_med_001480.jsp&mid=WC0b01ac058001d124. Accessed 29 Nov 2012

2. Bainbridge JW, Smith AJ, Barker SS et al (2008) Effect of gene therapy on visual function in leber's congenital amaurosis. N Engl J Med 358:2231–2239

3. MacLaren RE, Groppe M, Barnard AR et al (2014) Retinal gene therapy in patients with choroideremia: initial findings from a phase 1/2 clinical trial. Lancet 383:1129–1137

4. Michalakis S, Mühlfriedel R, Tanimoto N et al (2010) Restoration of cone vision in the CNGA3−/− mouse model of congenital complete lack of cone photoreceptor function. Mol Ther 18:2057–2063

5. Sanofi-Genzyme. Safety and Tolerability Study of AAV2- sFLT01 in Patients With Neovascular Age-Related Macular Degeneration (AMD). http://clinicaltrials.gov/ct2/show/NCT01024998

6. Feuer WJ, Schiffman JC, Davis JL et al (2016) Gene therapy for leber hereditary optic neuropathy: initial results. Ophthalmology 123:558–570

7. Conlon TJ, Deng WT, Erger K et al (2013) Preclinical potency and safety studies of an AAV2-mediated gene therapy vector for the treatment of MERTK associated retinitis pigmentosa. Hum Gene Ther Clin Dev 24:23–28

8. Alves CH, Pellissier LP, Wijnholds J (2014) The CRB1 and adherens junction complex proteins in retinal development and maintenance. Progr Ret Eye Res 40:35–52

9. Tsang SH, Burke T, Oll M et al (2014) Whole exome sequencing identifies CRB1 defect in an unusual maculopathy phenotype. Ophthalmology 121:1773–1782

10. Tepass U, Theres C, Knust E (1990) crumbs encodes an EGF-like protein expressed on apical membranes of Drosophila epithelial cells and required for organization of epithelia. Cell 61:787–799

11. Pellissier LP, Hoek RR, Vos RM et al (2014) Specific tools for targeting and expression in Müller glial cells. Mol Ther Methods Clin Dev 1:14009

12. Pellissier LP, Quinn PM, Alves CH et al (2015) Gene therapy into photoreceptors and Müller glial cells restores retinal structure and function in CRB1 retinitis pigmentosa mouse models. Hum Mol Genet 24:1–15

13. Alves CH, Bossers K, Vos RM et al (2013) Microarray and morphological analysis of early postnatal CRB2 mutant retinas on a pure C57BL/6J genetic background. PLoS One 8:1–17

14. Alves CH, Pellissier LP, Vos RM et al (2014) Targeted ablation of Crb2 in photoreceptor cells induces retinitis pigmentosa. Hum Mol Genet 23:3384–3401

15. Alves CH, Sanz Sanz A, Park B et al (2013) Loss of CRB2 in the mouse retina mimics human retinitis pigmentosa due to mutations in the CRB1 gene. Hum Mol Genet 22:35–50

16. Pellissier LP, Alves CH, Quinn PM et al (2013) Targeted ablation of Crb1 and Crb2 in retinal progenitor cells mimics leber congenital amaurosis. PLoS Genet 9:e1003976

17. van de Pavert SA, Kantardzhieva A, Malysheva A et al (2004) Crumbs homologue 1 is required for maintenance of photoreceptor cell polarization and adhesion during light exposure. J Cell Sci 117:4169–4177

18. Pellissier LP, Lundvig DM, Tanimoto N et al (2014) CRB2 acts as a modifying factor of CRB1-related retinal dystrophies in mice. Hum Mol Genet 23:3759–3771

19. van Rossum AG, Aartsen WM, Meuleman J et al (2006) Pals1/Mpp5 is required for correct localization of Crb1 at the subapical region in polarized Müller glia cells. Hum Mol Genet 15:2659–2672

20. Klimczak RR, Koerber JT, Dalkara D et al (2009) A novel adeno-associated viral variant for efficient and selective intravitreal transduction of rat Müller cells. PLoS One 4:e7467

21. Dalkara D, Byrne LC, Lee T et al (2012) Enhanced gene delivery to the neonatal retina through systemic administration of tyrosine-mutated AAV9. Gene Ther 19:176–181

Chapter 11

Dual AAV Vectors for Stargardt Disease

Ivana Trapani

Abstract

Stargardt disease (STGD1), due to mutations in the large *ABCA4* gene, is the most common inherited macular degeneration in humans. Attempts at developing gene therapy approaches for treatment of STGD1 are currently ongoing. Among all the vectors available for gene therapy of inherited retinal diseases, those based on adeno-associated viruses (AAV) are the most promising given the efficacy shown in various animal models and their excellent safety profile in humans, as confirmed in many ongoing clinical trials. However, one of the main obstacles for the use of AAV is their limited effective packaging capacity of about 5 kb. Taking advantage of the AAV genome's ability to concatemerize, others and we have recently developed dual AAV vectors to overcome this limit. We tested dual AAV vectors for *ABCA4* delivery, and found that they transduce efficiently both mouse and pig photoreceptors, and rescue the *Abca4–/–* mouse retinal phenotype, indicating their potential for gene therapy of STGD1. This chapter details how we designed dual AAV vectors for the delivery of the *ABCA4* gene and describes the techniques that can be explored to evaluate dual AAV transduction efficiency in vitro and in the retina, and their efficacy in the mouse model of STGD1.

Key words Stargardt disease, Gene therapy, AAV vectors, Dual AAV hybrid, Dual AAV *trans*-splicing

1 Introduction

Stargardt disease (STGD1; MIM#248200), the most common autosomal recessive early-onset macular degeneration in humans [1], is caused by mutations in *ABCA4* [coding sequence (CDS): 6822 bp], which encodes the photoreceptor (PR)-specific all-trans-retinal transporter [1, 2]. In the absence of a functional ABCA4 protein, vitamin A aldehyde forms bis-retinoid adducts that are deposited in retinal pigment epithelial (RPE) cells during the process of disc shedding and phagocytosis. Consequently, abnormally high levels of lipofuscin pigments accumulate in the RPE, triggering RPE-cell death and causing secondary PR degeneration [1]. This event leads to the rapid and progressive loss of central vision, color vision, and discriminate fine vision experienced by STGD1 patients.

Direct gene replacement represents an attractive therapeutic option for treatment of an autosomal recessive disease as STGD1, since delivering a wild-type functioning copy of the *ABCA4* gene to diseased PR would theoretically result in restoration of visual function. However, the identification of an efficient vector for the delivery of the *ABCA4* gene to the retina has been hampered by both the large size of the *ABCA4* CDS and the localization of the ABCA4 protein to the PR cell layer that requires the use of vectors able to transduce this specific layer. Indeed, while the ability of vectors with high packaging capacity, such as lentiviruses (LV), adenoviruses (Ad), and nonviral vectors, to efficiently transduce adult PR remains controversial [3, 4], vectors based on adeno-associated viruses (AAV), which have higher PR transduction capability and have been successfully used in various human trials for ocular diseases [3, 5, 6], have a canonical packaging capacity of about 4.7 kb [7, 8] and therefore would not be able to package the large *ABCA4* CDS. Others and we, however, have recently shown that AAV packaging capacity can be successfully expanded, in order to deliver large genes (i.e., genes with a CDS larger than 5 kb) to the retina, through the use of dual AAV vectors [9–12]. This approach relies on the use of two separate (dual) AAV vectors, each one carrying a half of a large gene. Upon coinfection of the target cell from both vectors, the two halves will be reconstituted because of the ability of AAV genomes to concatamerize via intermolecular recombination. Various dual AAV strategies have been described (referred to as trans-splicing, overlapping and hybrid dual vector strategies; Fig. 1) and have been used to efficiently deliver large genes to different tissues [13–15]. In the trans-splicing approach, the 5′-half vector has a splice donor (SD) signal at the 3′ end, while the 3′-half vector carries a splice acceptor (SA) signal at the 5′end that allow trans-splicing of a single large mRNA molecule following tail-to-head concatemerization of the two AAV [13]. In the overlapping approach, the dual AAV genomes share overlapping sequences, thus the reconstitution of the large gene expression cassette relies on homologous recombination [14]. The third dual AAV approach (hybrid) is a combination of the two previous approaches and it is based on the addition of a highly recombinogenic exogenous sequence (recombinogenic region or RR) to the trans-splicing vectors, in order to increase their recombination efficiency [15–17]. This recombinogenic sequence is placed downstream of the SD signal in the 5′-half vector and upstream of the SA signal in the 3′-half vector, so that, after recombination, it is spliced out from the mature RNA. The recombinogenic sequences used so far in order to induce the recombination between dual AAV hybrid vectors derive either from a region of the alkaline phosphatase gene (AP) [15, 17] or from the phage F1 genome (AK) [16]. We have compared dual AAV strategies side-by-side in the mouse and pig
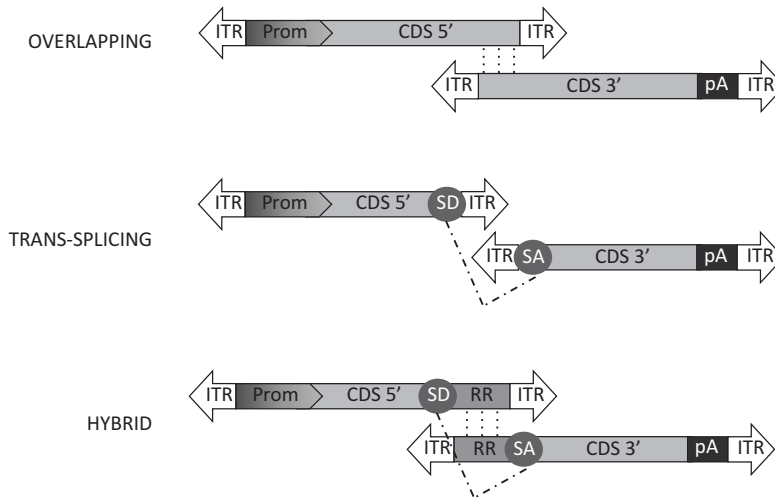
Fig. 1 Schematic representation of dual AAV vector strategies. *ITR*: inverted terminal repeats, *Prom* promoter, *CDS* coding sequence, *SD* splicing donor signal, *SA* splicing acceptor signal, *RR* recombinogenic region, *pA* polyadenylation signal. Pointed lines show overlapping regions available for homologous recombination, dashed lines show the splicing occurring between SD and SA

retina and have found that dual AAV trans-splicing and hybrid AK vectors transduce efficiently PR and reduce lipofuscin accumulation in *Abca4−/−* mice [9, 12]. Thus, they can be explored for treatment of STGD1 disease.

Here, the rationale behind the cloning strategies we used to generate dual AAV vectors is described as well as the techniques that can be used to assess dual AAV efficiency in vitro and in vivo, both in the mouse and pig retina.

2   Materials

2.1   Generation of Dual AAV Construct

1. Plasmid pZac2.1-CMV-*hABCA4*-SV40: The plasmid (Fig. 2) has been generated using as backbone the pZac2.1 plasmid, a kind gift of Dr. James M. Wilson (Department of Medicine, Perelman School of Medicine, University of Pennsylvania). It includes: inverted terminal repeats (ITR) from AAV serotype 2; the Cytomegalovirus (CMV) immediate-early enhancer/promoter region followed by a chimeric intron (U47119.2 bp 857–989) composed of the 5′-donor site from the first intron of the human β-globin gene and the branch and 3′-acceptor site from the intron that is between the leader and the body of an immunoglobulin gene heavy chain variable region; the full-length human *ABCA4* (*hABCA4*) CDS (NM_000350.2, bp 105–6926), with a 3×flag
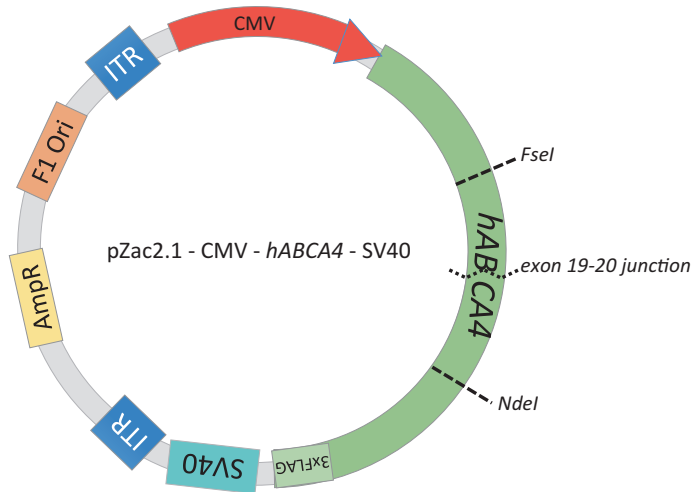
Fig. 2 Schematic representation of pZac2.1-CMV-*hABCA4*-SV40. *ITR* inverted terminal repeats, *CMV* cytomegalovirus immediate-early enhancer/promoter, *hABCA4* human *ABCA4* coding sequence, *3×flag* 3×flag tag, *SV40* polyadenylation signal, *F1 Ori* phage F1 replication origin, *AmpR* ampicillin resistance

tag at the 3′end before the stop codon; the SV40 polyadenylation signal.

2. Plasmid pAAV2.1 [18], used as DNA template for the amplification of the AK sequence.

3. Mutagenesis primer 1: primer 5′-GGAGCTGGGAAAACC ACCACCTTCAATTGAGGAACCCCTAGTG ATGGAGTTGG-3′ of which the first half aligns to the end of exon 19, and the second half to the 3′ITR of plasmid pZac2.1-CMV-*hABCA4*-SV40. Additionally, the MfeI restriction site is included in the middle of the primer (underlined sequence), in order to allow further cloning of the SD and AK region in the plasmid generated after mutagenesis.

4. Mutagenesis primer 2: primer 5′-CCAACTCCATCACTAGGGGTTCCTCAATTG AAGGTGGTGGTTTTCCCAGCTCC-3′, reverse complementary of mutagenesis primer 1.

5. Mutagenesis primer 3: plus strand primer 5′-CCAACTCCATCACTAGGGGTTCCTGGATCCGTC CATCCTGACGGGTCTGTTGC-3′ of which the first half aligns to the 5′ITR and the second half to the beginning of exon 20 of plasmid pZac2.1-CMV-*hABCA4*-SV40. Additionally, a BamHI restriction site is included in the middle of the primer (underlined sequence) in order to allow further cloning of the SA and AK region.

6. Mutagenesis primer 4: primer 5′-GCAACAGACCCGTCAGG ATGGACGGATCCAGGAACCCCTAGTGATGGAG TTGG-3′, reverse complementary of mutagenesis primer 3.

7. Forward h*ABCA4* primer 1: primer 5′-ACGGAGGATCCAGAGCACCCAG-3′ annealing to a region of the h*ABCA4* CDS upstream of the FseI restriction site. The FseI site is used for further cloning of the PCR product into the vector backbone.

8. Reverse h*ABCA4* primer 2: primer 5′-<u>AGAAACGCAAGAGTC TTCTCTGTCTCGACAAGCCCAGTTTCTATT GGTCTCCTTAAACCTGTCTTGTAACCTT GATACTTAC</u>AAGGTGGTGGTTTTCCCAGCTCC-3′ annealing to the end of exon 19 and carrying a 5′tail which includes the SD (underlined sequence).

9. Forward AK primer 3: primer 5′-<u>GTAAGTATCAAGGTTACA AGACAGGTTTAAGGAGACCAATAGAAACTGGGC TTGTCGAGACAGAGAAGACTCTTGCGT TTCT</u>GGGATTTTTCCGATTTCGGC-3′ annealing to the AK region and carrying a 5′ tail, which includes the SD (underlined sequence).

10. Reverse AK primer 4: primer 5′-<u>CAATTG</u>GAAAGATGCCACCTGAAATTATAAACG-3′ annealing to the end of the 32-bp long region which follows the AK sequence and carrying a 5′ tail which includes the MfeI restriction site (underlined sequence). The MfeI site is used for further cloning of the PCR product into the vector backbone.

11. Forward AK primer 5: primer 5′-<u>GGATCC</u>GGGATTTTTCCGATTTCGGC-3′ annealing to the AK region and carrying a tail that includes the BamHI restriction site (underlined sequence). The BamHI site is used for further cloning of the PCR product into the vector backbone.

12. Reverse AK primer 6: primer 5′-<u>CTGTGGAGAGAAAGGCAAA GTGGATGTCAGTAAGACCAATAGGTG CCTATC</u>GAAAGATGCCACCTGAAATTATAAACG-3′ annealing to the end of the 32-bp long region which follows the AK sequence and carrying a tail, which includes the SA (underlined sequence).

13. Forward h*ABCA4* primer 7: primer 5′-<u>GATAGGCACCTATTGGTCTTACTGACATCCACT TTGCCTTTCTCTCCACAGG</u>TCCATCCT GACGGGTCTGTTGC-3′ annealing to the beginning of exon 20 and carrying a tail, which includes the SA (underlined sequence).

14. Reverse *hABCA4* primer 8: primer 5′-AAGGTCAGCCAGCGTCTCCTCC-3′ annealing to a region of the *hABCA4* CDS after the NdeI restriction site. The NdeI site is used for further cloning of the PCR product into the vector backbone.

15. Reverse SD primer 9: primer 5′-<u>CAATTG</u>AGAAACGCAAGAGTCTTCTCTGTCTC-3′ annealing to the end of the SD and carrying a tail, which includes the MfeI restriction site (underlined sequence). The MfeI site is used for further cloning of the PCR product into the vector backbone.

16. Forward SA primer 10: primer 5′-<u>GGATCC</u>GATAGGCACCTATTGGTCTTACTGACA-3′ annealing to the beginning of the SA and carrying a tail, which includes the BamHI restriction site (underlined sequence). The BamHI site is used for further cloning of the PCR product into the vector backbone.

17. QuickChange II XL Site-Directed Mutagenesis Kit (Agilent Technologies).

18. dNTPs mix.

19. 10× Pfu buffer.

20. Pfu DNA Polymerase.

21. Taq DNA Polymerase.

22. TOPO-TA cloning kit (Thermo Fisher Scientific).

23. One shot TOP10 chemically competent *E. coli* cells (e.g., from Thermo Fisher Scientific).

24. Restriction enzymes: FseI, MfeI, BamHI, NdeI.

25. 10× T4 DNA Ligase Buffer.

26. T4 DNA Ligase.

27. 15 mL conical centrifuge tubes.

28. Plasmid miniprep kit.

29. LB medium: 10 g tryptone, 5 g yeast extract, 10 g NaCl per liter. Sterilize by autoclaving. Once the LB medium is at room temperature, supplement with the appropriate antibiotic.

2.2 Evaluation of Transduction Efficiency in HEK293 Cells

1. pΔF6 helper plasmid, which contains the adenovirus *E2A*, *E4*, and *VA* RNA helper genes [19].

2. 6-well plates.

3. 50 mL polypropylene tubes.

4. 1.5 mL centrifugation tubes.

5. 0.3 M $CaCl_2$. Sterilize by using 0.22 μm filter.

6. 2× Hepes Buffered Saline (2× HBS): 50 mM HEPES, 280 mM NaCl, 1.5 mM Na_2HPO_4. Dissolve in H_2O. Adjust pH to 7.1. Sterilize by using 0.22 μm filter (*see* **Note 1**).

7. DMEM growing medium: Dulbecco's modified Eagle's medium (DMEM) with sodium pyruvate, L-glutamine and high glucose, supplemented with 10% fetal bovine serum and antibiotics/antimycotic (100 U/mL Penicillin, 100 μg/mL Streptomycin, 0.25 μg/mL Amphotericin B).

8. Serum-free DMEM: DMEM with pyruvate, L-glutamine, and high glucose, without serum and without antibiotics/antimycotic.

2.3 ABCA4 Protein Extraction

1. 1.5 mL centrifugation tubes.

2. Protein assay kit.

3. Bucket with ice.

4. Liquid nitrogen or dry ice ethanol slurry to freeze cell lysates.

5. RIPA lysis buffer: 150 mM NaCl, 1% NP40, 0.5% sodium deoxycholate, 0.1% SDS, 1 mM EDTA, 50 mM Tris–HCl pH 8, supplemented with Protease Inhibitor Cocktail 1× (cOmplete, EDTA-free Protease Inhibitor Tablets, Roche) and 1 mM phenylmethylsulfonyl (PMSF).

6. Benchtop centrifuge.

2.4 Western Blot Procedure

1. 6% polyacrylamide gel.

2. PVDF membrane.

3. Anti-3×flag antibody (Monoclonal ANTI-FLAG® M2, Sigma-Aldrich).

4. HRP-conjugated secondary antibody.

5. Chemiluminescent substrate.

6. 2× sample buffer: 0.5 M Tris–HCl pH 6.8, 20% Glycerol, 2% SDS, 0.02% Bromophenol blue, 8 M Urea, 10% 2-mercaptoethanol.

7. Running buffer: 25 mM Tris base, 192 mM Glycine, 0.1% SDS.

8. Transfer buffer: 25 mM Tris base, 192 mM Glycine, 20% methanol.

9. TBST: 20 mM Tris–HCl pH 7.5, 150 mM NaCl, 0.05% Tween 20.

10. Blocking buffer: 5% milk in TBST.

11. Electrophoresis and protein blotting apparatus.

12. CCD camera-based imager.

2.5 Evaluation of Transduction Efficiency In Vivo

1. 4 week-old C57BL/6J mice.

2. Scissors and forceps for eye injection and dissection.

3. 30 G needle.

4. Hamilton syringe equipped with a 33 G needle.

5. PBS + 5% glycerol: PBS supplemented with 5% glycerol. Used here as the AAV vector storage buffer and thus as buffer to dilute the AAVs. In case that the AAV storage buffer is different than use that buffer to dilute the vectors.

6. Anesthetic.

7. 0.5% Tropicamide.

8. Antibiotic cream for ocular use.

9. Stereoscopic microscope.

2.6 Injection of Dual AAV Vectors in the Pig Retina

1. Large White pigs.

2. Endotracheal tube (Magill type).

3. 23 G needle.

4. 1 mL syringe with 30-G needle.

5. Trocars.

6. Light fibers.

7. Subretinal injection needle: An extendible 41 G (23 G/0.6 mm) subretinal injection needle (D.O.R.C. Dutch Ophthalmic Research Center, Zuidland, The Netherlands) connected to a 1 mL syringe.

8. Scalpel, scissors and forceps for eye dissection.

9. Corneal lens.

10. PBS + 5% glycerol: PBS supplemented with 5% glycerol. Used here as the AAV vector storage buffer and thus as buffer to dilute the AAVs. In case that the AAV storage buffer is different than use that buffer to dilute the vectors.

11. Anesthetic.

12. 2% Sevoflurane: 2% Sevoflurane mixed with air/oxygen.

13. 5% Povidone-iodine solution.

14. 2% Hypromellose.

15. Gentomil/Bentelan: mix 1 volume of 40 mg/mL Gentomil with 1 volume of 0.75 mg/mL Bentelan.

16. Stereoscopic microscope.

2.7 Evaluation of the Number of Lipofuscin Granules in the Mouse Model of STGD1 by Electron Microscopy

1. 1 month-old *Abca4*−/− mice.

2. 2 mL centrifuge tubes.

3. Scissors, forceps and scalpel for eye dissection.

4. Bucket with ice.

5. 25 × 75 × 1 mm Glass slides.

6. Parafilm.

7. Grid support for EM sections (Formvar support film hexagonal, 100 mesh, copper grids).

8. 0.4 M PHEM buffer: 240 mM PIPES, 100 mM HEPES, 8 mM MgCl₂, 40 mM EGTA. Adjust pH at 6.9 with NaOH.

9. Fixative solution: 2% paraformaldehyde (PFA), 0.2% glutaraldehyde (GTA), 0.1 M PHEM.

10. Storage solution: 0.5% PFA, 0.1 M PHEM.

11. 12% gelatin in 1× PBS (pH 7.4); 5% gelatin in 1× PBS (pH 7.4); 2% gelatin in 1× PBS (pH 7.4).

12. 2.3 M sucrose in 0.1 M sodium phosphate buffer at pH 7.4.

13. 0.15% Glycine: 0.15% glycine in 1× PBS.

14. 2% Uranyl acetate. Prepare in water.

15. Mixture of Uranyl Acetate and methylcellulose: 0.4% Uranyl acetate dissolved in 1.8% methyl cellulose.

16. Electron microscope such as a FEI Tecnai-12 electron microscope equipped with a VELETTA CCD digital camera.

17. iTEM software: Transmission Electron Microscopy imaging platform iTEM software.

18. Rotating wheel.

3   Methods

To generate dual AAV plasmids, we use the pZac2.1-CMV-*hABCA4*-SV40 plasmid as starting backbone (Fig. 2). The plasmid includes the *hABCA4* CDS with a 3×flag tag at the 3′-end in order to allow efficient protein detection by Western Blot (WB). The two separate dual AAV plasmids (5′ and 3′) contain either the promoter, followed by the N-terminal portion of the transgene CDS (5′ plasmid), or the C-terminal portion of the transgene CDS, followed by the polyadenylation signal (3′ plasmid).

Dual AAV vectors which rely on splicing for transgene reconstitution, such as dual AAV trans-splicing and hybrid vectors, are generated by splitting the gene at an endogenous exon–exon junction. Thus, we split the *hABCA4* CDS between exons 19–20 (5′ half: NM_000350.2, 105–3022 bp; 3′ half: NM_000350.2, bp 3023–6926; *see* **Note 2**), which is approximately in the middle of the CDS, in order to generate two half vectors of approximately the same length, taking also into account the length of the regulatory elements. The SD and SA signals contained in dual AAV trans-splicing

andhybridvectorplasmidsareasfollows:5′-GTAAGTATCAAGGTTA C A A G A C A G G T T T A A G G A G A C C A A T A G A A A C TGGGCTTGTCGAGACAGAGAAGACTCTTGCGTTTCT-3′ (SD; U47120.2, bp 890–971) whose sequence is included in reverse *hABCA4* primer 2 and in forward AK primer 3; 5′-GATAGGCACCTATTGGTCTTACTGACATCCA CTTTGCCTTTCTCTCCACAG-3′ (SA; U47120.2, bp 972–1022) whose sequence is included in forward h*ABCA4* primer 7 and reverse AK primer 6. The SD must be placed right after the end of exon 19, while the SA must be placed right before the beginning of exon 20, so that no additional bases are included in the *hABCA4* CDS after recombination and splicing.

The recombinogenic region we use in hybrid AK vectors is derived from the phage F1 genome (Gene Bank accession number: J02448.1; bp 5850–5926; sequence: 5′-GGGATTTTTCCGATTTCGGCCTATTGGTTAAAAAATG A G C T G A T T T A A C A A A A A T T T A A C G C GAATTTTAACAAAAT-3′). This sequence is found in the F1 origin of replication of many commonly used plasmids, including pAAV2.1. For cloning purposes, the AK sequence is followed by a 32 bp-long region (sequence: attaacgtttataatttcaggtggcatctttc) in each of the dual AAV hybrid AK vectors.

3.1 Cloning strategy of the Plasmid Used to Produce 5′ Hybrid AK AAV Vector

1. Using mutagenesis primers 1 and 2 and the protocol described in the mutagenesis kit, generate a plasmid backbone which includes only the promoter and the *hABCA4* CDS up to exon 19, by deletion mutagenesis of pZac2.1-CMV-*hABCA4*-SV40 plasmid (*see* **Note 3**). Design primers so that the first half aligns to the end of exon 19, and the second half to the 3′ITR. Thus, mutagenesis using these primers results in the deletion of the second half of the *hABCA4* CDS, and of all the remaining bases that are included in the original backbone, between the end of the *hABCA4* CDS and the 3′ ITR.

2. Follow the steps below to generate a fragment including the SD and AK region by overlapping PCR. Set up the first PCR reaction by mixing 10× Pfu buffer, dNTPs, forward h*ABCA4* primer 1, reverse h*ABCA4* primer 2, Pfu DNA polymerase, Taq DNA polymerase, DNA template (plasmid generated in step 1 or pZac2.1-CMV-*hABCA4*-SV40 plasmid), and water in a final volume of 50 μL (*see* Tables 1 and 2).

3. Set up the second PCR reaction by mixing 10× Pfu buffer, dNTPs, forward AK primer 3, reverse AK primer 4, Pfu DNA polymerase, Taq DNA polymerase, DNA template (pAAV2.1), and water in a final volume of 50 μL (*see* Tables 1 and 2).

4. Set up the third PCR reaction by mixing as DNA template 1/10th of the first PCR, 1/10th of the second PCR, 10× Pfu buffer, dNTPs, forward h*ABCA4* primer 1, reverse AK primer

Table 1
PCR protocol

Reagent	Quantity
10× PFU buffer	5 µl
Primers (*see* **Note 4**)	500 nM
dNTPs mix	0.2 mM (each nucleotide)
Pfu DNA polymerase	1.5 U
Taq DNA polymerase	1 U
DNA template	50 ng
H_2O	Up to 50 µL

Table 2
PCR cycling steps

Temperature	Time	Cycle
95 °C	5 min	1
95 °C	45 s	35
3–5 °C below primers' Tm (around 55 °C)	30 s	
68 °C	2 min/kb	
72 °C	7 min	1

Tm melting temperature

4, Pfu DNA polymerase, Taq DNA polymerase and water in a final volume of 50 µL (*see* Tables 1 and 2). This overlapping PCR is used for the amplification of the 5′ hybrid AK full-length product.

5. Subclone the product of the overlapping PCR in the TOPO cloning vector according to the protocol specified by the provider.

6. Transform in TOP10 cells according to the protocol specified by the provider.

7. Pick 5–10 colonies and culture them overnight in 15 mL conical centrifuge tubes with 5 mL LB medium containing an appropriate antibiotic.

8. Using a plasmid miniprep kit, isolate the plasmid DNA from the colonies and analyse the DNA by restriction analysis to identify positive clones (i.e., colonies which contain the overlapping PCR product cloned in the TOPO vector).

9. Sequence the DNA of the positive clones using primers specific for the vector. For this, provide the plasmid DNA and primers to a sequence service provider.

10. Digest the TOPO vector containing the overlapping PCR by FseI and MfeI restriction enzymes.

11. Clone the obtained fragment in the plasmid generated by mutagenesis in step 1 (digested with FseI and MfeI restriction enzymes), according to the ligase protocol detailed in Table 3.

12. Transform the whole volume of ligation in TOP10 cells, according to the protocol specified by the provider.

13. Pick 5–10 colonies, culture them overnight, isolate plasmid DNA from the colonies and analyse DNA by restriction analysis to identify positive clones.

14. Amplify a positive clone in order to obtain an adequate amount of plasmid DNA for AAV vector production (*see* **Note 6**).

3.2 Cloning Strategy of the Plasmid Used to Produce 3′ Hybrid AK AAV Vector

1. Using the mutagenesis primers 3 and 4 and the protocol described in the mutagenesis kit, generate a plasmid backbone which includes the *hABCA4* CDS from exon 20 to the end, the 3×flag tag and SV40 polyA by deletion mutagenesis of pZac2.1-CMV-*hABCA4*-SV40 plasmid (*see* **Note 3**). Design primers so that the first half aligns to the 5′ITR and the second half to the beginning of exon 20. Thus, mutagenesis using these primers results in deletion of the first half of the *hABCA4* CDS and all the remaining bases that are included in the original backbone between the end of the 5′ ITR and the beginning of the *hABCA4* CDS.

2. Follow the steps below to generate a fragment including the AK region and the SA by overlapping PCR. Set up the first PCR reaction by mixing 10× Pfu buffer, dNTPs, forward AK primer 5, reverse AK primer 6, Pfu DNA polymerase, Taq

Table 3
Ligase protocol

Reagent	Quantity
Backbone DNA	25 ng
Insert DNA	Molar ratio of 3:1 of insert to vector (*see* **Note 5**)
10× T4 DNA Ligase Buffer	2 μL
T4 DNA Ligase	2 μL
H_2O	Up to 20 μL

Keep 30 min at room temperature and then overnight at 16 °C

DNA polymerase, DNA template (pAAV2.1) and water in a final volume of 50 μL (*see* Table 1).

3. Set up the second PCR reaction by mixing 10× Pfu buffer, dNTPs, forward h*ABCA4* primer 7, reverse h*ABCA4* primer 8, Pfu DNA polymerase, Taq DNA polymerase, DNA template (plasmid generated in step 1 or pZac2.1-CMV-h*ABCA4*-SV40 plasmid), and water in a final volume of 50 μL (*see* Table 1).

4. Set up the third PCR reaction by mixing as DNA template 1/10th of the first PCR, 1/10th of the second PCR, 10× Pfu buffer, dNTPs, forward AK primer 5, reverse h*ABCA4* primer 8, Pfu DNA polymerase, Taq DNA polymerase, and water in a final volume of 50 μL (*see* Table 1). This overlapping PCR is used for the amplification of the 3′ hybrid AK full-length product.

5. Subclone the product of the overlapping PCR in the TOPO cloning vector according to the protocol specified by the provider.

6. Transform in TOP10 cells according to the protocol specified by the provider.

7. Pick 5–10 colonies and culture them overnight in 15 mL conical centrifuge tubes with 5 mL LB medium containing an appropriate antibiotic.

8. Using a plasmid miniprep kit, isolate the plasmid DNA from the colonies and analyse the DNA by restriction analysis to identify positive clones.

9. Sequence the DNA of the positive clones using primers specific for the vector. For this, provide the plasmid DNA and primers to a sequence service provider.

10. Digest the TOPO vector containing the overlapping PCR by BamHI and NdeI restriction enzymes.

11. Clone the obtained fragment in the plasmid generated by mutagenesis in step 1, (digested with BamHI and NdeI restriction enzymes), according to the ligase protocol detailed in Table 3.

12. Transform the whole volume of ligation in TOP10 cells, according to the protocol specified by the provider.

13. Pick 5–10 colonies, culture them overnight, isolate plasmid DNA from the colonies and analyse DNA by restriction analysis to identify positive clones.

14. Amplify a positive clone in order to obtain an adequate amount of plasmid DNA for AAV vector production (*see* **Note 6**).

3.3 Cloning Strategy of Plasmids Used to Produce Dual AAV trans-Splicing Vectors

Dual AAV trans-splicing vectors are designed to be identical to hybrid vectors except for the absence of the AK recombinogenic region. Thus, the corresponding plasmids are generated as detailed below.

3.3.1 5′ Plasmid

1. Set up a PCR reaction by mixing 10× Pfu buffer, dNTPs, forward h*ABCA4* primer 1, reverse SD primer 9, Pfu DNA polymerase, Taq DNA polymerase, DNA template (5′ hybrid AK plasmid generated in Subheading 3.1) and water in a final volume of 50 μL (*see* Tables 1 and 2).

2. Subclone the product of the PCR in the TOPO cloning vector according to the protocol specified by the provider.

3. Transform in TOP10 cells according to the protocol specified by the provider.

4. Pick 5–10 colonies and culture them overnight in 15 mL conical centrifuge tubes with 5 mL LB medium containing an appropriate antibiotic.

5. Isolate plasmid DNA from the colonies and analyse DNA by restriction analysis to identify positive clones.

6. Sequence the DNA of the positive clones using primers specific for the vector.

7. Digest the TOPO vector containing the overlapping PCR by FseI and MfeI restriction enzymes.

8. Clone the obtained fragment in the 5′ hybrid AK plasmid (generated in Subheading 3.1), digested with FseI and MfeI restriction enzymes, according to the ligase protocol detailed in Table 3.

9. Transform the whole volume of ligation in TOP10 cells, according to the protocol specified by the provider.

10. Pick 5–10 colonies, culture them overnight, isolate plasmid DNA from the colonies and analyse DNA by restriction analysis to identify positive clones.

11. Amplify a positive clone in order to obtain an adequate amount of plasmid DNA for AAV vector production (*see* **Note 6**).

3.3.2 3′ Plasmid

1. Set up a PCR reaction by mixing 10× Pfu buffer, dNTPs, forward SA primer 10, reverse *hABCA4* primer 8, Pfu DNA polymerase, Taq DNA polymerase, DNA template (3′ hybrid AK plasmid generated in Subheading 3.2) and water in a final volume of 50 μL (*see* Tables 1 and 2).

2. Subclone the product of the PCR in the TOPO cloning vector according to the protocol specified by the provider.

3. Transform in TOP10 cells according to the protocol specified by the provider.

4. Pick 5–10 colonies and culture them overnight in 15 mL conical centrifuge tubes with 5 mL LB medium containing an appropriate antibiotic.

5. Isolate plasmid DNA from the colonies and analyse DNA by restriction analysis to identify positive clones.

6. Sequence the DNA of the positive clones using primers specific for the vector.

7. Digest the TOPO vector containing the overlapping PCR by BamHI and NdeI restriction enzymes.

8. Clone the obtained fragment in the 3′ hybrid AK plasmid (generated in Subheading 3.2), digested with BamHI and NdeI restriction enzymes, according to the ligase protocol detailed in Table 3.

9. Transform the whole volume of ligation in TOP10 cells, according to the protocol specified by the provider.

10. Pick 5–10 colonies, culture them overnight, isolate plasmid DNA from the colonies and analyse DNA by restriction analysis to identify positive clones.

11. Amplify a positive clone in order to obtain an adequate amount of plasmid DNA for AAV vector production (*see* **Note 6**).

3.4 Evaluation of Transduction Efficiency in HEK293 Cells

1. Produce AAV2 vectors from the four plasmids generated in Subheadings 3.1, 3.2, 3.3.1 and 3.3.2 (*see* **Note 7**), and determine the titer.

2. Test dual AAV vector transduction efficiency in HEK293 cells according to the following steps. All the steps have to be carried out in a cell culture hood using proper aseptic culture practices.

3. Plate 1×10^6 HEK293 cells in 6-wells plates, in order to reach an optimal confluence for AAV infection of about 70% on the day after. Keep the cells in DMEM growing medium.

4. The day after, change the medium with 2 mL of fresh DMEM growing medium, then transfect cells with pΔF6 helper plasmid using the calcium phosphate method (*see* **Note 8**). Specifically: prepare a mix of 0.3 M $CaCl_2$ and pΔF6 helper plasmid (150 μL of $CaCl_2$ and 1.5 μg of pΔF6 helper plasmid are required for each well) and mix thoroughly. In a 50 mL polypropylene tube prepare 2× HBS (150 μL are required for each well) and slowly (drop-wise) add the mix of $CaCl_2$ and pΔF6 helper plasmid while bubbling air through HBS with a pipette (*see* **Note 9**); wait at least 5 min, until fine precipitates will form in the solution, then add 300 μL of the mix in each well, without removing the medium.

5. Four hours after transfection remove the medium and wash the cells with serum-free DMEM.

6. Incubate the cells with the infection mix (*see* **Note 8**) which is composed of each of the dual AAV vectors at a multiplicity of infection (MOI; *see* **Note 10**) of 10^5 genome copies (GC)/

cell (total MOI 2×10^5 GC/cell) and serum-free DMEM up to 700 μL (*see* **Note 11**).

7. Two hours post-infection add 2 mL of DMEM growing medium.

8. Harvest the cells 72 h post-infection in 1.5 mL centrifugation tubes.

9. Centrifuge at $2500 \times g$ for 5 min at 4 °C.

10. Directly proceed to protein extraction or store the cell pellet at -80 °C.

3.5 ABCA4 Protein Extraction

All the steps have to be performed at 4 °C.

1. Lyse the cell pellet (deriving from one well of the 6-well plate) in 30–50 μL of RIPA lysis buffer.

2. Keep the lysate 30 min on ice.

3. Perform a freeze and thaw step by freezing on liquid nitrogen or dry ice ethanol slurry and thawing on ice.

4. Isolate protein lysate from the cell pellet by centrifugation at $16{,}000 \times g$ for 10 min at 4 °C and transfer it to a new 1.5 mL centrifugation tube.

5. Measure the protein concentration in the lysate using an appropriate protein assay kit. Use 30–50 μg of proteins for further Western blot analysis as described in the next section.

3.6 Western Blot Procedure

1. Add a volume of 2× sample buffer to the protein lysate.

2. Keep the mix obtained 15 min at 37 °C.

3. Run the samples on a 6% polyacrylamide gel in running buffer at 130 V for about 3 h.

4. Transfer the proteins from the gel to a PVDF membrane by overnight blotting (*see* **Note 12**) in transfer buffer at 30 V in a cold room and the day after for 1 h at 100 V, still in a cold room.

5. Remove the membrane from the blotting apparatus.

6. Block 1 hour in blocking buffer at room temperature.

7. Incubate with anti-3×flag antibodies (to detect the 3×flag tag located at the C-terminus of the ABCA4 protein produced from dual AAV vectors) diluted 1:1000 in blocking buffer for 2 h at room temperature (*see* **Note 13**).

8. Remove the antibody and wash the membrane three times for 5 min with TBST.

9. Incubate the membrane with HRP-conjugated secondary antibody diluted in blocking buffer for 45 min at room temperature.

10. Remove the secondary antibody and wash the membrane three times for 10 min with TBST.

11. Apply the chemiluminescent substrate to the blot and capture chemiluminescent signals using a CCD camera-based imager.

12. Blot the membrane with an appropriate normalizer of high molecular weight (*see* **Note 14**).

3.7 Evaluation of Transduction Efficiency In Vivo

3.7.1 Injection of Dual AAV Vectors in the Mouse Retina

1. Produce AAV8 vectors from the plasmids generated in Subheadings 3.1, 3.2, 3.3.1 and 3.3.2 (*see* **Note 7**), and determine the titer.

2. Prepare the dual AAV vector mix by mixing freshly thawed vectors. A dose of at least 1×10^9 GC of each vector per eye is recommended; depending on the titer of the vector preparations, use the highest dose achievable taking into account that the final volume that will be injected in the subretinal space is 1 μL and that the same number of GC of each vector must be contained in this volume. As an example, if a mix of vector A and B has to be injected and vector A has a titer of 3×10^{12} GC/mL and vector B has a titer of 7×10^{12} GC, the maximum dose of 2, 1×10^9 GC of each vector per eye can be used by mixing 0.7 μL of vector A and 0.3 μL of vector B (*see* **Note 15**). If in need of diluting vectors, use the same solution in which the vectors are dissolved (i.e., PBS or PBS + 5% glycerol).

3. Anesthetize C57BL/6J mice (*see* **Note 16**) and apply 1–2 drops of 0.5% tropicamide on mouse eyes in order to dilate the pupils.

4. Place the mouse under the microscope and pull out slightly the eye from the globe by applying a small pressure around the eye.

5. Perform subretinal injection as previously described [20]. Briefly, carefully cut the conjunctiva at the level of the limbus, and perform a sclerotomy through the use of a 30 G needle; finally introduce the needle (33 G) of a Hamilton syringe in the subretinal space in the temporal side through the space created by the sclerotomy and release 1 μL of vector solution.

6. After removal of the syringe, apply an antibiotic cream on the eyes of the mice.

7. At least 1 month post-injection sacrifice the mice, remove the eye completely intact by cutting at the level of the optic nerve, remove the cornea, the lens and the vitreous with the help of scissors and forceps, and harvest the neural retina (*see* **Note 17**).

8. Immediately freeze and store the retinas at −80 °C or lyse them in 30–50 μL of lysis buffer and proceed to WB analysis as described in Subheadings 3.5 and 3.6. A maximum amount of 200 μg should be used in WB analysis to avoid overloading of the gel.

9. After blotting and incubation of the membrane with 3×flag antibodies to detect the 3×flag tag included in the ABCA4 protein, blot the membrane also with an appropriate normalizer of high molecular weight (*see* **Note 18**).

1. Prepare vector mix just before injections taking into account that a dose of 1×10^{11} GC of each vector per eye is recommended and 100 µL of vectors mix solution will be injected in the subretinal space. Also, needles used for injections in pigs have a large dead volume, so it is recommended to prepare at least 250 µL of vectors mix solution per each eye. If in need of diluting vectors, use the same solution in which vectors are dissolved (i.e., PBS or PBS + 5% glycerol).

2. Anesthetize Large White pigs and perform tracheal intubation to keep pigs under general anesthesia with 2% sevoflurane.

3. Apply povidone–iodine solution periocularly and on the cornea, before and after the injection procedure.

4. Perform subretinal injection with the help of a microscope as previously described [21]. Briefly, perform two sclerotomies with a 23 G needle in the temporal and in the nasal side of the eye (3–4 mm from the limbus).

5. Position a trocar on each side of the eye, in order to allow the insertion of a light fiber from the temporal side and of the subretinal needle from the nasal side.

6. Load 250 µL of vector mix solution in a 1 mL syringe connected to the subretinal injection needle.

7. Slowly inject 100 µL in the subretinal space, in the nasal area, illuminating the posterior pole with the light fiber, without vitreous removal, under direct observation with a stereoscopic microscope and the help of a lens placed on the cornea through a film of 2% hypromellose.

8. After injection, remove about 0.1 mL of aqueous humor, using a 1 mL syringe with 30-G needle, in order to avoid an increase in intraocular pressure.

9. At the end of surgery, after removal of the light fiber, subretinal needle and trocars, release 500 µL of Gentomil/Bentelan solution in the conjunctiva. Additionally, systemic antibiotic administration is advised.

10. One month post-injection sacrifice the pigs by exposure to a lethal dose of anesthetic.

11. Remove the eye completely intact by cutting at the level of the optic nerve, remove the cornea, the lens and the vitreous with the help of scalpel and forceps, and harvest the neural retina, separating the putative site of injection from the remaining part of the retina (*see* **Notes 17** and **19**).

12. Immediately freeze and store the retinas at −80 °C or lyse them in 150 µL (each of the region of the retina, or use 300 µL if lysing whole retinas) of lysis buffer and proceed to WB analysis as described in Subheadings 3.5 and 3.6. A maximum

amount of 200 μg should be used in WB analysis to avoid overloading of the gel.

13. After blotting of the membrane with 3×flag antibodies to detect the 3×flag tag included in the ABCA4 protein, blot the membrane also with an appropriate normalizer of high molecular weight (*see* **Note 18**).

3.8 Evaluation of the Efficacy in the Mouse Model of STGD1

The efficacy is evaluated by counting the number of lipofuscin granules, which accumulate in the RPE of *Abca4−/−* mice compared to WT [22], by electron microscopy (EM).

1. Perform subretinal injection of dual AAV vectors in *Abca4−/−* mice (*see* **Note 20**), as described in Subheading 3.7.1 (*see* **Note 21**).

2. At least 3 months later, sacrifice the mice, mark the temporal (injected) side of the eyes before harvesting and place the eyes in fixative solution.

3. Fix the eyes overnight in the dark then wash three times for 5 min in 0.1 M PHEM buffer and proceed with embedding in gelatin or store the eyes in storage solution.

4. Prepare the eyes for embedding: remove the cornea and the lens from the eye and dissect the area of interest (temporal half of the eye). If an AAV expressing a marker gene has been injected along with dual AAV vectors, dissect the area of interest by looking at marker gene expression (i.e., brown dots if using tyrosinase).

5. Keep the dissected area in 2% gelatin for 30 min at 37 °C.

6. Change to 5% gelatin for 30 min at 37 °C.

7. Change to 12% gelatin for 30 min at 37 °C.

8. Proceed to embedding in a thin slab of 12% gelatin (obtained by putting a drop of gelatin between two glass slides, covered with parafilm and distanced by 0.2–0.3 mm spacers).

9. Keep the glass slides on ice for 30 min.

10. Remove the gelatin block from the glass slides, move it in a 2 mL centrifuge tube filled with 2.3 M sucrose and leave overnight on a rotating wheel at 4 °C.

11. The day after remove the sample from the wheel and store at 4 °C or proceed to sectioning.

12. Section the gelatin block ($T = -120$ °C; thickness = 60 nm) and transfer the section ribbon on grid support for EM.

13. Wash the grids two times for 2 min with 0.15% glycine.

14. Wash the grids eight times for 1 min with H_2O.

15. Incubate the grids on ice, with 2% Uranyl Acetate for 6 min.

16. Wash the grids on ice with a mixture of Uranyl Acetate and methyl cellulose.

17. Incubate the grids on ice with a mixture of Uranyl Acetate and methyl cellulose for 6 min.

18. Pick up and dry the grids, and store them in a grids box.

19. Acquire electron microscopy images using a FEI Tecnai-12 electron microscope equipped with a VELETTA CCD digital camera at the 20,000× magnification.

20. Use the images to count the number of lipofuscin granules within each field of view ($25~\mu m^2$) using iTEM software.

4   Notes

1. Solutions do not need to be freshly made for each transfection. They can be stored at $-20~^{\circ}C$ for long periods or at $4~^{\circ}C$ for shorter.

2. The splitting site can influence the efficiency of the splicing, thus it is recommended to use the same exon-exon junction we have successfully tested.

3. The mutagenized plasmid should be wholly sequenced to double-check that both a precise deletion has occurred and that no additional mutations have been included in the plasmid during the mutagenesis reaction.

4. The highest grade of primer purification after synthesis should be used for primers intended for cloning (SDS-page or HPLC).

5. Nanograms of insert to be used can be calculated considering the relative length of the backbone and insert, according to the formula: required mass insert (g) = desired insert to backbone molar ratio × mass of backbone (g) × ratio of insert to backbone lengths. As an example, if the backbone is 3000 bp-long and the insert is 1000 bp-long, 25 ng of insert should be used in the ligase according to the protocol provided [required mass insert (g) = $3 \times 25 \times 10^{-9} \times 1000/3000$].

6. Plasmid intended to be used for AAV vector production should be purified with a kit that ensures removal of endotoxins during plasmid preparation.

7. AAV vectors are produced by triple transfection of HEK293 cells followed by two rounds of $CsCl_2$ purification, according to the published protocol [23]. For the in vitro experiments, produce AAV2 vectors which efficiently transduce HEK293 cells [24], while produce AAV8 vectors for the experiments performed in vivo in the mouse and pig retina, since this serotype efficiently transduces photoreceptors [21, 25] but poorly infects HEK293 cells. Suspend AAV vectors in PBS + 5%

glycerol, aliquot and store at −80 °C until use. Given the small volumes needed for subretinal injections, it is suggested to prepare 20 μL aliquots of the vectors.

8. In order to check the efficiency of transfection and infection procedures it is advisable to use one well of the plate for transfection of a plasmid encoding for a reporter gene (in parallel with helper plasmid transfection, using the same reagents and transfection protocol) and one well of the plate in which cells have been transfected with the helper plasmid for further infection with an AAV vector encoding for a reporter gene (in parallel with dual AAV infection, using same reagents, infection protocol and AAV serotype).

9. Extensive bubbling is crucial for correct precipitates formation and consequently effective transfection. Thus, to promote bubbling, it is suggested to prepare a mix of at least 5 mL of $CaCl_2$ + 5 mL of HBS, even if in need of transfecting few wells.

10. MOI corresponds to the number of viral particles per cell; as an example, a MOI of 1 means infecting with 1 AAV vector per cell.

11. Infections must be performed in the minimum amount of medium that completely covers the bottom of the plates; if scaling up the plate format for the infection, use an adequate amount of medium, without exceeding.

12. Assemble the transfer sandwich making sure no air bubbles are trapped in the sandwich.

13. Overnight incubation at 4 °C might be explored to enhance detection of low amounts of protein.

14. Filamin A protein might be used as normalizer or loading control for WB on cellular lysates.

15. It is suggested to prepare a total mix of at least 30 μL to avoid handling too small volumes and to be sure that the needle of the syringe will be completely submerged in the mix, avoiding intake of air.

16. It is important to check that the mouse strain that will be used in expression studies does not carry any gene causative of retinal degeneration (as example, C57BL/6N have been found to carry the rd8 mutation of the *Crb1* gene [26]).

17. Since *ABCA4* is physiologically expressed only in PR, dissection of the neural retina from the RPE is suggested to evaluate specifically dual AAV-mediated *ABCA4* expression in PR. However, when using a ubiquitous promoter, such as the CMV, that will drive *ABCA4* expression both in PR and in the RPE, cross-contamination of the neural retina with RPE during dissection process may result in a WB signal that cannot be precisely ascribed to PR. Thus, to more precisely assess *ABCA4*

expression in PR, it is advisable to use a promoter that drives gene expression exclusively in PR, such as the rhodopsin promoter [25].

18. Dysferlin protein might be used as normalizer or loading control for WB on retinal lysates.

19. A record of the area in which injection was performed should be taken at the time of surgery in order to allow dissection of the injection site from the uninjected portion of the retina. This is crucial to enrich the sample with ABCA4 expression for further WB analysis. If then intense ABCA4 expression is found in the enriched area in WB analysis, an equal volume of enriched and not enriched samples can be pulled together for further WB analysis in order to show expression in the whole retina.

20. The use of *Abca4−/−* mice on an albino background for electron microscopy analysis is preferable since lipofuscin granules in the RPE might be more easily identified on an albino than on a pigmented background.

21. For electron microscopy analysis, coinjection of a virus that expresses a gene that allows tracking of the injection site at harvesting is suggested (at a dose of 1:5 or less of dual AAV dose). If using albino mice, the tyrosinase gene might be included [27].

Acknowledgments

References

1. Molday RS, Zhang K (2010) Defective lipid transport and biosynthesis in recessive and dominant Stargardt macular degeneration. Prog Lipid Res 49:476–492

2. Allikmets R, Singh N, Sun H et al (1997) A photoreceptor cell-specific ATP-binding transporter gene (ABCR) is mutated in recessive Stargardt macular dystrophy. Nat Genet 15:236–246

3. Trapani I, Puppo A, Auricchio A (2014) Vector platforms for gene therapy of inherited retinopathies. Prog Retin Eye Res 43:108–128

4. Dalkara D, Goureau O, Marazova K et al (2016) Let there be light: gene and cell therapy for blindness. Hum Gene Ther 27:134–147

5. Trapani I, Banfi S, Simonelli F et al (2015) Gene therapy of inherited retinal degenera-

tions: prospects and challenges. Hum Gene Ther 26:193–200

6. Carvalho LS, Vandenberghe LH (2015) Promising and delivering gene therapies for vision loss. Vis Res 111:124–133

7. Colella P, Auricchio A (2012) Gene therapy of inherited retinopathies: a long and successful road from viral vectors to patients. Hum Gene Ther 23:796–807

8. Lipinski DM, Thake M, MacLaren RE (2013) Clinical applications of retinal gene therapy. Prog Retin Eye Res 32:22–47

9. Trapani I, Colella P, Sommella A et al (2014) Effective delivery of large genes to the retina by dual AAV vectors. EMBO Mol Med 6:194–211

10. Dyka FM, Boye SL, Chiodo VA et al (2014) Dual adeno-associated virus vectors result in efficient in vitro and in vivo expression of an oversized gene, MYO7A. Hum Gene Ther Methods 25:166–177

11. Lopes VS, Boye SE, Louie CM et al (2013) Retinal gene therapy with a large MYO7A cDNA using adeno-associated virus. Gene Ther 20:824–833

12. Colella P, Trapani I, Cesi G et al (2014) Efficient gene delivery to the cone-enriched pig retina by dual AAV vectors. Gene Ther 21:450–456

13. Yan Z, Zhang Y, Duan D et al (2000) Trans-splicing vectors expand the utility of adeno-associated virus for gene therapy. Proc Natl Acad Sci U S A 97:6716–6721

14. Duan D, Yue Y, Engelhardt JF (2001) Expanding AAV packaging capacity with trans-splicing or overlapping vectors: a quantitative comparison. Mol Ther 4:383–391

15. Ghosh A, Yue Y, Lai Y et al (2008) A hybrid vector system expands adeno-associated viral vector packaging capacity in a transgene-independent manner. Mol Ther 16:124–130

16. Trapani I, Colella P, Sommella A et al (2013) Effective delivery of large genes to the retina by dual AAV vectors. EMBO Mol Med 6:194–211

17. Ghosh A, Yue Y, Duan D (2011) Efficient transgene reconstitution with hybrid dual AAV vectors carrying the minimized bridging sequences. Hum Gene Ther 22:77–83

18. Auricchio A, Hildinger M, O'Connor E et al (2001) Isolation of highly infectious and pure adeno-associated virus type 2 vectors with a single-step gravity-flow column. Hum Gene Ther 12:71–76

19. Zhang Y, Chirmule N, Gao G et al (2000) CD40 ligand-dependent activation of cytotoxic T lymphocytes by adeno-associated virus vectors in vivo: role of immature dendritic cells. J Virol 74:8003–8010

20. Liang FQ, Anand V, Maguire AM et al (2001) Intraocular delivery of recombinant virus. Methods Mol Med 47:125–139

21. Mussolino C, della Corte M, Rossi S et al (2011) AAV-mediated photoreceptor transduction of the pig cone-enriched retina. Gene Ther 18:637–645

22. Weng J, Mata NL, Azarian SM et al (1999) Insights into the function of Rim protein in photoreceptors and etiology of Stargardt's disease from the phenotype in abcr knockout mice. Cell 98:13–23

23. Doria M, Ferrara A, Auricchio A (2013) AAV2/8 vectors purified from culture medium with a simple and rapid protocol transduce murine liver, muscle, and retina efficiently. Hum Gene Ther Methods. 24:392–398

24. Dong X, Tian W, Wang G et al (2010) Establishment of an AAV reverse infection-based array. PLoS One 5:e13479

25. Allocca M, Mussolino C, Garcia-Hoyos M et al (2007) Novel adeno-associated virus serotypes efficiently transduce murine photoreceptors. J Virol 81:11372–11380

26. Mattapallil MJ, Wawrousek EF, Chan CC et al (2012) The Rd8 mutation of the Crb1 gene is present in vendor lines of C57BL/6N mice and embryonic stem cells, and confounds ocular induced mutant phenotypes. Invest Ophthalmol Vis Sci 53:2921–2927

27. Gargiulo A, Bonetti C, Montefusco S et al (2009) AAV-mediated tyrosinase gene transfer restores melanogenesis and retinal function in a model of oculo-cutaneous albinism type I (OCA1). Mol Ther 17:1347–1354

Optogenetic Retinal Gene Therapy with the Light Gated GPCR Vertebrate Rhodopsin

Benjamin M. Gaub, Michael H. Berry, Meike Visel, Amy Holt, Ehud Y. Isacoff, and John G. Flannery

Abstract

In retinal disease, despite the loss of light sensitivity as photoreceptors die, many retinal interneurons survive in a physiologically and metabolically functional state for long periods. This provides an opportunity for treatment by genetically adding a light sensitive function to these cells. Optogenetic therapies are in development, but, to date, they have suffered from low light sensitivity and narrow dynamic response range of microbial opsins. Expression of light-sensitive G protein coupled receptors (GPCRs), such as vertebrate rhodopsin, can increase sensitivity by signal amplification, as shown by several groups. Here, we describe the methods to (1) express light gated GPCRs in retinal neurons, (2) record light responses in retinal explants in vitro, (3) record cortical light responses in vivo, and (4) test visually guided behavior in treated mice.

Key words Retinitis pigmentosa, Congenital blindness, Retinal gene therapy, Optogenetics, Translational medicine, Visual prosthetics, Light-gated receptors

1 Introduction

Inherited retinal degenerative diseases are a significant unmet medical problem, affecting one in 3000 people worldwide [11–13]. There is currently only one FDA approved treatment for retinal degeneration, the Second Sight Electronic prosthesis [14]. There are currently a few Phase I/II gene therapy clinical trials started, nearly all for patients in the early stages of monogenic disease where there are surviving photoreceptors to treat. These trials, which are encouraging, are mostly limited to "gene replacement" for disease resulting from recessive null mutations in causative genes with a coding region below 8 kb, the size cutoff for AAV or lentiviral vectors.

In retinal disease, many retinal interneurons survive in a physiologically and metabolically functional state for long periods

(years), providing an opportunity for treatment by genetically adding a light sensitive function to these cells [15, 16]. One approach used by several groups is to add a light-receptive function to the surviving inner retinal neurons by expressing a microbial opsin [1, 2, 3, 5, 7–10]. In 2014, the FDA approved a clinical trial for RST-001 (RetroSense Inc.), an intravitreal AAV2 vector to transfer Channelrhodopsin-2 (ChR2) to retinal ganglion cells [17]. GenSight, Inc., is beginning a clinical trial using intravitreal AAV to deliver ChrimsonR to cone inner segments [4] in patients with severe vision deficit from rod cell death, and loss of the light-sensitive cone outer segments.

Poor light sensitivity is one of the biggest challenges to the optogenetic vision restoration. The threshold intensity required to activate ChR2-sensitized bipolar cells and ganglion cells is 10^{15} photons/cm^2 s [9, 10] (*see* Fig. 1). Halorhodopsin (NpHR) expressed in cones has slightly better light sensitivity, requiring a minimum of 10^{13} photons/cm^2 s to generate a measurable photocurrent [3]. In comparison, activation threshold of the endogenous photopigments in rods (10^6 photons/cm^2 s) and cones (10^{10} photons/cm^2 s) is substantially lower [9].

Furthermore, microbial opsins have limited sensitivity range—ChR2 and NpHR only adapt to intensity changes of 2–3 orders of magnitude, whereas rods and cones adjust their responses to 8–9 orders of magnitude [3, 4]. ChR2 and NpHR operating as a single unit (without a GPCR cascade), require very high intensity light for stimulation. Additionally, the bright light intensity must be carefully regulated so as to not saturate the cell response, which could cause failure of the cells to follow high frequency stimulation [18, 19].

Recently, Acucela, Inc. has licensed a human rhodopsin based optogenetic gene therapy [20] for treatment of RP from the Univ. of Manchester [21], which promises to have higher sensitivity than ChR2 variants. In their study, AAV-mediated expression of rhodopsin into both RGCs and inner nuclear layer neurons generated reproducible responses to light pulses at the intensities as low as 10^{12} photons/cm^2 s, within the range of the irradiance encountered in our daily life. We have found very similar sensitivities by AAV mediated expression of rhodopsin in specific retinal cell classes (*see* Fig. 1) [22].

In all these approaches, the early responses from patients will tell us much about what is needed for a workable retinal prosthetic. While awaiting those exciting results, it is clear that these approaches have shortcomings: (1) microbial gene expression in a mammalian tissue is a potential concern, (2) once expressed, the opsin cannot be silenced in case of adverse reaction, and (3) microbial opsins operate over a narrow range of light and only at very high intensity, an intensity that is likely to cause light damage to the surviving retinal cells over time.

Light-sensitivity of natural and artificial photoreceptor systems
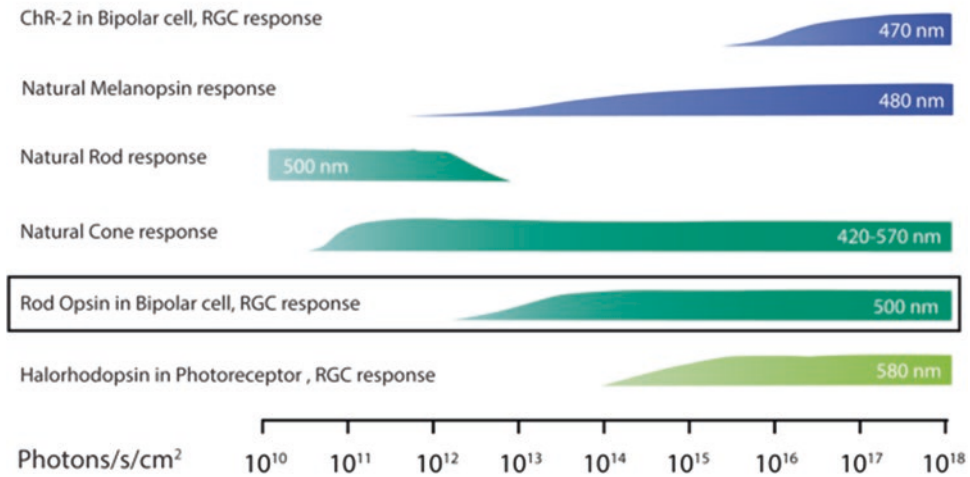
Fig. 1 Comparison of the light sensitivities of natural and artificial photoreceptor systems. Rod and cone photoreceptor sensitivities and melanopsin-expressing retinal ganglion cell sensitivity are compared with those of halorhodopsin (NpHR), wild-type channelrhodopsin 2 (ChR2), and vertebrate rhodopsin installed in various cell types. Light sensitivities are given in photons/cm^2 s The wavelengths for the respective therapeutic approaches are color-coded and indicated as numbers in white. All optogenetic channel light sensitivities are based on in vitro retinal whole-mount recordings from retinal ganglion cells (Figure modified from [27])

Here, we describe a gene therapy based method to deliver the light gated mammalian GPCR vertebrate rhodopsin to the retina of blind mice. We show how to verify expression of rhodopsin in retinal tissue and how to probe the treated retina for light responses in vitro. Further, we describe in detail how to test light responses in vivo, first by recording visually evoked responses in the visual cortex and second, by testing visually guided behavior in treated mice.

2   Materials

2.1   Intraocular AAV Injection

1. Retinal degeneration mice: rd1, rd10 strains. Control mice with wildtype retina on similar genetic background: C57/BL-J.

2. 1 μl of AAV >10^{13} vg/ml per eye to be injected.

3. 72 mg/kg Ketamine and 64 mg/kg xylazine for general anesthesia.

4. 0.5% Proparacaine, 2.5% phenylephrine, 1% tropicamide for topical anesthesia of the cornea.

5. Sharp 30-G needle (disposable tuberculin syringe).

6. Blunt 32 G 1-cm Hamilton syringe.

7. Operating Microscope with foot-controlled motorized focus.

8. 1% phenol red in PBS.

9. Heating pad.

10. See video of injection procedure at JOVE [23].

2.2 Verification of Gene Expression

1. Microscope slides and coverslips.

2. 4% paraformaldehyde (PFA).

3. Phosphate Buffered Saline (PBS).

4. Fine forceps.

5. Fine scissors.

6. Agarose.

7. Vibratome sectioning device.

8. Vectashield mounting medium with DAPI.

9. Fluorescent microscope with digital imaging camera, computer and software.

10. Blocking buffer: 10% normal goat serum (NGS), 1% BSA, 0.5% Triton X-100 in PBS (pH 7.4).

11. Appropriate combinations of primary and secondary antibodies (optional).

2.3 In Vitro Multielectrode Array (MEA) Recordings of Retina Response

1. Dissection stereomicroscope.

2. Darkroom with dim red light.

3. Fine scissors, forceps and scalpel.

4. Small incubator.

5. Organotypic cell culture inserts (Millicell, Millipore).

6. 60-channel perforated MEA1060 multi electrode array system with constant vacuum pump (Multi Channel Systems).

7. MEA chamber pMEA 100/30iR-Tpr (Multi Channel Systems).

8. Mesh weight (Slice grids, Scientific Instruments).

9. Ames media (Sigma).

10. Constant perfusion system to supply oxygenated Ames media (32 °C).

11. Heating system for media.

12. Illumination system for optogenetic stimulation (DG-4, Sutter Instruments).

13. Green band pass filter 510/50 nm (Thorlabs).

14. Upright microscope.

15. MCS rack software (Multi Channel Systems).

16. Analysis software: Offline Sorter (Plexon).

2.4   In Vivo Visually Evoked Potential (VEP) Recordings of Cortical Response

1. 2 mg/kg Chlorprothixene.

2. 1.5 g/kg Urethane for general anesthesia.

3. Isoflurane for general anesthesia.

4. Temperature controller, rectal probe, and heating pad.

5. 1% Tropicamide.

6. Silicone oil.

7. Syringe with 25 G needle.

8. Fine forceps and scissors.

9. Acrylic glue (Ortho-Jet BCA).

10. Betadine solution.

11. Marker pen.

12. Small ruler.

13. Handheld dental drill with foot pedal control.

14. Custom made metal head plate.

15. Borosilicate glass (1.5 mm OD, 1.16 mm ID, Warner Instruments).

16. Horizontal puller (Sutter Instruments).

17. Artificial cerebrospinal fluid (ACSF): 124 mM NaCl, 2.5 mM KCl, 2.0 mM $MgSO_4$, 1.25 mM KH_2PO_4, 26 mM $NaHCO_3$, 10 mM glucose, 4 mM sucrose, 2.5 mM $CaCl_2$. Note: When the components are first mixed, the ACSF solution may be slightly milky, but it should clear when aerated with 95% O_2, 5% CO_2, after which the pH of the medium should be 7.4.

18. Microscope and micromanipulator.

19. LED light source with fiber optic light guide (455 nm, 15 mW/cm², Thorlabs).

20. Axoclamp 200B amplifier (Axon Instruments).

21. I/O board (Lab-PC-1200, National Instruments).

22. Custom made acquisition software written in MatLab.

2.5   Visually Guided Behavior: Open Field Test

1. Plastic box (dimensions l = 60 cm, w = 40 cm, h = 30 cm) with a light compartment (l = 25 cm, w = 40 cm, h = 30 cm) with white walls and a dark compartment (l = 35 cm, w = 40 cm, h = 30 cm) with black walls and small area between the two compartments (h = 5 cm, w = 10 cm).

2. Ethanol.

3. Light source (custom 5 × 6 LED array (447.5 nm Rebel LED, Luxeon star).

4. Video camera.

2.6 Visually Guided Behavior: Forced 2-Choice Water Maze Task	1. Y-maze (or modified radial arm maze).
	2. Transparent escape platform.
	3. Ethanol.
	4. Light source (custom LED array (5 × 6 LEDs, 447.5 nm Rebel LED, Luxeon star).
	5. Video camera.
	6. 6 cm diameter glass beaker.
2.7 Visually Guided Behavior: Light Cued Fear Conditioning	1. Coulbourn shock chamber Habitest with test cage.
	2. Ethanol.
	3. Light source (custom 5 × 6 LED array (447.5 nm Rebel LED, Luxeon star).
	4. Freeze-frame acquisition software.

3 Methods

3.1 DNA Preparation and AAV Production

1. For targeted expression of vertebrate rhodopsin in ON-bipolar cells, prepare a plasmid containing a 4× repeat of the metabotropic glutamate receptor 6 promoter (4×grm6) followed by the rat rhodopsin gene tagged C-terminally with a yellow fluorescent protein. The DNA cassette should be flanked on either side by inverted terminal repeat (ITR) domains. Package and purify Adeno associated virus serotype 2 with the rAAV2/2(4YF) capsid following the protocol of Visel et al. [24]

2. For further instructions on DNA preparation and AAV packaging and purification, *see* **Notes 1–3** and refer to the methods paper by Visel et al. [24]

3.2 Intraocular AAV Injection

1. To prepare for intraocular injection, anesthetize mice by intraperitoneal injection of 72 mg/kg ketamine and 64 mg/kg xylazine. When the mice are not responding to toe pinch anymore, anesthetize the eyes with a drop of 0.5% proparacaine and dilate the pupils with a drop of 2.5% phenylephrine followed by a drop of 1% tropicamide. Wait for >1 min between drug applications.

2. For intravitreal injections (*see* **Note 4**), make an incision posterior of the ora serrata using a sharp 30-G needle. Then feed a 1–2 μl volume containing about 5×10^{11} viral genomes of AAV diluted in PBS (with 1% phenol red as contrast agent) through the incision site and inject into the vitreous using a blunt 32 G Hamilton syringe. It is critical to avoid damaging the lens with the syringe as this will lead to cataracts. Leave the Hamilton needle tip in the eye for >60 s to allow homogenization and reduce the efflux.

3.3 Tissue Preparation and Verification of Expression

1. Verify gene expression 4–6 weeks post injection by fluorescent imaging (*see* **Note 5**).

2. To isolate the retina, sacrifice mice, enucleate the eyes and fix in 4% paraformaldehyde for 1 h. Remove the cornea by making a circular incision around the ora serrata using scissors. Place two forceps around the edges of the eyecup and carefully tear the retina from the sclera. Make radial cuts to flatten the retina thereby forming the typical clover-leaf shape. Then use retinal whole mounts for antibody staining (*see* **Note 5**). Alternatively, mount whole mounts directly on a glass slide using Vectashield mounting medium with DAPI to stain cell nuclei. Now these retinas are ready for imaging, ideally with a confocal microscope.

3. To prepare retinal sections, embed whole mount retinas in agarose and make transverse sections of 150 μm thickness using a vibratome device at medium speed with maximum vibration. Mount retinal slices on glass slides using Vectashield or stain with antibodies.

4. For antibody staining (*see* **Note 5**), incubate whole mounts or sections in blocking buffer for 2 h at RT on a shaker. Apply primary antibodies over night at 4 °C or for 4 h at RT and apply secondary antibodies for 2 h at RT. It is important to wash the tissue 3×10 min with PBS between antibody applications and before imaging to reduce fluorescence background.

3.4 In Vitro Multielectrode Array (MEA) Recordings of Retina Response

1. For MEA experiments, use mice 6–10 weeks after AAV injection. First, prepare whole mounts as described in Subheading 3.3.2 with modifications. Place the cloverleaf retina onto an organotypic membrane (Millipore) instead of glass slide and do not fix the samples as this would kill biological activity. Place the excised retina photoreceptor cell side down on the Millipore membrane, add a drop of Ames medium on the retina and transfer the filter to an incubator to let the retina settle for >30 min prior to experiments. Perform dissection and experiments in a dark room with minimal red light to prevent bleaching of 11-*cis*-retinal (*see* **Note 6**).

2. Take the Millipore membrane with the whole mounted retina and use a scalpel to cut around the edges of the retina and leave ~5 mm of margin. Use forceps to place the retina ganglion cell side down in the center of the MEA array. In order to prevent the retina from floating and to improve electrode contact and signal-to-noise, place a mesh weight on the retina. The contact of tissue and electrodes can be further improved by applying vacuum to the base of the retina through the MEA chamber using the constant vacuum pump. All the tubing to and from

the MEA chamber and vacuum pump must be preloaded with buffer. It is important that no air bubbles enter the tubing as they interfere with the constant vacuum. During recording, provide a constant perfusion of oxygenated Ames media (32 °C) to the recording chamber to support neural activity.

3. The retina is now ready to be stimulated with light. Optogenetic stimulation requires strong light sources that emit only the desired wavelength of light. This can be achieved with an LED system which emits monochromatic light or bandpass filtered white light from an arc lamp. If possible, couple the illumination through the imaging objective and calibrate light intensities using a handheld power meter.

4. Acquire data with MCS rack software at 25 kHz frequency and filter data below 300 Hz and above 2000 Hz. Simultaneously record light stimulation parameters as TTL pulses. When finished with acquisition, convert voltage traces to spike trains offline. Apply principal components analysis using an offline sorting software (e.g., Plexon) to sort spikes recorded at one electrode into single units, and define them as "cells." Export single unit spike clusters to MatLab for further analysis.

3.5 In Vivo Visually Evoked Potential (VEP) Recordings of Cortical Response

1. To prepare for VEP recordings, anesthetize mice. Induce anesthesia with 5% isoflurane for 3 min and then reduce to 0.5–1%. Inject mice with chlorprothixene (2 mg/kg, intraperitoneally), wait 5 min and then inject mice with urethane (1.5 g/kg, intraperitoneally). Supplement the anesthesia throughout the surgery with 0.5–1% isoflurane. Dilate pupils with 1% tropicamide, then add a drop of silicon oil to prevent the eyes from drying out. Maintain body temperature of anesthetized mice using a DC temperature controller with rectal probe and a heating pad set to 37 °C.

2. Clean mouse head with betadine solution for disinfection. Grab the scalp with forceps at center of head half way between eyes and ears and remove scalp with scissors. Then use a syringe with 25G needle to clean the skull by scratching to remove the muscle and membrane. This step is very important otherwise the glue will not hold. With a small ruler, locate the visual cortex by coordinates (1.7 mm lateral to midline and 0.7 mm anterior to lambda) and mark the location with a pen. Apply glue around the marked location and attach a small custom made metal head plate by pressing for ~30 s. Wait 10 min for the glue to cure. Use a handheld drill with foot pedal control to make a small craniotomy and durotomy over the primary visual cortex. Supply a drop ACSF every 2–3 min to prevent the tissue of drying out. Take care to avoid damaging blood vessels.

3. Pull electrodes with a resistance of 3 MΩ from borosilicate glass (1.5 mm OD, 1.16 mm ID) using a horizontal puller and fill them with ACSF.

4. Transfer mice to the microscope and place them on a heating pad. Then, position the ACSF-filled electrode over the craniotomy and slowly lower it to a final depth of 400 μm, to layer 4 of the visual cortex.

5. To stimulate the retina, use an LED system or a band pass filtered white light source coupled to a fiber optic guide. Position the end of the fiber optic guide 1 cm away from the contralateral eye.

6. Stimulate the eye and record visually evoked potentials. Amplify responses at 10 kHz frequency, band pass filter at 2 kHz, digitize using an I/O board in a computer and average responses over multiple trials of optogenetic stimulation. Export, analyze and graph the voltage traces in MatLab.

3.6   Visually Guided Behavior: Open Field Test

1. Begin by spraying the box meticulously with ethanol to prevent odor from previous experiments to impact visually guided behavior.

2. Position the light source (*see* **Note 7**) over the light compartment.

3. Bring mice into the testing room in their home cages, transfer them to the open field box (*see* **Note 8**) with their littermates and allow them to habituate to the new environment for 45 min. Then, put mice back in their home cage and test them individually.

4. First, place a mouse in the light compartment of the box in a randomized starting position and allow a maximum of 3 min for the mouse to discover that there is a second compartment.

5. Start the trial (5 min) as soon as the mouse crosses into the dark compartment, and record the time spent in the light compartment. Mice that cross the opening only once and stay in the dark compartment for entire time (5 min) are disqualified.

6. Use permanent records (video) to analyze the percent of time spent in the light and dark compartment.

3.7   Visually Guided Behavior: Forced 2-Choice Water Maze Task

1. First, spray the maze meticulously with ethanol to prevent odor from previous experiments to impact visually guided behavior.

2. Fill the Y-maze with water at 20 °C (*see* **Note 9**).

3. Place a light source (*see* **Note** 7) at the end of one of the "escape arms" that cues the location of the escape platform. Add the platform directly under the light source.

4. Position a video camera above the maze to make permanent records of the experiment. A wide angle lens is preferable (e.g., GoPro camera).

5. Bring mice into the testing room in their home cages and transfer them into new cages located on a heating pad and next to a space heater to warm the mice after every trial. Keep the room dark for the entire time of the experiment.

6. Habituate mice to the maze one day before the start of an 8-day trial. Place mice onto the platform for 1 min. Then release the mice at increasing distances from the platform and finally release them from the chute for ten trials. Repeat with the platform on the opposite side.

7. Additionally, habituate the mice each day before the start of the experiment by placing them onto the platform for 1 min on both sides and returning them to the cage.

8. For each trial, remove mice from their cage, place them in a glass beaker (6 cm diameter) and then slowly (10–60 s) lower them into the water opposite of the divider. It is important that the mouse decides when to exit the beaker. If the beaker is lowered too fast, mice are stressed and will not perform well. Give the mouse a maximum of 60 s to find the platform. Trials in which mouse found the hidden platform without entering the alternative arm first are counted as correct trials. Trials in which the mouse explored the alternative arm first or takes longer than 60 s to find the platform are counted as failed trials.

9. After the trial, dry the mouse with paper towels, place it into a warm chamber with a space heater and allow it to rest for at least 3 min before the next trial. All mice perform ten trials per session with two sessions a day, with a total of 20 trials per mouse per day for 8 consecutive days. Move the platform and the light cue between trials according to the following pattern: LRRLRLLRLR and RLLRLRRLRL on alternating days.

3.8 Visually Guided Behavior: Light Cued Fear Conditioning

1. Prior to the experiment, inject control mice with sham injections (PBS) to control for the virus treatment.

2. The experiment is done over three consecutive days: habituation on day 1, training on day 2 and testing on day 3.

3. Start every day by spraying the Habitest chamber meticulously with ethanol to prevent odor from previous experiments to impact visually guided behavior.

4. On day 1, bring the animals into the testing room in their home cages and then acclimatize them individually to the Coulbourn shock chambers for 30 min.

5. On day 2, train the mice by subjecting them to paired or unpaired light cued fear conditioning. Training consists of 5 min habituation to the chamber followed by three shock trials at 0.7 mA. For paired trials synchronize the 20 s light cue (*see* **Note 10**) with 3× 2 s foot shocks at 4 s inter-shock-interval with 40 s inter trial interval. For unpaired trials, provide the same amount of foot shocks and light cues but in a random order without synchronization. These brief, low current shocks provide the minimal aversive stimulus to create a fearful memory associated with a light cue.

6. On day 3, test the animals in a fear probe trial. Change the floor of the chamber from the shock grid to a solid floor. Then allow the mice to habituate to the chamber for 5 min, and then present the same light stimulation protocol as on day 2, but without shock, while recording their movement and behavior with the Freeze-frame software.

7. Use the video recordings to analyze conditioned fear behavior (time spent freezing, a typical rodent fear response) associated with the learned light cue.

4   Notes

1. In order to construct a genomic plasmid for gene therapy, begin with a plasmid containing internal terminal repeat domains (ITR) and add promoter element, gene of interest and fluorescent reporter gene. If expression should be limited to one target cell type, use cell specific promoter elements (e.g., 4×grm6). Otherwise use generic promoter elements (CMV, EF1-alpha, hsyn). For DNA preparation it is important to transform the DNA into competent bacteria that lack recA (e.g., SURE2 or STBL 3) and grow the bacteria for <12 h to minimize homologous recombination which can render the ITRs nonfunctional.

2. Package and purify AAVs following the protocol described by Visel et al. [24]. The choice of serotype is critical as this will determine the cells that the virus is targeting. For targeting ON-bipolar cells, we have found best results with the quadruple tyrosine mutant AAV2(4YF). It is also important to consider the route of delivery (subretinal vs. intravitreal) when choosing a serotype. AAV serotypes that penetrate deep into the retina like 7 m8 [25] or AAV2(4YF) [26] are crucial when choosing the route or intravitreal injection.

3. Determine the titer of AAVs via qPCR relative to inverted repeat domains (ITR) standard. Titers for these viruses should range between 10^{12}-10^{14} viral genomes/ml.

4. Two routes of intraocular AAV delivery are commonly used: subretinal and intravitreal injections. Intravitreal injections are preferred over subretinal injections as they are technically easier to deliver and produce pan-retinal expression in contrast to subretinal injections which produce a very local expression around the site of virus deposition covering less than a quarter of the retina.

5. Antibody staining is required if the gene of interest is not tagged with a fluorescent reporter, otherwise no staining are required. In case the gene of interest is expressed in the distal layers (RGC or photoreceptor layer), whole mount imaging may be sufficient. For expression in inner retinal neurons, agarose sections are required.

6. After removal of the retina from the retinal pigment epithelium RPE, the ligand for rhodopsin, 11-*cis*-retinal cannot be replenished. To prevent bleaching of 11-*cis* retinal, retinas must be handled in dark rooms under red light.

7. For visually guided behavior experiments, it is important to have very strong light sources in order to have a homogenous illumination in a large area (e.g., light compartment of open field test: $A = 0.1$ m^2). This can be achieved by custom built LED arrays (we used a 5×6 LED array).

8. It is extremely important to handle the mice gently to minimize stress. Stress-induced fear masks any learned behavior and will overwrite what the mice may have previously learned.

9. Warm water will be less aversive leading to floating of mice. Cold water will put too much stress on the mice.

10. Using this behavioral paradigm, one can test for several levels of visual restoration. Begin with simple light recognition (light on vs. off) and then increase the difficulty of the task by testing for spatial pattern recognition (moving vs. static stimuli) or temporal pattern recognition (flashing vs. static stimuli).

References

1. Henriksen BS, Marc RE, Bernstein PS (2014) Optogenetics for retinal disorders. J Ophthalmic Vis Res 9:374–382

2. Marc R, Pfeiffer R, Jones B (2014) Retinal prosthetics, optogenetics, and chemical photoswitches. ACS Chem Neurosci 5:895–901

3. Busskamp V, Duebel J, Balya D et al (2010) Genetic reactivation of cone photoreceptors restores visual responses in retinitis pigmentosa. Science 329:413–417

4. Busskamp V, Picaud S, Sahel JA et al (2012) Optogenetic therapy for retinitis pigmentosa. Gene Ther 19:169–175

5. Nirenberg S, Pandarinath C (2012) Retinal prosthetic strategy with the capacity to restore normal vision. Proc Natl Acad Sci U S A 109:15012–15017

6. Doroudchi MM, Greenberg KP, Zorzos AN et al (2011) Towards optogenetic sensory

replacement. Conf Proc IEEE Eng Med Biol Soc 2011:3139–3141

7. Doroudchi MM, Greenberg KP, Liu J et al (2011) Virally delivered channelrhodopsin-2 safely and effectively restores visual function in multiple mouse models of blindness. Mol Ther 19:1220–1229

8. Thyagarajan S, van Wyk M, Lehmann K et al (2010) Visual function in mice with photoreceptor degeneration and transgenic expression of channelrhodopsin 2 in ganglion cells. J Neurosci 30:8745–8758

9. Lagali PS, Balya D, Awatramani GB et al (2008) Light-activated channels targeted to ON bipolar cells restore visual function in retinal degeneration. Nat Neurosci 11:667–675

10. Bi A, Cui J, Ma YP et al (2006) Ectopic expression of a microbial-type rhodopsin restores visual responses in mice with photoreceptor degeneration. Neuron 50:23–33

11. Berger W, Kloeckener-Gruissem B, Neidhardt J (2010) The molecular basis of human retinal and vitreoretinal diseases. Prog Retin Eye Res 29:335–375

12. Shintani K, Shechtman DL, Gurwood AS (2009) Review and update: current treatment trends for patients with retinitis pigmentosa. Optometry 80:384–401

13. Curcio CA, Owsley C, Jackson GR (2000) Spare the rods, save the cones in aging and age-related maculopathy. Invest Ophthalmol Vis Sci 41:2015–2018

14. Ho AC, Humayun MS, Dorn JD et al (2015) Long-term results from an epiretinal prosthesis to restore sight to the blind. Ophthalmology 122:1547–1554

15. Mazzoni F, Novelli E, Strettoi E (2008) Retinal ganglion cells survive and maintain normal dendritic morphology in a mouse model of inherited photoreceptor degeneration. J Neurosci 28:14282–14292

16. Haverkamp S, Michalakis S, Claes E et al (2006) Synaptic plasticity in CNGA3($-/-$) mice: cone bipolar cells react on the missing cone input and form ectopic synapses with rods. J Neurosci 26:5248–5255

17. RetroSense Therapeutics Phase I/II Clinical Trial for RST-001; trial #NCT02556736. www.clinicaltrials.gov.

18. Grossman N, Nikolic K, Grubb MS et al (2011) High-frequency limit of neural stimulation with ChR2. Conf Proc IEEE Eng Med Biol Soc 2011:4167–4170

19. Grossman N, Nikolic K, Toumazou C et al (2011) Modeling study of the light stimulation of a neuron cell with channelrhodopsin-2 mutants. IEEE Trans Biomed Eng 58:1742–1751

20. Cehajic-Kapetanovic J, Eleftheriou C, Allen AE et al (2015) Restoration of vision with ectopic expression of human rod opsin. Curr Biol 25:2111–2122

21. http://www.acucela.com/Read-About-Us/Press-Releases/160404_RP

22. Gaub BM, Berry MH, Holt AE (2015) Optogenetic vision restoration using rhodopsin for enhanced sensitivity. Mol Ther 23:1562–1571

23. Westenskow PD, Kurihara T, Bravo S et al (2015) Performing subretinal injections in rodents to deliver retinal pigment epithelium cells in suspension. J Vis Exp 95:52247

24. Flannery JG, Visel M (2013) Adeno-associated viral vectors for gene therapy of inherited retinal degenerations. Methods Mol Biol 935:351–369

25. Dalkara D, Byrne LC, Klimczak RR et al (2013) In vivo-directed evolution of a new adeno-associated virus for therapeutic outer retinal gene delivery from the vitreous. Sci Transl Med 5:189ra176

26. Petrs-Silva H, Dinculescu A, Li Q et al (2011) Novel properties of tyrosine-mutant AAV2 vectors in the mouse retina. Mol Ther 19:293–301

27. Mutter M, Benkner B, Münch T (2017) Optogenetik als mögliche Therapie bei degenerativen Netzhauterkrankungen. Med Genet 29:239–247

Chapter 13

CRISPR Repair Reveals Causative Mutation in a Preclinical Model of Retinitis Pigmentosa: A Brief Methodology

Wen-Hsuan Wu, Yi-Ting Tsai, Sally Justus, Galaxy Y. Cho, Jesse D. Sengillo, Yu Xu, Thiago Cabral, Chyuan-Sheng Lin, Alexander G. Bassuk, Vinit B. Mahajan, and Stephen H. Tsang

Abstract

CRISPR/Cas9 genome engineering is currently the leading genome surgery technology in most genetics laboratories. Combined with other complementary techniques, it serves as a powerful tool for uncovering genotype–phenotype correlations. Here, we describe a simplified protocol that was used in our publication, *CRISPR Repair Reveals Causative Mutation in a Preclinical Model of Retinitis Pigmentosa*, providing an overview of each section of the experimental process.

Key words CRISPR, Genome engineering, sgRNA construct design, Retinitis pigmentosa, Electroretinogram, Fundoscopy, Optical-coherence tomography

1 Introduction

In our publication, *CRISPR Repair Reveals Causative Mutation in a Preclinical Model of Retinitis Pigmentosa* [1], we identified which of two potentially pathogenic variants in a retinitis pigmentosa (RP) mouse model is responsible for the phenotype, namely, a rapid dysgenesis of the retina postnatally, eventually leading to blindness. This publication resolved a century-long debate on whether a mutation in the phosphodiesterase 6 beta (*Pde6b*) gene or a viral insertion (*Xmv*-28) was responsible for the retinal degeneration, both of which are present in the mouse model. This discovery was only made possible by CRISPR genome engineering technologies. Here, we provide a brief description of the methods we used to conduct these experiments. While this protocol is specific to the aims of our previous paper, we hope that its overarching themes, tips, and techniques can be repurposed for readers and inform or inspire their own CRISPR-based discoveries (*see* **Note 1**).

2 Materials

2.1 sgRNA
Construction

1. sgRNA Oligos (Integrated DNA Technologies Custom DNA oligos, *see* Table 1).
2. T4 DNA ligase reaction buffer, 10×.
3. T4 polynucleotide kinase.
4. pSpCas9(BB) (we used pX335-U6-Chimeric_BB-CBh-hSpCas9n(D10A) in this paper, Addgene plasmid ID: 42,335).
5. Tango buffer (Fermentas/Thermo Scientific) or FastDigest buffer.
6. FastDigest BbsI (BpiI) (Fermentas/Thermo Scientific).
7. DTT, 10 mM.
8. ATP, 10 mM.
9. T7 DNA ligase (New England BioLabs).
10. PlasmidSafe ATP-dependent DNase (Epicentre).
11. 10× PlasmidSafe buffer.
12. One Shot Stbl3 chemically competent *E. coli* (Life Technologies).
13. Lysogeny Broth (LB) medium supplemented with 100 μg/ml ampicillin. Prepare from a 100 mg/mL ampicillin stock.
14. LB agar plates supplemented with 100 μg/ml ampicillin.
15. ddH$_2$O.

2.2 sgRNA In Vitro
Validation

1. pSpCas9(BB)-sgRNA constructs.
2. DMSO.
3. Primers (*see* Tables 2 and 3).
4. Phusion Hot Start II High-Fidelity DNA Polymerase (Thermo Scientific).
5. dNTP.
6. ddH$_2$O.
7. AccuGENE™ 10× TBE Buffer.
8. UltraPure Agarose.
9. UltraPure DNase/RNase-free distilled water.
10. Cas9 protein (PNA Bio).
11. 10× Cas9 nuclease buffer (NEB).
12. RNasin Plus RNase Inhibitor.

2.3 Zygote Injection

1. FVB/N male and superovulated female mice.
2. M16 medium (Specialty Media).

Table 1
Donor template sequence for CRISPR-mediated correction of the Y347X mutation

ssODN	Sequence (5′ → 3′)
NdeI-Pde6b ssODN	AACAATGCAAGCATTCATTCCTTCGACCTCTGTTCTTTTCCCACAGC ACACCCCCGGCTGATCACTGGGCCCTGGCCAGTGGCCTTCCAACAT ATGTAGCTGAGAGTGGCTTTGTGAGTGTCCCTCTCCAGGCCTTGGC CTCTACTGGCCAGTGCTATGATATGTGCTAGCCTGCTACCTCCTATT AGCACATCCTGCTA

Table 2
Oligo sequences for *Pde6b* sgRNA construction

sgRNA oligos	Sequence (5′ → 3′)
sgRNA1-foward	CACCGCCACTTTCTGCTACTTAGGT
sgRNA1-reverse	AAACACCTAAGTAGCAGAAAGTGGC
sgRNA2-foward	CACCGCTCCAGGCCTTGGCCTGTAC
sgRNA2-reverse	AAACGTACAGGCCAAGGCCTGGAGC
sgRNA3-foward	CACCGAGGGCCCAGTGATCAGCCGG
sgRNA3-reverse	AAACCCGGCTGATCACTGGGCCCTC
sgRNA4-foward	CACCGCCAACCTAAGTAGCAGAAAG
sgRNA4 reverse	AAACCTTTCTGCTACTTAGGTTGGC

Table 3
Primer sequences for PCR

Primers	Sequence (5′ → 3′)
T7-sgRNA1-foward	TTAATACGACTCACTATAGGGCCACTTTCTGCTACTTAGGT
T7-sgRNA2-foward	TTAATACGACTCACTATAGGGCTCCAGGCCTTGGCCTGTAC
T7-sgRNA3-foward	TTAATACGACTCACTATAGGGAGGGCCCAGTGATCAGCCGG
T7-sgRNA4-foward	TTAATACGACTCACTATAGGGCCAACCTAAGTAGCAGAAAG
sgRNA-reverse	AAAAGCACCGACTCGGTG
RD1-check-F	CAAGAAGGCAGTAGGATTCCG
RD1-check-R	TTGTCTTGCCTGCTTCTCATC
#10	ATGTACCGCCAGCGCAATGG
#JS610	CCCCGCCTTCTCAACAACCTGGGACGGGAG
#80	CTCTGTTTCTCTCCTGATACG
#81	ACCTGCATGTGAACCCAGTATT

2.4 Detection of Gene Correction or Disruption	1. Phusion Hot Start II High-Fidelity DNA Polymerase (Thermo Scientific).
	2. Primers (*see* Tables 2 and 3).
	3. dNTP.
	4. ddH$_2$O.
	5. NdeI restriction enzyme.
2.5 Kits	1. QIAprep or other spin miniprep kit.
	2. QIAQuick or other PCR purification kit.
	3. MEGAshortscript or other shortscript T7 Transcription kit.
	4. MEGAclear or other transcription cleanup kit.
	5. DNeasy or other blood and tissue kit.
	6. Surveyor Mutation Detection Kit (Integrated DNA Technologies).
	7. Zero Blunt TOPO PCR Cloning Kit (Life Technologies).
2.6 Electroretinogram Recordings	1. 100 mg/mL Ketamine.
	2. 20 mg/mL Xylazine.
	3. PBS.
	4. Heating pad.
	5. 1% Tropicamide ophthalmic solution.
	6. 2.5% Phenylephrine ophthalmic solution.
	7. 0.5% Proparacaine hydrochloride ophthalmic solution.
	8. 2.5% Goniosol hypromellose ophthalmic demulcent solution.
2.7 Fundoscopy Imaging	1. 100 mg/mL Ketamine.
	2. 20 mg/mL Xylazine.
	3. PBS.
	4. 1% Tropicamide ophthalmic solution.
	5. 2.5% Phenylephrine ophthalmic solution.
	6. 0.5% Proparacaine hydrochloride ophthalmic solution.
	7. Systane Gel (Lubricant Eye Gel, Alcon).
	8. 100 mg/mL AK-Fluor sodium fluorescein (Akorn Inc.).
2.8 Equipment	1. Burian-Allen bipolar mouse contact lens electrodes (Hansen Lab, La Jolla, California).
	2. Espion Electroretinogram (ERG) Diagnosys equipment (Diagnosys LLC).
	3. Ganzfeld dome (Diagnosys LLC).

4. Spectralis scanning laser confocal ophthalmoscope (OCT-SLO Spectralis 2; Heidelberg Engineering).

5. Red LED headlight (Rayovac SPHLTLED-BB Sportsman 22 Lumen 3 in 1 Headlight).

3 Methods

3.1 Single-Stranded Oligodeoxynucleotide (ssODN) Donor Template Design

1. Design and order custom ssODN donor templates that do not harbor disease-causing mutations in the gene of interest (Table 1). Instead, the sequences may contain silent mutations that can dually serve as sites for restriction enzyme cleavage during tests like RFLP assays, for example.

2. Dilute the ssODN with nuclease-free water to 10 μM. Store at −20 °C.

3.2 Single Guide RNA (sgRNA) Design

1. Use a CRISPR guide design software to develop the sequence. There are many software options and websites available for this purpose. We use Benchling (www.benchling.com), but other options include http://tools.genome-engineering.org, https://www.atum.bio/eCommerce/cas9/input, etc.

2. Each site should offer detailed instructions for designing the guide using the software, but generally:

   (a) Input the target genomic DNA sequence.

   (b) Aim to find a guide sequence as close to the target site as possible.

   (c) Enhance sgRNA specificity by targeting the mutation site itself and by placing the mutation within 12 bps of the 3′ end of the sgRNA sequence.

3. Order oligos as specified by the Benchling website (Table 2). *See* **Note 2**

3.3 sgRNA Construction

3.3.1 Prepare the Inserts

1. Resuspend sgRNA oligos with ddH$_2$O to 100 μM and prepare the following mixture in order to phosphorylate and anneal the sgRNA oligos:

Ingredients	Quantity (μL)
ddH$_2$O	6.5
T4 PNK	0.5
10× T4 PNK buffer	1
sgRNA top (100 μM)	1
sgRNA bottom (100 μM)	1
Total	10

2. Anneal oligos with the following thermocycling parameters: 37 °C for 30 min, then 95 °C for 5 min, and finally ramp down to 25 °C at 5 °C per min.

3. Dilute to 1:200 (i.e., 1 μl of oligo to 199 μl RT ddH$_2$O).

3.3.2   Cloning the sgRNAs into Plasmid

1. Prepare the ligation reaction based on the parameters below, then incubate for 1 h while cycling 6 times, with alternating periods of 37 °C for 5 min and 23 °C for 5 min.

Ingredients	Quantity (μL)
ddH$_2$O	to 20
T7 ligase	0.5
Tango buffer or FastDigest buffer, 10×	2
DTT, 10 mM	1
ATP, 10 mM	1
FastDigest *Bbs*I	1
Diluted oligo duplex	2
pSpCas9(BB), 100 ng	×
Total	20

2. Use PlasmidSafe exonuclease to remove any lingering linearized DNA (optional, *see* below for mixture parameters).

Ingredients	Quantity (μL)
Ligation reaction	11
ATP, 10 mM	1.5
PlasmidSafe buffer, 10×	1.5
PlasmidSafe exonuclease	1
Total	15

3. Incubate at 37 °C for 30 min followed by 70 °C for 30 min.

3.3.3   Transforming Plasmid into Competent Cells

1. Transform the plasmid into *E. coli* according to the protocol accompanying the cells.

2. The next day, pick 2–3 colonies and inoculate into 3 mL of LB medium with 100 μg/mL of ampicillin. Incubate at 37 °C and shake overnight.

3. Following the manufacturer's instructions, isolate the plasmid using the QIAprep spin miniprep kit.

4. Use the U6-Fwd primer to sequence from the U6 promoter and verify the sequence.

3.4 In Vitro Validation of sgRNA Targeting

1. To prepare the T7-sgRNA template, use PCR amplification with the appropriate primer pair (Table 3) following the parameters below to add the T7 promoter sequence to the sgRNA template.

Ingredients	Quantity (per reaction, µL)	Final
pSpCas9-sgRNA (5 ng/µL)	2	10 ng
Forward primer (10 µM)	1	0.2 µM
Reverse primer (10 µM)	1	0.2 µM
5× HF buffer	10	1×
DMSO	1.5	
Phusion high-fidelity DNA polymerase	0.5	–
dNTP (2.5 mM)	4	200 µM
ddH$_2$O	30	–
Total	50	

2. Perform the PCR cycles as follows:

Cycle number	Denature	Anneal	Extend
1	98 °C, 2 min		
2–36	98 °C, 5 s	65 °C, 5 s	72 °C, 7 s
37			72 °C, 2 min

3. Use a TBE buffer and 2% weight/volume (wt/vol) agarose gel to run the PCR product. The product size should be roughly 120 bp.

4. Following the manufacturer's instructions, use the PCR purification kit to purify the T7-sgRNA PCR product.

5. Following the manufacturer's instructions, use the MEGAshortscript T7 kit for *in vitro* transcription of sgRNA, using the purified PCR product as the template.

6. Following the manufacturer's instructions, use the MEGAclear kit to purify the sgRNA. Elute the sgRNA with nuclease-free water.

7. Verify its quality by running on a gel (2% wt/vol agarose gel with TBE buffer) and assessing bands for possible sgRNA degradation.

8. Using RNase-free water, dilute the sgRNA to 500 ng/µL.

9. Prepare the target template: Using the appropriate primer pair (Table 3), perform a PCR-amplification using the following parameters:

Ingredients	Quantity (per reaction, μL)	Final
Genomic DNA template from FVB/N mice (5 ng/μL)	2	10 ng
Forward primer (10 μM)	1	0.2 μM
Reverse primer (10 μM)	1	0.2 μM
5× HF buffer	10	1×
DMSO	1.5	
Phusion high-fidelity DNA polymerase	0.5	–
dNTP (2.5 mM)	4	200 μM
ddH$_2$O	30	–
Total	50	

10. Perform the PCR cycles as follows:

Cycle number	Denature	Anneal	Extend
1	98 °C, 5 min		
2–36	98 °C, 5 s	63 °C, 8 s	72 °C, 20 s
37			72 °C, 3 min

11. Run the PCR product on a gel (1.5% wt/vol agarose gel in TBE buffer). Verify its concentration and size (~845 bp is expected).

12. Following the manufacturer's instructions, use the PCR purification kit to purify the PCR product.

13. Complex the Cas9 protein, sgRNA, and target template together under the following conditions:

Ingredients	Quantity (per reaction, μL)	Final
Cas9 protein, 1 mg/mL	0.6	600 ng
sgRNA, 500 ng/μL	1	500 ng
Cas9 buffer (NEB), 10×	2	1×
Target template	x	400 ng
RNAsin, 40 U/μL	0.1	0.2 U/μl
ddH$_2$O	to 20	
Total	20	

14. Incubate at 37 °C for 2 h, then at 70 °C for 30 min.

15. Run on a gel (2% wt/vol agarose gel with TBE buffer) to estimate sgRNA efficiency.

3.5 Zygote Injection and Generation of Mice

This involves pronuclear injection and oviduct transfer, which are standard procedures that are beyond the scope of this chapter. Briefly:

1. Superovulate FVB/N females by mating with FVB/N males and obtain oocytes.

2. Inject 3 ng/μL of sgRNA plasmid, 3 ng/μL of Cas9 protein, and 1 μM of ssODN into the FVB/N inbred zygotes under a depression slide chamber.

3. Culture zygotes in M16 (Specialty Media) overnight and transfer surviving zygotes into oviducts of 0.5-day postcoitum, pseudopregnant B6×CBA F1 females.

4. Separate male and female offspring into individual cages at 3 weeks after birth.

5. Backcross offspring into the FVB/N background to assess the percentage/efficiency of the repair through germline transmission. *See* **Note 3**

3.6 Detection of Gene Correction or Disruption

3.6.1 Purification of the Gene-Edited PCR Fragments

1. To identify CRISPR/Cas9-mediated gene correction or disruption in the $Pde6b^{rd1}$ locus, isolate DNA by performing tail clipping per institutional guidelines.

2. Following the manufacturer's instructions, use the blood and tissue kit to isolate genomic DNA from the samples.

3. Amplify extracted DNA by PCR under the following conditions using gene-specific primers (Table 3):

Ingredients	Quantity (per reaction, μL)	Final
Tail DNA	x	10 ng
Forward primer (10 μM)	1	0.2 μM
Reverse primer (10 μM)	1	0.2 μM
5× HF buffer	10	1×
dNTP (2.5 mM)	4	200 μM
Phusion high-fidelity DNA polymerase	0.5	
DMSO	1.5	
ddH$_2$O	To 50	
Total	50	

4. Perform the PCR cycles as follows:

Cycle Number	Denature	Anneal	Extend
1	98 °C, 5 min		
2–36	98 °C, 5 s	63 °C, 8 s	72 °C, 20 s
37			72 °C, 3 min

5. Following the manufacturer's instructions, use the PCR purification kit to purify the PCR products.

3.6.2 (Option A)

To identify homology-directed repair (HDR) events with additional restriction enzyme sites (RFLP assay):

1. Digest the PCR products with the corresponding enzyme (in this case, we used *Nde*I). Incubate at 37 °C, 1 h.

2. Run the digested samples on a gel (1.5% wt/vol agarose gel with TBE buffer).

3. Verify the donor-targeted allele. There should be two smaller fragments cleaved upon enzyme treatment. In our example, the targeted one would be cleaved into ~340 and 500 bp fragments, while the untargeted one would be intact, with a size of 845 bp.

3.6.3 (Option B)

To identify nonhomologous end joining (NHEJ) events, analyze PCR products using the Surveyor® Mutation Detection Kit according to the manufacturer's instructions, here briefly:

1. Denature and reanneal the PCR products by using the following conditions: 95 °C for 10 min, then 95 °C ramp down to 25 °C at 5 °C per min.

2. Create the SURVEYOR nuclease S digestion mixture:

Ingredients	Quantity (per reaction, μL)	Final
Annealed heteroduplex	X	200-400 ng
SURVEYOR nuclease S	1	
SURVEYOR enhancer S	1	
MgCl$_2$ solution supplied with kit, 0.15 M	0.1×	
Total	Y (10–40)	

3. Mix thoroughly and incubate at 42 °C for 1 h.

4. Add 0.1Y µL of Stop solution from the kit.

5. Run the digested samples on a gel (1.5% wt/vol agarose gel with TBE buffer).

6. Verify the NHEJ events by detecting two smaller fragments cleaved upon enzyme treatment.

3.6.4   (Option C)

To identify the detailed sequence change and calculate the percentage of HDR/NHEJ events after Cas9/sgRNA treatment, subclone PCR products by using the Zero Blunt® TOPO® PCR Cloning Kit:

1. Prepare TOPO cloning reaction:

Ingredients	Quantity (per reaction, µL)
PCR product	0.5-4
Salt solution	1
H_2O	0–3.5
TOPO vector	1
Total	6

2. Mix gently and incubate at room temperature for 5 min.

3. Transform into competent *E. coli* according to the protocol accompanying the cells.

4. Spread each transformation on a LB agar plate with ampicillin (100 µg/mL). Incubate at 37 °C overnight.

5. Pick >16 colonies from each plate and inoculate into 3 mL of LB medium with 100 µg/mL of ampicillin. Incubate at 37 °C and shake overnight.

6. Following the manufacturer's instructions, purify the plasmids by using the spin miniprep kit.

7. Use the M13 forward primer (5′-GTAAAACGACGGCCAG-3′) or M13 reverse primer (5′-CAGGAAACAGCTATGAC-3′) for Sanger sequencing.

8. Calculate the editing efficiency as (no. of modified clones)/ (no. of total clones).

3.7   Electroretinogram Recordings

1. Dark-adapt mice overnight.

2. Administer one drop of 1% Tropicamide ophthalmic solution and 2.5% Phenylephrine ophthalmic solution in each eye to dilate. Apply 0.5% Proparacaine hydrochloride ophthalmic solution to numb the cornea. Allow ten minutes to pass.

3. Use an anesthetic solution (1 mL of 100 mg/mL ketamine and 0.1 mL of 20 mg/mL xylazine in 8.9 mL PBS) at a concentration of 0.1 mL/10 g BW to anesthetize mice via intraperitoneal injection.

4. Place mouse on a heating pad to maintain body temperature at 37 °C.

5. Place Burian-Allen bipolar mouse contact lens electrodes on each cornea and apply 2.5% Goniosol Hypromellose Ophthalmic Demulcent Solution.

6. Place reference electrodes subcutaneously in the anterior scalp between the eyes. Place ground electrodes on the mouse's back.

7. Use the Espion ERG Diagnosys equipment to simultaneously obtain recordings from both eyes. For rod and maximal rod and cone responses, use white light pulses of 0.00130 and 3 cd × s/m² (White-6500K). Be sure to obtain recordings under dim red light illumination, which allows the investigator to observe the experiment while not affecting the test and light stimuli.

8. Light-adapt mice in the Ganzfeld dome for 10 min.

9. Use flashes of 30 cd × s/m² (Xenon) to obtain cone cell recordings and suppress rod responses by using a background illumination of 30 cd/m² (White-6500K).

3.8 Fundoscopy Imaging

1. Administer one drop of 1% Tropicamide ophthalmic solution and 2.5% Phenylephrine ophthalmic solution in each eye to dilate. Apply 0.5% Proparacaine Hydrochloride ophthalmic solution to numb the cornea. Allow ten minutes to pass.

2. Anesthetize mice by intraperitoneal injection of ketamine/xylazine as described above (Subheading 3.7, **step 3**).

3. Place mouse on a heating pad to maintain body temperature at 37 °C.

4. Apply a lubricating ophthalmic gel on the eye not being tested to protect against drying.

5. Perform fundoscopy imaging procedures using the Spectralis scanning laser confocal ophthalmoscope using a 30° lens.

6. Perform OCT imaging procedures using Spectralis and the 55° lens.

3.9 Xmv-28 Insertion Verification

1. Order primers that span the *Pde6b* and *Xmv*-28 sequences: primer pair 1 = #10 and #JS610 for the 5′ junction, and primer pair 2 = #80 and #81 for the 3′ junction (Table 3) [2].

2. Amplify FVB/N genomic DNA with/without CRISPR-editing by PCR under the following conditions using junction-specific primers (Table 3):

Ingredients	Quantity (per reaction, µL)	Final
Genomic DNA template from FVB/N mice (5 ng/µL)	2	10 ng
Forward primer (10 µM)	1	0.2 µM
Reverse primer (10 µM)	1	0.2 µM
5× HF buffer	10	1×
DMSO	1.5	
Phusion high-fidelity DNA polymerase	0.5	–
dNTP (2.5 mM)	4	200 µM
ddH$_2$O	30	–
Total	50	

3. Perform the PCR cycles as follows:

Cycle number	Denature	Anneal	Extend
1	98 °C, 5 min		
2–36	98 °C, 5 s	60 °C, 5 s	72 °C, 90 s
37			72 °C, 10 min

4. Confirm presence of insertion by running the PCR product on a gel (0.8% wt/vol agarose gel in TBE buffer). Verify the product size (3.3 kb for 5′ junction and 2.4 kb for 3′ junction, respectively).

4 Notes

1. Our protocols for CRISPR, sgRNA/template design, ERG acquisition, histology, etc. closely follow that set forth in the following publications, which we highly recommend readers to review [3–6].

2. When designing the gRNA, a mutation that creates a novel PAM sequence is ideal. This is because if a mutation can create a PAM (ex: AGG), then the wild type form (ex: AGT) is unlikely to be recognized by Cas9 because of the lack of a PAM. In this way, Cas9 is more likely to be specific and only edit the allele with the mutation.

3. Regarding Subheading 3.5: *Zygote injection and generation of mice*, the method we have described has been reported by several others to be an effective strategy. Yet, for our experiments, injection of the sgRNA and Cas9 protein did not work efficaciously. We therefore altered our method by injecting 5 ng/µL of plasmid and 1 µM of ssODN in a pronuclear fashion, an alternative that worked well for us and may be considered if the traditional sgRNA + Cas9 injection strategy does not work.

Acknowledgments

Disclaimer

While we may reference specific companies, products, and/or brands in this manuscript, these suggestions should serve only as examples. We are not endorsed by, nor do we endorse, any particular company, product, or brand, and there are a variety of options than can be used to achieve the same experimental ends.

References

1. Wu WH, Tsai YT, Justus S et al (2016) CRISPR repair reveals causative mutation in a preclinical model of retinitis pigmentosa. Mol Ther 24:1388–1394

2. Bowes C, Li T, Frankel WN et al (1993) Localization of a retroviral element within the rd gene coding for the beta subunit of cGMP phosphodiesterase. Proc Natl Acad Sci U S A 90:2955–2959

3. Yang H, Wang H, Jaenisch R (2014) Generating genetically modified mice using CRISPR/Cas-mediated genome engineering. Nat Protoc 9:1956–1968

4. Ran FA, Hsu PD, Wright J et al (2013) Genome engineering using the CRISPR-Cas9 system. Nat Protoc 8:2281–2308

5. Koch SF, Tsai YT, Duong JK et al (2015) Halting progressive neurodegeneration in advanced retinitis pigmentosa. J Clin Invest 125:3704–3713

6. Zhang L, Du J, Justus S et al (2016) Reprogramming metabolism by targeting sirtuin 6 attenuates retinal degeneration. J Clin Invest 126:4659–4673

In-Depth Functional Analysis of Rodents by Full-Field Electroretinography

Vithiyanjali Sothilingam, Regine Mühlfriedel, Naoyuki Tanimoto, and Mathias W. Seeliger

Abstract

Full-field electroretinography (ERG) belongs to the gold-standard of electrophysiological test systems in ophthalmology and reflects the sum response of the entire retina to light stimulation. The assessment of the retinal function is a fundamental diagnostic technique not only in the clinical ophthalmology it is also indispensable in the ophthalmic research, in particular, in therapeutic approaches where the in vivo follow up of the benefit after treatment is absolutely necessary. Several current therapeutic approaches have demonstrated long-lasting amelioration in respective disease models and show promise for a successful translation to human patients. In this chapter we provide electroretinography protocols of experimental data which may serve as informative features for upcoming gene therapeutic approaches and clinical trials.

Key words Electroretinography, Gene therapy, Rodents, Mouse, Rod, Cone

1   Introduction

Electroretinography (ERG) is a non-invasive electrophysiological method which is standardized by the International Society for Clinical Electrophysiology of Vision (ISCEV) since 1989 for clinical application to facilitate a global comparability of the ERG protocols [1–3]. In basic ophthalmic research, ERG is also a well established functional diagnostic method to assess outer retinal functionality and is comparable to human use [4, 5]. The establishment of specific protocols is an important but often underestimated factor to monitor successful molecular therapy in retinal degenerations and essential for the translation to human patients [6–9]. In the disease model of retinitis pigmentosa or achromatopsia where predominantly one type of photoreceptors (PR), either cone or rod, is affected and the corresponding electrical response of the PR subtype is completely abolished, the detection of even minor improvements is required following a therapeutic intervention. However, the mostly unaffected counterpart needs a well-designed

set of ERG test conditions to optimize sensitivity and specificity of such protocols in preparation of human clinical trials [7–9]. In this chapter, we show details about the experimental procedure during ERG examinations and appropriate protocols designed to use in therapeutic interventions.

2   Materials

1. Full-field ERG system: a signal amplification system, a PC-based control and recording unit, a monitor screen (*see* **Note 1**). The ERG measurement in mice needs an additional set up if the ERG system for human application is used.

2. A small box with two manipulators (for the active electrodes which should be adjustable in three dimensions to facilitate positioning).

3. Two active electrodes (*see* **Notes 2** and **3**) and two short needle electrodes used as a reference and a ground electrode.

4. A heating pad on the small box (maintains stable body temperature throughout the experiment).

5. Mydriatic drops (e.g., Mydriaticum Stulln, Pharma Stulln) for pupil dilation.

6. Methylcellulose (e.g., Methocel 2%, Omnivision GmbH) for eye moistening.

7. Anesthesia: Ketamine (66.7 mg/kg body weight), xylazine (11.7 mg/kg body weight), Normal Saline (0.9% NaCl).

8. Electronic scale (set to minimum one position after the decimal point).

9. Mouse cage and cage lid (*see* **Note 4**).

10. Large box: To allow continuous dark adaptation of mice during ERG measurement. The mice cages are kept in a container and are additionally covered with a dark-colored, thick blanket.

11. Dim-red light: To preserve dark adaptation of mice during ERG examination the room has to be completely dark and the minimum light source which should be used is a noninterfering dim-red light (e.g., battery-operated bicycle lamp).

3   Methods

3.1 Preparation Before ERG Examination

The arrangements often begin one day before the analysis. For the overnight dark adaptation (at least longer than 6 h) of mice the room has to be completely dark, meaning that even after a period of time (ca. 20 min) the room is dark. Optimally the examination room should have a double-door system so that one can enter or

leave the room without incidence of light which would disturb the dark adaptation during investigation.

3.2 ERG Recording Day

1. To allow continuous dark adaptation, first one should enter the room using a dim-red light and without other light entering.

2. Before other arrangement begins, insert the mice cages into a large container, close it and covered it with a light-impermeable blanket. The following steps can then be carried out under regular lighting.

3. The ERG equipment has to be turned on and anesthesia be prepared. Afterward the room light is again turned off and all other preparations are performed using dim-red light.

4. The mouse is weighed and the appropriate amount of anesthetic is given subcutaneously to the mouse. Then insert the mouse into a cage and wait until narcotized.

5. For the dilation of the pupil mydriatic eye drops are applied to both eyes.

6. The anesthetized mouse is placed symmetrically on a small box which is heated to body temperature (*see* **Note 5**).

7. The first (disposable stainless) needle electrode is applied subcutaneously as a reference at the forehead region and the second ground electrode equally at the back near the tail.

8. The positioning of the active electrodes includes moistening of these electrodes with methylcellulose and positioning of them on the surface of both corneas (*see* **Note 6**).

9. After the impedance of each electrode is checked (*see* **Note 7**), the small box is placed into the full-field bowl so that the eyes are placed well into the center and the ERG measurement can be started.

3.3 ERG Protocols

Essential aspects that determine the contribution of the retinal neurons to ERG include stimulus conditions, background illumination (which influences retinal adaptation levels) and duration of the stimulus. Therefore it is necessary that appropriate ERG protocols have to be tailored in order to specifically analyze visual signals of retinal neurons. ERG recordings are usually divided into two groups according to the frequency of stimuli, the so-called single flash which represents an intensity series and the flicker ERG with a change in frequency from very low to high. These measurements are performed either under dark-adapted (scotopic) or light-adapted (photopic) conditions, including a static background light of 30 cd $\times$ s/m² . For a fast estimation of retinal functionality single flash protocols are a minimum requirement (Fig. 1). However, for a thorough analysis of major bipolar cell contributions of the rod and cone pathways specific flicker protocols are required [11].
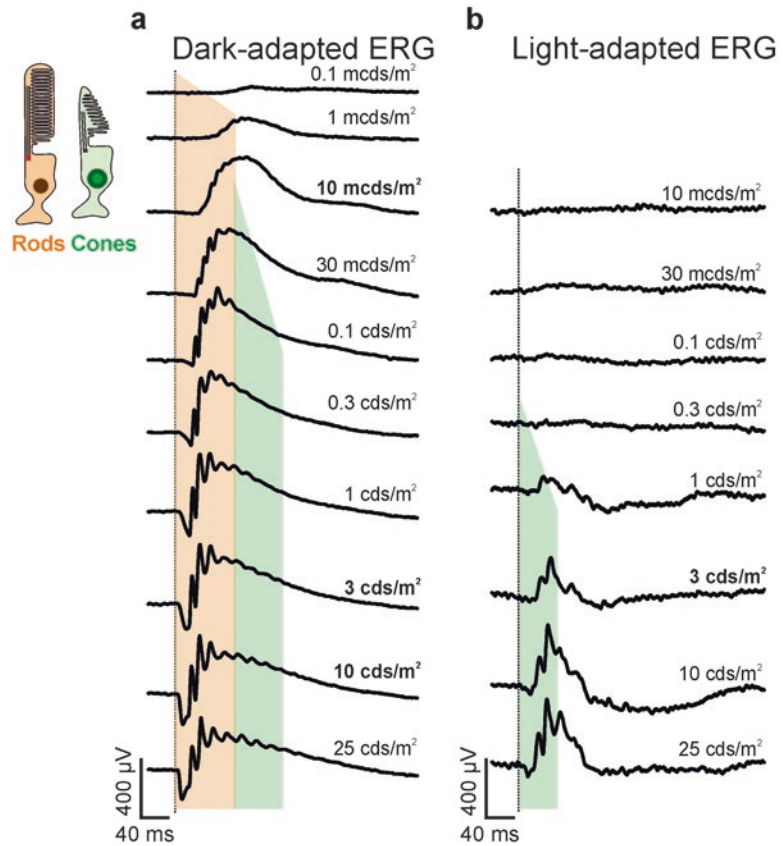
Fig. 1 Single flash ERG intensity series (adapted from [10]). (**a**) Dark-adapted (scotopic) and (**b**) light-adapted (photopic) recording series of a C57BL/6 mouse. Light levels up to 10 mcd × s/m² reflect pure rod system activity (orange marked area) and ERG traces above 10 mcd × s/m² represent mixed rod and cone system activities (orange and green marked area). Light-adapted ERG measurements under a steady background illumination of 30 cd × s/m² starting at 0.01 cd × s/m² allow to obtain information exclusively about cone system contribution (green marked area). The rod system is usually saturated and cannot react under these conditions [4, 5]. ISCEV standards are pointed out in bold letters

Especially, the combination of both single-flash and flickering ERG paradigms are valuable for discrimination of the functional pathology of animal models with negative ERG [12, 13]. Importantly, the designed murine ERG intensity and flicker series in our laboratory meet the standards of the International Society for Clinical Electrophysiology of Vision (ISCEV) for clinical full-field electroretinography which guarantee a high compatibility. The ISCEV standards are hereinafter highlighted in bold [2, 3].

<table>
<tr><td>

3.3.1 Stimulation Strength

</td><td>

1. Scotopic single flash intensity series includes steps at 0.0001, 0.001, **0.01**, 0.03, 0.1, 0.3, 1.0, **3.0**, **10.0**, and 30.0 cd × s/m² (Fig. 1a).

2. Scotopic flicker frequency series at **3.0** cd × s/m² ISCEV standard flash (SF) intensity includes frequencies at 0.5, 1, 2, 3, 5, 7, 10, 12, 15, 18, 20, and 30 Hz.

   After a 10 min adaptation to a static background light of 30 cd/m² the light-adapted (photopic) protocol series starts.

3. Photopic single flash intensity series: 0.01, 0.03, 0.1, 0.3, 1.0, **3.0**, 10.0, and 30.0 cd × s/m² (Fig. 1B).

4. Photopic flicker frequency series at **3.0** ISCEV SF intensity (from 0.5 to **30** Hz) contains equal intermediate frequency steps as in scotopic flicker series.

</td></tr>
</table>

3.3.2 Stimulation Duration and Filter Parameters

These parameters should be adjusted to ensure minimal fluctuations of the baseline and signal to noise ratio. Our recommendation for the single flash protocol is to average ten responses with inter-stimulus intervals of 5 (for <1.0 cd × s/m²) or 17 s (for 1.0–30 cd × s/m²). For the flicker protocols, responses are averaged either 20 times (for 0.5–3 Hz) or 30 times (for 5 Hz and above). For all four protocols the band-pass filter cut-off frequencies are 0.3 and 300 Hz analog to human ISCEV standard.

3.4 ERG Data Analysis and Presentation

The electroretinogram in response to a flash of light is a biphasic ERG waveform with an initial negative component, the a-wave, and a subsequent positive component, called b-wave (Fig. 2). A third component of the ERG are the oscillatory potentials (OPs), a number of higher-frequent and low amplitude wavelets on top of the b-wave varying in size and number with increasing stimulus intensities. The initial a-wave is dominated by photoreceptor outer segment activity and the following b-wave component reflects the activity of ON bipolar cells [4, 5, 14].
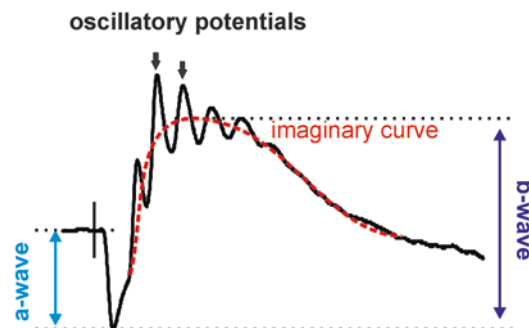
Fig. 2 Major ERG components. A typical dark-adapted ERG waveform at a higher light intensity consists of an a-wave (negative deflection) and a b-wave (positive deflection) including oscillatory potentials (black arrows)

1. For a first evaluation of the overall retinal functionality the b-wave amplitude (in microvolt) and latency (time, expressed in milliseconds, between the start of the stimulus and the peak of the b-wave) of single flash ERG responses are measured (*see* **Note 8**).

2. For specific questions, the a-wave but also the positive deflection of the flicker ERG responses is analyzed (*see* **Note 9**).

3. For an adequate overview of the data distribution, we suggest a nonparametric presentation of the data as a box-and-whisker-plot, including the 5, 25, 50 (median), 75, and 95% quantiles. The values of the amplitude/latency of the ERG data are then plotted verse the intensity/frequency on a graph.

4. Additionally, it is recommended to show a representative response series (e.g., treated verse untreated eye) from each group. In some other cases, an overlay of the responses may provide information about the configuration of the ERG waveform (*see* **Note 10**).

4   Notes

1. ERG systems for clinical application can be used for rodents, however they should comply with the current industrial standard issued by the ISCEV.

2. We use ring electrode made of gold wire.

3. ERG responses are obtained from both eyes simultaneously to verify proper positioning of active electrodes and comparing ERG responses between right and left eyes, e.g., it is particularly necessary when the untreated eye is used as an internal control [6–8].

4. Depending on the mouse line, sometimes a mouse jumps heavily during anesthesia, thus the cage should be covered with a cage lid. Do not keep mice in cage with litter to avoid corneal injury. Disposable soft wipes are used in our lab to cover the bottom of the cage.

5. The symmetrical positioning is important for equal stimulation of both eyes.

6. The distance between the active electrode and the cornea is an essential parameter which influences the noise level as well as the fluctuation of the signal baseline.

7. The impedance of the active electrodes is a good indicator for the right positioning. Large impedances usually mean that the contact between active electrode and cornea is too distant, whereas very small impedances may mean that the electrodes are strongly attached to the corneal surface and may influence the ocular circulation.

8. Due to large oscillations in murine ERG, the maximal positive deflection may not resemble the peak of b-wave. Therefore, it is suggested to fit an imaginary curve on the b-wave (*see* Fig. 2) which roughly runs through the midpoints between minimum and maximum of oscillations [4, 5].

9. In contrast to single flash responses, the a- and b-wave analogues and oscillations of the b-wave analogue diminish with increasing flicker frequency in a flicker frequency series. For this reason, the amplitude of the flicker responses is measured from the trough to the peak of each response for all frequencies.

10. The comparison of the waveforms by a superposition is indispensable in cases where the time course of the voltage change cannot be fully analyzed and described by the quantitative analysis of the response amplitudes [15–18].

References

1. Marmor MF, Arden GB, Nilsson SE et al (1989) Standard for clinical electroretinography. Arch Ophthalmol 107:816–819

2. Marmor MF, Holder GE, Seeliger MW et al (2004) Standard for clinical electroretinography (2004 update). Doc Ophthalmol 108:107–114

3. McCulloch DL, Marmor MF, Brigell MG et al (2015) ISCEV Standard for full-field clinical electroretinography (2015 update). Doc Ophthalmol 130:1–12

4. Tanimoto N, Muehlfriedel RL, Fischer MD et al (2009) Vision tests in the mouse: functional phenotyping with electroretinography. Front Biosci (14):2730–2737

5. Tanimoto N, Sothilingam V, Seeliger MW (2013) Functional phenotyping of mouse models with ERG. Methods Mol Biol 935:69–78

6. Janssen A, Min SH, Molday LL et al (2008) Effect of late-stage therapy on disease progression in AAV-mediated rescue of photoreceptor cells in the retinoschisin-deficient mouse. Mol Ther 16:1010–1017

7. Michalakis S, Mühlfriedel R, Tanimoto N et al (2010) Restoration of cone vision in the CNGA3−/− mouse model of congenital complete lack of cone photoreceptor function. Mol Ther 18:2057–2063

8. Koch S, Sothilingam V, Garcia Garrido M et al (2012) Gene therapy restores vision and delays degeneration in the CNGB1(−/−) mouse model of retinitis pigmentosa. Hum Mol Genet 21:4486–4496

9. Sothilingam V, Garcia Garrido M, Jiao K et al (2015) Retinitis pigmentosa: impact of different Pde6a point mutations on the disease phenotype. Hum Mol Genet 24:5486–5499

10. Sothilingam V (2016) Dissection of visual signalling based on functionally specific rod photoreceptor mutants. Dissertation, Eberhard Karls Universität Tuebingen. http://dx.doi.org/10.15496/publikation-12184

11. Tanimoto N, Sothilingam V, Kondo M et al (2015) Electroretinographic assessment of rod- and cone-mediated bipolar cell pathways using flicker stimuli in mice. Sci Rep 5:10731

12. Tanimoto N, Michalakis S, Weber BH et al (2016) In-depth functional diagnostics of mouse models by single-flash and flicker electroretinograms without adapting background illumination. Adv Exp Med Biol 854:619–625

13. Tanimoto N, Akula JD, Fulton AB et al (2016) Differentiation of murine models of "negative ERG" by single and repetitive light stimuli. Doc Ophthalmol 132:101–109

14. Frishman LJ (2006) Origins of the electroretinogram. In: Heckenlively JR, Arden GB (eds) Principles and practice of clinical electrophysiology of vision, 2nd edn. The MIT Press, Cambridge, MA, pp 139–183

15. Knop GC, Seeliger MW, Thiel F et al (2008) Light responses in the mouse retina are prolonged upon targeted deletion of the HCN1 channel gene. Eur J Neurosci 28:2221–2230

16. Sothilingam V, Michalakis S, Garcia Garrido M et al (2016) HCN1 channels enhance rod system responsivity in the retina under conditions of light exposure. PLoS One 11:e0147728

17. Beck SC, Schaeferhoff K, Michalakis S et al (2010) In vivo analysis of cone survival in mice. Invest Ophthalmol Vis Sci 51:493–497

18. Schaeferhoff K, Michalakis S, Tanimoto N et al (2010) Induction of STAT3-related genes in fast degenerating cone photoreceptors of cpfl1 mice. Cell Mol Life Sci 67:3173–3186

Chapter 15

Advanced Ocular Injection Techniques for Therapy Approaches

Regine Mühlfriedel, Marina Garcia Garrido, Christine Wallrapp, and Mathias W. Seeliger

Abstract

Treatment approaches for inherited eye diseases require local therapeutic molecule delivery by intraocular injection. One important factor that can influence the study outcome is the quality of intraocular administration. The intracompartmental structure (e.g., vitreous) of the eye allows a sustainable release of therapeutic biologicals using an intravitreal delivery. The protocol described here aims at providing the details relevant to perform a transscleral *pars plana* intravitreal transfer in small eyes using a genetically modified stem cell system. The fact that cells and therewith visually distinct particles are implanted, allows for the assessment of the implantation site and the distribution, and possibilities for temporal follow up studies—hence, valuable information becomes available which can be used to fine-tune the intravitreal delivery technique.

Key words Intraocular delivery, Transscleral *pars plana* injection, Retina, Mouse eye, Photoreceptor cells, Intravitreal implantation, In vivo imaging, Micro CellBeads®

1 Introduction

The accessibility for routine surgery and its immune privileged state make the eye an ideal target for intraocular therapeutic treatments of inherited eye diseases. Depending on the aetiology, the progression of disease and the availability of therapeutic compounds or vector systems, two different local application routes are suitable for therapeutic treatments. As many inherited vision-threatening eye diseases are caused by mutations in photoreceptor and/or retinal pigment epithelium (RPE) genes, the therapy for such diseases requires local viral vector delivery by subretinal administration [1–5]. The subretinal space is an excellent target because subretinal delivery places injected material in contact with the plasma membrane of the photoreceptor (PhR) and the RPE cells. In genetic diseases, specific restoration of gene function by gene replacement approaches would seem an ideal therapeutic strategy [6–13]. Recombinant, replication-

deficient adeno-associated viral (rAAV) vectors are increasingly being used in gene therapy trials in the central nervous system [14–17] and are currently among the most frequently used viral vector systems in clinical trials for ocular disorders, e.g., Leber congenital amaurosis (LCA) linked to RPE65 deficiency [18–23], Choroideremia [24] and Achromatopsia [25]. The genetic heterogeneity, the often late diagnosis of retinal disorders and the high treatment costs could be a drawback for this treatment strategy. For that reasons, neuroprotection outlines a therapeutic strategy for treatment of retinal neurodegenerative disease that is independent of the mutation and applicable regardless of the primary genetic defect and the aetiology of the degeneration. The intracompartmental structure (e.g., vitreous) of the eye allows for a sustainable release of therapeutic biologicals, e.g., neurotrophic factors preventing any systemic effects of substances using an intravitreal delivery. The development of efficient ocular delivery micro systems is of great importance for the achievement of sustained long life neuroprotective effects of proteins [26–30]. However, there are other studies that have not succeeded to restore function [31, 32], likewise neurotrophic factors were failing to bring any benefit when tested in human clinical trials for, for example, Parkinson disease (GDNF, [33]) or amyotrophic lateral sclerosis (CNTF, [34]). Apart from disease model-specific factors, one important factor that can influence the study outcome is the quality of intraocular administration. Since there are no large animal models available for most retinal disorders, genetically modified mouse models are commonly used in preclinical proof-of-concept studies. However, because of the relatively small murine eye, adverse effects of the ocular delivery procedure itself may interfere with the therapeutic outcome. To overcome limiting effects of subretinal delivery, a detailed protocol for optimized subretinal injection technique was described recently [35]. The protocol presented here, aims at providing the details of a procedure for the transscleral *pars plana* intravitreal transfer in small eyes using a genetically modified stem cell system (micro CellBeads®, provided by CellMed AG, a BTG company). CellBeads® were designed as cell-based implants for a sustained local delivery of bioactive factors or markers [36–40]. For the use in preclinical studies, the mean diameter of the corebead was miniaturized from 400 to 160–180 μm. Each micro CellBead consists of about 50–70 factor-secreting mesenchymal stem cells encapsulated in a spherically shaped immuno-isolating alginate matrix, they can easily be visualized and the assessment of the implantation, localization and distribution for such type of biological cell compounds is possible. This system has provided valuable properties which can be used for the fine-tuning of the intravitreal delivery. The intravitreal injection technique described here should be applicable in experiments involving any type of cell solution serving as biological compounds in neuroprotective approaches.

2   Materials

2.1   Anaesthesia, Solutions and Agents

1. Ketamine/xylazine: Mixture of ketamine (working solution: 66.7 mg/kg) and xylazine (working solution: 11.7 mg/kg).

2. Bioactive compounds stored at −80 °C.

3. Eagle's minimum essential medium (EMEM): EMEM supplemented with 10% FCS and 2 mM L-glutamine.

4. Ringer's solution (Sigma-Aldrich).

5. Tropicamide eye drops.

6. Hydrogel: Carbomer hydrogel (Vidisic®).

7. Ointment: Dexamethason and Gentamicin ointment (Dexamytrex®).

8. Frozen micro CellBeads® aliquots (cryopreserved miniaturized CellBeads® in 10% DMSO, 2 ml vial, provided by CellMed AG, a BTG company, Alzenau, Germany).

2.2   Surgical Instruments and Supplies

1. Operating microscope.

2. 1 ml insulin syringes (BD Microlance TM).

3. 26-gauges sterile needles.

4. Sterile curved surgical forceps.

5. Glass coverslips (7–10 mm in diameter).

6. Cell strainer (100 μm nylon, BD Falcon).

7. Cell culture dishes (35 × 10 mm, CELLSTAR®).

8. Warming blanket.

9. Water bath at 37 °C.

3   Methods

3.1   Preparation of the Cell Suspension for Intravitreal Delivery

1. Quickly thaw the frozen aliquot containing about 500 CellBeads® in a water bath at 37 °C.

2. Transfer completely the content of the vial in a small cell culture dish (35 × 10 mm) filled with 2 ml EMEM.

3. Incubate the CellBeads® in EMEM for about 5 min by room temperature.

4. To remove the excess of DMSO, put the CellBeads® into a cell strainer and wash them with 1 ml Ringer's solution for five times.

5. By rinsing carefully, transfer the CellBeads® in a new cell culture dish filled with 1 ml Ringer's solution (CellBeads® should be covered completely by the buffer).

6. The CellBeads® can be kept in the buffer at room temperature and used within the next 4 h in the experiment.

3.2 Anaesthesia and Preparation of Mice

1. Before starting the experiment, sterilize the surgical instruments and needles by incubating them with 70% ethanol for 10–15 min. Rinse needles three times with sterile water.

2. Anaesthetize the mouse by subcutaneous injection of the prepared mixture of ketamine and xylazine. The mouse will develop adequate anaesthesia in approximately 5 min.

3. For pupillary mydriasis apply tropicamide eye drops on both eyes. The pupil is fully dilated within 2–3 min. If necessary, another drop of tropicamide has to be placed on the cornea when the pupil is not adequately dilated up to that point in time. After dilation, it should take less than 5 min to complete the surgery.

3.3 Injection Procedure

Intravitreal injection is performed under direct visualization using an operating microscope.

1. Shortly before implantation of CellBeads®, fill a 1 ml insulin syringe with about 20 μl of CellBeads® suspension containing approximately 30 CellBeads® and attach the sterile needle. Prevent air bubbles in the solution (*see* **Note 1**).

2. Position the mouse with its nose facing away (e.g., application in the ventral part) or toward (e.g., application in the dorsal part) the surgeon and its right eye facing up toward the ring light and the microscope.

3. Drop the hydrogel on the cornea of both eyes. Cover the right eye with a glass coverslip. Visualize the fundus in such a way that its blood vessels and the optic nerve head could be clearly seen (*see* **Note 2**). This serves as a means to assess the condition of the eye before injection and as a control for the postoperative condition of the retina. The coverslip is not removed during the surgery procedure.

4. Grasp the *Tunica conjunctiva* with the forceps at the favoured site (e.g., dorsal part) and place the sterile needle at the inferior site of the *Ora serrata*. The tip of the needle should be positioned with the aperture facing upward (Fig. 1).

5. Advance the needle transsclerally *ab externo* into the vitreous. Inject the micro CellBeads® suspension as soon as the tip of the needle breaches the sclera/RPE/retina slowly with low pressure under manual control. Because of a large injection volume, the optimized position for injection can be found directly in the upper vitreous space of the optic nerve head. The injection in the intravitreal space results in a visible distribution of cell material (e.g., CellBeads®, Fig. 2a, *see* **Notes 3–5**). The needle and the syringe cannot be used twice.
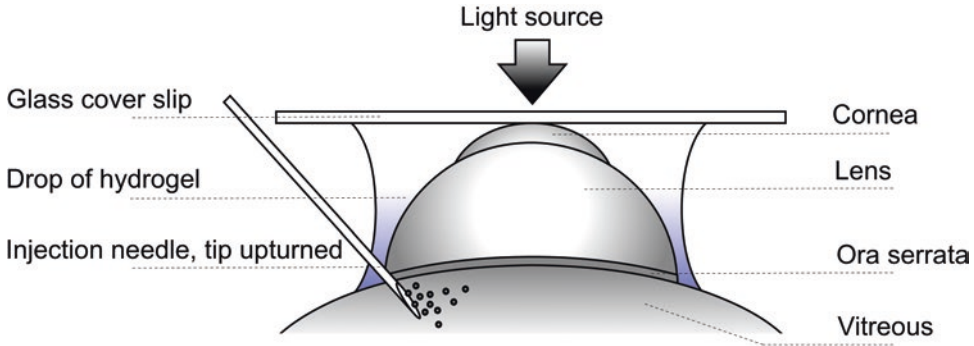
Fig. 1 Technical setup for the intraocular injection. The fundus is visualized by means of a contact lens system consisting of a drop of hydrogel on the cornea, covered with a glass coverslip. The tangential position of the needle is shown just before lancing transsclerally the RPE/retina at the site of the *Ora serrata*. Adapted from [35]
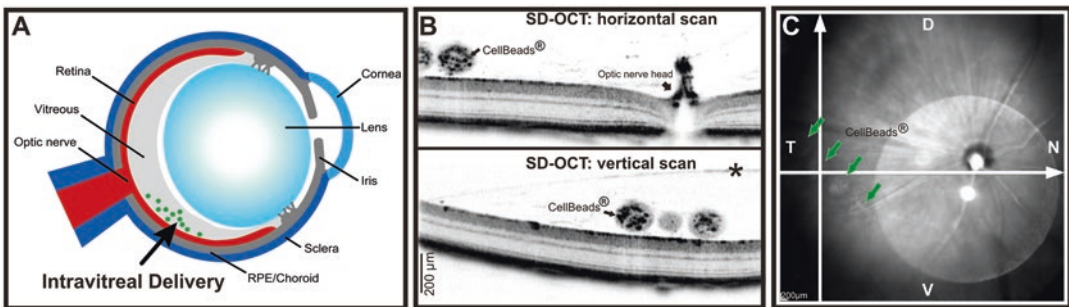
Fig. 2 Schematic representation of intravitreal delivery by using factor-secreting mesenchymal stem cells encapsulated in a spherically shaped immuno-isolating alginate matrix (micro CellBeads®). Cartoon of the eye representing an intravitreal delivery by using released bioactive compounds following a transscleral injection (**a**). In vivo monitoring of implanted micro CellBeads® at 10 days post-delivery using the noninvasive diagnostic SD-OCT technique (**b** and **c**). Representative virtual SD-OCT cross sections (SD-OCT horizontal and vertical scans) reveal detailed structures of the capsule and the encapsulated mesenchymal cells and the integrity of the retina next and underneath the implanted micro CellBeads® (**b**). Following implantation of five micro CellBeads®, infrared fundus imaging confirms their epiretinal localization without any visible adverse side effects (**c**). In vivo images were taken with the equipment set of 30° field of view and with the software Heidelberg Eye Explorer HEYEX version 5.3.3.0. Asterisk indicates the boundary layer between lens and vitreous, respectively. N = nasal, T = temporal, D = dorsal, V = ventral, respectively

6. Slowly withdraw the needle. Remove the glass coverslip and the hydrogel drop. Clean the eye surface carefully. Take care to prevent any direct contact to the cornea due to the risk of neovascularization development.

7. Optional: Monitor and assess the quality of intraocular injection, retinal morphology, as well as the injection site using the in vivo imaging techniques (e.g., SD-OCT and cSLO, Fig. 2b, c).

8. Protocol the injection site, volume, concentration (e.g., numbers of implanted micro CellBeads®), as well as the side effects.

9. Apply antibiotic ointment to the corneas to prevent from eventual inflammatory reaction and drying eyes while the animal recovers from anaesthesia.

10. Place the animal until awakening on a warming blanket at 37 °C. Put the animal recovered from anaesthesia back in the cage.

3.4 Postoperative Treatment

1. Provide antibiotic ointment two times daily for 48 h. Opacity of the eye is mostly due to injuries of the lens and/or cornea via the needle tip (*see* **Note 6**). These animals should be excluded from further studies.

4 Notes

1. Air bubbles in the solution can be avoided by rinsing (slowly) the needle several times with buffer solution and replacing the buffer with the cell suspension before starting the experiment.

2. Because of the small size of the mouse eye, the successful intraocular injection is not easy to evaluate, specifically for newcomers in this field. The usage of an operation microscope offers possibilities for a well-controlled intraocular procedure. Additionally, the in vivo imaging is a very helpful technique allowing the improvement of the quality and the fine tuning of the injection itself. The criteria described in the text could be readily observed during fundus examination during the procedure as well as following post injection using cSLO and SD-OCT. There are several causes of incorrect delivery into the vitreal space (*see* **Notes 3–5**).

3. By using the transscleral route of administration, retinal and choroidal vessels can be injured by the needle tip resulting in haemorrhages. As a solution, a glass coverslip can be used during the injection, thus fundus including retinal vessels can be well outlined. In this way, the optimum combination of the site where the fine forceps hold the eye and the position where the needle breaks the RPE/retina can be found. It is possible to inject by passing in between two retinal vessels to avoid their injury by too high pressure.

4. By using the transscleral as well the transcorneal route of administration, material can accidentally be injected subretinally. A subretinal injection results in a retina detachment by a bleb formation causing mislocalization of cell material (Fig. 3). This can be avoided by controlling the position of the needle tip which should be clearly visible under the microscope.

5. By using the transscleral as well the transcorneal route of administration, material can be injected into the lens resulting
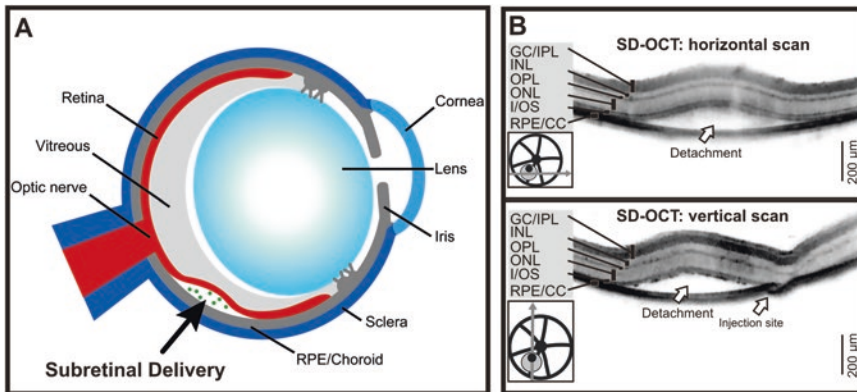
Fig. 3 Schematic representation of cavity formation due to the subretinal gene delivery. Cartoon of the eye representing a cavity formation between the RPE layer and the retina at the ventral part of the retina following a transscleral injection. (**a**) Monitoring of the retinal detachment post subretinal injection using rAAV gene delivery. Detailed in vivo SD-OCT imaging of the retinal architecture of a subretinally injected eye. The quality of subretinal injection and route of administration can be proven by the imaging of retinal detachment between the photoreceptor cell layer (IS/OS) and the RPE (**b**). Representative horizontal and vertical SD-OCT scans show the ablation size as well as the injection site immediately 10 min post injection (**b**, upper and lower pictures). Total volume of 1.0 μl rAAV (recombinant adeno-associated viral) particles at post natal day P14 was injected

in damages and incorrect administration of the bioactive compounds. Too high pressure during the injection results in fine ruptures of the retinal layers. Furthermore, the tip of the needle can easily break through the inner retina/ganglion cells. As there is no further barrier, the tip of the needle can easily penetrate the vitreous resulting in an incorrect injection in the lens. As a consequence, the lens shows immediately an opacity which can clearly be seen under the microscope and does not disappear during the procedure. The difference between a needle tip located either subretinally or intravitreally can be visualized by the properties of reflectance: when located intravitreally, tips appear more clear and bright as compared to a subretinal location.

6. The postoperative treatment with antibiotic ointment is important to prevent dry eyes resulting in neovascularizations of the cornea. This process leads to negative and irreversible side effects resulting in difficulties for performing in vivo imaging.

Acknowledgment

References

1. Timmers AM, Zhang H, Squitieri A et al (2001) Subretinal injections in rodent eyes: effects on electrophysiology and histology of rat retina. Mol Vis 7:131–137

2. Johnson CJ, Berglin L, Chrenek MA et al (2008) Technical brief: subretinal injection and electroporation into adult mouse eyes. Mol Vis 14:2211–2226

3. Buch PK, Bainbridge JW, Ali RR et al (2008) AAV-mediated gene therapy for retinal disorders: from mouse to man. Gene Ther 15:849–857

4. Bainbridge JW, Mistry A, Schlichtenbrede FC et al (2003) Stable rAAV-mediated transduction of rod and cone photoreceptors in the canine retina. Gene Ther 10:1336–1344

5. Liang FQ, Anand V, Maguire AM et al (2001) Intraocular delivery of recombinant virus. Methods Mol Med 47:125–139

6. Alexander JJ, Umino Y, Everhart D et al (2007) Restoration of cone vision in a mouse model of achromatopsia. Nat Med 13:685–687

7. Michalakis S, Mühlfriedel R, Tanimoto N et al (2010) Restoration of cone vision in the CNGA3-/- mouse model of congenital complete lack of cone photoreceptor function. Mol Ther 18:2057–2063

8. Koch S, Sothilingam V, Garcia Garrido M et al (2012) Gene therapy restores vision and delays degeneration in the CNGB1(-/-) mouse model of retinitis pigmentosa. Hum Mol Genet 21:4486–4496

9. Busskamp V, Duebel J, Balya D et al (2010) Genetic reactivation of cone photoreceptors restores visual responses in retinitis pigmentosa. Science 329:413–417

10. Schlichtenbrede FC, da Cruz L, Stephens C et al (2003) Long-term evaluation of retinal function in Prph2Rd2/Rd2 mice following AAV-mediated gene replacement therapy. J Gene Med 5:757–764

11. Janssen A, Min SH, Molday LL et al (2008) Effect of late-stage therapy on disease progression in AAV-mediated rescue of photoreceptor cells in the retinoschisin-deficient mouse. Mol Ther 16:1010–1017

12. Palfi A, Millington-Ward S, Chadderton N et al (2010) Adeno-associated virus-mediated rhodopsin replacement provides therapeutic benefit in mice with a targeted disruption of the rhodopsin gene. Hum Gene Ther 21:311–323

13. Sun X, Pawlyk B, Xu X et al (2010) Gene therapy with a promoter targeting both rods and cones rescues retinal degeneration caused by AIPL1 mutations. Gene Ther 17:117–131

14. McCown TJ (2005) Adeno-associated virus (AAV) vectors in the CNS. Curr Gene Ther 5:333–338

15. Marks WJ Jr, Ostrem JL, Verhagen L et al (2008) Safety and tolerability of intraputaminal delivery of CERE-120 (adeno-associated virus serotype 2-neurturin) to patients with idiopathic Parkinson's disease: an open-label, phase I trial. Lancet Neurol 7:400–408

16. Stieger K, Colle MA, Dubreil L et al (2008) Subretinal delivery of recombinant AAV serotype 8 vector in dogs results in gene transfer to neurons in the brain. Mol Ther 16:916–923

17. den Hollander AI, Black A, Bennett J (2010) Lighting a candle in the dark: advances in genetics and gene therapy of recessive retinal dystrophies. J Clin Invest 120:3042–3053

18. Cideciyan AV, Hauswirth WW, Aleman TS et al (2009) Human RPE65 gene therapy for Leber congenital amaurosis: persistence of early visual improvements and safety at 1 year. Hum Gene Ther 20:999–1004

19. Simonelli F, Maguire AM, Testa F et al (2010) Gene therapy for Leber's congenital amaurosis is safe and effective through 1.5 years after vector administration. Mol Ther 18:643–650

20. Pang J, Boye SE, Lei B et al (2010) Self-complementary AAV-mediated gene therapy restores cone function and prevents cone degeneration in two models of Rpe65 deficiency. Gene Ther 17:815–826

21. Bainbridge JW, Smith AJ, Barker SS et al (2008) Effect of gene therapy on visual function in Leber's congenital amaurosis. N Engl J Med 358:2231–2239

22. Maguire AM, Simonelli F, Pierce EA et al (2008) Safety and efficacy of gene transfer for Leber's congenital amaurosis. N Engl J Med 358:2240–2248

23. Hauswirth WW, Aleman TS, Kaushal S et al (2008) Treatment of Leber congenital amaurosis due to RPE65 mutations by ocular subretinal injection of adeno-associated virus gene vector: short-term results of a phase I trial. Hum Gene Ther 19:979–990

24. MacLaren RE, Groppe M, Barnard AR et al (2014) Retinal gene therapy in patients with choroideremia: initial findings from a phase 1/2 clinical trial. Lancet 383:1129–1137

25. Fischer D, Wilhelm B, Michalakis S et al (2016) Successful delivery of rAAV8.CNGA3 in a patient with CNGA achromatopsia. Paper presented at the ARVO 2016, Seattle 1–5 May 2016, Retinal Prosthetics and Novel Therapies 462, Number: 5207

26. Gauthier R, Joly S, Pernet V et al (2005) Brain-derived neurotrophic factor gene delivery to muller glia preserves structure and function of light-damaged photoreceptors. Invest Ophthalmol Vis Sci 46:3383–3392

27. Hauck SM, Ekström PA, Ahuja-Jensen P et al (2006) Differential modification of phosducin protein in degenerating rd1 retina is associated with constitutively active Ca2+/calmodulin kinase II in rod outer segments. Mol Cell Proteomics 5:324–336

28. LaVail MM, Yasumura D, Matthes MT et al (1998) Protection of mouse photoreceptors by survival factors in retinal degenerations. Invest Ophthalmol Vis Sci 39:592–602

29. Wenzel A, Grimm C, Samardzija M et al (2005) Molecular mechanisms of light-induced photoreceptor apoptosis and neuroprotection for retinal degeneration. Prog Retin Eye Res 24:275–306

30. LaVail MM, Unoki K, Yasumura D et al (1992) Multiple growth factors, cytokines, and neurotrophins rescue photoreceptors from the damaging effects of constant light. Proc Natl Acad Sci U S A 89:11249–11253

31. Towne C, Setola V, Schneider BL et al (2011) Neuroprotection by gene therapy targeting mutant SOD1 in individual pools of motor neurons does not translate into therapeutic benefit in fALS mice. Mol Ther 19:274–283

32. Lhériteau E, Libeau L, Mendes-Madeira A et al (2010) Regulation of retinal function but nonrescue of vision in RPE65-deficient dogs treated with doxycycline-regulatable AAV vectors. Mol Ther 18:1085–1093

33. Nutt JG, Burchiel KJ, Comella CL et al (2003) Randomized, double-blind trial of glial cell line-derived neurotrophic factor (GDNF) in PD. Neurology 60:69–73

34. Bongioanni P, Reali C, Sogos V (2004) Ciliary neurotrophic factor (CNTF) for amyotrophic lateral sclerosis/motor neuron disease. Cochrane Database Syst Rev (3):CD004302

35. Mühlfriedel R, Michalakis S, Garcia Garrido M et al (2013) Optimized technique for subretinal injections in mice. Methods Mol Biol 935:343–349

36. Heile AM, Wallrapp C, Klinge PM et al (2009) Cerebral transplantation of encapsulated mesenchymal stem cells improves cellular pathology after experimental traumatic brain injury. Neurosci Lett 463:176–181

37. Zhang R, Zhang H, Xu L et al (2011) Intravitreal cell-based production of glucagon-like peptide-1. Retina 31:785–789

38. Klinge PM, Harmening K, Miller MC et al (2011) Encapsulated native and glucagon-like peptide-1 transfected human mesenchymal stem cells in a transgenic mouse model of Alzheimer's disease. Neurosci Lett 497:6–10

39. Weber C, Pohl S, Poertner R et al (2010) Production process for stem cell based therapeutic implants: expansion of the production cell line and cultivation of encapsulated cells. Adv Exp Med Biol 123:143–162

40. Sieving PA, Caruso RC, Tao W et al (2006) Ciliary neurotrophic factor (CNTF) for human retinal degeneration: phase I trial of CNTF delivered by encapsulated cell intraocular implants. Proc Natl Acad Sci U S A 103:3896–3901

Neutralizing Antibodies Against Adeno-Associated Virus (AAV): Measurement and Influence on Retinal Gene Delivery

Mélissa Desrosiers and Deniz Dalkara

Abstract

Adeno-associated viral vectors have become widely used in the clinic for retinal gene therapy. Thanks to AAVs impeccable safety profile and positive functional outcomes in its clinical application, interest in retinal gene therapy has increased exponentially over the past decade. Although early clinical trials have shown there is little influence of neutralizing antibodies on the performance of AAV when vector is administered into the subretinal space, recent findings suggest neutralizing antibodies may play a role when AAV is delivered via the intravitreal route. These findings highlight the importance of microenvironment on gene delivery and stress the need for a versatile assay to screen subjects for the presence of AAV-neutralizing antibodies. Measuring NAb titers against AAV prior and after gene therapy will help us better understand the impact of preexisting immunity on gene transfer, especially when the vector is administered intravitreally.

Key words Neutralizing antibody assay, AAV vectors, Serum, Intravitreal, Subretinal

1 Introduction

AAVs are one of the most widely used vectors in gene therapy. They are nonpathogenic, and display little immunogenicity making them ideal for therapeutic gene delivery in several organs. Nevertheless, their use in the clinic has been hampered by patient's preexisting immunity and development of immunity following vector administration [1]. Systemic injection of AAV in individuals with high titers of neutralizing antibodies (NAbs) impedes gene delivery. For these reasons, most studies in humans and large animal models choose to exclude subjects with preexisting immunity [1]. However, the role of NAbs in AAV transduction of tissues considered to be immune privileged, such as the eye, is less clear.

The progress in retinal gene therapy has been accelerated by the positive outcomes of the clinical trials for Leber's congenital amaurosis [2–4] and choroideremia [5]. The immune privileged

nature of the eye along with its confined structure made it possible to employ low doses of AAV in clinical trials ensuring the safety of AAV in the retina. Until now, the published literature relating to clinical trials of AAV gene therapy in the eye describes immune reactions before and after subretinal injections of AAV (Table 1). It is now well established that the subretinal space has an immune privilege [6–8], and that both eyes are independent regarding humoral immunity [7]. The presence of neutralizing antibodies in the serum is not a no go for gene therapy in the subretinal space [6] as shown by the safety of readministration of AAV in contralateral eyes of subjects previously treated for LCA [8]. However, when the cellular targets of gene therapy lie within the inner retina [9] or when the retina has fragile architecture [10, 11] it is preferable to use intravitreal injection route. According to recent findings, intravitreal space is less immune privileged compared to the subretinal space [6, 12]. Even though the correlation between NAb titers against AAV in serum and in aqueous/vitreous humor is not well established [7, 13], the nonhuman primate study by Maclachlan and coworkers recognized that preexisting antibody titers against AAV2 may impact successful transduction via the vitreous. More recently, Kotterman et al. showed that serum NAb titer higher than 1/10 leads to weak retinal expression after intravitreal delivery of AAV [12]. They consider that Nab titers as low as 1:100 can interfere with the expression of the transgene in macaques after intravitreal delivery.

As a context for our protocol for measuring NAb titers in serum, we present a summary of screens for neutralizing activity conducted in humans and large animals in view of the injection route and AAV serotype in Table 1. As shown, for most of the studies the NAb assay was used to assess the presence of neutralizing antibodies against AAV serotype 2 via subretinal injection. The methods proposed in most studies and the protocol we detail here both measure neutralizing ability of serum toward AAV serotype 2. We chose to focus on serum as opposed to vitreous humor as it can be collected in a noninvasive way without compromising the eye. We test the ability of serum to inhibit transduction of HEK293T cells by AAVs carrying luciferase as a reporter gene as this has the advantage of being robust and quantitative compared to methods based on cell counting. Our method employs serial dilutions of blood sera mixed with a fixed amount of AAV (quantified in viral genomes). It is crucial to use an appropriate multiplicity of infection (MOI) that allows a proper dynamic range for a given serotype in order to have an accurate readout. In Fig. 1 we show a typical MOI curve for AAV serotype 2 on HEK293T cells. Based on this MOI curve, we chose the MOI for the no-serum control. The plates always include a no serum control as well as standard from animals having had previous AAV exposure (Fig. 2).

Table 1
Summary of neutralizing antibody screens in humans and large animal models in view of the injection route and AAV serotype

Publication	Type of injection	Serotype	NAb assay type (reporter, cell type, MOI)	nAb Titer determination	Cutoff
[2, 14, 15]	SR	AAV2	Unilateral injection	β-Gal, HEK cell, data unavailable	Dilution range resulting in <50% inhibition of maximum activity	Subjects with neutralizing antibodies to AAV2 above 1:1000 were excluded
[8, 16]	SR	AAV2	Contralateral eye follow-up study of [2]	β-Gal, HEK cells, data unavailable	Dilution range resulting in <50% inhibition compared to the maximum activity control	Two individuals had high (>1:1000) baseline NAb to AAV2. The rest of the subjects had low NAb titer (<1:10)
[3, 17]	SR	AAV2	Unilateral injection	GFP, HEK cells, data unavailable	Dilution of serum that yields 50% of the number of GFP positive cells relative to wells where no serum was incubated with vector	No mention of selection of patient based on NAb status
[18, 19]	SR	AAV2	Unilateral injection	GFP, HEK cells, MOI 5000 vg WITH AdV	Test serum dilution that resulted in 50% inhibition of transduction by GFP with the positive control set at 0% inhibition	Of the 21 patients who received the treatment; • 9 were considered negative (NAb >1:20). • 5 were considered positive with a low NAb titer (1:20–1:100) • 7 had a NAb titer <1:100
[20–22]	SR	AAV2	Unilateral injection	–	Titering of NAbs was performed by ELISA	Exclusion criteria: AAV antibody titers greater than two standard deviations above normal at baseline
[5]	SR	AAV2	Unilateral injection	–	–	No mention of patient selection based on NAb titers
[23]	SR	AAV2	Unilateral injection	–	–	No mention of selection of patient based on NAb titers

Table 1
(continued)

Publication	Type of injection	Serotype	Species	NAb type (reporter, cell type, MOI)	Serum	Eye
[7]	SR	AAV2	*Dogs*	β-Gal, HEK 293, MOI 6800 vg	Before first injection: naive Second injection (15 days later): <1:100	–
[7]	SR	AAV2	*NHP*: previously exposed to AAV2 in other studies	β-Gal, HEK 293, MOI 6800 vg	Serum NAb ranged from negligible (1:1) to high (1:250)	Anterior chamber NAb concentrations before injection were negligible (1:1–1:3) in all four NHPs
[24]	SR	AAV2, 8	*NHP*	β-Gal, Huh7 cells, MOI 10 000 vg	All animals in the study were negative for AAV-neutralizing antibodies at enrollment (<20). The highest titer post injection is 1:640	The highest titer post injection in ocular fluid is 1:160
[12]	IVT	AAV2, 5, 8, 9	*NHP* previously injected with AAV	GFP, HEK, MOI 2×10^3	The presence of NAB titers of 1:10 or greater in the serum resulted in weak or no expression of the transgene	The level of anti-AAV antibodies in the serum is positively correlated with anti-AAV antibody levels in the vitreous fluid ($r = 0.3$)
[25]	SR/IVT		*NHP*	–	ELISA	–

Ref		Vector	Animal	Transgene, cells, MOI	NAb titers	
[26]		AAV5	*NHP*	mCherry, ARPE19, MOI 10^4	All NAb titers <1:10 at the beginning of the experiment. Of the 3 animals one rose to 1:640 post injection (but had surgical complication)	–
[27]	IVT with vitrectomy	AAV2 4YF	*Dog*	mCherry, ARPE19, MOI 5×10^3	4 weeks after injection, NAB titers were up to >81,920 Serum of a naive animal scored at 1:5	–
[28]	SR/IVT	AAV2–7m8 and AAV8bp2	*NHP*	GFP, HEK, MOI AAV2 7m8 = 10^4 AAVBP2 = 10^5	4 weeks after injection, NAb titers were between 1:3.16 and 1:10 in serum and 1:3.16 and 1:100 in the vitreous	–

MOI curve for AAV2 on HEK cells
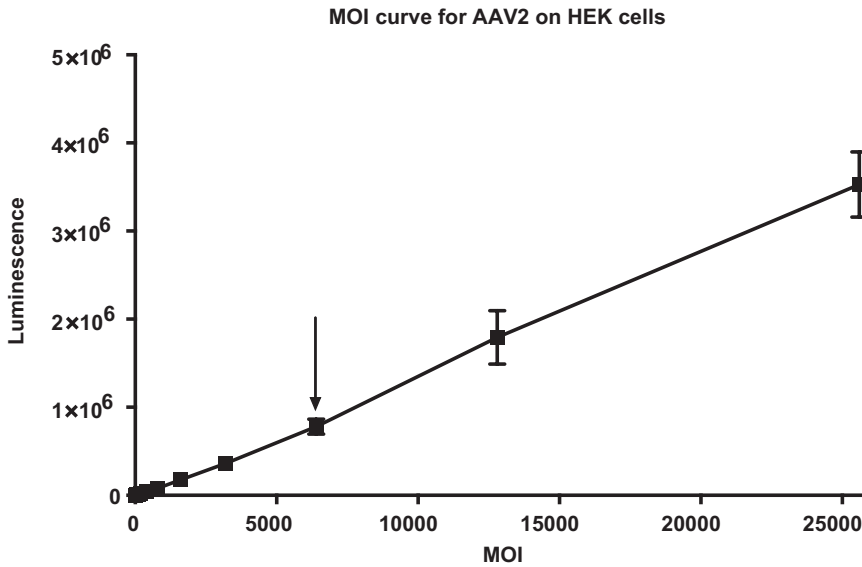
Fig. 1 A typical AAV2-HEK cell infection curve. The arrow indicates the MOI used in our protocol

The samples are compared to the no-serum control, which provides the maximum transduction efficiency for a given serotype under the given conditions. The readout is usually percent transduction efficiency compared to the no-serum control. A typical range of serums from five random macaques is shown in Fig. 3. Data obtained after addition of sera show increase in luciferase levels as the albumin content of serum increases transduction levels (Fig. 3a) [29]. The higher the NAbs in a given sample the lower the serum dilution will be. For example a NAb titer of 1/10 is considered low and compatible with subsequent intravitreal AAV injections. As an example, the outcome after intravitreal delivery of 5 × 10E11 vg of AAV2-GFP in the eyes of macaques BC758 and CB723 whose serum Nab titers are shown in Fig. 3a are shown in Fig. 3b, c. This data, agrees with the notion that serum NAb titers higher than 1/10 lead to weak transgene expression after AAV mediated gene delivery in macaques.

The method we describe here will be useful for screening for the presence of NAbs in large animal models to be used in AAV-mediated retinal gene delivery experiments. It can be readily adapted to derivatives of AAV2 such as tyrosine mutants [30, 31] or 7mer insertion variants [32] of this serotype. However, care should be taken in adapting our protocol to detect NAbs against other AAV serotypes—as some AAV serotypes like AAV8 or AAV5 lead to poor HEK cell transduction and thus require very high MOI [33, 34]. The use of the optimal amount of AAV particles per cell for each AAV serotype makes the assay more sensitive but compromises the comparison of NAb titers between different AAV serotypes.
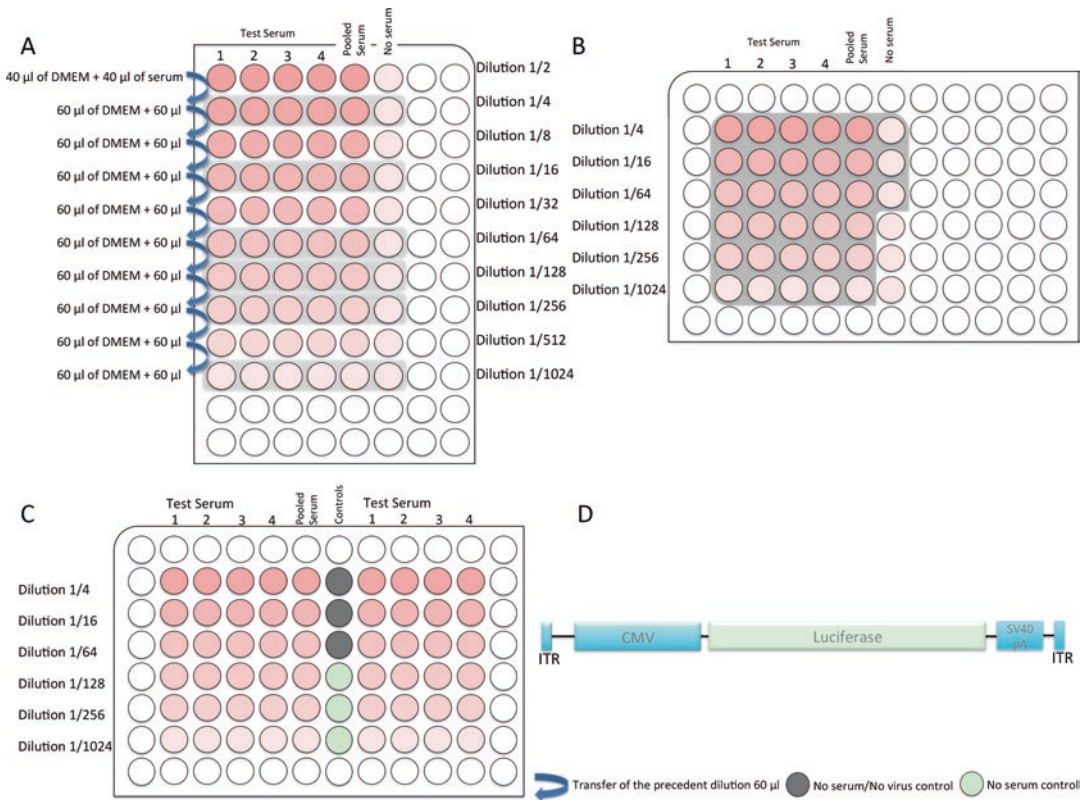
Fig. 2 Overview of the plates' layout. (**a**) Plate A, shows the sample dilutions. This configuration gives the opportunity to use multichannel pipette to transfer required dilution (in gray) to the plate B. (**b**) Plate B, shows in gray the wells where the virus dilution is added. (**c**) Plate C contains the cells. The location of the control, standard and sample are highlighted. (**d**) AAV transgene construct used in this assay

The full to empty AAV particle ratio of the AAV vector preparation and the methods used for determining the physical titer of the vector stock [35] may affect the reproducibility of the results between different laboratories. Lastly, it is also important to employ caution when transposing results from serum NAb titers to humoral responses in other compartments such as aqueous or vitreous humor.

2   Materials

1. HEK 293T cell line (*see* **Note 1**).

2. Cell culture 96 wells white plate with clear bottom.

3. Complete DMEM: DMEM medium supplemented with 10% de-complemented FBS.

4. DMEM medium.
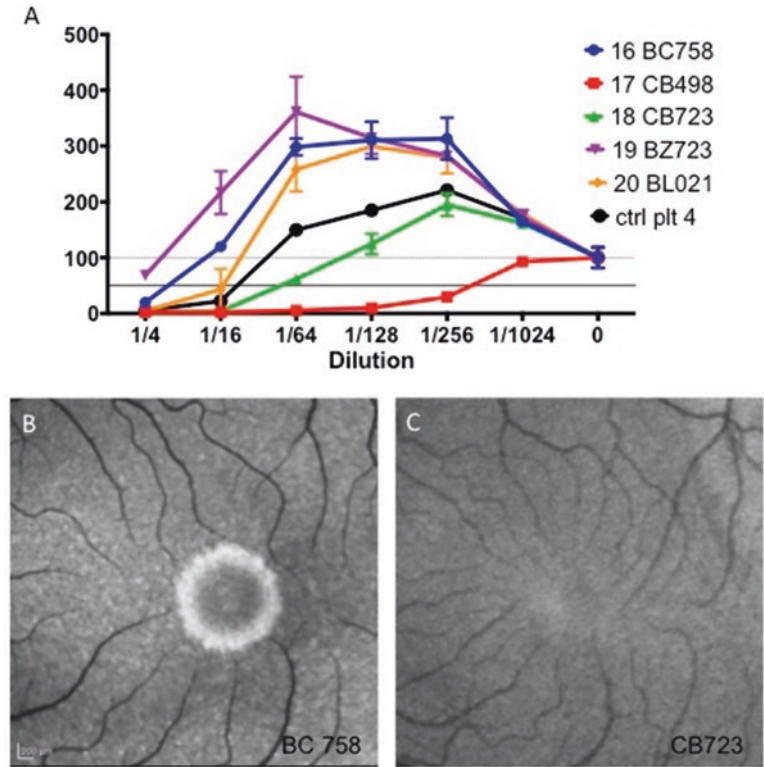
Fig. 3 (**a**) Graph of a typical neutralizing antibodies assay. (**b**) Post-injection fluorescent fundus images of BC758 after intravitreal injection with 5[11] vg AAV2-GFP. (**c**) Post-injection fluorescent fundus images of CB723 after intravitreal injection with 5[11] vg AAV2-GFP

5. 0.05% Trypsin–EDTA.

6. PBS: PBS without calcium and magnesium.

7. Malassez cell.

8. Multichannel pipette (for volume of 100, 60, 40, and 25 μL).

9. Conical bottom 96 wells plate.

10. AAV2-CMV-Luciferase (*see* **Notes 2** and **3**) thawed on ice.

11. Sera to be tested.

12. Control Serum (*see* **Note 4**).

13. Revelation kit for Luciferase, including a lysis buffer for cells, and reagent for revelation.

14. Luminometer plate reader.

15. Statistical analysis software.

3 Methods

3.1 Cell Plating

1. Rinse the HEK 293T cells with PBS, trypsin the cells, and count them using a Malassez cell (*see* **Note 5**).

2. Prepare a 10 mL dilution of 700,000 cells/mL in complete DMEM (*see* **Note 6**).

3. Using a multichannel pipette, distribute 100 μL of the cell suspension per well, in a white 96-well plate, so to have 70,000 cells per well.

4. Return the cells into the incubator for at least 4 h (37 °C/5% CO_2).

3.2 Dilution of the Sera

1. Use a new 96 well plate (Plate A). Turning the plate sideways put 40 μL of the serum to test in the first well of each column. Add 40 μL of the standard and 40 μL of DMEM, in the last two columns of the plate (*see* **Note 4**) (*see* Fig. 1a). This last column with DMEM will be used as a no-serum control.

2. In the first line of the plate, add 40 μL of DMEM in every well and mix thoroughly.

3. Pipette 60 μL of DMEM in all the wells of the column with the serum, up to the last dilution (*see* **Note 7**).

4. Mix well and transfer 60 μL of the first column of cells containing the serum into the following column. Continue this two-fold serial dilutions until reaching the last dilution to be used.

5. Transfer 40 μL of the dilutions to use onto a new plate (Plate B).

3.3 Dilution of the Virus/ Incubation/Infection

1. Calculate the volume of virus required V (μL) (*see* **Note 1**).

   MOI = multiplicity of infection

   V = Virus to use

   VP/W = Virus particle per well

   VP/P = Virus particle per plate

   T = titer on the virus, in vector genome per μL

   $$\text{MOI} \times 70{,}000 \text{cells/well} = \text{VP/W}$$

   $$\frac{\text{VP/W}}{12.5 \mu L} = \frac{\text{VP/P}}{2000 \mu L}$$

   $$\frac{\text{VP/P}}{T} = V\left(\mu L\right)$$

2. Dilute V in 2 mL of DMEM.

3. Add 40 μL of the virus dilution on every well of the Plate B except for three wells, which will serve as no-virus controls (*see* Fig. 1b).

4. Add 40 µL of DMEM in the three wells not receiving the virus dilution.

5. Seal the plate with Parafilm.

6. Put the plate in the fridge for 2 h.

7. Observe the cells under a microscope; most cells should have settled on the bottom of the plate. Manipulate the plate carefully to avoid any detachment of cells.

8. Using a multichannel pipette, transfer 25 µL of the virus/serum dilution to the well of the cell's plate in duplicate, except for the control and standard (*see* Fig. 1c) (*see* **Note 8**). Be careful to not detach the cells when pipetting.

9. Return the cells to the incubator.

3.4 Revelation

1. 24 h later, prepare the lysis solution according to the instruction of the kit used (*see* **Note 9**).

2. Remove the medium of the cells.

3. Carefully rinse the cells with PBS.

4. Add the lysis solution. Pipette carefully to lyse all the cells of the well. Once the lysis is done, the plate can be transferred to the Luminometer plate reader.

5. Add the luciferase reagent. Read the plate immediately.

3.5 Analysis of the Results

1. Subtract from all the wells the mean of the background (i.e., the no virus control).

2. Using an appropriate spreadsheet computer application, plot a graph with the percentage of luminescence on the Y axis, 100% being the no serum control (*see* **Note 10**).

4 Notes

1. This protocol is for the detection of antibodies against AAV serotype 2 and derivatives. If one had to detect antibodies against another serotype, we strongly recommend using a cell line that is efficiently infected with the serotype [34]. Wang et al. [36] concluded recently that the cell type is not important in the output of the nAb assay, but we found that having a cell line that is efficiently infected by the serotype tested increases the sensitivity of the assay. The MOI (multiplicity of infection) used to do the NAb assay should be as low as possible [37]. To define the MOI required, one should setup a Virus-Cell infectivity curve, with increased MOI. The MOI chosen should be at the lower end of the curve, but high enough to show an increase from noninfected cells. The chosen MOI might vary

according to the AAV preparation (and the method used for its dosage), the virus serotype, the cell type and the plate reader used in the assay. This is why we recommend laboratories to establish this curve with their in house conditions.

2. We use a AAV2 virus for the NAb assay for animals to be injected with AAV2 7m8 and other mutant like AAV2 3YF. We found that point mutation and 7mer insertions of the capsid does not change the output of the NAb assay for these serotypes. However, care should be taken if other mutants are used.

3. One could also use GFP or β-Galactosidase as reporter. We found that luciferase is more sensitive and reliable than GFP. The AAV encoding luciferase should be kept frozen in single use aliquots.

4. On every plate there should be a standard, made from pooled serum. This pooled serum should be frozen in aliquots for single use. The NAb of this sample must be constant on every plate, validating the stability of the results, even between experiments set many months apart.

   Every plate will also have both the "no serum" and the "no virus" conditions, in triplicate. The no virus condition is the background level, and should be subtracted from all the results. The no serum condition is considered as the maximum infection and will be set as the 100% infection when analyzing the results.

5. All the steps of this procedure should be carried under a cell culture hood, in a sterile manner, until the **step 4** of Subheading 3.4.

6. This procedure analyzes up to four sera in duplicate per plate, plus the appropriate control and standard. Scale-up according to the number of serum you want to test.

7. The dilution to use should be determined according to expected results: Searching for naïve animals, we recommend focusing on low dilution (1:4, 1:8, 1:16, 1: 32, 1:64, 1:128), so to detect low antibody levels. If looking at NAb level of immunized animals, we recommend extending dilution (1:16, 1:64, 1:128, 1:256, 1:512, 1:1024), over a wider range. Represented on figure 2 is a series of dilutions that is suitable for every case. Note that the lowest dilution used within this protocol is 1:4.

8. We notice that evaporation on the external wells of the plate seem to have an influence on the quantity of luminescence produce in the end. We prefer not to use these wells.

9. Since the luciferase reaction is dependent on temperature, be careful to use solution at RT. Thaw frozen solution many hours in advance. Keep solution away from light.

10. As explained recently by Wang et al. [29] the sample from naïve serum show a percentage of luminescence higher than 100% in the sample incubate with serum. It can be explained by AAV capsid's interaction with human serum albumin which increases infection both in vivo and in vitro. Sample from non-human primate also exhibit this increased infection.

References

1. Mingozzi F, High KA (2007) Immune responses to AAV in clinical trials. Curr Gene Ther 7:316–724

2. Maguire AM, Simonelli F, Pierce EA et al (2008) Safety and efficacy of gene transfer for Leber's congenital amaurosis. N Engl J Med 358:2240–2248. https://doi.org/10.1056/NEJMoa0802315

3. Bainbridge JWB, Smith AJ, Barker SS et al (2008) Effect of gene therapy on visual function in Leber's congenital amaurosis. N Engl J Med 358:2231–2239. https://doi.org/10.1056/NEJMoa0802268

4. Cideciyan AV, Aleman TS, Boye SL et al (2008) Human gene therapy for RPE65 isomerase deficiency activates the retinoid cycle of vision but with slow rod kinetics. Proc Natl Acad Sci U S A 105:15112–15117. https://doi.org/10.1073/pnas.0807027105

5. MacLaren RE, Groppe M, Barnard AR et al (2014) Retinal gene therapy in patients with choroideremia: initial findings from a phase 1/2 clinical trial. Lancet 383:1129–1137. https://doi.org/10.1016/S0140-6736(13)62117-0

6. Li Q, Miller R, Han P-Y et al (2008) Intraocular route of AAV2 vector administration defines humoral immune response and therapeutic potential. Mol Vis 14:1760–1769

7. Amado D, Mingozzi F, Hui D et al (2010) Safety and efficacy of subretinal readministration of a viral vector in large animals to treat congenital blindness. Sci Transl Med 2:21ra16. https://doi.org/10.1126/scitranslmed.3000659

8. Bennett J, Wellman J, Marshall KA et al (2016) Safety and durability of effect of contralateral-eye administration of AAV2 gene therapy in patients with childhood-onset blindness caused by RPE65 mutations: a follow-on phase 1 trial. Lancet 388:661–672. https://doi.org/10.1016/S0140-6736(16)30371-3

9. Cwerman-Thibault H, Augustin S, Ellouze S et al (2014) Gene therapy for mitochondrial diseases: Leber Hereditary Optic Neuropathy as the first candidate for a clinical trial. C R Biol 337:193–206. https://doi.org/10.1016/j.crvi.2013.11.011

10. Byrne LC, Oztürk BE, Lee T et al (2014) Retinoschisin gene therapy in photoreceptors, Müller glia or all retinal cells in the Rs1h−/− mouse. Gene Ther 21:585–592. https://doi.org/10.1038/gt.2014.31

11. Park TK, Wu Z, Kjellstrom S et al (2009) Intravitreal delivery of AAV8 retinoschisin results in cell type-specific gene expression and retinal rescue in the Rs1-KO mouse. Gene Ther 16:916–926. https://doi.org/10.1038/gt.2009.61

12. Kotterman MA, Yin L, Strazzeri JM et al (2014) Antibody neutralization poses a barrier to intravitreal adeno-associated viral vector gene delivery to non-human primates. Gene Ther 22:116–126. https://doi.org/10.1038/gt.2014.115

13. Maclachlan TK, Lukason M, Collins M et al (2011) Preclinical safety evaluation of AAV2-sFLT01- a gene therapy for age-related macular degeneration. Mol Ther 19:326–334. https://doi.org/10.1038/mt.2010.258

14. Maguire AM, High KA, Auricchio A et al (2009) Age-dependent effects of RPE65 gene therapy for Leber's congenital amaurosis: a phase 1 dose-escalation trial. Lancet 374:1597–1605. https://doi.org/10.1016/S0140-6736(09)61836-5

15. Testa F, Maguire AM, Rossi S et al (2013) Three-year follow-up after unilateral subretinal delivery of adeno-associated virus in patients with Leber congenital amaurosis type 2. Ophthalmology 120:1283–1291. https://doi.org/10.1016/j.ophtha.2012.11.048

16. Bennett J, Ashtari M, Wellman J et al (2012) AAV2 gene therapy readministration in three adults with congenital blindness. Sci Transl Med 4:120ra15. https://doi.org/10.1126/scitranslmed.3002865

17. Bainbridge JWB, Mehat MS, Sundaram V et al (2015) Long-term effect of gene therapy on Leber's congenital amaurosis. N Engl J Med 372:1887–1897. https://doi.org/10.1056/NEJMoa1414221

18. Rakoczy EP, Lai CM, Magno AL et al (2015) Gene therapy with recombinant adeno-associated vectors for neovascular age-related macular degeneration: 1 year follow-up of a phase 1 randomised clinical trial. Lancet 386:2395–2403. https://doi.org/10.1016/S0140-6736(15)00345-1

19. Constable IJ, Pierce CM, Lai CM et al (2016) Phase 2a randomized clinical trial: safety and post hoc analysis of subretinal rAAV. sFLT-1 for wet age-related macular degeneration. EBioMed 14:168–175. https://doi.org/10.1016/j.ebiom.2016.11.016

20. Hauswirth WW, Aleman TS, Kaushal S et al (2008) Treatment of Leber congenital amaurosis due to RPE65 mutations by ocular subretinal injection of adeno-associated virus gene vector: short-term results of a phase I trial. Hum Gene Ther 19:979–990. https://doi.org/10.1089/hum.2008.107

21. Jacobson SG, Cideciyan AV, Ratnakaram R et al (2012) Gene therapy for Leber congenital amaurosis caused by RPE65 mutations: safety and efficacy in fifteen children and adults followed up to three years. Arch Ophthalmol 130:9–24. https://doi.org/10.1001/archophthalmol.2011.298.Gene

22. Cideciyan AV, Hauswirth WW, Aleman TS et al (2009) Human RPE65 gene therapy for Leber congenital amaurosis: persistence of early visual improvements and safety at 1 year. Hum Gene Ther 20:999–1004. https://doi.org/10.1089/hum.2009.086

23. Ghazi NG, Abboud EB, Nowilaty SR et al (2016) Treatment of retinitis pigmentosa due to MERTK mutations by ocular subretinal injection of adeno-associated virus gene vector: results of a phase I trial. Hum Genet 135:327–343. https://doi.org/10.1007/s00439-016-1637-y

24. Vandenberghe LH, Bell P, Maguire AM et al (2011) Dosage thresholds for AAV2 and AAV8 photoreceptor gene therapy in monkey. Sci Transl Med:3, 88ra54. https://doi.org/10.1126/scitranslmed.3002103

25. Jacobson SG, Boye SL, Aleman TS et al (2006) Safety in nonhuman primates of ocular AAV2-RPE65, a candidate treatment for blindness in Leber congenital amaurosis. Hum Gene Ther 17:845–858. https://doi.org/10.1089/hum.2006.17.845

26. Boye SE, Alexander JJ, Boye SL et al (2012) The human rhodopsin kinase promoter in an AAV5 vector confers rod- and cone-specific expression in the primate retina. Hum Gene Ther 23:1101–1115. https://doi.org/10.1089/hum.2012.125

27. Boyd RF, Boye SL, Conlon TJ et al (2016) Reduced retinal transduction and enhanced transgene-directed immunogenicity with intravitreal delivery of rAAV following posterior vitrectomy in dogs. Gene Ther 23:548–556. https://doi.org/10.1038/gt.2016.31

28. Ramachandran P, Lee V, Wei Z et al (2016) Evaluation of dose and safety of AAV7m8 and AAV8BP2 in the non-human primate retina. Hum Gene Ther. https://doi.org/10.1089/hum.2016.111

29. Wang M, Sun J, Crosby A et al (2016) Direct interaction of human serum proteins with AAV virions to enhance AAV transduction: immediate impact on clinical applications. Gene Ther. https://doi.org/10.1038/gt.2016.75

30. Zhong L, Li B, Mah CS et al (2008) Next generation of adeno-associated virus 2 vectors: point mutations in tyrosines lead to high-efficiency transduction at lower doses. Proc Natl Acad Sci U S A 105:7827–7832. https://doi.org/10.1073/pnas.0802866105

31. Petrs-silva H, Dinculescu A, Li Q et al (2011) Novel properties of tyrosine-mutant AAV2 vectors in the mouse retina. Mol Ther 19:293–301. https://doi.org/10.1038/mt.2010.234

32. Dalkara D, Byrne LLC, Klimczak RR et al (2013) In vivo-directed evolution of a new adeno-associated virus for therapeutic outer retinal gene delivery from the vitreous. Sci Transl Med 5:189ra76. https://doi.org/10.1126/scitranslmed.3005708

33. Hurlbut GD, Ziegler RJ, Nietupski JB et al (2010) Preexisting immunity and low expression in primates highlight translational challenges for liver-directed AAV8-mediated gene therapy. Mol Ther 18:1983–1994. https://doi.org/10.1038/mt.2010.175

34. Calcedo R, Wilson JM (2013) Humoral immune response to AAV. Front Immunol 4:341. https://doi.org/10.3389/fimmu.2013.00341

35. Lock M, McGorray S, Auricchio A et al (2010) Characterization of a recombinant adeno-associated virus type 2 reference standard material. Hum Gene Ther 21:1273–1285. https://doi.org/10.1089/hum.2009.223

36. Wang M, Crosby A, Hastie E et al (2015) Prediction of adeno-associated virus neutralizing antibody activity for clinical applica-tion. Gene Ther 22:984–992. https://doi.org/10.1038/gt.2015.69

37. Wang L, Calcedo R, Bell P et al (2011) Impact of pre-existing immunity on gene trans-fer to nonhuman primate liver with adeno-associated virus 8 vectors. Hum Gene Ther 22:1389–1401. https://doi.org/10.1089/hum.2011.031

Chapter 17

Screening for Neutralizing Antibodies Against Natural and Engineered AAV Capsids in Nonhuman Primate Retinas

Timothy P. Day, Leah C. Byrne, John G. Flannery, and David V. Schaffer

Abstract

Adeno-associated virus (AAV) has shown promise as a therapeutic gene delivery vector for inherited retinal degenerations in both preclinical disease models and human clinical trials. The retinas of nonhuman primates (NHPs) share many anatomical similarities to humans and are an important model for evaluating AAV gene delivery. Recent evidence has shown that preexisting immunity in the form of neutralizing antibodies (NABs) in NHPs strongly correlates with weak or lack of AAV transduction in the retina when administered intravitreally, work with translational implications. This necessitates prescreening of NHPs before intravitreal delivery of AAV. In this chapter, we describe a method for screening NHP serum for preexisting NABs.

Key words Adeno-associated virus, Retinal gene therapy, Retinitis pigmentosa, Nonhuman primates, Translational medicine, Neutralizing antibodies, Serum screen

1   Introduction

AAV-mediated gene therapy has enjoyed recent success ranging from multiple proof-of-concept experiments to human clinical trials [1–3]. Animal models are currently the best way to optimize application of AAV vectors, as they recapitulate many of the cellular barriers and tissue structures encountered in the final therapeutic application, in a manner unattainable in vitro. Small animal models, such as rodents, remain important to the development of human gene therapy; however, for several reasons including important structural and functional differences, they cannot predict transduction efficiency in humans. Large animals—such as dogs, pigs, or nonhuman primates (NHPs)—more effectively evaluate the clinical potential of AAV for treatment of retinal degeneration patients and provide key insights. Specifically, the eye of the NHP has nearly identical anatomy compared to humans, with a cone-rich macula and cone-only fovea. The biological and immunological

features of NHPs are also closer to humans, and the surgical procedures for the eye are similar. In the NHP, AAV can be delivered to the retina via subretinal or intravitreal injection. Subretinal injection involves creating a fluid filled space or "bleb" between the apical side of the RPE and the photoreceptors, leading to a concentrated volume of virus in a small space, and resulting in a restricted area of transduction. Consequently, this localized injection does not treat the entire retina, and there are some associated risks associated with making the retinal detachment. By comparison, intravitreal injection is a less invasive procedure, as it does not require a through-retinal needle penetration (retinotomy) with the retinal detachment, and allows for the potential of panretinal expression [4]. That said, intravitreal injections create greater exposure of the viral capsid proteins to the immune system as they more readily exit the eye through the trabecular meshwork outflow pathway into the circulation. Vectors introduced into the vitreous must cross through the inner limiting membrane and multiple cell layers to reach either the photoreceptors or RPE [4, 5].

The tropism of AAV in the NHP retina depends upon several factors including the serotype, route of administration, promoter, and dose. Therefore, it is critical to choose the correct vector for the desired outcome. Subretinal injection of AAV2 in NHPs leads to photoreceptor and RPE transduction for at least 1 year [6, 7]. The ability to target foveal photoreceptors has been reported to be dose-dependent, with lower doses leading only to RPE transduction and higher doses leading to expression in both RPE and photoreceptors. The limited photoreceptor expression observed outside the fovea was determined to be predominantly rods [5, 8]. Subretinal injection of AAV2 has most notably been used in the treatment of Leber's congenital amaurosis (LCA2) in human clinical trials. Intravitreal injection of AAV2 (driving expression from a ubiquitous chicken beta actin, i.e., CBA, or CMV promoter) in NHPs leads to a disc of expression centered on the fovea with only Müller glia and especially retinal ganglion cells (RGCs) transduced. Variable expression in the periphery in Müller glia and RGCs was observed. In addition, RGC-specific expression was achieved using the hCx36 promoter [9]. RGC expression has been used to restore light response to the NHP retina with channelrhodopsin expressed in RGCs [10, 11].

In addition to AAV2 vectors, subretinal delivery of AAV5 leads to transduction of both the photoreceptor cells and the RPE, with greater transduction efficiency observed in the photoreceptors [12]. Photoreceptor specificity can be achieved with the hGRK1 promoter, which has been shown to have strong expression with no evidence of gross pathology after injection [13]. Most notably, subretinal delivery of an AAV5 vector was used to produce trichomatic vision in a primate model of red–green color blindness [14]. Subretinal delivery of AAV7 results in modest levels of pho-

toreceptor transduction. AAV7 is outperformed by AAV8 for rod transduction and outperformed by AAV9 for cone transduction in the NHP retina [4]. Subretinal delivery of AAV8 leads to expression in RPE, photoreceptors, and Muller glia with the relative efficiency of transduction in the three classes of cells dependent upon the dose. Rod photoreceptors were transduced with higher efficiency than cones and foveal cones were transduced at a higher efficiency than extrafoveal cones in NHPs [8]. Subretinal delivery of AAV9 led to strong expression in cones both centrally and peripherally in NHP retinas with limited rod expression observed in the periphery [4]. This transduction pattern is thought to be due to the level of galactose found on the surface of cones, the receptor for AAV9 [15].

Despite the promise of subretinal delivery in clinical studies to date, it would be preferable to utilize intravitreal administration to avoid the risk associated with subretinal surgery and to potentially transduce the full surface area of the retina. However, natural evolution likely did not select AAV for its capacity to infect the retina, and as a result naturally occurring AAV variants isolated from healthy, extraocular tissues, would be expected to yield vectors with significant limitations in gene transfer to either healthy or diseased retina. To overcome this obstacle, viruses can be engineered for advantageous delivery properties for human ocular tissue. In particular, successful intravitreal injection will require the engineering of AAV variants to penetrate the physical barrier of the inner limiting membrane [5]. In general, two methodologies have been approached to engineer better AAV vectors for retinal gene therapy: rational design and directed evolution.

The rational design approach applies fundamental molecular biology knowledge to the improvement of the viral capsid. Zhong et al. showed that epidermal growth factor receptor protein tyrosine kinase-mediated phosphorylation of tyrosine residues on the AAV leads to degradation of the virus via ubiquitination [16]. This insight resulted in the design of tyrosine to phenylalanine AAV mutants, which increase transduction efficiency by attenuating proteasome degradation [17, 18]. The utility of the tyrosine mutant vector was recently observed in a NHP model. For example, when a GFP transgene with a modified mGluR6 promoter was packaged in an AAV2 based tyrosine mutant, some transduction was observed in difficult-to-reach bipolar cells in NHP retinas after intravitreal injection [10]. In addition, low level transduction in a small number of foveal cones has been reported with tyrosine mutant AAV2 vector [17–19].

While rational design has led to improvements in AAV retinal transduction, in general rational engineering relies upon detailed mechanistic knowledge of the full gene delivery pathway—from point of administration to arrival in a target nucleus—to enable capsid modifications to overcome critical steps that limit transduc-

tion. Unfortunately, the requisite breadth and depth of knowledge is not available for most tissue and cellular targets in a primate system. As a result, a vector engineering strategy that does not rely on a priori mechanistic knowledge but can instead still lead to advantageous characteristics is required, and fortunately directed evolution is such an approach. Directed evolution is a vector engineering strategy in which large genetic libraries of AAV variants are generated through a variety of methods and selected via a selection pressure, such as successful retinal gene delivery. In this process, multiple iterations of selection lead to a convergence on novel AAV variants that have the selected properties [20]. For example, directed evolution in the mouse retina led to 7m8, a variant of AAV2 with an additional peptide sequence that is capable of pan-retinal expression in the mouse when injected from the vitreous as well as improved expression in the NHP retina including increased expression across the retina and inside the fovea. Multiple studies have shown that 7m8 has increased transduction efficiency compared to tyrosine mutants [10, 21]. Additional engineering in larger animal models offers the promise of further improvement.

An alternate engineering approach involved the generation of hybrid AAV vectors that combined fragments of novel AAV capsid sequences isolated from primates mixed with AAV8. These novel hybrid recombinant vectors were screened, and two were shown to transduce ganglion cells in ex vivo macaque retinal explants. The majority of the transduced ganglion cells were found at the edges of the explant, with limited expression in the center [22]. This supports the idea that the inner limiting membrane acts as a barrier to AAV and that on the edges it was disrupted by the dissection [5].

These examples illustrate the importance of NHP models for evaluating AAV gene delivery in the retina. Despite the immune privilege of tissue in the eye both preexisting and development of immunity post-injection are obstacles to AAV gene delivery.

Dose escalation studies of subretinally delivered AAV showed a dose-related increase in neutralizing antibodies in serum but not in the anterior chamber until high doses (10^{11} viral genomes) were delivered [8]. A biodistribution study of intravitreally delivered AAV2 showed high levels of vector DNA in the injected eye but low levels of vector DNA in the spleen and lymph nodes, as well as other organs [19]. After subretinal vector delivery, DNA has been found in lacrymal and nasal fluids for 3–4 days and in serum for up to 15–20 days [23]. This has been associated with a retinal hemorrhage during subretinal surgery [13].

Evidence in the literature demonstrates that the immune response to the viral capsid following subretinal injection does not impede the readministration of AAV subretinally to the contralateral eye in both NHP studies and human clinical trials [24–26]. Intravitreal injection, on the other hand, led to NABs against the capsid and a humoral immune response that prevented transgene

expression when the viral vector was subsequently delivered intravitreally (but not when administered subretinally) to the contralateral eye. Subretinal injection did not block transgene expression upon readministration in the contralateral eye with either subretinal or intravitreal injection [27]. A study of preexisting immunity to AAV showed that there is both cross-reactivity of NABs against different AAV serotypes and that preexisting NABs against AAV in primate serum samples correlate with weakened or no gene expression following intravitreal injection of AAV in the NHP retina [28]. Therefore, prescreening primates for NABs against AAV is specifically necessary for proper evaluation of intravitreally administered AAV vectors in the retina, both to characterize NABs before and after a subretinal surgery and especially for intravitreal injection. The following method describes a screening protocol for NABs against AAV in NHP serum samples.

The neutralizing antibody assay allows for the detection of NABs in the serum against AAV serotypes that could impede the expression of transgenes delivered by AAV via intravitreal injection. In this assay, serum from multiple NHPs is collected and then serially diluted. An AAV virus carrying a transgene for a fluorescent reporter is incubated with the serially diluted serum. This incubated AAV is then used to infect a cell line in a 96-well plate. The plate is then imaged for GFP expression. If expression of the fluorescent reporter is impeded by highly diluted serum, then it can be determined that there is a high level of NABs present in that animal. Conversely, if GFP expression is not reduced in high levels of serum then the animal has a low level of NABs present and is a suitable candidate for intravitreal injection.

2 Materials

2.1 Serum Processing

1. Primate serum in red top vacutainer.
2. Collection tubes.
3. Ice.
4. Pipet.
5. Cryovials.
6. Benchtop centrifuge with swing-out rotor and carriers.

2.2 Quantification of NAB Titers

1. Greiner CELLSTAR 96-well polystyrene black plate with clear bottom.
2. Greiner CELLSTAR 96-well plate polystyrene plate—clear.
3. HEK 293 Cells ATCC #CRL-1573.
4. Packaged AAV with a fluorescence reporter driven by a ubiquitous promoter.

5. 1.5 mL Eppendorf tubes.

6. Multichannel pipet.

7. Disposable pipetting reservoir.

8. DMEM media.

9. Fetal bovine serum.

10. Dulbecco's phosphate-buffered saline (D-PBS).

11. Hoechst nuclear stain (2′-(4-hydroxyphenyl)-5-(4-methyl-1-piperazinyl)-2,5′-bi-1H-benzimidazole trihydrochloride hydrate).

12. ImageXpress Micro Cellular Imaging and Analysis System.

3 Methods

3.1 Serum Processing

1. A trained professional should perform blood collection with all proper safety measures in place, including an approved animal use protocol, necessary equipment for the animal's safety, and appropriate personal protective equipment. The blood sample is taken from a peripheral vein with blood collected in a red top Vacutainer.

2. Once blood is collected, place tubes upright in a rack and incubate at room temperature for 30 min. Do not exceed 1 h.

3. Centrifuge the blood samples for 15 min at $1000 \times g$ and do not use brakes to stop the centrifuge.

4. Use a pipette to aspirate off the serum and pool in a collection tube. Keep this collection tube on ice (*see* **Note 1**).

5. If not using serum samples immediately, aliquot the serum into cryovials, then freeze and store at −80 °C.

3.2 In Vitro Quantification of NAB Titers

1. Before beginning the procedure, ensure that you have sufficient AAV with the capsid of interest that is packaged with a fluorescent reporter (usually eGFP) driven by a ubiquitous promoter and that has already been titered (*see* **Note 2**).

2. Twenty four hours before the serum incubation, pass HEK 293 cells into a 96-well black plate with clear bottom at a density of 1.5×10^4 cells/well in 100 µl DMEM + 10% FBS (*see* **Note 3**). Incubate the cells for 24 h at 37 °C with 5% CO_2. The following day, cells should be approximately 70–80% confluent.

3. On the day of serum incubation, heat-inactivate FBS by heating at 56 °C for 30 min. Then mix DMEM + 1% heat inactivated FBS media.

4. Dilute serum samples in DMEM + 1% heat inactivated FBS using the following dilutions of primate serum: 1:2, 1:10, 1:25, 1:50, 1:100, 1:250, 1:500, 1:1000, 1:2500, and 1:5000.

Make the dilutions in 1.5 mL Eppendorf tubes (*see* **Notes 4** and **5**). Each dilution should be tested in triplicate for each primate sample using 60 µL per well. Therefore, prepare at least 200 µL of each dilution (180 µL to be used and 20 µL to allow for pipetting error).

5. Transfer each dilution from the Eppendorf tube into the three replicate wells with 60 µL of dilution per well to a sterile 96-well plate (clear).

6. Include controls on the plate. Use 3 wells with virus but without serum for a positive GFP control and 3 wells without virus for a negative GFP control.

7. Make a stock solution of virus that will be incubated with serum. Dilute virus to ~2000 MOI in DMEM + 1% heat inactivated FBS (*see* **Notes 6** and **7**). Make 60 µL per dilution for each well and include overages for pipetting error. For example, testing one primate sample would require 1.8 mL of diluted virus (10 serum dilutions *3 replicates of each dilution *60 µL of diluted virus).

8. Add 60 µL of the virus stock solution to each well of the incubation plate. Each well will now have a total volume of 120 µL.

9. Mix by gently pipetting up and down.

10. Incubate at 37 °C in 5% CO_2 for 1 h.

11. Add 50 µL from each serum–virus mixture to each well of the plated cells in the first 96-well plate that was seeded the day before.

12. Incubate for 48 h at 37 °C with 5% CO_2.

13. Dilute Hoechst nuclear stain 1:4000 in D-PBS.

14. Remove media from each well of 96-well plate and add 100 µL of diluted Hoechst stain to each well.

15. Image the plate using a high content fluorescence imager such as the ImageXpress Micro Cellular Imaging and Analysis System. This will allow for automated reading of the 96-well plate. The accompanying MetaXpress Image Analysis Software (or alternate software such as CellProfiler) can be used to determine the number of transduced cells in each well (*see* **Notes 8** and **9**).

16. Average the results from the three replicates for each dilution. Validate that controls have high expression level, and determine the dilution at which less than 50% of cells have fluorescent expression. This is reported as the neutralizing antibody titer. See Fig. 1 for an example plate image.

Specifically for intravitreally administered AAV vectors, there is a strong effect of preexisting NABs on transgene expression. Neutralization of 50% of GFP expression at dilutions of 1:10 to
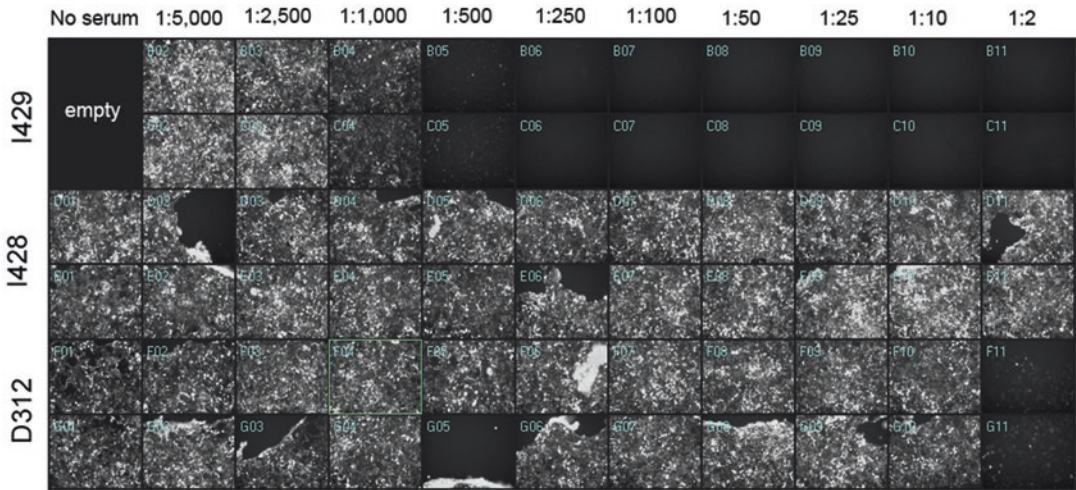
Fig. 1 Example of imaged 96-well plate. Sera from three different animals were serially diluted and infected with AAV2-CMV-GFP. In this example, animal I428 is the best candidate for intravitreal injection of AAV with no loss of GFP expression at the highest serum concentration. The empty boxes indicate a negative control. The green box represents an ideal well for effective imaging

1:50 can negatively affect transgene expression in NHPs, with reports of neutralization at a dilution of 1:10 resulting in zero transgene expression. See Table 1 of reference [28]. It is ideal to only utilize NHPs with no detectable NABs present. In addition, NAB analysis is important for characterizing animals receiving sub-retinal injection, including seroconversion following administration. In summary, this protocol is useful for characterizing the potential for animal neutralization of administered AAV vector, both for intraocular injection and in general.

4   Notes

1. When pipetting serum, be careful not to disturb the cell layer or aspirate any cells. After collecting the serum, hold the tube to the light and look for turbidity. If turbid, repeat the centrifugation and pipet serum to a new tube.

2. For an in-depth guide to AAV vector packaging and purification please refer to this reference [29].

3. The cell count, correct confluency, and consistency in each well are very important. Use a hemocytometer or other method to correctly count the number of cells. Using a multichannel pipet and a disposable pipetting reservoir will also increase accuracy and consistency.

4. Screen multiple NHPs at one time. Each primate sample requires 30 wells to screen for one AAV serotype or variant, so three primate samples can be screened in one plate, including controls. To ensure that a sufficient number of animals are seronegative against AAV, a rough guideline is that three NHPs should be screened to identify one for utilization in the AAV experiment. For example, if an experiment requires three animals then screen at least nine. However, this guideline may vary depending on the animal facility.

5. When transferring the serial dilution, the same pipet tip can be used throughout if pipetting is started with the most dilute sample to the least dilute sample. The carryover from the lower dilution will be negligible, and not changing tips will speed up the process.

6. Virus titer is very important to determine the correct MOI. In addition, the transduction efficiency can differ between serotypes, with different promoters, or between different cell types. If doing the experiment for the first time, consider testing the transduction efficiency of the AAV to be used at multiple MOIs to determine what would be optimal for that particular case.

7. MOI of 2000 is determined as follows: Wells are seeded with 1.5×10^4 cells. Assuming one cell division cycle there are roughly 3×10^4 cells/well after 24 h. Therefore, 6×10^7 viral genomes in 60 μL of DMEM + 1% heat inactivated FBS are needed.

8. If NABs are present at a sufficiently high concentration, then AAV transduction will be inhibited, and there will be a reduction in GFP expression. Determine the lowest serum dilution that leads to less than 50% GFP expression in the well compared to positive control.

9. Cell imaging is one of many methods, and alternatives include flow cytometry or a luciferase assay, with the appropriate transgene payload, to determine the serum dilution which inhibits AAV transduction [13, 30].

Acknowledgments

References

1. Maguire AM, Simonelli F, Pierce EA et al (2008) Safety and efficacy of gene transfer for Leber's congenital amaurosis. N Engl J Med 358:2240–2248

2. Bainbridge JW, Smith AJ, Barker S et al (2008) Effect of gene therapy on visual function in Leber's congenital amaurosis. N Engl J Med 358:2231–2239

3. Simonelli F, Maguire AM, Testa F et al (2010) Gene therapy for Leber's congenital amaurosis is safe and effective through 1.5 years after vector administration. Mol Ther 18:643–650

4. Vandenberghe LH, Bell P, Maguire AM et al (2013) AAV9 targets cone photoreceptors in the nonhuman primate retina. PLoS One 8:e53463

5. Dalkara D, Kolstad KD, Caporale N et al (2009) Inner limiting membrane barriers to AAV-mediated retinal transduction from the vitreous. Mol Ther 17:2096–2102

6. Bennett J, Maguire AM, Cideciyan AV et al (1999) Stable transgene expression in rod photoreceptors after recombinant adeno-associated virus-mediated gene transfer to monkey retina. Proc Natl Acad Sci U S A 96:9920–9925

7. Jacobson SG, Boye SL, Aleman TS et al (2006) Safety in nonhuman primates of ocular AAV2-RPE65, a candidate treatment for blindness in leber congenital amaurosis. Hum Gene Ther 17:845–858

8. Vandenberghe LH, Bell P, Maguire AM et al (2011) Dosage thresholds for AAV2 and AAV8 photoreceptor gene therapy in monkey. Sci Transl Med 3:88ra54

9. Yin L, Greenberg K, Hunter JJ et al (2011) Intravitreal injection of AAV2 transduces macaque inner retina. Invest Ophthalmal Vis Sci 52:2775–2783

10. Lu Q, Ganjawala TH, Ivanova E et al (2016) AAV-mediated transduction and targeting of retinal bipolar cells with improved mGluR6 promoters in rodents and primates. Gene Ther 23:680–689

11. Sengupta A, Chaffiol A, Macé E et al (2016) Red-shifted channelrhodopsin stimulation restores light responses in blind mice, macaque retina, and human retina. EMBO Mol Med 8:1248–1264

12. Lotery AJ, Yang GS, Mullins RF et al (2003) Adeno-associated virus type 5: transduction efficiency and cell-type specificity in the primate retina. Hum Gene Ther 14:1663–1671

13. Boye SE, Alexander JJ, Boye SL et al (2012) The human rhodopsin kinase promoter in an AAV5 vector confers rod- and cone-specific expression in the primate retina. Hum Gene Ther 23:1101–1115

14. Mancuso K, Hauswirth WW, Li Q et al (2009) Gene therapy for red–green colour blindness in adult primates. Nature 461:784–787

15. Bell CL, Vandenberghe LH, Bell P et al (2011) The AAV9 receptor and its modification to improve in vivo lung gene transfer in mice. J Clin Invest 121:2427–2435

16. Zhong L, Li B, Jayandharan G et al (2008) Tyrosine-phosphorylation of AAV2 vectors and its consequences on viral intracellular trafficking and transgene expression. Virology 381:194–202

17. Petrs-Silva H, Dinculescu A, Li Q et al (2009) Novel properties of tyrosine-mutant AAV2 vectors in the mouse retina. Mol Ther 19:293–301

18. Petrs-Silva H, Dinculescu A, Li Q et al (2008) High-efficiency transduction of the mouse retina by tyrosine-mutant AAV serotype vectors. Mol Ther 17:463–471

19. Ye GJ, Budzynski E, Sonnentag P et al (2015) Safety and biodistribution evaluation in cynomolgus macaques of rAAV2tYF-CB-hRS1, a recombinant adeno-associated virus vector expressing retinoschisin. Hum Gene Ther Clin Dev 26:165–176

20. Kotterman MA, Schaffer DV (2014) Engineering adeno-associated viruses for clinical gene therapy. Nat Rev Genet 15:445–451

21. Dalkara D, Byrne LC, Klimczak RR et al (2013) In vivo-directed evolution of a new adeno-associated virus for therapeutic outer retinal gene delivery from the vitreous. Sci Transl Med 5:189ra76

22. Charbel Issa P, De Silva SR, Lipinski DM et al (2013) Assessment of tropism and effectiveness of new primate-derived hybrid recombinant AAV serotypes in the mouse and primate retina. PLoS One 8:e60361

23. Weber M, Rabinowitz J, Provost N et al (2003) Recombinant adeno-associated virus serotype 4 mediates unique and exclusive long-term transduction of retinal pigmented epithelium in rat, dog, and nonhuman primate after subretinal delivery. Mol Ther 7:774–781

24. Amado D, Mingozzi F, Hui D et al (2010) Safety and efficacy of subretinal readministration of a viral vector in large animals to treat congenital blindness. Sci Transl Med 2:21ra16

25. Bennett J, Ashtari M, Wellman J et al (2012) AAV2 gene therapy readministration in three adults with congenital blindness. Sci Transl Med 4:120ra15

26. Bennet J, Wellman J, Marshall KA et al (2016) Safety and durability of effect of contralateral-eye administration of AAV2 gene therapy in patients with childhood-onset blindness caused by RPE65 mutations: a follow-on phase 1 trial. Lancet 388:661–672

27. Li Q, Miller R, Han PY et al (2008) Intraocular route of AAV2 vector administration defines humoral immune response and therapeutic potential. Mol Vis 14:1760–1769

28. Kotterman MA, Yin L, Strazzeri JM et al (2014) Antibody neutralization poses a barrier to intravitreal adeno-associated viral vector gene delivery to non-human primates. Gene Ther 22:116–126

29. Flannery JG, Visel M (2012) Adeno-associated viral vectors for gene therapy of inherited retinal degenerations. Methods Mol Biol 935:351–356

30. Rapti R, Louis-Jeune V, Kohlbrenner E et al (2009) Neutralizing antibodies against AAV serotypes 1, 2, 6, and 9 in sera of commonly usedanimal models. Mol Ther 20:73–83

Chapter 18

Subretinal and Intravitreal Retinal Injections in Monkeys

Daniyar Dauletbekov, K. Ulrich Bartz-Schmidt, and M. Dominik Fischer

Abstract

Ocular anatomy and physiology in cynomolgus monkeys (*Macacca fascicularis*) are very similar to that found in the human visual system. Therefore and despite significant ethical and economical implications, these animals constitute an excellent model system for toxicology and biodistribution studies in the development of new and meaningful treatment strategies for ocular disorders. The methods for delivery of investigational new drugs (INDs) to the ocular tissue are virtually identical to the methods used in clinical practice. This protocol explains in detail the method of applying INDs to the vitreous cavity or the subretinal space in monkeys.

Key words Vitreoretinal surgery, Injection, Retina, Monkeys

1 Introduction

The two classical routes of local intraocular delivery historically include intravitreal and subretinal injections. Intravitreal injection delivers a therapeutic agent inside the vitreal cavity allowing its distribution across the surface of the retina. While the diffusion of the IND can still be limited by several anatomical barriers, such as the vitreous (if no vitrectomy was performed) or the inner limiting membrane, cells of the inner retinal layers can potentially be reached very efficiently. Bioavailability at the level of photoreceptors in the outer retina, at the level of the retinal pigment epithelium (RPE) or the choroidal vasculature, however, depends on numerous factors and might not reach therapeutic levels for some INDs. The first intravitreal injection was reported by Ohm in 1911 who introduced air into the vitreous cavity to treat retinal detachment [1]. The intravitreal administration of pharmaceutical agents was started by using penicillin to treat endophthalmitis [2], and intravitreal drug delivery became a very frequently used technique with the introduction of drugs antagonizing the vascular endothelial growth factor (VEGF) [3, 4].

Subretinal injections release the therapeutic agent into the potential space between the photoreceptors and the RPE, thus

directly targeting these cell populations. The first experimental subretinal injections were reported in the 1970s in cats in order to investigate the subretinal drainage transport [5, 6]. Lately, the subretinal mode of delivery received wide interest with the advent of gene therapy based on adeno-associated viral (AAV) vectors delivering therapeutic DNA into the subretinal space [7]. The success of such vectors became evident in a number of successful clinical trials treating hereditary retinal disorders [8–11]. Although, the subretinal route is considered as more traumatic due to the need to penetrate the retina and induce a temporary retinal detachment, experimental studies on cynomolgus monkeys assessing subretinal injection of balanced salt solution showed complete recovery of the retina [12, 13]. Once basic biomechanic principles are appropriately considered to minimize stress and strain of neuroretinal tissue, subretinal injections can be applied safely in the (pre)clinical setting [14].

As intravitreal and subretinal techniques of injection can vary in different laboratories, a description of a standardized technique of injection in cynomolgus monkeys, which closely mimic human anatomy and physiology, could be useful for a wide audience of researchers.

2 Materials

2.1 Operating Room

For intravitreal injections:

1. Operating table.

2. Light source for transillumination.

   Additional equipment for subretinal injections:

3. Anesthesia machine for general anesthesia and monitoring of vital parameters.

4. Operating microscope.

5. Foot pedal controlled vitrectomy machine (e.g., PentaSys II, Ruck GmbH).

6. Light source for endoillumination.

2.2 Animal and Equipment for Individual Injections

For intravitreal injections:

1. 10% and 1% povidone–iodine solution.

2. Surgical drapes.

3. Lid speculum.

4. Conjunctival forceps.

5. 30G Injection cannula.

6. 1 mL polyacrylamide syringe.

7. Optional: paracentesis blade.

8. Animal: Cynomolgus monkey (*Macacca fascicularis*).

Additional equipment for subretinal injections:

9. Valved trocars for minimal invasive vitreoretinal surgery (MIVS).

10. Endo-illumination and vitrectomy cutter.

11. Wide field (for vitrectomy) and high magnification (for sub-retinal injection) viewing systems (BIOM or contact lenses).

12. 41G extendable cannula (e.g., DORC 1270.EXT).

13. 41G fixed (Luer-Lok) injection cannula.

14. Indenter.

15. Optional: triamcinolone or brilliant blue dye.

2.3 Drugs

1. For intravitreal injection, topical anesthesia with 2% conjucain eye drops.

   For subretinal injections only:

2. For subretinal injection, general anesthesia is the method of choice in monkeys such as with gas (e.g., isoflurane).

3. A long lasting amide agent (e.g., bupivacaine) can be used for (additional) local anesthetic blocking.

4. Methocel: 2% Hydroxypropylmethylcellulose.

5. 125 mg Cefuroxime to be administered to the operated eye.

6. 2 mg Dexamethasone to be administered to the operated eye.

7. Postoperative antibiotic (e.g., 0.5% Moxifloxacine) eye drops.

8. Anti-phlogistic (e.g., 1% Prednisolone) eye drops.

9. BSS Plus sterile irrigation solution (e.g., Alcon).

3 Methods

*3.1 Preparing
the Animal*

To achieve best results it is important to fully dilate the pupils of the animal and to ensure deep anesthesia with as little body movement due to heart beat and respiratory excursions as possible. Once the animal is anesthetized, care has to be taken to prevent cornea exposure/edema.

1. Anesthetize the animal.

2. Put the animal onto the operating table and bring the animal into stable supine position and head in comfortable reach of the surgeon.

3. Scrub eyelids and peri-ocular tissue with 10% povidone–iodine solution.

4. Apply 1% povidone–iodine solution to flush out the conjunctival fornices.

5. Place a sterile drape over the head of the animal and around the eye.

6. Place methocel onto the corneal epithelium to negate the refractive power of the air corneal interface and reduce the risk of corneal dehydration.

7. Position the anesthetized animal under operating microscope with the eye to be injected under view. Operating microscope is used later for coaxial visualization of the target tissue. For subretinal surgery, a binocular indirect ophthalmomicroscope (BIOM) or contact lens systems (Landers for wide field and Kilp for high magnification) can both be used together with a stereoscopic diagonal inverter and an optional videorecording device.

3.2 Intravitreal Injection

1. For intravitreal injection, apply topical anesthesia with 2% conjucain eye drops.

2. Using light source apply transillumination to confirm ciliary band and pars plana.

3. Penetrate the sclera at the pars plana in the superotemporal quadrant using the 30G cannula attached to the 1 mL polyacrylamide syringe and inject slowly without approximating the lens.

4. If volumes of >50 μL (0.05 mL) are injected, check pulsation of the central retinal artery and or measure intraocular pressure (IOP).

5. Optional: perform anterior chamber tap with a sharp blade for paracentesis to reduce IOP if necessary.

3.3 Subretinal Injection

1. Connect the animal to the anesthesia machine for general anesthesia and monitoring of vital parameters.

2. For (additional) local anesthetic blocking, a long lasting amide agent can be used (e.g., bupivacaine).

3. Clamp the temporal canthus to achieve hemostasis for 60 s.

4. Use sharp scissors to perform temporal canthotomy.

5. Place lid speculum.

6. Using light source apply transillumination to confirm ciliary band and pars plana.

7. Using conjunctival forceps to immobilize the conjunctiva, place valved trocar for infusion line in the temporal inferior quadrant and double-check location of trocar to rule out infusion into the suprachoroidal space (*see* **Note 1**).

8. Ensure full tonization of the globe and continue with placing the second and third trocar in the pars plana of the superior temporal and superior-nasal quadrant respectively (*see* **Note 2**).

9. Under wide field viewing, perform core vitrectomy using foot pedal controlled vitrectomy machine and induce posterior hyaloid detachment.

10. Complete vitrectomy as much as possible, using indenter when needed without compromising the lens.
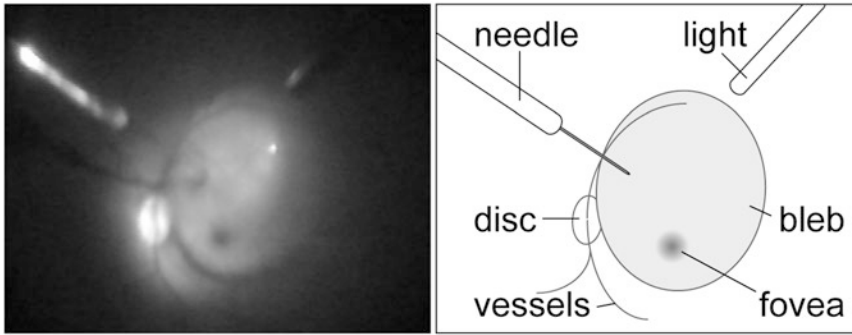
Fig. 1 Frame from a videorecording during subretinal injection in cynomolgus monkey. Left panel shows the frame with a 41 G needle penetrating the retina just central of the superior arcade and about one disc diameter away from the superotemporal disc margin. This placement of the retinotomy usually results in a central placement of the bleb including the fovea. Right panel reflects the same situation as illustration

11. Triamcinolon or brilliant blue dye may be used to visualise vitreous or posterior hyaloid membrane where appropriate.

12. Switch to high magnification viewing system and induce localized retinal detachment in the target area by subretinal injection of BSS Plus using the 41G extendable cannula (e.g., DORC 1270.EXT) attached to a 1 mL polyacrylamide syringe (Fig. 1) (*see* **Notes 3** and **4**).

13. Switch to use the 41G fixed cannula (Luer-Lok) attached to a 1 mL polyacrylamide syringe and inject a preloaded and defined volume of the IND into the preformed bleb.

14. Once the IND has been placed successfully, carefully check the periphery for retinal breaks using the indenter before removing instruments and trocars.

15. Before recovery, subconjunctival 125 mg cefuroxime and 2 mg dexamethasone can be administered to the operated eye.

16. Postoperative prophylactic treatment consists of antibiotic (e.g., 0.5% Moxifloxacine), and antiphlogistic (e.g., 1% Prednisolone) eye drops given *ter in die* (tid) each in the treated eye for 2 weeks.

17. Leave sclerotomies and canthotomy to heal without stitches (*see* **Note 5**).

4 Notes

1. The sclera is tougher to penetrate than in other species (e.g., *Homo sapiens*), necessitating a greater force vector. Extra care has to be taken to maintain the intended angle and rotational position of the trocar and eye ball and not to injure adjacent structures such as the lens.

2. Tonization of the globe is of paramount importance during the subsequent trocar placement for the same reasons as above.

3. Highest injection force is needed during the initial phase of bleb induction, while the counteracting adhesive force between RPE and neuroretina falls off exponentially with increasing bleb size [7]. In order to minimize secondary changes (e.g., shearing off RPE cells from Bruch's membrane), use as little injection pressure as possible and quickly reduce pressure once a bleb starts to rise.

4. Subretinal delivery is often used in studies of gene therapy using viral vectors. A recent study showed that the addition of surfactant 0.001% Pluronic F-68 (PF-68) in the vector solution significantly reduced the vector genome loss in the injection system by about 50% [13]. Considering such a significant loss of viral genomes, the use of PF-68 could be considered when viral particles are injected.

5. Stitches induce further foreign body sensation and lead to extensive digito-ocular manipulation by the animals followed by increased risk of hypotony and infection.

References

1. Ohm J (1911) Über Die Behandlung Der Netzhautablösung Durch Operative Entleerung Der Subretinalen Flüssigkeit Und Einspritzung von Luft in Den Glaskörper. Albrecht Von Graefes Arch Ophthalmol 79:442–450

2. Feigenbaum A, Kornbluth W (1945) Intravitreal injection of penicillin in a case of incipient abscess of the vitreous following extracapsular cataract extraction; perfect cure. Ophthalmologica 110:300–305. http://www.ncbi.nlm.nih.gov/pubmed/21024385

3. Moreno SF, Paloma JB (2008) Therapeutic anti-VEGF in age-related macular degeneration: ranibizumab and bevacizumab controversy. Br J Ophthalmol 92:866–867. http://www.ncbi.nlm.nih.gov/pubmed/18523097

4. Rosenfeld PJ, Brown DM, Jeffrey SH et al (2006) Ranibizumab for neovascular age-related macular degeneration. New Engl J Med 355:1419–1431. https://doi.org/10.1056/NEJMoa054481

5. Stürm R, Rokos L (1975) Influence of occlusion of retinal vessels on the transport of 22Na and 131J-Iodo-O-Hippurate out of the subretinal space (experiments performed on cats) (author's transl). Albrecht Von Graefes Arch Klin Exp Ophthalmol 197:119–127. http://www.ncbi.nlm.nih.gov/pubmed/1082262

6. Gloor BP, Rokos L, Leuenberger R (1975) Transport of 131J-Iodo-O-Hippurate and 22Na out of the retroretinal space in experimental non rhegmatogenous detachment of the retina (Author's Transl). Albrecht Von Graefes Arch Klin Exp Ophthalmol 197:107–117. http://www.ncbi.nlm.nih.gov/pubmed/1082261

7. Liang FQ, Anand V, Maguire AM et al (2001) Intraocular delivery of recombinant virus. Methods Mol Med 47:125–139. https://doi.org/10.1385/1-59259-085-3:125

8. Bainbridge JW, Alexander J, Smith AJ, Susie S, Barker SS et al (2008) Effect of gene therapy on visual function in leber's congenital amaurosis. N Engl J Med 358:2231–2239. https://doi.org/10.1056/NEJMoa0802268

9. Hauswirth WW, Aleman TS, Kaushal S et al (2008) Treatment of leber congenital amaurosis due to RPE65 mutations by ocular subretinal injection of adeno-associated virus gene vector:

short-term results of a phase I trial. Hum Gene Ther 19:979–990. https://doi.org/10.1089/hum.2008.107

10. Maguire AM, Francesca Simonelli F, Eric A, Pierce EA et al (2008) Safety and efficacy of gene transfer for leber's congenital amaurosis. New Engl J Med 358:2240–2248. https://doi.org/10.1056/NEJMoa0802315

11. MacLaren RE, Groppe M, Barnard AR et al (2014) Retinal gene therapy in patients with choroideremia: initial findings from a phase 1/2 clinical trial. Lancet 383:1129–1137. https://doi.org/10.1016/S0140-6736(13)62117-0

12. Nork TM, Murphy CJ, Kim CB et al (2012) Functional and anatomic consequences of subretinal dosing in the cynomolgus macaque. Arch Ophthalmol 130:65–75. https://doi.org/10.1001/archophthalmol.2011.295

13. Invest Ophthalmol Vis Sci. 2017 Aug 1;58(10):4155–4160. doi: 10.1167/iovs.17-22402

14. Fischer MD, Hickey DG, Singh MS et al (2016) Evaluation of an optimized injection system for retinal gene therapy in human patients. Hum Gene Ther 27:150–158. https://doi.org/10.1089/hgtb.2016.086

Part III

Clinical Protocols and Retinal Gene Therapy Vector Testing on Human Retina

Chapter 19

Production of iPS-Derived Human Retinal Organoids for Use in Transgene Expression Assays

Peter M. Quinn, Thilo M. Buck, Charlotte Ohonin, Harald M.M. Mikkers, and Jan Wijnholds

Abstract

In vitro retinal organoid modeling from human pluripotent stem cells is becoming more common place in many ophthalmic laboratories worldwide. These organoids mimic human retinogenesis through formation of organized layered retinal structures that display markers for typical retinal cell types. Pivotally these humanized retinal models provide a stepping stone to the clinic as therapeutic tools and are expected to provide a promising alternative to current animal models. Thus pluripotent stem cell based healthy as well as diseased human retinal organoids are attractive for use in drug potency assays and gene augmentation therapeutics. Here we outline an established protocol for generation of these retinal organoids and how they can be used in conjunction with adeno-associated virus vectors for transgene expression assays.

Key words Retinal organoids, human Induced Pluripotent Stem Cells (hiPSCs), Adeno-Associated Virus (AAV), Potency assays

1 Introduction

Human retinal organoids are one of the plethora of organotypic in vitro models, which faithfully capture, at least in part in vivo development of the endocrine, digestive, respiratory, nervous, and sensory systems of the human body and as such are amenable to be studied in a diseased context also [1, 2]. The mammalian retina initiates from the eye field at the anterior neural plate forming optic sulci, which further develop into optic vesicles as envaginates of the diencephalon moving out to the surface ectoderm. The optic vesicles then fold into themselves, becoming optic cups. With the outer sheet developing further into the retinal pigment epithelium (RPE) and the inner sheet continuing to develop into a multilayered neural retina [3]. Human retinal organoids were first produced using human embryonic stem cells (ESCs) and subsequently using human induced pluripotent stem cells (hiPSCs).

Both pluripotent stem cells showed faithful recapitulation of human retinogenesis [4, 5]. These pluripotent stem cells form aggregates, which are called embryoid bodies (EBs), that mimic gastrulation like processes and thus have the potential to form all three germ layers [6]. Subsequently the cells within these EBs are further directed into a neural and then retinal specific fate. Very similar to the development of a human eye the EBs progress from an early eye field state, through to optic vesicles and subsequently multilayered optic cups with attached RPE [4, 5]. These iPSC models have a tremendous promise as they allow infinite access to previously limited or inaccessible eye material. iPSC-based eye models can be exploited to study basic eye development, provide a potential source of tissue genotype specific material for cell transplantation purposes, are a substitute to animal models, and are ideal for transgene and biological expression assays of drug targets and gene augmentation vectors. For example RPE differentiated from hiPSCs derived from a choroideremia patient with a defect in Rab escort protein 1 (REP1) was transduced with a AAV2/5-CAG-CHM vector which restored the REP1 defective RPE to a normal cellular phenotype [7].

Retinal gene therapies are using adeno-associated virus (AAV) as a delivery vector for clinical trials targeted to *RPE65*, *CNGA3*, and *REP1* genes aimed at treating Leber congenital amaurosis 2 (LCA2), achromatopsia, and choroideremia, respectively [8–10]. Development of these gene therapies have given insights into required therapeutic dosage and dose limiting toxicity in the retina. However further testing of different AAV serotypes and promoter combinations is pivotal to improve cell targeting, transduction and coverage which in turn will reduce toxic factors and promote long term efficacy [11, 12]. Diseases such as retinitis pigmentosa 12 (RP12) and LCA8 caused by mutations in the Crumbs homolog 1 (CRB1) gene may require gene augmentation in multiple cell types adding an extra layer of complexity to therapeutic development [13–15]. With maintenance of the Crumbs proteins in the adjacent photoreceptors and Müller glia cells required for a functional retina [15]. However the localization of these proteins between the mouse and human is reversed [15–17]. Thus using humanized healthy and diseased retinal organoid models to test transgene expression is a critical addition to the therapeutic pipeline bridging proof of concept work done in mice toward clinical application by removing potential interspecies differences [12].

In this chapter we describe the basic protocols for the maintenance, passaging, and long-term storage of hiPSCs; the formation of EBs from hiPSCs and subsequently their differentiation to retinal organoids. Further, we show how these hiPSC-derived retinal organoids can be used in potency assays for testing transgene expression upon AAV vector infection.

2 Materials

2.1 Solutions and Media

1. Matrigel.

2. mTeSR (StemCell Technologies).

3. Gentle Cell Dissociation Reagent (StemCell Technologies).

4. mFreSR (StemCell Technologies).

5. DMEM/F12: DMEM/F12 containing L-glutamine, Sodium Pyruvate, Phenol Red and without HEPES.

6. DMEM A: DMEM containing High Glucose, No Phenol Red, without Sodium Pyruvate and with HEPES.

7. DMEM B: DMEM containing High Glucose, Sodium Pyruvate, GlutaMAX, Phenol Red and without HEPES.

8. mTeSR/blebbistatin: 2 mL mTeSR supplemented with 0.4 μL blebbistatin. Final concentration of 10 μM, use freshly prepared. Prepare a 50 mM ± blebbistatin (Abcam) stock in DMSO. Store up to 1 month at −20 °C.

9. Neural Induction Medium 1 (NIM-1): 48.95 mL DMEM/F12 supplemented with 0.5 mL 100× N2 supplement, 0.5 mL 100× Minimum Essential Media-Non Essential Amino Acids (MEM NEAAs), 10 μL 10 mg/mL Heparin (Sigma). Combine, mix gently and sterile filter (0.22 μm). Store for 2 weeks at 4 °C.

10. mTeSR/NIM-1(3:1): Three volumes of mTeSR mixed with one volume of NIM-1.

11. mTeSR/NIM-1(1:1): Mix equal volumes of mTeSR with NIM-1.

12. DMEM/F12 A (3:1): Mix equal volumes of DMEM A with DMEM/F12.

13. DMEM/F12 B (3:1): Mix equal volumes of DMEM B with DMEM/F12.

14. Neuronal Induction Medium 2 (NIM-2): 96 mL DMEM/F12 A (3:1) supplemented with 2 mL 50× B27 Supplement (without Vitamin A), 12.5 μL 100× Sodium Pyruvate, 1 mL 100× NEAA, 1 mL 100× antibiotic–antimycotic (10,000 units/mL of penicillin, 10,000 μg/mL of streptomycin, 25 μg/mL of Amphotericin B). Combine, mix gently and sterile filter (0.22 μm). Store for 2 weeks at 4°C.

15. Retinal Lamination Medium (RLM): 107.25 mL DMEM/F12 B (3:1) supplemented with 12.5 mL embryonic stem cell-qualified FBS, 2.5 mL 50× B27 Supplement (without Vitamin A), 1.25 mL 100× MEM NEAAs, 1.25 mL 100× antibiotic–antimycotic (10,000 units/mL of penicillin, 10,000 μg/mL of streptomycin, 25 μg/mL of Amphotericin B), 0.25 mL taurine

(100 μM final concentration). Prepare from a 50 mM stock of taurine, store stock at 4°C for 6 months. Combine and sterile filter (0.22 μm). Store RLM for 2 weeks at 4 °C.

16. Retinal Lamination Medium 1 (RLM-1): RLM supplemented with 0.1 μL 10 mM retinoic acid (1 μM final concentration) per mL. Prepare from a stock 10 mM all-trans retinoic acid in DMSO, store at -20°C for 1 year. Make RLM-1 fresh each time.

17. Retinal Lamination Medium 2 (RLM-2): RLM supplemented with 0.05 μL 10 mM retinoic acid (0.5 μM final concentration) per mL. Prepare from a stock 10 mM all-trans retinoic acid in DMSO, store at −20 °C for 1 year. Make RLM-2 fresh each time.

18. Phosphate buffered saline (PBS): 2.6 mM KH_2PO_4, 26 mM Na_2HPO_4, 145 mM NaCl, pH 7.2.

19. 4% Paraformaldehyde (PFA): 4% PFA in PBS.

20. 5% Sucrose: 5% sucrose in PBS.

21. 30% Sucrose: 30% sucrose in PBS.

22. Cryo-embedding media, Tissue-Tek® O.C.T. compound.

23. 1% sodium dodecyl sulfate (SDS).

24. Autoclave bags.

25. 0.001% Poloxamer-188 in PBS.

26. Agarose-coated plates: Add 1 g of agarose to 100 mL ultrapure water and heat in the microwave to dissolve. Autoclave to sterilize. Add enough hot 1% agarose to wells so it covers also the sides. Immediately aspirate the agarose with the same serological pipette, leaving a thin film coating base and partially side walls of the well. Close lid and wait a few minutes.

2.2 Materials and Supplies

1. hiPSCs.

2. Serological pipettes.

3. 6-well culture plates.

4. 24-well culture plates.

5. 96-well culture plates.

6. Parafilm.

7. Cell scraper.

8. Cryovials.

9. CoolCell container with a reproducible freezing rate of −1 °C per hour.

10. 15 mL conical tubes.

11. 27 G Needle.

12. P10, P200, and P1000 pipette tips.

13. Molecular grade agarose.

14. $10 \times 10 \times 5$ mm Cryomold® biopsy, square.

15. 9 cm Petridish.

16. Dry ice.

17. Inverted light and phase contrast microscope.

18. Protective equipment when dealing with viral vector: gloves, safety goggles, lab coat, Biosafety level 2 laboratory, and laminar flow hood.

2.3 Viral Vector

1. AAV2/5 CMVmin-*GFP* (*see* **Note 1**).

3 Methods

3.1 Culturing of Human Induced Pluripotent Stem Cells

3.1.1 Matrigel Coating Cultureware

1. Defrost an aliquot of Matrigel on ice.

2. Dilute the aliquot in 25 mL of DMEM/F12. Check the recommended dilution factor of the aliquot.

3. Use a precooled pipet tip and add 1 mL of diluted Matrigel to each well of a 6-well plate and swirl for even coating (*see* **Note 2**).

4. Incubate at room temperature for at least 1 h before use.

5. If not used immediately, store Parafilm-sealed culture ware at 4 °C for up to 3 months (*see* **Note 3**).

6. Before using plates they should be at room temperature and excess Matrigel should be removed just before seeding with cells.

3.1.2 Thawing Cryopreserved Cells (see Notes 4 and 5).

1. Defrost the cells quickly in a 37 °C water bath with occasional gentle agitation.

2. Add 1 mL of mTeSR slowly to the thawed contents and transfer to a 15 mL conical tube.

3. Add a further 8 mL of warm mTeSR slowly to the side of the 15 mL conical tube with intermittent agitation.

4. Wait 3–5 min for aggregates to sink, or centrifuge cells at 100 x *g* for 2 minutes at RT.

5. Aspirate as much medium as possible without disturbing the pellet and carefully reconstitute in mTeSR (*see* **Note 6**).

6. Plate 2 mL into one Matrigel coated well of a 6-well plate.

7. In the incubator distribute the aggregates by agitation of plate front to back and side to side several times, and incubate at 37 °C with 5% CO_2 (*see* **Note 7**).

8. Leave undisturbed and do not change medium the day after passaging.

9. From day 2 onward, remove the differentiated areas if required and daily feed with 2 mL mTeSR (*see* **Note 9**).

10. Passage the undifferentiated cells (phase bright centers) 5–10 days after thawing. The passaging is dependent on cell survival and initial plating density (*see* **Note 10**).

3.1.3 Passaging of Undifferentiated Cells

1. Have both Matrigel coated 6-well plates and mTeSR medium warmed to room temperature (*see* **Note 4)**.

2. Passage the undifferentiated cells when they have phase bright centers. Remove differentiated parts by scraping with a pipette tip under an inverted light microscope (*see* **Notes 8–10**).

3. Aspirate medium of each well and add 1 mL of Gentle Cell Dissociation Reagent (stored at RT), incubate 4–8 min at RT (dependent on cell line). When gaps at colony borders start to appear the incubation should be stopped.

4. Aspirate and add 1 mL of mTeSR medium and gently detach the colonies by scraping with a cell scraper and pipette into a 15 mL conical tube.

5. Rinse the wells with an additional 1 mL of mTeSR to collect any remaining aggregates and let them settle in the 15 mL conical flask (*see* **Note 5**).

6. Carefully pipette 2–3 times with a P1000 pipette tip to break up aggregates so they are more uniform in size and transfer to coated wells at the desired density, typically about 1:10 to 1:40.

7. In the incubator distribute the aggregates by agitation of plate front to back and side to side (*see* **Note 7**).

8. Do not change medium the day after passaging.

3.1.4 Cryopreserving Cells

1. Cryopreservation should take place when hiPSC colonies are ready for passaging (*see* **Note 9**) and taken up to **step 5** of Subheading 3.1.3.

2. Thaw the required amount of mFreSR (1 mL per well) and keep on ice.

3. Centrifuge the sunken aggregates in the 15 mL conical tube at $300 \times g$ for 5 min at RT.

4. Aspirate as much medium as possible without disturbing the pellet and carefully reconstitute in 1 mL of cold mFreSR per well using a serological pipette (*see* **Note 5**).

5. Transfer 1 mL of cell aggregates (1 well) mixture into labeled cryovials using a 2 mL serological pipette.

6. Freeze cell aggregates by placing the cryovials in a CoolCell container that is put thereafter into a −80 °C freezer. Store the cryovials long-term in liquid nitrogen.

3.2 Differentiation of Human Induced Pluripotent Stem Cells

1. At the start of the differentiation, referred to as differentiation day 0 (DD0), remove the medium from the small aggregates of hiPSCs (from **step 5** of Subheading 3.1.3).

3.2.1 Embryoid Body Generation

2. Carefully pipette 2–3 times with a P1000 pipette tip to break up aggregates so they are more uniform in size and transfer to a 15 mL conical tube to sink. Remove medium.

3. Add 2 mL of mTeSR/blebbistatin medium and incubate o.n in 1 well of an agarose coated 6-well plate (*see* **Note 11**).

4. Transfer aggregates to a 15 mL conical tube, let them sink. Remove the medium, add 2 mL mTeSR/NIM-1(3:1) and incubate o.n. in 1 well of an agarose coated 6-well plate.

5. Transfer aggregates to a 15 mL conical tube, let them sink. Remove the medium, add 2 mL mTeSR/NIM-1(1:1) and incubate o.n in 1 well of an agarose coated 6-well plate.

6. Transfer aggregates to a 15 mL conical tube, let them sink. Remove the medium, add 2 mL NIM-1 and incubate o.n in 1 well of an agarose coated 6-well plate.

7. Change medium every other day till DD7 (*see* Fig. 1).

3.2.2 Embryoid Body Plating (See Note 12)

1. EBs are collected in a 15 mL conical tube and left 5 min to sink and aspirate medium.

2. Add 2 mL of NIM-1 per well to Matrigel-coated 6-well plates.

3. Aspirate excess medium from the EBs and resuspend in fresh NIM-1.

4. Plate approximately at a density of 20 aggregates per cm^2.

5. Plates should be then placed in an incubator and EBs evenly distributed by agitation of plates front to back and side to side and change medium every other day.

6. Change to NIM-2 at DD16 and incubate at 5% CO_2 at 37 °C.

7. Medium should be changed every day until DD28 at which point neural epithelial cell fate has been acquired and the neural rosette structures can be excised (*see* Fig. 1). The neural rosettes are ready to be dislodged to allow them to mature in floating culture and develop into optic vesicles. They will already be growing as partially attached 3-dimensional structures with an outgrowth of flat cells attached to the Matrigel.
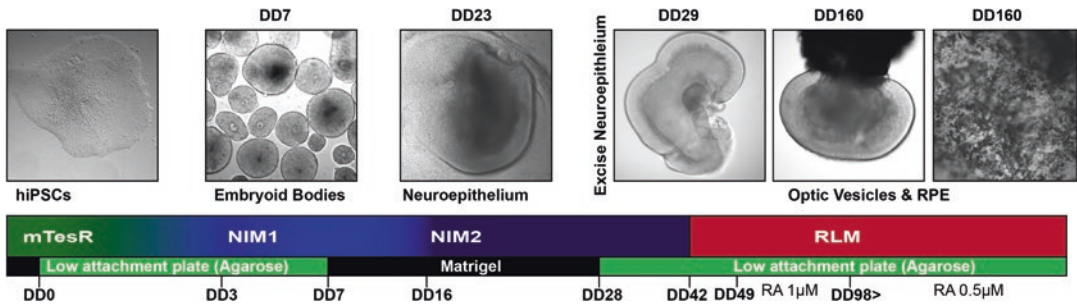
Fig. 1 Timeline of retinal differentiation. hiPSCs are directed to form embryoid bodies through the addition of blebbistatin and a transition from mTeSR to neural induction medium 1 (NIM-1). At differentiation day (DD)7 these embryoid bodies are plated and attached to Matrigel where they differentiate toward a neuroepithelium fate. At DD16 the medium is switched from NIM-1 to NIM-2. Subsequently these neuroepithelia can be excised and sorted into those of a retinal organoid fate and are maintained in a low attachment environment with agarose-coated wells. At DD42 retinal lamination medium (RLM) is used to aid in the lamination of the optic vesicles, and the addition of retinoic acid at DD49 helps to promote photoreceptor maturation. Attached RPE is also visibly present

3.2.3 Optic Vesicle Generation

1. Use a pipet with P1000 tip as a high-pressure medium gun to flush loose at their base the neural rosettes for their dislodgment. As an alternative, use a needle point and cut the neural rosettes away from the plate's surface. The outgrowth of flat cells remains attached to the Matrigel and will be discarded. This is how the borders for excision can be identified.

2. Collect the floating neural rosettes into a 15 mL conical tube using a 5 mL serological pipette and allow them to sink over a 1–3 min period.

3. Aspirate the remaining medium, resuspend in 2 mL NIM-2 medium per well of agarose coated 6-well plate (*see* **Note 11**) and incubate o.n. at 5% CO_2 at 37 °C.

4. From excision onward, Optic Vesicles should be maintained in agarose coated wells (*see* Fig. 1).

3.3 Sorting, Maturation and Maintenance of hiPSC Derived Retinal Organoids

1. Under an inverted light microscope, manually remove with a truncated P200 pipet tip the forebrain organoids from the 96-well at DD33 (*see* **Notes 8** and **13**). Discard if not needed.

2. Transfer the retinal organoids and medium with a truncated P200 pipet tip to a 15 mL conical tube and allow them to sink over a 1–3 min period.

3. Aspirate the medium, resuspend the retinal organoids in 4 mL NIM-2 medium and transfer 2 mL in each of two fresh agarose-coated 6-well plates (*see* **Note 14**).

4. Check daily, change NIM-2 medium twice per week or earlier in case that the medium starts to turn yellow until DD41.

5. Switch to RLM medium between DD42 and DD48.

6. Switch to RLM-1 between DD49 and DD97 (*see* **Note 15**).

7. From DD98 use retinal lamination medium 2 (RLM-2) for long term culturing instead of RLM-1 (*see* Fig. 1).

3.4 AAV Infection of hiPSC Derived Retinal Organoids

3.4.1 Preparation of the Virus (See Note 16)

1. Centrifuge the concentrated virus suspension shortly and store on ice.

2. Prime the pipette tip in 0.001% Poloxamer-188 before pipetting the viruses.

3. Add the AAV2/5-CMVmin-*GFP* to 50 μL of RLM-2 (medium used dependent on time point chosen for infection) with a final concentration of 1.75×10^{10} genome copies (*see* **Note 17**).

3.4.2 AAV Infection of Retinal Organoids

1. Take two retinal organoids from the cultured stock of organoids and transfer to one agarose-coated well of a 96-well plate.

2. Remove excess medium.

3. Add the 50 μL of RLM-2 (medium used dependent on time point chosen for infection) containing the AAV2/5-CMVmin-*GFP* to the well containing the two retinal organoids (*see* **Note 18**).

4. Incubate for 24 h at 5% CO_2 at 37 °C.

5. Add 50 μL of RLM-2 (medium used dependent on time point chosen for infection) to the 96-well with viral vector particles.

6. Incubate for 24 h at 5% CO_2 at 37 °C.

7. Transfer organoids to a 15 mL conical tube, let them sink, and remove medium. Wash three times in 1 mL PBS and resuspend in 2 mL of RLM-2 (medium used dependent on time point chosen for infection).

8. Transfer the retinal organoids to one well of a 24-well agarose-coated plate.

9. Change the medium twice a week for maintenance (*see* **Note 19**). In our example we infected DD160 retinal organoids and analyzed GFP expression 11 days later at DD171 (*see* Fig. 2). The hiPSC derived retinal organoids are then ready for further tissue processing and analysis (*see* **Note 20**).

3.5 Tissue Processing of hiPSC Derived Retinal Organoids

Tissue processing of hiPSC derived retinal organoids requires some care due to the greater fragility of this tissue and is similar to dealing with excised retinal material from mice. Special care must be taken when processing the tissue for freezing particularly limiting water content, which leads to water crystallization and tissue artifacts.

1. Place a preferred number of retinal organoids in a 15 mL tube and let them sink and remove access medium.
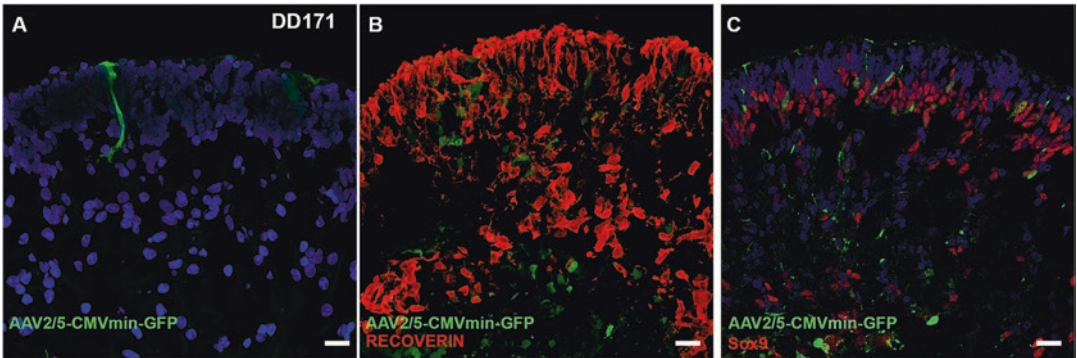
Fig. 2 AAV infected hiPSC-derived retinal organoids. Retinal organoids 10 days after infection (DD171) with AAV2/5-CMV-*GFP* (**a**). GFP staining AAV2/5-CMV-*GFP* expression does not overlap with recoverin staining (**b**) but does overlap Sox9 (**c**) staining. Scale bar: 20 μm

2. Wash the retinal organoids shortly in PBS.

3. Fixation: Add 500 μL of 4% PFA for 30 min at room temperature.

4. Wash the retinal organoids shortly in PBS and aspirate.

5. For sucrose embedding, incubate the retinal organoids in 5% sucrose for 30 min and aspirate.

6. Incubate the retinal organoids in 30% sucrose for approximately 30 min (until the retinal organoids have sunk).

7. In a petri dish place a blob of cryo-embedding media and transfer the retinal organoids on top using a truncated P1000 pipette (in as minimal amount of solution as possible).

8. Gently mix by swirling the retinal organoids into the cryo-embedding media with a pipette tip. Thus removing all excess of sucrose solution.

9. The retinal organoids can then be placed into a cryomold containing fresh cryo- embedding media and freeze it over dry ice.

10. Store at −80 °C until ready for sectioning on a cryotome cryostat (7–10 μm).

4   Notes

1. AAV2/5-CMVmin-*GFP*-WPRE-pA viral particles contain: Two inverted terminal repeats (ITRs) each of 145 bp of adeno-associated virus 2 (AAV2), a 0.26 kb minimal cytomegalovirus (CMV) promoter, the cDNA for green fluorescent protein (*eGFP*), a WPRE element for woodchuck hepatitis posttranscriptional regulatory element (WPRE), and a polyadenylation (pA) sequence of SV40 virus. The *GFP* expression vector is packaged in AAV serotype 5 particles [15].

2. Pipet tips can be cooled by pipetting up and down in ice-cold DMEM/F12 prior to pipetting Matrigel.

3. Do not use wells if the Matrigel coating is uneven or if the diluted solution evaporates from sealed or warmed-up plates before they are used.

4. Have mTeSR and precoated Matrigel plates warmed to room temperature (Approx. 1 h) before starting any protocol. Alternatively plates can be placed in the incubator to warm up for 15 min. Do not warm mTeSR in a 37 °C water bath.

5. Avoid breaking up the cell aggregates into very small pieces during thawing, transfer, plating and cryopreservation steps as this will minimize the start-up efficiency. Ideally use a serological pipette with larger bore size (2 or 5 mL).

6. Addition of a Rock Inhibitor (e.g., Y-27632 or Fasudil) enhances survival of thawed pluripotent stem cells, particular if cell aggregates are not maintained [18, 19]. The content of one cryo tube should be diluted according to the desired density.

7. Uneven distribution of aggregates may result in increased differentiation of iPSCs.

8. Keep plates with organoids or iPSCs less than 15 min outside the incubator to keep the pH and temperature of the medium in an acceptable range.

9. Remove differentiated areas by scraping with a pipette tip. This should be done after the initial 24 h after plating and before passaging. Apply a fluid scraping motion, long strokes as opposed to small scratching motions.

10. Cells are ready to be passaged if a colony has a phase bright center and takes up the field of view (binocular) using a 10× objective of the microscope.

11. Low attachment plates can be created by thinly agarose-coating of wells and will help increase final yield. Do not use unevenly coated agarose wells, replace agarose culture regularly. If agarose "lifts," medium can be seen underneath, then move the retinal organoids into a new well.

12. Avoid excessive and too forceful pipetting of EBs and retinal organoids at all stages. This leads to cell damage and may affect the outcome of the experiment.

13. Retinal and forebrain organoids exhibit distinct morphological characteristics. Those that have a horseshoe type appearance are retinal organoids as opposed to those with a homogenous uniform look throughout, which are forebrain organoids.

14. At this stage a number of aggregates can be kept together in 6-well plates. Aggregate number can be adjusted so that the NIM-2 medium does not turn yellow within 3–4 days.

15. The original protocol [4] recommends to switch to RLM-1 (containing 1 μM of retinoic acid) at DD70 which promotes rod development by repressing cone-specific gene expression. The original protocol [4] uses at DD98 RLM-2 containing N2-supplement instead of B27 supplement. The method that we describe here produces cone but not rod photoreceptors.

16. Take care of the viral trash. Dispose tips contaminated with AAV in 1% SDS. Transfer infected retinas to a fresh 24-well plate before starting the cryopreservation steps. And dispose the plate in an autoclavable bag sprayed with 1% SDS. AAVs can survive on plastics for weeks [20].

17. Pipetting AAV virus can be improved if the AAV is stored in 0.001% poloxamer-188 in PBS and the pipette tip is first equilibrated in 0.001% poloxamer-188 (Pluronics) in PBS.

18. Use less than 10 μL virus in PBS in the 50 μL viral mix not to change the RLM concentration too much which can lead to tissue degradation.

19. Depending on AAV capsid used it takes days or weeks before maximum levels of expression is reached. Optimal expression levels must be determined dependent on AAV capsid used. The GFP onset in organoids can be monitored by live-cell imaging.

20. In case that direct GFP fluorescence is low, you can boost the GFP signal by performing immunohistochemistry using a primary antibody against GFP and a fluorescent dye-labeled secondary antibody.

Acknowledgment

References

1. Clevers H (2016) Modeling development and disease with organoids. Cell 165:1586–1597

2. Lancaster MA, Knoblich JA (2014) Organogenesis in a dish: modeling development and disease using organoid technologies. Science 345:1247125

3. Heavner W, Pevny L (2012) Eye development and retinogenesis. Cold Spring Harb Perspect Biol 4(12):a008391. https://doi.org/10.1101/cshperspect.a008391.

4. Zhong X, Gutierrez C, Xue T et al (2014) Generation of three-dimensional retinal tissue

with functional photoreceptors from human iPSCs. Nature Comm 5:4047

5. Nakano T, Ando S, Takata N et al (2012) Self-formation of optic cups and storable stratified neural retina from human ESCs. Cell Stem Cell 10:771–785

6. ten Berge D, Koole W, Fuerer C et al (2008) Wnt signaling mediates self-organization and axis formation in embryoid bodies. Cell Stem Cell 3:508–518

7. Cereso N, Pequignot MO, Robert L et al (2014) Proof of concept for AAV2/5-mediated gene therapy in iPSC-derived retinal pigment epithelium of a choroideremia patient. Mol Ther Methods Clin Dev 1:14011

8. Fischer MD, Wilhelm B, Michalakis S et al (2016) Successful delivery of rAAV8. CNGA3 in a patient with CNGA3 achromatopsia. ARVO Annual Meeting Abstract. Invest Ophthalmol Vis Sci 57:5207. ARVO AnnualMeeting Abstract

9. Edwards TL, Jolly JK, Barnard AR et al (2016) Visual acuity after retinal gene therapy for choroideremia. N Engl J Med 374:1996–1998

10. Maguire AM, Simonelli F, Pierce EA et al (2008) Safety and efficacy of gene transfer for leber's congenital amaurosis. N Engl J Med 358:2240–2248

11. Koch SF, Tsai YT, Duong JK et al (2015) Halting progressive neurodegeneration in advanced retinitis pigmentosa. J Clin Invest 125:3704–3713

12. Vandenberghe LH, Auricchio A (2012) Novel adeno-associated viral vectors for retinal gene therapy. Gene Ther 19:162–168

13. den Hollander AI, ten Brink JB, de Kok YJ et al (1999) Mutations in a human homologue of Drosophila crumbs cause retinitis pigmentosa (RP12). Nat Genet 23:217–221

14. Richard M, Roepman R, Aartsen WM et al (2006) Towards understanding CRUMBS function in retinal dystrophies. Hum Mol Genet 15:235–243

15. Pellissier LP, Quinn PM, Alves CH et al (2015) Gene therapy into photoreceptors and Muller glial cells restores retinal structure and function in CRB1 retinitis pigmentosa mouse models. Hum Mol Genet 24:3104–3118

16. Pellissier LP, Lundvig DM, Tanimoto T et al (2014) CRB2 acts as a modifying factor of CRB1-related retinal dystrophies in mice. Hum Mol Genet 23:3759–3771

17. van Rossum AG, Aartsen WM, Meuleman J et al (2006) Pals1/Mpp5 is required for correct localization of Crb1 at the subapical region in polarized Muller glia cells. Hum Mol Genet 15:2659–2672

18. Baharvand H, Salekdeh GH, Taei A et al (2010) An efficient and easy-to-use cryopreservation protocol for human ES and iPS cells. Nat Protoc 5:588–594

19. Claassen DA, Desler MM, Rizzino A (2009) ROCK inhibition enhances the recovery and growth of cryopreserved human embryonic stem cells and human induced pluripotent stem cells. Mol Reprod Dev 76:722–732

20. Reuter JD, Fang X, Ly CS et al (2012) Assessment of hazard risk associated with the intravenous use of viral vectors in rodents. Comp Med 62:361–370

Chapter 20

AAV Serotype Testing on Cultured Human Donor Retinal Explants

Thilo M. Buck, Lucie P. Pellissier, Rogier M. Vos, Elon H.C. van Dijk, Camiel J.F. Boon, and Jan Wijnholds

Abstract

This protocol details on a screening method for infectivity and tropism of different serotypes of adeno-associated viruses (AAVs) on human retinal explants with cell-type specific or ubiquitous green fluorescent protein (*GFP*) expression vectors. Eyes from deceased adult human donors are enucleated and the retinas are isolated. Each retina is punched into eight to ten 6-mm equal pieces. Whatman™ paper punches are placed on the retinas and the stack is transferred onto 24-well culture inserts with the photoreceptors facing the membrane. AAVs are applied on the retinal explant punches to allow transduction for 48 h. Retinas are nourished by a serum-free Neurobasal®-A based medium composition that allows extended culturing of explants containing photoreceptor inner and outer segments. The protocols include quality control measurements and histological staining for retina cells. The cost and time effective procedure permits AAV transgene expression assays, RNAi knockdown, and pharmacological intervention on human retinas for 21 days ex vivo.

Key words Adeno-Associated Virus (AAV), Explant, Human, Neural retina tissue culture, Organotypic, Photoreceptors, Retinal Müller glial cell, Postmortem, Potency assays

1 Introduction

The first recombinant adeno-associated viral (rAAV) gene rescue therapies have been administered to patients in clinical trials [1, 2]. Preliminary clinical results are promising, but these still have to be converted into medication. Though, for the AAV gene therapy product Glybera (UniQure, Amsterdam, The Netherlands), for lipoprotein lipase deficiency, European market approval has been obtained. And recently in 2017 the FDA approved the investigational AAV gene therapy product Luxturna™ (Spark Therapeutics, Philadelphia, USA) for *RPE65*-mediated inherited retinal disease. The prediction of the cell tropism of different rAAV serotypes and variants on human retinas has been a hurdle. rAAV transduction

information of mice has little predictive value for human tissue because the distribution and specificity of receptors hijacked by rAAVs to infect cells differ between species. Yet information on rAAV serotype infection and both onset and levels of expression in human retinal cell types is limited because adult retinas rapidly lose their morphology during ex vivo culturing. Generally, the gene therapy vector protein expression is detectable a week after infection [3, 4]—provided the AAV particles applied have a sufficient titer—and peaks at around 5 weeks [5, 6]. Currently, a fair comparison of cell tropism and infectivity of AAV serotypes and variants with different promoter strengths and onset of expression can only be assessed in monkey studies. Here, we provide a technique to screen rAAVs on cell tropism and infectivity on human retinal explants. This technique can also be employed for neurodegeneration, neuroprotection, and cell transplantation assays.

Many variables influence the success of a retina culture. Differences of the maximum days in culture depend on the species and the age of retina. For example, cultured organotypic neonate mouse retinas last up to 27 days [7, 16]. Young adulthood retinas of rats and neonate retinas of chickens have been cultured for up to 7 days [8–10]. However, adult mammalian material, such as human, mouse, and pig retinas have only been cultured for short-term (up to 10 days) [10–14]. Recently, human retinas have been cultured in floating culture for 4 weeks [19]. Many cell, molecular, and morphological changes take place once the retina is cultured ex vivo. Changes include the deactivation of the shedding and regeneration of the outer segments (OS) of photoreceptors (PRCs), loss of cells with a successive retinal thinning, collapse of the outer plexiform layer (OPL), and Müller glia stress as identified by the upregulation of glial fibrillary acidic protein (GFAP) [12, 13]. The health of the retina needs to be thoroughly monitored and recorded. This can be achieved at the end by immunohistochemistry (retina cells, cell apoptosis, and cell cycling, *see* Table 1), morphological description (retinal layer thickness), and comparing it to control samples at the day of dissection; but also by inspecting it for tissue shrinkage and medium usage.

Diverse techniques can be employed to reduce retinal degeneration and culture intervariability, such as to use only fresh tissue (<72 h postmortem), to keep the tissue until dissection in Phosphate buffered saline (PBS) or Hanks' Balanced Salt Solution (HBSS) buffers at 4 °C (<24 h), to minimally manipulate the retina during dissection, to use serum-free medium compositions with supplements similar to in vivo retina environments, to change medium conditionally and frequently, to set the incubator to the optimal temperature (34–37 °C) and air composition (oxygen: ambient or reduced oxygen to 3%), and to work clean [11–14]. The only two serum-free medium for retina cultures described are R-16 and Neurobasal®-A medium [12, 14, 15].

Table 1
List of primary antibodies and chemical dyes for immunohistochemistry

Antibody	Anti-	Dilution	Company e.g.	Main staining property
Calbindin	Rabbit	1/250	AnaSpec	Strongly horizontal cells/INL-OPL; lower amacrine/INL
Calretinin	Rabbit	1/500	Chemicon	Amacrine/INL; displaced amacrine and ganglion cells/GCL
CRB1	Rabbit	1/250	Home made	Subapical region
Cone arrestin	Rabbit	1/500	Millipore	Cone photoreceptors
PKCα	Mouse	1/250	BD Biosciences	Rod bipolar cells
GFAP	Rabbit	1/200	DAKO	Stressed Müller glial cells and gliosis
Glutamine Synthetase	Mouse	1/200	BD Biosciences	Müller glial cells
p27^{kip1}	Rabbit	1/150	Millipore	Müller glial cells and cell cycle inhibitor protein
SOX9	Rabbit	1/250	Millipore	Müller glial nuclei/INL; astrocyte nuclei/GCL; RPE nuclei
Recoverin	Rabbit	1/500	Chemicon	Rod and cone photoreceptor somas and segments
Rhodopsin	mouse	1/250	Millipore	Outer segment and weakly soma of rods
CD45	Mouse	1/250	Emelca Bioscience	Activated microglia or macrophage/monocyte lineage cells
Rhodamine PNA	N/A	1/200	Vector	Cone outer segments. Added with second Antibody Buffer.
Caspase 3 (cleaved)	Rabbit	1/250	Cell Signaling	Cell apoptosis
Phospho-Histone H3	Rabbit	1/100	Millipore	Mitosis Marker

The authors have no preferences for distributors or companies. Antibodies and chemical dyes can be obtained from various sources

2 Materials

2.1 Solutions and Media

1. Explant medium: 300 μL 50× B-27 Supplement (Invitrogen), 150 μL 100× N-2 Supplement (Invitrogen), 30 μL 50 mM Taurine, 120 μL 200 mM L-glutamine, 150 μL 100 mM sodium pyruvate, 18.45 μL 1 mM N-Acetyl-L-cysteine, 150 μL 100× antibiotic–antimycotic (10,000 units/mL penicillin, 10,000 μg/mL streptomycin, 25 μg/mL Amphotericin B) in a final volume of 15 mL Neurobasal®-A medium (Invitrogen). Aliquot into 5 mL and store at 4 °C and use up within 5 days. Warm up aliquots only once.

2. Hanks' Balanced Salt Solution (HBSS). HBSS liquid containing Ca^{2+} and Mg^{2+}.

3. Sterile distilled water.

4. MilliQ autoclaved water.

5. Phosphate buffered saline (PBS): 2.6 mM KH_2PO_4, 26 mM Na_2HPO_4, 145 mM NaCl, pH7.0–7.2.

6. Dulbecco's Phosphate buffered saline with Ca^{2+} and Mg^{2+} (DPBS): 0.9 mM $CaCl_2$, 0.49 mM $MgCl_2$–6·H_2O, 2.67 mM KCl, 1.47 mM KH_2PO_4, 137.93 mM NaCl, 8.6 mM Na_2HPO_4–7·H_2O, pH 7.0–7.2.

7. 4% Paraformaldehyde (PFA) in PBS.

8. 5% Sucrose in PBS.

9. 30% Sucrose in PBS.

10. Cryo-embedding media, Tissue-Tek® O.C.T. compound.

11. 1% Sodium dodecyl sulfate (SDS).

12. Ethanol absolute 99.99%.

13. 70% ethanol in milliQ water (70% EtOH): 70 mL Ethanol absolute, 30 mL milliQ water.

14. 10% Poloxamer-188 surfactant solution, sterile.

15. 0.001% Poloxamer-188 in DPBS. Filter-sterilized. Stored in 1 mL aliquots at −20 °C.

2.2 Materials and Supplies

1. 12 mm filter diameter; 0.4 μm pore Hydrophilic Polytetrafluoroethylene (PTFE) Millicell Cell Culture Inserts (Millipore; catalogue number PICM01250).

2. Whatman™ 3MM Chr Chromatography Paper. Clean a 2-hole punch with warm water and soap, and 70% ethanol. Punch the Whatman™ 3MM paper. Autoclave the 6-mm punches.

3. 24-well culture plates, flat bottom.

4. Surgical instruments: Lancet. 11 cm Iris Scissor, curved. 18 cm Operating scissor, sharp/blunt, curved. Dressing forceps. Tissue forceps. 6 mm Surgical punch with adapter (*see* **Note 1**).

5. P1000, P200, P20, P10 pipette tips and single-channel pipette set.

6. Standard pipette gun and serological pipettes.

7. 37 °C 5% CO_2 incubator.

8. Parafilm.

9. Sucrose.

10. Superfrost Plus microscope slides.

11. 15 mL conical tubes.

12. 9 cm petridish.

13. $10 \times 10 \times 5$ mm Cryomold® biopsy, square.

14. Dry-Ice.

15. Cryostat.

16. 70 mm thickness Antiroll glass.

17. Carbon steel microtome blades C-35 pfm.

18. 20% Bovine Serum Albumin (BSA) dissolved in PBS.

19. Triton X-100.

20. (Goat) Serum.

21. Blocking Buffer: to prepare 10 mL, mix 1 mL normal goat serum, 0.04 mL Triton X-100, 0.5 mL 20% BSA, and 8.46 mL PBS.

22. Primary Antibody Buffer: to prepare 10 mL, mix 0.03 mL (goat) serum, 0.04 mL Triton X-100, 0.5 mL 20% BSA, 9.43 mL PBS, and primary Antibody.

23. Second Antibody Buffer: to prepare 10 mL, mix 0.5 mL 20% BSA, 9.5 mL PBS, and fluorescent dye-conjugated secondary Antibody directed against the primary Antibody.

24. VECTASHIELD HardSet Antifade Mounting Medium with 4′,6-Diamidin-2-phenylindol (DAPI; Vector Labs).

25. Protective equipment: gloves, safety goggles, lab coat, Biosafety level 2 laboratory, and laminar flow hood.

2.3 Recombinant Adeno-associated Virus with Transgene Expression Cassette

1. Recombinant AAV particles to be tested at a titer of $>10^{12}$ genomic copies per mL, e.g., rAAV2.CMV.*EGFP*.WPRE.pA packaged into serotype AAV9 capsids. The expression vector contains for example the two inverted terminal repeats (ITRs) of AAV2, the ubiquitous immediate early CMV promoter (CMV), the cDNA for *EGFP*, the woodchuck hepatitis virus post-transcriptional regulatory element (WPRE), and a bovine growth hormone polyadenylation sequence (pA).

2. The virus was produced as previously reported [3]. In short, HEK293T cells were triple transfected by Ca-phosphate transfection method with the helper plasmid pAAV9 from the Vector Core University of Pennsylvania, the helper plasmid pAdΔF6 [17], and a pAAV2.CMV.*EGFP*.WPRE.pA transfer plasmid. The cells were lysed and harvested 72 h post-transfection. AAVs were purified by an iodixanol gradient and concentrated by amplicon-spin columns. AAVs were tested on purity by SDS-PAGE Silver Staining and the genomic copies per mL (titer) were measured against a standard by qPCR.

3   Methods

3.1   Culturing of Postmortem Human Retina

The tissue was collected in agreement with the guidelines of the ethics committee of the LUMC. Patient anonymity was strictly maintained. All tissue samples were handled in a coded fashion, according to Dutch national ethical guidelines (Code for Proper Secondary Use of Human Tissue, Dutch Federation of Medical Scientific Societies).

3.1.1   Dissecting Out the Eye

1. Within 24 h after the death of a human donor removal of the entire globe of the eye and its contents, with preservation of all other periorbital and orbital structures, was performed.
2. The optic nerve was cut at 1 cm distance from the eye globe.
3. Eyes were transported and stored in HBSS at 4 °C.
4. A suture was put through an eye muscle to differentiate right and left eyes (*see* **Note 2**).
5. The eye was stored in cold HBSS in the fridge (*see* **Note 3**).

3.1.2   Prepare Medium and 24-well Culture Plate (>1 h Before Dissection)

1. Prepare fresh medium and warm it up in a water bath (*see* **Note 4**).
2. Add 15 mL milliQ autoclaved water between 24 wells. Place in incubator (*see* **Note 5**).
3. Add 300 μL medium to the eight wells in the middle of the plate. Leave the outside wells empty.
4. Add the inserts.
5. Gently shake the plate until all the inserts are wet.
6. Place it back in the incubator for at least 30 min before adding the retina pieces (*see* **Note 6**).

3.1.3   Dissecting Out a Retina from a Postmortem Human Eye

1. Place the eye for 30 s in 70% EtOH in a 50 mL tube or 6 cm dish to prevent infections.
2. Rinse off the EtOH with cold HBSS.
3. Place the eye in a 6 cm dish in cold HBSS (*see* **Note 7**).

4. Remove the extraocular tissue (such as muscles, epithelia layers, visible blood vessels) with the operating scissor and the tissue forceps until you only see the white sclera.

5. Fix the eye against the side of the dish with the help of a forceps (*see* **Note 8**).

6. Use the lancet or a surgical blade and slowly make a small cut around 0.5 cm below the lens slightly below the ciliary body (where you can see a color difference (*see* **Note 9** and Fig. 1a).

7. Subsequently cut around the eye with the Iris Scissor (*see* **Note 10** and Fig. 1b).

8. Cut the optic nerve preferably from the inside of the eye (between retinal pigment epithelium (RPE) and retina). If the retina is still attached then you can also cut the optic nerve from the outside (*see* **Note 11** and Figs. 1c, d).

9. Remove the lens with the vitreous attached.

10. Make three cuts spaced evenly from the edge to the optic nerve.

11. Carefully flatten the eye by pushing in the sides so they flip upward. Now, the retina detaches slowly from the RPE (*see* Figs. 1c, e).

12. Remove the sclera with the RPE attached to another dish. The retina with the ganglion cell layer (GCL) facing up should float in clean cold HBSS solution (*see* **Note 12** and Fig. 1e).

13. Locate the fovea (yellowish dot, avascular zone, ~1.5 mm diameter, ~5 mm from the optic disc). Make punches starting from the fovea going outwards. You should be able to make 8–14 punches (*see* Fig. 1g,h).

14. Place the Whatman™ paper punches on each retina (*see* **Note 13** and Fig. 1g,h).

15. Take out the previously prepared 24 well plate with inserts and medium from the incubator.

16. Carefully place the retina pieces on the inserts (Whatman™ paper facing upwards, PRCs downwards) and put it back in the incubator (*see* **Note 14**).

17. Take retina pieces for control and process them: Fixate (cold 4% PFA, 30 min), cryo-protect (cold 5% sucrose in PBS, 30 min; then cold 30% sucrose in PBS, 30 min) and freeze in O.C.T Tissue Tek on dry ice (*see* **Note 15**).

3.1.4 Culturing Retina Punches

1. Conditionally change medium daily. Remove 150 μL and replace it with fresh 150 μL prewarmed CO_2 equilibrated medium.

2. End the culture at desired endpoint (7–21 days) as described under **step 17** of Subheading 3.1.3.
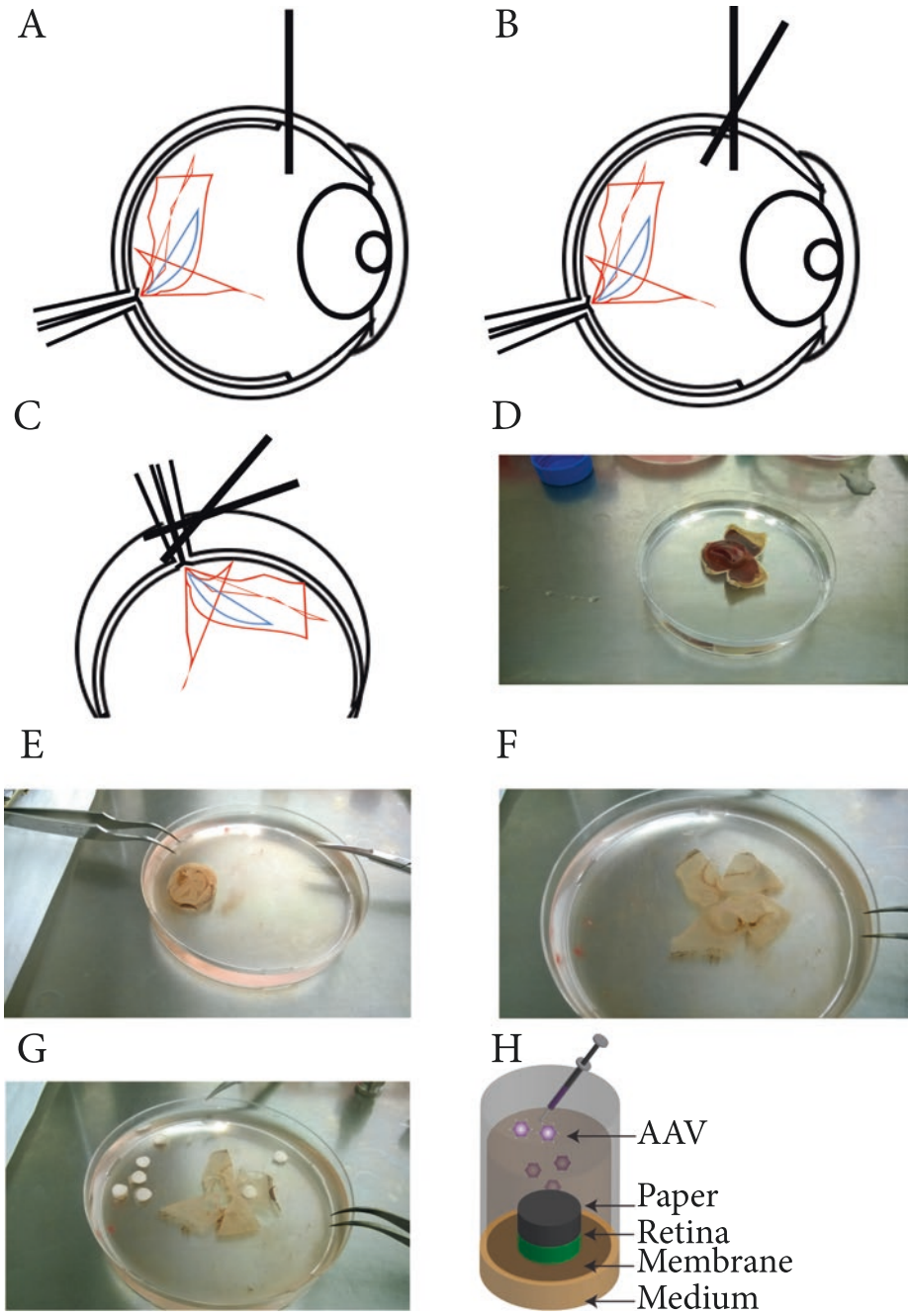
Fig. 1 Dissecting out a human retina and placement of the retina on the insert. (**a**) Stance at the border of the retina and the ciliary body. You can see color change from black to white. (**b**) Make long cuts with a scissor. (**c**) Cut off the optic nerve to free the retina. (**d**) Eye with the retina removed. You can see the retinal pigmented epithelium in black. (**e**) The retina without retinal pigmented epithelium. (**f**) Flattened out retina. (**g**) Punches made from the Ganglion cell layer side and Whatman paper placed on the top. (**h**) Culture system. AAVs are applied on the Whatman™ paper from the top and the PRCs face on the membrane

3.2 AAV Infection of Postmortem Donor Retinas

3.2.1 Preparation of the Virus (1 h Before Infection)

1. Warm up 50 μL medium per punch to be infected.

2. Centrifuge the concentrated virus suspension shortly and store on ice.

3. Prime the pipette tips in 0.001% poloxamer-188 in PBS solution (*see* **Note 16**).

4. Prepare the 50 μL infection mix: Add 3.4×10^{11} genome copies of AAV2/9.CMV.*GFP* to a final volume of 50 μL prewarmed medium (*see* **Note 17**).

3.2.2 AAV Infection of Postmortem Donor Retinas (~3 h After Retina Dissection)

1. Remove 150 μL of each 24 well.

2. Pipette the 50 μL infection mix on top of the Whatman™ paper in the inserts.

3. Incubate the retina with the AAVs for 48 h.

4. Remove medium and add 300 μL fresh prewarmed equilibrated medium .

5. Conditionally change the medium every day as described at **step 1** of Subheading 3.1.3. and end the culture at the desired endpoint as described at **step 17** of Subheading 3.1.3.

3.3 Workflow: Tissue Processing of Postmortem Donor Retinas

1. Prepare a fresh 24-well plate. Add 300 μL of 4% PFA, PBS, 5% sucrose, and 30% of sucrose to separate wells (horizontally).

2. Lift off the retinas with the Whatman™ paper attached from the insert (*see* **Note 18**).

3. Wash/dip the insert in the PBS well.

4. Move it to the 4% PFA in PBS well for 30 min (continue as described in **step 17** of Subheading 3.1.3 and in Fig. 2; *see* **Note 19**). Then quickly wash it in PBS.

5. Set the cryostat to −18/20 °C. Cool down the blade, antiroll glass (70 mm), the sample(s) at least for 1 h before cutting in the cutting chamber to −18/20 °C. And set the cutting thickness to 8 μm.

6. In the meantime, label 1–15 Superfrost slides per two samples. (Initials, date, experiment, and slide number).

7. Freeze the sample on a freezing block on the thin edge as depicted (*see* Fig. 2)

8. Orientate the block horizontally (*see* Fig. 2).

9. Cut as described for example in Fischer et al. [18]. In short: cut one section and move it on slide #1. Cut one section and move it on slide #2 (*see* Fig. 2).

10. Dry sections between 1 to 18 h before storing them at −20 °C or −80 °C (*see* **Note 20**).

11. Staining guideline: air dry glasses for 1 h.

12. Wash 1× in PBS.
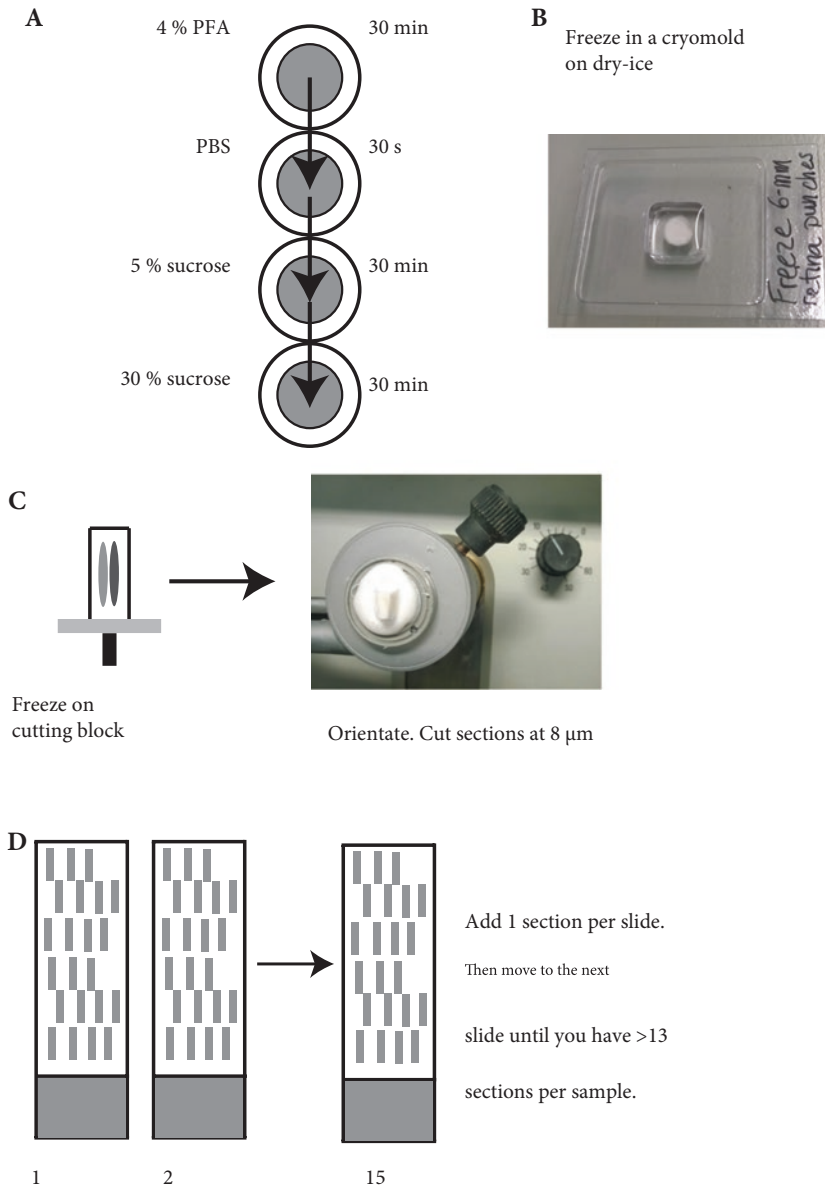
Fig. 2 Workflow for tissue processing. (**a**) Fixing process and cryopreservation. (**b**) Freeze in a cryomold for better orientation. (**c**) Flip the block and then freeze it on the cutting block (see image) to get all retina layers on one section. (**d**) Add one section per slide and then move to the next slide. You can add two samples per slide to have an internal control for immunohistochemistry staining

13. Incubate in blocking buffer for 30–60 min. Dip off the medium. Incubate with 150–200 μL/slide of primary antibody buffer with the appropriate primary antibody dilution (*see* Table 1). Incubate in a humid chamber at 4 °C overnight. Wash 3× for 15 min in PBS. Add 200–300 μL of the second Antibody buffer with the appropriate second antibody dilution
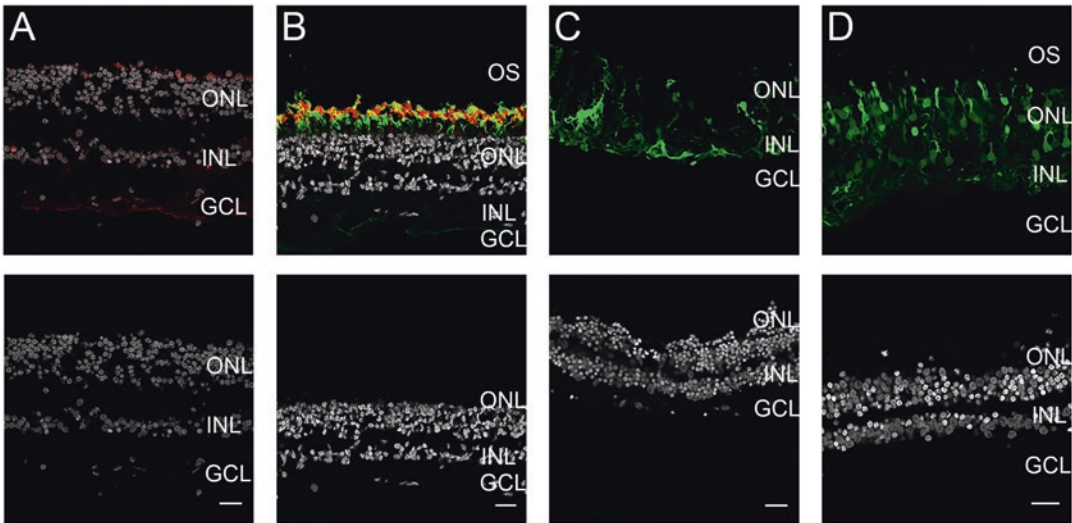
Fig. 3 Expected results. (**a**) Poor dissection or tissue without outer segments present (stained with PNA in red). (**b**) Good dissection and tissue with outer segments present (stained with Rhodopsin in red and PNA in green). (**c**) Retinal explant infected by AAV2/9.CMV.*EGFP*, 21 days after infection (GFP in green). (**d**) Retinal explant infected with AAV2/9.CMV.*EGFP*, 14 days after infection (GFP in green). Retinal layers: Outer Nuclear Layer (ONL), Inner Nuclear Layer (INL), Ganglion Cell Layer (GCL). Nuclear staining (DAPI) in gray. Scale bar: 25 μm

for 40–60 min (*see* **Note 21**). Wash 3× for 15 min in PBS. Dip off excess PBS and mount with one drop (30 μL) of VECTASHIELD HardSet Antifade Mounting Medium with DAPI. Harden at room temperature for 3 h or at 4 °C for >48 h (storage condition).

14. Image on a confocal (or fluorescent) microscope at >20× magnification (*see* Fig. 3 and **Note 22**).

4   Notes

1. Clean surgical tools with warm water and soap. Then, wash with 70% EtOH.

2. Eye(s) should be enucleated within 24 h after death, to obtain the best results.

3. Retina should be dissected out within 36 h after dissection, to obtain the best results.

4. You can also warm up the medium by placing it in the incubator with unscrewed cap. This allows activation of the sodium bicarbonate buffer in a 5% CO_2 environment.

5. This ensures that the plate is an evenly humid chamber for all retinas.

6. If the dissection is in another room with incubator than your standard culture room then take the prepared 24-well plate

wrapped in parafilm to the dissection room and place it there in the incubator. Don't move a dissected retina in a 6 cm plate. It will shear off all the OS of the retinas.

7. HBSS medium provides the glucose to cells while keeping the pH in check under atmospheric conditions.

8. A second person can support the fixation with an additional forceps.

9. Cutting below the ciliary body helps to remove the vitreous body and the RPE from the retina.

10. Make large cuts to minimize the physical shearing on the retina during dissection.

11. The older the material and human donor, the stickier the retina. Cold HBSS (without magnesium, calcium) can help detaching the retina from the RPE.

12. You can conditionally replace the medium to keep the temperature low.

13. The punches should easily attach to each piece. Autoclaving the punches can cause punches to stick to each other. Use forceps to take only one punch at a time.

14. Try to minimize pressure and area touched with the forceps. Work quick (<5 min) so the medium stays warm and the pH of the medium stays intact (*see* Fig. 1).

15. *See* Fig. 1 for detailed tissue processing steps.

16. This helps to prevent AAV attachment to the plastic tip.

17. Different AAVs are differently effective in infecting retinal cells. Other AAVs can infect as low as 10^7 genome copies per infection mix. Limit the amount added to the medium to 15 μL added not to dilute the medium to much.

18. The retinas never attached to the inserts so cutting out the inserts is not necessary. When handling retinas, minimize the contact (touch only sides). You can also select Whatman™ punches where not the complete retina is attached to so you can manipulate on areas where no retina is attached to it.

19. After the cryopreserving step in 30% sucrose and the tissue dropped to the bottom, then you can store it for a few days in the fridge. We always immediately freeze it. At this step you can also peel off the Whatman™ paper. Yet we did not find a difference in staining if it was carefully peeled off or not. We decided not to peel it off anymore to have less artifacts introduced by the peeling off.

20. It is a good practice to stain one section directly after cutting with 1% toluidine blue in milliQ water or anti-fade mounting medium with DAPI to quickly assess the tissue morphology under a light or fluorescent microscope.

21. If not enough liquid is on the slide then you can place parafilm or a cover slide on top of it. It helps to get even distribution of the second antibody on the slide.

22. Compare the outer segments (OS) of PRCs after dissection and at the time of harvest with for example PNA and Rhodopsin staining (*see* Fig. 3). We observed that OS seem to be relevant in the AAV infection pathway to photoreceptors (unpublished).

Acknowledgment

References

1. Kumar SR, Markusic DM, Biswas M et al (2016) Clinical development of gene therapy: results and lessons from recent successes. Mol Ther Methods Clin Dev 3:16034

2. Carvalho LS, Vandenberghe LH (2015) Promising and delivering gene therapies for vision loss. Vis Res 111:124–133

3. Pellissier LP, Hoek RM, Vos RM et al (2014) Specific tools for targeting and expression in Müller glial cells. Mol Ther Methods Clin Dev 1:14009

4. Van Wyk M, Hulliger EC, Girod L et al (2017) Present molecular limitations of ON-bipolar cell targeted gene therapy. Front Neurosci 11:161

5. Wu Z, Asokan A, Samulski RJ (2006) Adeno-associated virus serotypes: vector toolkit for human gene therapy. Mol Ther 14:316–327

6. Thomas CE, Storm TA, Huang Z et al (2004) Rapid uncoating of vector genomes is the key to efficient liver transduction with pseudotyped adeno-associated virus vectors. J Virol 78:3110–3122

7. van Rossum AG, Aartsen WM, Meuleman J et al (2006) Pals1/Mpp5 is required for correct localization of Crb1 at the subapical region in polarized Müller glia cells. Hum Mol Genet 15:2659–2672

8. Barr-Nea L, Barishak RY (1970) Tissue culture studies of the embryonal chicken retina. Investig Ophthalmol 9:447–457

9. Aartsen WM, Arsanto JP, Chauvin JP et al (2009) PSD95β regulates plasma membrane Ca(2+) pump localization at the photoreceptor synapse. Mol Cell Neurosci 41:156–165

10. Johnson TV, Bull ND, Martin KR (2011) Organotypic explant culture of adult rat retina for in vitro investigations of neurodegeneration, neuroprotection and cell transplantation. Protocol Exchange:1–28. https://doi.org/10.1038/protex.2011.215

11. Fernandez-Bueno I, Fernandez-Sanchez L, Gayoso MJ et al (2012) Time course modifications in organotypic culture of human neuroretina. Exp Eye Res 104:26–38

12. Johnson TV, Martin KR (2008) Development and characterization of an adult retinal explant organotypic tissue culture system as an in vitro intraocular stem cell transplantation model. Invest Ophthalmol Vis Sci 49:3503–3512

13. Bull ND, Johnson TV, Welsapar G et al (2011) Use of an adult rat retinal explant model for screening of potential retinal ganglion cell neuroprotective therapies. Invest Ophthalmol Vis Sci 52:3309–3320

14. Wang J, Kolomeyer AM, Zarbin M et al (2011) Organotypic culture of full-thickness adult porcine retina. J Vis Exp 49:2655. https://doi.org/10.3791/2655

15. Romijn HJ (1988) Development and advantages of serum-free, chemically defined nutrient media for culturing of nerve tissue. Biol Cell 63:263–268

16. Caffé AR, Ahuja P, Holmqvist B et al (2001) Mouse retina explants after long-term culture in serum free medium. J Chem Neuroanat 22:263–273

17. Gao G-P, Alvira MR, Wang L et al (2002) Novel adeno-associated viruses from rhesus monkeys as vectors for human gene therapy. Proc Natl Acad Sci U S A 99:11854–11859

18. Fischer AH, Jacobson KA, Rose J et al (2008) Cryosectioning tissues. Cold Spring Harb Protoc 3:8–10

19. Osborne A, Hopes M, Wright P et al (2016) Human organotypic retinal cultures (HORCs) as a chronic experimental model for investigation of retinal ganglion cell degeneration. Exp Eye Res 143:28–38

Chapter 21

Human Retinal Explant Culture for Ex Vivo Validation of AAV Gene Therapy

Harry O. Orlans, Thomas L. Edwards, Samantha R. De Silva, Maria I. Patrício, and Robert E. MacLaren

Abstract

Recombinant adeno-associated viral (AAV) vectors have been successfully employed as the mode of gene delivery in several clinical trials for the treatment of inherited retinal diseases to date. The design of such vectors is critical in determining cellular tropism and level of subsequent gene expression that may be achieved following viral delivery. Here we describe a system for living retinal tissue extraction, ex vivo culture, viral transduction and assessment of transgene expression that may be used to assess viral constructs for gene therapy in the human retina at a preclinical stage.

Key words Gene therapy, Human retina, AAV, Culture

1 Introduction

Gene therapy with AAV has shown substantial promise in the treatment of inherited retinal disease. An excellent safety profile has been demonstrated for these vectors in numerous clinical trials within a variety of organ systems [1]. At the time of writing, eight gene replacement phase I clinical trials using AAV are underway for inherited retinal diseases attributable to mutations in the RPE65 (Leber's congenital amaurosis), REP1 (choroideremia), MERTK (retinitis pigmentosa) and CNGA3 (achromatopsia) genes [2–5]. Among other factors, vector design is critical for the success or otherwise of human gene therapies. The ideal vector should deliver sufficient DNA to allow restoration of function without inducing toxicity or significant off-target effects. Central to this are the concepts of cellular tropism and transduction efficiency [6]. Tropism, or cellular specificity, of AAVs is determined by capsid pseudotype and choice of promoter, while the eventual level of transgene expression within any particular cell may be augmented by inclusion of nontranslated elements within the recombinant AAV expression cassette such as the Woodchuck Hepatitis Virus

Posttranscriptional Regulatory Element (WPRE) [7, 8], or through the use of self-complementary AAV genomes [9, 10]. Efficient viral transduction is desirable for clinical application as it allows for the delivery of a lower number of viral particles to achieve any given level of transgene expression, which in turn reduces the risk of potential dose-dependent toxicity and immune reaction.

Given the near infinite number of potential AAV designs that may be employed for any particular clinical application, the use of laboratory based assays to evaluate and compare AAVs is essential before an optimized vector may be brought to clinical trial. While cell and small animal-based models are useful and have until now formed the basis of preclinical AAV assessment, transgene expression in such tissues does not necessarily reflect the situation in the human subject. Indeed, significant inter-species variation has been reported in terms of both AAV tropism and eventual levels of transgenic protein expression [11]. Furthermore, in vivo animal experiments are frequently lengthy, costly and may culminate in inconclusive results.

In this chapter, we describe a method for the extraction of living human retinal tissue for ex vivo assessment of putative human gene therapy vectors. Human retinal tissue may be acquired for this purpose from consenting adults who are undergoing clinically indicated retinectomy [12, 13]. In some respects, this represents the ultimate preclinical model, being in fact the target tissue in question. It is in other respects, however, an imperfect model for a number of reasons. Firstly, the tissue is, almost by definition, abnormal, having been extracted from patients who may have a history of complex retinal detachment, proliferative vitreoretinopathy, and/or advanced diabetic eye disease. Additionally, the tissue is often ischemic and in cases where the retinectomized area has been detached for any considerable length of time, the outer retina may be degenerate or absent in its entirety. This of course limits the utility of this assay, in certain circumstances, for assessment of photoreceptor-targeted treatments. Relatively healthy full-thickness retinal tissue may however be acquired for this purpose from larger retinal tears that may be encountered, for example, in patients undergoing vitreoretinal surgery for nondiabetic vitreous hemorrhage, or acute rhegmatogenous retinal detachment.

The organotypic culture system described below is based largely upon that described by Johnson and Martin for ex vivo culture of the rat retina in the context of retinal stem cell therapy [14]. Briefly, the method involves extraction of retinal fragments at the time of surgery which are then cultured in a Neurobasal-A based medium. After one day in culture, the fragments are transduced with the vector(s) under assessment. This may be an AAV designed for clinical application or an equivalent vector containing a reporter gene such as green fluorescent protein (GFP). If a reporter AAV is used, the retinal fragments may be imaged by

fluorescence microscopy while in culture to assess the timing and degree of transgene expression over the course of the culture period. At the end of the culture period, which in our experience may be up to two weeks, the explants may be fixed, embedded, and sectioned for immunohistochemistry and confocal microscopy. Alternatively, tissue can be processed for mRNA or protein expression analysis.

2   Materials

Complete Neurobasal-A culture medium must be prepared in advance of surgical extraction of tissue. Supplements may be aliquoted and stored at −20 °C until use at which point they should be thawed at room temperature, added to Neurobasal-A and the resulting "complete" medium stored at 4 °C. Concentrations of supplements specified below refer to those of the final complete medium. Preparation of culture medium and handling of human tissue should be performed under aseptic conditions in a positive-pressure tissue culture hood.

2.1 Surgical Procedure

1. Vitreoretinal forceps.
2. 23/25/27-G Vitrectomy cutter.
3. Valved cannula to insert the vitrectomy cutter.
4. 7/0 Vicryl box suture.
5. Sterile 20 G forceps.
6. Vitrectomy machine.
7. Balanced salt solution (BSS) : 0.64% sodium chloride, 0.075% potassium chloride, 0.048% calcium chloride dihydrate, 0.03% magnesium chloride hexahydrate, 0.39% sodium acetate trihydrate, 0.17% sodium citrate dihydrate, sodium hydroxide and/or hydrochloric acid (to adjust pH), and water. The pH is approximately 7.5.
8. 10 mL syringe.
9. Sterile bung to seal the 10 mL syringe.

2.2 Tissue Handling and Explant Culture

1. Complete Neurobasal-A Culture Medium : Neurobasal-A with phenol red supplemented with 100 units/mL Penicillin, 100 μg/mL Streptomycin, 0.8 mM L-Glutamine, 2% 50× B27 supplement, 1% 100× N2 supplement, store at 4 °C.
2. 10 cm diameter petri dish.
3. 24-well culture plate.
4. Organotypic culture inserts (0.4 μm pore size; Falcon, Thermo Fisher Scientific).

5. 3 mL Pasteur pipettes.

6. Sterile scissors.

7. Sterile forceps.

8. Sterile scalpel.

9. Pipettes and filter tips.

10. Humidified tissue culture incubator set to 34 °C with 5% CO_2.

11. Positive-pressure tissue culture hood.

2.3 Viral Transduction

1. AAV aliquot stored at −80 °C and thawed immediately prior to use.

2. Complete Neurobasal-A culture medium, as described above.

3. Sterile forceps.

2.4 Immuno-histochemistry

1. 3 mL disposable sterile Pasteur pipettes.

2. 4% Paraformaldehyde (PFA) in PBS.

3. 30% Sucrose solution in PBS.

4. Optimal Cutting Temperature medium (OCT).

5. Vinyl specimen mold trays, 15mm × 15mm × 5mm (Tissue-Tek Cryomold, Sakura).

6. Dry ice.

7. Cryotome.

8. Poly-L-lysine-coated glass slides.

9. Marker pen.

10. 0.01M phosphate buffered saline (PBS): 0.95 g/L 10 mM phosphates as sodium phosphates, 0.201 g/L 2.68 mM KCL, and 8.12 g/L 140 mM NaCl, pH 7.45. Prepared from PBS tablets. Solid PBS tablet to be dissolved in 500 mL distilled water.

11. PBS/serum blocking solution: PBS supplemented with 0.1% Triton X-100, 10% donkey serum.

12. PBS/Triton primary antibody solution: PBS supplemented with 0.1% Triton X-100, 2% donkey serum, primary antibody.

13. PBS/Tween washing solution: PBS supplemented with 0.05% Tween 20.

14. PBS/Triton secondary antibody solution: PBS supplemented with 0.1% Triton X-100, 2% serum, secondary antibody.

15. 12.3 mg/mL Hoechst 33342.

16. Antifade mounting reagent.

3   Methods

3.1   Legal Aspects and Ethical Approval

Legislation regarding the retention of human tissue for research purposes in the UK is enshrined within the Human Tissue Act 2004 which outlines the need for ethical approval for all such research. The process of ethical review is therefore a legal requirement before conducting research on human tissue in the UK as it is in many other countries including the United States. In the USA, this process is overseen by Institutional Review Boards (IRBs— further information may be found within the US Food and Drug Administration (FDA) website www.fda.gov), while in the UK, ethical review is regulated by the NHS Health Research Authority (HRA). All necessary information may be found online at www.hra.nhs.uk.

3.2   Patient Consent

Under the Human Tissue Act, 2004, written consent should be obtained for patients from whom tissue is to be extracted and retained for research purposes. However, in cases where the researcher is unable to identify an individual from his/her tissue, and the tissue is used for a specific study for which ethical approval has been granted, the Act states that additional consent is not necessarily required. It is however considered best practice to do so. Comprehensive guidelines on the principles and processes involved with consent for research purposes have been outlined by the General Medical Council of the UK (GMC), and are available via their web page www.gmc-uk.org. Briefly, the following principles apply for patient consent with regard to retention of human retinal tissue:

1. Consent must be valid. Informed consent should be sought from patients with capacity without pressure or coercion.

2. Individuals retain the right to withdraw consent at any time.

3. Sharing information. Adequate information should be provided and tailored to individual patient needs. A participant information sheet should be provided. Guidance on the design and recommended content of such forms is available from the National Research Ethics Service, UK.

4. Information should be given in a way and language that patients can understand.

5. Those who seek consent should have an adequate understanding of the research in question.

6. Records of written consent should be retained by the researcher. Consent should be confirmed through a study-specific consent form.

3.3 Surgical Procedure

Retinal tissue may be extracted by one of two methods: direct extraction via a sclerostomy with vitreoretinal forceps or with the automated cutter and manual aspiration (*see* **Note 1**). The approach adopted should be guided by experience of the surgeon, nature of the required retinectomy and availability of a surgical assistant.

3.3.1 En Bloc Retinectomy Extraction

1. Perform a thorough vitrectomy with close shaving over the planned biopsy region.
2. Outline the extent of the planned biopsy with endodiathermy, paying particular attention to retinal vessels (*see* **Note 2**).
3. Insert the 23/25/27-gauge vitrectomy cutter through a valved cannula, reduce the cut rate to for example less than 500 cuts/min, and perform an en bloc retinectomy inside the diathermied outline (*see* **Note 3**).
4. Allow the retinectomized specimen to drift onto the posterior pole.
5. Remove the cutter and lower the infusion pressure to less than 15 mm Hg to reduce turbulence of the tissue during withdrawal of the instruments.
6. Make a conjunctival incision to expose sclera for an MVR sclerostomy.
7. Preplace a 7/0 vicryl box suture at the sclerostomy site before making a new circumferentially oriented 20 G MVR incision.
8. Keeping the low infusion rate (to minimize turbulent movement of the biopsied tissue), insert 20 G forceps and extract the tissue fragment, taking care while drawing the specimen through the sclerostomy.
9. Place the specimen directly into balanced salt solution (BSS) for transfer into culture (*see* **Note 4**).

3.3.2 Extraction Via the Cutter with Manual Aspiration

1. Perform **steps 1–3** as above.
2. Connect the aspiration line to a 10 mL syringe which should be held by an assistant.
3. Reduce the vitrector cut rate to a minimum, e.g., 100 cuts/min (*see* Fig. 1), and while an assistant manually aspirates with the syringe, take individual bites of the area to be retinectomized (*see* **Note 5**).
4. Once an adequate number of retinal fragments have been acquired, remove the syringe and apply a sterile bung. The sealed syringe containing the retinal specimens should now be removed from the operating room and taken directly for culture (*see* **Note 4**).

3.4 Ex Vivo Handling of Retinal Tissue

All handling of samples should be performed under aseptic conditions in a positive-pressure tissue culture hood.
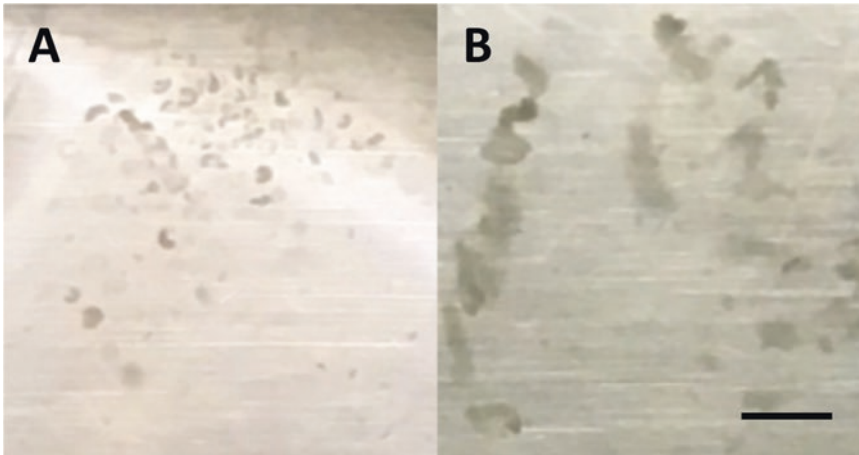
Fig. 1 Effect of cutter speed on size of extracted retinal fragments. Photograph (**a**) illustrates the size of retinal fragments obtained with maximal cut rate as may be used during routine vitreoretinal surgery. Photograph (**b**) shows the larger fragments that may be acquired when the cut rate is reduced to a minimum, in this case 100 cuts/min, scale bar 2 mm

3.4.1 Ex Vivo Handling of Retinal Tissue

1. Carefully empty the specimen jar containing the retinal fragments suspended in BSS into a 10 cm diameter petri dish, note that small retinal fragments may adhere to the sides of the container. Excess BSS may be removed with a pipette.

2. If a large piece of retina has been excised en bloc, divide this by cutting it into fragments of the required size using a scalpel (*see* **Note 6**). If fragments were acquired using the cutter, larger fragments of near uniform shape and size should be identified and selected for subsequent culture (*see* **Note 7**).

3. Prepare Pasteur pipettes for transfer of fragments by removing the tip using sterile scissors such that the new opening is of sufficient size to accommodate retinal fragments without traumatizing the tissue (*see* Fig. 2) (*see* **Note 8**).

4. Transfer each retinal fragment to be cultured into an individual culture insert. This is done by drawing the fragment suspended in BSS into the tip of the modified Pasteur pipette. Maintain pressure on the bulb of the pipette while transferring the tissue then firmly expel the fragment in suspension into the insert (*see* **Note 9**).

3.4.2 Ex Vivo Culture and Viral Transduction

1. Fill wells of a 24-well plate (such that an individual well is prepared for each explant to be cultured) with 400 μL prewarmed complete Neurobasal-A culture medium.

2. Using sterile forceps, place the inserts containing retinal fragments into prepared wells and pipette an additional 50–100μL of complete Neurobasal-A medium into each of the inserts (*see* **Note 10**).
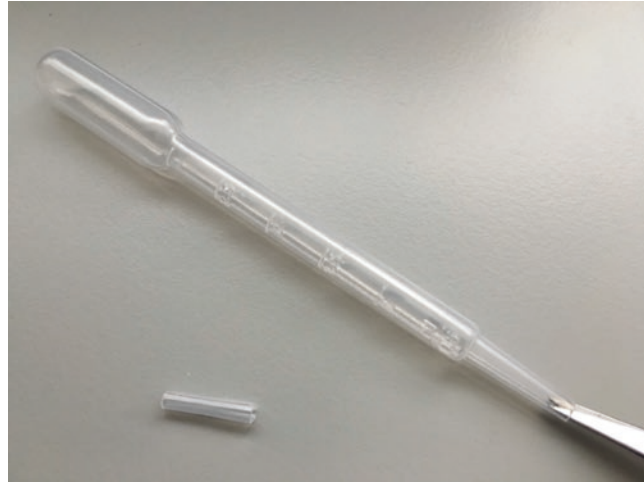
Fig. 2 Preparation of a Pasteur pipette for handling of retinal fragments. Sterile scissors should be used to remove the tapered tip of the pipette to allow a wider opening through which retinal fragments may pass in suspension. The scissors should then be opened forcibly within the newly created opening so that the end of the pipette splays outward rather than inward. This manoeuvre removes any internal shelves in which retinal fragments may become entrapped during transfer of tissue

3. Replace the 24-well plate lid and incubate the explants in a humidified tissue culture incubator set to 34 °C with 5% CO_2.

4. After approximately 24 h in culture, replace the 400 µL of media within the well with fresh prewarmed complete Neurobasal-A (*see* **Note 11**).

5. Transduce each experimental retinal fragment with 10^{10} genome particles of the AAV to be tested by pipetting the virus in solution directly into the media within the insert (*see* **Note 12**). A proportion of the explants should be allocated as untransduced negative controls. After transduction, return the plate to the 34 °C incubator.

6. On alternate days following viral transduction, and until the designated end of the culture period, replace 400 µL of complete Neurobasal-A within each well with fresh media (*see* **Note 11**).

3.5 En Face Fluorescence Microscopy and Image Analysis (See Note 13 and Fig. 3)

1. For quantitative fluorescence imaging, select the appropriate objective for the microscope so that the entire explant can be visualized within a single field of view.

2. Position the 24 well plate on the viewing platform of the microscope with the lid left in place and for each explant, acquire a set of images under standardised conditions (*see* **Note 13**). This would normally consist of a transmission image (e.g., with a 0.5 s exposure), followed by fluorescence images using appropriate filters at a range of exposure times (*see* **Note 14**).
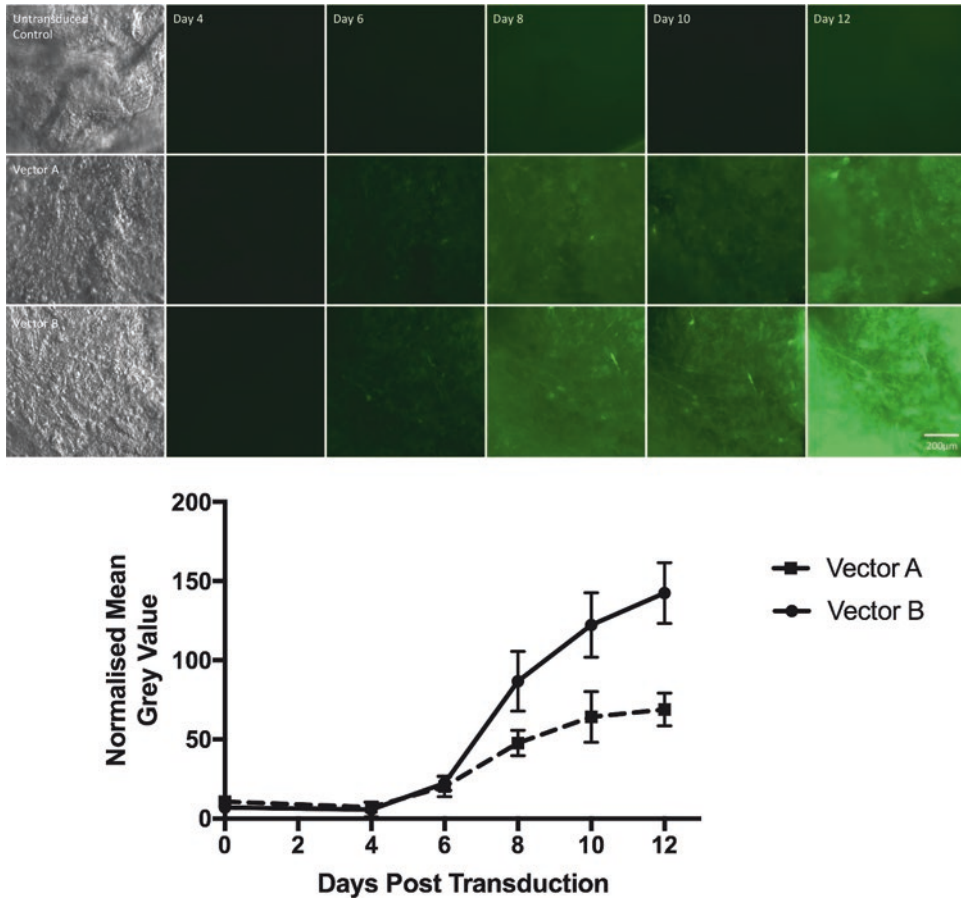
Fig. 3 Comparison of two AAV constructs expressing GFP. The fluorescence micrographs above show changes in fluorescence seen with time after transduction with two viral constructs expressing GFP under the control of a strong ubiquitous promoter. Transmission images on Day 0 are shown to the left. The graph illustrates how mean grey values normalized for background fluorescence calculated from such images can be used to compare vectors

3. After imaging is complete, return the plate to the 34 °C incubator.

4. To begin the process of image analysis, load the transmission microscopy image of the first untransduced sample into ImageJ (*see* **Note 15**).

5. Define an area of interest and save this to the manager (*see* **Note 16**).

6. Open the equivalent fluorescence image, apply the region of interest from the manager panel and measure the grey value (*see* **Note 17**).

7. Repeat **steps 5**–**7** for all images.

8. Prior to analysis, correct for background fluorescence by subtracting the mean grey value of the untransduced control from that of transduced samples ("Normalized mean grey value").

3.6 Immuno-histochemistry

1. At the end of the designated culture period, transfer the retinal fragments into 4% PFA using a modified Pasteur pipette. Leave to fix for 30 min then transfer the fragments into 30% sucrose solution for a minimum of 1 h.

2. Next, transfer each retinal fragment into PBS for a brief wash before transferring into individual vinyl specimen mold trays. Excess PBS around the fragment may be removed with a pipette.

3. Fill the tray with OCT ensuring that each fragment is completely submerged and suitably orientated for sectioning (*see* **Note 18**).

4. Mark the position of the fragment on the edges of each tray with a pen before placing it on dry ice (*see* **Note 19**).

5. After freezing, the previously placed markers may be extended over the frozen OCT to indicate the position of the tissue (*see* Fig. 4). Trays should be stored at −80 °C prior to sectioning.

6. When ready to section the retinal fragments, remove the frozen OCT from the plastic mold and mount along a thin edge.

7. Section on a cryotome to a thickness of 12–18μm onto poly-L-lysine-coated slides (*see* **Note 20**) which may then be stored at −20 °C.

8. Immunohistochemistry may then be performed according to standard protocols. For example, following hydration wash 3 × 5 min in PBS.

9. Block retinal sections for 1 h at room temperature in PBS/serum blocking solution.

10. After a further 3 × 5 min washes, incubate slides at 4 °C overnight with PBS/Triton primary antibody solution.

11. Subsequently wash for 3 × 5 min with PBS/Tween washing solution.

12. Incubate for 2 h at room temperature with the species–appropriate PBS/Triton secondary antibody solution.

13. Counter-stain sections with Hoechst 33342 1:5000 and mount with an antifade reagent.

14. Retinal sections may be viewed on a confocal microscope with laser excitation wavelengths appropriate to the fluorophores used. Overlapping XY optical sections of approximately 0.5μm thickness may then be acquired through the specimen (*see* Fig. 5).
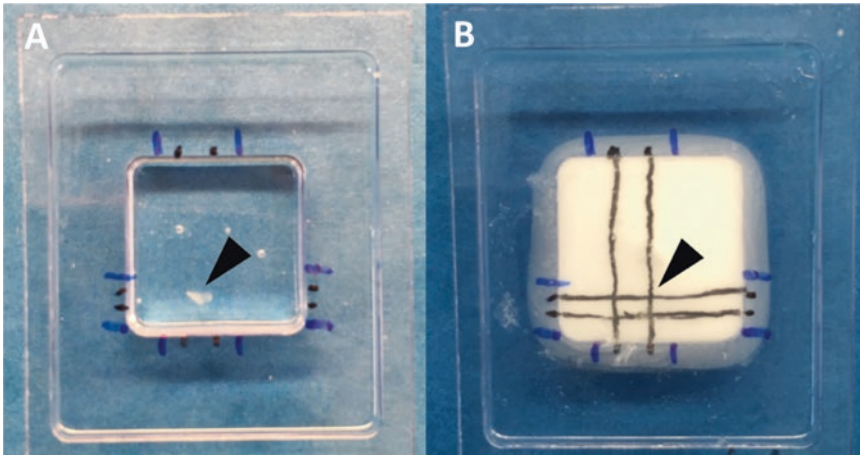
Fig. 4 Placement of tissue fragments within OCT for sectioning. Tissue should be orientated within OCT in a flat conformation so that perpendicular retinal cross sections may be achieved (Panel **a**). The position of the retinal fragment should be marked prior to freezing, after which the marks may be extended across the frozen block (Panel **b**). Black arrows indicate the position of the explant within the OCT
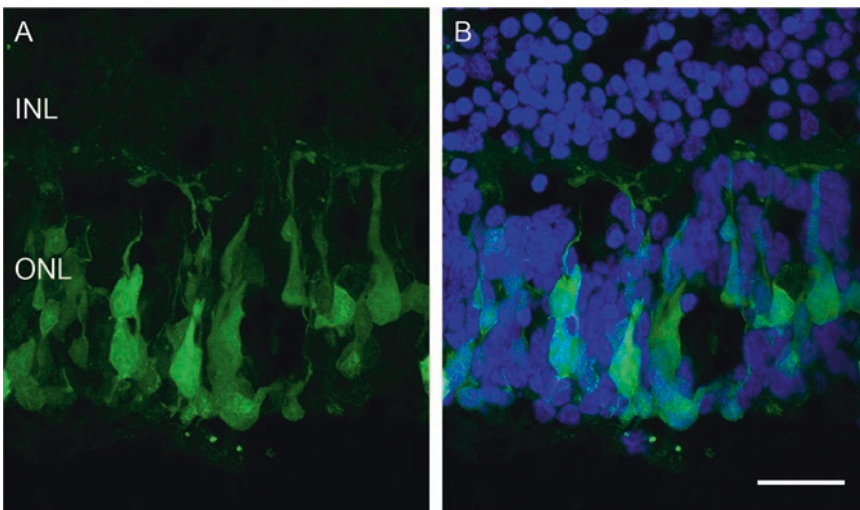
Fig. 5 Transduction of human photoreceptors using AAV2/2.GFP Confocal microscopy image taken of a human retinal explant following transduction with rAAV2/2.GFP, tissue fixation, sectioning and counterstaining with Hoechst 33,342. (**a**) GFP expression as a marker of retinal photoreceptor transduction, (**b**) composite image with Hoechst 33,342, scale bar 25 μm. INL: Inner nuclear layer; ONL: Outer nuclear layer

4   Notes

1. In either case, it is important to thoroughly clear all attached vitreous from the retina targeted for biopsy prior to retinectomy, as residual gel may cause biopsied fragments to curl and not lie flat in tissue culture.

2. This may not be required for small horseshoe tear amputations.

3. This step can alternatively be performed using 23 G scissors.

4. If any delay is anticipated between tissue extraction and placement into culture, the tubes or syringes containing the specimen(s) should be placed on ice.

5. If an assistant is unavailable, an alternative approach is to reflux specimens from the cutter into a sterile dish outside of the eye.

6. Before cutting the retinal fragments, excess BSS should be aspirated using a pipette so that the fragment in question is resting directly against the base of the petri dish and is not curled or folded. Manipulation through resuspension in BSS may be required to achieve this.

7. Certain fragments may show a tendency to curl or fold at this stage which may in part be due to residual vitreous on their surface. If possible, avoid selecting such specimens for culture. Fragments with obvious vitreous attachments should similarly be avoided.

8. The process of cutting the pipette tip may create an internal shelf at the new opening. If this is not corrected, retinal fragments will tend to get trapped within the tip of the pipette. This shelving effect may be remedied by forcibly opening the tips of the scissors within the new pipette opening so that the plastic straightens or slightly splays externally (*see* Fig. 2). This manoeuvre may need to be performed in several meridians to ensure that no internal shelf remains before the pipette is used for tissue transfer.

9. After expelling the retinal fragment into the culture insert, confirm that the fragment is now sitting within the insert and has not become trapped within the pipette. Not infrequently, the tissue may be incarcerated at the tip opening or within the pipette. If this occurs, release the tissue by passing BSS in and out of the opening then repeat the transfer process. Before doing so, it may be necessary to modify the pipette tip further with sterile scissors (see above) to remove any residual internal shelving.

10. The final fluid level should be high enough to completely cover the explant. This ensures diffusion of vital gasses and nutrients between the culture medium and the explant over its entire surface. Higher fluid levels should not be used if possible as this may encourage movement of the tissue from the porous base of the insert. Avoid trapping air beneath the insert by tilting it as it is placed into the well. Bubbles beneath the insert may interfere with diffusion to the lower surface of the explant and may adversely affect quantification of fluorescence from

subsequent images. If a bubble is noted, the insert should be lifted and repositioned back into the well.

11. To change the media, culture inserts should be removed with sterile forceps to reduce the risk of contamination. When changing media, be careful not to disturb the retinal fragment within the insert, particularly if performing en face fluorescence microscopy during the culture period. In this case, it is advantageous to maintain the tissue fragment in a similar conformation to ensure consistency of imaging.

12. In our experience, this dose of virus consistently produces a detectable level of GFP expression and allows comparison between constructs. Transduction efficacy will be affected by size of the retinal explant and AAV capsid and genome. If comparing gene therapy vectors, the transduction process should ideally be completed in a blinded fashion.

13. Quantitative *en face* fluorescence microscopy may be performed in instances where the vector to be tested expresses a fluorescent protein such as GFP. Images should be taken under standardized conditions of ambient lighting with consistent acquisition parameters. Our experience suggests that measurements are most consistent with ambient lights switched off.

14. Since the final level of fluorescent protein expression is unknown at the outset of the experiment, we would suggest acquiring images at a range of exposure times at each time point (e.g., 0.5 s, 1 s, 2 s, 5 s, 10 s). At the end of the experiment, the exposure time selected for further analysis should be that which produces images with the highest signal without reaching saturation.

15. ImageJ software is freely available to download courtesy of the National Institute of Health (NIH), USA via the following URL: https://imagej.nih.gov.

16. If viral constructs are to be compared using this assay, the mean grey value must reflect the average level of fluorescence within the retina [15]. For this to be valid, the area of retina analysed (the so-called "region of interest") must consist entirely of flat unfolded retina (*see* Fig. 6). The inclusion of folded retina will artificially increase measured fluorescence as multiple layers of retina will contribute to this value in such circumstances. To define an area of interest, select the freehand tool icon and draw around the largest area of contiguous flat, single-layered retina. This selection should then be added to the Region of Interest (ROI) Manager (Select Edit>Selection>Add to Manager).

17. Transferring the ROI from the transmission to the fluorescence micrograph avoids any operator-dependent bias when defining the region of fluorescence to be included in the
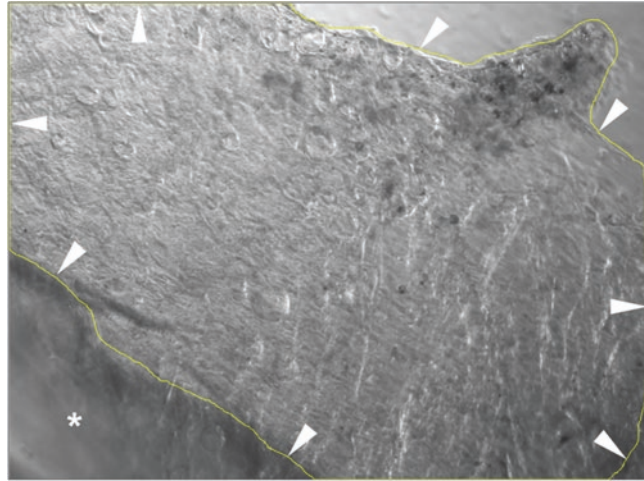
Fig. 6 Defining a region of interest from a transmission microscopy image. The region of interest used should be the greatest contiguous area of retina that is flat and not folded. The ROI in the above image is indicated by white arrows. An area of retina that is curled and out of focus is marked by a white asterisk. This region has not been included in the ROI

analysis. To measure mean grey value, select Analyse>Measure. A results panel will appear displaying the area of the ROI, the mean grey value and the minimum and maximum grey values. The scale within which grey value is measured will depend on the digital resolution of the image in question. Grey value for an 8-bit image for example will range between 0 and 256.

18. The retinal tissue should be orientated so as to be parallel with the base of the tray and suspended so that it lies approximately half way through the depth of the OCT. To achieve this, a pipette tip may be used to create currents within the viscous OCT that carry the fragment to the desired orientation. Avoid touching the tissue directly.

19. As the retinal fragments are very small and transparent, marking the OCT is advisable before proceeding with tissue sectioning. These marks allow the operator to know approximately how much OCT must be shaved before the specimen is encountered.

20. The OCT block may be shaved rapidly down to the preplaced markers. It is useful to have a light microscope on hand to confirm the presence of tissue sections on slides as the OCT block is sectioned further.

Acknowledgments

References

1. Mingozzi F, High KA (2011) Therapeutic in vivo gene transfer for genetic disease using AAV: progress and challenges. Nat Rev Genet 12:341–355

2. Smith J, Ward D, Michaelides M et al (2015) New and emerging technologies for the treatment of inherited retinal diseases: a horizon scanning review. Eye 29:1131–1140

3. Bainbridge JWB, Smith AJ, Barker SS et al (2008) Effect of gene therapy on visual function in Leber's congenital amaurosis. N Engl J Med 358:2231–2239

4. MacLaren RE, Groppe M, Barnard AR et al (2014) Retinal gene therapy in patients with choroideremia: Initial findings from a phase 1/2 clinical trial. Lancet 383:1129–1137

5. Ghazi NG, Abboud EB, Nowilaty SR et al (2016) Treatment of retinitis pigmentosa due to MERTK mutations by ocular subretinal injection of adeno-associated virus gene vector: results of a phase I trial. Hum Genet 135:327–343

6. Mcclements ME, Maclaren RE (2013) Gene therapy for retinal disease. Transl Res 161:241–254

7. Loeb JE, Cordier WS, Harris ME et al (1999) Enhanced expression of transgenes from adeno-associated virus vectors with the woodchuck hepatitis virus posttranscriptional regulatory element: implications for gene therapy. Hum Gene Ther 10:2295–2305

8. Patricio MI, Barnard AR, Orlans HO et al (2017) Inclusion of the woodchuck hepatitis virus posttranscriptional regulatory element enhances AAV2 mediated transduction of mouse and human retina. Mol Ther Nucleic Acids (in press)

9. McCarty DM (2008) Self-complementary AAV Vectors; advances and applications. Mol Ther 16:1648–1656

10. Petersen-Jones SM, Bartoe JT, Fischer AJ et al (2009) AAV retinal transduction in a large animal model species: comparison of a self-complementary AAV2/5 with a single-stranded AAV2/5 vector. Mol Vis 15:1835–1842

11. Asokan A, Schaffer DV, Samulski RJ (2012) The AAV vector toolkit: poised at the clinical crossroads. Mol Ther 20:699–708

12. Tolmachova T, Tolmachov OE, Barnard AR et al (2013) Functional expression of Rab escort protein 1 following AAV2-mediated gene delivery in the retina of choroideremia mice and human cells ex vivo. J Mol Med 91:825–837

13. De Silva SR, Issa PC, Singh MS et al (2016) Single residue AAV capsid mutation improves transduction of photoreceptors in the Abca4−/− mouse and bipolar cells in the rd1 mouse and human retina ex vivo. Gene Ther 23:767–774

14. Johnson TV, Martin KR (2008) Development and characterization of an adult retinal explant organotypic tissue culture system as an in vitro intraocular stem cell transplantation model. Invest Ophthalmol Vis Sci 49:3503–3512

15. Issa PC, Singh MS, Lipinski DM et al (2012) Optimization of in vivo confocal autofluorescence imaging of the ocular fundus in mice and its application to models of human retinal degeneration. Invest Ophthalmol Vis Sci 53:1066–1075

Chapter 22

Visual Acuity Testing Before and After Intravitreal Injection of rAAV2-ND4 in Patients

Bin Li and Chenmian Wu

Abstract

Gene therapy in ophthalmology has developed rapidly, and there has been a breakthrough in the treatment of Leber's hereditary optic neuropathy. After receiving an intravitreal injection of rAAV2-ND4, patients followed up over a certain time period showed a definite increase in visual acuity. Visual acuity testing is critical for assessing the efficacy of rAAV2-ND4 intravitreal injection.

Key words Visual acuity test, Snellen chart, LogMAR chart, Children, Low vision

1 Introduction

Vision is the basic function of the eyes. Decreased visual acuity is the most common loss of visual function caused by a disease affecting the eyes, and is one of its most important manifestations. Therefore, visual acuity testing and recording is a necessary component of all eye examinations and hence, of primary importance.

In the clinic, a newspaper can be placed at an appropriate distance to allow the patient to use both his eyes (while wearing glasses if necessary) to discern large, medium, and small letters in order to assess the visual acuity. Testing is usually performed using a special typeface, such as Jaeger or Law. The best way to test distance vision is with the Snellen chart or a news headline of an equivalent scale. The best distance for testing is at 6 m or 20 feet, unless the patient is unable to discern the letter in the first row.

Visual acuity testing and recording for individuals with low vision can be performed at a shorter distance. If one eye cannot distinguish any letter, it can be recorded as "counting fingers," "hand motion," "light perception," or "no light perception" based on the response of the patient to further vision assessment.

Visual acuity testing before and after rAAV2-ND4 intravitreal injection follows the basic guidelines and procedures of eye examinations.

2 Materials

2.1 Snellen Chart

A Snellen chart is an eye chart that can be used to measure visual acuity. Snellen charts are named after the Dutch ophthalmologist Herman Snellen who developed the chart in 1862 [1].

Visual acuity is determined by the smallest target that can be seen clearly and discerned at a given distance. The commonly used Snellen chart is composed of a series of random letters that become progressively smaller with each row.

2.2 LogMAR Chart

The LogMAR chart is an eye chart composed of alphabet letters invented by the National Vision Research Institute of Australia in 1976 [2]. Its advantage is that a more accurate assessment of visual acuity can be performed, compared to other eye charts (such as the Snellen chart). Thus, the LogMAR chart is widely used by optometrists, ophthalmologists, and vision scientists. In scientific research, especially, the LogMAR chart is recommended for testing the visual acuity (*see* **Note 1**).

2.3 Materials for Children

For children old enough to cooperate, the tumbling E eye chart, the Landolt C eye chart, Cardiff cards and the "E" cube are selected to perform testing methods comparable to the adult Snellen chart.

3 Methods

3.1 Snellen Chart

A quiet environment should be selected for visual acuity testing. The eye chart should be fixed onto a well-lit, clean wall surface at eye level. To avoid glare, there should not be any window in the vicinity of the eye chart. The illumination of the wall should be at least 1/5 of the illumination of the eye chart.

Generally, 6 m, or 20 feet, is considered the ideal distance for testing distance vision. At a distance of 6 m, the light reflected by an object can be assumed to be parallel and generally does not require functional eye movement for accommodation. When testing in a room at a distance less than 6 m, a mirror can be used to increase the testing distance. In addition, the vision chart can be proportionately shrunken to compensate for the insufficient distance in a small room.

During the testing process, the examiner gently places an eye cover over one of the patient's eyes, and then asks the patient to

read the eye chart, recording the smallest row of letters that the patient is able to discern. The result of visual acuity testing is given as a fraction. The numerator represents the distance between the patient and the eye chart, and the denominator represents the distance required by an individual with normal vision to clearly discern the letters. For example, if a patient can clearly see the 20/20 row of letters at a distance of 20 feet, visual acuity is recorded as 20/20. If the patient can clearly see the 20/60 row of letters at a distance of 20 feet, visual acuity is recorded as 20/60. A visual acuity of 20/60 means that the patient can see all four letters from a distance of 20 feet that a normal individual can see from a distance of 60 feet. If the patient cannot identify only one or two letters in a given row, that row can still be recorded. For example, if the patient can read the 20/20 row but cannot identify one of the letters, visual acuity is recorded as 20/20-1.

3.2   LogMAR Chart

As its name suggests, the LogMAR chart records visual acuity as the logarithm of the minimum angle of resolution. If the patient is able to resolve differences as small as 1 min of visual angle, the score is recorded as LogMAR 0; if the patient is able to resolve differences as small as 2 min of visual angle, the score is recorded as LogMAR 0.3 (since $\log_{10}1 = 0$ and $\log_{10}2 = 0.3$).

Each letter has a score value of 0.02 logarithmic units. There are five letters per line, so that each row represents a change in visual acuity of 0.1 logarithmic units. The formula for calculating the score is as follows:

LogMAR visual acuity score = 0.1 + LogMAR of the smallest line distinguishable − 0.02 × (number of letters read).

3.3   Early Treatment of Diabetic Retinopathy Study (EDTRS) Chart

Data from the ETDRS were used to select letter combinations that give each line the same average difficulty, without using all letters on each line.

The ETDRS eye chart has a convenient conversion relationship with the standard logarithmic visual acuity chart and the Snellen eye chart (*see* Table 1). When the visual acuity of the patient is between 20/20 and 20/200, the testing distance should be 4 m; when visual acuity is between 20/200 and 20/400, the testing distance should be 2 m; and when visual acuity is 20/400 or below, the testing distance should be 1 m. The ETDRS eye chart eliminates the inaccuracy associated with methods such as "counting fingers," for expressing visual acuity. Thus, it is selected for testing in patients treated with intravitreal injection of rAAV2-ND4, especially those who suffer from very poor visual acuity (*see* **Notes 1**, and **2**).

Table 1
Comparison of visual acuity scales

Foot	Meter	Decimal	LogMAR
20/200	6/60	0.10	1.00
20/160	6/48	0.125	0.90
20/125	6/38	0.16	0.80
20/100	6/30	0.20	0.70
20/80	6/24	0.25	0.60
20/63	6/19	0.32	0.50
20/50	6/15	0.40	0.40
20/40	6/12	0.50	0.30
20/32	6/9.5	0.63	0.20
20/25	6/7.5	0.80	0.10
20/20	6/6	1.00	0.00
20/16	6/4.8	1.25	−0.10
20/12.5	6/3.8	1.60	−0.20
20/10	6/3	2.00	−0.30

3.4 Visual Acuity Testing in Children

For very young children, only a rough visual acuity assessment is possible. Fortunately, most children stare at light sources and track movement of light sources with both eyes. The accuracy of this type of eye movement can help the examiner better assess the vision of the child. Slightly older children may extend a hand to reach for a toy. Because the size of a toy that can induce a child to extend his hand differs (such as a rolling white ball of different size), the examiner can assess the child's visual acuity to a certain extent. During the examination process, assistance and information provided by the child's mother is invaluable for a smooth testing process (such as the guidance the mother gives the child or the sizes of toys that the child can discern). With the participation of specialty physicians and technicians, even more objective visual acuity testing can be conducted, including prioritizing visual testing methods, electrophysiology, and so on.

Older children are more suited for standard examination. The examiner can select testing methods that are more comparable to the adult Snellen chart, such as Sheridan-Gardiner testing, the tumbling E eye chart, the Landolt C eye chart, Cardiff cards, and so on. The most convenient testing method is to use a cube with

the letter E printed at 6/6 to 6/36 on each of the six sides, and for the examiner to show each side of the cube to the child. This method can be used to train parents of children to distinguish the elements of the tumbling E eye chart, and can be used with illiterate patients or patients not familiar with the alphabet.

The testing in children should be performed with precautions (*see* **Note 3**).

4   Notes

1. As a gene therapy procedure, some Leber's hereditary optic neuropathy patients received intravitreal injection of rAAV2-ND4 [3, 4]. Visual acuity testing was conducted before and after the procedure. The change in visual acuity is an important basis for assessing the effectiveness of rAAV2-ND4 intravitreal injection. In order to obtain even more accurate and credible results, the visual acuity tests in this study have slight modifications from general visual acuity tests as follows:

   Preference for the LogMAR eye chart. The original intent behind the design of LogMAR eye chart was to assess visual acuity with greater accuracy than other types of eye charts. Every row in the LogMAR eye chart has the same number of letters, effectively standardizing letters of different sizes. It uses the Sloan font, in which the differentiation between every letter is similar. The spacing and letter size between rows change logarithmically; hence, the LogMAR eye chart can be used even at nonstandard distances. In addition, the final score from the LogMAR eye chart is calculated based on all the letters that were recognized. The LogMAR eye chart is best adapted to the research objectives of this study and is amenable to statistical analysis. It is believed that LogMAR visual acuity changes greater than 0.3 are significant.

   If the ETDRS eye chart is needed for visual acuity testing of specific patients with low vision, the distance for testing should be consistent before and after rAAV2-ND4 intravitreal injection. For example, if a patient was tested at a distance of 2 m before rAAV2-ND4 intravitreal injection, he/she should be tested at 2 m after the injection and not at 2.5 m or 4 m. This method is expected to eliminate interference from the ability of the eye to accommodate and help the examiner intuitively observe the smallest improvements in visual acuity.

   Use of the Snellen chart is not recommended. There are two reasons for the same. Visual symbols in the Snellen eye chart have different perspectives from different directions. Patients with low vision find it difficult to discern even the largest letters.

   In this study, many patients were children or adolescents [3, 4]. Due to anxiety or a sensitive mental state, some patients may recite

the eye chart from memory in an attempt to obtain a better score on the visual acuity test. Therefore, during multiple tests, different eye charts should be selected in order to eliminate this source of error. During the testing process, using the other eye to peek at the chart is also a common cause for a falsely high visual score. Therefore, in order to ensure the authenticity of the test, the examiner should absolutely prevent this type of behavior from occurring during the visual acuity testing process.

Measures that can be taken to ensure this include the following: (a) using different eye charts to test each eye, each chart having a different order of letters, which can eliminate the error caused by the patient memorizing the eye chart; (b) making sure that the opposite eye is well covered before allowing the patient to see the eye chart, which will prevent the patient from using the opposite eye to peek at the eye chart; (c) making sure that the patient is tested in a quiet environment without onlookers, which will prevent the patient from feeling awkward or unhappy with a low score; and (d) before and after receiving gene therapy, the patient should be tested in an identical environment, including illumination, testing distance, and so on, which will reduce errors introduced by environmental factors.

2. Patients with Leber's hereditary optic neuropathy present with a rapid decline in vision at onset. Many patients already have low vision before receiving rAAV2-ND4 intravitreal injection.

Pupil dilation before vision assessment is not recommended in patients with low vision. Before examination, the refractive status of the patient should be confirmed in order to exclude large errors.

Projection equipment is not recommended for visual acuity testing of patients with low vision. The main reason for this is the low number of, and contrast between, letters available for testing patients with low vision. When using the Snellen eye chart to test patients with low vision, the examiner can hold a handheld eye chart at 10 feet or closer from the patient's eyes.

The dominant and nondominant eyes should be clearly indicated during vision testing of patients with low vision. Amsler grid is the traditional method for assessing the central visual field. Although its sensitivity is suboptimal, it can be used to examine visual acuity in patients with low vision, especially for identifying the dominant eye.

3. In most Leber's hereditary optic neuropathy patients, the onset is in childhood or adolescence. Some patients may exhibit poor results during visual acuity testing, thus increasing the difficulty of testing. Visual acuity testing in children must abide by the following guidelines.

It should be used when the motivation, intelligence, or suitability of the child to be tested is in doubt, because this type of testing does not involve the child differentiating between visual symbols.

If testing is conducted by substituting an independent single letter for an entire row, visual acuity testing results may be inaccurate. For example, for children with disuse amblyopia, the results of testing with a single letter may be 20/40 or 20/50, but may only be 20/200 with an entire row of letters.

When testing using an entire row of letters, the difficulty in discerning different letters in the same row may differ. Usually, L is the letter that is easiest to recognize, and B is the most difficult to recognize. The letters X, C, F, and E are the next most difficult to recognize.

If the child wears glasses, both uncorrected and corrected vision should be measured and compared.

The testing period should not be too long. Children are easily distracted, and often vision testing cannot be completed because loss of interest or attention causes the child to lose concentration.

Children that do not understand the tumbling E eye chart testing method should be trained at home. Parents can use cards or cubes printed with the letter E to train their children. The training process can be made into a game, with the letter E representing a table, and the child being asked which direction the legs of the table are pointing.

References

1. Snellen H (1873) Probe Buchstaben Zur Bestimmung Der Sehschärfe. Peters, Berlin
2. Bailey IL, Lovie JE (1976) New design principles for visual acuity letter charts. Am J Optom Physiol Optic 53:740–745
3. Wan X, Pei H, Zhao MJ et al (2016) Efficacy and safety of rAAV2-ND4 treatment for Leber's hereditary optic neuropathy. Sci Rep 6:21587
4. Yang S, Ma SQ, Wan X et al (2016) Long-term outcomes of gene therapy for the treatment of Leber's hereditary optic neuropathy. EBioMedicine 10:258–268

Chapter 23

Recording and Analysis of the Human Clinical Electroretinogram

Mathieu Gauvin, Allison L. Dorfman, and Pierre Lachapelle

Abstract

The electroretinogram (ERG) represents the biopotential that is produced by the retina in response to a light stimulus. To date, it remains the best diagnostic tool to objectively evaluate the functional integrity of the normal or diseased retina. In the following pages we briefly review the necessary requirements in order to record and analyze the conventional clinical ERG.

Key words Electroretinogram, ERG methods, ERG stimulus, ERG analysis, Human

1 Introduction

In contrast to the ECG, the ERG is an evoked potential meaning that a stimulus (usually a flash of light) is required to generate it. This electrical potential is usually picked up with an active electrode placed on the eye (i.e., the cornea or conjunctiva) or on the skin around the eye. The ERG signal is usually obtained in photopic (or light-adapted) and scotopic (or dark-adapted) conditions to assess cone- and rod-mediated function, respectively [1, 2]. The response thus obtained (*see* Fig. 1a) is usually quantified by measuring the amplitude and timing of its two major components, namely the a-wave (the short latency negative wave) which signals the activation of the photoreceptors and the b-wave (the larger positive wave that follows) which is claimed to arise from the combined activities of the bipolar and Müller cells [3, 4]. Low voltage high-frequency oscillations are also seen on the ascending limb of the b-wave. They are referred to as the oscillatory potentials (OPs), and their origin remains debated [5, 6].

Retinal function can be altered as a result of different pathological processes which may or may not alter the ERG, and consequently, the ERG can provide significant diagnostic information regarding a variety of retinal disorders. Moreover, the
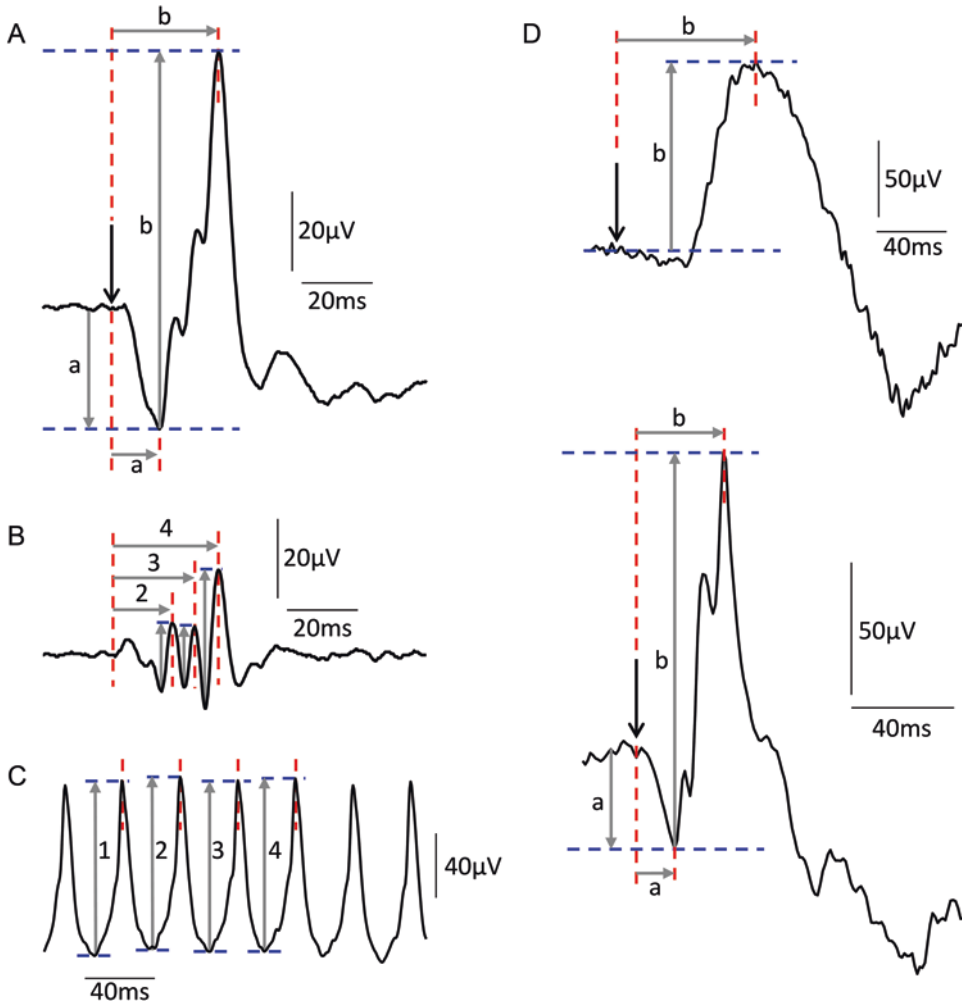
Fig. 1 Representative example of the the traditional time domain measurements of the photopic a- and b-waves (**a**) and OPs (**b**). Measurements of the a- and b-waves are indicated by the corresponding letter (**a**), while that of OP2, OP3 and OP4 are indicated by the corresponding numbers (**b**). Amplitude and peak time measurements are illustrated by the vertical and horizontal arrows, respectively. Measurement of the first four peaks of the photopic flicker ERG (**c**). Measurements of peaks 1, 2, 3, and 4 are indicated by the corresponding numbers (**c**). Measurements of the a- and b-waves amplitude and peak time of the scotopic ERG (**d**: pure-rod ERG; **e**: mixed rod-cone ERG)

ERG can also be used to monitor disease progression, evaluate retinal toxicity associated with pharmaceutical agents, or to assess the role of specific receptors, molecules or genes on retinal function [7–9]. Of interest, since 1989, the International Society for Clinical Electrophysiology of Vision (ISCEV) has introduced basic guidelines (latest update in 2015 [10]) regarding the materials and suggested protocols for recording the full-field ERG [10]. The latter recommendations have been instrumental in harmonizing visual electrophysiology clinics

and laboratories worldwide. The fundamental materials and methods necessary for proper recording of the full-field ERG will be presented in the following pages.

2   Materials

A list of specialized equipment and supplies necessary for carrying out the methods described in Subheading 3 is provided in this section.

2.1   Electrodes

1. Active electrodes and connectors (*see* **Notes 1** and **2**).
2. Reference electrodes and connectors (*see* **Notes 1** and **2**).
3. Common (ground) electrodes and connectors (*see* **Notes 3** and **2**).

2.2   Recording Devices and Light Stimuli

1. Xenon or light-emitting diode (LED) flash (*see* **Note 4**).
2. Spherical reflective dome, a.k.a. Ganzfeld dome (*see* **Note 4**).
3. Signal Amplifiers (*see* **Note 4**).
4. Computer and supporting software (*see* **Note 4**).

2.3   Calibration and Instruments

1. Photometer (*see* **Note 5**).
2. Function generator (*see* **Note 6**).

2.4   Supplies and Accessories

1. Alcohol swabs (*see* **Note 7**).
2. Abrasive gel (*see* **Note 7**).
3. EEG gel or paste (*see* **Note 7**).
4. Dilating eye drops (*see* **Note 8**).
5. Anaesthetic eye drops (*see* **Note 9**).
6. Cotton-swab.
7. Petroleum jelly.
8. Medical Gauze.
9. Medical tape.
10. Saline water.
11. Small cleaning brush and soap.

3   Methods

3.1   Preparation of Human Subjects

1. Begin with a thorough explanation of the procedures to be carried out on the subject/patient. For all research subjects, ensure that consent is obtained with the use of institutional ethics board-approved consent/assent (in the case of pediatric age-groups) forms. In both subjects and patients, it is important to take note of any medications either currently being

taken or taken in the past, as certain medications have been shown to adversely affect the ERG (*see* **Note 11**).

2. In order to reduce variability in pupil diameter as well as to maximize the amount of light which will reach the retina, pupils should be maximally dilated prior to beginning ERG testing, and pupil size noted. Dilation drops usually take effect within 30 min or so with 1% tropicamide ophthalmic solution, and sometimes more rapidly with phenylephrine ophthalmic solution. The effects of dilation can last over a few hours, or sometimes more. In addition, side effects as a result of dilation also exist (*see* **Note 8**).

3. Prior to positioning of the electrodes, the subject is prepared (*see* **Note 7**) by gently cleaning the skin using an alcohol swab in the regions where skin electrodes will be pasted (*see* point 4 for positions). An exfoliating gel is subsequently used on the same areas and is applied with either a medical gauze pad or a cotton swab in order to remove dead skin which, if not removed, could ultimately prevent good contact with the electrodes.

4. Once the skin has been cleaned, reference electrodes can be prepared for pasting onto the skin. The first of three large gold-cup electrodes should be filled with a generous amount of conductive electrode paste (*see* **Notes 1** and **3**). The back of the electrode should be covered with the paste as well, and then firmly pressed onto a small piece of medical gauze. The cup portion of the electrode should then be pasted onto the temple and secured with medical grade tape. The latter will be used as the first of two reference electrodes. For bilateral ERG recordings, this last step should be repeated, though now the electrode will be placed on the opposite temple. Each reference electrode will be used for the eye on the same side (e.g., the left reference electrode will be the left eye reference and vice-versa). Lastly, the same technique is used for placement of the ground (common) electrode, which should be firmly positioned in the middle of the forehead or earlobe.

5. You may now proceed to the installation of the active DTL electrodes (*see* **Note 1** and **3**). Ask the patient to tilt the head back (and preferably to place it against the headrest if there is one), to open the eyes as wide as possible, and to maintain their gaze in the superior position. Secure the first side of the DTL electrode nasally near the internal canthus using a small piece of medical tape. Then, using one of your hands, delicately extend the lower lid to expose the sclera, and place the fibre (loosely) on the exposed sclera using your other hand. You may use a wet cotton-swab to help with the positioning or to move the eyelashes out of the DTL fibre's way.

6. Once in position, ask the subject to blink several times, and the DTL fibre should now be naturally sitting deep inside the lower lid conjunctival sac (*see* **Note 9**). This position yields minimal DTL electrode displacement (from eye movements or blinks) and prevents corneal abrasion as the DTL will not be in contact with the cornea (*see* **Note 10**). Now, take the other side of the DTL fibre which is coated in double sided medical tape and stick it right over the reference electrode montage. Once this is done, the DTL fibre that remains will need to be rolled around the wedged out portions of a small gold-cup electrode (we use a gold-plated 5 mm cup electrodes; Grass Technologies, Warwick, RI). The small gold cup with the DTL that has been rolled around it can then be secured with a piece of medical tape over the tape that is already covering the reference electrode montage. To electrically isolate the exposed DTL section that is not on the eye, you may apply a little bit of petroleum jelly on the skin near the exposed DTL fibre (e.g., between the external canthus and the temple). If the recording is being performed bilaterally, repeat the above steps to install the second active DTL electrode.

7. All of the electrode wire connectors can now be plugged into the respective amplifier inputs (*see* **Notes 1** and **2**). In order to facilitate placement of the head with respect to the Ganzfeld stimulator, the leads can be placed at the back of the patient's/subject's head.

3.2   ERG Recordings

1. Before proceeding with the ERG recording, electrode impedance should be verified for each channel in use (*see* **Note 12**). If the impedance is within acceptable limits (i.e., <5 kΩ), proceed directly to **step 3**. If the impedance is too high, attempt steps defined in **Notes 7** and **12**.

2. Subjects/patients should be assisted with correct placement of the chin on the chin rest (*see* **Note 13**). One also needs to ensure that the head rest on the chair is properly height adjusted, so that the subject/patient is easily able to rest their head throughout the recording session if/when necessary. The latter also helps to ensure that minimal movement will take place throughout the recording which will thus minimize potential unwanted electrode movement or displacement. If the person carrying out the recording is seated in another room (i.e., preferred setup), advise the subject/patient that communication will take place with the use of an intercom system through which constant contact will be kept with the subject/patient being tested.

3. Advise the subject/patient that they are required to fixate on the fixation mark located directly in the Ganzfeld (usually a

small red LED) (*see* **Note 14**). Proper placement and fixation should be verified through the camera which is built in to most systems. Should any further adjustments to positioning be required (i.e., adjustment of the chair height, centering of the face with respect to the Ganzfeld, etc.), this must be done prior to the commencement of the ERG recording.

4. Once the above has been achieved, advise the subject/patient that recording will begin. Once the recording has begun, anesthetic drops (*see* **Note 9**) can be administered on the cornea in the event that the subject/patient is noted to blink frequently to the point where myoclonic artifacts are visualized to contaminate the response.

5. Given that the patients/subjects are presumably coming into the clinic from a light environment, it is preferable to begin with recording of the photopic (light adapted) ERG for assessment of cone function. To achieve the latter, first ensure that the background light is turned on inside the Ganzfeld with a background intensity set to 30 cd/m^{-2} (*see* **Note 5**) to adequately desensitise the rod photoreceptors. Note that the lighting in the room should be off. The gain of the amplifier's channels should be sufficiently high to bear a measurable response, and the recording bandwidth should be set to 0.3–500 Hz for the ERG and to 75–500 Hz for the oscillatory potentials (*see* **Note 15**).

6. Using the supporting acquisition software (as per protocols developed either by or with the help of the supplier), begin the recording. The ISCEV standards recommend the use of white light flashes set at 3 cd.s.m.$^{-2}$ in intensity in order to elicit the photopic ERG (*see* **Note 5**). Average as many responses as desired (we usually average at least 10–15 responses) until a clean measurable signal is obtained, such as that exemplified in Fig. 1a (*see* **Note 16**). The latter can be increased to an average of 100 flashes or so in patients with advanced retinal degeneration, but due to the severely attenuated amplitude of their responses (in some cases), it might be difficult or impossible to obtain a clear recording in some patients. One can also repeat **step 6** using different stimulus intensities in order to obtain the photopic luminance-response function curve (*see* **Note 17**).

7. Once the photopic ERG recordings are completed and the traces have been saved, the 30 Hz flicker ERG (*see* an example of tracing in Fig. 1c) can be recorded next, given that it too is a light-adapted response.

8. Following the latter, and once the traces are saved, the scotopic recording protocol should be used. The background light in the Ganzfeld should turn off automatically once the scotopic protocol is opened, and the lights in the room will remain

off as well (just as they were for the photopic and flicker ERG protocols). Following a period of dark-adaptation (at least 20 min), record an ERG using a dim stimulus intensity of 0.01 cd.s.m.$^{-2}$ (i.e., to obtain the pure rod response, as illustrated at Fig. 1d) and then obtain another ERG using a brighter intensity of 3 cd.s.m.$^{-2}$ (i.e., to obtain the combined responses of both the rod and cone systems; rod dominated, as illustrated at Fig. 1e). Again, **step 8** can be repeated (i.e., without repeating dark-adaptation) using additional stimulus intensities to obtain the scotopic luminance-response function curve (*see* **Note 17**).

9. Once all recordings have been completed and saved, the electrodes can be delicately removed. The latter is much easier on the subject/patient if a wet towel is used, as the medical tape can occasionally be somewhat difficult to remove. Any remaining electrode paste can be removed simultaneously.

10. If reusable gold-cup electrodes are being used (*see* **Notes 1 and 3**), they should now be cleaned using gentle soap and a brush (a toothbrush works quite well) to remove all residual conductive paste.

11. Proceed with ERG analysis (*see* Subheading 3.3).

3.3 ERG Analysis

1. In clinics, the ERG analysis is generally based on the amplitude (usually microvolts) and peak time (milliseconds) of the a-wave, b-waves, and OPs evoked in both light (**step 4** in the previous section) and dark (**step 5** in the previous section) adaptation states. The functional diagnosis of retinopathies is usually confirmed once the amplitude and/or the peak time of the a-wave and/or b-wave and/or OPs are significantly altered (Also *see* **Note 8**) [4, 10, 11]. However, in order to achieve this goal, it is important to establish a normative database with responses obtained from age-matched control subjects.

2. By convention (*see* [10]), the a-wave amplitude should be measured from the prestimulus baseline to the most negative trough of the ERG that precedes the b-wave (Fig. 1a). Likewise, the b-wave is measured from the a-wave to the most positive peak that follows it (Fig. 1a). Similarly, the amplitude of each OP is measured from trough to peak (Fig. 1b). The peak time of the a- and b-waves is measured from flash onset to the through/peak of the a- and b-waves (Fig. 1c). Furthermore, the peak time of each OP is measured from flash onset to the peak of each respective OP (Fig. 1d).

3. Additional analyses can be performed in the time-frequency domain. These advanced analyses have previously been shown to be diagnostically relevant (*see* **Note 18**).

4   Notes

1. The ERG records potential differences, and hence, a minimum of two electrodes is needed to record the signal. Namely, an active electrode connected to a positive input of the recording system, and a reference electrode connected to a negative input. In our clinic, we use the Dawson, Trick, and Litzkow (DTL) conductive fibre electrode (27/7 X-Static silver-coated conductive nylon yarn, Noble Biomaterials Inc.) as the active electrodes, whereas skin electrodes (Grass gold-plated 1 cm cup electrodes; Grass Technologies) are used as the reference electrodes.

2. An additional electrode should be used as a ground electrode (also referred to as the common electrode) and should be plugged into the common input of the recording system. It provides electrical protection to the patient. In our clinic, a skin electrode (Grass gold-plated 1 cm cup electrodes; Grass Technologies) is used for the common electrode.

3. Note that beside the electrode types mentioned in **Notes 1** and **2**, other types of electrodes can be used to obtain high-quality recordings (*see* the latest version of the ISCEV standards for details [10]). For example, in young infants (or apprehensive patients/subjects) a skin electrode pasted on the lower lid can be used as the active electrode. However, use of the latter will generate noisier responses. Normally an increase in the number of averaged responses should help remove unwanted noise (also *see* **Note 19**). While no visual electrophysiology clinic or laboratory is bound to the use of any one type of active recording electrode, it is important to note that they cannot be used interchangeably as different electrodes have been shown to yield responses of different amplitudes [12, 13]. Consequently, it is important to ensure that results obtained with the use of a particular electrode type are compared to others collected using the same electrode type. Similarly, when considering findings reported in the literature, take note of the active electrode in use so that fair comparisons can be made.

4. Currently, most modern ERG recording systems are digital and include the Ganzfeld stimulator (which encompasses the stimulating xenon/LED flash stimulus, the background light and the reflective dome), amplifiers, bandpass filters, computer and supporting software as a whole integrated system. In our clinic, we have used the Espion (Diagnosys LLC) and UTAS (LKC Technologies) visual electrophysiology recording systems. Note that ISCEV standards also include some guidelines regarding technical requirements of ERG recording equipment [10].

5. The intensity of the background light and/or flash stimulus might be altered with time due to the normal wear and tear. It

is therefore imperative that the user periodically callibrates the flash stimulus and background using an apropriate photometer. All measurements should be taken where the eye would normally be located in a real recording context. In our clinic, we use the IL1700 (International Light Technologies). Systems are also, on occasion, self-calibrating and will thus notify the user if a problem is detected with the stimulator, amplifier or otherwise. For additional guidelines and details, the user can consult the manufacturer of their system as well as the latest ISCEV technical notes [14].

6. You may use a function generator (such as a sine wave generator) to test or debug the amplifier function. Simply connect the negative and positive outputs of the generator to the reference and active electrodes amplifier's inputs. Connect the ground of the generator to the amplifier's common electrode input. Set the output voltage of the function generator to its minimum level (i.e., usually a few millivolts). Turn on the recording system, set the gain of the amplifier to the smallest gain value, and start a new recording session. Activate the function generator and compare the wave amplitude set on the generator and the one displayed on the recording system. If differences are observed, there is likely a problem with either the amplifier or the electrodes. Replace the electrodes. If there is still a problem, call your ERG system supplier for technical assistance.

7. To optimise ionic current flow and decrease the impedance between the skin electrodes and the surface of the skin, EEG gel or paste (we use the Ten20 electrode paste; Weaver and Company) must be utilised together with proper skin preparation. Skin preparation includes cleaning with an alcohol swab and the use of an abrasive gel (we use NuPrep gel; Weaver and Company) to remove the natural layer of dead skin.

8. One very rare side effect of dilation drop is spontaneous angle-closure glaucoma. Because of this inherent risk, an ophthalmologist should look at the depth of the anterior chamber of the patient' eyes before dilation (to confirm that the subject/patient is risk-free). Beyond helping to determine if the subject or patient is a suitable candidate for dilation, the ophthalmological exam is necessary, in conjunction with the ERG, in order to obtain the most accurate diagnosis possible. It is for this reason that the ERG is most frequently looked at alongside family history, patient's complaints, fundus imaging, color vision testing, OCTs and visual fields, for example.

9. While the DTL electrode is widely well tolerated, on very rare occasions, some subjects might find it slightly uncomfortable, which might results in frequent blinkings. In those cases, a single drop of anaesthetic eye drops [we use Alcaine (Alcon Inc.)] can be employed.

10. Each electrode should maintain good contact, positioning and acceptable impedance (<5 kΩ) throughout the recording session (also *see* **Note 20**). Note that DTL electrode movement can cause fluctuation of the ERG signal and can consequently affect the resulting amplitude. As such, we recommend that the experimenter confirm the proper positioning of the DTL by visual inspection prior to and at the end of the recording [15]. Should any shifting have occurred throughout the recording session, the latter should be noted.

11. Given that the menstrual cycle has been shown to contribute to variations in the ERG amplitude [16], ask your female patients about the dates pertaining to her last menstrual period and note this for comparison with future clinical ERG testing.

12. Before recording, the electrode impedances should be measured (i.e., automatically measured and displayed on most ERG systems), and baseline traces should be observed to ensure that the noise level is acceptable. If the noise is abnormally high in amplitude, the experimenter might try to unplug/replug the electrodes' wires into the respect inputs of the amplifier and verify the impedance again. If the impedance is still high, it is possible that there is a troublesome contact with one of the electrodes and it is best to try and replace one or more (if necessary) of the electrodes. If nothing solves the problem, the electrodes can be disconnected from the patient and fully emerged in saline (NaCl) water while connected to the amplifier to simulate an optimal electrode contact. The latter will allow for the identification of a faulty electrode through verification of baseline tracings. Faulty electrodes should subsequently be discarded, and if electrodes are not the problem, consider troubleshooting amplifiers, connectors and other components of the recording system. Seek assistance from your supplier if necessary.

13. For pediatric electrophysiological testing, the young subject/patient is often seated on the parent or guardian's lap. In this case, ensure that the parent or guardian's head is resting comfortably against the headrest of the medical chair, and have the Ganzfeld placed as close as possible to the subject/patient. Many Ganzfeld units are equipped with a mobile arm that allows for simplified movement of the unit to accommodate candidates for testing that are too young to maintain their chin on the chin rest. A Ganzfeld which is easily moved about the mobile arm is also especially useful for testing infants who are too young to have head control, where they can remain in the arms of the person supporting them while the Ganzfeld is brought as close to the face as it would have been had they been positioned on the chin-rest. In fact, a mobile Ganzfeld arm has even been used to render the ERG recording system compatible

in the operating room, where it can be used at the patient's bedside during surgical procedures. Furthermore, having the Ganzfeld unit resting on a mobile table (on wheels) can also be advantageous for use in subjects/patients that are wheelchair bound, where, when used in combination with the mobile arm of the Ganzfeld, the subject/patient need to be moved out of their chair. The latter set-up makes testing possible for virtually any subject or patient coming into the clinic or laboratory.

14. Most modern ERG recording systems house an infrared camera inside the Ganzfeld which allows for convenient monitoring of the subject/patient and to determine whether they are blinking excessively, not fixating or closing their eyes. If any of the latter occurs, pause the recording, inform the subject/patient or guardian and allow for some time to blink or rest. Resume recording thereafter.

15. Selecting the proper filter bandwidth is important for signal acquisition and for noise reduction. The sampling frequency should be set to at least two times the highest frequency of the signal. If using a bandpass of 0.3–500 Hz, the maximal frequency will be approximately 500 Hz, and the sampling frequency should thus be of 1000 Hz (1000 data points per second) to reproduce a good quality waveform. For additional details regarding the amplifier gains and bandpass filter parameters, the latest ISCEV standards can be consulted [12].

16. Some systems will allow the clinician/experimenter to reject responses from the average in real time. You may thus remove any responses that are out of range or contaminated by eye blinks. This will lead to a cleaner recording. The latter can also be achieved post hoc.

17. The relationship between the amplitude of the ERG components and the flash luminance can also be used to derive meaningful clinical information. It is well known that the use of progressively brighter stimuli will result in a linear increase of the scotopic and photopic a-wave amplitudes [17, 18]. Likewise, the amplitude of the scotopic b-wave gradually augments with progressively brighter flash intensities, following a sigmoidal luminance-response function, which can be fit using the Naka-Rushton eq. [19]. In contrast, the photopic b-wave gradually increases, reaches a maximal value and then decreases before reaching a plateau [17, 20]. The above luminance-response function curve is referred to as the photopic hill and can be altered as a result of several retinal conditions, and as such is used for clinical diagnosis [21].

18. Of interest, our laboratory recently identified novel ERG descriptors derived from the discrete wavelet transform (DWT). These novel descriptors are physiologically meaningful, diagnostically relevant and usable over a wide range of signal amplitudes and

morphologies. Selected descriptors can quantify distinct retinal events (such as the ON and OFF retinal pathway, for example), and can be independently affected by a given disease process. These descriptors can be used to better characterize the different ways by which the ERG can be altered as a result of normal and pathological conditions [7, 22–25].

19. When the 50/60-cycles power line interference corrupts the response, avoid the use of a notch filter. Rather, try to twist the electrode cables (by braiding the wires), which is an efficient means by which to reduce this kind of noise. To reduce electromagnetic interferences even more, averaging responses at random interstimulus interval periods can also be efficient.

20. Note that excessively long recording time (greater than 2 h) may cause artefacts due to drying conductive gel and/or fatigue and anxiety in the subject/patient. Resting or blinking time can be incorporated as required.

References

1. Sieving PA, Murayama K, Naarendorp F (1994) Push-pull model of the primate photopic electroretinogram: a role for hyperpolarizing neurons in shaping the b-wave. Vis Neurosci 11:519–532

2. Miller RF, Dowling JE (1970) Intracellular responses of the Muller (glial) cells of mudpuppy retina: their relation to b-wave of the electroretinogram. J Neurophysiol 33:323–341

3. Hood DC, Birch DG (1990) A quantitative measure of the electrical-activity of human rod photoreceptors using electroretinography. Vis Neurosci 5:379–387

4. Heckenlively JR, Arden GB (2006) Principles and practice of clinical electrophysiology of vision. MIT Press, Cambridge, MA

5. Yonemura D, Tsuzuki K, Aoki T (1962) Clinical importance of the oscillatory potential in the human ERG. Acta Ophthalmol Suppl 70:115–123

6. Lachapelle P (1994) The human suprathreshold photopic oscillatory potentials: method of analysis and clinical application. Doc Ophthalmol 88:1–25

7. Gauvin M, Chakor H, Koenekoop RK et al (2016) Witnessing the first sign of retinitis pigmentosa onset in the allegedly normal eye of a case of unilateral RP: a 30-year follow-up. Doc Ophthalmol 132:213–229

8. Fornaro P, Calabria G, Corallo G (2002) Pathogenesis of degenerative retinopathies induced by thioridazine and other antipsychotics: a dopamine hypothesis. Doc Ophthalmol 105:41–49

9. Nakamura M, Skalet J, Miyake Y (2003) RDH5 gene mutations and electroretinogram in fundus albipunctatus with or without macular dystrophy – RDH5 mutations and ERG in fundus albipunctatus. Doc Ophthalmol 107:3–11

10. McCulloch DL, Marmor MF, Brigell MG et al (2015) ISCEV Standard for full-field clinical electroretinography (2015 update). Doc Ophthalmol 130:1–12

11. Miyake Y (2006) Electrodiagnosis of retinal disease. Springer-Verlag, Tokyo

12. Lachapelle P, Benoit J, Little JM et al (1993) Recording the oscillatory potentials of the electroretinogram with the DTL electrode. Doc Ophthalmol 83:119–130

13. Coupland SG, Janaky M (1989) ERG electrode in pediatric patients: comparison of DTL fiber, PVA-gel, and non-corneal skin electrodes. Doc Ophthalmol 71:427–433

14. Brigell M, Bach M, Barber C et al (2003) Guidelines for calibration of stimulus and recording parameters used in clinical electrophysiology of vision. Doc Ophthalmol 107:185–193

15. Hebert M, Vaegan, Lachapelle P (1999) Reproducibility of ERG responses obtained with the DTL electrode. Vis Res 39:1069–1070

16. Brule J, Lavoie MP, Casanova C et al (2007) Evidence of a possible impact of the menstrual cycle on the reproducibility of scotopic ERGs in women. Doc Ophthalmol 114:125–134

17. Rufiange M, Rousseau S, Dembinska O (2002) Cone-dominated ERG luminance-response function: the Photopic Hill revisited. Doc Ophthalmol 104:231–248

18. Levin LA, Di Polo A (1966) Ocular neuroprotection. Marcel Dekker, New York

19. Naka KI, Rushton WA (1966) S-potentials from colour units in the retina of fish (Cyprinidae). J Physiol 185:536–555

20. Wali N, Leguire LE (1992) The photopic hill: a new phenomenon of the light adapted electroretinogram. Doc Ophthalmol 80:335–345

21. Garon ML, Dorfman AL, Racine J et al (2014) Estimating ON and OFF contributions to the photopic hill: normative data and clinical applications. Doc Ophthalmol 129:9–16

22. Gauvin M, Lina JM, Lachapelle P (2014) Advance in ERG analysis: from peak time and amplitude to frequency, power, and energy. Biomed Res Int 2014:246096

23. Gauvin G, Little JM, Lina JM et al (2015) Functional decomposition of the human ERG based on the discrete wavelet transform. J Vis 15:14

24. Gauvin M, Dorfman AL, Trang N et al (2016) Assessing the contribution of the oscillatory potentials to the genesis of the photopic ERG with the discrete wavelet transform. Biomed Res Int 2016:2790194

25. Gauvin M, Sustar M, Little JM et al (2017) Quantifying the ON and OFF contributions to the flash ERG with the discrete wavelet transform. Transl Vis Sci Technol 6:3

Chapter 24

Recording and Analysis of Goldmann Kinetic Visual Fields

Mays Talib, Gislin Dagnelie, and Camiel J.F. Boon

Abstract

Goldmann kinetic perimetry is a commonly used method of evaluating the peripheral visual field. Ongoing gene therapy trials have targeted the central retina, but have nonetheless often included Goldmann kinetic perimetry as part of extensive preinterventional and postinterventional assessment. Future gene therapy trials may target the entire retina through intravitreal injections, as have drug therapeutic trials, further necessitating the evaluation of function across the entire retina. In the following pages, we will briefly review the necessary steps to perform and quantify the visual field, using the conventional Goldmann perimeter and the Field Digitizer software (version 4.20; Johns Hopkins Technology Ventures, Baltimore, USA), respectively.

   Key words Goldmann visual field, Kinetic perimetry, Peripheral visual field, Quantitative visual field analysis

---

1   Introduction

One of the principal descriptors of visual function is the visual field, i.e., the area within which a subject can obtain visual information while steadily fixating the gaze on a central point. A decrease in the visual field can be one of the earliest symptoms in several inherited retinal diseases, including retinitis pigmentosa [1, 2]. The process of recording the visual field is called perimetry. Different forms of perimetry include static perimetry, where stationary stimuli are projected at different locations, typically in the central 10° or 30° radius of the visual field, and local intensity thresholds are measured by modifying the light intensity of the stimulus based on the patients' response. In kinetic perimetry, stimuli of fixed size and intensity are moved by the examiner from nonseeing areas of the visual field into seeing areas of the visual field, measuring the full peripheral and central visual field. A commonly used strategy for assessing the peripheral visual field in ongoing natural history studies and gene therapy trials is Goldmann perimetry [3–6], but in recent years modern semiautomated perimeters such as the

Octopus 900 have also been used. The Goldmann perimeter is a hemispheric dome with a 30 cm radius and fixed background light intensity (luminosity) of 31.5 apostilb (10 cd/m²) [7]. The perimeter contains a mobile target of changeable size and luminosity that is projected onto the inside of the bowl and can be moved in all directions by moving a pantograph arm. The patient presses a buzzer when the target first becomes visible or disappears and reappears; this response is used to determine the boundaries of the visual field for that particular target; such a closed contour boundary is called an isopter (i.e., line of equal visibility). A built-in telescope allows for the direct viewing of the patient's fixation. The pantograph arm moves across a paper chart on the operator side of the perimeter, allowing the operator to register the target position (*see* **Note 1**).

Although ongoing subretinal gene therapy trials have targeted the central retina [3, 8, 9], possible intravitreal gene therapy administration in the future could target the whole retina [10, 11], further necessitating the Goldmann visual field (GVF) to evaluate the potential therapeutic effect. In an oral 9-cis-retinoid trial, aimed at targeting the whole retina, treatment effect on the visual field size was demonstrated with GVFs in several patients [12]. In the remainder of this chapter we will be referring to the GVF, but it should be understood that the same procedures can be applied to kinetic visual fields recorded with other perimeters.

In clinical practice, the clinician requesting the GVF is predominantly interested in qualitative analysis of the visual field and changes therein. In a (gene) therapeutic trial setting, as seeing retinal area becomes a potential outcome measure to be evaluated, a researcher may wish to perform quantitative analysis of the visual field, transformed to retinal area. Several methods have been developed to quantify the seeing visual field area and scotoma size, using computer algorithms [13–17]. In this chapter, we will describe the use of the Digital Field Analyser software developed by Dagnelie [13], which converts areas in the GVF chart to retinal areas by taking into account the distortions associated with plotting perimetry data on a planar chart, while the stimuli were presented in a spherical bowl, as well as the nonconformity of the human eye to the perimeter bowl. This programme digitizes isopters in the visual field map, converting the enclosed area into the retinal seeing or non-seeing area in mm²; it has been used in several studies on the natural history of inherited retinal dystrophies associated with mutations in candidate genes for (gene) therapy [5, 6, 12]. Minimal training of the digitizing researcher is required in order to reliably determine the isopter size [18], and test–retest variability was shown to be limited in a clinical retinitis pigmentosa population [19]. The essential materials and methods required for the proper performance and plotting of the GVF, and the subsequent digitization of the GVF will be presented in this chapter.

2 Materials

2.1 Performing the Goldmann Kinetic Perimetry

1. The Goldmann perimeter.
2. Wide-aperture lenses for correcting the refractive error, especially up to 30° eccentricity.
3. Visual field plotting chart.
4. Color markers, to mark the target isopters: blue (V4e), red (III4e; I3d), black (I4e), green (I3e).
5. An eye patch, in order to test each eye individually. Alternatively, use 5 × 5 cm gauze.
6. Micropore tape.

The available targets (light stimuli) vary in size and luminance. The Roman numbers indicate the stimulus size. The available stimulus sizes are depicted in Table 1. The Arabic numbers and the lower case letters indicate the light intensity. For each Arabic number lower than 4, the light intensity is reduced by 5 dB (Table 2). For each lower case letter earlier in the alphabet than e, the light intensity is reduced by 1 dB. The stimulus luminance for 0 dB value is 4800 apostilb, which equates to a V4e target calibrated at 1000 apostilb [7].

Table 1
Stimuli sizes for the Goldmann perimeter

Target	V	IV	III	II	I	0
Size (mm^2)	64	16	4	1	0.25	0.0625

Table 2
Luminance values in apostilbs for the Goldmann perimeter

Object	4	3	2	1
e	1000	315	100	31.5
d	800	250	80	25
c	630	200	63	20
b	500	160	50	16
a	400	125	40	12.5

1000 apostilb (asb) = 315 cd/m^2; 315 asb = 100 cd/m^2; 100 asb = 31.5 cd/m^2; 31.5 asb = 10 cd/m^2

3 Methods

3.1 Preparation of the Patient or Subject

1. Prior to testing, instruct the patient on the purpose and process of the examination. Explain that you will be moving a white light stimulus into his/her field of vision, while the patient fixates on the central point, and that the patient should indicate when he sees the stimulus by pushing the attached button box. When pushing the button, the patient should feel or hear a click. Newer button boxes may produce a clearly audible buzz. Explain to the patient that this test evaluates their peripheral field, and that they should therefore not wait until they see the stimulus sharply and clearly, but that they should push the button as soon as they see the light stimulus. Explain that some stimuli may appear brighter or dimmer than others.

2. Measure and note the pupil diameter.

3. The fixation distance for the Goldmann perimeter is 30 cm, i.e., reading distance; especially in pseudophakic and severely presbyopic subjects this requires a near add of ~3 diopters (D). In calculating the trial frame addition, a minor lens addition may be sufficient in emmetropic subjects (Table 3) [7, 20]. For patients with astigmatism greater than 1 D, a second lens may be added, correcting for the full cylindric error. If the astigmatism is less than 1 D, use the spherical equivalent of the refractive error. Some myopic patients may perform the examination unaided or with their contact lenses [21]. Place any addition in the lens holder of the perimeter. The patient's own reading glasses should *not* be used during testing, as the frame may obstruct a portion of the visual field, and as the reading glasses are intended for the patient's preferred reading distance, which may not be at 30 cm.

4. Cover one eye using an eye patch or 5 × 5 cm gauze and micropore tape, making sure that there are no nasal or lateral openings (*see* **Note 2**). Start with the eye that has (subjectively) better function. In the case of equal function, start with the right eye.

5. Adjust the chin rest, shown in Fig. 1a, such that the center of the patient's eye is viewed through the telescope (Fig. 1b, green arrow). From the patient's viewpoint, this means that the chinrest is positioned completely to the left in order to view the right eye, and vice versa for the left eye. From the examiner's viewpoint, this means that the chinrest is positioned to the right side of the telescope in order to view the right eye, and to the left side of the telescope in order to view the left eye.

6. Place the patient's head against the forehead strap. The sagittal axis of the patient's head must be vertical, i.e., perpendicular to

Table 3
Trial frame lens addition by age

Age (years)	Add to distance refractive error (diopters)
30–39	+1.00
40–44	+1.50
45–49	+2.00
50–54	+2.50
55–59	+3.00
≥60	+3.25

Source: Rowe et al. [23]; Barton et al. [20]
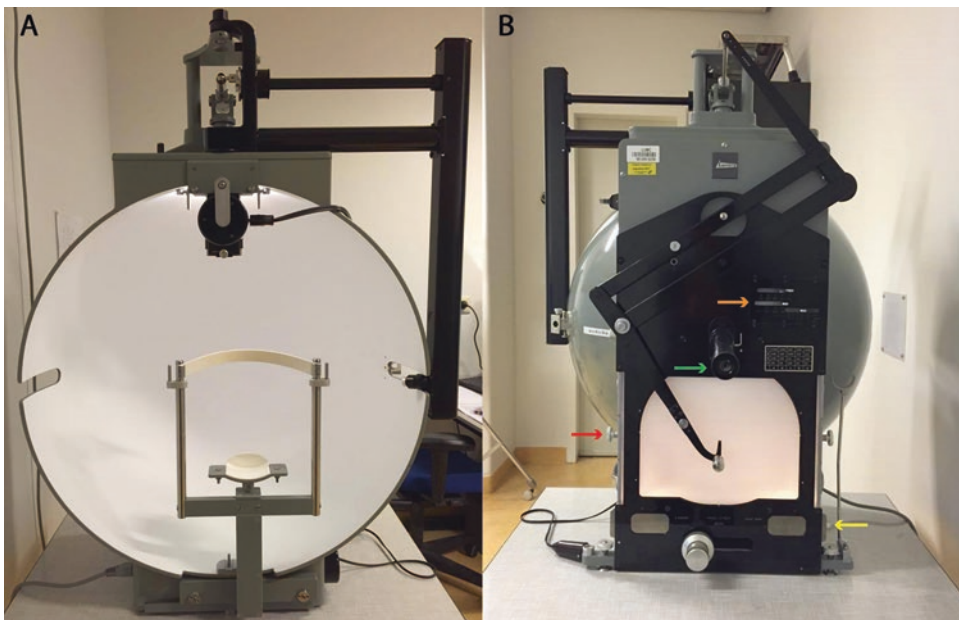
Fig. 1 The Goldmann perimeter. (**a**) The hemispheric bowl from the patient's perspective, showing the chin rest and forehead strap. (**b**) The examiner's control panel. The operator arm of the pantograph is seen at the center of the frame. The perimetry chart is slid into the frame, and the slot can be widened and tightened by turning the buttons lateral to the frame (*red arrow*). The examiner views the patient's fixation through the telescope (*green arrow*). The large button at the bottom (*white arrow*) can be turned to elevate or depress the chin rest of the patient, and it can be moved along the slot, to move the chin rest to the left or right. The examiner adjusts the stimulus size and luminance via the sliders at the top (*orange arrow*). The turning latch (*yellow arrow*) can be turned or pushed down in order to present the target in the bowl

the chin rest, to prevent a misrepresentation of the blind spot on the perimetry plotting chart. Emphasize to the patient the importance of maintaining this position throughout the examination.

7. Adjust the chair to the patient's comfort. Uncomfortable seating may distract the patient during the examination.

8. Let the patient adapt to the background luminance of the perimeter for approximately 5 min. For information on usual test duration, *see* **Note 3**.

3.2 Preparation of the Test

The target illuminance and background illuminance of the Goldmann perimeter should be calibrated as part of a daily routine in the case of daily use. The calibration procedure is described in the manual of each Goldmann perimeter.

The luminance of the room should be mesopic, i.e., dimmer than the background illuminance inside the perimeter bowl, but not completely dark.

1. Slide the visual field plotting chart in the assigned slot of the frame on the examiner's side of the Goldmann perimeter (Fig. 1b). The buttons located laterally to the grooves of this frame can be turned to release tension on the frame, in order to slide the plotting chart more easily.

2. Turn the buttons lateral to the frame back to provide a snug fit for the plotting chart, to prevent it from moving along with the movements of the pantograph during the test.

3. Make sure that the vertical and horizontal marks on the edges of the perimetry chart are aligned with the notches on all four sides of the frame.

3.3 Mapping the Field of Vision

1. Start with the largest, brightest stimulus: the V4e target. The size and luminance of the stimulus can be controlled via the three sliders shown in Fig. 1b (orange arrow).

2. The stimulus is presented to the subject when the examiner pushes the turning latch on the side of the device, lateral to the chart slot, shown in Fig. 1b (yellow arrow). *See* **Note 4** for further information on this turning latch.

3. Tell the patient to press the button as soon as the light becomes visible, and to press it again if at any time the target disappears or reappears; explain to the patient that it is common for the light to disappear in some parts of the visual field, and that the purpose of the test is to find such areas.

4. Move the stimulus/target centripetally from the most peripheral margin, along a straight line, into the area of vision, toward the central point of fixation. Press the pantograph onto the

frame background surface with your hand, to ensure a steady movement of the stimulus.

5. For each target, examine at least 12 meridians. The horizontal and vertical meridians are usually evaluated by examining 5–10° on each side of the horizontal and vertical meridian, instead of at 0° of the meridian. *See* **Note 5** for further information on the meridians to examine.

6. Move the stimulus with a constant speed of approximately 2–3°/s (*see* **Note 6**), but not faster [22]. In areas suspicious of a scotoma, the stimulus may be moved slower, as well as in areas of suspicion or inconsistent detection by the patient.

7. When a patient presses the button, mark the point where the target was located at that moment (*see* **Note 7**). Account for the reaction time by slightly adjusting the location of the mark.

8. Then proceed to a target that the patient only perceives within their central 30°, which is usually the I2e, but may be a brighter target in older patients, e.g., I4e, or a dimmer target in younger patients [20]. In all cases, measure at least the V4e, the smallest seeing target within the central 30°, and an intermediate target in between. Note the largest target that the patient did not see anymore.

9. During testing, the examiner should pay attention to the fixation of the patient to the central point, and note this in the record, as this is important for interpreting the test result. Encourage the patient to keep their gaze fixated at the central fixation target.

3.4 Mapping a Scotoma

1. The physiological blind spot is usually determined using the I4e target, as the isopter for this target is located approximately 10° outside of the blind spot, which is located 15° temporally from the central fixation point. Starting from the non-seeing area, move the target outward in ≥8 different directions.

2. Likewise, once you have identified an area of decreased sensitivity, map this area by presenting a stimulus starting from the center of the scotoma, and moving the target outward in ≥8 different directions, that contain the clock hours 12, 2, 4, 6, 8, 10, and other clock hour directions where appropriate.

3.5 Notes on the Perimetry Plotting Chart

Make the following notes on the perimetry chart for each eye, in addition to the patient age, and patient ID or study ID:

1. Fixation quality during the test.

2. The pupil diameter.

3. The trial frame addition.

4. Level of attention/fatigue.

5. The test duration.

6. Any relevant notes regarding cooperation.

After making sure that the notes on the chart are complete, save the chart according to the hospital procedure (*see* **Note 8**), and shut off the Goldmann perimeter (*see* **Note 9**).

3.6   Interpreting the Goldmann Visual Field

1. Assess the isopters size and compare this to age-matched ranges (*see* **Note 10**). From the central fixation point, the normal visual field usually reaches approximately 90° temporally, 50° nasally, and 50–60° superiorly and inferiorly, for the largest, brightest light (Fig. 2).

2. Evaluate any focal defects within the isopter area other than the blind spot.

3. Classify the type of defect. In RP patients, concentric constriction or a midperipheral ring scotoma is common, and in later disease stages, only a central island of vision may remain. Describe any (mid-) peripheral remnants of visual field and their localization and size. In retinal dystrophies primarily affecting cones, a (para)central scotoma may be present.
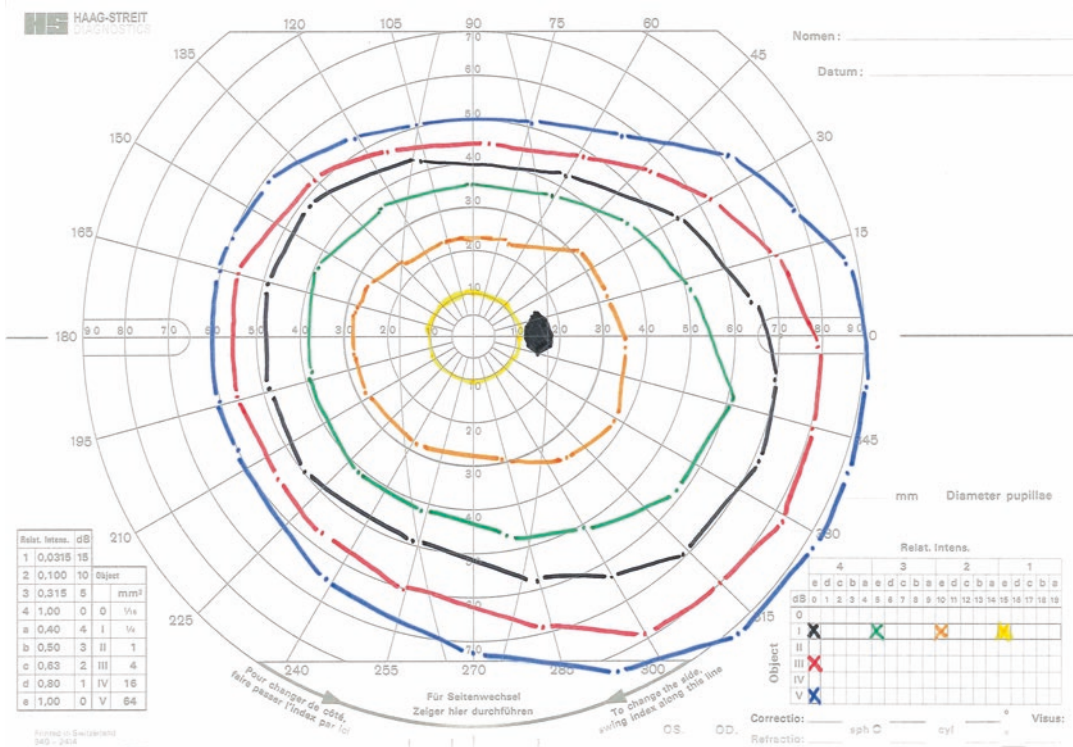
Fig. 2 Normal Goldmann kinetic perimetry isopters for a healthy 20–30 year old person. For a 50–60 year old person, it is expected that the largest isopters decrease in radius by approximately 10°

4. If the Goldmann visual field is not digitized and quantitatively analyzed, one may describe the size of the remaining visual field or scotoma size by noting the horizontal and vertical diameter in degrees.

3.7 Quantitative Analysis of the Goldmann Visual Field

1. The FieldDigitize 4.20 software (Johns Hopkins Technology Ventures, Baltimore, USA) must be installed (*see* **Note 11**).

2. Open FieldDigitizeRelease.4.20.

3. The digitizing researcher must now enter his/her initials and select the image (upload the GVF).

4. The program now automatically refers the researcher to the "Basic Info Form." In the current version of the software the Study ID in this form must be a six-digit number.

5. The researcher is now asked to calibrate the image by first selecting the center of the chart, followed by points along the right (90°), top (70°), left (90°), and bottom (70°) axes. More information on the calibration process is found under **Note 12**.

6. The program now automatically refers the researcher to the "Contour Information Form," where the researcher fills in information on the used target. Scotomas can be digitized by clicking "non-seeing" under "visual field."

7. The researcher now proceeds to trace the isopter of interest, or "contour". This is done by following the contour and clicking on each point that was marked during the test; note that the software will assume that these points are connected by the shortest line on the retina.

8. After finishing a contour by clicking on the point where digitizing was started, the program automatically asks the user if they wish to start another contour. If selected yes, the "Contour Information Form" automatically reappears.

9. When finishing this GVF, the user is given the option to save the contours. If the user chooses not to save the contours, they must fill in the reason in the assigned text box.

10. The program automatically computes seeing- and non-seeing retinal areas, after an automatic topological data checking procedure that ensures that no isopters crossed, or other obvious plotting or digitizing mistakes were made.

11. The calculated visual field areas are saved under the "Area Result" folder.

12. For each contour separately, and for the summed areas, the contour information, seeing retinal area in mm^2, the bowl area in degrees squared and steradians, and the logarithm of the seeing retinal area (under "log summed areas") are given.

4   Notes

1. Performing and mapping the peripheral visual field by Goldmann perimetry requires a trained and skilled examiner. For example, the examiner may find it challenging to operate the pantograph, observe the patient's fixation, and mark the isopter edges all at the same time. This requires some practice.

2. In the case of significant drooping of the eyelid, the examiner may tape the excess skin tissue.

3. In the case of a visual field with no complicated defects, the GVF examination by a skilled examiner usually takes approximately 20 min for both eyes. In the case of a patient with complicated visual field defects, e.g., a retinitis pigmentosa patient, the examination usually takes approximately 30 min for both eyes. For the Octopus 900 perimeter (Haag-Streit Inc., Koeniz, Switzerland), the test duration is similar to Goldmann perimetry, if the Octopus 5°/s or Octopus 10°/s setting is chosen, but slower if the Octopus 3°/s setting is chosen [23].

4. The turning latch shown in Fig. 1b (yellow arrow) can be either turned or pushed down. When turned, the stimulus light is turned on, and remains turned on until the examiner turns it back off. When pushed down instead of turned, the stimulus light is on as long as the examiner pushes it down. This last option is usually used. The examiner pushes the latch while moving the stimulus from the non-seeing area of the visual field into the seeing area of the visual field. As soon as the patient sees the stimulus and pushes the button in his/her hand, the examiner releases the latch, and starts the same procedure for the next meridian. One instance where the examiner may wish to turn the latch and thus keep the stimulus light on, instead of pushing it down, is if the patient only has a central island of remaining visual field, or if the examiner performs a final verifying scan of the (mid-) periphery, moving the pantograph in a perusing manner. However, experienced examiners may choose to continue the centripetal trace to the center of the visual field, marking any further isopter crossings such as mid-peripheral ring scotomas along the way.

5. When the examiner has finished testing at least 12 meridians for the V4e target, and proceeds to test a smaller target, it is best to follow 12 new meridians for this smaller target, each meridian path positioned between two meridian paths tested for the larger target. This will test more points along the isopter borders.

6. For accurately determining the blind spot and small scotomatous areas, a slower speed may be appropriate [23]. In other

cases, the examiner should be cautious of the so-called "technician factor," which introduces bias by varying the stimulus speed based on the examiner's expectation of the patient's response [24].

7. In the case of patients who alternatingly see and do not see one or more area(s): note this in the patient record or on the GVF printout.

8. Each hospital or clinic may have its own scanning policy, but make sure to save a digital scan of the GVF.

9. After using the Goldmann perimeter, make sure to turn off the background luminance for longer preservation of the device elements.

10. As with static perimetry, it is important to compare current GVFs to prior GVFs in order to identify disease progression or, in the case of a (gene therapy) trial, treatment effect.

11. The FieldDigitize 4.20 software can also be used to analyze the seeing (and non-seeing) retinal areas of kinetic visual fields measured with other perimeters, e.g., the Octopus 900 (Haag-Streit Inc., Koeniz, Switzerland).

12. When digitizing GVFs, the program may reject the calibration of the image if the image scan is warped. In this case, an image should be rescanned or resized using any software that can correct the distortion. Also, the software makes certain assumptions about the layout of the chart, so if consistent errors occur, the scan settings may have to be adjusted. Avoid warping the image when cropping or resizing it.

References

1. Berson EL, Sandberg MA, Rosner B et al (1985) Natural course of retinitis pigmentosa over a three-year interval. Am J Ophthalmol 99:240–251

2. Grover S, Fishman GA, Anderson RJ et al (1997) Rate of visual field loss in retinitis pigmentosa. Ophthalmology 104:460–465

3. Bainbridge J, Mehat MS, Sundaram V et al (2015) Long-term effect of gene therapy on Leber's congenital amaurosis. N Engl J Med 372:1887–1897

4. Bennett J, Wellman J, Marshall KA et al (2016) Safety and durability of effect of contralateral-eye administration of AAV2 gene therapy in patients with childhood-onset blindness caused by RPE65 mutations: a follow-on phase 1 trial. Lancet 388:661–672

5. Talib M, van Schooneveld MJ, van Genderen MM et al (2017) Genotypic and phenotypic characteristics of CRB1-associated retinal dystrophies: a long-term follow-up study. Ophthalmology. https://doi.org/10.1016/j.ophtha.2017.01.047

6. Pierrache LH, Hartel BP, van Wijk E et al (2016) Visual prognosis in USH2A-associated retinitis pigmentosa is worse for patients with usher syndrome type IIa than for those with nonsyndromic retinitis pigmentosa. Ophthalmology 123:1151–1160

7. Rowe F (2016) Visual fields via the visual pathway, 2nd edn. CRC Press, Boca Raton, FL

8. MacLaren RE, Groppe M, Barnard AR et al (2014) Retinal gene therapy in patients with choroideremia: initial findings from a phase 1/2 clinical trial. Lancet 383:1129–1137

9. Maguire AM, Simonelli F, Pierce EA et al (2008) Safety and efficacy of gene transfer for Leber's congenital amaurosis. N Engl J Med 358:2240–2248

10. Pellissier LP, Quinn PM, Alves CH et al (2015) Gene therapy into photoreceptors and Muller glial cells restores retinal structure and function

in CRB1 retinitis pigmentosa mouse models. Hum Mol Genet 24:3104–3118

11. Wassmer SJ, Carvalho LS, György B et al (2017) Exosome-associated AAV2 vector mediates robust gene delivery into the murine retina upon intravitreal injection. Sci Rep 7:45329

12. Koenekoop RK, Sui R, Sallum J et al (2014) Oral 9-cis retinoid for childhood blindness due to Leber congenital amaurosis caused by RPE65 or LRAT mutations: an open-label phase 1b trial. Lancet 384:1513–1520

13. Dagnelie G (1990) Conversion of planimetric visual field data into solid angles and retinal areas. Clin Vis Sci 5:95–100

14. Zahid S, Peeler C, Khan N et al (2014) Digital quantification of Goldmann visual fields (GVFs) as a means for genotype-phenotype comparisons and detection of progression in retinal degenerations. Adv Exp Med Biol 801:131–137

15. Odaka T, Fujisawa K, Akazawa K et al (1992) A visual field quantification system for the Goldmann Perimeter. J Med Syst 16:161–169

16. Trost DC, Woolson RF, Hayreh SS (1979) Quantification of visual fields for statistical analysis. Arch Ophthalmol 97:2175–2180

17. Linstone FA, Heckenlively JR, Solish AM (1982) The use of planimetry in the quantitative analysis of visual fields. Glaucoma 4:17–19

18. Barry MP, Bittner AK, Yang L et al (2016) Variability and errors of manually digitized Goldmann visual fields. Optom Vis Sci 93:720–730

19. Bittner AK, Iftikhar MH, Dagnelie G (2011) Test-retest, within-visit variability of Goldmann visual fields in retinitis pigmentosa. Invest Ophthalmol Vis Sci 52:8042–8046

20. Barton JS, Benatar M (2003) Field of vision: a manual and atlas of perimetry, 1st edn. Humana Press, Totowa, NJ. 335p

21. Koller G, Haas A, Zulauf M et al (2001) Influence of refractive correction on peripheral visual field in static perimetry. Graefes Arch Clin Exp Ophthalmol 239: 759–762

22. Johnson CA, Keltner JL (1987) Optimal rates of movement for kinetic perimetry. Arch Ophthalmol 105:73–75

23. Rowe FJ, Rowlands A (2014) Comparison of diagnostic accuracy between Octopus 900 and Goldmann kinetic visual fields. Biomed Res Int 2014:214829

24. Ramirez AM, Chaya CJ, Gordon LK et al (2008) A comparison of semiautomated versus manual Goldmann kinetic perimetry in patients with visually significant glaucoma. J Glaucoma 17:111–117

Chapter 25

Measuring Central Retinal Sensitivity Using Microperimetry

Mays Talib, Jasleen K. Jolly, and Camiel J.F. Boon

Abstract

Microperimetry is an increasingly often used method of assessing the sensitivity of the central macula, analyzing fixation capabilities and loci, and accurately combining structural and functional information, even in the absence of stable fixation. Ongoing gene therapy trials have targeted the central retina, and utilized microperimetry as a main outcome measure for changes in retinal function. In retinal treatment planning, microperimetry has been used to assess the potential therapeutic window of opportunity. In the following pages, we briefly review the necessary steps to perform the Macular Integrity Assessment (MAIA) microperimetry.

Key words Microperimetry, MAIA, Retinal sensitivity

1 Introduction

Microperimetry is a psychophysical method for mapping the central sensitivity across the visual field. It correlates visual function measurements to exact locations in the central retina, allowing for an overlay of structural and functional information, by combining three different techniques in one exam: fundus imaging, retinal sensitivity mapping, and fixation capabilities analysis [1]. In the last decades, microperimetry is increasingly often used in the diagnosis and follow-up of several retinal disorders [2], including age-related macular degeneration [3, 4], choroideremia [5], and retinitis pigmentosa [6]. Important assets of microperimetry include the ability to reliably test macular function even in patients without foveal fixation [7], to assess fixation stability, and to localize fixation points on the retina, known as preferred retinal loci (PRL), topographically representing fixation attempts. This poses a substantial advantage in inherited retinopathies and age-related macular degeneration, where loss of fixation stability poses a challenge for conventional perimetry methods [8, 9]. Furthermore,

microperimetry may detect early changes in retinal function, even in the absence of visual acuity changes [10, 11].

Several microperimetry devices have been developed: the Macular Integrity Assessment (MAIA, CenterVue, Padova, Italy) and MAIA Scotopic, the MP-1 and MP-3 (Nidek, Padova, Italy), and the Optos OCT SLO (Optos Plc., Dunfermline, UK). In the remainder of this chapter we refer to the MAIA microperimeter, but amended procedures can be followed with the other devices. The decibel scales of these different microperimetry instruments are not comparable or interchangeable, as the MAIA has the largest stimulus attenuation range (0–36 dB; Fig. 1) and the highest available stimulus intensity (318.47 cd/m², or 1000 apostibls) [12]. Therefore, to monitor disease progression, the same instrument should be used at baseline and follow-up.

Microperimetry testing with the MAIA is a largely automated process (*see* **Note 1**), including automatic image focusing on the retina, correcting for refractive errors between −15 and +10 diopters. However, automation should be used as a starting point rather than an endpoint to minimise sources of error or inaccuracies. During testing, stimuli with similar size to the Goldmann III (4 mm²) are presented to the subject over different locations within the central 36° of the retina, against a 4 apostilbs (1.27 cd/m²) background. The luminance of the presented stimuli varies within the 36 dB dynamic range. During testing, a real-time fundus image is generated with a confocal Scanning Laser Ophthalmoscope (SLO), and changes in fixation are registered 25 times per second during examination. Automated eye tracking corrects for eye movements, and ensures that the light stimulus and the retinal location on the fundus image correspond throughout the test. Both supra-threshold and full-threshold testing strategies are available, and the most appropriate strategy choice depends on the extent of pathology.

Both the MAIA and Nidek MP-1 microperimetry devices have therapeutic biofeedback modules to provide (re)fixation training to patients as a part of low vision rehabilitation. This rehabilitative option, although an important aspect of these microperimetry devices [13, 14], is beyond the scope of this chapter.

Ongoing and planned gene therapy trials have adopted microperimetry as an outcome measure in assessing pretreatment characteristics and therapeutic effect [15, 16]. Moreover, it has been used to assess implications for future gene therapy, e.g., the potential therapeutic window of opportunity, in phenotyping studies and retinal treatment planning [17–19]. The fundamental materials and methods necessary for proper performance of microperimetry will be presented in the following pages.
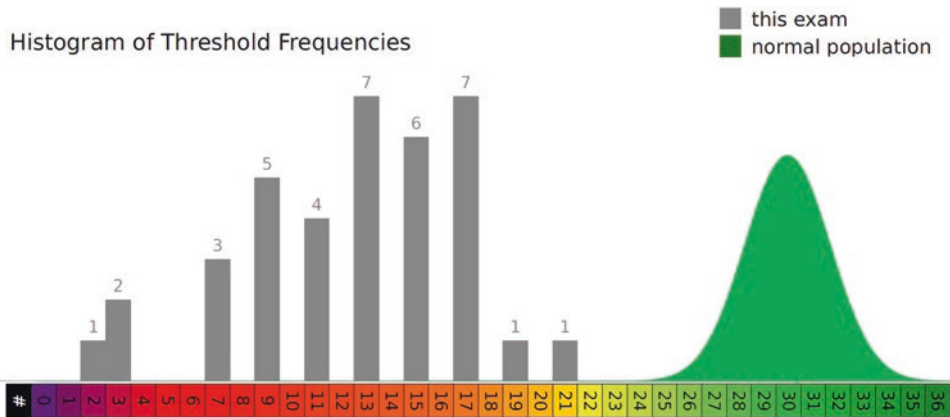
Fig. 1 The Macular Integrity Assessment (MAIA) dB color scale and an example of the accompanying histogram of threshold frequencies. The colors are coded according to the MAIA normative database, with "green" signifying normal values, "yellow" suspect values, "red" abnormal values, and "black" signifying a scotoma. The *green normal curve* shows the distribution in the normative database, while the *grey bars* show an example of the threshold (sensitivity) distribution in a patient with retinitis pigmentosa

2   Materials

1. The MAIA microperimeter (MAIA, Centervue, Padova, Italy).

2. A computer or laptop with image storage software for exporting the obtained microperimetry examination and the complementary printout.

3. An eye patch, in order to test each eye individually. Alternatively, use 5 × 5 cm gauze; the newer versions have an inbuilt eye patch.

4. Micropore tape.

5. Alcohol for disinfecting the chinrest and forehead strap.

3   Methods

3.1   Preparation of the Patient or Subject

1. The patient's pupils do not have to be dilated. Performing the test with or without pupil dilation will yield similar and consistent results (*see* **Note 2**) [20]. The MAIA operates with a minimum pupil diameter of 2.5 mm.

2. Prior to testing, instruct the patient on the purpose and process of the examination. The examiner may do this while the patient is in dark-adaptation (*see* **Note 3**). Explain that this examination tests the ability to perceive light stimuli and to fixate at a steady target, that the patient should press the pushbutton when he/she sees a small flashing light appearing anywhere, and that some lights may be dimmer than others. The

patient should not wait to see the light sharply and crisply, but press if they believe they see a light as the test will push to the limits of vision, so many lights will be very faint. It is normal that some stimuli are not seen, and there may be long periods where the subject does not need to press the button. Explain that it is important to not move the head or eyes during testing.

3. Cover the eye not being tested using an eye patch or 5×5 cm gauze and micropore tape, making sure that there are no nasal or lateral openings. Start with the eye that has (subjectively) better vision, or, in the case of a trial setting, start with the control eye.

4. Adjust the chair to the patient's comfort. Uncomfortable seating may distract the patient during the examination.

3.2 Preparation of the Test

1. The room should be darkened/mesopic. This reduces glare and makes it easier to perform the test. The screen has a setting to switch it to darkroom mode, making it red and reducing a source of troublesome light.

2. Input patient details in the microperimeter.

3. Select the "expert" test with the 10-2 standard grid, which tests the retinal sensitivity on 37 different points on the retina.

4. Follow-up exams are performed by clicking the "follow-up" option next to the baseline test. When performing a follow-up microperimetry exam, it is important to obtain a similar fundus image to the baseline image. Selecting the "follow-up" protocol ensures automatic alignment of the fundus images between examinations. It also ensures the same retinal points are tested at subsequent examinations.

5. The examiner is responsible for inspecting the proper functioning of the push-button. To do so, the examiner pushes the button and checks on the test screen if the "Button" indicator turns orange upon pushing the button.

3.3 Performing Microperimetry

1. Subjects first adapt to the low light conditions in a process called dark-adaptation. There is no current consensus about the ideal adaptation time to be adopted prior to testing, and adaptation times in the literature vary highly, although it is common to have the subject adapt to the dark for at least 5 min (*see* **Note 3**). Generally, the subjects should be at least 10 min away from any glare sources in order to achieve consistent high sensitivity. The examiner can start the adaptation process while instructing the patient on the study.

2. Select the test mode, grid, and eye to be tested (*see* **Note 4**). More information on the test duration for each mode is given

in **Note 5**. *See* **Notes 6–9** for information on selecting the appropriate test mode.

3. Before starting the wanted test, start a test run in both eyes to negate the learning curve. An appropriate mode to perform this test run is the "4 levels fixed" mode. These results will not be used in later analysis. After both eyes have performed this test run, run the wanted test mode.

4. Center the machine using the centering control on the touch screen on the newest version of the MAIA (green text on device, Fig. 2), or using the arrow keys on the control panel below the screen on the older version of the MAIA (red text on device), and ask the patient to inform you when the small red fixation ring is visible. Autoalignment can be used to start this process.

5. Move the microperimeter closer to the eye, using the control panel, until the fundus image fills the screen without any distortion in the image. Distortion signals you are too close, black areas signal you are too far away.

6. Click start to capture the fundus image. If the image is not clear, rerun autofocus. If after two autofocus runs the image remains unclear, adjust the image using the manual focus option (*see* **Note 10**). At follow up examinations, the focus should be matched to the baseline image as closely as possible to ensure microperimetry is being conducted in the same
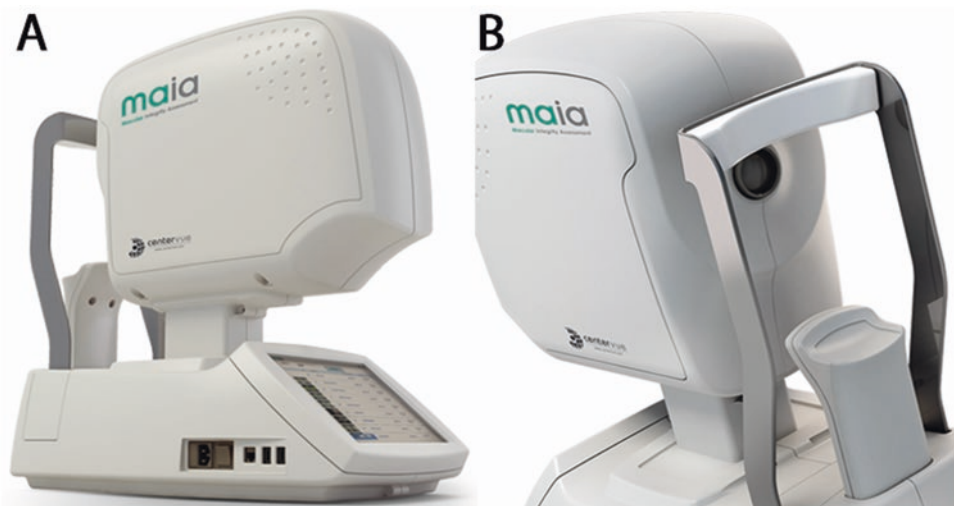
Fig. 2 The Macular Integrity Assessment (MAIA) microperimetry device. (**a**) The device from the operator's perspective. The touch screen is used to enter patient information, to select test strategy, the eye to be examined, to follow screen prompts, and to center and focus the fundus image on the screen. The older device has *red text* instead of *green text*, and has a control panel below the screen, which is used to center the fundus image by moving the four-direction button, and to focus the fundus image by using the two-direction button. (**b**) The device from the patient's perspective, showing the chinrest and forehead strap

plane. If this is not the case, there will be greater variability in the sensitivity.

7. Inform the patient that the test is about to start.

8. Follow the screen prompts and start the test.

9. Monitor the patient's fixation, head and eye movements, and the image clarity throughout the test. The focus must not be altered once the test starts, but the machine can be moved left, right, up or down.

10. Periodically encourage the patient to maintain their concentration and keep their gaze fixated at the central red circle throughout the test. Offer encouragement.

11. When eye tracking is lost, the microperimeter produces an audio alarm signal (*see* **Note 11**). In this case, pause the examination and if required, recenter the fundus image using the arrow keys. During testing, do not change the image focus using the depth button. After recentering the image, restart the examination. More information on pausing the test is given in **Note 12**.

12. After test completion, an automatic screen prompt allows for export and/or print of the test. When the examiner chooses to "print" the test, a printout containing the outcome parameters of interest is generated. When the examiner chooses to "export" the test, an overview of the pointwise sensitivity is generated. This overview also appears in the printout.

13. Some patients may not be able to perform the MAIA microperimetry with the standard fixation target due to a central scotoma. Information on overcoming this problem is given in **Note 13**.

14. Considerations regarding microperimetry in children are given in **Note 14**.

For a brief overview of the different steps in performing microperimetry with the Nidek MP-1 device, *see* **Note 15**.

3.4 Interpretation of the Parameters

1. The reliability index, shown at the top left of the printout page, should be at least 85%.

2. The so-called Preferred Retinal Locus (PRL, *see* **Note 16**), visible as a cloud of green points in every MAIA test, signifies the region enclosing the patient's eye movements while trying to fixate. The PRL designates the location of fixation. Normal subjects use the fovea for fixation, while patients affected by a pathology affecting the central retina develop eccentric fixation, using extrafoveal areas. PRL provides information on the location and stability of a patient's fixation.

3. Fixation stability is represented in two ways:

First way: The percentage of fixation points located within a 1°
(P1) and 2° (P2) radius distance. P1 (%) and P2 (%) are
given in numerical values on the printout, and are catego-
rized on a color grid representing stable (green bar; >75%
of fixation points within P1), relatively unstable (yellow
bar; <75% of fixation points within P1, but >75% of fixa-
tion points within P2), or unstable fixation (red bar; <75%
of fixation points located within P2).

Second way: Bivariate contour ellipse area (BCEA) indices are
automatically calculated in degrees^2. This ellipse encom-
passes the proportion (95% and 63%) of the cloud of fixa-
tion points within the standard deviations of the horizontal
and vertical eye positions during the fixation attempt. The
BCEA provides a more accurate estimate of the fixation
stability.

4. The fixation graph at the bottom of the printout shows the eye
movement amplitude (degrees) with time (minutes), visualiz-
ing changes in fixation during the examination.

5. Macular Integrity Index: this is a numerical value that only
appears in examinations performed with the full-threshold 4-2
strategy and the standard MAIA stimuli grid, and is unique to
the MAIA microperimeter. It represents the probability that a
response is normal, suspect or abnormal, compared to age-
adjusted normative data. It does not indicate the disease sever-
ity, and it does not have a direct relationship with the mean
threshold value for the sensitivity in dB.

6. A high test-retest variability has been reported in microperim-
etry results, particularly at the border of scotomas and degen-
erated areas [21, 22]. This should be taken into account when
assessing disease progression.

4 Notes

1. Although microperimetry is largely an automated test, a skilled
examiner is required to set up the machine parameters and to
monitor the patient responses during the test.

2. Pupil dilation does not have a significant effect on the mean
threshold sensitivity, pointwise threshold sensitivity, and fixa-
tion stability (as measured by 95% BCEA) in healthy eyes and
in eyes of patients with choroideremia [20]. Because a nonsig-
nificant effect of pupil dilation was found on the peripheral
points, it is recommended that pupils are undilated for clinical
trials, but they can be either dilated or undilated for clinical
work. Note that even in the undilated state, the pupil size
should at least be 2.5 mm, as a smaller size would lead to a

mismatch of pupillary aperture with the MAIA viewing piece, which would affect the measured sensitivity threshold. As microperimetry is tested in a mesopic environment, a mesopic-adapted eye will likely meet this pupil size requirement.

3. There is no current consensus on the optimal dark-adaptation time, and both phenotyping studies and gene therapy trials have used different dark adaptation times prior to microperimetry, varying from 5 to 45 min [16, 23, 24]. Often, the dark adaptation time, if applicable, is not mentioned in the available literature.

4. The "4-2" mode and the "10-2" grid have caused confusion with new microperimetry users in the past. The "4-2" projection strategy describes the staircase psychophysical method, whereas "10-2" is the grid pattern covering the central 20° in diameter, with 2° spacing between points.

5. The typical duration for the suprathreshold tests is 2 min per eye for the "fast" and "scotoma finder" modes, and 3 min per eye for the "4 levels fixed" mode. The typical duration for the full-threshold strategy "4-2" is less than 6 min per eye in absence of pathology, but around 10 min per eye when pathology is present. Test durations have been shown to be significantly longer for children than adults. In each case, the duration of the exam should not exceed 15 min per eye. Customised grids can be required with points added and subtracted before commencing.

6. The supra-threshold mode "fast" is used to screen patients with no known disease. Measures two levels of sensitivity (27 and 25 dB).

7. The supra-threshold test mode "scotoma finder" is used to examine highly pathologic patients with one level of sensitivity (0 dB).

8. The supra-threshold test mode "4 levels fixed" is used to examine pathologic patients, using four levels of sensitivity (0, 5, 15, and 25 dB). This mode is also suitable as a test-run in both eyes, to negate the learning curve in microperimetry.

9. The full-threshold 4-2 test mode is used to examine retinal sensitivity in detail.

10. The manual focus can also be used to fine-tune the image. This is especially helpful in cases of high corneal distortion or media opacities.

11. On occasion, the image looks acceptable, but the machine will still produce the audible alarm signal. In this case, check whether the patient has rotated their head, sat back, or moved head position.

12. The patient may pause the test at any time for up to 5 min in total per test. During any pause, the patient must remain in the darkened room. When the eye moves out of tolerance the test is automatically paused until the eye moves back into tolerance.

13. The MAIA has an option for cross-shaped dynamic multifixation targets, which can be used in patients with a central scotoma who have substantial difficulties seeing the standard central fixation target, which is a red circle with a 0.76° diameter. In this case, the multifixation target, comprising a 5 × 5 grid with a 2.4° diameter, allows the patient to perform the microperimetry examination by fixating on an eccentric fixation target [25].

14. MAIA microperimetry has been shown to be feasible in children aged 9–12 years [23]. However, children have consistently lower fixation stability than adults, and make more frequent and larger eye movements [23]. Test results for pointwise sensitivity and mean sensitivity are slightly less reliable than in adults. Children under the age of 9 are usually physically too small to be seated comfortably at the MAIA microperimeter, but a minimum feasible age for microperimetry has not been established yet [23]. Considerations such as an overall lack of attentiveness should be taken into account when performing microperimetry in children and when analyzing the printout.

15. With the Nidek MP-1 system, preparation of the subject and performance of the test are mostly similar, but involve several differences:

    The image is not an SLO image, but an infra-red image.

    (a) To center the image and to move the device closer to the patient's eye, until the fundus fills the screen, a control stick is used instead of a control button panel.

    (b) If necessary, the most accurate refractive error can be entered, in order to optimize the image focus.

    (c) If the image is too dark or too saturated, the intensity of the infrared light may be manually adjusted by using the infrared power slide.

    (d) When the image is optimized, the button on top of the control stick is pushed to initiate testing.

    (e) After finishing the test, the examiner is asked if he/she wishes to test additional stimuli. This is usually not necessary.

    (f) Color retinography is then performed with a bright flash. In order to optimize the image focus, move the optical head back and forth. To align the two on-screen targets,

move the optical head slightly left/right. Inform the patient that a bright flash will appear. Push the button on the control stick to perform the color retinography.

(g) Overlay the microperimetry examination onto the color retinography by choosing either the semiautomatic or manual registration, depending on the obtained image quality.

16. Preferred Retinal Loci (PRL) provide information on the location and stability of a subject's fixations, and provides a target for biofeedback training: patients with macular degeneration and loss of foveal sensitivity can be trained to relocate their PRL to an area with better sensitivity, which may lead to an improvement in fixation parameters, visual acuity, reading speed, and vision-related quality of life [26, 27].

References

1. Midena E (2013) Microperimetry and multimodal retinal imaging. Springer Science & Business Media, Germany. 196p

2. Acton JH, Greenstein VC (2013) Fundus-driven perimetry (microperimetry) compared to conventional static automated perimetry: similarities, differences, and clinical applications. Can J Ophthalmol 48:358–363

3. Rohrschneider K, Gluck R, Becker M et al (1997) Scanning laser fundus perimetry before laser photocoagulation of well defined choroidal neovascularisation. Br J Ophthalmol 81:568–573

4. Meleth AD, Mettu P, Agrón E et al (2011) Changes in retinal sensitivity in geographic atrophy progression as measured by microperimetry. Invest Ophthalmol Vis Sci 52:1119–1126

5. Simunovic MP, Xue K, Jolly JK et al (2017) Structural and functional recovery following limited iatrogenic macular detachment for retinal gene therapy. JAMA Ophthalmol 135:234–241

6. Battu R, Khanna A, Hegde B et al (2015) Correlation of structure and function of the macula in patients with retinitis pigmentosa. Eye (Lond) 29:895–901

7. Chen FK, Patel PJ, Xing W et al (2009) Test-retest variability of microperimetry using the Nidek MP1 in patients with macular disease. Invest Ophthalmol Vis Sci 50:3464–3472

8. Cideciyan AV, Swider M, Aleman TS et al (2012) Macular function in macular degenerations: repeatability of microperimetry as a potential outcome measure for ABCA4-associated retinopathy trials. Invest Ophthalmol Vis Sci 53:841–852

9. Wu Z, Ayton LN, Guymer RH et al (2013) Intrasession test-retest variability of microperimetry in age-related macular degeneration. Invest Ophthalmol Vis Sci 54:7378–7385

10. Midena E, Vujosevic S, Convento E et al (2007) Microperimetry and fundus autofluorescence in patients with early age-related macular degeneration. Br J Ophthalmol 91:1499–1503

11. Liu H et al (2015) Retinal sensitivity is a valuable complementary measurement to visual acuity—a microperimetry study in patients with maculopathies. Graefes Arch Clin Exp Ophthalmol 253:2137–2142

12. Markowitz SN, Reyes SV (2013) Microperimetry and clinical practice: an evidence-based review. Can J Ophthalmol 48:350–357

13. Verboschi F, Domanico D, Nebbioso M et al (2013) New trends in visual rehabilitation with MP-1 microperimeter biofeedback: optic neural dysfunction. Funct Neurol 28:285–291

14. Morales MU, Saker S, Amoaku WM (2015) Bilateral eccentric vision training on pseudovitelliform dystrophy with microperimetry biofeedback. BMJ Case Rep. https://doi.org/10.1136/bcr-2014-207969

15. Zobor D, Werner A, Stanzial F et al (2017) The clinical phenotype of CNGA3-related achromatopsia: pretreatment characterization in preparation of a gene replacement therapy trial. Invest Ophthalmol Vis Sci 58:821–832

16. MacLaren RE, Groppe M, Barnard AR et al (2014) Retinal gene therapy in patients with

choroideremia: initial findings from a phase 1/2 clinical trial. Lancet 383:1129–1137

17. Sundaram V, Wilde C, Aboshiha J et al (2014) Retinal structure and function in achromatopsia: implications for gene therapy. Ophthalmology 121:234–245

18. Aboshiha J, Dubis AM, Cowing J et al (2014) A prospective longitudinal study of retinal structure and function in achromatopsia. Invest Ophthalmol Vis Sci 55:5733–5743

19. Testa F, Rossi S, Sodi A et al (2012) Correlation between photoreceptor layer integrity and visual function in patients with Stargardt disease: implications for gene therapy. Invest Ophthalmol Vis Sci 53:4409–4415

20. Han RC, Jolly JK, Xue K et al (2016) Effects of pupil dilation on MAIA microperimetry. Clin Exp Ophthalmol. https://doi.org/10.1111/ceo.12907.

21. Wu Z, Jung CJ, Ayton LN et al (2015) Test-retest repeatability of microperimetry at the border of deep scotomas. Invest Ophthalmol Vis Sci 56:2606–2611

22. Dimopoulos IS, Tseng C, MacDonald IM (2016) Microperimetry as an outcome measure in choroideremia trials: reproducibility and beyond microperimetry as an outcome measure in CHM trials. Invest Ophthalmol Vis Sci 57:4151–4161

23. Jones PR, Yasoubi N, Nardini M et al (2016) Feasibility of Macular Integrity Assessment (MAIA) microperimetry in children: sensitivity, reliability, and fixation stability in healthy observers. Invest Ophthalmol Vis Sci 57:6349–6359

24. Salvatore S, Fishman GA, McAnany JJ et al (2014) Association of dark-adapted visual function with retinal structural changes in patients with Stargardt disease. Retina 34:989–995

25. Morales MU, Villani GM, Turra F et al (2014) Dynamic multifixation target for microperimetry to use in patients with large central scotoma. Invest Ophthalmol Vis Sci 55:4139–4139. ARVO Annual Meeting Abstract

26. Scuderi G, Verboschi F, Domanico D et al (2016) Fixation improvement through biofeedback rehabilitation in Stargardt disease. Case Rep Med 2016:4264829

27. Ueda-Consolvo T, Otsuka M, Hayashi Y et al (2015) Microperimetric biofeedback training improved visual acuity after successful macular hole surgery. J Ophthalmol 2015:572942

Inspection of the Human Retina by Optical Coherence Tomography

Thomas Theelen and Michel M. Teussink

Abstract

Optical coherence tomography (OCT) is a high-resolution, three-dimensional, noninvasive imaging modality to examine the human retina. Since the introduction of spectral domain (SD-) OCT—the currently most used variant of OCT—previously unknown details of in vivo retinal morphology of a broad variety of pathologies have become visible. This chapter explains the basic principles of the OCT technology, deals with possible pitfalls in OCT examination or analysis, and hints at the use of OCT technology in functional imaging.

Key words Optical coherence tomography, Scattering, Reflection, Speckle, Decorrelation, Human, Retina

1 Introduction

1.1 Basic Principles of Optical Coherence Tomography (OCT)

OCT is a relative new imaging technique based on interferometry to capture three-dimensional images of the retina in high resolution. With spectral-domain (SD-) OCT, which became available for routine clinical examinations in 2005, the three-dimensional structure of the human retina could be observed in vivo on a micrometer scale [1, 2]. OCT rapidly became one of the most frequently used imaging modalities in ophthalmology because of the easy identification of important pathological features such as subretinal fluid, distortions and thinning of retinal layers. A generic OCT system schematic is shown in Fig. 1. In a simple Michelson interferometer implementation (which time-domain OCT and SD-OCT have in common), a beam of low-coherence, near-infrared light is directed into a 2 × 2 fiber optic coupler to split the incident light. Light coming from the reference fiber is directed to a mirror and redirected back into the same fiber. Light coming from the sample fiber is focused on the sample and the tissue is scanned in two dimensions. The light reflected back from the retina is mixed with reference light returning from the mirror, and spectral interference of these light beams at the surface of the
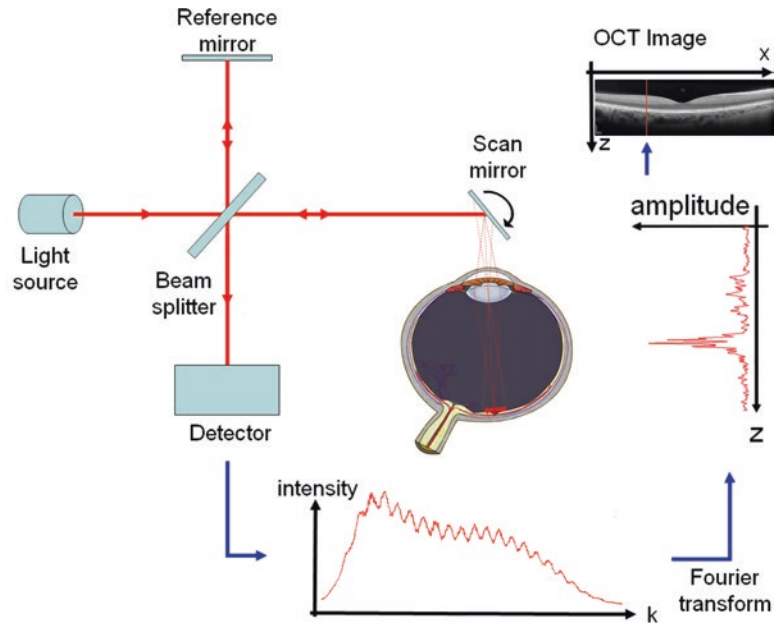
Fig. 1 Basic spectral domain OCT system schematic and processing workflow

detector is measured [3]. In SD-OCT, a diffractive grating spectrally separates the returning light into narrow bandwidths, which are focused on 1024 or 2048 separate photoreceptive elements of a high-speed line-scan camera. The received signals, representing intensity versus wave number, are processed by inverse Fourier transformation into electric field magnitude (i.e., reflectivity) versus sample depth. These individual depth profiles are called A-scans. A-scans acquired along one lateral direction form B-scans, and scanning in two directions at a particular depth produces C-scans.

SD-OCT has a much higher signal-to-noise ratio and a better depth resolution than time domain OCT. The former advantage enables depth profiles to be acquired at a far greater speed, which in turn makes SD-OCT less dependent on artifacts caused by eye movements. Therefore, SD-OCT is the predominantly used OCT technology in current clinical practice.

An OCT B-scan of a healthy human retina obtained with a commercial SD-OCT system is displayed in Fig. 2. These images are typically displayed in log-scale intensity, where the original values are a measure of the number of photons reflected (backscattered). The different appearance of retinal layers on SD-OCT scans is caused by several optical effects.

1. Differences in the refractive indices at the interface between two materials cause reflectance.
2. Diffuse reflective properties of tissues.
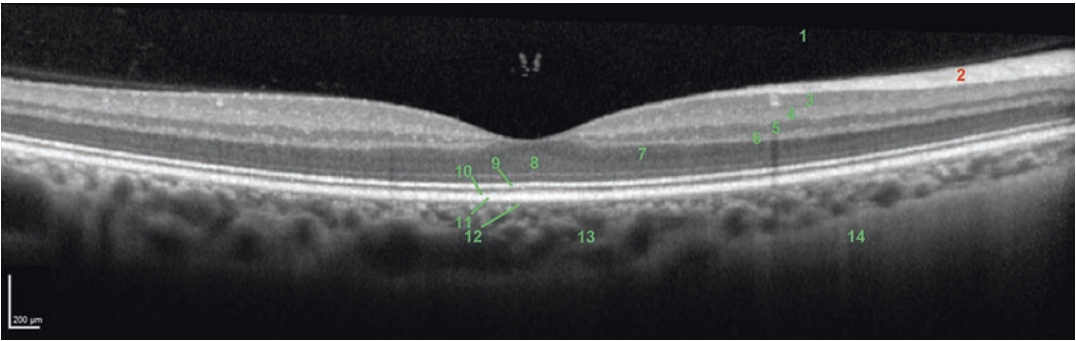
Fig. 2 Fovea-centered SD-OCT scan of a healthy eye, showing various optical layers of the retina. In this image, lighter pixels represent higher backscattering (i.e., reflectivity). Vitreous (1), retinal nerve fiber layer (2), ganglion cell layer (3), inner plexiform layer (4), inner nuclear layer (5), outer plexiform layer (6), Henle fiber layer (7), outer nuclear layer (8), photoreceptor inner/outer segment junction (9), photoreceptor outer segment—RPE interdigitation zone (10), RPE/Bruch's membrane complex (11), choriocapillaris (12), choroid (13), sclera (14). The retina is displayed anatomically incorrect for better visualization of the layers; in reality the retina is flatter. Scale bar to the bottom left. Nomenclature according to the International Nomenclature for Optical Coherence Tomography [4]

3. Angle between optical surfaces and incident OCT beam.

4. Birefringence, i.e., reflectivity is dependent on the light polarization state [5].

A single SD-OCT scan typically has a lot of speckle noise due to random interference effects. Averaging can improve image quality for morphological assessment. To do this, however, one has to ensure that the scans to be averaged are acquired at the same retinal location. Therefore, eye trackers have been implemented in SD-OCT systems. Of note, averaged OCT scans may no longer be used for quantitative analyses of tissue reflectivity. In addition, averaging may lead to blurring, causing the effective axial resolution to decrease as more scans are being used for averaging. Figure 3 exemplifies how averaging can improve the OCT image quality.

2   Materials

OCT systems are provided by several manufacturers. Please refer always to the user manuals provided with the device. Below general materials and instructions to perform OCT and OCT angiography imaging are provided.

1. Spectral Domain-OCT.

2. OCT angiography imaging system.

3. Alcohol swabs.

4. Dilating eye drops (optional).

5. Artificial tears (optional).
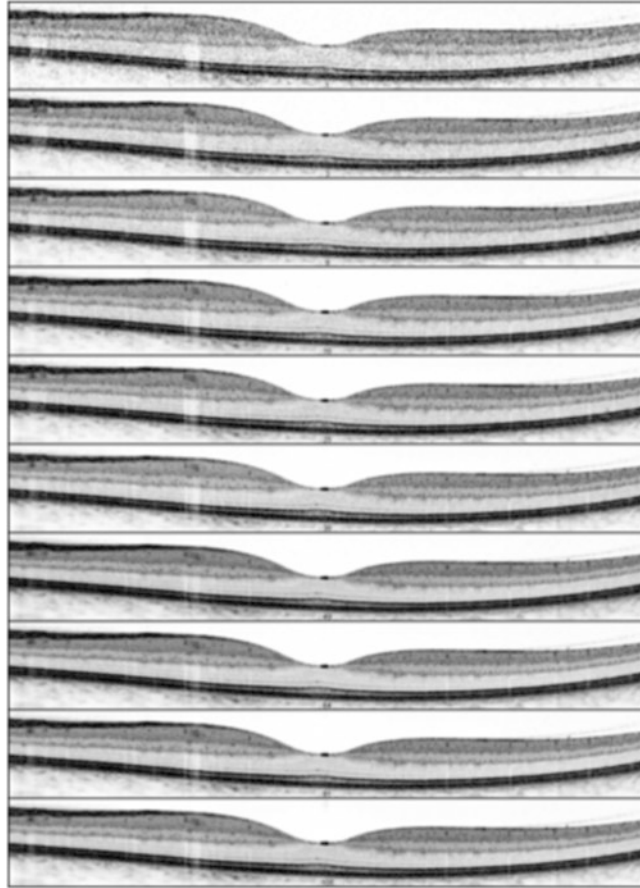
Fig. 3 Effect of B-scan averaging on the quality of SD-OCT scans. Number of averaged scans are 1, 3, 9, 16, 25, 36, 49, 64, 81, and 100 scans (from top to bottom row). Note that the greatest improvement is reached by nine averaged scans. More averaging only leads to minor additional quality (higher signal-to-noise ratio) with increased loss of axial resolution

3   Methods

3.1   Preparation of Human Subjects

1. A careful explanation of the procedures to be carried should precede any examination.

2. In general, OCT and OCT angiography scans may be taken without pharmacological pupil dilation. However, in case of bad image quality, pupil diameter maximization can be useful. Details on pupil dilation and possible side effects are provided in Chapter 23.

3. If pupil dilation is not desired or image quality is still insufficient despite a maximized pupil, one may apply artificial tear drops to improve the optical surface of the eye. In some cases, repeated application during long-lasting examinations is necessary to achieve an enduring optical effect. In general, we advise to use preservation-free single-dose eye drops.

3.2 OCT Recordings

1. Before positioning the subject for OCT recording, ensure that the head rest is properly cleaned with a soft alcohol swab.

2. The examiner must ensure that the head rest and the chair are properly height adjusted, to prevent unintended movements of the subjects examined due to an uncomfortable position.

3. If an eye with good central vision is examined, the use of an internal fixation target is the best option. However, in case of severe vision decrease, one may better use an external fixation light for the other eye with good vision. If both eyes have bad visual acuity one could use the external fixation target excentrically according to the subjects normal fixation area.

4. Every OCT device has its own recording protocol. Please refer to the manufacturers' user manuals. It is important to perform a quality check after each recorded OCT scan and repeat with artificial tears of pupil dilation if necessary (*see* **Notes 1** and **2**).

3.3 OCT Applications

3.3.1 SD-OCT as a Tool to Detect Retinal Disease Biomarkers

OCT allows for qualitative and quantitative assessment of retinal diseases. For example, the identification of focal thinning of the nerve fiber layer can be important for the early diagnosis of glaucoma [6, 7]. Of particular clinical interest is the strong reflectivity of the photoreceptor-RPE complex. With modern SD-OCT devices, four reflective bands may be observed in this complex in the healthy. These include reflections from the external limiting membrane, the inner-outer segment junction, photoreceptor outer segment tips, and the zone where outer segment tips interdigitate with RPE cell protrusions (interdigitation zone) [8]. Frequently however, the latter two are visualized as a single band. Disruptions, thickness changes, and reflectivity changes of the photoreceptor bands have been linked to loss of visual function in numerous retinal diseases. However, the absence of particular bands (e.g., the inner–outer segment junction band) does not necessarily indicate loss of structure, because optical changes may occur without tissue loss [9].

3.3.2 Functional OCT

Early in OCT development, its potential for numerous functional applications beyond structural imaging was recognized [10]. Presently, some of the most advanced applications include OCT's sensitive to birefringence (polarization-sensitive OCT), oxygenated hemoglobin (spectroscopic OCT), enhanced contrast of targeted molecules (contrast enhanced OCT) [11, 12], tissue elasticity (shear wave imaging OCT) [13], blood flow (OCT angiography), and stimulus-evoked intrinsic optical signals (IOS) indicative of hemodynamic activation and/or phototransduction (IOS-fOCT). Currently, only OCT angiography has been introduced in clinical practice and is commercially available from several manufacturers.
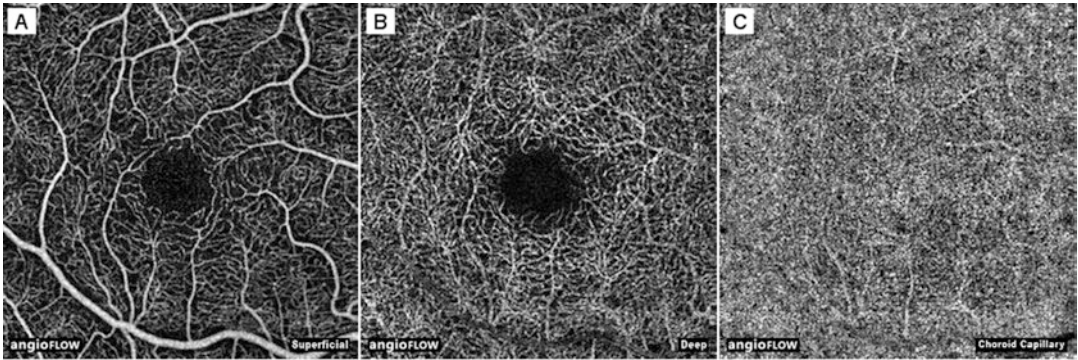
Fig. 4 OCT-A images of a healthy subject obtained with a commercial device based on the SSADA technique, displaying axially average flow in three vascular compartments. Superficial retina showing the retinal vessels and capillary beds, including the inner limiting membrane, retinal nerve fiber layer, and ganglion cell layers (**a**). Deep retina, showing the deeper inner retinal capillary beds, including the inner plexiform layer, inner nuclear layer, and outer plexiform layer (**b**). Choriocapillaris, showing the choroidal capillary bed, defined as 10 μm below Bruch's membrane directly below the RPE (**c**)

3.3.3 OCT angiography (OCT-A)

In OCT-A, blood flow is discriminated from static tissue by analyzing phase changes [14–17] or intensity changes [18, 19] in the OCT signal caused by moving light-scattering particles, i.e., intravascular blood cells. Phase-based methods are insensitive to motion normal to the incident beam (i.e., axial motion) and require phase-sensitive detection. Intensity-based methods make use of rapid fluctuations in the scattering pattern of blood flow, caused by a stream of randomly distributed blood cells through the imaging volume (voxel), leading to decorrelation of reflections in proportion to particle velocity. In OCT-A, speckle noise produces high decorrelation values throughout the flow image regardless of the actual sample reflectivity. Because of the randomness of these speckles, generated by the interference of waves with random phases [10], simply averaging of multiple images of the same location suffices to suppress speckle (Fig. 3). One intensity-based method, split-spectrum amplitude decorrelation angiography (SSADA), demonstrated high gains in the signal-to-noise ratio of flow detection due to an equalized sensitivity to flow in all three dimensions by equalizing the axial and lateral resolution [20]. The SSADA-technique is therefore used in various commercialized SD-OCTs (Fig. 4).

OCT-A devices offer a multitude of clinical biomarker sensing properties.

1. Scattering information of the underlying morphological OCT.

2. Noninvasive information of blood-flow within vessels.

3. Three-dimensional vessel structure information.

A major drawback is that OCT-A cannot detect serum flow and leakage. However, novel algorithms combining scattering and flow information may help to overcome this disadvantage in the future [21].

4   Notes

Current OCT devices allow for ultrahigh-quality scans—if applied correctly to the examined eye. Ocular conditions, OCT positioning, and focusing faults may still seriously affect the quality of the received images. Here, practical advice is given to get the optimum out of an OCT scan.

1. Ocular conditions (*see* Fig. 5). Compared to visible light, the infrared light used in OCT fortuitously is relatively insensitive to ocular media clouding/opacities. Dry eye syndrome and severe cataract are nevertheless frequent reasons for increased scattering leading to a low signal-to-noise ratio (SNR) and bad images.

2. Application faults (*see* Fig. 6). The examiner has to pay attention to the right position and focus of the OCT scanning device according to the patients' pupil. Defocus of the device, the wrong distance to the cornea and non-pupil centered imaging may result in incorrect scans, change of tissue reflectivity, and segmentation errors.
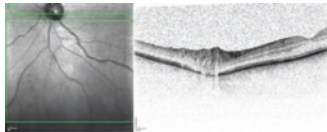
Condition	Consequence	Example	Solution
Dry eye	Increased speckle Segmentation faults		Apply artificial tears
Severe cataract	Increased speckle noise Segmentation faults		Maximal mydriasis

Fig. 5 Ocular conditions decreasing optical coherence tomography (OCT) image quality
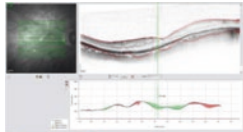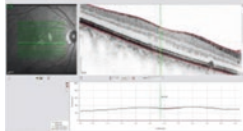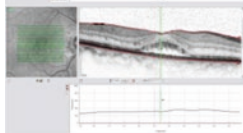
Condition	Consequence	Example	Solution
Wrong distance	Decreased tissue reflectivity Decreased SNR Vignetting (shadowing)		Increase / decrease camera-cornea distance until uniform illumination
Decenter	Tilted OCT scan Affected tissue reflectivity Segmentation errors		Center according to uniform illumination on fundus image and horizontal OCT scan
Defocus	Increased speckle noise Decreased SNR Segmentation errors		Re-focus fundus image on retinal vessels

Fig. 6 Examination faults leading to image deterioration in optical coherence tomography (OCT). *SNR* signal-to-noise ratio

References

1. Wojtkowski M, Srinivasan V, Ko T et al (2004) Ultrahigh-resolution, high-speed, fourier domain optical coherence tomography and methods for dispersion compensation. Opt Express 12:2404–2422

2. Nassif N, Cense B, Park B et al (2004) In vivo high-resolution video-rate spectral-domain optical coherence tomography of the human retina and optic nerve. Opt Express 12:367–376

3. Izatt J, Choma MA, Dhalla AH (2015) Theory of optical coherence tomography. In: Drexler W, Fujimoto JG (eds) Optical coherence tomography: technology and applications, 2nd edn. Springer International, Cham, pp 65–94

4. Staurenghi G, Sadda S, Chakravarthy U et al (2014) International nomenclature for optical coherence tomography P. Proposed lexicon for anatomic landmarks in normal posterior segment spectral-domain optical coherence tomography: The in*oct consensus. Ophthalmology 121:1572–1578

5. Lujan BJ, Roorda A, Knighton RW et al (2011) Revealing Henle's fiber layer using spectral domain optical coherence tomography. Invest Ophthalmol Vis Sci 52:1486–1492

6. Leung CK (2014) Diagnosing glaucoma progression with optical coherence tomography. Curr Opin Ophthalmol 25:104–111

7. Weinreb RN, Khaw PT (2004) Primary open-angle glaucoma. Lancet 363:1711–1720

8. Kocaoglu OP, Lee S, Jonnal RS et al (2011) Imaging cone photoreceptors in three dimensions and in time using ultrahigh resolution optical coherence tomography with adaptive optics. Biomed Opt Express 2:748–763

9. Scoles D, Flatter JA, Cooper RF et al (2015) Assessing photoreceptor structure associated with ellipsoid zone disruptions visualized with optical coherence tomography. Retina 36:91–103

10. Fercher AF, Drexler W, Hitzenberger CK et al (2003) Optical coherence tomography–principles and applications. Rep Prog Phys 66:239–303

11. Adler DC, Huang SW, Huber R et al (2008) Photothermal detection of gold nanoparticles using phase-sensitive optical coherence tomography. Opt Express 16:4376–4393

12. Lee TM, Oldenburg AL, Sitafalwalla S et al (2003) Engineered microsphere contrast agents for optical coherence tomography. Opt Lett 28:1546–1548

13. Wang S, Larin KV (2014) Shear wave imaging optical coherence tomography (swi-oct) for ocular tissue biomechanics. Opt Lett 39:41–44

14. Zhao Y, Chen Z, Saxer C et al (2000) Phase-resolved optical coherence tomography and optical doppler tomography for imaging blood flow in human skin with fast scanning speed and high velocity sensitivity. Opt Lett 25:114–116

15. Wang RK, Jacques SL, Ma Z et al (2007) Three dimensional optical angiography. Opt Express 15:4083–4097

16. Wang XJ, Milner TE, Nelson JS (1995) Characterization of fluid flow velocity by optical doppler tomography. Opt Lett 20:1337–1339

17. Chen Z, Milner TE, Dave D et al (1997) Optical doppler tomographic imaging of fluid flow velocity in highly scattering media. Opt Lett 22:64–66

18. Barton J, Stromski S (2005) Flow measurement without phase information in optical coherence tomography images. Opt Express 13:5234–5239

19. Mariampillai A, Standish BA, Moriyama EH et al (2008) Speckle variance detection of microvasculature using swept-source optical coherence tomography. Opt Lett 33:1530–1532

20. Jia Y, Tan O, Tokayer J et al (2012) Split-spectrum amplitude-decorrelation angiography with optical coherence tomography. Opt Express 20:4710–4725

21. Cunha-Vaz J, Santos T, Ribeiro L et al (2016) OCT-Leakage: a new method to identify and locate abnormal fluid accumulation in diabetic retinal edema. Invest Ophthalmol Vis Sci 57:6776–6783

Chapter 27

Vector Shedding and Immunogenicity Sampling for Retinal Gene Therapy

Alun R. Barnard, Anna N. Rudenko, and Robert E. MacLaren

Abstract

There has been recent growth in the number and magnitude of clinical trials for various forms of retinal gene therapy. Because of regulatory requirements, and to better understand vector safety profiles, there is a need for standardised and effective methods to collect, process, and store biological samples taken from trial patients that can be used to assess the dissemination of the vector within bodily fluids and any systemic cellular and humoral immune responses.

Key words Viral vector shedding, Immunogenicity, AAV, Gene therapy, Clinical trials

1 Introduction

In most countries and territories, there is a regulatory requirement to assess the potential risk to third parties and to the environment from any medicine containing or consisting of GMO/GMMs (genetically modified organisms/microorganisms), before authorization to market the product is granted [1–3]. This is true even for medicines that are based on wild-type viruses that are nonpathological or "safe," such as vectors derived from AAV (adeno-associated virus). Part of the risk assessment will involve inspection of the biological properties of the wild-type and modified vector (such as replicative ability, potential for gene transfer/recombination, etc.) but an important component will also be empirical data on how the vector disseminates into the environment, through the secretions and/or excreta of the patient receiving treatment. This latter component is defined as vector shedding. The types of secretions and/or excreta of the trial participant that are collected should be tailored to the specific route of administration, for example, a tear sample is most useful for ocular gene therapy, but others samples such as saliva, urine and faeces may also be included. Peripheral blood and related products are also often included as vector shedding samples, although these materials are not

considered true excreta since they do not shed into the environment spontaneously. As gene therapy becomes a more widespread and mainstream treatment strategy for a number of retinal diseases, with more investigative clinical trials taking place [4–9], it would be useful to have standardised materials and methodologies for the accurate collection of vector shedding samples.

Consideration should also be made as to the best methods for detecting the presence of vector in samples. For viral GMMs, it is accepted that direct methods of detection (such as culturing) may not be applicable and indirect monitoring techniques, such as detection of viral DNA by polymerase chain reaction (PCR), may be necessary. Although PCR is limited, insofar as it will determine whether the GMM nucleic acids are detected and not necessarily indicate the presence of an intact GMM, the use of quantitative PCR (qPCR) methods can determine if the amount of GMM nucleic acid is changing over time. This is useful, as a sample type that shows decreasing copy-numbers over time might confirm that, although the initial vector that is delivered is being shed, this is reducing and no replication of vector is taking place. Other advantages of using qPCR-based assays are that they are sensitive, reproducible, and rapid. Whatever molecular method is chosen for vector shedding analysis, it should be validated, quality controlled and compared against appropriate standards. If a PCR-based assay is chosen, then a great advantage is that shedding samples may be minimally processed, frozen, and stored for later analysis. However, care must be taken to preserve the vector DNA (or RNA) in samples and reduce the activity of DNase/RNase enzymes that might be present in the sample or introduced from the environment.

Another important aspect in the assessment of regulatory approval and the future management of patients is the degree to which a GMO medicine elicits a systemic immune response. For subretinal gene therapy using AAV, the low vector dose and direct administration into an immune privileged site are likely to limit immune responses as compared to, say, hepatic portal vein delivery of vector for gene therapy for hemophilia. However, to better understand the full safety profile of any potential GMO medicine it is important in early clinical trials to look for markers of systemic cellular and humoral immune activation, even if these do not necessarily manifest as a noticeable immune response in the patient. There are several assays to study immune responses. The most common methods measure the specific antibody content of serum or plasma fractions of peripheral blood, either by directly quantifying these by Enzyme-Linked ImmunoSorbent Assay (ELISA) or indirectly with a cell-based neutralizing antibody assay. Specific immune-cell fractions can also be isolated from blood for use in an ex vivo assay of adaptive immune responses, for example peripheral blood mononuclear cells (PBMCs) can be

isolated for use in enzyme-linked immunosorbent spot (ELISPOT) assays. Whatever immunoassays are ultimately used, they should be validated, quality controlled and compared against appropriate standards wherever possible. From a sampling perspective, it is important that standardised methods exist for collection, processing and storage, in order to reduce variability and preserve quality.

The schedules of sample collection for vector shedding and immunological assessment will likely overlap but will likely have a different overall duration and temporal resolution. For trials involving nonreplicating vectors, such as AAV, vector shedding will be most important in the period immediately following vector administration and sampling will be most intensive during this period and may be reduced or discontinued later in the trial. To our knowledge, the only vector shedding sample for AAV retinal gene therapy that has tested positive for vector DNA to date has been a tear sample collected on the day immediately after administration [8].

For immunological assessment sampling, although it is important to obtain a baseline sample for these tests, cellular and humoral adaptive immune responses to the vector and transgene product may develop later, especially if immune suppression is given around the time of vector administration. Thus, this sampling may be more evenly spaced throughout the duration of the trial and may continue after vector shedding sampling has been discontinued. The methods for collection and processing of samples are described below. These are intended to be accessible to a range of individuals, but it assumed they will normally be carried out by clinical research nurses who have some ophthalmic training and phlebotomy experience.

2 Materials

It is best to use materials that are individually wrapped and single-use. Wherever possible, they should be certified as sterile and free of pyrogens, DNA, RNases, DNases, and PCR inhibitors. All materials should be used by the expiry date on the packaging. Materials should be stored at room temperature (unless stated otherwise) and be kept in a separate area away for direct sunlight, high humidity, and away from potential exposure to viral vectors. Most components of the kits described below can be assembled together and "bagged up" so they are ready in advance of sampling. The kits described aim to split the sample into three identical aliquots for long-term storage. This allows for retesting if there are problems during analysis.

2.1 Tear Sampling Kit	1. HydraFlock Mini Tip swab in peel pouch (Medical Wire and Equipment), or similar (×2, one for each eye).

2. Biopur 1.5 mL Safe-Lock cryosafe tubes (Eppendorf), or similar, ×4.

3. Biopur 1.5 mL Safe-Lock cryosafe tubes prefilled with 1 mL Phosphate-Buffered Saline (PBS, pH 7.4, without calcium, magnesium, or Phenol Red, ThermoFisher Scientific). Sample tubes should be chilled to 2–8 °C and kept on ice prior to sampling (×2).

4. Sufficient cryosafe adhesive labels (*see* **Note 1**).

5. Graduated pipettes (e.g., individually wrapped, certified sterile 1.0 mL graduated Pasteur pipette from STARLAB), ×2.

6. Sterile, disposable forceps, ×2.

7. Sterile, disposable scissors, ×2.

2.2 Saliva Sampling Kit

1. Saliva Collection Aid (Salimetrics).

2. Biopur 2 mL Safe-Lock cryosafe tubes (Eppendorf), ×3.

3. Sufficient cryosafe adhesive labels (*see* **Note 1**).

4. Graduated pipette (e.g., individually wrapped, certified sterile 1.0 mL graduated Pasteur pipette from STARLAB).

2.3 Urine Sampling Kit

1. Sterile urine collection container/cup (up to 100 mL).

2. Biopur 2 mL Safe-Lock cryosafe tubes (Eppendorf), ×3.

3. Sufficient cryosafe adhesive labels (*see* **Note 1**).

4. Graduated pipette (e.g., individually wrapped, certified sterile 1.0 mL graduated Pasteur pipette from STARLAB).

2.4 Faeces Sampling Kit

1. We have taken the view that this type of sample is not necessary following ocular gene therapy, and to date no regulatory authority, from a variety of countries, has requested that we include it.

2.5 Blood Collection Kit

1. Venepuncture set (Vacutainer® Blood Collection Set).

2. Gold top Vacutainer® blood collection tubes (BD: 5 mL, 13 × 100 mm Vacutainer® SST™ II Advance plastic tube, gold Hemogard™ closure, contains silica clot activator and gel), ×2.

3. Lavender top Vacutainer® blood collection tube (BD: 4 mL, 13 × 75 mm Vacutainer® plastic tube, lavender Hemogard™ closure, contains dipotassium EDTA salt).

2.6 Blood Processing Kit

1. Biopur 2 mL Safe-Lock cryosafe collection tubes (Eppendorf), ×3.

2. Sufficient cryosafe adhesive labels (*see* **Note 1**).

3. Graduated pipette (e.g., individually wrapped, certified sterile 1.0 mL graduated Pasteur pipette from STARLAB).

2.7 Serum Processing Kit

1. Biopur 2 mL Safe-Lock cryosafe tubes (Eppendorf), ×3.
2. Sufficient cryosafe adhesive labels (*see* **Note 1**).
3. Graduated pipette (e.g., individually wrapped, certified sterile 1.0 mL graduated Pasteur pipette from STARLAB).

2.8 Other Necessary Items/Equipment

1. Disinfectant that is effective against nonenveloped viruses (e.g., Distel High Level Laboratory Disinfectant manufactured by Tristel).
2. Decontamination solution for the degradation/deactivation of DNA and RNA (e.g., DNA-ExitusPlus™ manufactured by AppliChem GmbH).
3. Cryosafe and solvent-resistant, permanent marker pen (e.g., fine tip, black VWR Lab Marker) to write on cryosafe adhesive labels. A label printer may be used instead, but labels should be cryosafe and the printed text should be solvent-resistant.
4. Rack for Safe-Lock tubes, which has been previously treated with a disinfectant against nonenveloped viruses and decontaminant for the degradation/deactivation of DNA and RNA.
5. Rack for Vacutainer® blood collection tubes, which has been previously treated with a disinfectant against nonenveloped viruses and decontaminant for the degradation/deactivation of DNA and RNA.
6. Calibrated bench-top centrifuge, with a timer and capable of speeds generating a relative centrifugal force (RCF) of at least 1100.

3 Methods

Throughout the sampling and processing procedures it is important to wear gloves and other personal protective equipment (PPE). These will be identical to those of standard precautions used by clinical staff for routine handling of blood or tissue samples that could potentially harbour blood-borne viruses or other pathogens [10]. A minor difference is that disposable PPE (especially gloves) should be changed between sample types (and between eyes when sampling tears) to help minimise the potential for carry-over/contamination between samples.

The need to collect these samples is not immediately obvious, so it is important to explain the procedure to the trial participant and why it is required. It is standard practice to create worksheets to document the identity, sample type, visit type and date, timing

and chain of custody of samples. Identities should be recorded using an anonymous Participant Identifier specific to the trial participant concerned.

3.1 Tear Sampling and Processing

1. Perform check of necessary materials against list detailed above.

2. Confirm that no eye drops have been applied to the trial participant's eyes within the preceding hour. Do not proceed if this is not the case: the collection must be delayed.

3. Use adhesive cryolabels and cryomarker to label the 2× tubes prefilled with 1 mL PBS.

4. Make sure the participant is sitting comfortably with the head well supported. Ask the participant to look up throughout the procedure (and so avoiding touching the cornea). Always hold the swab parallel to the cornea to avoid injury if the participant moves unexpectedly (*see* Fig. 1).

5. Starting with the right eye, gently pull the lower lid down and gently touch the whole length of the flocked tip of the swab on the inside of the lower eyelid (the lower fornix) at the outer aspect (*see* **Note 2**).

6. Place the entire swab tip in the appropriate labeled tube (containing 1 mL of chilled PBS). Use sterile scissors to cut the swab shaft approximately 3.5 cm from the tip. Close tube cap tightly.

7. Repeat the process for the other eye (left) with a separate swab, scissors and labeled sample tube (*see* **Note 3**).

8. Vigorously shake the tubes with swab tips inside and then incubate on ice for at least 5 min. Further processing can be delayed by up to 30 min provided the tubes are kept chilled (2–8 °C).

9. Use adhesive cryolabels and cryomarker to label the 4× unused Safe-Lock cryosafe collection tubes identically (two tubes per eye).

10. Use sterile disposable forceps to remove the swab tip from the PBS solution in one of the tear fluid sample tubes. Squeeze residual moisture back into tube by pressing the swab to the inner side of the tube.

11. Use a sterile graduated pipette to transfer the tear fluid sample so that approximately equal amounts of sample (~0.33 mL) are divided between the 3× individual (but identically labeled for the same eye) Safe-Lock cryosafe collection tubes.

12. Using a fresh sterile forceps and pipette, repeat the process of removing the swab tip and dividing the tear fluid sample taken
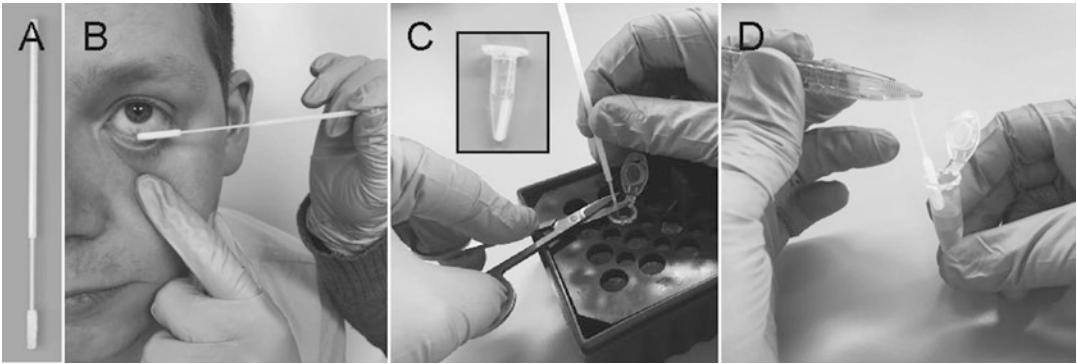
Fig. 1 Sampling method for tears. (**a**) full view of unpackaged HydraFlock® Mini Tip swab. There is a thicker plastic handle and toward the tip the shaft is thinner to allow it to be cut more easily. (**b**) during sampling the swab is held parallel to surface of the face, the lower lid is gently pulled down and the whole length of the flocked tip of the swab is touched on the inside of the lower eyelid (the lower fornix) at the outer aspect. (**c**) the tip of the swab is then immersed in prechilled PBS in a 1.5 mL cryosafe tube. This swab is held in place while the thin part of the shaft is cut just above the level of the end of the tube. The tube cap can then be tightly closed—the inset image shows the swab tip in place in the tube. (**d**) after vigorously shaking the capped tubes with swab tips inside and incubating on ice for at least 5 min, the tube can then be opened and sterile disposable forceps used to remove and discard the swab tip (the tip should be pressed to the inner side of the tube to release residual PBS solution back into tube)

from the other eye. Close the caps of the Safe-Lock cryosafe collection tubes tightly.

13. Discard all single-use materials as clinical waste (*see* **Note 4**).

3.2 Saliva Sampling and Processing

1. Perform check of necessary materials against list detailed above.

2. Confirm that the trial participant has followed instructions not to have anything to eat or drink for 30 min prior to collection of the sample. Do not proceed if this is not the case: the collection must be delayed.

3. Remove the Saliva Collection Aid (SCA) from packaging and place it securely into a freshly opened 2 mL Safe-Lock cryosafe collection tube (*see* Fig. 2).

4. Instruct the participant to allow saliva to pool in the mouth. (Some find it helpful to imagine eating their favorite food.)

5. Ask the participant to tilt their head forward and gently force/allow saliva to pass (drool) through the SCA into the Safe-Lock cryosafe collection tube (*see* **Note 5**).

6. Continue the process until the Safe-Lock cryosafe collection tube is filled to a volume of 1 mL.

7. Remove the SCA from the first filled Safe-Lock cryosafe collection tube and close the cap of the tube tightly.

8. Place the SCA in a new Safe-Lock cryosafe collection tube.
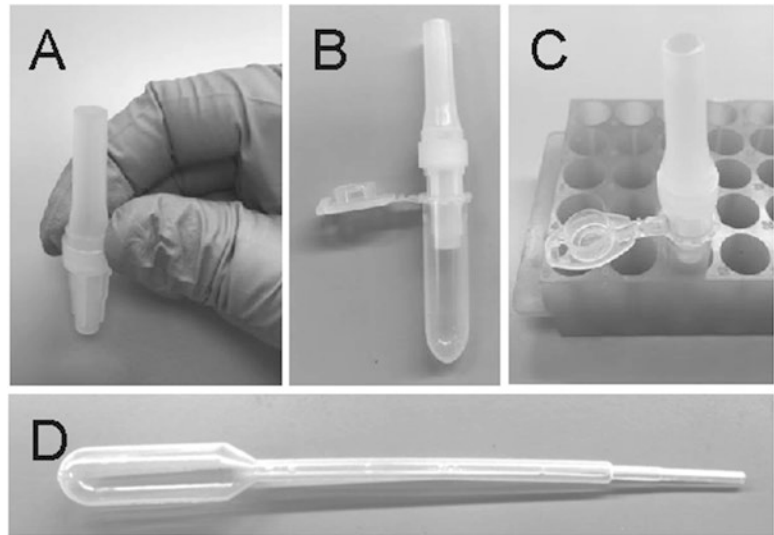
Fig. 2 Sampling materials for saliva. (**a**) the saliva collection aid (SCA) is a tube type device, to be handled by the middle collar. (**b**) plastic ridges allow the tube to be inserted snugly into a 2 mL collection tube. (**c**) the SCA-tube assembly can be stood in a tube rack, ready for immediate use. (**d**) a sterile, Pasteur-style, graduated pipette as shown here can be used to transfer saliva so approximately equal amounts of sample (0.5–1 mL) are contained in three individual 2 mL cryo-safe collection tubes

9. Repeat the process above: instruct the participant to allow saliva to pool in his mouth then drool through the SCA into the Safe-Lock cryosafe collection tube until filled to a volume of 1 mL.

10. Remove the SCA from the second filled Safe-Lock cryosafe collection tube and close the cap of the tube tightly.

11. Place the SCA in a new Safe-Lock cryosafe collection tube.

12. Repeat the process above again: instruct the participant to allow saliva to pool in his mouth then drool through the SCA into the Safe-Lock cryosafe collection tube until filled to a volume of 1 mL.

13. Remove the SCA from the third filled Safe-Lock cryosafe collection tube and close the cap of the tube tightly.

14. In total, 3×1 mL samples of saliva should be collected. If this is not possible, at least 3×0.5 mL of saliva must be collected but salivary stimulants must not be used. A sterile, disposable pipette can be used to transfer saliva so approximately equal amounts of sample (0.5–1 mL) are contained in three individual 2 mL cryosafe collection tubes.

15. Use adhesive cryolabels and cryomarker to label the 3× filled and sealed Safe-Lock cryosafe collection tubes identically.

16. Discard all single-use materials as clinical waste (*see* **Note 4**).

3.3   Urine Sampling and Processing

1. Perform check of necessary materials against list detailed above.

2. Instruct the participant to provide a sample of mid-stream urine by disregarding the initial flow of the voided urine and then, without disrupting the flow, collecting approximately 10 mL of urine in the sterile container (*see* **Note 6**).

3. Using a sterile graduated pipette, transfer 1 mL of urine into each of the 3 × 2 mL Safe-Lock cryosafe collection tubes.

4. Close the caps of the Safe-Lock cryosafe collection tubes tightly.

5. Use adhesive cryolabels and cryomarker to label the 3× filled and sealed Safe-Lock cryosafe collection tubes identically.

6. Discard all single-use materials as clinical waste (*see* **Note 4**).

3.4   Blood Collection

1. Perform check of necessary materials against lists detailed above.

2. The drawing of blood (venepuncture) should be conducted according to local procedures and guidelines (*see* **Note 7**).

3. Collect first Vacutainer® blood collection tubes, 2× Gold top Vacutainer® blood collection tube. This tube must be gently inverted five times after collection.

4. Collect second Vacutainer® blood collection tubes, 2× Lavender top Vacutainer® blood collection tube. This tube must be gently inverted 8–10 times after collection.
   FILL TUBES COMPLETELY to ensure a standard dilution of anticoagulant/additive.

5. Unprocessed Gold top Vacutainer® blood collection tubes should be stored at room temperature (18–25 °C) before processing—they MUST NOT BE CHILLED OR FROZEN.

3.5   Anticoagulated Blood Sample Processing

1. Perform check of necessary materials against lists detailed above.

2. Carefully open the Vacutainer® tube containing the whole blood sample.

3. Using a sterile graduated pipette, transfer 1 mL of blood into each of the 3 × 2 mL Safe-Lock cryosafe collection tubes.

4. Close the caps of the Safe-Lock cryosafe collection tubes tightly.

5. Use adhesive cryolabels and cryomarker to label the 3× cryosafe collection tubes identically.

6. Discard all single-use materials as clinical waste (*see* **Note 4**).

3.6   Processing Blood to Obtain a Serum Sample

1. Perform check of necessary materials against lists detailed above.

2. Check the condition of the centrifuge and that a recent calibration/validation has been performed.

3. Allow the blood to clot in the 2× Gold top Vacutainer® 5 mL blood collection tubes for a minimum of 30 min in a vertical

position. Ensure the formation of a dense clot and proceed to processing within a maximum of 2 h of collection.

4. Place the 2× Gold top Vacutainer® 5 mL blood collection tubes in the centrifuge rotor and ensure that the rotor is balanced.

5. Centrifuge at room temperature at a speed generating an RCF of 1100–1300 for 10 min for swing-head rotors or 15 min for a fixed-angle rotor (*see* **Note 8**).

6. Check that the serum has been successfully separated from the clot by the intermediate gel layer (*see* **Note 9**).

7. Carefully open the Vacutainer® tubes containing the separated serum samples.

8. Using a sterile graduated pipette, transfer an equal volume (~1 mL) of serum into each of the 3 × 2 mL Safe-Lock cryosafe collection tubes.

9. Close the caps of the Safe-Lock cryosafe collection tubes tightly.

10. Use adhesive cryolabels and cryomarker to label the 3× cryosafe collection tubes identically.

11. Discard all single-use materials as clinical waste (*see* **Note 4**).

3.7 Sample Storage

1. Promptly transfer the samples to the storage area for immediate freezing (*see* **Note 10**).

2. Processed samples should be stored frozen at colder than −60 °C. The frozen storage should have limited/controlled access and temperature monitoring in place.

3. Follow local processes for the logging of entry of samples.

4. The final action would be to complete any sample worksheets with the time at which samples have been frozen and to store worksheets in a secure locked cabinet.

4 Notes

1. Many types of label may be used, but it is important that the label and adhesive are certified cryosafe (i.e., they do not degrade or fall off when frozen to ultralow temperatures of colder than −60 °C). They should also fit on a 1.5 mL tube but allow writing in a font size that is legible.

2. The foreign object sensation may cause the participant to blink. This should not be discouraged and the swab should be withdrawn and then the tip touched gently again on the lower fornix after blinking has ceased. The swabs used here are designed for very rapid absorption (much faster and more effective than cotton or rayon fibre buds) so it is not necessary to hold the swab in place for an extended duration or to rub

against the surface. Conversely, the sample is released very effectively when immersed in liquid.

3. After tear samples have been taken, it may not be possible to process them immediately but will be more practical to continue with collection of other samples and come back to this later. The delay between collection and processing should be kept as short as possible, and during this time the tear samples should be kept on ice to maintain the integrity of any potential vector DNA.

4. Used materials may normally be disposed of via normal clinical waste routes. Sharps should be placed in appropriate containers (sharps bins) and other contaminated disposable equipment/material should go in normal biohazard yellow bags for disposal, unless it is suspected that the patient may substantially shed viable GMMs after administration (unlikely in ocular gene therapy), in which case potential GMMs in the waste may have to be inactivated using physical or chemical methods, before disposal.

5. Collecting saliva is not a quick process, especially on a patient's first attempt. We recommend against the use of oral stimulants when collecting saliva samples due to the possibility of causing assay interference or increasing variability in general. Instead, good communication is key, with the patient asked to remain calm and allowing some time for saliva to pool in the mouth before attempting to drool through the collection aid. Passing saliva into the tube should be a passive process and it does help if the patient is told to bend their head and/or body far forward to allow gravity to do the work. If the patient is too forceful in pushing saliva from their mouth, this causes the sample to be become excessively frothy.

6. There is no logical reason why a "midstream" urine sample is needed for vector shedding, but since this is the established method for urinalysis in general (it reduces bacterial contamination from skin commensals), it is arguably easier just to follow the status quo.

7. Venepuncture should be conducted using as large a gauge hypodermic needle as possible (i.e., 21 G), to prevent hemolysis of the sample. Blood collection systems from other manufacturers can be substituted here, if this fits with local practice and guidelines. However, the tube volume and additive should be as close as possible to those given. If other clinical samples are taken in the same venepuncture session, then they should be added to the collection list in accordance with the manufacturer's guidance on the order of draw for multiple tubes. For Vacutainer® blood collection tubes this can be found at www.bd.com/vacutainer/pdfs/plus_plastic_tubes_wallchart_orderofdraw_VS5729.pdf.

8. A swing-head rotor centrifuge is preferred for better separation and barrier formation but a fixed-angle rotor is acceptable if that is all that is available. If the centrifuge shows only revolutions per minute (RPM), a conversion to RCF must be performed. The radius of the rotor is needed for this calculation, which can often be found in the centrifuge handbook or manufacturer's website. Various online tools can then be used to perform the calculation, for example, http://www.hettich-centrifuge.co.uk/support.html.

9. Tubes should not be recentrifuged once the barrier has formed—to improve the serum quality after a poor separation, transfer the serum into a new Gold top Vacutainer® 5 mL blood collection tube and repeat the centrifugation step.

10. To maintain the DNA integrity of vector shedding samples it is important to proceed with processing and subsequent freezing as soon as possible. If immediate freezing is not possible, the processed samples should be immediately chilled at 2–8 °C and maintained at this temperature for no longer than necessary (ideally less than 2 h before freezing). A prefrozen chiller rack (e.g., StarChill MCT from Starlabs) or ice box may be used, but any reusable equipment must be thoroughly cleaned and treated with a disinfectant against nonenveloped viruses and an agent for the degradation/deactivation of DNA and RNA between uses.

Acknowledgments

References

1. U.S. Department of Health and Human Services, Food and Drug Administration, Center for Biologics Evaluation and Research (2015) Design and analysis of shedding studies for virus or bacteria-based gene therapy and oncolytic products: guidance for industry. https://www.fda.gov/downloads/BiologicsBloodVaccines/GuidanceComplianceRegulatoryInformation/Guidances/CellularandGeneTherapy/UCM404087.pdf. Accessed Aug 2015

2. Scientific Advisory Committee on Genetic Modification, Health and Safety Executive, UK (2007) The SACGM compendium of guidance, part 6: guidance on the use of genetically modified microorganisms in a clinical setting. http://www.hse.gov.uk/biosafety/gmo/acgm/acgmcomp/part6.pdf. Accessed Jan 2007

3. International Conference on Harmonisation of Technical Requirements for Registation of Pharmaceuticals for Human Use (2009) ICH considerations: general principles to address virus and vector shedding. http://www.ich.org/fileadmin/Public_Web_Site/ICH_Products/Guidelines/Multidisciplinary/M6/Concept_Paper/Considerations_on_Viral_Vector_Shedding.pdf. Accessed June 2009

4. Bainbridge JW, Smith AJ, Barker SS et al (2008) Effect of gene therapy on visual function in Leber's congenital amaurosis. N Engl J Med 358:2231–2239

5. Ghazi NG, Abboud EB, Nowilaty SR et al (2016) Treatment of retinitis pigmentosa due to MERTK mutations by ocular subretinal injection of adeno-associated virus gene vector: results of a phase I trial. Hum Genet 135:327–343

6. Hauswirth WW, Aleman TS, Kaushal S et al (2008) Treatment of leber congenital amaurosis due to RPE65 mutations by ocular subretinal injection of adeno-associated virus gene vector: short-term results of a phase I trial. Hum Gene Ther 19:979–990

7. MacLaren RE, Groppe M, Barnard AR et al (2014) Retinal gene therapy in patients with choroideremia: initial findings from a phase 1/2 clinical trial. Lancet 383:1129–1137

8. Maguire AM, Simonelli F, Pierce EA et al (2008) Safety and efficacy of gene transfer for Leber's congenital amaurosis. N Engl J Med 358:2240–2248

9. Wan X, Pei H, Zhao MJ et al (2016) Efficacy and safety of rAAV2-ND4 treatment for Leber's hereditary optic neuropathy. Sci Rep 6:21587

10. World Health Organization (2007) Standard precautions in health care: aide-memoire. http://www.who.int/csr/resources/publications/EPR_AM2_E7.pdf. Accessed Oct 2007

INDEX